U.S. DEPARTMENT OF THE INTERIOR
U.S. GEOLOGICAL SURVEY

GEOLOGIC HAZARDS IN THE SUMMIT RIDGE AREA OF THE SANTA CRUZ MOUNTAINS, SANTA CRUZ COUNTY, CALIFORNIA, EVALUATED IN RESPONSE TO THE OCTOBER 17, 1989, LOMA PRIETA EARTHQUAKE: REPORT OF THE TECHNICAL ADVISORY GROUP

Technical Advisory Group
on the
Santa Cruz Geologic Hazard Investigation

Report Prepared
for the
Federal Emergency Management Agency

1991

U.S. Geological Survey Open-File Report 91-618

TECHNICAL ADVISORY GROUP

Members:

David K. Keefer, (Report Editor), U.S. Geological Survey, Menlo Park, Calif.
Arijs A. Rakstins, (Project Manager), U.S. Army Corps of Engineers, San Francisco, Calif.
Gary B. Griggs, University of California, Santa Cruz, Calif., and Gary B. Griggs and Associates, Santa Cruz, Calif.
Edwin L. Harp, U.S. Geological Survey, Golden, Colo.
Paia Levine, County of Santa Cruz, Santa Cruz, Calif.
Colin C. McAneny, U.S. Army Corps of Engineers, Vicksburg, Miss.
Thomas E. Spittler, California Division of Mines and Geology, Santa Rosa, Calif.
Gerald E. Weber, University of California, Santa Cruz, Calif. and Weber and Associates, Watsonville, Calif.

Additional Contributors:

John M. Andersen, U.S. Army Corps of Engineers, Vicksburg, Miss.
Mary E. Hynes, U.S. Army Corps of Engineers, Vicksburg, Miss.
Jeffrey M. Nolan, Weber and Associates, Watsonville, Calif.
H. M. Taylor, U.S. Army Corps of Engineers, Vicksburg, Miss.

This is a technical report prepared for the Federal Emergency Management Agency at the request of the County of Santa Cruz to determine the geologic hazards that may have resulted from the Loma Prieta earthquake. Neither the Federal Emergency Management Agency nor any of the institutions or individuals participating in the Technical Advisory Group have any control on the use of this report by the County of Santa Cruz or other parties.

TABLE OF CONTENTS

CHAPTER I. INTRODUCTION

The magnitude 7.1 Loma Prieta earthquake, which occurred at 5:04 p.m. Pacific daylight time on October 17, 1989, was the largest seismic event in the San Francisco Bay-Monterey Bay region of California since 1906. The earthquake ruptured a 25-mile-long segment of the San Andreas fault in the Santa Cruz Mountains and had a hypocenter 10 miles east-northeast of Santa Cruz at a depth of 11 miles. At least 67 deaths, 3,757 injuries, and $6 billion to $7 billion of property damage have been attributed to the earthquake (Plafker and Galloway, 1989; San Francisco Chronicle, October 17, 1990, p. A5; San Francisco Chronicle, October 11, 1991, p. A4). Among other effects, the earthquake caused thousands of ground failures, including landslides, soil-liquefaction features, and zones of ground cracking throughout an area of approximately 5,400 square miles (Plafker and Galloway, 1989). The types and distribution of these ground failures were similar to those produced by other worldwide, historical earthquakes of approximately the same magnitude (Keefer, 1984).

A. Initial Post-Earthquake Investigations in Santa Cruz County

Immediately following the earthquake, geologic investigations of the earthquake effects were begun throughout the epicentral region. In Santa Cruz County, emergency geologic-hazard evaluations were initiated the day after the earthquake by personnel from the U.S. Geological Survey (USGS), U.S. Army Corps of Engineers (COE), California Division of Mines and Geology (CDMG), California Department of Transportation, University of California at Berkeley (UCB), University of California at Santa Cruz (UCSC), County of Santa Cruz (SCC), and numerous other government agencies and private-sector consulting firms. Many initial observations of landslides, ground cracks, and other ground failures in the epicentral region, including Santa Cruz County, were described in reports by Plant and Griggs (1990), Seed and others (1990), Spittler and Harp (1990), Spittler and others (1990), and Manson and others (in press). In all, geologic information in these reports was provided by more than 90 different individuals.

Within a few days after the earthquake, available data indicated that ground failures in Santa Cruz County had caused substantial damage and created potentially serious, continuing hazards to life and property. In particular, a zone with numerous ground cracks and large landslides was identified in the Summit Ridge area of the Santa Cruz Mountains, along the northeastern boundary of the county. This zone was between the San Andreas and Zayante faults and extended from just west of California Highway 17 approximately 5 miles southeast to Skyland Ridge. Results of initial surveys indicated that more detailed and systematic investigations of this area would be needed to determine the nature and extent of any potential hazards. The initial surveys also showed that the public agencies within Santa Cruz County did not have the resources to perform such investigations in a timely manner without assistance. SCC therefore requested assistance from the California Office of Emergency Services.

B. Formation of the Technical Advisory Group (TAG)

CDMG responded to the SCC request for emergency assistance by sending geologists and engineering geologists to coordinate geologic studies being conducted by various agencies and individuals, to complete a systematic reconnaissance, and to catalog the data being collected. On October 28, 1989, at a public hearing convened by Congressman Leon Panetta, the Federal Emergency Management Agency (FEMA), COE, and USGS also became involved in this effort and formulated the program that became known as the "Santa Cruz Geologic Hazard Investigation."

A Technical Advisory Group (TAG), composed of representatives from the USGS, COE, CDMG, SCC, UCSC, and local consulting firms was formed to direct the investigation. Members of the TAG were chosen for their technical expertise in the various fields needed to carry out a comprehensive investigation. As indicated in a Memorandum For Record (500-4b) of November 10, 1989, issued at the FEMA Disaster Field Office, which was coordinating Federal disaster response, initial members appointed to the TAG were Paia Levine (SCC), Edwin L. Harp (USGS), Colin McAneny (COE), William M. Brown III (USGS), Gary B. Griggs (UCSC and Gary B. Griggs and Associates), Thomas E. Spittler (CDMG), and Gerald E. Weber (Weber and Associates and UCSC).

This memorandum also indicated that other people with appropriate expertise would be expected to serve on the TAG as the work of the TAG progressed into different phases, and the TAG membership has changed somewhat during the course of the investigation in response to changing project needs. The current TAG, responsible for issuing this report, includes all of the original members except William M. Brown III, who was replaced by David K. Keefer (USGS) soon after the TAG was formed. In addition, Arijs A. Rakstins (COE) was added to the TAG as the project manager. Four other technical experts were retained by the TAG as consultants and contributing authors on specific aspects of the work: John M. Andersen (COE), Mary E. Hynes (COE), Jeffrey M. Nolan (Weber and Associates), and H. M. Taylor (COE). In addition, the TAG was assisted on several occasions by Robert Brumbaugh, Kenneth Harrington (COE), Martin Hudson (University of California at Davis--UCD), Kevin Schmidt (USGS), and Tak Yamashita (COE). At the request of the SCC Board of Supervisors, Alan D. Tryhorn, a geologic consultant retained by some residents of the Summit Ridge area, attended some TAG meetings as an observer.

C. Objectives of Investigation and Scope of Report

The charge for the "Santa Cruz Geologic Hazard Investigation" was given in a FEMA Action Tasker (fig. 1.1), developed at a Disaster Field Office meeting on November 8, 1989 (Memorandum For Record, Disaster Field Office (500), dated November 9, 1989). This charge was as follows:

> "Provide geotechnical advice and resource support to Santa Cruz County for the following:
>
> A. Mapping & survey of area-wide hazards
>
> B. Foundation investigation & instrumentation including required inclinometers, piezometers, rain gauges & assoc. lab procedures
>
> C. Preliminary modeling and hazard analysis for determination of safety hazards & emergency measures required"

FIGURE 1.1--Action Tasker from Federal Emergency Management Agency outlining charge to Technical Advisory Group for Santa Cruz Geologic Hazard Investigation.

ACTION TASKER

MISSION AREA

DSR DFA HMT TECH ASST

TO:	EOC LOG NO:	SUSPENSE
CORPS OF ENGINEERS	#051	IMMEDIATE

SUBJECT: TECHNICAL ASSISTANCE TO SANTA CRUZ COUNTY FOR INVESTIGATION OF GEOLOGIC HAZARDS RESULTING FROM THE LOMA PRIETA EARTHQUAKE

ACTION REQUIRED

PROVIDE GEOTECHNICAL ADVICE AND RESOURCE SUPPORT TO SANTA CRUZ COUNTY FOR THE FOLLOWING:

A. MAPPING & SURVEY OF AREA-WIDE HAZARDS

B. FOUNDATION INVESTIGATION & INSTRUMENTATION INCLUDING REQUIRED INCLINOMETERS, PIEZOMETERS, RAIN GAUGES & ASSOC. LAB PROCEDURES

C. PRELIMINARY MODELING AND HAZARD ANALYSIS FOR DETERMINATION OF SAFETY HAZARDS & EMERGENCY MEASURES REQUIRED

COORDINATE

- USGS WILL PROVIDE TECHNICAL ADVICE ON SCOPE OF INSTRUMENTATION AND ANALYSIS.

- CALIFORNIA DIVISION OF MINES & GEOLOGY WILL ALSO PROVIDE SUPPORT TO SANTA CRUZ COUNTY.

- A TASK GROUP INVOLVING SANTA CRUZ COUNTY, USGS, COE, AND CDMG WILL WORK TOGETHER TO COMPLETE THESE TECHNICAL INVESTIGATIONS.

- COE WILL BE RESPONSIBLE FOR A/E CONTRACTING SUPPORT.

Encl 3

This Action Tasker also outlined participation of the various government agencies as follows (fig. 1.1):

> "-USGS will provide technical advice on scope of instrumentation and analysis.
>
> -California Division of Mines & Geology will also provide support to Santa Cruz County.
>
> -A task group involving Santa Cruz County, USGS, COE, and CDMG will work together to complete these technical investigations.
>
> -COE will be responsible for A/E contracting support."

As indicated by the last statement above, it was anticipated that parts of the investigation would be carried out by various private-sector firms acting under contract.

The area covered by the investigation was determined based on criteria established by FEMA for Federal funding of technical assistance and on the geologic data that were available in the first few weeks after the earthquake. The agreement to provide Federal funds was based on the urgency of the need for technical assistance, the emergency nature of concern for public health and safety, the extent of public infrastructure in the affected area, and the public costs potentially involved in an emergency that might develop in the future as a result of earthquake-related ground damage.

In the Summit Ridge area of Santa Cruz County, preliminary geologic evidence available within the first few weeks after the earthquake indicated the presence of extensive zones of ground cracks and large landslides. Concern at that time about possible additional ground cracking and slope movements within the Summit Ridge area was heightened by the imminent approach of the annual rainy season and the likelihood of large aftershocks. By contrast, the preliminary evidence suggested that most other earthquake-induced

ground failures that had been identified within Santa Cruz County affected relatively small areas and damaged or threatened one or a small number of properties and were, therefore, of a size typically investigated and mitigated by individual property owners. In addition, few of these other hazard areas involved public infrastructure.

It is important to emphasize that the selection of the Summit Ridge area for detailed study, while other areas were left for privately-funded investigations, was based on data available at the time selections were made and investigation resources were allocated, a few weeks after the earthquake. It is also important to note that the purpose of this publicly funded study was to identify and delineate the extent of the potential hazards and to serve as a guide in planning and decision making in the study area. This study thus was not intended to substitute for or replace appropriate, site-specific geologic and engineering investigations required for individual construction projects or other site-specific purposes.

Components of the Santa Cruz Geologic Hazard Investigation, carried out in the Summit Ridge area and reported herein, are as follows:

* Detailed mapping of ground cracks caused by the Loma Prieta earthquake was carried out by 54 investigators. Forty of these investigators were from the USGS (including three visiting scientists) and CDMG; the remaining 14 were from SCC, the COE, and from the private-sector firms of Leighton and Associates, Weber and Associates, J. M. Nolan Consultant, and Dames and Moore. This mapping, based entirely on ground-based field observations and measurements, was verified and compiled by Thomas E. Spittler (CDMG) and Edwin L. Harp (USGS) at a scale of 1:4800, on a planimetric base prepared by SCC, which shows property boundaries and cultural features (Spittler and Harp, 1990). Details of the mapping method and compilation procedures were discussed in that report. Preliminary versions of this mapping were used for planning other components of the investigation. For the present report, the final version of this mapping was registered with 1:6,000 orthophoto and topographic bases, the latter enlarged by Towill, Inc. from 1:24,000-scale USGS quadrangle maps. As discussed in Chapter III, the maps of ground cracks registered with the topography

were the base used for plotting inferred, approximate boundaries of large landslides in the Summit Ridge area that experienced movement during the Loma Prieta earthquake. The maps of ground cracks compiled by Spittler and Harp (1990) were also used in the detailed analysis of structurally controlled ground cracks, as discussed in Chapter IV.

* Topographic profiles along 12 selected transects were surveyed in the field by Towill, Inc. and Majors Engineering and compiled at scales of 1:1200 and 1:4800 (1:120 and 1:480 for one short profile) for use in preparing geologic cross sections and in performing slope-stability analyses.

* A program of surface monitoring of potential post-earthquake slope movements was undertaken by Gary B. Griggs and Associates. This program involved placing 51 quadrilateral arrays of survey stakes and eight continuously recording strain gages across ground cracks or zones of ground cracks that preliminary evidence indicated were associated with large landslides. Details of this program were described by Griggs and others (1990) and Griggs and Marshall (1991) and are summarized in Chapter VI.

* Data on landslides occurring in and around the Summit Ridge area before the 1989 earthquake, primarily associated with previous earthquakes or winter rainfall, were compiled from existing historical documents and the scientific literature by Jeffrey S. Marshall (Gary B. Griggs and Associates) and David K. Keefer (USGS). These data are presented in Chapter II, and much of this information was also included in Griggs and others (1990).

* The post-earthquake status of water wells in the Summit Ridge area was surveyed by Robert Brumbaugh (Brumbaugh, 1990). Information in this survey came primarily from accounts volunteered by individual well owners and operators. Locations of some of the wells were also field checked, but no systematic downhole instrumental survey of well conditions was undertaken. Information on post-earthquake well status was obtained for 157 of the 239 known wells in the area. Of these 157 wells, 33 were reported to have been damaged by the 1989 earthquake (Brumbaugh, 1990). Relevant portions of these data are discussed in Chapters III and VII.

* Trenching investigations, to determine subsurface characteristics of ground-crack features, were carried out by Weber and Associates. Two trenches were excavated and logged at localities chosen by the TAG in consultation with Weber and Associates. In addition, data were evaluated from 25 other trenching investigations in the Summit Ridge area, on file with SCC or with the Loma Prieta Elementary School District. Results of the trenching investigations are presented in Chapter V.

* A program of subsurface exploration and borehole monitoring in the upper Schultheis Road and Villa Del Monte areas was carried out by William Cotton and Associates, Inc. This program consisted of drilling, sampling, logging, and instrumenting 18 boreholes and preparing four geologic cross sections. As part of this program, William Cotton and Associates, Inc. also reviewed and compiled pertinent, existing geologic and water-well data, performed localized engineering-geologic surface mapping and profiling, evaluated the pertinent topographic profiles prepared by Towill, Inc. and Majors Engineering, and formulated a geologic interpretation of landslide boundaries and depths. Instruments installed in the boreholes were inclinometers for recording slope movements and piezometers for recording pore-water pressures. Initial monitoring of the instruments was also carried out by William Cotton and Associates, Inc., and subsequent monitoring was accomplished by Robert Brumbaugh and others under the supervision of the TAG. Interpretive cross sections prepared from these subsurface data were used as input for analyzing slope stability. The scope and results of the drilling program, including complete borehole logs, were presented in a report by William Cotton and Associates, Inc. (1990), and results and interpretations from this subsurface exploration and monitoring are summarized in Chapter VII.

* Two other types of subsurface exploration and monitoring were undertaken on an experimental basis in the Upper Schultheis Road area. These investigations--shallow geophysical profiling and installation and monitoring of a tiltmeter--were discussed, respectively, by Williams and King (1990) and Horath (1990). The results of the geophysical profiling had not been fully interpreted in time for inclusion in this report. The tiltmeter, installed in an effort to detect potential post-earthquake

movement, recorded negligible movements during the monitoring period, extending from March 28 through August 7, 1990.

* Samples of earth materials in the Summit Ridge area were subjected to laboratory tests to determine grain-size characteristics, Atterberg liquid and plastic limits, specific gravities, water contents, unit weights, shear strengths and stress-strain properties. Tests were performed in the COE South Pacific Division Laboratory in Sausalito, California (U.S. Army Corps of Engineers South Pacific Division Laboratory, 1991) and are discussed in Appendix A. Samples to be tested were chosen by COE personnel in consultation with the TAG. Preliminary recommendations for appropriate samples for testing were provided by William Cotton and Associates, Inc.

* Analytical slope-stability modeling was performed and is discussed in Chapter VIII. This modeling simulated slope-stability conditions, associated both with earthquake shaking and with various ground-water/pore-water pressure regimes for various depths and geometries of sliding surfaces slopes, along three cross sections in the Upper Schultheis Road and Villa Del Monte areas.

* A public meeting on the study was held on June 6, 1991. Several comments and documents were received from the public before, during, and after this meeting, including a report by the Villa Del Monte Emergency Homeowners' Association Technical Committee, entitled "Tectonic Upthrust A Critique of Cotton's & Griggs' Reports." These comments and documents were reviewed by the TAG.

* The final component of the study was an evaluation by the TAG of the nature and severity of the geologic hazards in the Summit Ridge area associated with the ground cracking and slope movements that occurred during the Loma Prieta earthquake. This evaluation is presented in Chapter IX.

This report was reviewed by I. M. Idriss (Professor of Civil Engineering, UCD), Robert L. Schuster (Geologist, USGS), and Nicholas Sitar (Professor of Civil Engineering, UCB). In addition to these reviewers, we wish to thank Robert Brumbaugh, Kenneth Harrington,

Martin Hudson, Kevin Schmidt, Tak Yamashita, and numerous residents of the Summit Ridge area for their cooperation and assistance with this investigation.

D. References Cited

Brumbaugh, R., 1990, Santa Cruz well history survey: Santa Cruz, Calif., Report to Santa Cruz County Planning Department.

Griggs, G.B. and Marshall, J.S., 1991, Ground Crack Monitoring Program- December 1990-July 1991. Report to the Army Corps of Engineers.

Griggs, G. B., Rosenbloom, N. A., and Marshall, J. S., 1990, Investigation and monitoring of ground cracking and landslides initiated by the October 17, 1989 Loma Prieta earthquake: Santa Cruz, Calif., Gary B. Griggs and Associates, Final Report to the U.S. Army Corps of Engineers.

Horath, F., 1990, Summary of tiltmeter data, slope movement investigation, Schultheiss Road landslide: Santa Cruz, Calif., Applied Geomechanics, Inc., Report for U.S. Army Corps of Engineers, 14 p.

Keefer, D. K., 1984, Landslides caused by earthquakes: Geological Society of America Bulletin, v. 95, no. 4, p. 406-421.

Manson, M. W., Keefer, D. K., and McKittrick, M. A., compilers, in press, Landslides and other geologic features in the Santa Cruz Mountains, California, resulting from the Loma Prieta earthquake of October 17, 1989: California Division of Mines and Geology, Preliminary Report 29.

Plafker, G., and Galloway, J. P., eds., 1989, Lessons learned from the Loma Prieta, California, earthquake of October 17, 1989: U.S. Geological Survey Circular 1045, 48 p.

Plant, N., and Griggs, G. B., 1990, Coastal landslides caused by the October 17, 1989 earthquake Santa Cruz County, California: California Geology, v. 43, no. 4, p. 75-84.

Seed, R. B., Dickenson, S. E., Reimer, M. F., Bray, J. D., Sitar, N., Mitchell, J. K., Idriss, I. M., Kayen, R. E., Kropp, A., Harder, L. F., Jr., and

Power, M. S., 1990, Preliminary report on the principal geotechnical aspects of the October 17, 1989 Loma Prieta earthquake: University of California at Berkeley, College of Engineering, Earthquake Engineering Research Center Report No. UCB/EERC-90/05, 137 p.

Spittler, T. E., and Harp, E. L., 1990, Preliminary map of landslide features and coseismic fissures in the Summit Road area of the Santa Cruz mountains triggered by the Loma Prieta earthquake of October 17, 1989: U.S. Geological Survey Open-File Report 90-688 (also released as California Division of Mines and Geology Report 90-6), 29 p. + 3 plates.

Spittler, T. E., Harp, E. L., Keefer, D. K., Wilson, R. C., and Sydnor, R. H., 1990, Landslide features and other coseismic fissures triggered by the Loma Prieta earthquake, central Santa Cruz Mountains, California, *in* McNutt, S. R., and Sydnor, R. H., eds., The Loma Prieta (Santa Cruz Mountains), California earthquake of 17 October 1989: California Division of Mines and Geology, Special Publication 104, p. 59-66.

U.S. Army Corps of Engineers South Pacific Division Laboratory, 1991, Report of Soil Tests, Santa Cruz Landslide Study, Santa Cruz County, CA: Sausalito, Calif., Division Laboratory, 51 p.

William Cotton and Associates, Inc., 1990, Schultheis Road and Villa Del Monte areas geotechnical exploration Santa Cruz County, California: Los Gatos, Calif., William Cotton and Associates, Inc. Report for U.S. Army Engineers, 2 vols.

Williams, R. A., and King, K. W., 1990, Summary of seismic-reflection/refraction investigations on Schultheis Road landslide, Santa Cruz County: Golden, Colo., U. S. Geological Survey, Technical letter dated August 17, 1990, 5 p.

CHAPTER II. PHYSICAL AND CULTURAL SETTING OF THE SUMMIT RIDGE AREA

A. Location, Topography, and Vegetation

The area covered by the Santa Cruz Geologic Hazard Investigation is adjacent to the northeastern boundary of Santa Cruz County, approximately 50 miles southeast of San Francisco, 10 miles south of San Jose, and 10 miles north of Santa Cruz (fig. 2.1). The area encompasses those portions of the Summit Ridge area most affected by ground cracks and landslides that occurred during the Loma Prieta earthquake. Boundaries of the area were chosen by the TAG and coincide with major topographic or cultural features wherever possible. The study area is bounded on the west by Hutchinson Road; on the north and northeast by the Santa Cruz County boundary, Summit Road, and Highland Way (Montgomery Road); on the east by Skyland Ridge and Amaya Ridge; and on the south and southwest primarily by Hester Creek, Burns Creek, and Mountain Charlie Gulch, with local departures from these creek channels to encompass landslides and zones of ground cracking in the Redwood Lodge and Laurel township areas (fig. 2.2). These boundaries enclose an area of approximately 6.4 square miles.

Much of the northern and northeastern boundary of the study area coincides with the crest of the Santa Cruz Mountains, an 80-mile-long mountain range that separates the San Francisco Bay region to the north and east from the Monterey Bay region to the south and west. The highest point in the Santa Cruz Mountains is the summit of Loma Prieta (altitude 3791 feet above mean sea level), 3.8 miles east of the study area. Within the study area itself, altitudes range from approximately 520 feet to 2167 feet. The study area includes parts of Skyland Ridge, the features locally known as "Summit Ridge" and "Amaya Ridge," and several adjacent ridges and valleys. Slopes range from gently rolling to locally steep. Surveyed profiles in the area show average slope inclinations of ridge flanks are typically in the range between 10 and 25°. Many of the ridge flanks also exhibit irregular, benched topographic profiles along which segments steeper than this average alternate with gentler segments. Much of the Summit Ridge area is covered with dense forests, dominated in some zones by coast redwood (*Sequoia sempervirens)* and in others by various species of oak (*Quercus).*

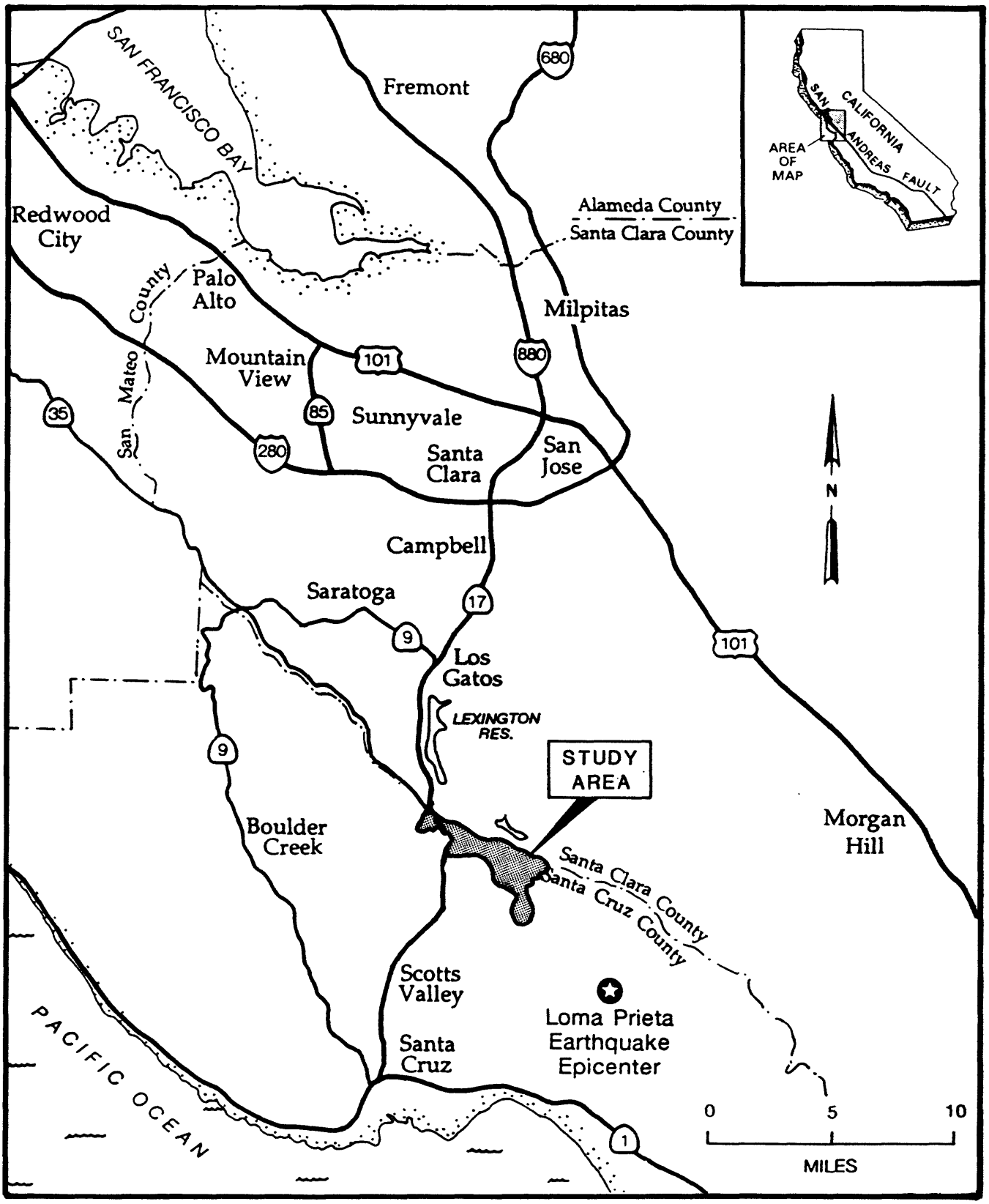

FIGURE 2.1 –Location of study area in the San Francisco Bay–Monterey Bay region.

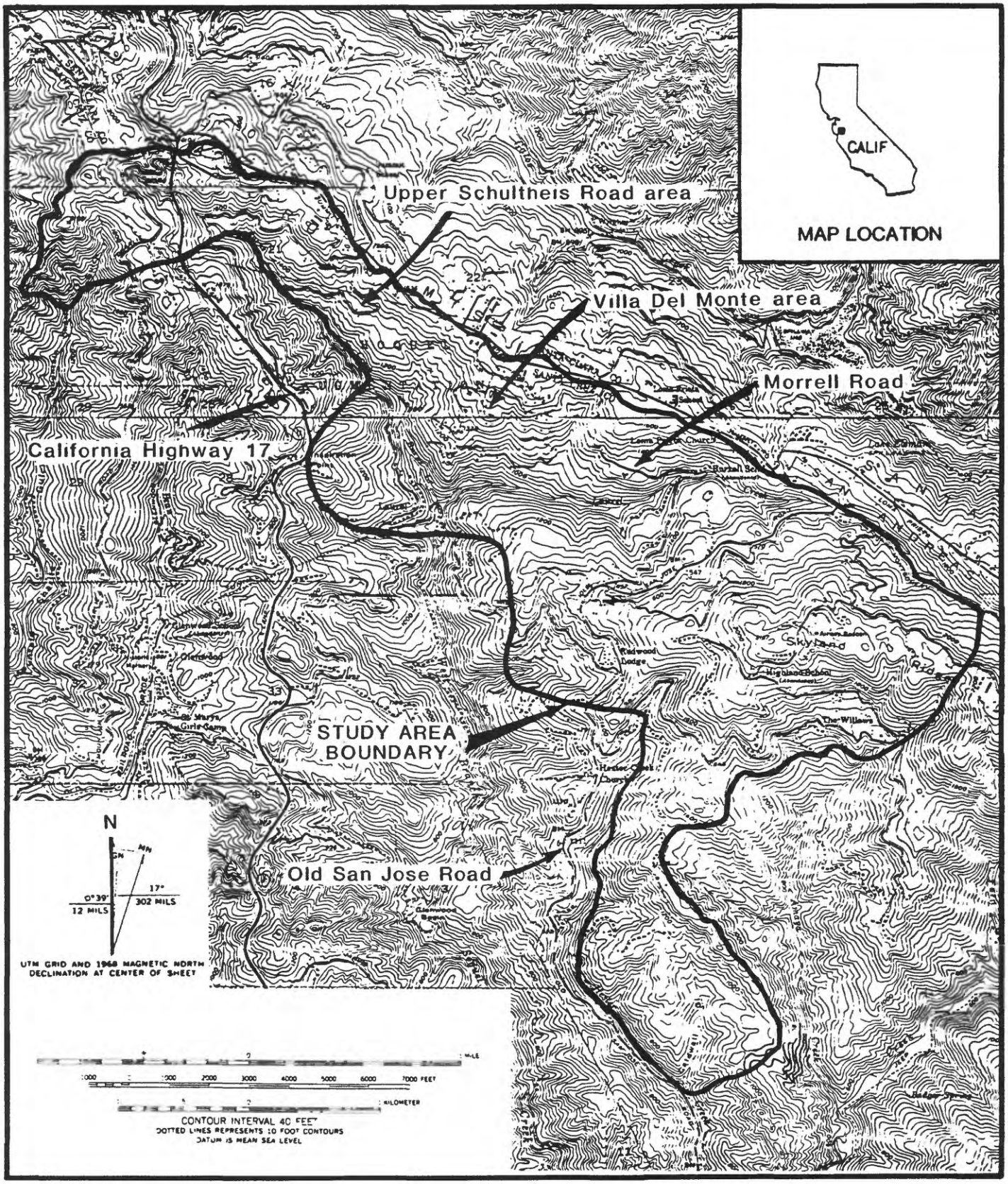

FIGURE 2.2 –Topography, drainage, and major roads in the Summit Ridge area and boundary of study area. Base maps from U.S. Geological Survey Laurel, Calif. and Los Gatos, Calif. 7.5–minute topographic quadrangles.

Nonforested areas are typically covered by chaparral or grassland vegetation.

B. Climate and Rainfall

The Santa Cruz Mountains have a Mediterranean climate, characterized by warm, dry summers and cool, rainy winters. Temperatures rarely exceed 100° Fahrenheit or fall below freezing, and virtually all precipitation occurs as rain. This rain is generated by storms that originate over the Pacific Ocean and pass through the region, almost always between the months of November and April, inclusive, when 90 percent of the precipitation occurs. Precipitation is highly variable from place to place and year to year and depends on the number, severities, and paths of the storms that pass through the region. Figure 2.3 shows a composite 73-year record of annual rainfall as recorded at gages in and near the Summit Ridge area for water years 1919 through 1991, inclusive.

Mean annual precipitation in the Summit Ridge area is 45 to 50 inches (Rantz, 1971). However, rainfall during the 3 years preceding the Loma Prieta earthquake as well as during the 2 years after the event was below normal. Annual precipitation in the Summit Ridge area during the 1987-1991 water years was 32, 25, 29, 30, and 35 inches, respectively (fig. 2.3), or 71, 56, 64, 67, and 78 percent of normal. By contrast, maximum annual rainfall during the 73-year period of record was 87 inches (fig. 2.3), almost double the mean and almost triple the total received in the year after the Loma Prieta earthquake. The earthquake also occurred near the end of the dry summer season; the only precipitation recorded in the Summit Ridge area between June 1 and October 17, 1989, was 1.2 inches of rain that fell between September 16 and 29. Thus, ground conditions in the Summit Ridge area were unusually dry at the time of the earthquake.

C. Population and Infrastructure

The Summit Ridge area was settled by people other than Native Americans beginning early in the nineteenth century. The area currently retains a rural to locally suburban character despite its proximity to an urban metropolis of 5.9 million people in the San

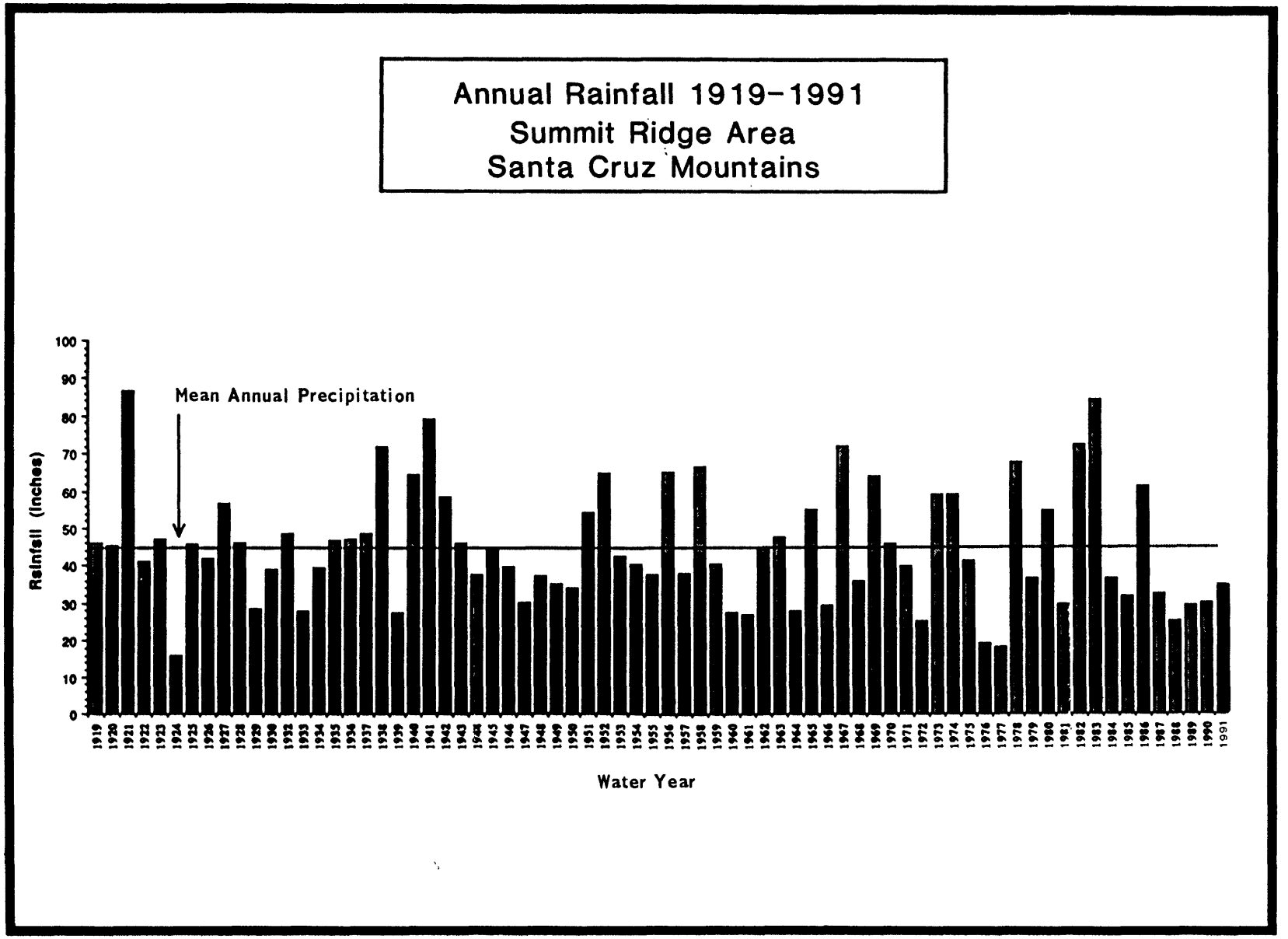

FIGURE 2.3 -Annual precipitation in the Summit Ridge area for water years 1919-1991. Data from Wrights gage, supplemented with data from Schultheis and Burrell gages for last 4 years. Data for 1919-1990 from Griggs and others (1990). 1991 data from Burrell gage.

Francisco Bay region. The Summit Ridge area is inhabited by approximately 4,000 people, many of whom live in the Villa Del Monte neighborhood, which contains 195 lots and approximately 165 single-family homes, or in the Redwood Lodge-Summit Woods area, where approximately 100 lots are located. In addition to the several hundred private residences, one public school and several churches are located in the Summit Ridge area.

Major north-south transportation arteries through the Summit Ridge area are California Highway 17 (a four-lane controlled-access highway) and Old San Jose Road (also called "San Jose-Soquel Road"); the main east-west artery is Summit Road. Fire protection and emergency response within this unincorporated area of Santa Cruz County are provided by the California Division of Forestry and Fire Protection and the SCC Sheriff's Department, respectively. Water service is provided by small mutual water companies and by individual wells and in-stream intakes.

D. Geologic Setting

Bedrock in this part of the central Santa Cruz Mountains consists primarily of Tertiary, marine sedimentary rocks--mostly sandstones, mudstones, siltstones, and shales. These rocks, which generally strike northwest, have been intensely folded and locally faulted so that they typically dip steeply, are vertical, or are even overturned. The most recent USGS geologic quadrangle mapping in the study area (Clark and others, 1989, with landslide boundaries revised by McLaughlin and Clark, 1990, unpublished data; McLaughlin and others, in press) is shown in figure 2.4. This geologic mapping was still ongoing at the time of this writing, and so it is possible that some geologic contacts and other information will be revised by the authors of the quadrangle maps as that work progresses.

The geologic structure of the Summit Ridge area is dominated by northwest-striking faults and folds (fig. 2.4). A portion of the 800-mile-long San Andreas fault passes along the northeastern boundary of the study area. Two other major, named faults in the area are the Butano and the Zayante (fig. 2.4). The Butano fault branches off from the San Andreas fault near the Summit Road-Old San Jose Road intersection; from that point the Butano fault strikes northwest through the study area, along and adjacent to Summit

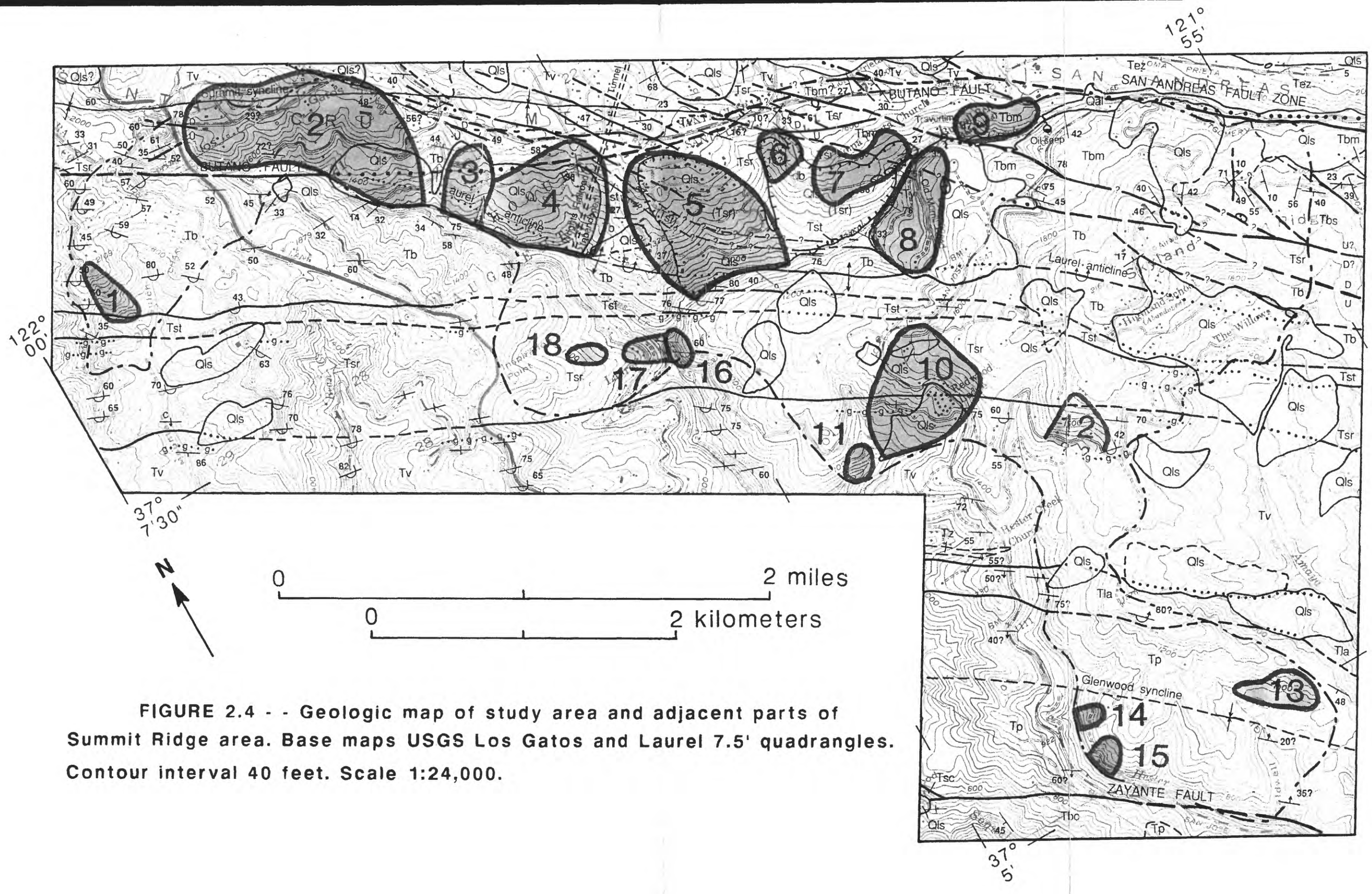

FIGURE 2.4 - - Geologic map of study area and adjacent parts of Summit Ridge area. Base maps USGS Los Gatos and Laurel 7.5' quadrangles. Contour interval 40 feet. Scale 1:24,000.

FIGURE 2.4--Geologic map of study area and adjacent parts of Summit Ridge area. Compiled from Clark and others (1989, with landslide boundaries revised by McLaughlin and Clark,1990, unpublished data) and McLaughlin and others (in press). Boundaries of landslides and landslide complexes that moved during Loma Prieta earthquake determined as described in Chapter III of this report.

DESCRIPTION OF ROCK UNITS
(modified from Clark and others, 1989)

SURFICIAL DEPOSITS

Qal ALLUVIUM (HOLOCENE AND UPPER PLEISTOCENE)--Unconsolidated gravel, sand, and silt deposited by streams.

Qls LANDSLIDE DEPOSITS (HOLOCENE AND PLEISTOCENE)--Debris consisting of a mixture of colluvium and intact masses of rock, displaced down slope by gravity. Additional landslide information can be found on the map by Cooper-Clark and Associates (1975) and in Wieczorek and others (1988).

UNITS SOUTHWEST OF SAN ANDREAS FAULT

Tp PURISIMA FORMATION (PLIOCENE)--Thick bedded to massive, locally cross-bedded, weakly consolidated, bluish-gray fine- to medium-grained sandstone with abundant andesitic detritus, and very thick-bedded, yellowish-gray, tuffaceous and diatomaceous siltstone. Locally contains scattered cetacean bones and molluscan lenses diagnostic of inner neritic depths and of Pliocene age. As much as 2,700 feet thick along Glenwood syncline.

Tla LAMBERT SHALE (LOWER MIOCENE)--Thin- to medium-bedded and faintly laminated olive-gray organic mudstone with pale-yellowish-brown phosphatic laminae and lenses in lower part. Formation grades upward to thin-bedded sandy siltstone with thin to thick interbeds of micaceous fine- to medium-grained arkosic sandstone. Approximately 1,500 feet of Lambert crop out along Mountain Charlie Gulch and as much as 1,800 feet along Hinckley Creek to the southeast. Fish scales and fragments are common, and benthic foraminifers are diagnostic of bathyal depths and of the early Miocene Saucesian Stage.

Tv VAQUEROS SANDSTONE (LOWER MIOCENE AND OLIGOCENE)--Thick-bedded to massive, yellowish-gray, fine- to coarse-grained arkosic

sandstone with thick glauconitic sandstone bed in lower part. The Vaqueros is as much as 2,700 feet thick. Benthic foraminifers from the lower part are diagnostic of bathyal depths and of an early Zemorrian (Oligocene) age.

Tz ZAYANTE SANDSTONE (LOWER MIOCENE AND OLIGOCENE)--Thick- to very thick-bedded poorly sorted, reddish muddy sandstone, greenish sandy siltstone, and cobble conglomerate with abundant granitic detritus, probably nonmarine. Locally intertongues with Vaqueros Sandstone. (Present within boundaries of geologic map but not within study area.)

SAN LORENZO FORMATION (OLIGOCENE AND UPPER EOCENE)

Tsr Rices Mudstone Member--upper part is light-gray nodular mudstone, which is locally bioturbated and glauconitic and yields fish scales and benthic foraminifers diagnostic of upper middle bathyal depths and an early Zemorrian (Oligocene) age. Along Soquel Creek and to the east in the Loma Prieta quadrangle, lower part is massive fine-grained glauconitic arkosic sandstone with *Pitar* locally abundant and mollusks characteristic of inner neritic depths and of a Refugian (late Eocene) age. The Rices Mudstone Member varies from 1,300 feet to as much as 1,800 feet thick.

Tst Twobar Shale Member--thin-bedded and laminated olive-gray shale with very thin lenses and laminae of very fine arkosic sandstone, containing bathyal benthic foraminifers assignable to the Narizian Stage of the late Eocene. From 200 feet to as much as 450 feet thick along Laurel Creek.

BUTANO SANDSTONE (UPPER, MIDDLE, AND LOWER EOCENE)

Tb Yellowish-gray, medium-bedded to massive fine- to medium-grained arkosic sandstone with thin interbeds of olive-gray siltstone and shale. As much as 700 feet of Butano Sandstone crops out along the axis of Laurel anticline, but there its base is not exposed. In the northeastern part of Laurel quadrangle, about 200 feet of massive Butano Sandstone overlies Butano mudstone (Tbm).

Tbm Dark-gray, thin-bedded nodular mudstone commonly with fist scales along bedding planes, with interbedded thin to thick, locally graded, arkosic sandstone. Planktic and benthic foraminifers from Soquel

Creek are diagnostic of bathyal depths and of a probable late Eocene (Narizian) age.

Tbs Thick-bedded to massive, fine- to coarse-grained arkosic sandstone exposed at base of section along Soquel Creek. Between the San Andreas and Zayante faults, the basement of the Butano is not exposed.

Tbc Very thick-bedded to massive, light-gray, granular, medium- to coarse-grained arkosic sandstone with thick to very thick interbeds of sandy pebble conglomerate containing granitic boulders as long as 3 feet. As much as 3,600 feet of section crops out south of the Zayante fault in western part of Laurel quadrangle, where it rests unconformably on Salinian granitic basement rocks. (Present within boundaries of geologic map but not within study area.)

MAFIC BASEMENT(?) ROCKS BETWEEN ZAYANTE AND SAN ANDREAS FAULT ZONES

d b DIABASE AND GABBRO OF LAUREL CREEK (JURASSIC?)--Fine- to medium-grained intrusive diabase and gabbro, brecciated and sheared, discontinuously exposed for about 1,000 feet along northwest-trending fault which crosses Laurel Creek about 0.1 mile downstream from where Old Morrill Road crosses Laurel Creek north of its junction with Old San Jose Road. Diabase is in fault contact with mudstone of the Butano Sandstone, with the Rices Mudstone Member of the San Lorenzo Formation, and with the Vaqueros Sandstone. Diabase and gabbro have a peculiar "clot-like" cumulate texture, and are lithologically similar to undated diabase and gabbro northeast of the San Andreas fault along Highland Way and Eureka Canyon Roads to the east in Loma Prieta quadrangle. Rock is locally chloritized, and cut by quartz veinlets.

UNIT NORTHEAST OF SAN ANDREAS FAULT

Te_2 MARINE SANDSTONE AND SHALE (EOCENE)--Massive to thin-bedded, coarse- to fine-grained, yellowish-orange to white weathering, quartzo-feldspathic sandstone, silty sandstone, and silty dark-brown to greenish-brown, brown to gray weathering mudstone. Unit is extensively hydrothermally altered and quartz veined within Laurel quadrangle. (Present within boundaries of geologic map but not within study area.)

MAP SYMBOLS

(modified from Clark and others, 1989, except for landslides associated with Loma Prieta earthquake)

Contact, dashed where approximate, dotted where concealed

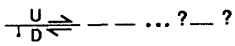

Fault, dashed where approximate, dotted where concealed, queried where uncertain. Ball and bar denote down-thrown block, or U and D denote up and down-thrown blocks. Direction and amount of dip of fault plane shown locally. Horizontal arrows denote relative horizontal movement

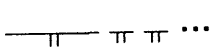

Fault at low-angle to bedding, interpreted as low-angle normal fault, double-bars on down-dropped side

Thrust fault, bars on upper plate

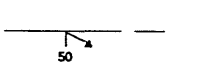

Direction and amount of dip of fault, and plunge of lineation on fault plane

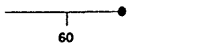

Bedding, ball denotes that facing direction is known from sedimentary structures

Vertical bedding, ball denotes facing direction as determined from sedimentary structures

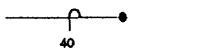

Overturned bedding, ball denotes that facing direction is known from sedimentary structures

Bedding, strike and dip direction approximated from air photos, from long-distance sighting, or averaged in area where strike or dip highly variable

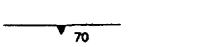

Shear foliation

Vertical shear foliation

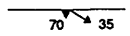

Shear foliation, showing plunge of lineation on shear surface

Folds

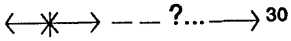

Synclinal axis, showing direction and amount of plunge, dashed where approximate, dotted where concealed, queried where uncertain

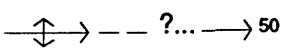

Anticlinal axis, showing direction and amount of plunge, dashed where approximate, dotted where concealed, queried where uncertain

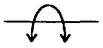

Overturned anticline

Drill hole

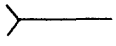

Mine adit

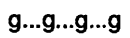

Glauconitic marker bed

Travertine Spring

Closed depression

Landslide, arrows indicate direction of movement

Topographic escarpment, line above barbs denotes top of escarpment

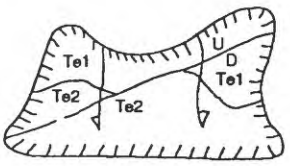

Large landslide, consisting of one or more blocks of intact rock rotationally displaced downslope from a prominent main scarp. Arrows indicate direction of movement; stratigraphy and structure of intact blocks delineated where mapped.

Large landslide or landslide complex inferred to have moved during 1989 Loma Prieta earthquake. Numbers signify landslide or landslide complex described in Chapter III of this report. 1 is Majestic Drive landslide, 2 Old Santa Cruz Highway landslide complex, 3 Upper Schultheis Road landslide, 4 Ralls Drive landslide, 5 Villa Del Monte landslide complex, 6 Taylor Gulch landslide, 7 Upper Morrell Road landslide, 8 Lower Morrell Road landslide complex, 9 Burrell landslide complex, 10 Upper Redwood Lodge Road landslide complex, 11 Long Branch landslide, 12 Stetson Road landslide, 13 Amaya Ridge landslide, 14 Hester Creek North landslide, 15 Hester Creek South landslide, 16 Lower Redwood Lodge Road landslide, 17 Lower Schultheis Road East landslide, 18 Lower Schultheis Road West landslide.

Ridge. The Zayante Fault passes along part of the southern boundary of the study area. Major, named folds in the study area are the Laurel Anticline, the Summit Syncline, and the Glenwood Syncline (fig. 2.4).

The sedimentary rocks within the study area have been divided into five geologic formations--the Butano Sandstone, San Lorenzo Formation, Vaqueros Sandstone, Lambert Shale, and Purisima Formation (Clark and others, 1989, with landslide boundaries revised by McLaughlin and Clark, 1990, unpublished data; McLaughlin and others, in press). All these rocks are typically poorly to moderately cemented; contain numerous shear surfaces; and are locally deeply weathered, intensely fractured, or both. Surface outcrops of bedrock within the Summit Ridge area are few; the rocks are typically mantled by deposits of colluvial and residual soil as much as several tens of feet thick.

On the south flank of Summit Ridge, on Skyland Ridge, and in the Redwood Lodge-Summit Woods area, rocks of the Butano Sandstone, San Lorenzo Formation, and Vaqueros Sandstone predominate (fig. 2.4). The Vaqueros Sandstone is predominantly thick-bedded to massive, arkosic and glauconitic sandstone. The San Lorenzo Formation has been divided into the Rices Mudstone Member (nodular mudstone and massive arkosic sandstone) and the Twobar Shale Member (thin-bedded and laminated shale with very thin lenses and laminae of very fine, arkosic sandstone). The Butano Sandstone within the study area has also been divided into three members: a unit consisting of medium-bedded to massive, arkosic sandstone with thin interbeds of siltstone and shale, a unit consisting of nodular mudstone interbedded with arkosic sandstone, and a unit consisting of thick-bedded to massive, arkosic sandstone (Clark and others, 1989, with landslide boundaries revised by McLaughlin and Clark, 1990, unpublished data; McLaughlin and others, in press).

The overall trend of bedding and structure on the south flank of Summit Ridge and on Skyland Ridge is northwest-southeast (fig. 2.4). The Laurel Anticline trends approximately N45°W through this area to a point southeast of the California State Highway 17-Summit Road intersection, where the anticlinal axis is truncated by the Butano fault, which strikes N60°-65°W (fig. 2.4). The anticline is overturned to the southwest in places, and bedding generally dips steeply to the southwest, steeply to the northeast, or is overturned to the northeast (fig. 2.4). North of the Laurel Anticline, the Summit

Syncline, trending N60°-65°W, passes through the northern part of the area to a point near Morrell Road, where this structure is truncated by a fault, trending N45°W, which also offsets the Butano fault. In the Villa Del Monte and Morrell Road areas, several other northwest-striking faults also extend across the Butano fault and the Summit Syncline (fig. 2.4).

In the southern part of the study area, bedrock has been mapped as Lambert Shale and Purisima Formation (Clark and others, 1989, with landslide boundaries revised by McLaughlin and Clark, 1990, unpublished data; see fig. 2.4). Lambert Shale consists of thin- to medium-bedded, organic mudstone grading upward to sandy siltstone with interbeds of arkosic sandstone. Purisima Formation rocks are thick-bedded to massive, weakly consolidated sandstone, and very thick-bedded, tuffaceous and diatomaceous siltstone. The northwest-trending Glenwood Syncline is the dominant fold structure in this part of the study area (fig. 2.4). Bedding northeast of the synclinal axis dips predominantly steeply to the southwest but is locally vertical or overturned to the northeast; bedding southwest of the axis dips predominantly steeply to the northeast.

E. Seismicity

The San Francisco Bay-Monterey Bay region is one of the most seismically active in the world. The region is transected by numerous active and potentially active faults (fig. 2.5), including the San Andreas, which passes through and under the Summit Ridge area (fig. 2.4) and which produced the Loma Prieta earthquake. The San Andreas and associated faults form part of the boundary between two of the earth's large crustal plates--the Pacific and the North American. Northward movement of the Pacific plate relative to the North American plate has produced a virtually continuous history of instrumentally-recorded seismicity in the region. In addition to myriad small and moderate-sized seismic events, 23 earthquakes of magnitude 6.0 or greater have occurred in the region since 1836; two of these were approximately as large as the Loma Prieta earthquake (M 7.0 in 1838 and M 7.0 in 1868) and one was substantially larger (M 8.3 in 1906) (Wesnousky, 1986; U.S. Geological Survey, 1990).

The Working Group on California Earthquake Probabilities (1990) has released probability estimates for future large earthquakes that may be produced by rupture on certain faults in

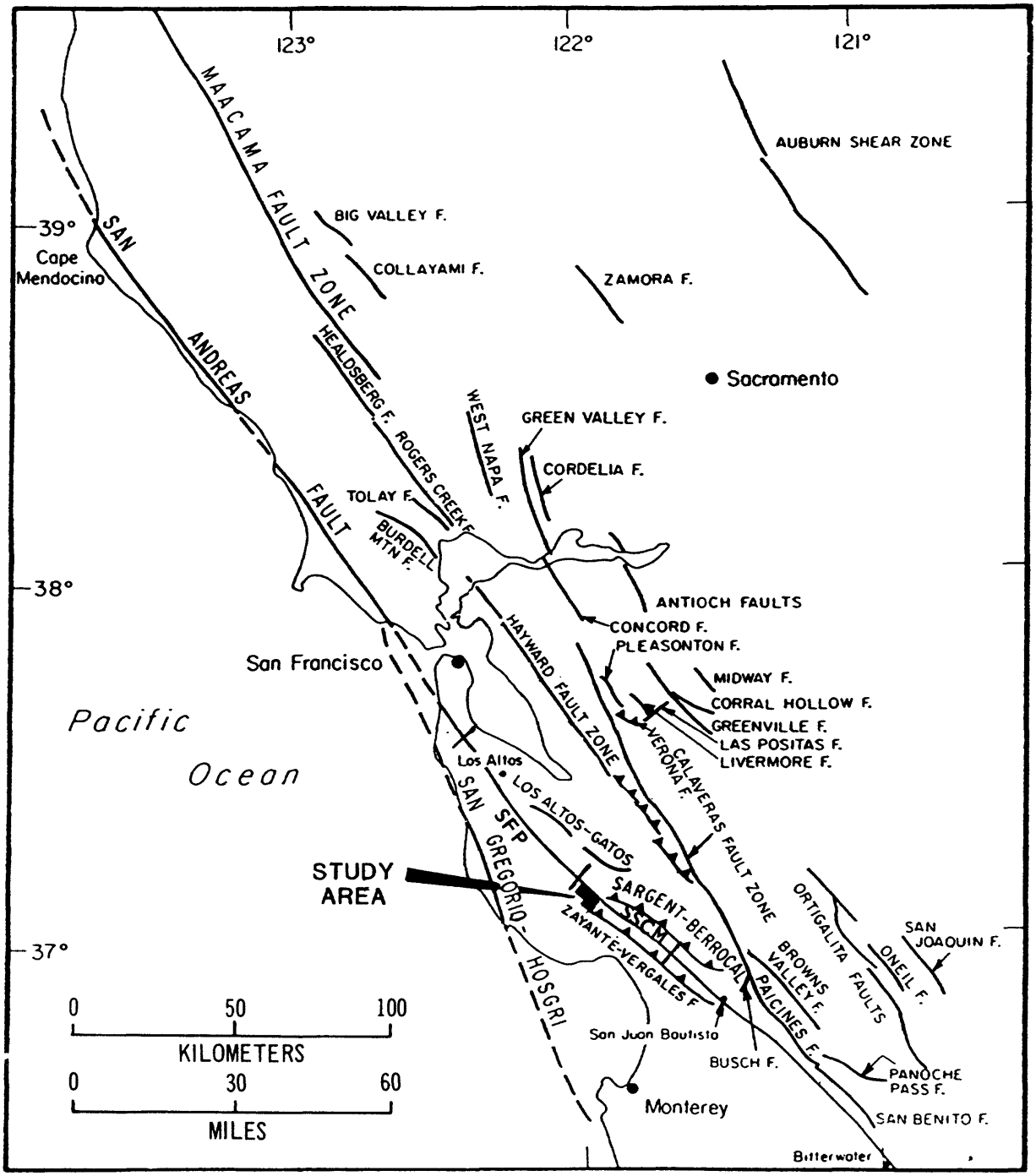

FIGURE 2.5 –Faults in the San Francisco Bay–Monterey Bay region and surrounding area of California (modified from Wesnousky, 1986). Segmentation of San Andreas fault from Working Group on California Earthquake Probabilities (1990, p. 2). SFP is San Francisco Peninsula segment; SSCM is Southern Santa Cruz Mountains segment, which ruptured to produce Loma Prieta earthquake.

the San Francisco Bay Region. These estimates cover three segments of the San Andreas fault, two segments of the Hayward fault, and the Rodgers Creek fault (fig. 2.5). The overall probability of another M 7 or larger earthquake during the next 30 years, produced by rupture somewhere on one of these fault segments, is judged to be 67 percent.

The southern Santa Cruz Mountains segment of the San Andreas fault, which produced the Loma Prieta event, is judged to have a very low probability (less than 1 percent) of producing another M 7 earthquake in the next 30 years (Working Group on California Earthquake Probabilities, 1990). However, the San Francisco Peninsula segment is judged to have a 30-year probability for a M 7 earthquake of 23 percent (Working Group on California Earthquake Probabilities, 1990), and this segment extends southward from near Lower Crystal Springs Reservoir to just north of the point where the fault crosses California Highway 17, approximately 2 miles north of the study area. Shaking in both Santa Cruz and San Jose from a M 7 earthquake on this fault segment is estimated to be potentially as severe as shaking from the Loma Prieta earthquake (U.S. Geological Survey, 1990). In addition, the Zayante fault, which passes through the southern tip of the study area, and the Sargent-Berrocal fault zone, which passes within 4000 feet of the area (fig. 2.5), were both judged by Wesnousky (1986) to be capable of producing earthquakes as large as the Loma Prieta event. Within the Summit Ridge area itself, both the Zayante fault and the Butano fault were judged by Hall and others (1974) to have a moderate potential for future surface rupture, whereas the San Andreas fault was judged to have a high potential for future surface rupture.

F. The Loma Prieta Earthquake

The Loma Prieta earthquake, which began 15 seconds after 5:04 p.m. Pacific daylight time on October 17, 1989, had a Richter surface-wave magnitude (M_S) of 7.1. The earthquake hypocenter was at a depth of approximately 11 miles and was located at 37° 2' N latitude and 121° 53' W longitude, 4.1 miles southeast of the study area (fig. 2.1). The earthquake is inferred to have ruptured a 25-mile-long segment of the San Andreas fault extending from near the Pajaro Gap east of Watsonville northwestward through the Summit Ridge area to just north of California Highway 17 (Plafker and

Galloway, 1989; Working Group on California Earthquake Probabilities, 1990; see fig. 2.5).

Whereas most of the San Andreas fault is relatively straight in plan view and near-vertical in cross section, within the Santa Cruz Mountains the fault bends. In addition, the distribution of Loma Prieta aftershocks indicated that the fault dips approximately 70° to the southwest and extends under the Summit Ridge area (Plafker and Galloway, 1989). Because of the bend and non-vertical dip, the fault slip at depth had both right-lateral, strike-slip; and vertical, compressional components. The inferred fault slip at depth was 6.2 feet right lateral, 4.3 feet reverse, and 7.5 feet total (Plafker and Galloway, 1989). No throughgoing, right-lateral, surface fault-rupture has been found. Instead, areas adjacent to the segment of the fault that produced the earthquake exhibited complex patterns of coseismic fissures, owing at least partly to the bend in the fault here.

During the earthquake, ground shaking in the Summit Ridge area was violent as indicated by eyewitness accounts and such effects as the snapping of large redwood trees, movement of heavy vehicles, and destruction of residences and other structures. At the Corralitos CDMG Strong Motion station, 700 feet from the San Andreas fault and 7.6 miles southeast of the study area, horizontal ground accelerations as strong as 64 percent of gravity and vertical accelerations as strong as 47 percent of gravity were recorded (Shakal and others, 1989).

Analyses of geodetic data indicated that the earthquake produced zones of ground-surface subsidence northeast of the San Andreas fault and uplift southwest of the fault, in and around the Summit Ridge area (McNally and others, 1989; Plafker and Galloway, 1989; Anderson, 1990; Lisowski and others, 1990; Schwartz and others, 1990). Three studies that produced contour maps of calculated uplift and subsidence were made, based on modeling in which the Earth was idealized as an elastic half-space and the fault rupture was idealized as a slip on a dipping, rectangular cut buried in the half space (Lisowski and others, 1990) or as a planar, uniform slip fault embedded in the half space (Anderson, 1990 referencing preliminary modeling reported in McNally and others (1989)). A preliminary contour map was also included in Plafker and Galloway (1989) but the modeling assumptions were not reported in detail.

Generalized contours showing distribution of calculated uplift and subsidence from Anderson (1990) are shown in figure 2.6. Calculated maximum subsidence was approximately 6 inches; calculated maximum uplift was approximately 22 inches. This maximum calculated uplift occurred approximately 1.2 miles southwest of the San Andreas fault and decreased uniformly from there toward the fault (Anderson, 1990). In the study area, maximum calculated uplift of approximately 22 inches occurred only in the southeastern corner (fig. 2.6). The calculated uplift decreased to approximately 18 inches in the Redwood Lodge area and to between 6 and 14 inches along the crest of Summit Ridge. According to this modeling, the base of Summit Ridge was uplifted a few inches more than the crest of the ridge; interpolation between the generalized contours on figure 2.6 suggests that the base of the ridge may have been uplifted 4 to 8 inches more than the crest.

The analysis of Lisowski and others (1990), as well as preliminary analyses reported in McNally and others (1989), and Plafker and Galloway (1989) produced contour patterns similar to that in figure 2.6, with absolute amounts of calculated uplift and subsidence differing from those shown in figure 2.6 by at most a few inches. The largest calculated maximum uplift was between 26 and 30 inches, according to the preliminary analysis of McNally and others (1989). The maximum calculated uplift according to the preliminary analysis reported in Plafker and Galloway (1989) was 18 inches, and the maximum calculated uplift according to Lisowski and others (1990) was between 16 and 20 inches.

It is important to note that these calculated amounts of uplift and subsidence were based on modeling of idealized conditions rather than on measurements. The only measured elevation change in the vicinity of Summit Ridge described in these reports was at a station on Loma Prieta, northeast of the San Andreas fault, which subsided approximately 4 to 8 inches relative to three other stations in the geodetic network (Lisowski and others, 1990) and probably subsided approximately 6 inches in absolute altitude (Schwartz and others, 1990).

G. Pre-1989 Landslides and Landslide Hazard Mapping

Pre-1989 landslide deposits are widespread in the Summit Ridge area as well as throughout much of the rest of the Santa Cruz

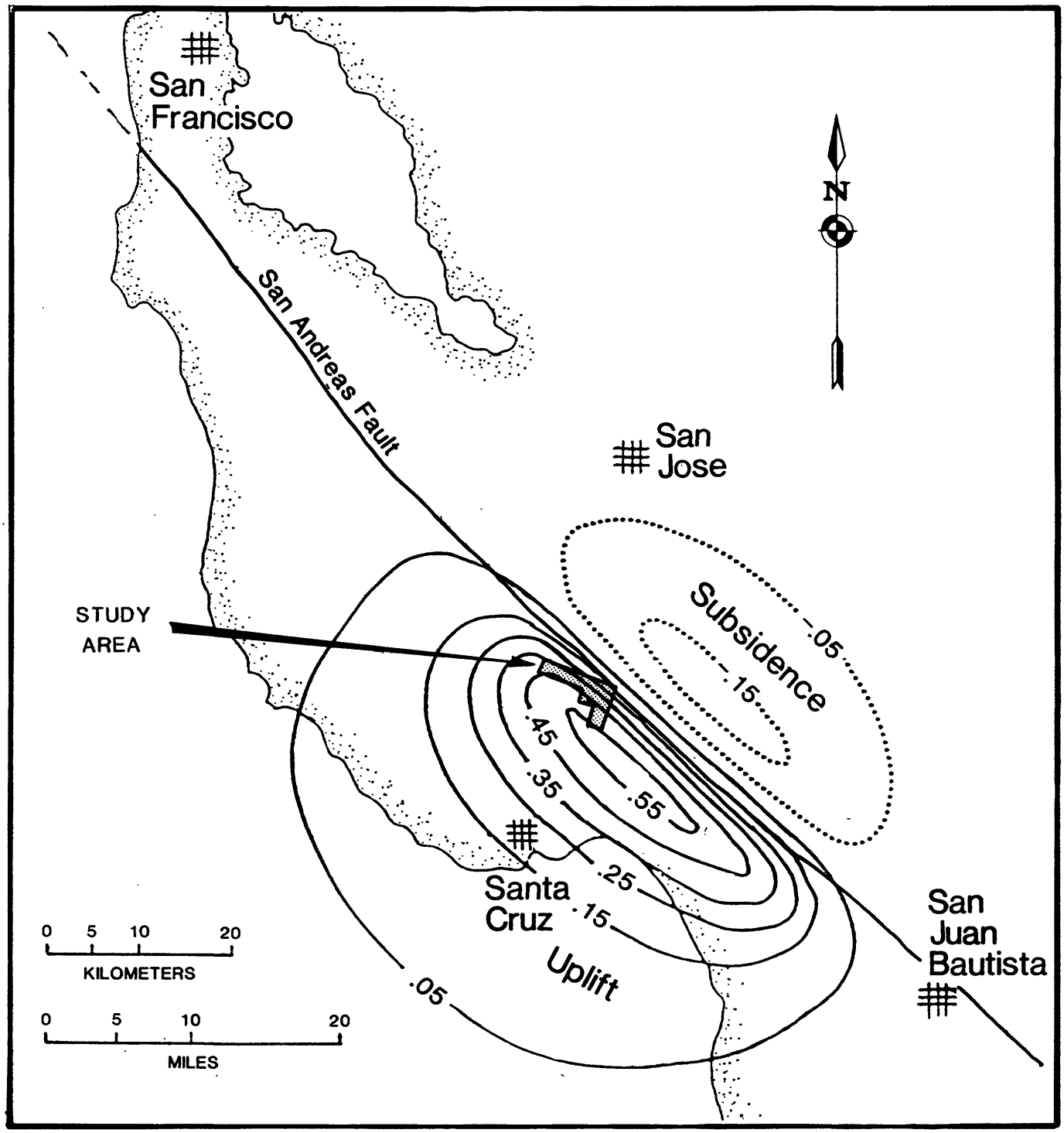

FIGURE 2.6 –Calculated coseismic uplift and subsidence associated with the Loma Prieta earthquake (modified from Anderson, 1990). Contours of equal uplift or subsidence in meters (1 meter=39.4 inches). Maximum uplift of 0.55 meters (22 inches) occurred along southern boundary of study area: uplift decreased through area to the north and west.

Mountains. Numerous landslides in the mountains have occurred in association with historical and recent earthquakes (Lawson and others, 1908; Youd and Hoose, 1978; Manson and others, 1990; Marshall, 1990), storms (Keefer and others, 1987; Ellen and Wieczorek, 1988), and other events, and active landsliding is one of the main geologic processes sculpting the mountain landscape. Landslides that are active or recurrent in these mountains are of many different types, including large, deep slumps and block slides; fluid and fast-moving debris flows; rock falls; debris slides; and failures in fill. In 1975, a landslide map (Cooper-Clark and Associates, 1975) was prepared for SCC as part of the County's state-mandated Seismic Safety Element in its General Plan. This section summarizes evidence of historical landslides in and around the Summit Ridge area and describes the 1975 landslide map and other pre-earthquake landslide mapping.

1. Landslides Caused by Previous Earthquakes

Landslides are known to have occurred in the Santa Cruz Mountains during both the October 8, 1865, earthquake (M 6.5) on the San Andreas fault and the October 21, 1868, earthquake (M 7.0) on the Hayward fault. However, the landslides in these events were not well documented, and the available historical information is fragmentary (Youd and Hoose, 1978; Marshall, 1990). Among the fragmentary accounts from the 1865 earthquake are reports of landslides from a few scattered localities including the Mountain Charlie area (Youd and Hoose, 1978; Marshall, 1990). Information from the 1868 earthquake is even more fragmentary, with known reports of landslides in the Santa Cruz Mountains only at Eagle Glen and Pescadero (Youd and Hoose, 1978; Marshall, 1990).

Documentation of landslides caused by the much larger April 18, 1906, San Francisco earthquake (M 8.3), while not complete, was substantially more extensive owing to one of the world's first scientific post-earthquake investigations (Lawson and others, 1908) as well as to information in many other reports, books, and newspaper articles. The 1906 earthquake caused thousands of landslides throughout an area of approximately 12,000 square miles (Keefer, 1984), including all of the Santa Cruz Mountains. In particular, the earthquake reactivated many pre-existing landslides (Lawson and others, 1908, v. 1, p. 385).

The severity of landsliding in and around the Summit Ridge area during the 1906 earthquake was described in general terms in an article in the Santa Cruz Morning Sentinel of May 1, 1906, (p. 2) as follows:

> *"From all reports, the higher altitudes of the Santa Cruz Mountains all the way from beyond Saratoga to Loma Prieta, on both slopes, appear to have been more seriously disturbed than many localities in the valleys and foothills. In places the roads are or were impassable, not only on account of great avalanches of stones and earth, but of wide deep cracks in the earth where the ground was rent asunder."*

More specific and detailed descriptions of the many reported ground cracks and landslides caused by the 1906 earthquake in and around the Summit Ridge area are given in table 2.1. Most locations given in the original reports were not precise enough to identify the specific hillsides where landslides occurred, and the reports were almost certainly incomplete, because landslides were not mapped in a systematic or comprehensive manner. However, even the incomplete and imprecise information available from the 1906 earthquake indicates that landslides occurred in many parts of the Summit Ridge area, including Summit Ridge, Skyland Ridge, the Morrell, Burrell, and Laurel areas, and along Old San Jose and Redwood Lodge roads. The reports indicate that several of these landslides were relatively large and that, in several localities, many landslides occurred. During the earthquake, two large, fast-moving avalanches of rock and soil killed 10 people near the Summit Ridge area; nine people were killed at Olive Springs, just south of the study area boundary, and one person was killed at Grizzly Rock, 6 miles northwest of the study area. The rock-and-soil avalanche at Olive Springs was reported to have been approximately 1,500 feet long, 400 feet wide, and 100 feet deep, and the avalanche at Grizzly Rock approximately 1,200 feet long, 240 feet wide, and 300 feet deep (table 2.1).

2. Landslides Associated with Rainfall

TABLE 2.1--Landslides and ground cracks in and around the Summit Ridge area produced by the April 18, 1906, earthquake (M 8.3) (modified from Youd and Hoose, 1978, table 6, and Marshall, 1990).

Location	Description and Original Reference
Alma	A landslide dammed Alma creek creating danger of flooding. (Santa Cruz Evening Sentinel, April 19, 1906, p. 5).
	"The ground around the [devastated Tevis] house and in the hills above, was opened in hundreds of places in fissures of from a few inches to three feet in width. The depth of these is not apparent as the ground is broken in a zigzag manner." (Santa Cruz Morning Sentinel, May 1, 1906, p. 2)
	"On the ranch of Dr. Tevis [presently the site of Alma College], about a mile from Alma Station, where the land is rolling and wooded, the ground was fissured and the bottom of an artificial lake was upheaved.... The cracks and fissures, of which there are many, run mostly north and south, and vary in length up to 100 feet, and in width from 0.5 inch or less to 20 inches. While a good many of the openings were parallel to the slopes and were caused by the ground starting to slide, others crost the roads and could be traced some distance up the banks. A board fence was splintered where it crost a fissure. The upheaval of the lake was caused by a closing together of the sides, shown by the heaving up of parts of the retaining dam at the lower end of the lake. The rise of the bottom is roughly 10 feet." (Lawson and others, 1908, p. 275)
Eva	A 10-acre slide dammed the creek at Eva station until the water crossed the railroad tracks following a new raised channel. (Santa Cruz Morning Sentinel, April 26, 1906, p. 8)
	A "huge earth slide dammed the creek at Eva station, creating a natural lake that blocked all [railroad] travel...for months." It took until December to remove the slide and lake. (Young, 1979, p. 39).
Alma to Wrights	The railroad between Alma and Wrights was impassable due to several landslides and boulders on the tracks. (Santa Cruz Morning Sentinel, April 26, 1906, p. 8)
	A landslide dammed Los Gatos Creek at the News Letter ranch, forming a lake with depth ranging from 50 to 100 feet. (Santa Cruz Morning Sentinel, May 1, 1906, p. 2)
Patchin to Wrights	"On the ridge road, about 5 miles northwest of Wright Station, the fault again shows slightly in a few 2-inch cracks.... Going down the slope from here to Wright, the cracks rapidly

become larger. ...At Patchin, 3 miles west of Wright Station, there are fissures over a foot wide trending mainly in the direct line of the fault (S. 33° E.). Several stretches of numerous small cracks alternating with a few long continuous fissures, mark the course from Patchin to Wright Station." (Lawson and others, 1908, p. 109-110)

"Just north of Wright's Station, on the west bank of Los Gatos Creek, there was a landslide 0.5 mile wide which had slid into the creek and dammed it. The top of this slide was near the Summit school-house and was close to the main fault-line." (Lawson and others, 1908, p. 276)

"The main fault fracture is about 500 feet northeast of the [Summit] hotel, and a secondary crack close to it had a downthrow of from 5 to 7 feet on the north or downhill side. The crack was about 4 feet wide here, and the line of fracture was parallel with the direction of the ridge. The Summit school-house was dropt 4 feet downhill from its original position toward the northeast." Just below the Summit school-house was the headscarp of the landslide that dammed Los Gatos Creek near Wright Station. (Lawson and others, 1908, p. 275-276)

"At Freely's place, 4 or 5 miles north of Morrell's some 15 acres of woodland have slid into Los Gatos Creek, making a large pond. There are many other slides in the neighborhood and many broken trees." (Lawson and others, 1908, p. 278)

"Into this [Los Gatos] creek, from the Freely ranch, some ten acres of land was thrown in a great landslide. At the head of the creek is the long tunnel which cuts under the saddle, from Wright's to Laurel." (Jordan, 1907, p. 27)

"Landslides were abundant, especially in the Santa Cruz Mountains, where the topography is more rugged. One slide, a few miles from Wright's Station, involved eight to ten acres of ground." (Carey, 1906, p. 297)

Wrights — "Large fissures and ridges" formed in the ground at Wrights. (Santa Cruz Evening Sentinel, April 21, 1906, p. 2)

Wrights to Laurel — The Wrights to Laurel railroad tunnel collapsed in the earthquake just hours before the planned inaugural run of the first standard gauge train along this previously narrow gauge line. Where the tunnel crosses the summit it was offset laterally five feet. Almost all other railroad tunnels in the Santa Cruz Mountains suffered some collapse or were blocked by slides at their entrances. (Payne, 1978, p. 49)

The Wrights to Laurel railroad tunnel cracked in middle and settled several inches out of line. (Young, 1979, p. 38-39)

"The tunnel floors have raised as much as three to four feet in places...." (Santa Cruz Morning Sentinel, April 26, 1906, p. 8)

Laurel to Glenwood — Minor slides blocked the Glenwood-Laurel tunnel. (Young, 1979, p. 39-39)

Four hundred feet of tunnel #3 between Laurel and Glenwood caved-in. (Santa Cruz Evening Sentinel, April 19, 1906, p. 5)

Morrell Ranch — "The Morrell ranch is located 1 mile south of Wright's Station.... the house itself was built exactly upon a fissure, which opened up under the house at the time of the earthquake. The house was completely wrecked, being torn in two pieces and thrown from its foundation....There was an apparent downthrow upon the northeast side of the fault, as seen in the orchard; but under the house the vertical movement was not so apparent. ...The fence and road near the house were crost by the fault and showed an offset which indicated a relative movement of the southwest side toward the southeast. ...The "splintering" of the main fracture raised a long, low ridge across which a creek had been forced to cut its way thru a vertical distance of 1.5 feet to get down to its original level." (Lawson and others, 1908, p. 276-277)

"The earthquake crack past thru [the Morrell] ranch, a branch of it going under the house. The main body of the house was thrown to the east, away from the crack, the ground there slumping several feet and the house being almost totally wrecked. All thru the orchard the rows of trees are shifted about 6 feet, those on the east side being farther north, and the east side, which is downhill, seems to have fallen. The crack is largely open and in one place is filled with water. This should be attributed to slumping. A little farther on, the crack passes thru a grassy hill on which there is no slumping. The Morrells say that this hill has been raised. What appears to be the fact is that the east side of the hill overrides the other. The whole top of the hill is more or less cracked for a width of about 10 feet. The east side is a little higher than the west side, and it looks as though the hill had been shoved together and raised, the east overriding. About 1 mile beyond Morrell's house, at the end of the ranch, there is a blacksmith shop, and the road is crost by the crack. Here there is a break of 3 or 4 feet like a waterfall, the east side being the lower; but this is part, I take it, of the general slumping of the east side of the crack where it stands near the ravine above Wright. Morrell's place is right over the Wright tunnel, the tunnel and the rocks near by being finely broken rock and very much subject to slides and other breaks." (Lawson and others, 1908, p. 277-278)

Burrell — "In the Burrell district there is one fissure in the hillside fully 3 feet wide. This crossed the road and tumbled Ingraham's store

building into the gulch." (Santa Cruz Morning Sentinel, April 24, 1906, p. 7)

"Near the Burrell school-house, 1.5 miles southeast of Wright Station, a crack extends across the road by a blacksmith shop and shows a downthrow of four feet on the northeast." (Lawson and others, 1908, p. 276)

Burrell [Laurel] Creek "Gulches appear to have been contracted as the bridges crossing them show that they were squeezed. The banks of Burrell Creek appear to have approached each other, so that the creek has become very much narrowed. Water pipes were broken and twisted, and filled with dirt." (Lawson and others, 1908, p. 276)

Highland "Half a mile to the northwest of the [Beecher] house [on Loma Prieta Avenue], a fissure 2 feet wide appeared.... The fissure runs from north to south, and the earth was piled up on the west side from 2 to 4 feet high across the road. On Highland, a mile to the west, a fissure 5 feet was opened at an elevation of 2,500 feet." (Lawson and others, 1908, p. 276)

Skyland "Large landslides occurred in the neighborhood." (Lawson and others, 1908, p. 278)

"The road between the King and Crane places has slid into the orchard below." (Santa Cruz Evening Sentinel, April 21, 1906, p. 4)

"There seems to have been a narrow strip, about two miles wide, east of Skyland, with Skyland as the center, where hardly a building remains standing or unbroken. ..."One section of road of about 3 miles long is hardly without a crack.... At one place in the road it has been lifted fully 5 feet." The road was still impassable after three days of heavy work by a crew of 6 men. (Santa Cruz Morning Sentinel, April 24, 1906, p. 7)

"...the cracks run up over the ridge just west of Skyland. Large fissures show in the orchards and fields on the eastern side of the ridge, but are not so evident on the western slope. Here instead, great landslides occurred, and redwoods were snapt off or uprooted." (Lawson and others, 1908, p. p.110)

"The slides which obliterated Fern Gulch at Skyland...lie to the west of the crack [fault]." (Lawson and others, 1908, p. 278)

On the western slopes of the ridge just west of Skyland, several earth-avalanches were caused by the shock; and great slides of a similar character occurred on both sides of Aptos Creek for 0.75 mile. Besides these, there were many smaller earth-avalanches in many parts of the Santa Cruz Mountains which can not be enumerated." (Lawson and others, 1908, p. 389-390)

"About Four Miles South of Wright Station" [probably near Laurel township] "The ridge...was full of cracks, ranging up to 2 and 3 feet in width, and in length from a few rods to 0.25 mile, all trending west of north to northwest. ...The canyon south of us was filled with landslides. In this canyon the stratification of the rocks is plainly shown. The strike is northwest-southeast and the dip is almost vertical. The cracks coincide in direction with the strike of the strata. Cold water was flowing from some of the cracks." (Lawson and others, 1908, p. 278)

San Jose-Soquel Road San Jose-Soquel road suffered extensive damage in the earthquake, but was reopened by July 4, 1906. (Payne, 1978, p. 17)

Redwood Lodge Road The earthquake "severely damaged Redwood Lodge Road and workmen took until June, 1906 to complete repairs." (Payne, 1978, p. 17)

Upper Soquel Creek A newspaper article of May 7, 1906 reported an eyewitness story that the headwaters of Soquel Creek were dammed by two landslides, forming a pond 100 feet deep. The upper Soquel Creek basin was reported ravaged by fallen trees and boulders as well as "great fissures and landslides. ...The roads were gone and in their stead were chaotic masses of debris from the hillsides." An article of May 9 corrected the account after the site was visited by another eyewitness. This second account claims the damming of the creek resulted not from landslides but from an upward vertical displacement of the creek bed of from 5 to 30 feet in places. the pond averaged 15 feet in depth not exceeding 20 feet. Many fissures in the ground near Soquel Creek were "now largely filled in." (Santa Cruz Evening Sentinel, May 7, 1906, p. 1, and May 9, 1906, p.1)

Hinckley Creek (Olive Springs) "The mountains are said to have come together and 17 lives...lost." [9 were actually killed.] (Santa Cruz Evening Sentinel, April 18, 1906, p. 1, and April 19, 1906, p. 7)

With the first severe shock of the earthquake, a landslide 500 feet wide, extending up to the ridgetop, descended with "extraordinary speed", burying the Loma Prieta lumber mill under a mass of rock and trees of "about 100 feet in depth at the worst places and gradually diminishing at the edges to 25 feet." Nine men were buried instantly while others, only several hundred feet away, were spared. "The mountainside where the land fell was swept bare of vegetation. Massive redwoods and pines were jammed on top of the mill in the gulch below. ...The landslide filled the water course. The stream was dammed and the water rose to a depth of sixty feet in the gulch. A pump was set to working and the water is now being used to wash away the earth from the machinery." Hundreds were involved in a massive digging effort in the following week, but only three bodies had been discovered by five days later. [More than a year passed before the last body was finally removed from the debris.] (Santa Cruz Morning Sentinel, April 26, 1906, p. 1)

The mill was buried under 60 feet of earth and trees, whereas the nearby bunkhouse, where nine men were sleeping, was buried under 10 to 15 feet of debris. (Patten, 1969, p. 79)

A second slide occurred during an aftershock at 11 p.m., April 19 interfering with rescue efforts. (Santa Cruz Evening Sentinel, April 21, 1906, p. 2)

"Near Olive Springs, 12 miles north of Santa Cruz, an earth-avalanche demolished Loma Prieta Mill and killed several men." (Lawson and others, 1908, p. 389)

"At Santa Cruz the inhabitants reported that near Olive Springs, 12 miles north of Santa Cruz, a landslide demolished Loma Prieta Mill and killed 9 men." (Lawson and others, 1908, p. 271)

"...the [fault] crack goes into Hinckley's Gulch, in which the Loma Prieta Mills are situated, and which are buried under the slides." (Lawson and others, 1908, p. 278)

"On the northern side of Bridge Creek Canyon there are typical cracks from 1 to 8 inches wide, and here also occurred a great landslide which buried the Loma Prieta Mill." (Lawson and others, 1908, p. 110)

"Wreck of Loma Prieta Sawmill, Hinckley's Gulch, Santa Cruz County." (Jordan, 1907, p. 30) [Picture caption]

"Site of Loma Prieta Sawmill, covered to a depth of 125 feet." (Jordan, 1907, p. 31) [Picture caption]

"Loma Prieta Lumber Company's Mill. The mill, boarding house and other buildings of the plant were situated in a gulch, and were overwhelmed by a portion of the mountain--1500 feet long, 400 feet wide and 100 feet deep which slid down upon them. The mill and everything in the gulch were forced up the opposite slope of the mountain and there buried to a depth of one hundred feet. Pine and redwood trees 100 feet high came down with the slide and are now standing over the mill site as though they had grown there. Nine men were killed." (Salinas Daily Index, April 25, 1906, p. 3)

"LOMA PRIETA CO'S LOSS. When the earthquake occurred yesterday morning it caused a large mountain of earth to slide into the canyon and completely covering the new mill. Continuing its course up the mountain on the other side it covered what is known as the bunk house and buried ten men, who were asleep at the time." (Salinas Daily Index, April 19, 1906, p. 3)

Castle Rock Ridge "A small landslide had moved across the road [8 miles north of Boulder Creek] which 20 men spent one and a half days clearing away. ...Up the road to the summit of Castle Rock Ridge no slides or cracks were observed." (Lawson and others, 1908, p. 268)

Deer Creek (Grizzly Rock--northeast of Boulder Creek) An extensive landslide descending from the eastern side of the valley buried the Deer Creek shingle mill, houses, trees, etc. Two people were killed. The site of the mill was estimated to be under 50 to 100 feet of earth. The slide apparently had two lobes, one moving to the west and the other to the east. A witness watched as large redwoods on the slide mass performed "all kinds of acrobatic feats." "Where formerly there was high hills and wooded lawns nothing now remains but a wide level stretch over a mile long and covered with the protruding tops of trees." (Santa Cruz Evening Sentinel, April 19, 1906, p.4)

An article reprinted from the "Mountain Echo" said that the crest of a spur ridge off of the main mountain summit northeast of Deer Creek failed and "swept in a semi-circular pathway of destruction for three-fourths of a mile toward Deer Creek. A fine redwood forest in its pathway, and the property of Isaiah Hartman of this place, was swept down like grain before the reaper. ...It was many minutes after the heavy series of earthquake shocks...that the avalanche was discovered to be approaching with the mighty roar of crashing timber and grinding rocks. When first seen it was over a quarter of a mile away across a flat country and no one dreamed it could reach the mill. It however, swept onward in a bending course with a solid wall of earth and redwood trees fifty or sixty feet high.... The mill cabins were crushed like eggshells and buried in the debris while the mill itself disappeared under the moving wall." One person was killed at the mill, while another was killed at a different site on the other side of a ridge one-half mile to the east. (Santa Cruz Evening Sentinel, April 23, 1906, p.1).

In a report of a visit to the site of the Deer Creek slide two months later, the base of the slide was encountered a half mile above the Santa Clara Lumber Co. mill near the site of a new shingle mill. An eyewitness to the slide said it took less than a minute for the slide to move from its origin 400 feet above and half a mile distant down onto the old shingle mill. The slide descended a winding gulch carrying a huge mass of rock, soil and large trees. (Santa Cruz Evening Sentinel, June 21, 1906, p.5)

"On Deer Creek, in the Santa Cruz Mountains, an extensive earth-avalanche started near Grizzly Rock and moved westward down a steep, narrow canyon for about 0.25 mile. (Plates 124D and 125A.) It then changed its course thru an angle of about 60^{o} as it entered a wider canyon of lower grade, and following this for another 0.25 mile, finally stopt at the Hoffmann Shingle Mill, which was wrecked. A fine growth of redwood, some 200 feet in height, was mowed down, and covered to the extent of 10 acres or more with from 30 to 60 feet of debris. The trees were from 3 to 10 feet in diameter. The main canyon was filled with earth and rock for an average width of 80 yards and a length of 400 yards. The entire area of the slide was about 25 acres. The difference in altitude between the point where the slide started and the shingle mill where it stopt, is 500 feet. According to Mr. G. A. Waring, the slide material has a depth of 300 feet and is composed of soil, clay, and shale. Mr. E. P.

Carey, who examined and photographed this interesting earth-avalanche, states that it originated in rock that broke away in pieces from the steeply inclined slope at the head of the gulch, leaving a large theater-like space, the bare, light-colored rock walls of which were in sharp contrast with the surrounding green vegetation. The movement was faster in the center or deepest part of the gorge than on the margins.. The rock was in general piled up higher along both sides than in the center, and many pieces became entangled in the standing or uprooted trees. A steep-walled tributary to the southeast of the main gulch supplied rock material to the main avalanche, and the 2 streams joined much as confluent glaciers do. The material involved in the avalanche showed every gradation from powder to angular pieces 30 feet or more in diameter. The surface was uneven throughout. Near the mill a man was killed by a tree that fell as the avalanche was advancing." (Lawson and others, 1908, p. 388)

"On Deer Creek a large landslide started from near Grizzly Rock and slid westward, but changed its direction 60° or more farther down toward the creek. The mill in the creek bottom below the slide was partly buried, and one man was killed. It is 500 feet from the mill in the gulch to the top, at the point where the slide started. The slide covered about 25 acres of ground, and destroyed a lot of virgin timber from 3 to 10 feet in diameter. The slide material, which is 300 feet deep, is composed of soil, clay, and shale." (Lawson and others, 1908, p. 267)

Bear Creek (NE of Boulder Creek) "On Bear Creek... a smaller slide [than the Deer Creek slide] had moved a few hundred feet, buried a hut, and killed one man. According to reports of men in this region, only a minute elapsed after the beginning of the earthquake before the slide was over. Down in the valley no cracks or other evidence of disturbance could be seen." (Lawson and others, 1908, p. 267)

Cauley [Connely?] Gulch "Mr. Carey also reports another earth-avalanche located on the Petty ranch, about 4 miles southeast of the one just described [Deer Creek landslide]. Here a huge rock mass, which embraces an area of about 12 acres at the headwaters of Cauley Gulch, broke away from a ledge and dropt, leaving a vertical scarp of 40 feet or more. The rock mass in this case was not shattered. It practically maintained its integrity. The narrow gulch below was unfavorable for free downward movement. As the block readjusted itself, its upper surface became nearly level, but was lower at the foot of the scarp than at its outer edge, thus indicating that it had suffered rotation." (Lawson and others, 1908, p. 388)

Grizzly Rock "The whole ridge west of the reservoirs [about 2 miles south of Congress Springs] was severely shaken, however, for cracks 4 or 5 inches wide opened near Grizzly Rock and several large slides occurred in its neighborhood. One water-pipe running north and south on the Beatty place was broken, while one trending east and west was unhurt. No cracks were found crossing the ridge between

Grizzly Rock and and White Rock. The cracks were next found on the road about a mile east of B.M. 2135 of the U.S. Geological Survey, but they do not show in the vineyard to the southeast." (Lawson and others, 1908, p. 109)

Original References Cited

Carey, E. P., 1906, The great fault of California and the San Francisco earthquake, April 18, 1906: Jour. Geography, v. 5, no. 7, p. 289-301.

Jordan, D. S., ed., 1907, The California earthquake of 1906: San Francisco, A. M. Robertson, 360 p.

Lawson, A. C., and others, 1908, The California earthquake of April 18, 1906: Report of the California State Earthquake Investigation Commission: Washington, D. C., Carnegie Institution, Publication 87 (reprint edition), 2 vols.

Patten, P. B., 1969, Oh, that reminds me..: Felton, Calif., Big Trees Press.

Payne, S. M., 1978, A howling wilderness, a history of the Summit Road area of the Santa Cruz Mountains 1850-1906: Santa Cruz, Calif., Loma Prieta Publishing Company.

Salinas Daily Index: Salinas, Calif., April 19, 1906, p. 3 and April 25, 1906, p. 3.

Santa Cruz Evening Sentinel: Santa Cruz, Calif. (various articles, see entries in text).

Santa Cruz Morning Sentinel: Santa Cruz, Calif. (various articles, see entries in text).

Young, John, V., 1979, Ghost towns of the Santa Cruz Mountains: Santa Cruz, Calif., Paper Vision Press.

As with the historical record of landslides caused by earthquakes, the record concerning landslides caused by rainfall in and around the Summit Ridge area is incomplete. Sources of data that are available include the following: (1) Marshall (1990) compiled information on landslides in the Santa Cruz Mountains before and after the 1865 and 1906 earthquakes. (2) Wieczorek and others (1988) mapped landslides in Santa Cruz County caused by the disastrous storm of January 3-5, 1982. (3) Keefer and others (1987) included the Summit Ridge area in a zone of high landslide concentration associated with the storm sequence of February 12-21, 1986, but did not report localities of individual landslides within that zone. (4) Griggs and others (1990) described a sample of landslide-related problems in the Summit Ridge area obtained from a review of SCC Public Works Department road-repair files and a field trip through the area with Ray Geyon, one of the department's senior staff members.

a. Landslides during winters immediately after earthquakes: Newspaper accounts indicate that heavy rains and flooding occurred in Santa Cruz County during the winter of 1866-67, one year after the 1865 earthquake. Concerning landslides, an article in the Santa Cruz Sentinel of December 29, 1866 (p. 2) stated that the mountain road between Santa Cruz and Santa Clara was impassable after heavy rains led to landslides, caved embankments, scoured gullies, and related effects (Marshall, 1990).

Landslides were evidently also abundant in the Santa Cruz Mountains during periods of winter rainfall after the 1906 earthquake. Landslides near Felton and Boulder Creek were reported from rainstorms in May 1906. More landslides were reported from Felton, Aptos, the mountains above Watsonville, and Chittenden Pass during a December 1906 storm that produced 3 to 10 inches of rainfall. Landslides occurred near Felton, Boulder Creek, and Corralitos as a result of storms in January and February of 1907, and landslides probably occurred throughout a large area of the Santa Cruz Mountains during a storm in March 1907 (Marshall, 1990).

The relation of landslides in those areas to ground cracking from the 1906 earthquake, if any, was not specifically determined, but to the north, in an area of Marin County affected by the earthquake, Lawson and others (1908, v. 1, p. 77) explicitly

connected ground cracking caused by the earthquake with landslides that occurred the following winter. They described this relation as follows:

> "Mention has already been made of numerous hillside cracks which marked incipient landslides. In such cases the downward motion apparently began during the earthquake agitation, but the momentum acquired was not sufficient to continue the motion after the earthquake stopt. In a very large number of these localities motion was resumed and landslides occurred during a period of excessive rainfall in the spring of 1907. * * * So far as my observation goes, all of the landslides having this history were wet, the material usually flowing freely down the slope as a thin mud. The probable explanation is that the cracks made in April, 1906, served to admit the water flowing over the surface during the rains of 1907, so that the material which was too dry to flow in 1906 acquired the proper consistency and continued its course the following year. The number of landslides which the earthquake induced in this indirect way is possibly as large as the number of landslides which were an immediate consequence of the shock."

b. Landslides caused by storm of January 3-5, 1982: The January 3-5, 1982, storm was one of the most destructive in the recorded history of the San Francisco-Monterey Bay region. The storm is also the only such event for which detailed and comprehensive data on landslide distribution are available. This storm, which produced as much as 24 inches of rain in 34 hours, caused more than 18,000 landslides and more than $66,000,000 in landslide-related damage throughout the region (Ellen and others, 1988). The mountainous areas of Santa Cruz County were among the most heavily damaged in the region. Near Ben Lomond, the Love Creek landslide--a large rock block slide--killed 10 people. Eight other landslides in Santa Cruz County also killed people (Ellen and others, 1988). Total landslide damage in the County was more than $26,000,000 (Creasey, 1988).

Most of the landslides triggered by the 1982 storm were debris flows--fluid, fast-moving, relatively shallow mixtures of unconsolidated earth and water. In Santa Cruz County, the highest concentrations of debris flows were in the central part of the county; concentrations were particularly high in the drainage basins of the San Lorenzo River, Branciforte Creek, Aptos Creek, Valencia Creek, and Soquel Creek (Wieczorek and others, 1988), which includes all but the westernmost tip of the study area.

Within the study area itself, approximately 20 debris flows were mapped (Wieczorek and others, 1988), and the number mapped was probably a minimum because the dense vegetation cover in many areas made detection of debris flows difficult. In addition to the mapped debris flows, the SCC road-repair records show that lower Schultheis and Redwood Lodge roads required repairs as a result of landslide damage in 1982 (table 2.2).

c. Other historical storms in the San Francisco-Monterey Bay region: Many other historical storms have also caused landslides throughout the San Francisco Bay-Monterey Bay region. Marshall (1990) documented landslides in the Santa Cruz Mountains during storms in January and March of 1906, before the 1906 earthquake. Areas of high landslide concentrations produced by the February 12-21, 1986, storm included the Summit Ridge area and adjacent parts of the Santa Cruz Mountains (Keefer and others, 1987). Brown (1988) reported that other storms produced significant landslide activity in parts or all of the San Francisco Bay-Monterey Bay region during the winters of 1949-50, 1955-56, 1961-62, 1962-63, 1964-65, 1966-67, 1968-69, 1969-70, 1972-73, 1974-75, and 1977-78. Documentation of landslides from these winter seasons, however, is fragmentary, and the number of landslides that occurred in the Summit Ridge area, if any, is unknown.

d. Landslides in the Summit Ridge area documented by records of road repairs: As reported by Griggs and others (1990), a review of SCC Public Works records and a field trip through the Summit Ridge area with Ray Geyon of that department provided additional data on landslides. During the field trip, in particular, it was noted that the types of landslide activity that had most concerned the road-repair crews were generally different than the

TABLE 2.2--Landslide-related damage to roads before the Loma Prieta earthquake (modified from Griggs and others, 1990)

Locality (See Fig. 2.7)	Description and Date of Damage
1	**Lower Schultheis Road--1982:** The slope below Lower Schultheis Road failed in 1982 approximately 0.3 miles east of the intersection with Laurel Road, destroying the roadway and requiring evacuation of local residents. A private company was retained to engineer the slope stabilization. Since repair work was completed in 1983(?), the road has settled at least an additional 2 feet. In 1989, earthquake-induced cracking was found across the road in this area, around the margins of the previous failure. This failure was on the northeastern flank of the larger Lower Schultheis East landslide.
2	**Redwood Lodge Road--Repeated Failures:** Over the years, Redwood Lodge Road has experienced many maintenance problems due to slope failure associated with heavy rainfall, in particular during 1983 and 1986. Numerous landslides, both large and small, have plagued the road along its entire length. The only one of these masses to show significant movement as a result of the October 17 Loma Prieta earthquake, was the Upper Redwood Lodge Road landslide complex, which encompasses several hundred feet of roadway west of the intersection of Redwood Lodge and Old San Jose Roads. This section of road, in particular, has a long history of repeated landslide damage and repair.
3	**Redwood Lodge Road--1981-82 and 1983:** A large landslide covered the road near the intersection of Laurel Creek and Burns Creek. Residents living below the damaged road were trapped and had to be evacuated. In subsequent years, the road was reconstructed, suffered additional failure during 1983, and was again reconstructed. Individual slide blocks still remain on the steep slope above the road. Slope instability in this area is typically associated with heavy rainfall and has been a concern for at least 30-40 years. The 1989 earthquake reactivated the landslide complex present along this stretch of Redwood Lodge Road. Cracks were opened along approximately 800 feet of steep hillside above the road and extended headward from the pre-existing main scarp.

4 **Morrell Road--1982-83:** A landslide, approximately 200 feet long and 200 feet wide, buried Morrell Road immediately south of the road's intersection with Laurel Creek. The main scarp of the landslide was approximately 30 feet above the road. SCC had to evacuate local residents and rebuild the road, which was covered with more than 20 feet of debris. The slope was stabilized in 1984. Cracks from the Lower Morrell landslide complex, associated with the Loma Prieta earthquake, crossed the road on both the right and left flanks of the 1982-1983 landslide.

5 **Morrell Road--1980:** Northwest of the intersection of Morrell Road with Laurel Creek, a stretch of the road moved downhill approximately 6 to 10 feet during a 2-year period. A house was moved to protect it from landslide damage. The slope moved relatively rapidly, forming large cracks and a 4-foot-high scarp across the road. However, the slide mass did not bulge below the road to compensate for the extensional movement associated with this scarp. SCC road crews graded and filled the roadway until the movement stopped. This area was on the eastern margin of the Upper Morrell Road landslide, which moved during the Loma Prieta earthquake.

6 **Morrell Road--Repeated Damage:** Although the area downslope from the 1989 Upper Morrell Road landslide has never been reported as a "problem" area, several stretches of the road have been patched repeatedly. SCC road-repair records did not identify this patching as landslide-related, but the repeated, slow offset of the road, may be related to a larger unstable, landslide feature. Cracks caused by the Loma Prieta earthquake crossed the road in several places. Some cut banks above and below the road have required cribbing and maintenance in the past, evidently because of local road-cut failures. Several of these features failed during the Loma Prieta earthquake.

7 **Villa Del Monte--1975-76 and Repeated Damage:** Within the Villa Del Monte area are several areas that have required SCC maintenance, most of which is evidently related to local cribbing or fill failures. In 1975-76, the hillside upslope from Skyview Terrace moved slowly downslope during a period of 2 years. SCC maintenance crews cleared the road approximately once a week during this time. This area is part of the Villa Del Monte landslide complex that moved during the Loma Prieta earthquake.

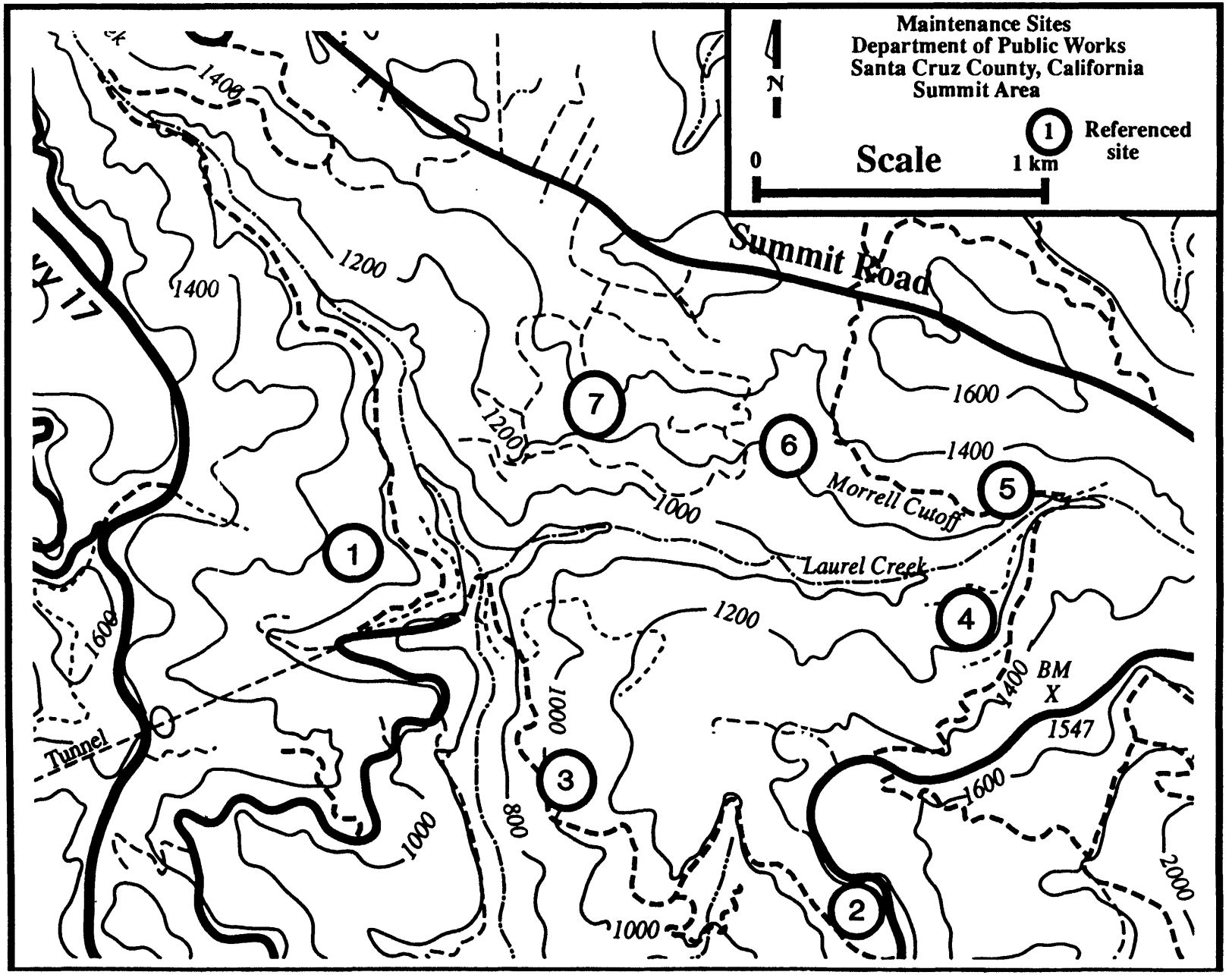

FIGURE 2.7 –Localities of landslides previous to the Loma Prieta earthquake that were documented by Santa Cruz County Public Works repair records. Locality descriptions in Table 2.2 (modified from Griggs and others, 1990).

types of landslide activity that occurred during the Loma Prieta earthquake. The road repairs were typically associated with cut-slope failures, relatively small slumps or slides, or failures involving man-made fill. Seven localities of landslide-related problems were identified (including one just outside the boundary of the study area); these localities are shown on figure 2.7 and described in table 2.2. Even though the types of landslide activity reported were different than those associated with the 1989 earthquake, all seven localities of road damage were also localities where earthquake-induced landslides and (or) ground cracks occurred in 1989.

3. Pre-Earthquake Landslide Mapping

In 1975, the "Preliminary Map of Landslide Deposits in Santa Cruz County, California" (fig. 2.8) was prepared by Cooper-Clark and Associates as part of the Seismic Safety Element of the SCC General Plan. This is the only official SCC map showing landslide distribution, and the map has been widely used to assess general slope-stability conditions for land-use planning.

The map was prepared solely from stereoscopic examination of vertical, black-and-white aerial photographs and thus is subject to several limitations in accuracy and precision. These include limitations in the size of landslide features that could be mapped (a minimum of 50 feet long or wide), difficulty in recognizing landslide deposits in areas of dense vegetation, degradation of recognizable landslide features with time after landslide movement, difficulty in differentiating landslide deposits from such similar-appearing features as alluvial terraces, and variations in the skill of personnel who interpreted the aerial photographs (Cooper-Clark and Associates, 1975). To reflect various degrees of certainty in identification, landslide deposits were classified as "definite" (D), "probable" (P), or "questionable" (?) (fig. 2.8).

This map was an important source of information on potential slope-stability concerns used by SCC planners in their initial assessments of project feasibility before the 1989 earthquake. For sites in the Santa Cruz Mountains, an initial check of the map was typically followed by a preliminary geologic-hazard assessment by the SCC geological staff. This assessment included a review of the map, a site visit to evaluate potential slope instability, and a stereographic examination of aerial photographs of the site. When

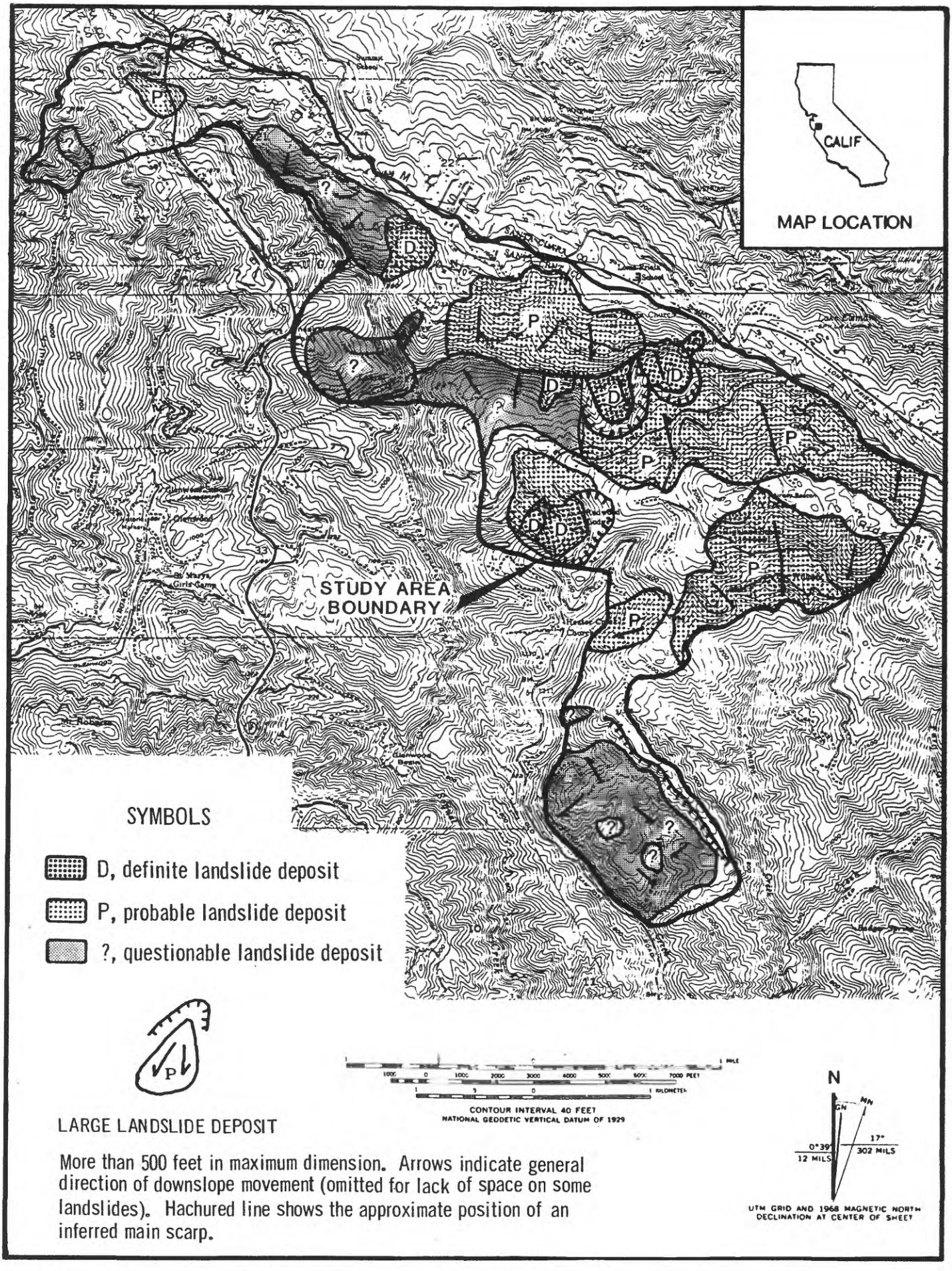

FIGURE 2.8 –Landslide deposits mapped by photointerpretation in the study area (from Cooper–Clark and Associates, 1975).

the Preliminary Map of Landslide Deposits showed a potential landslide hazard on or near the site (whether designated D, P, or ?), a full geologic report could be required.

The map shows 20 large landslide deposits in the study area (fig. 2.8). The largest of these covers more than 0.75 square miles, and together, definite, probable, or questionable landslide deposits cover approximately one-half of the study area. Many of the larger deposits are probably composite features formed over a long period of time by the movement of several, smaller, coalescing landslides and (or) retrogressive, headward growth.

Many large landslide deposits are also shown in the USGS geologic quadrangle maps that cover the study area (Clark and others, 1989, with landslide boundaries revised by McLaughlin and Clark, 1990, unpublished data; McLaughlin and others, in press; see fig. 2.4). Note that it is standard practice for geologic maps such as these quadrangle maps to emphasize bedrock distribution and thus to minimize portrayal of features such as landslides that cover the bedrock. In accordance with this practice, the geologic quadrangle maps portray fewer landslide deposits than does the map of Cooper-Clark and Associates (1975), which was specifically concerned with landslides.

A review by Griggs and others (1990) of 32 pre-earthquake geologic consulting reports concerned with the Summit Ridge area, on file with SCC, indicated that virtually all of the consultants who had worked in that area prior to the Loma Prieta earthquake recognized the landslide origin of irregular, benched topographic features there. Consultants had concluded that these features were "old" or "ancient" landslides that had probably formed during prior earthquakes, or perhaps during some period when the climate was wetter than at present. Approximately half the consultants stated that the potential for reactivation of these landslides was low to moderate, and approximately half of the consultants judged that these landslides could be remobilized by strong seismic shaking.

H. References Cited

Anderson, R. S., 1990, Evolution of the northern Santa Cruz Mountains by advection of crust past a San Andreas fault bend: Science, v. 249, no. 4967, p. 397-401.

Brown, W. M. III, 1988, Historical setting of the storm: Perspectives on population, development and damaging rainstorms in the San Francisco Bay region, *in* Ellen, S. D., and Wieczorek, G. F., eds., 1988, Landslides, floods, and marine effects of the storm of January 3-5, 1982, in the San Francisco Bay region, California: U.S. Geological Survey Professional Paper 1434, p. 7-15.

Clark, J. C., Brabb, E. E., and McLaughlin, R. J., 1989, Geologic map and structure sections of the Laurel 7-1/2' quadrangle, Santa Clara and Santa Cruz counties, California: U.S. Geological Survey Open-File Map 89-676, scale 1:24,000.

Cooper-Clark and Associates, 1975, Preliminary map of landslide deposits in Santa Cruz County, California, *in* Seismic Safety Element: Santa Cruz County Planning Department, scale 1:62,500.

Creasey, C. L., 1988, Landslide damage: A costly outcome of the storm, *in* Ellen, S. D., and Wieczorek, G. F., eds., 1988, Landslides, floods, and marine effects of the storm of January 3-5, 1982, in the San Francisco Bay region, California: U.S. Geological Survey Professional Paper 1434, p. 195-203.

Ellen, S. D., Wieczorek, G. F., Brown, W. M. III, and Herd, D. G., 1988, Introduction, *in* Ellen, S. D., and Wieczorek, G. F., eds., 1988, Landslides, floods, and marine effects of the storm of January 3-5, 1982, in the San Francisco Bay region, California: U.S. Geological Survey Professional Paper 1434, p. 1-5.

Ellen, S. D., and Wieczorek, G. F., eds., 1988, Landslides, floods, and marine effects of the storm of January 3-5, 1982, in the San Francisco Bay region, California: U.S. Geological Survey Professional Paper 1434, 310 p.

Griggs, G. B., Rosenbloom, N. A., and Marshall, J. S., 1990, Investigation and monitoring of ground cracking and landslides initiated by the October 17, 1989 Loma Prieta earthquake: Santa Cruz, Calif., Gary B. Griggs and Associates, Final Report to the U.S. Army Corps of Engineers.

Hall, N. T., Sarna-Wojcicki, A. M., and Dupre, W. R., 1974, Faults and their potential hazards in Santa Cruz County, California: U.S. Geological Survey Miscellaneous Field Studies Map MF-626, scale 1:62,500.

Keefer, D. K., 1984, Landslides caused by earthquakes: Geological Society of America Bulletin, v. 95, no. 4, p. 406-421.

Keefer, D. K., Wilson, R. C., Mark, R. K., Brabb, E. E., Brown, W. M. III, Ellen, S. D., Harp, E. L., Wieczorek, G. F., Alger, C. S., and Zatkin, R. S., 1987, Real-time landslide warning during heavy rainfall: Science, v. 238, no. 4829, p. 921-925.

Lawson, A. C., and others, 1908, The California earthquake of April 18, 1906: Report of the California State Earthquake Investigation Commission: Washington, D. C., Carnegie Institution, Publication 87 (reprint edition), 2 vols.

Lisowski, M., Prescott, W. H., Savage, J. C., and Johnston, M. J., 1990, Geodetic estimate of coseismic slip during the 1989 Loma Prieta, California, earthquake: Geophysical Research Letters, v. 17, no. 9, p. 1437-1440.

Manson, M. W., Keefer, D. K., and McKittrick, M. A., compilers, 1991, Landslides and other geologic features in the Santa Cruz Mountains, California, resulting from the Loma Prieta earthquake of October 17, 1989: California Division of Mines and Geology, Preliminary Report 29 (in press).

Marshall, J. S., 1990, History of landsliding associated with prior earthquakes in the Santa Cruz Mountains, *in* Griggs, G. B., Rosenbloom, N. A., and Marshall, J. S., 1990, Investigation and monitoring of ground cracking and landslides initiated by the October 17, 1989 Loma Prieta earthquake: Santa Cruz., Calif., Gary B. Griggs and Associates, Final Report to the U.S. Army Corps of Engineers, Appendix C.

McLaughlin, R. J., Clark, J. C., Brabb, E. E., and Helley, E. J., in press, Geologic map and structure sections of the Los Gatos 7 1/2' Quadrangle, Santa Clara County California: U.S. Geological Survey Open-File Map.

McNally, K. C., Lay, T., Protti-Quesada, M., Valensise, G., Orange, D., and Anderson, R. S., 1989, Santa Cruz Mountains (Loma Prieta) earthquake: Eos, v. 70, no. 45, p. 1463-1467.

Plafker, G., and Galloway, J. P, eds., 1989, Lessons learned from the Loma Prieta, California, earthquake of October 17, 1989: U.S. Geological Survey Circular 1045, 48 p.

Rantz, S. E., 1971, Mean annual precipitation and precipitation depth-duration-frequency data for the San Francisco Bay region, California: U.S. Geological Survey Open-File Report, 23 p.

Schwartz, S. Y., Orange, D. L., and Anderson, R. S., 1990, Complex fault interactions in a restraining bend on the San Andreas fault, southern Santa Cruz Mountains, California: Geophysical Research Letters, v. 17, no. 8, p. 1207-1210.

Shakal, A., Huang, M., Reichle, M., Ventura, C., Cao, T., Sherburne, R., Savage, M., Darragh, R., and Peterson, C., 1989, CSMIP strong-motion records from the Santa Cruz Mountains (Loma Prieta), California earthquake of 17 October 1989: California Division of Mines and Geology, California Strong Motion Instrumentation Program, Report OSMS 89-06, 195 p.

U.S. Geological Survey, 1990, The next big earthquake in the Bay Area may come sooner than you think: Menlo Park, Calif., U.S. Geological Survey, 23 p.

Wesnousky, S. G., 1986, Earthquakes, Quaternary faults, and seismic hazards of California: Journal of Geophysical Research, v. 91, no. B12, p. 12,587-12,631.

Wieczorek, G. F., Harp, E. L., Mark, R. K., and Bhattacharyya, A. K., 1988, Debris flows and other landslides in San Mateo, Santa Cruz, Contra Costa, Alameda, Napa, Solano, Sonoma, Lake and Yolo Counties, and factors influencing debris-flow distribution, *in* Ellen, S. D., and Wieczorek, G. F., eds., 1988, Landslides, floods, and marine effects of the storm of January 3-5, 1982, in the San Francisco Bay region, California: U.S. Geological Survey Professional Paper 1434, p. 133-161.

Working Group on California Earthquake Probabilities, 1990, Probabilities of large earthquakes in the San Francisco Bay region, California: U.S. Geological Survey Circular 1053, 51 p.

Youd, T. L., and Hoose, S. N., 1978, Historic ground failures in northern California triggered by earthquakes: U.S. Geological Survey Professional Paper 993, 177 p.

CHAPTER III. LANDSLIDES IN THE STUDY AREA PRODUCED BY THE LOMA PRIETA EARTHQUAKE

A. Data and Methods

In the Summit Ridge area, the Loma Prieta earthquake produced a complex pattern of ground cracks. Initial understanding of the mechanisms that created these cracks was complicated by the complexity and discontinuity of many of the cracks and of other, related surface features. However, within a few days after the earthquake, initial field observations suggested that several large landslides were among the earthquake-related features present in the Summit Ridge area. Preliminary identifications of major landslides were made based on repeated field observations and initial compilation of ground-crack mapping, primarily by personnel from the USGS, CDMG, and TAG.

The ground-crack mapping, which formed a primary basis for delineation of the various landslide masses, was progressively refined by repeated field checking and was officially released by CDMG and the USGS in the report by Spittler and Harp (1990). That report contained maps of the earthquake-induced ground cracks in the Summit Ridge area, plotted on the SCC planimetric base at a scale of 1:4,800, and a compilation of field notes from the 54 contributors who mapped the ground cracks. Those notes included descriptions of such characteristics of the ground cracks as linearity, displacements, and relations to pre-earthquake landslide deposits and other landform features.

Spittler and Harp (1990) indicated that most of the field mapping was carried out using as a base 1:6,000-scale aerial photography flown on October 27, 1989. In areas beyond that coverage, mapping was carried out on 1:4,800-scale enlargements of 1:24,000-scale USGS topographic maps, on 1:31,680-scale black-and-white aerial photographs taken in June 1989, or directly on the SCC planimetric base maps.

Spittler and Harp (1990) discussed the purpose, accuracy, and limitations of the crack mapping as follows:

"Location errors of fractures and other features were introduced through transfer problems and from the apparent scale errors in the county map base. Locations of features mapped from 1:6,000-scale airphotos are accurate to within 10 m [33 feet] where vegetation is sparse and to within 10-50 m [33 to 164 feet] where tree cover is dense. Outside the coverage of the 1:6,000-scale aerial photos, locations are less accurate. In areas with distinctive cultural or topographic features, the accuracy is estimated to be within 20 to 50 m [66 to 164 feet]. Where no distinct features are shown in the base maps or on the 1:31,680-scale aerial photos, and where the tree cover is dense, the location accuracy is estimated to be within 50 to 100 m [164 to 328 feet].

"Some landslide features and coseismic fissures may have been missed during the mapping because of dense vegetation, poor access, and the obliteration of many features due to repair work before mapping could be completed. The purpose of this map is to document the landslides and coseismic fractures in a systematic way and to display their distribution with a minimum of generalization. Because the features have been plotted by hand and not precisely surveyed at a large scale such as 1:500 or greater, some generalization has been incorporated in the mapping. Therefore these maps are useful as a reconnaissance tool and as a guide [sic] subsequent geologic and geotechnical investigations, but they are not sufficiently precise to serve as maps upon which to base site-specific engineering or planning decisions."

Using preliminary versions of these ground-crack maps, relevant features were checked in the field by personnel from the USGS, CDMG, and TAG to attempt to resolve possible ambiguities and to aid in interpretation of relations in critical areas. Using both preliminary and final versions of these maps, a detailed analysis of the origins of the ground cracks was undertaken, major ground cracks probably caused by other processes were distinguished from

landslide cracks (See Chapter IV), and major landslide masses were identified.

Twelve large landslides and landslide complexes in the study area were selected for surface monitoring by Gary B. Griggs and Associates to measure post-earthquake movement, if any. Selections of areas for monitoring were made in consultation with the TAG. As part of the monitoring program, these landslides and landslide complexes were observed repeatedly in the field, and general descriptions of these features were included in the report of Griggs and others (1990).

Landslides in the upper Schultheis Road and Villa Del Monte areas were additionally selected by the TAG for subsurface exploration and monitoring. Subsurface exploration and installation and initial monitoring of instruments there were performed by William Cotton and Associates, Inc. As part of that work, maps showing approximate, inferred boundaries of landslide features in those areas were presented in the report of William Cotton and Associates, Inc. (1990).

Additional data on ground movements in parts of the Summit Ridge area, which were used on a limited basis, were obtained from a survey of water wells. This survey, conducted and reported by Brumbaugh (1990), developed information in 239 water wells. The post-earthquake status was reported for 157 of these, of which 33 were reported to have been damaged by the earthquake. Methods used in this survey were described by Brumbaugh (1990) as follows:

> "The post-earthquake status of the water wells in this area was obtained by making site visits, phoning those not at home, and questioning neighbors and well drillers. Environmental Health permit requests were also used to obtain well status since the earthquake. The water levels in several of the wells were also measured to gain additional data on the wells."

Brumbaugh (1990) also stated that:

> "several wells in this area haven't been mechanically checked out since the earthquake and no

post-earthquake status was obtained where residents vacated their homes after the earthquake and no phone numbers were available."

Note that this survey did not include checking wells with a borehole camera or other means of independently verifying reports of well conditions.

These water-well data were not considered definitive for identifying areas where landslides had occurred because of limitations in these data. These limitations include: (1) most reports of damage, disturbance, or lack of disturbance were second hand, (2) many well locations were determined only approximately, (3) the causes of well damage or disturbance were typically unknown, (4) the extent to which reportedly undamaged wells were surveyed is unknown, and (5) the ground displacements that the wells could tolerate without visible indications of distress are also unknown. In some cases, where reports of water-well conditions were consistent for groups of several wells, they were used to locally refine locations of landslide boundaries. However, it is important to note that overall landslide recognition was based on surficial features and not on reports of water-well damage or other types of subsurface data.

For the purposes of the present report, the ground-crack maps in Spittler and Harp (1990), as well as other data, were plotted on topographic bases, prepared by Towill, Inc. by registering data on the SCC planimetric base with topographic contours from the USGS 1:24,000-scale Laurel and Los Gatos quadrangle maps (plates 3.1-3.4). These maps were plotted at a scale of 1:6,000. The pattern of ground cracks and their mapped relations to topography were then considered along with all of the other types of data discussed in this section to infer the approximate boundaries of large landslides and landslide complexes in the study area that moved during the Loma Prieta earthquake. The inferred landslide boundaries are subject to the same limitations in accuracy quoted above for the ground-crack mapping and additional limitations imposed by the transfer of ground-crack locations to the topographic base, by the interpretation of landslide boundaries from the ground cracks and other features, and by the interpolation of landslide boundaries between recognizable surface features. Errors due to the transfer process are judged to be minimal. Interpretation and interpolation of the

landslide boundaries were made using our best professional judgement, but potential errors in the locations of these interpreted boundaries cannot be determined quantitatively.

B. General Landslide Definitions and Characteristics

In this report, the term "landslide" is used to denote the "downward and outward movement of slope-forming materials composed of natural rock, soils, artificial fills, or combinations of these materials," as defined by Varnes (1958). This usage is also synonymous with the more general but perhaps less widely recognized term "slope movement" employed by Varnes (1978). During the Loma Prieta earthquake, ground cracks in the Summit Ridge area were almost certainly caused by several different mechanisms, including landslides. Other processes producing cracks may have included discontinuous, surface fault-rupture; slip along bedding planes; adjustments to the local tectonic uplift that accompanied the earthquake; extension or compression over active bedrock folds; and shaking-induced, ridge-top cracking.

The location and orientation of ground cracks produced by all these processes, including landslides, may be controlled by structures within rock and soil masses, such as bedding planes, faults, and other discontinuities, and many cracks produced by the earthquake in the Summit Ridge area show evidence of having been structurally controlled by such features. These structurally controlled cracks occurred both within and outside of landslides, as well as along landslide boundaries. Landslide boundaries and other landslide elements typically exhibit structural control even when the landslides have occurred without seismic or tectonic activity. Structural control of ground cracks in the Summit Ridge area is discussed in Chapter IV.

Terms used to describe various parts of large, deep-seated landslides are defined in figure 3.1. The landslide illustrated in this figure exhibits two main types of movement: The main body of the landslide is a rotational slump, which moved downslope on a concave-upward basal shear surface with a significant component of headward rotation; the foot of the landslide is an earth flow, which moved downslope partly by translation on the surface of separation and partly by distributed, internal shear, or flow (fig. 3.1). Figure 3.2 illustrates another type of large, deep-seated landslide--a block slide,

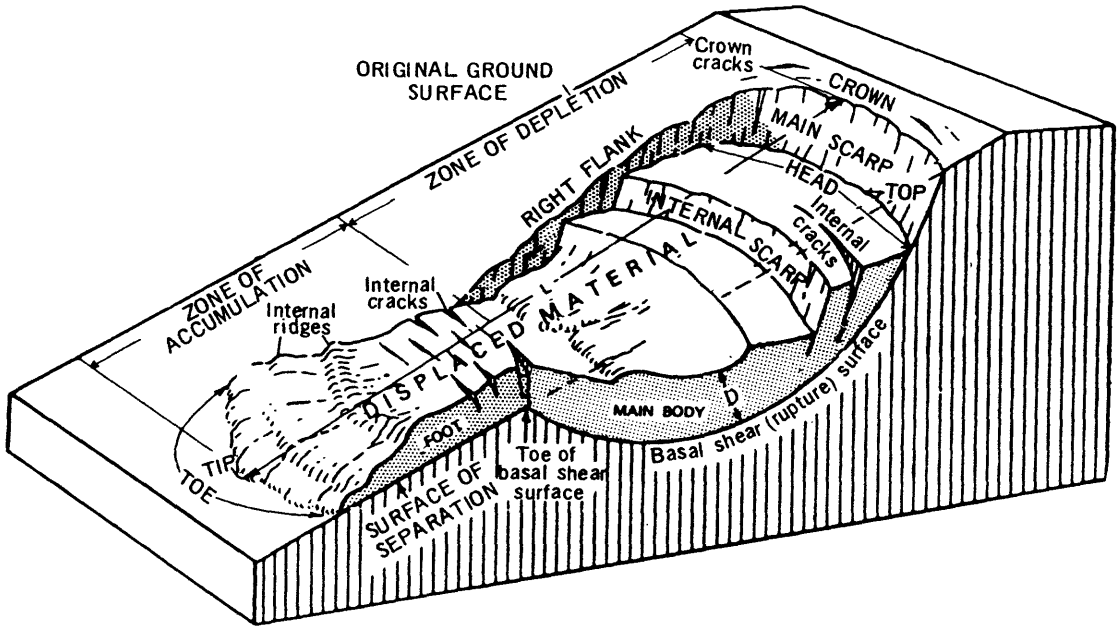

NOMENCLATURE FOR PARTS OF A LANDSLIDE

MAIN SCARP -A steep surface on the undisturbed ground around the periphery of the slide, caused by the movement of slide material away from undisturbed ground. The projection of the scarp surface under the displaced material becomes the basal shear surface.

INTERNAL SCARP -A steep surface on the displaced material produced by differential movements within the sliding mass.

HEAD -The upper parts of the slide material along the contact between the displaced material and the main scarp.

TOP -The highest point of contact between the displaced material and the main scarp.

TOE OF BASAL SHEAR SURFACE -The intersection (sometimes buried) between the lower part of the basal shear surface and the original ground surface.

TOE -The margin of displaced material most distant from the main scarp.

TIP -The point on the toe most distant form the top of the slide.

FOOT -That portion of the displaced material that lies downslope from the toe of the basal shear surface.

MAIN BODY -That part of the displaced material that overlies the basal shear surface between the main scarp and toe of the basal shear surface.

CROWN CRACKS - Cracks in the ground surface upslope from the crown.

CROWN -The material that is still in place, practically undisplaced and adjacent to the highest parts of the main scarp.

FLANK -The side of the landslide.

ORIGINAL GROUND SURFACE -The slope that existed before the movement which is being considered took place.

LEFT AND RIGHT -Compass directions are preferable in describing a slide, but if right and left are used they refer to the slide as viewed downslope from the crown.

SURFACE OF SEPARATION -The surface separating displaced material from stable material but not known to have been a surface on which failure occurred.

DISPLACED MATERIAL -The material that has moved away form its original position on the slope. It may be in a deformed or undeformed state.

ZONE OF DEPLETION -The area within which the displaced material lies below the original ground surface.

ZONE OF ACCUMULATION -The area within which the displaced material lies above the original ground surface.

LENGTH (L)-Distance from top to tip.

WIDTH (W) -Maximum distance from left flank to right flank, measured perpendicular to length.

DEPTH (D) -Maximum depth to the basal shear surface measured perpendicular to the ground surface.

BASAL SHEAR (or RUPTURE) SURFACE -Surface at base of main body on which landslide movement took place.

FIGURE 3.1 -Idealized slump and earth flow, showing nomenclature for parts of a landslide. (Modified from Varnes, 1978).

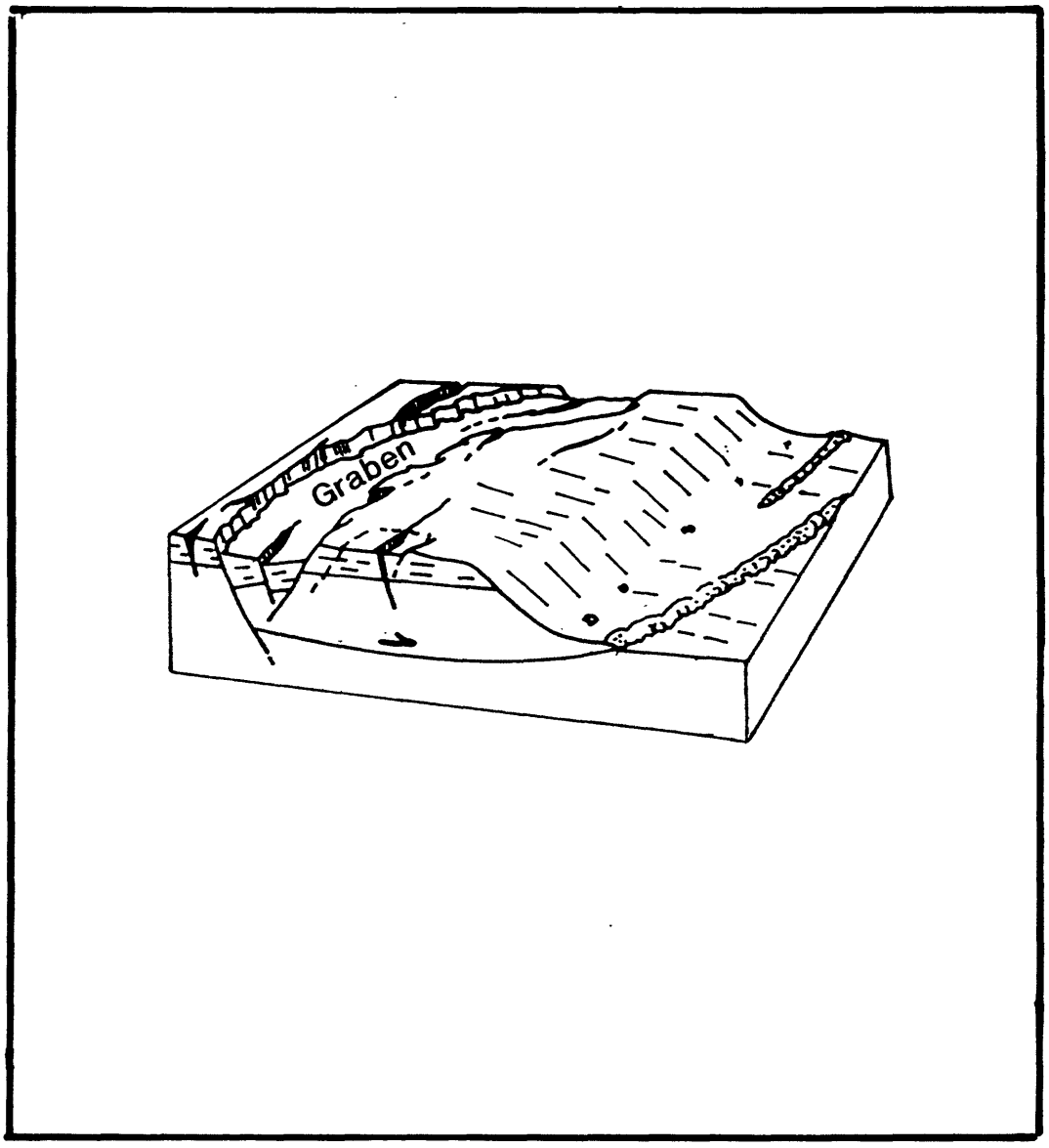

FIGURE 3.2 -Idealized block slide, which moved downslope primarily by translation on gently curved basal shear surface. Graben (down-dropped block of ground) present at head. Arrow shows direction of movement. (Modified from Varnes, 1978).

which moved downslope primarily by translation along a planar or gently curved shear surface. Ground-crack patterns and other surficial features in several parts of the Summit Ridge area indicate that the large landslides produced by the Loma Prieta earthquake were complex slumps, block slides, or combinations of the two types. (Earth flows were not observed in this area after the earthquake, and this type of landslide is included in figure 3.1 only for completeness in defining landslide nomenclature). The illustrations in figures 3.1 and 3.2 are highly idealized; few actual examples of such landslides exhibit all of the features illustrated, most actual landslides are irregular in shape, and many landslides are complex features that exhibit more than one type of movement--such as a combination of downslope translation and rotation.

Surficial features characteristic of completely developed slumps and block slides include, but are not limited to, the following:

* Main scarps at the upslope margins of slumps are typically arcuate, concave-downslope in plan view (fig. 3.1). Main scarps of block slides may be arcuate or linear, and some block slides have down-dropped blocks, called "grabens," at their heads (fig. 3.2). The overall trends of main scarps of both slumps and block slides are typically across the slope, approximately parallel or subparallel to the contours.

* Sets of discontinuous, crown cracks are typically present upslope and subparallel to main scarps (fig. 3.1).

* Flanks are defined by scarps or cracks trending downslope, or by en echelon sets of cracks, accompanied by local lateral ridges, compression features, or other indicators of relative movement. The overall trend of landslide flanks is typically approximately parallel or subparallel to the downslope direction.

* Zones of internal cracks and scarps may be present (fig. 3.1), sometimes defining completely detached blocks within landslides. However, some landslides exhibit major cracking only along the margins and may have large areas of internal ground surface that are relatively undeformed (fig. 3.2).

* Zones of bulging ground and (or) areas of compressional cracking may be present at the downslope margins.

* Topography within large landslides is commonly uneven, hummocky, disrupted, or benched (consisting of alternating steep and gentle stretches of slope). Zones of reversed slope inclination may also be present. An example of benched topography is shown in figure 3.3.

* Surface drainage may be disrupted, as evidenced by local ponding of water, small springs, and similar features.

* Most ground cracks and other surface features associated with landslides are located on ridge flanks and other slopes, although some areas of ridge tops and (or) flat valley floors may also be involved in some cases.

* Displacements across scarps and cracks in landslides, in aggregate, are consistent with downslope movement. Locally, however, scarps may also face upslope, as at the downslope margin of grabens (fig. 3.2) or the upslope margins of completely detached blocks within a landslide mass.

Note that recognition and identification of landslides is based on the overall patterns of ground cracks and other surficial features and does not rest on any one crack or other single feature. In addition, not all of the features described above are present on every slump or block slide; the degree of development of the landslide features depends on the local setting, material, and amount of displacement a landslide has undergone.

In particular, a slump or block slide that has moved only a short distance downslope may have discontinuous scarps or cracks along its head and flanks (fig. 3.4) yet may not have developed a zone of bulging ground at its toe. Much or all of the initial displacement of a landslide, evidenced by extension cracking at the head, may be accommodated by distributed internal compression of the landslide material without producing a visible bulge of ground at the toe, as illustrated in figure 3.5. The absolute amounts of displacement necessary for the development of continuous, through-going boundary cracks and compression features on landslides are not well known. However, as indicated in figure 3.5, several feet of displacement at the heads of landslides as large as many of those in the study area could be accommodated by small (less than one percent) compressive strains within the landslide material, with no

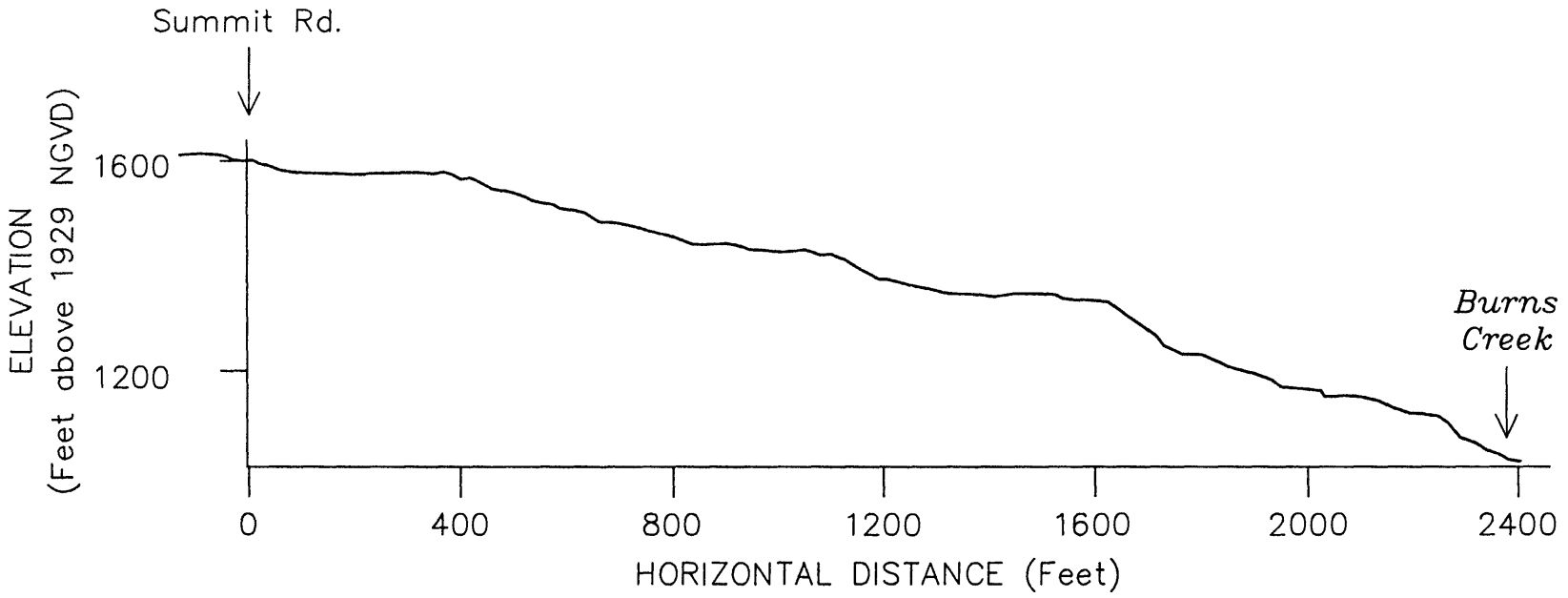

FIGURE 3.3 -- Example of benched topography. Note alternating steep and gently sloping stretches of hillside. Line 3, Upper Schultheis Road area, Surveyed by Majors Engineering, November 18, 1989.

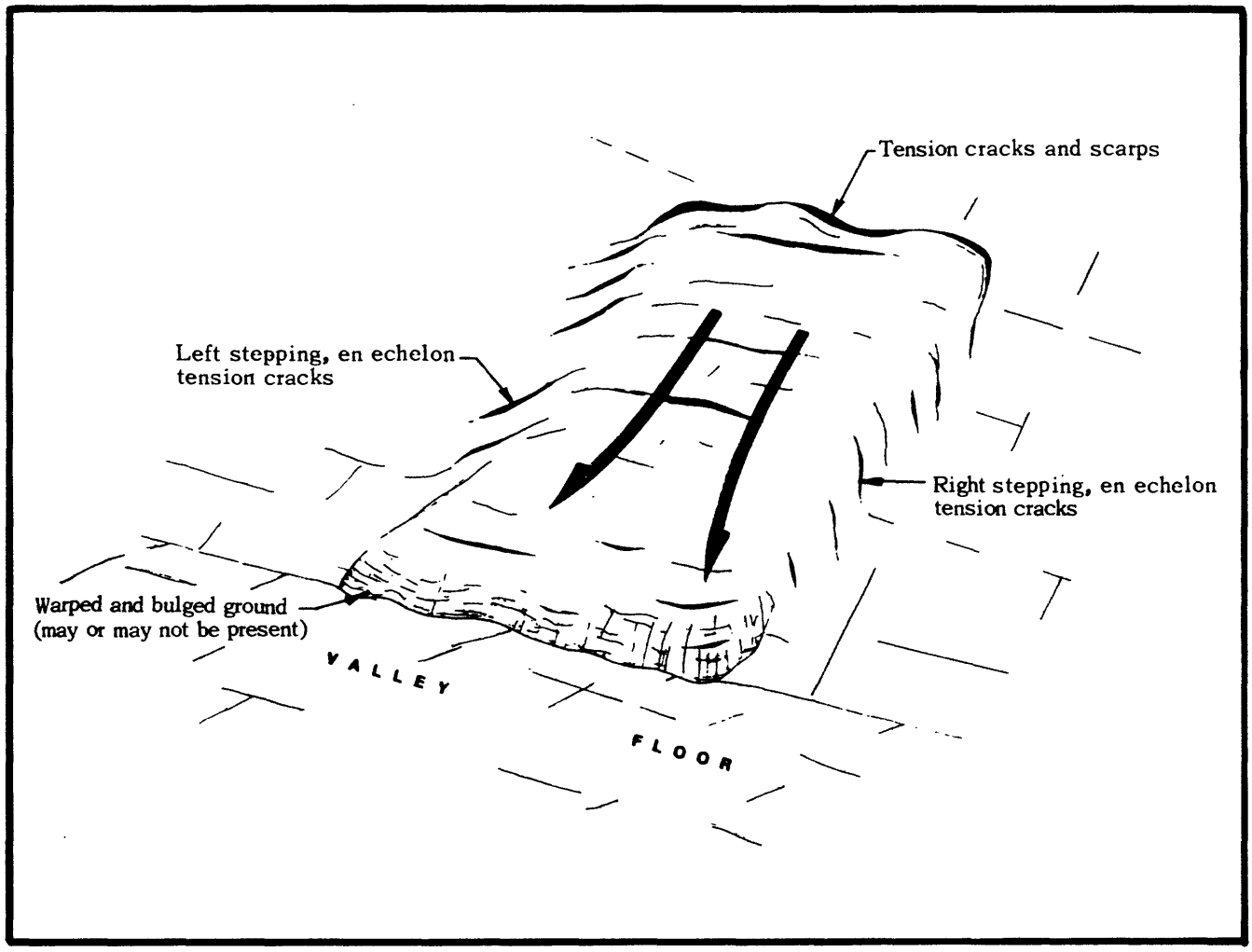

FIGURE 3.4 -Illustration of landslide that has moved only a short distance downslope. Note boundaries marked by discountinuous sets of cracks. Zone of bulging ground at toe may not be present. (Modified from William Cotton and Associates, Inc., 1990).

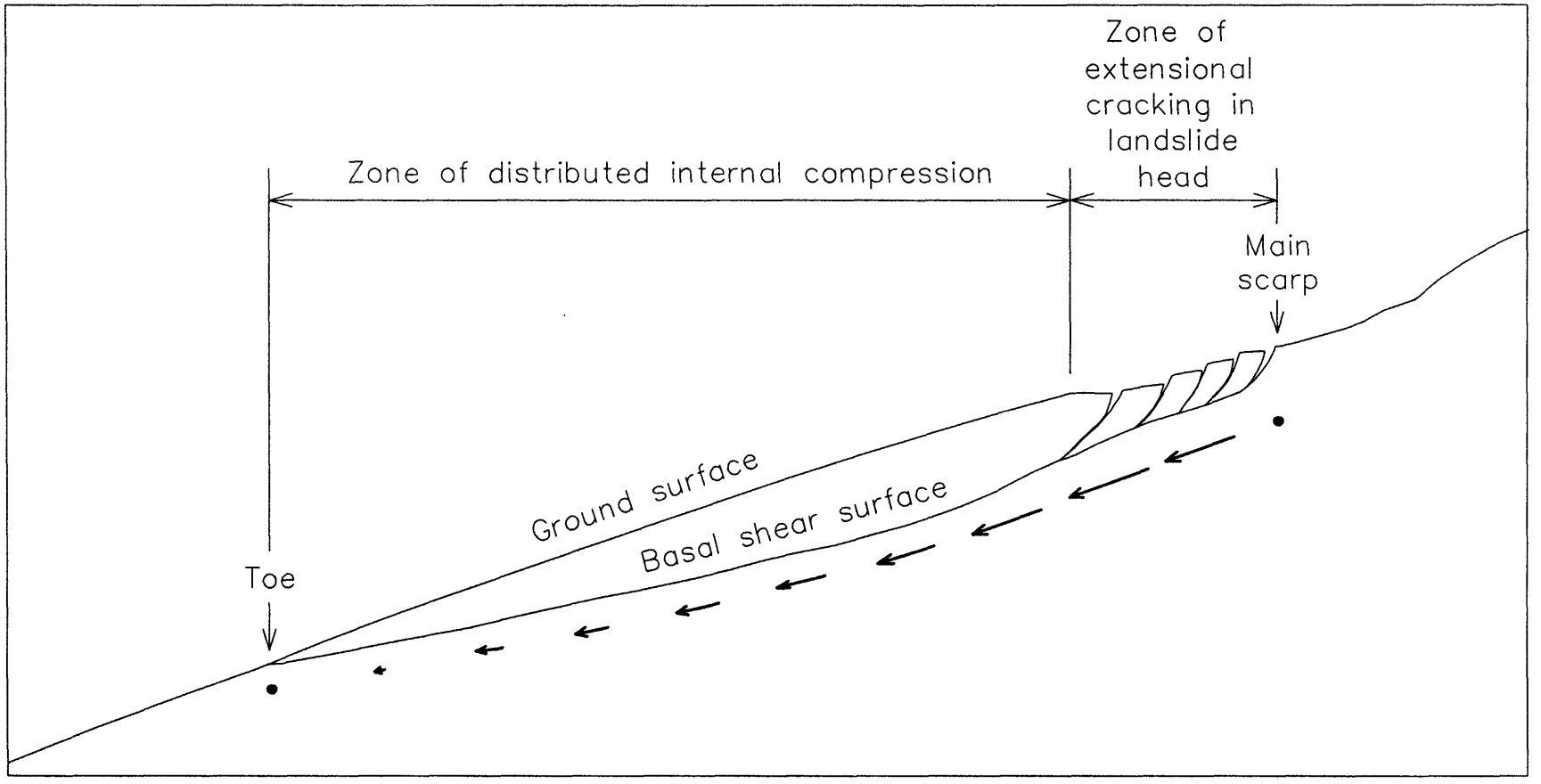

FIGURE 3.5 -- Idealized landslide cross section illustrating accomodation of extensional movement in head by distributed internal compression of remainder of landslide, with no bulging of ground surface at toe. Lengths of arrows below basal shear surface represent relative displacements of points along basal shear surface; dots indicate no displacement. As an example, within a landslide 3,000 feet long 6 feet of extensional displacement of the main scarp could be accomodated by 0.2 percent distributed, internal compressive strain of the landslide material, with no movement of the toe and no bulging of the ground surface (assuming a constant thickness of landslide material).

toe movement. Typically, therefore, when a landslide has moved only a short distance, cracks and scarps in the head, associated with extensional movement, are the best developed features and compressional features, associated with the toe, are the least developed features.

C. Summary of Characteristics of Landslides in the Study Area Caused by the Loma Prieta Earthquake

Within the study area, patterns of ground cracking in association with other data discussed above indicated that movement occurred on at least 18 large landslides and landslide complexes, with surface areas larger than 1 acre, during the Loma Prieta earthquake. The largest such landslide complex had an area of approximately 210 acres. The inferred locations and approximate boundaries of these 18 landslides and landslide complexes are shown in plates 3.1-3.4. Whereas these landslides and landslide complexes were scattered throughout the study area, most of the largest were on the south flank of Summit Ridge, in an area extending east from California Highway 17 to slightly east of Morrell Road.

The 18 large landslides and landslide complexes identified and portrayed in plates 3.1-3.4 are judged to be the minimum number that moved during the earthquake. As stated by Spittler and Harp (1990) and described in more detail in Section A of this chapter, some ground cracks and other types of features indicative of the presence of landslides may not have been recognized during mapping because of dense vegetation, lack of access, or obliteration of features by repair work before mapping could be completed.

In general, the landslides shown in plates 3.1-3.4 were marked at the surface by discontinuous zones of ground cracks and associated features. Typically, the features farthest upslope were zones of ground cracks and scarps, with trends approximately across the slope, that were arcuate, concave-downslope in plan view and exhibited features consistent with extensional and downslope displacements. Less commonly, cracks and scarps in such zones were gently curved, concave-downslope, or relatively linear. These zones of cracks and scarps were interpreted to be the main scarps and crown cracks associated with landslides.

Downslope from many of these zones were either zones of cracks and scarps with trends more nearly upslope-downslope or complex zones containing en echelon cracks. In some cases, the cracks trending more nearly upslope-downslope were continuous with the cross-slope-trending scarps and cracks farther upslope. These upslope-downslope-trending and en echelon cracks exhibited features consistent with the downslope displacements as expressed along landslide flanks, with components of right-lateral shear along right flanks and left-lateral shear along left flanks.

Downslope from some of the zones of cracks interpreted to be landslide flanks were local to relatively continuous compression features, trending approximately across slope, that are interpreted as being associated with landslide toes. In several cases where such features were not present, the patterns of other ground cracks suggested that the zones of downslope displacements extended all the way to the stream channels at the bases of the slopes. Many landslides and landslide complexes triggered by the earthquake also contained zones of internal cracks, internal ridges, or both.

In addition to the 18 large landslides and landslide complexes in the study area, several smaller landslides were triggered during the October 17 earthquake. Some of the smaller slumps and block slides are shown in plates 3.1-3.4. Other smaller, earthquake-induced landslides in the study area were mapped as part of a region-wide field reconnaissance conducted by CDMG and the USGS, the results of which were compiled by Manson and others (in press). Figure 3.6 shows the locations of those smaller landslides mapped in the study area, most of which were small rock falls, rock slides, soil falls, soil slides, slumps or block slides in fill, or reactivations of older landslides. Because these results were compiled from field-reconnaissance studies only, the available data include only general locations and descriptions of those landslides that were observed on a limited number of traverses through the area. Many other landslides of the types depicted in figure 3.6 probably also occurred in the study area during the earthquake but were not observed or mapped.

Earthquake-induced displacements on the large landslides in the study area were calculated from measurements of displacements across individual cracks and scarps reported in Spittler and Harp (1990), in Griggs and others (1990), or in unpublished data (particularly that of R. W. Jibson and D. K. Keefer of the USGS).

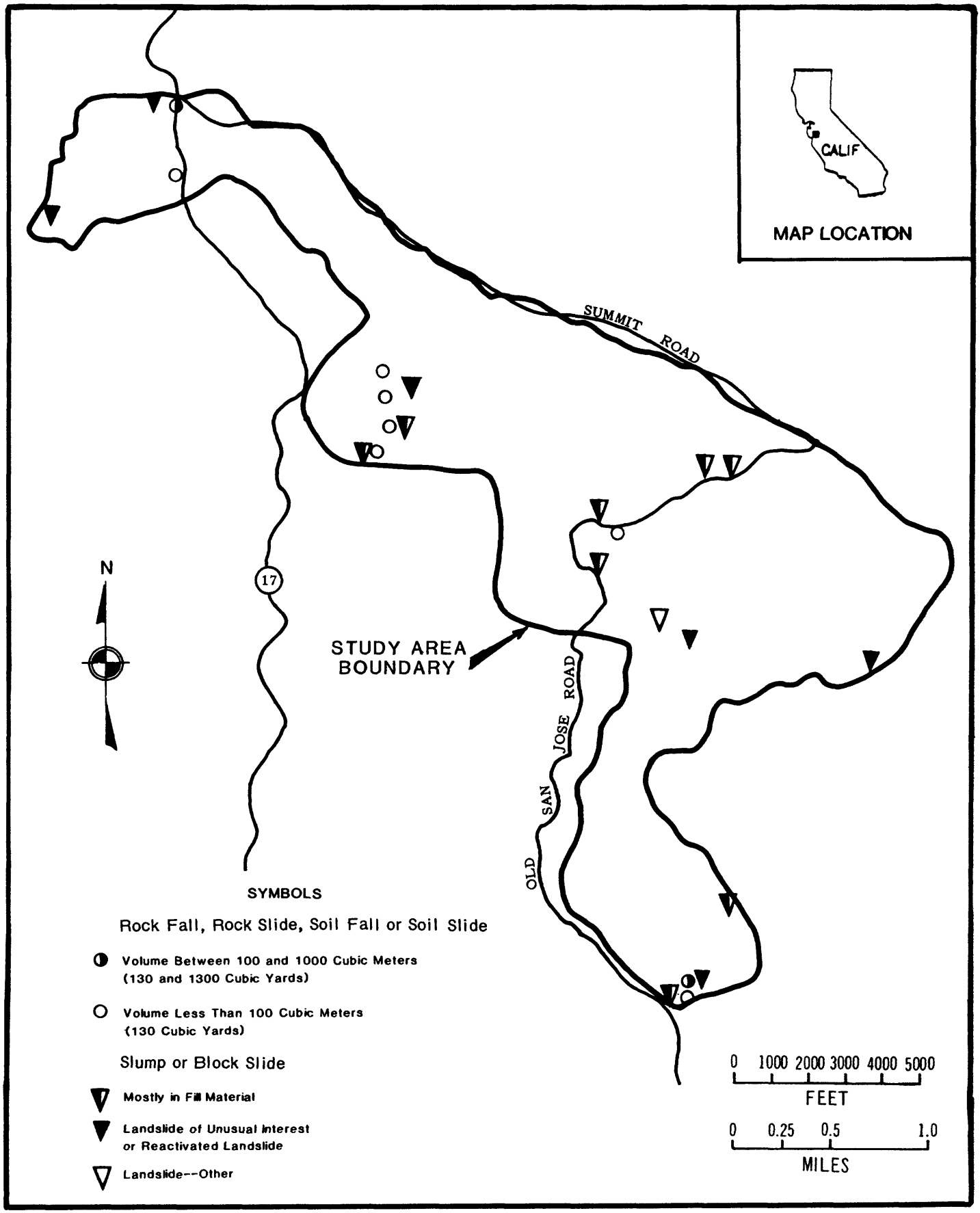

FIGURE 3.6 –Smaller landslides in study area triggered by Loma Prieta earthquake. (Modified from Mason and others, in press).

Displacements varied from place to place within the landslides; maximum calculated downslope displacements of individual landslides ranged from 10 inches to 8.1 feet. The morphological features of the landslides, including discontinuous boundary cracks, poorly developed compression features, and zones where little ground deformation was visible, were consistent with these limited displacements.

Even the limited displacements calculated for these landslides, however, were, in most cases, substantially larger than could be explained by the calculated absolute or local, differential, tectonic uplift produced by the earthquake (fig. 2.6). In addition, in many cases, including the south flank of Summit Ridge, the tilt imparted by this calculated tectonic uplift was in the opposite direction from the direction of measured slope movements. For example, the southern base of Summit Ridge was calculated to have been uplifted approximately 4 to 8 inches more than the crest of the ridge, imparting a local upslope tilt. Any ground cracks that might have occurred in direct response to this tilt would have shown relative upslope displacements limited to less than 8 inches of aggregate displacement as summed from bottom to top of the ridge flank. By contrast, the measured aggregate, downslope displacements of large earthquake-related landslides in that area were all more than 1 foot and locally were as much as 8.1 feet. Similarly, the downslope displacements of the other large earthquake-related landslides in the study area were too large and (or) were in the wrong direction to be attributed to the calculated tectonic uplift.

Eight of the 18 landslides and landslide complexes, including all but one of the largest, occurred on the south flank of Summit Ridge. The area of greatest concentration of landslides, along the south flank of the ridge approximately between California Highway 17 and Morrell Road, is also the part of the study area where the geologic structure is most complex, with intense folding and faulting of the rocks. Bedrock formations underlying this area include the Butano Sandstone, San Lorenzo Formation, and Vaqueros Sandstone (fig. 2.4). The map of Cooper-Clark and Associates (1975) and the USGS geologic quadrangle maps (Clark and others, 1989, with landslide boundaries revised by McLaughlin and Clark, 1990, unpublished data; McLaughlin and others, in press) also portray much of this area as being underlain by landslide deposits (figs. 2.4 and 2.8), and all of the landslides and landslide complexes that experienced movement during the earthquake in this area were partly or completely

superimposed upon the landslide deposits portrayed on one or more of these maps.

Major elements of geologic structure passing through the south flank of Summit Ridge and adjacent Skyland Ridge are the northwest-trending Laurel Anticline and Butano fault (fig. 2.4). The Butano fault truncates the axis of the Laurel Anticline in the vicinity of the Old Santa Cruz Highway, east of California Highway 17. In the westernmost part of the study area, west of this truncation, rocks southwest of the fault are Butano Sandstone and San Lorenzo Formation sediments that locally dip steeply southwest and locally are overturned and dip steeply northeast. The only large Loma Prieta-induced landslide mapped in this part of the study area moved in a direction oblique and almost opposite to the local dip of the bedding.

East of the truncation of the anticlinal axis, geologic structure along the south flank of Summit Ridge is more complex and is partly obscured by large mapped landslide deposits. Bedrock southwest of the Butano fault belongs primarily to the Butano Sandstone and San Lorenzo Formation, whereas bedrock nearer the ridge crest, northeast of the fault, has been mapped as Vaqueros Sandstone. Between Old Santa Cruz Highway and Morrell Road, the Laurel Anticline is locally overturned. Bedding in the middle of the ridge flank, between the Butano fault and the axis of the anticline typically dips to the northeast (into the hillside), whereas bedrock southwest of the axis dips either southwest (in the downslope direction) or is overturned to the northeast. Thus, the large earthquake-induced landslides in that area moved in directions locally subparallel to, locally opposite from, and locally oblique to the direction of bedrock dip. Failure, therefore, did not in general occur on bedding planes.

East of Morrell Road, the axis of the Laurel Anticline is largely overturned, and numerous subsidiary faults have been mapped; bedrock dips mapped in this area vary widely in direction, and relations between direction of landslide movement and geologic structure are thus obscured.

Farther south in the study area, in the Laurel township and Redwood Lodge neighborhoods, large Loma Prieta-induced landslides occurred on slopes underlain by mudstones and sandstones of the Rices Mudstone Member of the San Lorenzo Formation and by Vaqueros sandstones. Those rocks, lying between the axes of the Laurel Anticline and Glenwood Syncline, strike northwest and

typically are overturned to the northeast, but locally are vertical or dip to the southwest. Of the six large landslides in that area, one, or possibly two, moved in a direction approximately parallel to the local dip azimuth; movement of the others was oblique or opposite in direction to dip. The largest of these landslides is also at least partly coincident with older mapped landslide deposits (figs. 2.4 and 2.8).

In the southernmost part of the study area, the three large landslides that moved during the Loma Prieta earthquake were underlain by sandstones and siltstones of the Purisima Formation (fig. 2.4). These rocks lie on the limbs of the northwest-trending Glenwood Syncline. Bedding northeast of the synclinal axis, where one of the landslides occurred, dips to the southwest, and this landslide moved in the same azimuth as the dip. Bedding underlying the other two landslides, southwest of the axis, generally dips northeast, whereas the direction of landslide movement was east to southeast.

In most parts of the study area where large earthquake-induced landslides occurred, bedding dips are steep, typically significantly steeper than the local topographic slope. Thus, even in those cases where the direction of landslide movement was parallel or subparallel to the azimuth of bedrock dip, landslide movement was probably not controlled by true dip-slope conditions.

Throughout the study area, locations of landslides and landslide complexes that experienced movement during the Loma Prieta earthquake showed a high correlation with locations of large, pre-existing landslide deposits, as mapped by Cooper-Clark and Associates (1975). Of the 18 large landslides and landslide complexes that moved during the earthquake, all but one or two were wholly or partly within areas designated as "definite," "probable," or "questionable" landslide deposits on the 1975 map (figs. 2.8 and 3.7). The two exceptions were among the smaller of the earthquake-related landslides, with areas of 11 and 5 acres, and the possible downslope extension of one of them was within a "probable" landslide deposit, identified on the 1975 map. Of the 16 or 17 earthquake-related landslides and landslide complexes that occurred within landslide deposits depicted on the 1975 map, four were wholly or partly within "definite" landslide deposits, four or five were within "probable" deposits, 10 were within "questionable" deposits, and one was within a deposit that was not labeled. (Some of the earthquake-induced landslides were associated with more

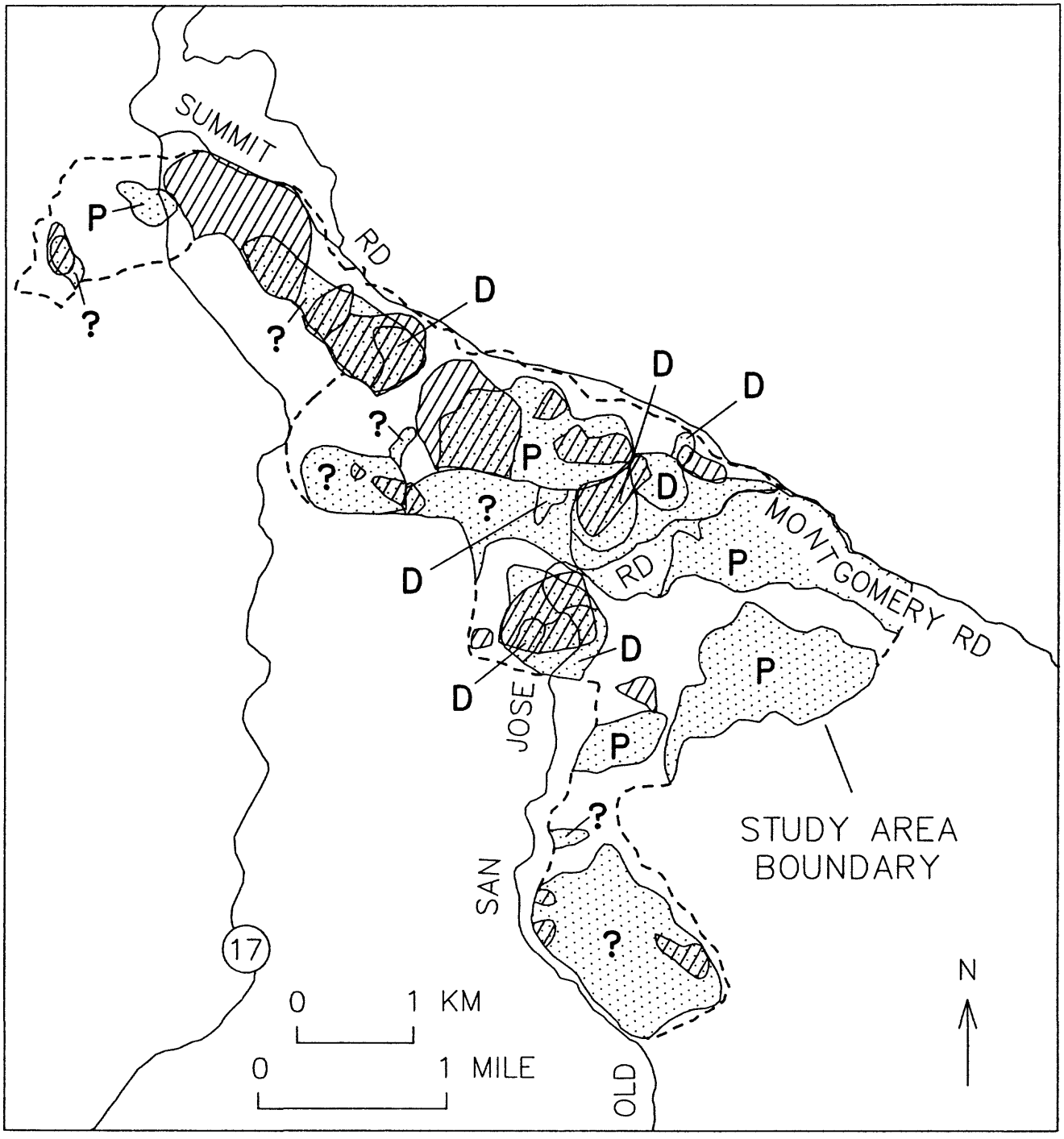

FIGURE 3.7 -- Generalized boundaries of landslides and landslide complexes inferred to have moved during the Loma Prieta earthquake (areas of diagonal stripes) compared to generalized landslide deposits and scarp areas (dotted patterns) mapped by Cooper – Clark and Associates (1975); D designates "definite", P "probable", and ? "questionable" landslide deposits and associated scarp areas as portrayed on 1975 map.

than one type of pre-existing landslide deposit, as depicted on the 1975 map.)

Conversely, 20 large landslide deposits were mapped within the study area by Cooper-Clark and Associates (1975), and 13 (or, possibly, 14) of those deposits produced large landslides during the Loma Prieta earthquake (fig. 3.7). The 20 landslide deposits mapped in 1975 in the study area included seven designated as "definite" five designated as "probable", seven designated as "questionable", and one that was unlabeled (figs. 2.8 and 3.7). Large earthquake-related landslides and landslide complexes occurred in six of the seven "definite" landslide deposits, one or two of the five "probable" deposits, five of the seven "questionable" deposits, and the sole unlabeled deposit.

Direct comparisons between the large landslides that experienced movement during the Loma Prieta earthquake and landslides triggered or reactivated by the 1906 San Francisco earthquake are difficult to make because of the incompleteness and imprecision in locations in the reports on the 1906 event. However, the reports of the 1906 earthquake do suggest that landslide activity in and around the Summit Ridge area was more widespread and severe in 1906 than in 1989. The greater landslide activity in 1906 is consistent with at least two major differences in conditions: (1) the 1906 earthquake (M 8.3) was much larger than the Loma Prieta event (M 7.1), releasing 60 times more seismic energy, and (2) ground-water levels within slopes were almost certainly higher during the 1906 earthquake than during the Loma Prieta event. Total rainfall during the 1905-06 winter was 124 percent of normal in Santa Cruz and 165 percent of normal in Santa Clara (Youd and Hoose, 1978); in addition, the 1906 earthquake occurred on April 18, late in the winter and after a period of exceptionally high rainfall in March. The 1989 Loma Prieta earthquake, by contrast, occurred at the end of the annual dry, summer period and followed three years of exceptionally low precipitation, when total annual rainfall was only 56 to 71 percent of normal.

D. Description of Large Landslides and Landslide Complexes in the Study Area That Moved as a Result of the Loma Prieta Earthquake

This section describes the large landslides and landslide complexes in the study area that moved during the Loma Prieta earthquake. These landslides and landslide complexes are described in geographic order beginning in the westernmost part of the study area, continuing from there east along Summit Ridge and Skyland Ridge, then proceeding south through the Redwood Lodge-Summit Woods area to Amaya Ridge, and from there west to the Laurel township area.

1. Majestic Drive Landslide

The Majestic Drive landslide is at the southern end of a spur ridge, which branches off Summit Ridge 0.6 miles southwest of the intersection of Summit Road and California Highway 17 (plate 3.1 and fig. 3.8). The crown, head, right flank, and uppermost left flank of the landslide are defined by a relatively continuous, 10- to 40-foot-wide zone of scarps and cracks that is arcuate, concave downslope in plan view. Downslope displacements across individual scarps and cracks at the head of the landslide were more than one foot.

The zone of cracks and scarps on the right flank of the landslide extends downslope approximately 1,000 feet, and the landslide mass is inferred to extend at least as far down the ridge flank as the downslope margin of this zone. As delineated on plate 3.1 and figure 3.8, the landslide mass is at least 1,000 feet long and 300 to 550 feet wide and has a surface area of at least 8 acres. The locations of the toe and lower left flank of the landslide, however, are uncertain, as no surface features marking their locations were mapped. Because no surface features marking a toe were evident, the landslide could extend an additional 400 feet farther downslope to the creek channel at the base of the ridge. The area between the downslope margin of the surface cracks and the creek channel is thus designated as a "possible landslide" in plate 3.1 and figure 3.8 and may encompass an additional area of 5 acres.

The average slope of the ridge flank down which this landslide moved is 20°; this slope also has a benched profile, with the several

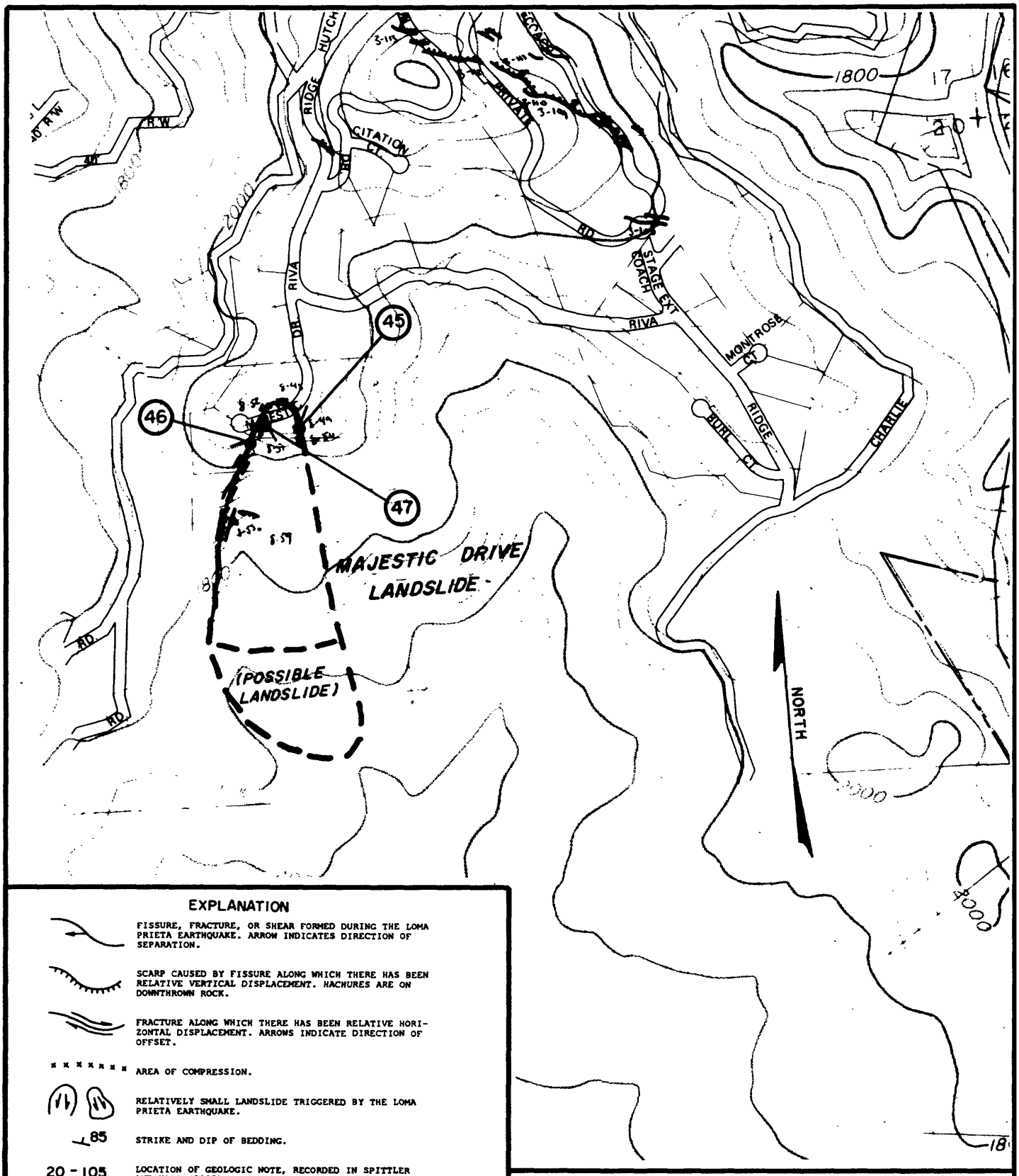

EXPLANATION

- FISSURE, FRACTURE, OR SHEAR FORMED DURING THE LOMA PRIETA EARTHQUAKE. ARROW INDICATES DIRECTION OF SEPARATION.
- SCARP CAUSED BY FISSURE ALONG WHICH THERE HAS BEEN RELATIVE VERTICAL DISPLACEMENT. HACHURES ARE ON DOWNTHROWN ROCK.
- FRACTURE ALONG WHICH THERE HAS BEEN RELATIVE HORIZONTAL DISPLACEMENT. ARROWS INDICATE DIRECTION OF OFFSET.
- AREA OF COMPRESSION.
- RELATIVELY SMALL LANDSLIDE TRIGGERED BY THE LOMA PRIETA EARTHQUAKE.
- 85 — STRIKE AND DIP OF BEDDING.
- 20 - 105 — LOCATION OF GEOLOGIC NOTE, RECORDED IN SPITTLER AND HARP (1990).
- APPROXIMATE, INFERRED BOUNDARY OF LARGE LANDSLIDE, LANDSLIDE COMPLEX, OR POSSIBLE LANDSLIDE THAT MOVED DURING THE LOMA PRIETA EARTHQUAKE.
- (4) — QUADRILATERAL ARRAY STATION # 4
- ● — ACTUAL STATION LOCATION
- ○ — REMOVED STATION

MAJESTIC DRIVE LANDSLIDE SURFACE STATIONS

SCALE 0 500 1000 FEET

FIGURE 3.8

gently sloping benches suggesting previous landslide movements. All but the uppermost part of the Majestic Drive landslide involves material previously designated by Cooper-Clark and Associates (1975) as belonging to a "questionable" landslide deposit (fig. 3.7).

Rocks underlying the Majestic Drive landslide are primarily sandstones, siltstones, and shales of the Butano Sandstone, which are overturned steeply to the northeast and therefore dip obliquely into the slope; the southwestern tip of the possible landslide area may be underlain by shales and sandstones of the Twobar Shale Member of the San Lorenzo Formation, which are also overturned steeply to the northeast (fig. 2.4).

2. Old Santa Cruz Highway Landslide Complex

The Old Santa Cruz Highway area (plate 3.1 and fig. 3.9) encompasses a zone of complex earthquake-induced landslides and structurally controlled cracks on the crest and south flank of Summit Ridge, extending 1 mile eastward from a point 1,000 feet east of the intersection of California Highway 17 and Summit Road. Downslope from near the ridge crest to Burns Creek, the zone of cracks and landslides extends for approximately 2,200 feet and thus encompasses approximately 0.33 square miles (210 acres).

The longest ground-cracking feature within the Old Santa Cruz Highway area is a nearly continuous, southeast-trending line of cracks and scarps, approximately 4,000 feet long, that crosses Summit Road 2,100 feet east of California Highway 17 and crosses Old Santa Cruz Highway 350 feet northeast of its junction with Schultheis Road (figs. 3.9 and 3.10). At least part of this zone was described as the "Tranbarger fracture" in Spittler and Harp (1990). Displacements across this feature vary along its length; maximum displacements are on the order of 2 feet downslope to the southwest, 2.5 feet shear (left-lateral), and 6 inches extension. A second, virtually continuous, 1,400-foot-long scarp strikes parallel to this zone and crosses Summit Road 1,600 feet farther east. Measurements across this latter scarp indicate 8 to 12 inches of movement downslope, to the southwest. Both of these long ground-crack features are discussed in more detail in Chapter IV, and results of a trenching study of the 1,400-foot-long scarp are discussed in Chapter V.

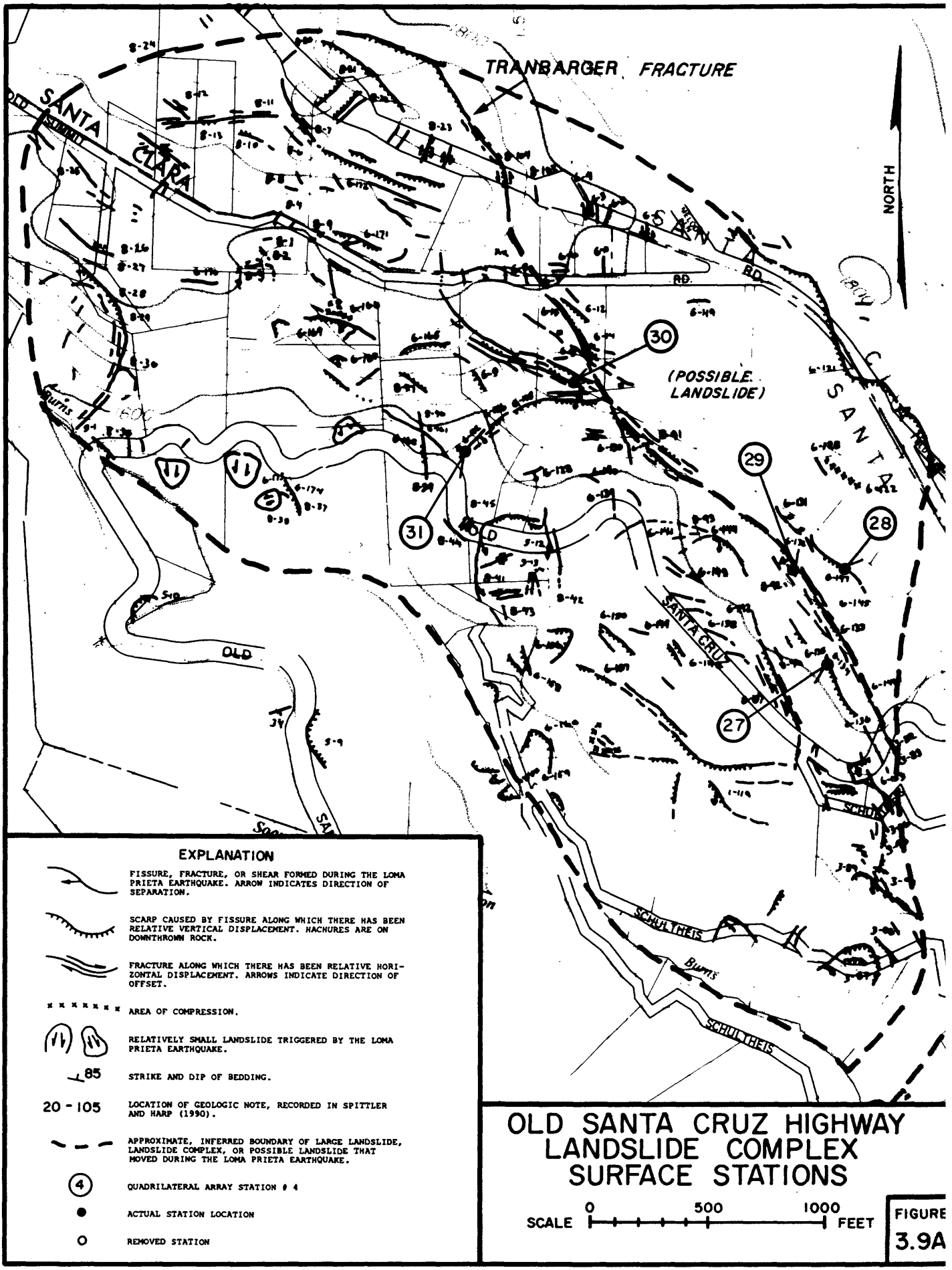

OLD SANTA CRUZ HIGHWAY LANDSLIDE COMPLEX SURFACE STATIONS

SCALE 0 500 1000 FEET

FIGURE 3.9A

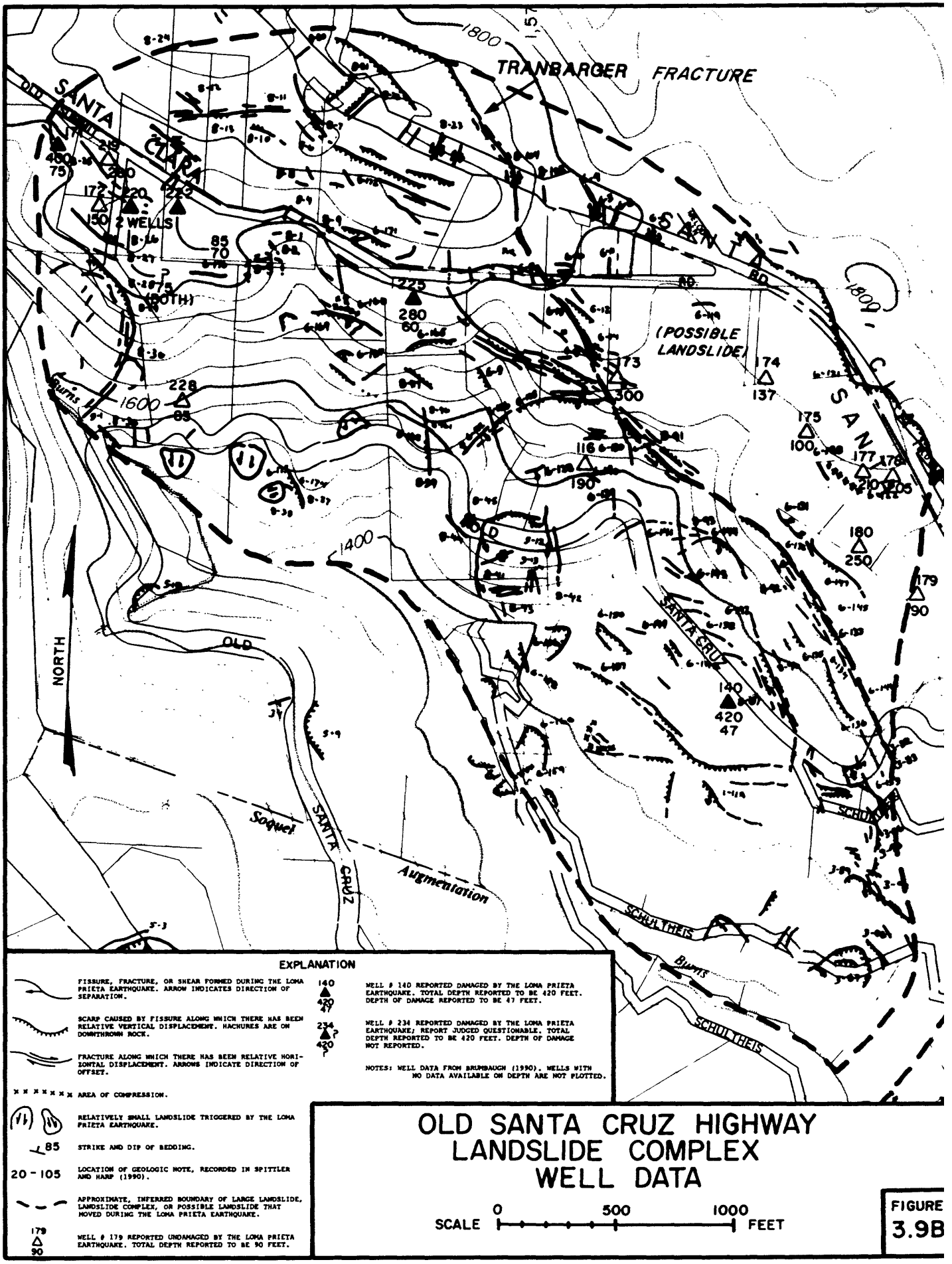
TRANBARGER FRACTURE
SANTA CLARA
OLD SANTA CRUZ HIGHWAY
(POSSIBLE LANDSLIDE)
NORTH
Soquel
SANTA CRUZ
Augmentation
SCHULTHEIS
BURTIS
SCHULTHEIS
1800
1600
1400
2 WELLS
EXPLANATION
FISSURE, FRACTURE, OR SHEAR FORMED DURING THE LOMA PRIETA EARTHQUAKE. ARROW INDICATES DIRECTION OF SEPARATION.
SCARP CAUSED BY FISSURE ALONG WHICH THERE HAS BEEN RELATIVE VERTICAL DISPLACEMENT. HACHURES ARE ON DOWNTHROWN ROCK.
FRACTURE ALONG WHICH THERE HAS BEEN RELATIVE HORIZONTAL DISPLACEMENT. ARROWS INDICATE DIRECTION OF OFFSET.
AREA OF COMPRESSION.
RELATIVELY SMALL LANDSLIDE TRIGGERED BY THE LOMA PRIETA EARTHQUAKE.
STRIKE AND DIP OF BEDDING.
LOCATION OF GEOLOGIC NOTE, RECORDED IN SPITTLER AND HARP (1990).
APPROXIMATE, INFERRED BOUNDARY OF LARGE LANDSLIDE, LANDSLIDE COMPLEX, OR POSSIBLE LANDSLIDE THAT MOVED DURING THE LOMA PRIETA EARTHQUAKE.
WELL # 179 REPORTED UNDAMAGED BY THE LOMA PRIETA EARTHQUAKE. TOTAL DEPTH REPORTED TO BE 90 FEET.
WELL # 140 REPORTED DAMAGED BY THE LOMA PRIETA EARTHQUAKE. TOTAL DEPTH REPORTED TO BE 420 FEET. DEPTH OF DAMAGE REPORTED TO BE 47 FEET.
WELL # 234 REPORTED DAMAGED BY THE LOMA PRIETA EARTHQUAKE; REPORT JUDGED QUESTIONNABLE. TOTAL DEPTH REPORTED TO BE 420 FEET. DEPTH OF DAMAGE NOT REPORTED.
NOTES: WELL DATA FROM BRUMBAUGH (1990). WELLS WITH NO DATA AVAILABLE ON DEPTH ARE NOT PLOTTED.
OLD SANTA CRUZ HIGHWAY
LANDSLIDE COMPLEX
WELL DATA
SCALE 0 500 1000 FEET

FIGURE 3.9B

FIGURE 3.10 –Segment of scarp forming part of "Tranbarger fracture," a 4,000–foot–long zone of scarps and cracks in the Old Santa Cruz Highway area. Photograph is taken from north edge of Summit Road; view is toward the northwest.

These two features have characteristics that are consistent with formation by landslide movement, formation by other, structurally controlled processes, or both, as discussed in more detail in Chapter IV. Characteristics consistent with a landslide origin are strikes approximately perpendicular to the slope inclination and measured displacements that, in nearly all places, are downslope, to the south and southwest (U.S. Geological Survey Staff, 1989; Spittler and Harp, 1990). Characteristics indicating structural control are (1) strikes parallel to other structurally-produced cracks, (2) the linearity and lengths of the features, (3) occasional uphill-facing scarp segments, and (4) location of the 1,400-foot-long scarp approximately over a fault mapped by McLaughlin and others (in press), as shown in figure 2.4.

If these two features are of landslide origin, the landslide movement is relatively deep and involves part of the ridge crest north of Summit Road near California Highway 17. Conversely, if the features are produced by other structurally controlled processes, these cracks could also have served as surfaces of weakness along which landslide movement took place later in the earthquake event. The seven reportedly undamaged wells between the two features (wells #173, 174, 175, 177, 178, 179, and 180 on fig. 3.9) and the linearity of the "Tranbarger fracture" where it crosses a deep valley north of Summit Road are consistent with either landslide movement on a basal shear surface several hundred feet deep at those localities or with movement produced by some other deep-seated process. Damage to the wells immediately east of California Highway 17 and south of Old Summit Road (wells #171, 220, and 222 on fig. 3.9), all reported disturbed at depths between 70 and 75 feet (Brumbaugh, 1990), suggests a 70- to 75-foot-deep landslide shear surface in that area.

Downslope and southwest of the two major zones of cracking are numerous, shorter, arcuate scarps and cracks and other features that indicate the presence of several smaller and shallower landslides (plate 3.1 and fig. 3.9). These scarps, cracks, and other features, which include localized areas of compression or bulging ground, are so numerous as to form a virtually continuous landslide complex between the "Tranbarger fracture" and Burns Creek. This area is thus designated as a "landslide complex" in plate 3.1 and figure 3.9, whereas the area between the two long crack features is designated as a "possible landslide."

Much of the Old Santa Cruz Highway area displays the uneven, hummocky topography and benched topographic profiles characteristic of landslide deposits. Average slope inclinations are on the order of 15 to 20°. The southeastern part of the area was designated as a "questionable" landslide deposit by Cooper-Clark and Associates (1975; fig. 3.7) and was also depicted as a landslide deposit on the USGS geologic quadrangle map (fig. 2.4).

The Butano fault is projected under this southeastern part of the Old Santa Cruz Highway area (fig. 2.4), but its local trend of N63°W is oblique to the trend of the main zones of ground cracking. Most of the area, which is northeast of the projected fault trace, is underlain by Vaqueros Sandstone. The northwest-trending axis of the Summit Syncline passes through the northeastern margin of the area. Bedrock dips within the Old Santa Cruz Highway area itself are shown as questionable by McLaughlin and others (in press); see figure 2.4. However, it is reasonable to infer from dips measured at nearby localities that rocks between the Butano fault and the synclinal axis dip to the northeast, into the slope, whereas rocks on the northwest side of the synclinal axis dip to the southwest. Underneath the pre-existing landslide deposit in the southeastern part of the Old Santa Cruz Highway area, southeast of the Butano fault, it is likely that the bedrock is Butano Sandstone, which is made up of sandstones, siltstones, and shales. Because the projected truncation of the axis of the Laurel Anticline occurs under this area, the dip of the bedrock there is not evident from the map information.

3. Upper Schultheis Road Landslide

The Upper Schultheis Road landslide is on the south flank of Summit Ridge, immediately east of the Old Santa Cruz Highway landslide complex and separated from it by less than 300 feet of ground with no observed cracks (plate 3.1). The crown of the landslide is 600 feet downslope from Summit Road and 1,200 feet south of the Summit Road-Old Santa Cruz Highway intersection (plate 3.1).

The crown, head, and upper western flank of the landslide are delineated by a continuous, complex main scarp that is arcuate and concave downslope in plan view (plate 3.1, figs. 3.11 and 3.12). The eastern flank of the landslide is marked by a set of discontinuous

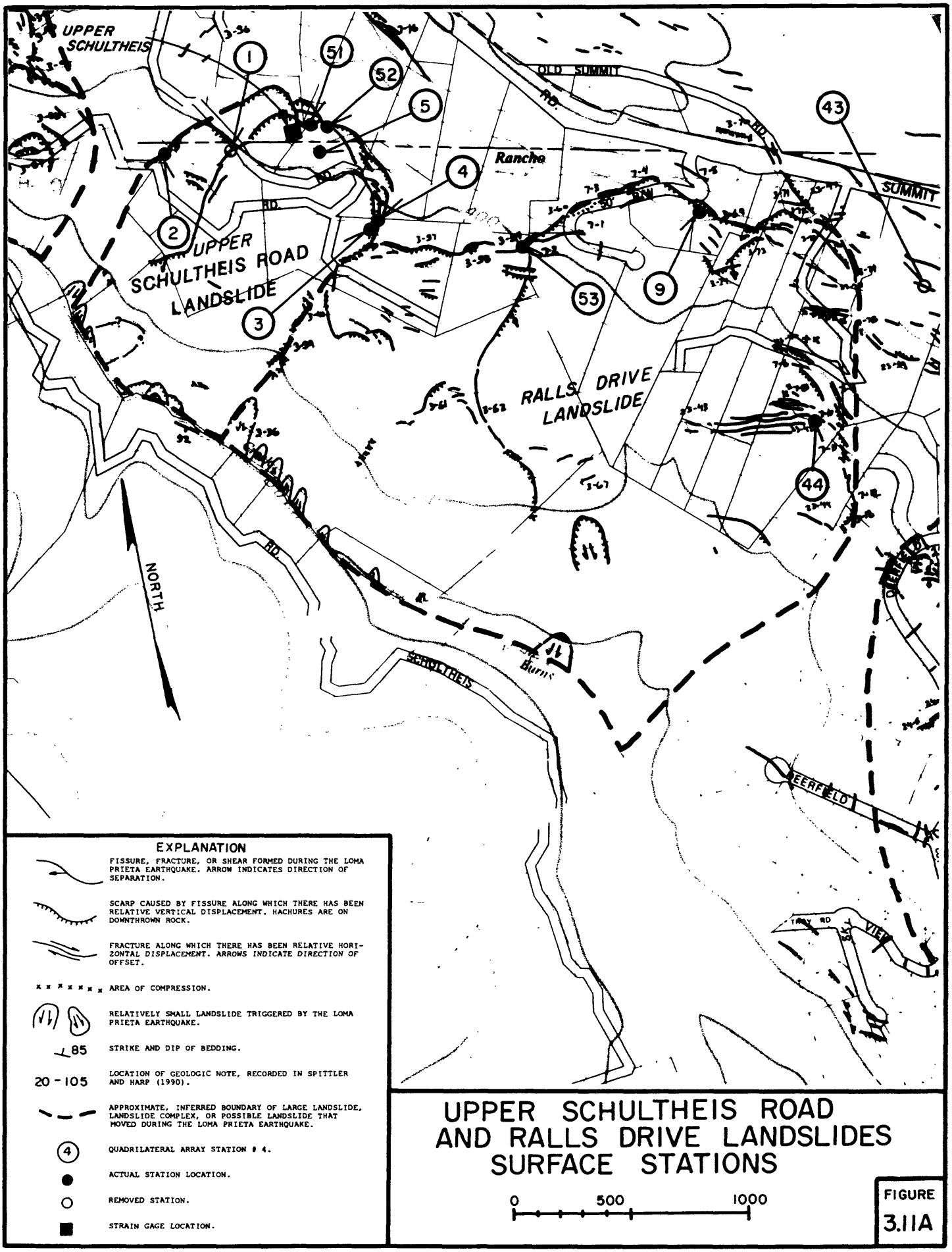

UPPER SCHULTHEIS ROAD AND RALLS DRIVE LANDSLIDES SURFACE STATIONS

FIGURE 3.11A

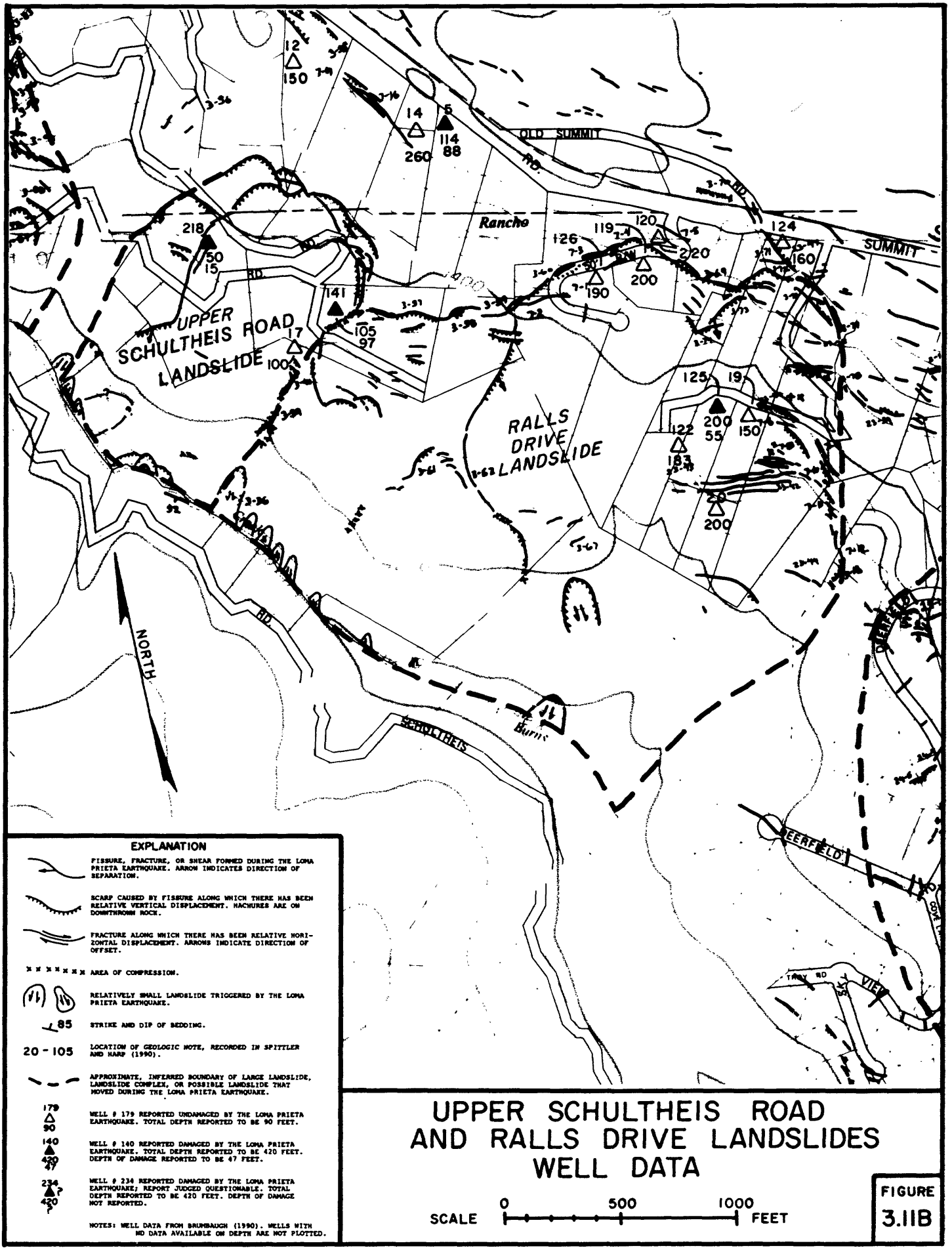

UPPER SCHULTHEIS ROAD AND RALLS DRIVE LANDSLIDES WELL DATA

FIGURE 3.11B

FIGURE 3.12 –Segment of arcuate, concave–downslope, ground–crack and scarp feature that forms the main scarp of the Upper Schultheis Road landslide. Photograph taken near crown of landslide; view is toward the east. Measurements near this locality showed 42 inches of extensional displacement and 18 inches of vertical displacement across this main scarp.

compression features and cracks that extend 900 feet downslope from the main scarp. Together, all these features encompass a landslide 950 feet wide. A few small compression features are present low on the slope above Burns Creek, but these are interpreted to be internal ridges on the basis of their lack of continuity, and the landslide probably extends downslope through the steep, heavily vegetated terrain below Schultheis Road to Burns Creek itself, where several smaller, local slope failures are present (fig. 3.11). The landslide thus defined is approximately 1,500 feet long and involves 31 acres.

A transect surveyed down the ridge flank through the Upper Schultheis Road landslide shows benched topography suggestive of previous landslide movement, with gently sloping meadows alternating with steeper stretches of slope, ending with a steep stretch immediately above Burns Creek, at the base of the ridge (fig. 3.3). The slope inclination averaged along the profile below the ridge crest is 15°. The arcuate main scarp of the Upper Schultheis landslide is partly coincident with the base of a steep stretch of slope that we infer on the basis of geomorphology to be the scarp of an older, pre-existing landslide. Both Cooper-Clark and Associates (1975) and McLaughlin and others (in press) also portray pre-existing landslide deposits with upslope boundaries at or near this scarp (figs. 2.4 and 3.7).

Displacements measured along a transect across the main scarp indicate that the head of the Upper Schultheis Road landslide moved 46 inches downslope. An additional 51 inches of total downslope displacement was measured across a series of internal fissures and scarps, striking approximately parallel to the slope contours, that extended 203 feet downslope from the main scarp. Measured displacement of landslide material was thus 97 inches (8.1 feet) (R. W. Jibson and D. K. Keefer, 1989, unpublished data).

Two of three known water wells within the landslide were reported to have been damaged during the earthquake. In well #218, along the right flank (fig. 3.11), an offset of 8 to 12 inches was reported to have occurred at a depth between 14 and 16 feet in a 30-inch-diameter casing; in well #141 (fig. 3.11), along the left flank, the pump motor was reportedly broken off the pump and the motor shaft bent to a 90°-angle at a depth of 97 feet (Brumbaugh, 1990).

All or nearly all of the area of the Upper Schultheis Road landslide was designated by Cooper-Clark and Associates (1975) as

being underlain by a "questionable" landslide deposit (fig. 3.7). The USGS geologic quadrangle map also portrayed most or all of the earthquake-related landslide as involving material from a previous landslide deposit (fig. 2.4). Beneath this landslide material, bedrock is composed of sandstones, siltstones, and shales belonging to the Butano Sandstone and Vaqueros Sandstone, which are separated by the Butano fault. This fault is projected to pass under the landslide 400 to 500 feet downslope from the crown. Upslope from the fault, Vaqueros Sandstone dips steeply northeast (fig. 2.4). Downslope from the fault, Butano Sandstone bedrock is folded around the axis of the Laurel Anticline, projected to pass a few hundred feet upslope from the landslide toe. Butano bedrock thus probably dips steeply northeast under most of the slope but steeply southwest under the landslide toe (fig. 2.4).

4. Ralls Drive Landslide

The Ralls Drive landslide is immediately east of the Upper Schultheis Road landslide, on the south flank of Summit Ridge (plate 3.1 and fig. 3.11). The main scarp of the landslide crosses Ralls Drive, and the crown is 100 feet south of Summit Road. Because the main scarp of the Ralls Drive landslide is virtually continuous with the main scarp of the Upper Schultheis Road landslide (plate 3.1 and fig. 3.11), these two landslides could as well be considered parts of a single landslide complex.

The main scarp of the Ralls Drive landslide (or "Ralls Drive" part of the "Upper Schultheis Road-Ralls Drive landslide complex") is a relatively continuous set of cracks and scarps. Some individual scarps are arcuate, concave downslope; others are linear and intersect to form an angular, or "zig-zag" pattern in plan view (plate 3.1 and fig. 3.11). Their linearity and the overall zig-zag pattern suggest that at least some segments of the main scarp and nearby ground cracks may have been structurally controlled. Part of the main scarp lies at the base of an older scarp.

Part of the eastern flank of the Ralls Drive landslide is delineated by a set of northwest-trending scarps and cracks arranged en echelon (fig. 3.11). The western flank of the landslide abuts the Upper Schultheis Road landslide. Approximately 800 feet east of this western flank is a major internal crack, striking approximately downslope, that divides the Ralls Drive landslide into

two main blocks. The smaller, western block formed on the spur ridge adjacent to the Upper Schultheis Road landslide, and the larger, eastern block formed around and under a short valley, tributary to Burns Creek. Both landslide blocks were moderately disrupted by internal scarps and cracks; the area of greatest disruption was adjacent to the eastern flank (fig. 3.11). Local indications of compression were present near the downslope termination of the crack separating the two blocks, particularly where this crack curved to the east.

The Ralls Drive landslide is on the order of 2,400 feet wide and at least 1,600 feet long. No visible surface feature marks the toe, but small internal scarps low on the slope suggest that the landslide extends an additional 500 to 1,400 feet downslope from the flank cracks to Burns Creek. The landslide thus has an area of approximately 120 acres.

Displacements measured across the main scarp and internal scarps are downslope, to the south, southeast, or southwest. These measurements indicate that the head of the western block moved downslope 22 to 40 inches, that the head of the eastern block moved downslope 11 to 38 inches, and that locally the most disrupted parts of the eastern block moved downslope as much as 71 inches.

Within the Ralls Drive landslide, one well (#125, fig. 3.11) was reported to have been damaged at a depth of 55 feet whereas five wells (#19, 20, 119, 122, and 126 in fig. 3.11), 150 to 200 feet deep, were reported undamaged by the earthquake. Three of these reportedly undisturbed wells are near the main scarp, and the other three are within the eastern block. The reported lack of damage to these wells could indicate either that movements of these parts of the landslide were not large enough or concentrated enough to damage the wells or that the basal shear surface is deeper than 150 to 200 feet. Damage to well #125 may then indicate a shallower, subsidiary shear surface or may be unrelated to landslide movement.

The average slope through the Ralls Drive landslide is on the order of 15°, but the slope is also irregular and contains benches and steeper segments, suggesting previous landslide activity. Most of the Ralls Drive landslide is underlain by material mapped by Cooper-Clark and Associates (1975) as landslide deposits. The western part of the landslide involves material designated as a "questionable" landslide deposit, and the eastern part involves material designated as a "definite" landslide deposit (fig. 3.7). The trace of the Butano

fault passes through the Ralls Drive landslide a few hundred feet downslope from the crown, and material downslope from the fault was also mapped as belonging to landslide deposits on the USGS geologic quadrangle map (fig. 2.4).

Upslope from the Butano fault, the Ralls Drive landslide is underlain by northeast-dipping Vaqueros Sandstone. Downslope from the fault, we infer from bedrock mapping immediately to the east that most of the landslide is underlain by sandstones, siltstones, and shales in the Butano Sandstone. A small portion of the landslide near the fault is apparently underlain by San Lorenzo Formation mudstones, sandstones, and shales (fig. 2.4). Because the axis of the Laurel Anticline is projected to pass near the base of the slope, most of the rocks downslope from the Butano fault probably also dip to the northeast. Dip of the rocks southwest of the anticlinal axis is probably to the southwest, based on nearby mapped dips (fig. 2.4). Two unnamed, northwest-striking fault segments are mapped through and near the head of the landslide (fig. 2.4). The strike of one of the faults is subparallel to some segments of the main scarp of the landslide; this relation and the linearity of these scarp segments indicate possible structural control.

5. Villa Del Monte Landslide Complex

The Villa Del Monte landslide is on the south flank of Summit Ridge, on the broad spur ridge between the Ralls Drive landslide and Taylor Gulch (plate 3.1 and fig. 3.13). Topographic profiles surveyed down the ridge flank in this area show average slope inclinations of between 12° and 15°, with numerous gently sloping benches alternating with steeper stretches of slope, especially in the central and eastern parts of the area. Slopes immediately upslope from Laurel (Burrell) Creek, at the base of the ridge, in particular, are relatively steep. Numerous roads and building sites have been located in this area to take advantage of the gently sloping benches, and the Villa Del Monte neighborhood, which contains approximately 165 homes, is the most densely populated part of the Summit Ridge area.

Whereas several distinct zones of ground cracks are present within the Villa Del Monte area, the preponderance of evidence indicates that all the major zones are part of a landslide complex that may have moved initially as a single unit. The major zones of ground

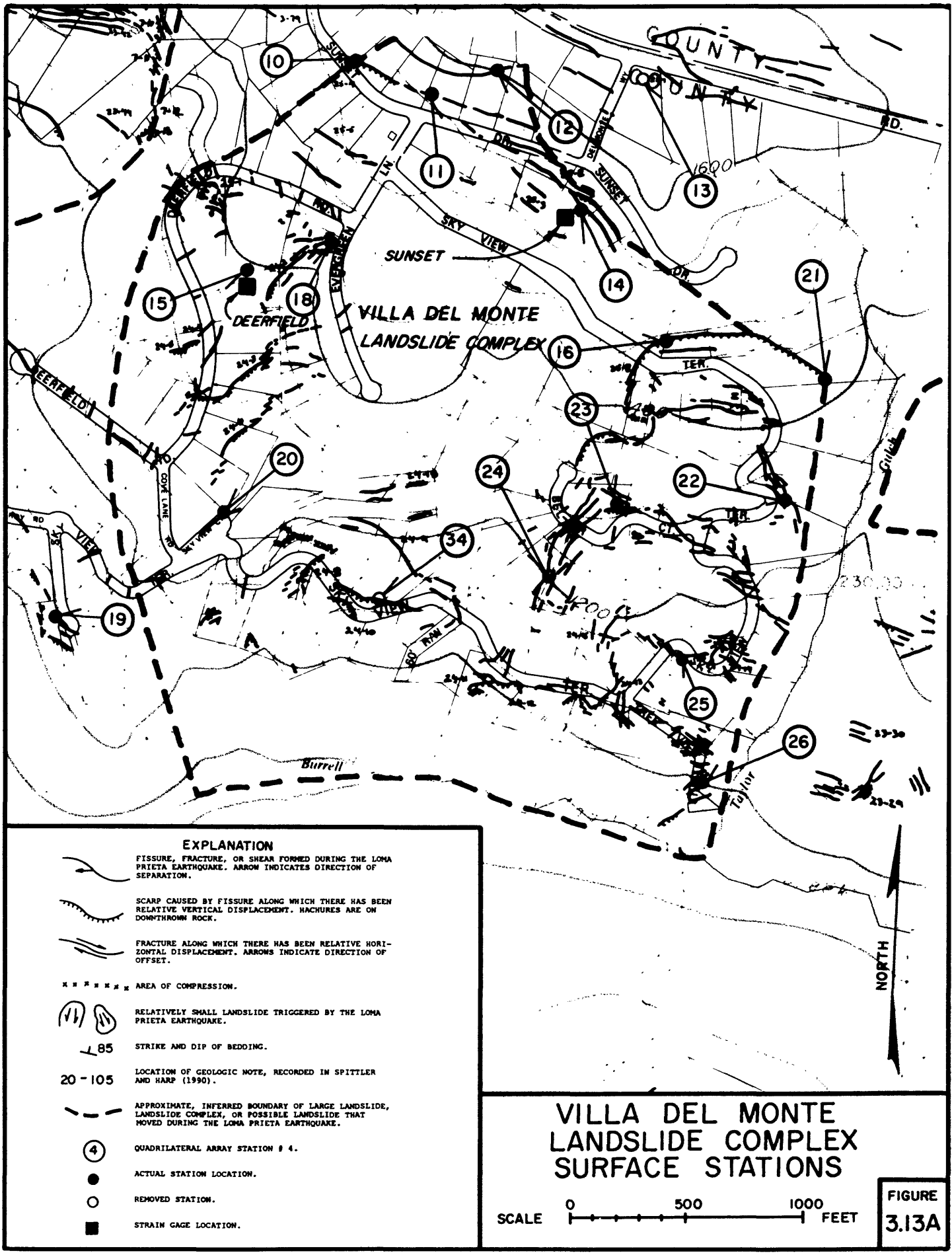
VILLA DEL MONTE
LANDSLIDE COMPLEX
SUNSET
DEERFIELD
SKY VIEW
EVERGREEN
COVE LANE
Burrell
Taylor
NORTH
EXPLANATION
FISSURE, FRACTURE, OR SHEAR FORMED DURING THE LOMA PRIETA EARTHQUAKE. ARROW INDICATES DIRECTION OF SEPARATION.
SCARP CAUSED BY FISSURE ALONG WHICH THERE HAS BEEN RELATIVE VERTICAL DISPLACEMENT. HACHURES ARE ON DOWNTHROWN ROCK.
FRACTURE ALONG WHICH THERE HAS BEEN RELATIVE HORIZONTAL DISPLACEMENT. ARROWS INDICATE DIRECTION OF OFFSET.
AREA OF COMPRESSION.
RELATIVELY SMALL LANDSLIDE TRIGGERED BY THE LOMA PRIETA EARTHQUAKE.
85
STRIKE AND DIP OF BEDDING.
20 - 105
LOCATION OF GEOLOGIC NOTE, RECORDED IN SPITTLER AND HARP (1990).
APPROXIMATE, INFERRED BOUNDARY OF LARGE LANDSLIDE, LANDSLIDE COMPLEX, OR POSSIBLE LANDSLIDE THAT MOVED DURING THE LOMA PRIETA EARTHQUAKE.
4
QUADRILATERAL ARRAY STATION # 4.
ACTUAL STATION LOCATION.
REMOVED STATION.
STRAIN GAGE LOCATION.
VILLA DEL MONTE
LANDSLIDE COMPLEX
SURFACE STATIONS
SCALE 0 500 1000 FEET
FIGURE
3.13A

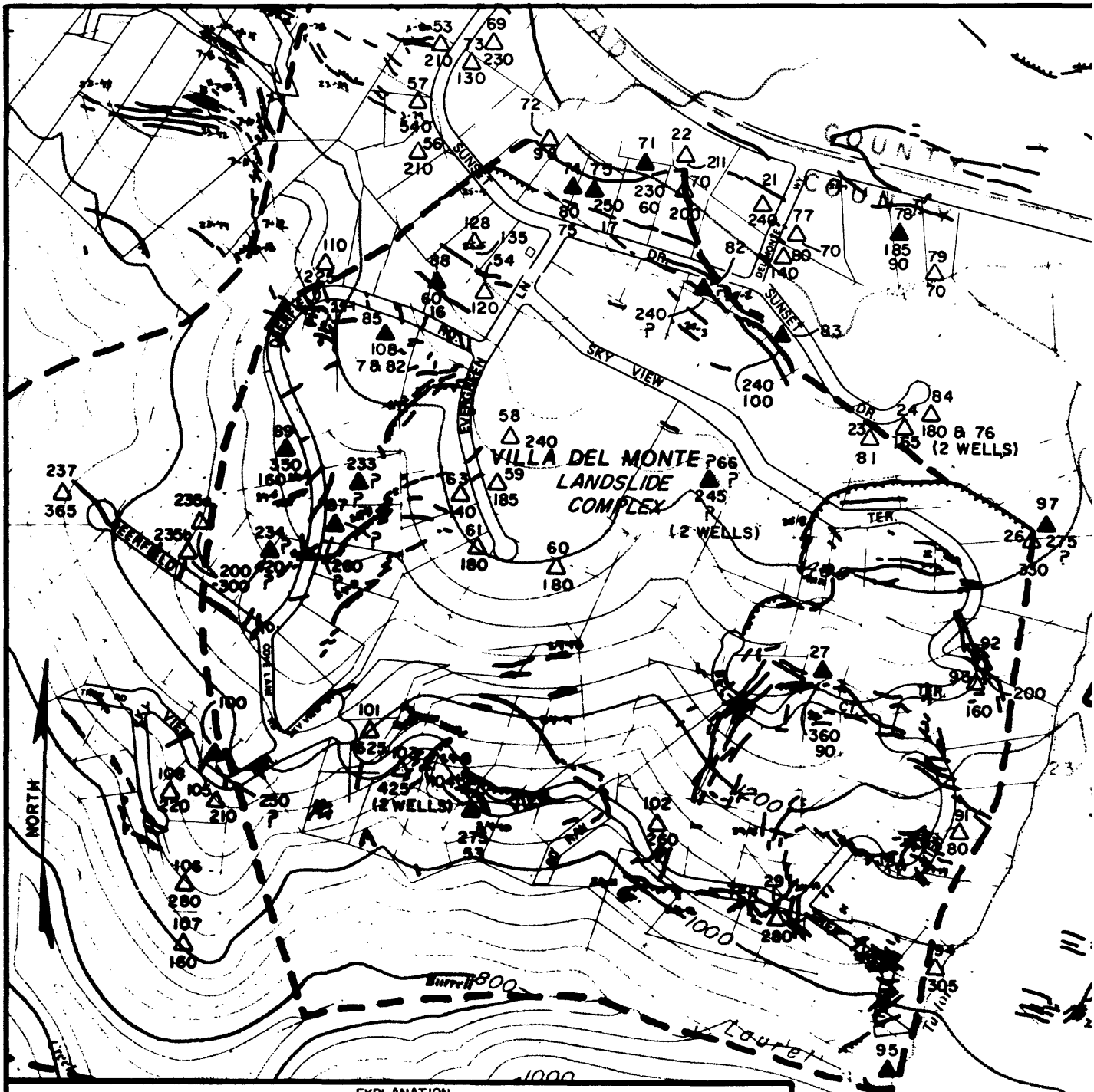

EXPLANATION

FISSURE, FRACTURE, OR SHEAR FORMED DURING THE LOMA PRIETA EARTHQUAKE. ARROW INDICATES DIRECTION OF SEPARATION.

SCARP CAUSED BY FISSURE ALONG WHICH THERE HAS BEEN RELATIVE VERTICAL DISPLACEMENT. HACHURES ARE ON DOWNTHROWN ROCK.

FRACTURE ALONG WHICH THERE HAS BEEN RELATIVE HORIZONTAL DISPLACEMENT. ARROWS INDICATE DIRECTION OF OFFSET.

AREA OF COMPRESSION.

RELATIVELY SMALL LANDSLIDE TRIGGERED BY THE LOMA PRIETA EARTHQUAKE.

85 STRIKE AND DIP OF BEDDING.

20 - 105 LOCATION OF GEOLOGIC NOTE, RECORDED IN SPITTLER AND HARP (1990).

APPROXIMATE, INFERRED BOUNDARY OF LARGE LANDSLIDE, LANDSLIDE COMPLEX, OR POSSIBLE LANDSLIDE THAT MOVED DURING THE LOMA PRIETA EARTHQUAKE.

179 / 90 WELL # 179 REPORTED UNDAMAGED BY THE LOMA PRIETA EARTHQUAKE. TOTAL DEPTH REPORTED TO BE 90 FEET.

140 / 420 / 47 WELL # 140 REPORTED DAMAGED BY THE LOMA PRIETA EARTHQUAKE. TOTAL DEPTH REPORTED TO BE 420 FEET. DEPTH OF DAMAGE REPORTED TO BE 47 FEET.

234 ? / 420 WELL # 234 REPORTED DAMAGED BY THE LOMA PRIETA EARTHQUAKE; REPORT JUDGED QUESTIONABLE. TOTAL DEPTH REPORTED TO BE 420 FEET. DEPTH OF DAMAGE NOT REPORTED.

NOTES: WELL DATA FROM BRUMBAUGH (1990). WELLS WITH NO DATA AVAILABLE ON DEPTH ARE NOT PLOTTED.

VILLA DEL MONTE LANDSLIDE COMPLEX WELL DATA

SCALE 0 500 1000 FEET

FIGURE 3.13B

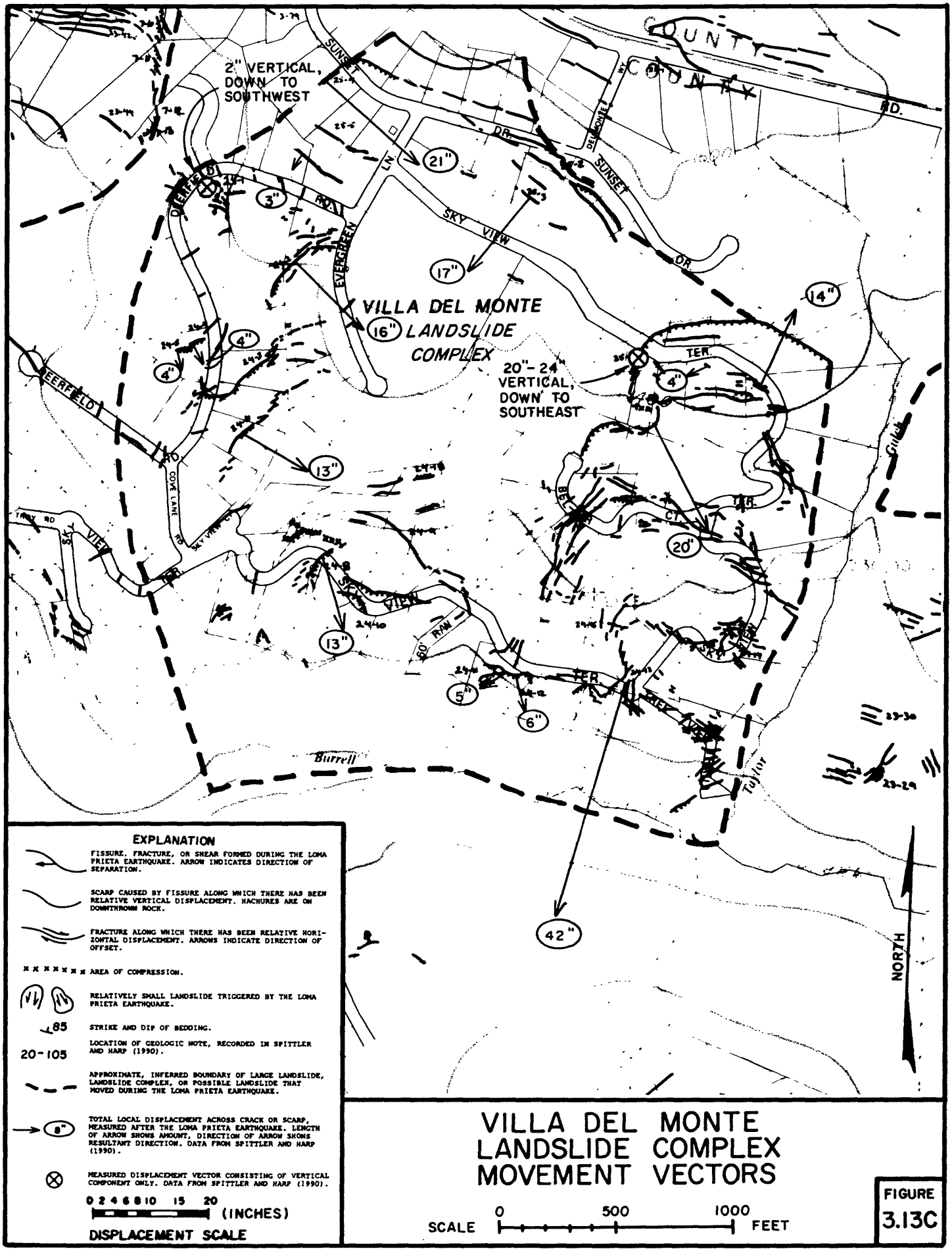

EXPLANATION

FISSURE, FRACTURE, OR SHEAR FORMED DURING THE LOMA PRIETA EARTHQUAKE. ARROW INDICATES DIRECTION OF SEPARATION.

SCARP CAUSED BY FISSURE ALONG WHICH THERE HAS BEEN RELATIVE VERTICAL DISPLACEMENT. HACHURES ARE ON DOWNTHROWN ROCK.

FRACTURE ALONG WHICH THERE HAS BEEN RELATIVE HORIZONTAL DISPLACEMENT. ARROWS INDICATE DIRECTION OF OFFSET.

AREA OF COMPRESSION.

RELATIVELY SMALL LANDSLIDE TRIGGERED BY THE LOMA PRIETA EARTHQUAKE.

85 STRIKE AND DIP OF BEDDING.

20-105 LOCATION OF GEOLOGIC NOTE, RECORDED IN SPITTLER AND HARP (1990).

APPROXIMATE, INFERRED BOUNDARY OF LARGE LANDSLIDE, LANDSLIDE COMPLEX, OR POSSIBLE LANDSLIDE THAT MOVED DURING THE LOMA PRIETA EARTHQUAKE.

8" TOTAL LOCAL DISPLACEMENT ACROSS CRACK OR SCARP, MEASURED AFTER THE LOMA PRIETA EARTHQUAKE. LENGTH OF ARROW SHOWS AMOUNT, DIRECTION OF ARROW SHOWS RESULTANT DIRECTION. DATA FROM SPITTLER AND HARP (1990).

MEASURED DISPLACEMENT VECTOR CONSISTING OF VERTICAL COMPONENT ONLY. DATA FROM SPITTLER AND HARP (1990).

0 2 4 6 8 10 15 20 (INCHES)

DISPLACEMENT SCALE

VILLA DEL MONTE LANDSLIDE COMPLEX MOVEMENT VECTORS

SCALE 0 500 1000 FEET

FIGURE 3.13C

cracks are along Sunset Drive, in the area of upper Skyview (or "Sky View") Terrace and Bel Air (or "Belair," "Bel-Air," or "Bel Aire") Court, along and east of Deerfield Road, and along lower Skyview Terrace (plate 3.1 and fig. 3.13). Additional, smaller zones of ground cracks along the westernmost extension of Deerfield Road and around the Troy Road-Skyview Terrace intersection (fig. 3.13) are probably associated with separate, smaller landslides.

a. Sunset Drive area: Cracks and scarps in the Sunset Drive area (figs. 3.13 and 3.14) extend approximately 1,400 feet across the slope; they cross Sunset Drive west of Evergreen Lane and again between Evergreen Lane and Del Monte Way (plate 3.1 and fig. 3.13), and they extend downslope from above Sunset Drive to near the Deerfield Road-Evergreen Lane intersection. Individual cracks and scarps are linear, arcuate and concave-downslope, or, in one case, concave-upslope in plan view. For part of its length, this zone of cracks and scarps crosses a gentle slope immediately downslope from a 9- to 15-foot-high bedrock scarp composed of intensely fractured sandstone. Displacements measured across individual cracks and scarps in this zone were downslope toward the southwest and southeast and were in the range between 3 and 21 inches (fig. 3.13). Whereas cracks and scarps in this area exhibit characteristics associated with a landslide, such as overall concave-downslope curvature of the zone in plan view and downslope displacements, a few northwest-striking cracks are also subparallel to local faults (fig. 2.4) and thus may also have been structurally controlled.

Six wells in this area were reported damaged (#71, 74, 75, 82, 83, and 88 in fig. 3.13). The damage to wells #71, 74, and 75, which involved collapsed casings at depths in the range between 17 and 75 feet (Brumbaugh, 1990), suggests that the crack immediately upslope from them (fig. 3.13) marks the uphill boundary of the landslide complex.

b. Upper Skyview Terrace-Bel Air Court area: The upper Skyview Terrace-Bel Air Court area, in the eastern part of the Villa Del Monte neighborhood, is the zone of most concentrated and pervasive ground cracking (plate 3.1, figs. 3.13 and 3.15). The cracks and scarps in the area extend approximately 1,100 feet across the slope and 2,200 downslope, from immediately above upper Skyview

FIGURE 3.14 –Ground crack in the Sunset Drive area of the Villa Del Monte landslide complex; crack is part of 1,400–foot-long zone of cracks and scarps that delineates, in part, the head of a large landslide. (Photograph by Kevin M. Schmidt, U.S. Geological Survey).

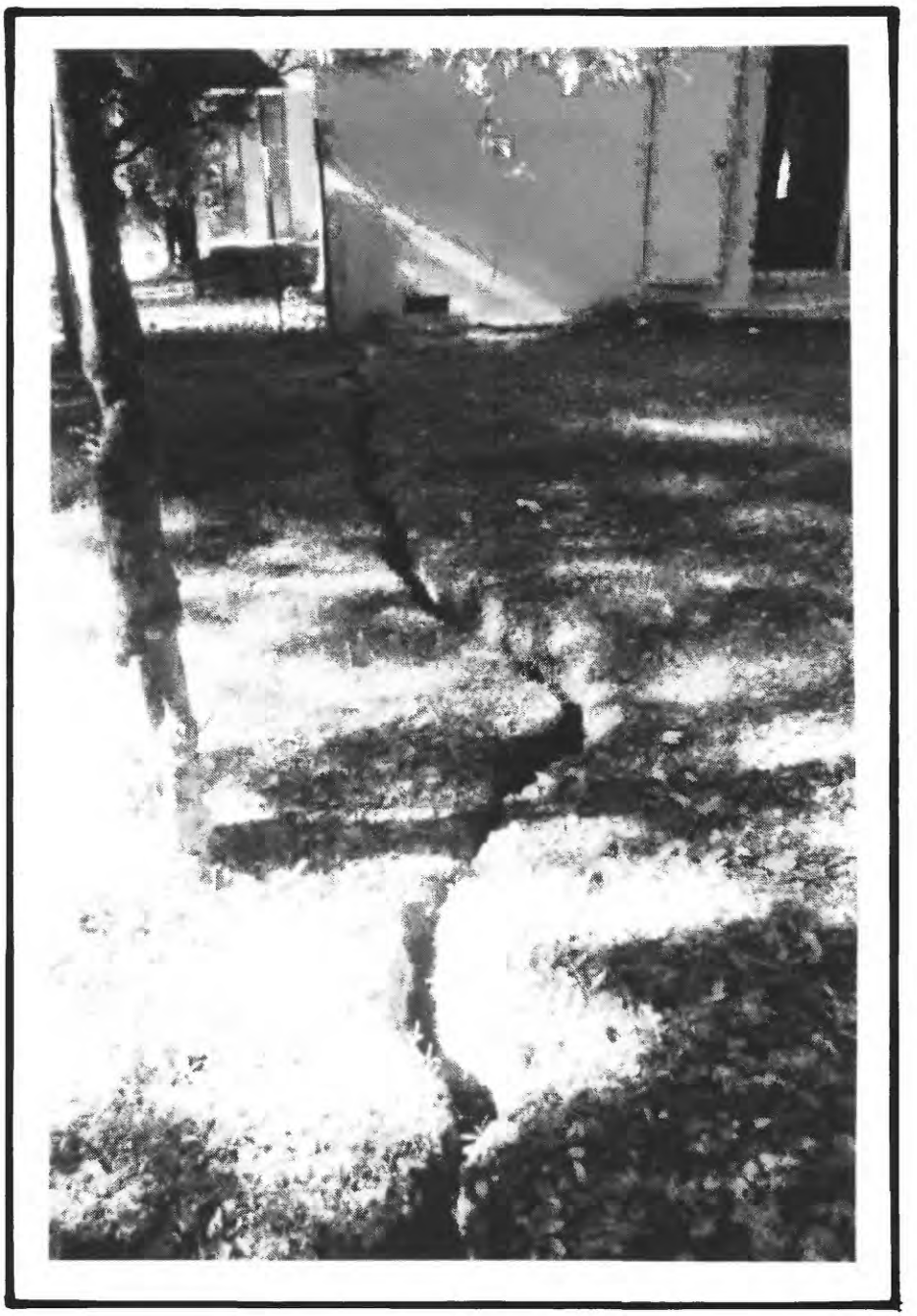

FIGURE 3.15 –Ground crack within landslide in Upper Skyview Terrace–Bel Air Court area that is part of the Villa Del Monte landslide complex. Ground crack, which passes beneath corner of house, showed 2 to 6 inches of extensional displacement and 2 inches of vertical displacement. Photograph taken near quadrilateral array #23; see figure 3.13 for location. (Photograph from Griggs and others, 1990).

FIGURE 3.16 (a) –Landslide features in Deerfield Road area of the Villa Del Monte landslide complex. Part of complex scarp several hundred feet long. This and adjacent scarps and ground cracks strike northeast and typically show displacements to the southeast. Photograph taken from just east of Deerfield Road; view is toward the northeast.

FIGURE 3.16 (b) –Landslide features in Deerfield Road area of the Villa Del Monte landslide complex. Compression feature, consisting of short ridge of compressed ground, marked by broken and buckled driveway pavement. Feature inferred to be internal ridge, formed due to differential movement of blocks within landslide complex. Photograph taken near Deerfield Road–Evergreen Lane intersection; view is toward the northwest.

scarps in this zone strike predominantly northeast, oblique to the regional bedrock structures (fig. 2.4), and displacement measurements indicate predominantly southeastward to locally southwestward movement of 2 to 16 inches (fig. 3.13). The strike of the main cracks within this zone and the predominant southeastward direction of movement indicate that this zone forms the western (or right) flank of a landslide, which moved downslope towards Laurel Creek.

All five wells in this zone, along Deerfield Road (wells #85, 88, 89, 233 and 234 in fig. 3.13) were reported to have been damaged. However, seven of the eight wells along westernmost Deerfield Road and westernmost Skyview Terrace (wells #105, 106, 107, 108, 235a, 235b, and 237 in fig. 3.13) were reportedly undamaged by the earthquake. This zone of undamaged wells suggests that the smaller zones of ground cracks farther west (fig. 3.13) were not part of the larger landslide; these westernmost ground cracks were almost certainly associated with smaller landslides, but the limits of the large landslide and of these smaller landslides in this area were poorly defined by the available data. In plates 3.1 and figure 3.13, the boundary of the larger landslide is inferred to lie generally in the area between the reportedly damaged and reportedly undamaged wells.

d. Lower Skyview Terrace area: Along lower Skyview Terrace, for a distance of approximately 1,300 feet east of Cove Lane Road, is a zone of mostly arcuate, concave-southward scarps and cracks (plate 3.1 and fig. 3.13). The zone extends approximately 700 feet from north to south, on both sides of lower Skyview Terrace. The water well within the area of most concentrated cracking (#104 in fig. 3.13) was reported damaged, while three nearby wells (#101, 102, and 103 in fig. 3.13), in less disturbed areas, were reported undamaged. This zone of scarps and cracks is interpreted to be a zone of internal cracks within a large landslide, on the basis of its position on the slope and its location relative to other ground cracks in the Villa Del Monte area. One measurement across a crack in this zone showed 13 inches of displacement downslope, toward the southeast (fig. 3.13).

e. Overall landslide dimensions, movement and setting: The Villa Del Monte landslide complex is inferred to extend downslope from the Sunset Drive area to Laurel Creek and thus has an overall length of 3,200 feet. The western margin of the landslide complex is inferred to be the western margin of the Deerfield Road area whereas the better-defined eastern margin is the eastern margin of ground cracking in the upper Skyview Terrace-Bel Air Court area (plate 3.1 and fig. 3.13). Thus the overall width is 3,000 feet, and the surface area is on the order of 170 acres. The pattern of ground cracking in the upper Skyview Terrace-Bel Air Court area indicates that this area contains the best defined landslide within the Villa Del Monte neighborhood and suggests that this landslide broke away from a larger landslide block and moved downslope as a distinct unit.

Between the Deerfield Road and upper Skyview Terrace-Bel Air Court areas, and downslope from the Sunset Drive area, is a large area with few ground cracks or damaged wells (fig. 3.13). The presence of such an interior zone with few ground cracks is consistent with the interpretation of this area as being involved in a large block slide that moved a short distance downslope; in such cases, deformation is typically concentrated along the landslide margins.

Displacements measured across individual cracks and scarps throughout the Villa Del Monte landslide complex were in the range between 2 and 42 inches, with most measurements showing local displacements of between 13 and 21 inches.

Cooper-Clark and Associates (1975) previously mapped the area of the eastern two-thirds of the Villa Del Monte landslide complex as a "probable" landslide deposit (fig. 3.7). On the USGS geologic quadrangle maps (Clark and others, 1989, with landslide boundaries revised by McLaughlin and Clark, 1990, unpublished data; McLaughlin and others, in press), all but the westernmost part of the landslide complex was shown as being underlain by a particularly large landslide deposit that stretches along Summit Ridge for 1 mile to the east; most of the northern, eastern and southern margins of the Villa Del Monte landslide complex correspond closely in location to the mapped boundaries of that deposit (fig. 2.4). In addition, the benched topography suggests previous landslide activity, and SCC road-repair records show

directly that previous landslide movement has occurred within the Villa Del Monte landslide complex (fig. 2.7 and table 2.2).

Bedrock projected under the mapped landslide deposit in the Villa Del Monte area consists of sandstones, mudstones, siltstones, and shales belong to the Butano Sandstone and San Lorenzo Formation (fig. 2.4). The axis of the Laurel Anticline is projected through the southwestern part of the landslide complex. Rocks northeast of this axis evidently dip obliquely into the slope, to the north and northeast, according to the nearest dip information that can be projected into this area. To the southwest of the axis, dip may be steeply to the southwest, locally overturned to the northeast, or both. Several northwest-striking faults are mapped through the crest and upper flanks of Summit Ridge, into and just north of the landslide complex.

6. Taylor Gulch Landslide

The Taylor Gulch landslide is on the east side of Taylor Gulch, which cuts into the southwestern flank of Summit Ridge. The landslide crosses Morrell Road (or "Morrill Road," or "Morrell Cutoff") 600 to 1,500 feet south of the Morrell Road-Summit Road intersection (plates 3.1 and 3.2 and fig. 3.17).

The crown, head, and flanks of the landslide are defined by an arcuate, concave-downslope scarp, 800 feet long, upslope from and east of Morrell Road (plates 3.1 and 3.2 and fig. 3.17); a discontinuous zone of cracks extends an additional 400 feet along the southern flank of the landslide. One displacement measurement across the main scarp indicated movement of 21 inches downslope, to the west. The landslide is disrupted by one zone of northwest-striking internal cracks, which are subparallel to unnamed faults mapped through this area (fig. 2.4) and which therefore may have been structurally controlled.

The toe of the landslide is not delineated by any observed surface feature, and so the downslope extent of the landslide can be inferred only within wide limits. The landslide is inferred to extend downslope at least as far as the downslope limit of ground cracking (fig. 3.17), and it is possible that the landslide extends downslope to the bottom of Taylor Gulch. The landslide is thus at least 900 feet wide and 500 feet long and covers at least 6 acres; if it extends to the

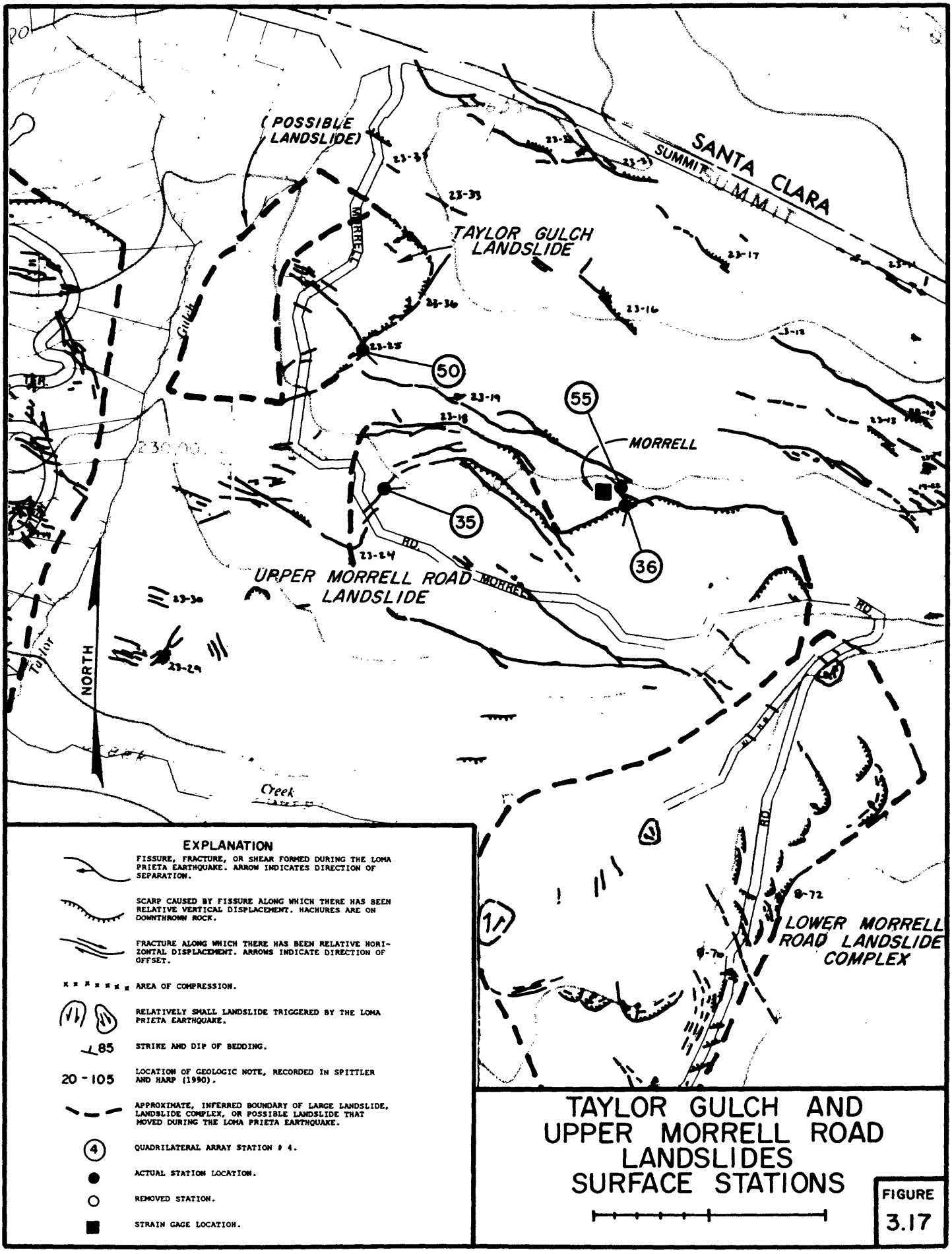

TAYLOR GULCH AND UPPER MORRELL ROAD LANDSLIDES SURFACE STATIONS

FIGURE 3.17

bottom of Taylor Gulch, it is 700 feet long and covers 14 acres. The average slope in this area is 16°.

The Taylor Gulch landslide involves material designated by Cooper-Clark and Associates (1975) as belonging to a "probable" landslide deposit (fig. 3.7) that was also designated as a large landslide deposit according to the USGS geologic quadrangle maps (fig. 2.4). Bedrock under the landslide is probably mostly mudstones and sandstones of the Rices Mudstone Member of the San Lorenzo Formation; partly mudstones and sandstones of the Butano Sandstone; and partly a small body of igneous diabase and gabbro. Two northwest-trending faults are projected through the area of the landslide, and bedrock structure at this locality is complex (fig. 2.4).

7. Upper Morrell Road Landslide

The Upper Morrell Road landslide is also on the south flank of Summit Ridge east of Taylor Gulch; ground cracks belonging to the landslide intersect Morrell Road 1,900 feet south of the Morrell Road-Summit Road intersection (plate 3.2 and fig. 3.17).

The head of the landslide is marked by two adjoining zones of ground cracks and scarps, each of which is arcuate, concave-downslope in plan view (figs. 3.17 and 3.18). Together these zones extend approximately 1,800 feet across the slope. As discussed in Chapter IV, the orientation of ground cracks in these zones and the relation of these cracks to others nearby suggest significant structural control. Displacement measurements across the main zones of cracks suggest that the landslide moved downslope as much as 6.6 feet. Southeast of these zones of cracks, a shorter, arcuate and concave-downslope scarp is inferred to mark part of the eastern flank of the landslide (fig. 3.17).

The toe of the Upper Morrell Road landslide is a gentle east-west-striking bulge in the ground surface, 1,400 feet long and 600 to 900 feet downslope from the main scarp. A zone of fractures and grabens located along the crest of this bulge is evidence of the local extension of the ground that accompanied the upward bulging of the landslide toe. Between the crown cracks and the toe, the landslide encompasses an area of approximately 35 acres.

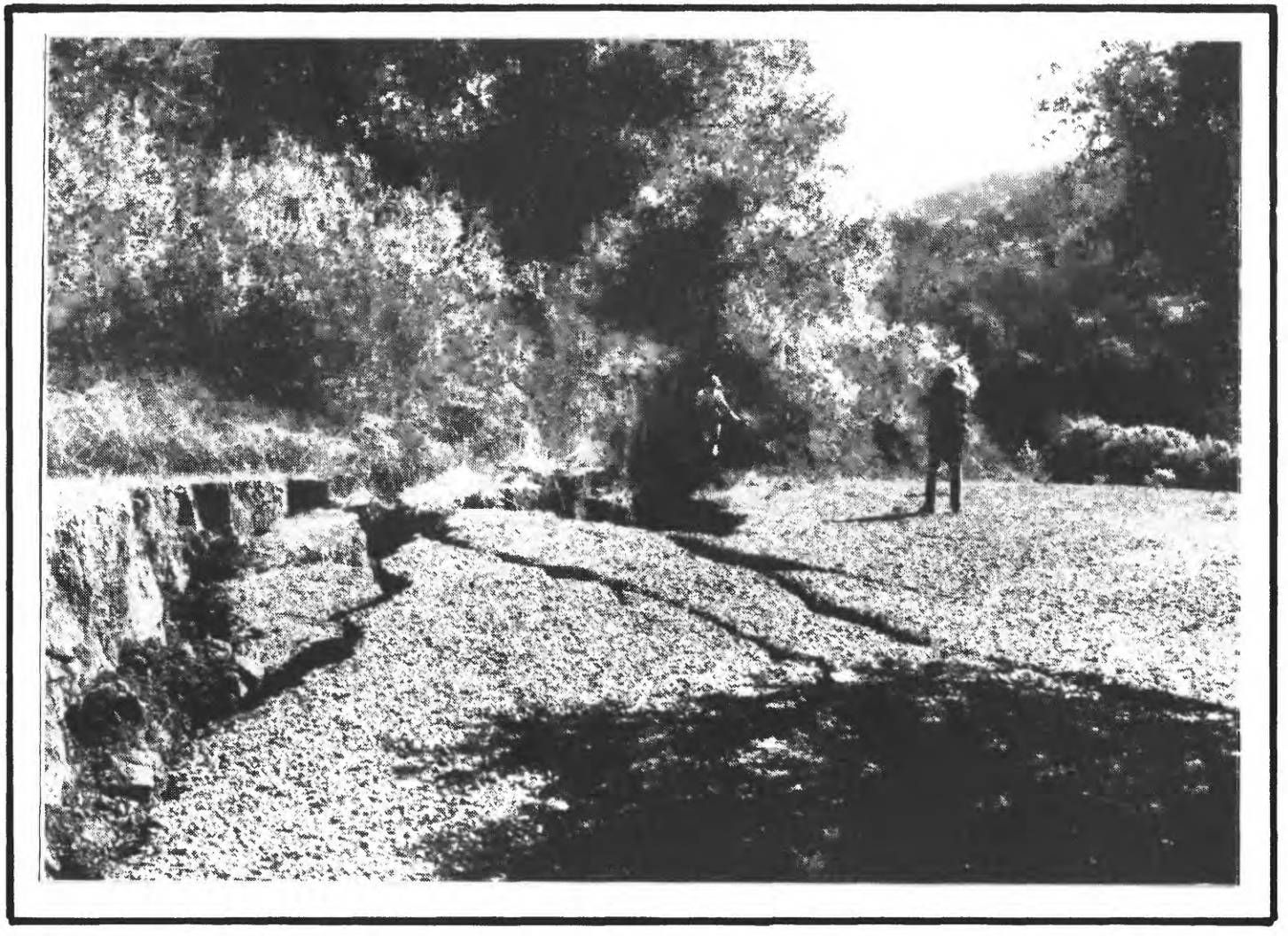

FIGURE 3.18 –Part of complex zone of ground cracks and scarps forming the main scarp of the Upper Morrell Road landslide. Zone shown where it crosses gravel road. Total width of zone is approximately 12 feet; individual cracks are as wide as approximately 80 inches and show as much as 12 inches of vertical displacement. View is toward the northeast.

Two profiles surveyed through the landslide show that the average slope is on the order of 15°. The topographic profiles also exhibit the benched form characteristic of landslide deposits. In agreement with the topographic indications of previous landslide activity, the map of Cooper-Clark and Associates (1975) shows that most or all of the Upper Morrell Road landslide involves part of a large, pre-existing landslide deposit (designated as "probable"; see fig. 3.7); the USGS geologic quadrangle map (Clark and others, 1989, with landslide boundaries revised by McLaughlin and Clark, 1990, unpublished data; see fig. 2.4) also shows this area as being underlain by landslide material. SCC road-repair records additionally suggest previous landslide damage to Morrell Road in this area (fig. 2.7 and table 2.2).

Bedrock underlying the Upper Morrell Road landslide is projected to be largely mudstones and sandstones of the Rices Mudstone Member of the San Lorenzo Formation (fig. 2.4). A small area under the center of the landslide toe is underlain by igneous diabase and gabbro; a small area along the eastern margin may be underlain by Vaqueros Sandstone; and a small area under the easternmost part of the landslide, northeast of a mapped fault, is underlain by mudstones and sandstones of the Butano Sandstone (fig. 2.4). The bedrock north of the landslide is also cut by northwest-striking faults, and the precise bedrock structure under the mapped, pre-existing landslide deposit is uncertain.

8. Lower Morrell Road Landslide Complex

This landslide complex stretches along Morrell Road, 0.6 to 0.9 miles southeast of its intersection with Summit Road. The complex contains many scarps and cracks, some of which occur in zones as much as 100 feet wide (plate 3.2 and Fig. 3.19). The longest scarps are arcuate, concave-downslope; some of the shorter scarps and cracks are more linear. The complex also contains at least three smaller, completely defined landslides. Together, scarps and other features delineate a landslide complex, approximately 1,500 feet long and 2,200 feet wide, that extends downslope from the prominent zone of scarps adjacent to Morrell Road to the creek at the base of the slope, encompassing an area of 54 acres. Displacements measured across individual scarps and cracks were as much as 13 inches; because the slope morphology and patterns of cracking indicate that the landslide complex is composed of many units, the

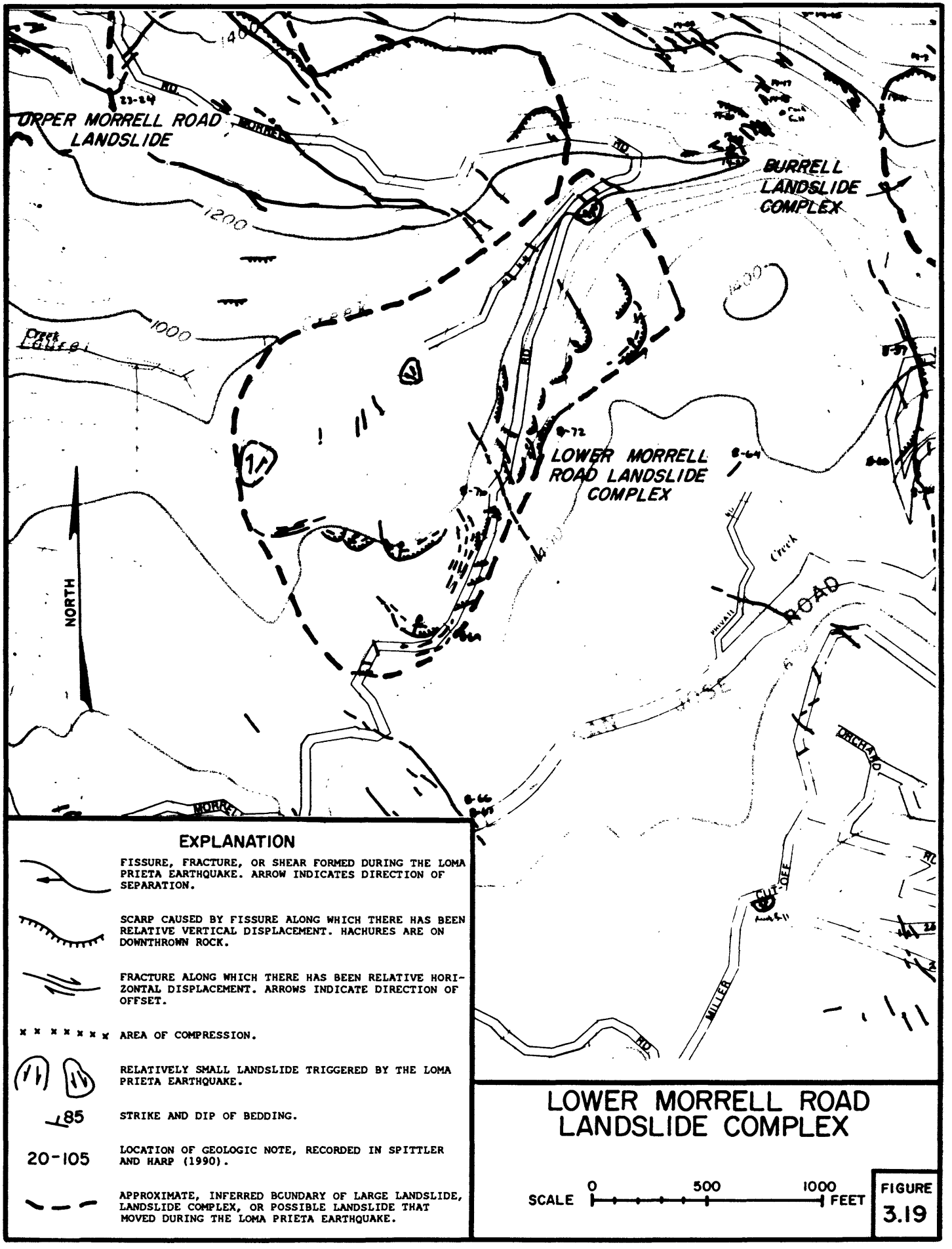
UPPER MORRELL ROAD LANDSLIDE
BURRELL LANDSLIDE COMPLEX
LOWER MORRELL ROAD LANDSLIDE COMPLEX
MORRELL
ROAD
NORTH
DRCHARD
MILLER
CUT-OFF
1400
1200
1000
800
EXPLANATION
FISSURE, FRACTURE, OR SHEAR FORMED DURING THE LOMA PRIETA EARTHQUAKE. ARROW INDICATES DIRECTION OF SEPARATION.
SCARP CAUSED BY FISSURE ALONG WHICH THERE HAS BEEN RELATIVE VERTICAL DISPLACEMENT. HACHURES ARE ON DOWNTHROWN ROCK.
FRACTURE ALONG WHICH THERE HAS BEEN RELATIVE HORIZONTAL DISPLACEMENT. ARROWS INDICATE DIRECTION OF OFFSET.
AREA OF COMPRESSION.
RELATIVELY SMALL LANDSLIDE TRIGGERED BY THE LOMA PRIETA EARTHQUAKE.
85
STRIKE AND DIP OF BEDDING.
20-105
LOCATION OF GEOLOGIC NOTE, RECORDED IN SPITTLER AND HARP (1990).
APPROXIMATE, INFERRED BOUNDARY OF LARGE LANDSLIDE, LANDSLIDE COMPLEX, OR POSSIBLE LANDSLIDE THAT MOVED DURING THE LOMA PRIETA EARTHQUAKE.
LOWER MORRELL ROAD LANDSLIDE COMPLEX
SCALE 0 500 1000 FEET
FIGURE 3.19

displacements almost certainly varied significantly from point to point.

A topographic profile surveyed downslope through the landslide complex shows a prominent, nearly level bench separating steeper sections above and below. The average slope is 15°. The map of Cooper-Clark and Associates (1975) showed this landslide complex as being within the source areas and deposits of "definite" landslides (figs. 2.8 and 3.7), and direct evidence of previous landslide movement there in 1982-83 is contained in SCC road-repair records (table 2.2 and fig. 2.7). The USGS geologic quadrangle map also showed this area to be underlain by a large landslide deposit (fig. 2.4). Bedrock relations are obscured by this mapped landslide deposit, but adjacent areas are underlain by sandstones, siltstones, and shales of the Butano Sandstone on the north, east and, south and by Vaqueros sandstones and San Lorenzo Formation sandstones, mudstones, and shales on the west. The Lower Morrell Road landslide complex lies northeast of the axis of the Laurel Anticline and so the dip may reasonably be inferred to be generally toward the northeast. A northwest-striking fault is also projected under the northern part of this landslide complex.

9. Burrell Landslide Complex

The Burrell landslide complex is on the south flank of Summit Ridge, 300 feet south of the Summit Road-Loma Prieta Avenue intersection (plate 3.2 and fig. 3.20). Scarps interpreted as landslide features within the complex were differentiated from other cracks in this area, interpreted as having been structurally controlled and formed by other processes, based on arcuate (vs. linear) form, occurrence at the upslope margin of a gently sloping topographic bench, and the occurrence of local compression features downslope from the arcuate scarps. The heads of two main landslides in this complex were thus delineated by two arcuate, concave-downslope scarps, which are separated by a zone of discontinuous cracks (plate 3.2 and fig. 3.20). A local compression feature downslope from the western margin of one of the arcuate scarps (locality 14-11 on plate 3.2 and fig. 3.20) delineates a portion of the landslide toe. Elsewhere the position of the toe is not marked by surface features, but the trend and location of the landslide-related features suggests that the complex may extend downslope to the channel of Laurel Creek. The complex is thus approximately 750 feet long and 1,500 feet wide and

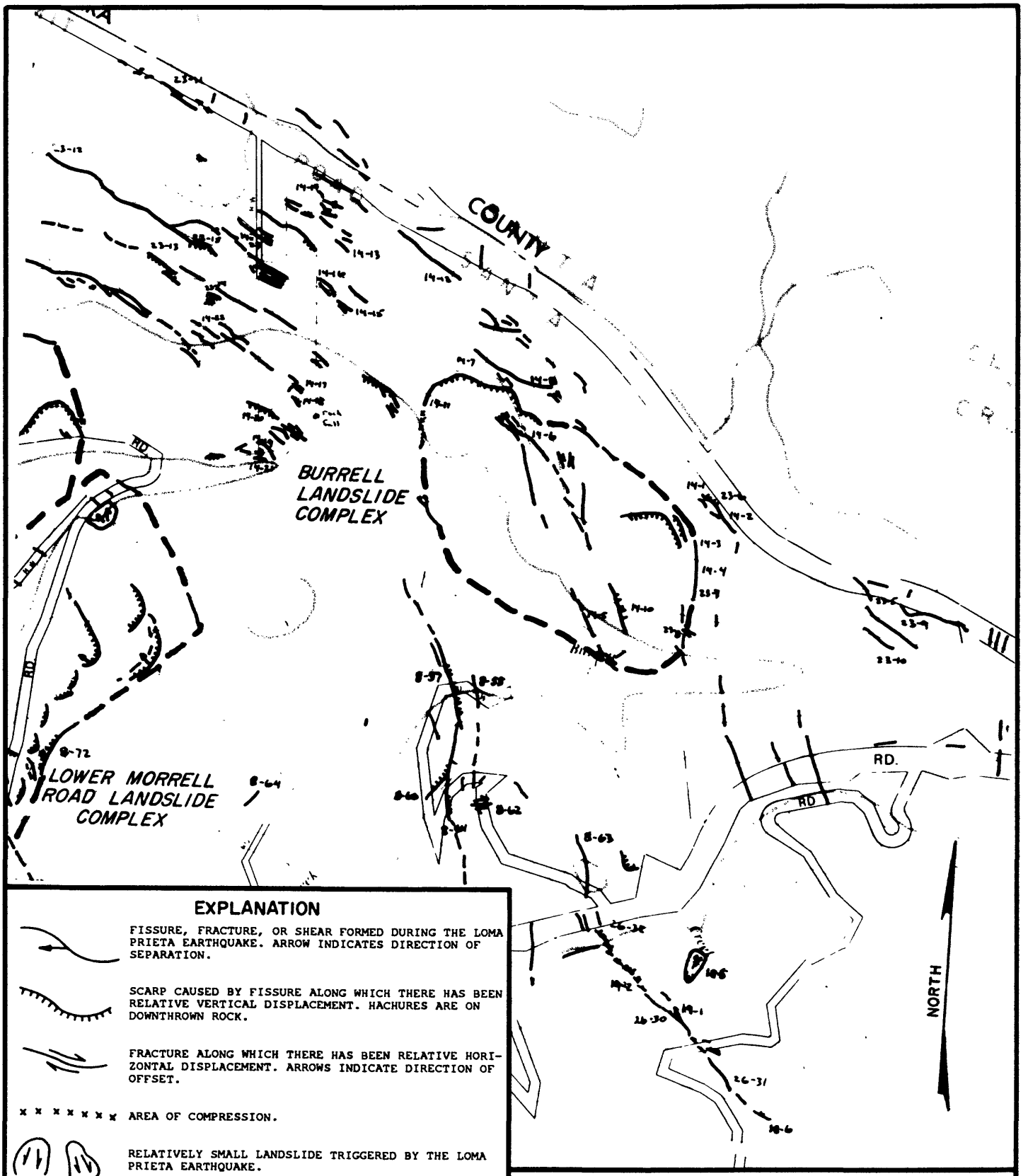

EXPLANATION

FISSURE, FRACTURE, OR SHEAR FORMED DURING THE LOMA PRIETA EARTHQUAKE. ARROW INDICATES DIRECTION OF SEPARATION.

SCARP CAUSED BY FISSURE ALONG WHICH THERE HAS BEEN RELATIVE VERTICAL DISPLACEMENT. HACHURES ARE ON DOWNTHROWN ROCK.

FRACTURE ALONG WHICH THERE HAS BEEN RELATIVE HORIZONTAL DISPLACEMENT. ARROWS INDICATE DIRECTION OF OFFSET.

AREA OF COMPRESSION.

RELATIVELY SMALL LANDSLIDE TRIGGERED BY THE LOMA PRIETA EARTHQUAKE.

85 — STRIKE AND DIP OF BEDDING.

20-105 — LOCATION OF GEOLOGIC NOTE, RECORDED IN SPITTLER AND HARP (1990).

APPROXIMATE, INFERRED BOUNDARY OF LARGE LANDSLIDE, LANDSLIDE COMPLEX, OR POSSIBLE LANDSLIDE THAT MOVED DURING THE LOMA PRIETA EARTHQUAKE.

BURRELL LANDSLIDE COMPLEX

SCALE 0 500 1000 FEET

FIGURE 3.20

encompasses approximately 22 acres. Downslope displacements measured across the major scarps were in the range between 11 and 28 inches.

The westernmost arcuate scarp is at the base of a pre-existing scarp that we interpret to be of landslide origin, and the western part of the landslide complex involves material shown as a "definite" landslide deposit by Cooper-Clark and Associates (1975; fig. 3.7). The area of landslide complex exhibits a benched topographic profile, which also suggests previous landslide activity. The average slope is on the order of 15 to 20°. Detailed trenching studies providing additional evidence of previous landslide activity here are discussed in Chapter V.

Bedrock underlying the Burrell landslide complex is mapped as mudstones and sandstones of the Butano Sandstone (fig. 2.4). The landslide complex lies between an unnamed, northwest-striking fault, which passes through the southwestern corner, and the San Andreas fault, which passes 500 feet to the northeast (fig. 2.4).

10. Upper Redwood Lodge Road Landslide Complex

The Upper Redwood Lodge Road landslide complex is in the Redwood Lodge area. The landslide crosses Old San Jose ("San Jose-Soquel") road between Summit Woods Drive and Redwood Lodge Road, 1.2 miles south of Summit Road (plates 3.1-3.4 and fig. 3.21).

The landslide complex was delineated primarily by three sets of discontinuous cracks and scarps that indicate the presence of at least three large, nested landslide blocks. The head of the landslide block farthest upslope and east is marked by a discontinuous set of northwest-trending, straight to slightly arcuate cracks and scarps that is approximately 1,900 feet long. The approximately N30°W strike of this zone is subparallel to the strike of ground cracks 1,200 feet to the northeast that are interpreted to have been structurally controlled (See Chapter IV), and these landslide-related cracks and scarps may also have been at least partly structurally controlled. The most prominent of these landslide-related cracks and scarps are in a nearly flat meadow at the base of a steep stretch of slope, and, for part of their length, they are associated with a pre-existing graben, on the order of 100 feet long, several feet wide, and a few feet deep. These relations and the geomorphology in this area lead us to infer

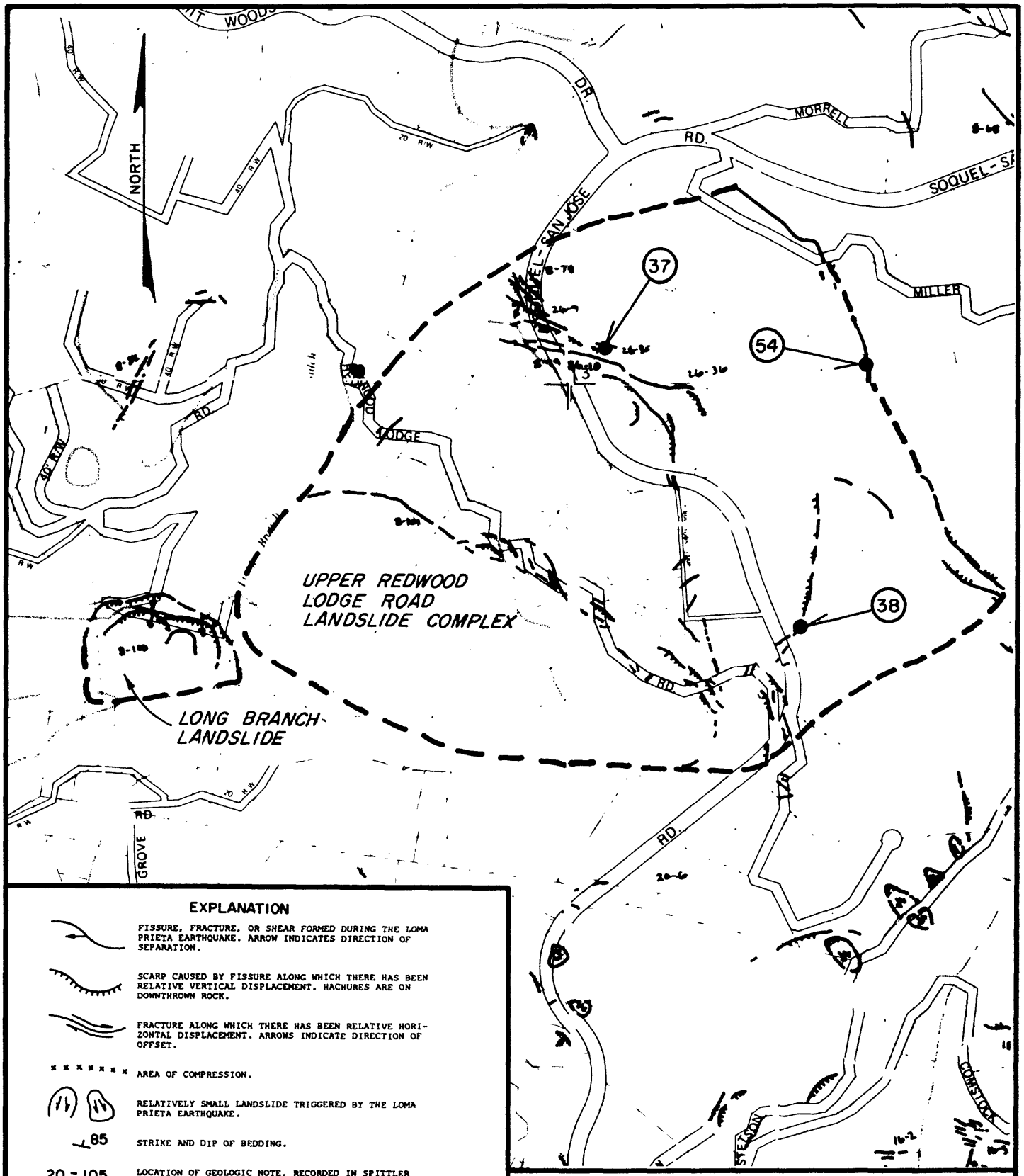

EXPLANATION

- FISSURE, FRACTURE, OR SHEAR FORMED DURING THE LOMA PRIETA EARTHQUAKE. ARROW INDICATES DIRECTION OF SEPARATION.
- SCARP CAUSED BY FISSURE ALONG WHICH THERE HAS BEEN RELATIVE VERTICAL DISPLACEMENT. HACHURES ARE ON DOWNTHROWN ROCK.
- FRACTURE ALONG WHICH THERE HAS BEEN RELATIVE HORIZONTAL DISPLACEMENT. ARROWS INDICATE DIRECTION OF OFFSET.
- AREA OF COMPRESSION.
- RELATIVELY SMALL LANDSLIDE TRIGGERED BY THE LOMA PRIETA EARTHQUAKE.
- 85 — STRIKE AND DIP OF BEDDING.
- 20 - 105 — LOCATION OF GEOLOGIC NOTE, RECORDED IN SPITTLER AND HARP (1990).
- APPROXIMATE, INFERRED BOUNDARY OF LARGE LANDSLIDE, LANDSLIDE COMPLEX, OR POSSIBLE LANDSLIDE THAT MOVED DURING THE LOMA PRIETA EARTHQUAKE.
- (4) — QUADRILATERAL ARRAY STATION # 4
- ● — ACTUAL STATION LOCATION
- O — REMOVED STATION

UPPER REDWOOD LODGE ROAD LANDSLIDE COMPLEX AND LONG BRANCH LANDSLIDE SURFACE STATIONS

SCALE 0 500 1000 FEET

FIGURE 3.21A

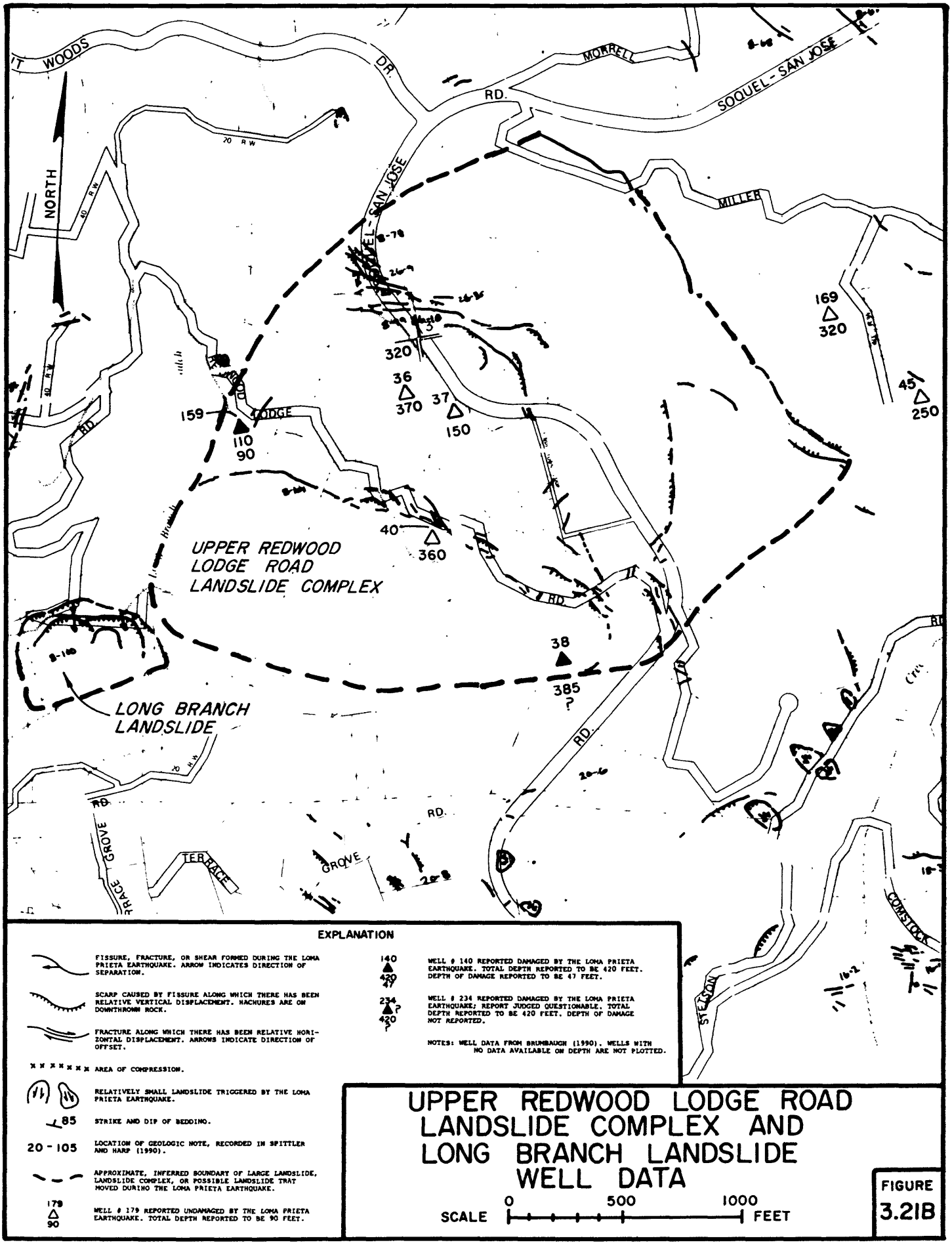
IT WOODS
DR.
RD.
MORRELL
SOQUEL - SAN JOSE
NORTH
20 R.W.
40 R.W.
MILLER
169
320
45
250
320
36
370
37
150
159
110
90
LODGE
UPPER REDWOOD
LODGE ROAD
LANDSLIDE COMPLEX
40
360
38
385
?
LONG BRANCH
LANDSLIDE
GROVE
TERRACE
COMSTOCK
STETSON
EXPLANATION
FISSURE, FRACTURE, OR SHEAR FORMED DURING THE LOMA PRIETA EARTHQUAKE. ARROW INDICATES DIRECTION OF SEPARATION.
SCARP CAUSED BY FISSURE ALONG WHICH THERE HAS BEEN RELATIVE VERTICAL DISPLACEMENT. HACHURES ARE ON DOWNTHROWN ROCK.
FRACTURE ALONG WHICH THERE HAS BEEN RELATIVE HORIZONTAL DISPLACEMENT. ARROWS INDICATE DIRECTION OF OFFSET.
AREA OF COMPRESSION.
RELATIVELY SMALL LANDSLIDE TRIGGERED BY THE LOMA PRIETA EARTHQUAKE.
85
STRIKE AND DIP OF BEDDING.
20 - 105
LOCATION OF GEOLOGIC NOTE, RECORDED IN SPITTLER AND HARP (1990).
APPROXIMATE, INFERRED BOUNDARY OF LARGE LANDSLIDE, LANDSLIDE COMPLEX, OR POSSIBLE LANDSLIDE THAT MOVED DURING THE LOMA PRIETA EARTHQUAKE.
179
90
WELL # 179 REPORTED UNDAMAGED BY THE LOMA PRIETA EARTHQUAKE. TOTAL DEPTH REPORTED TO BE 90 FEET.
140
420
47
WELL # 140 REPORTED DAMAGED BY THE LOMA PRIETA EARTHQUAKE. TOTAL DEPTH REPORTED TO BE 420 FEET. DEPTH OF DAMAGE REPORTED TO BE 47 FEET.
234
P
420
?
WELL # 234 REPORTED DAMAGED BY THE LOMA PRIETA EARTHQUAKE; REPORT JUDGED QUESTIONABLE. TOTAL DEPTH REPORTED TO BE 420 FEET. DEPTH OF DAMAGE NOT REPORTED.
NOTES: WELL DATA FROM BRUMBAUGH (1990). WELLS WITH NO DATA AVAILABLE ON DEPTH ARE NOT PLOTTED.
UPPER REDWOOD LODGE ROAD LANDSLIDE COMPLEX AND LONG BRANCH LANDSLIDE WELL DATA
SCALE
0
500
1000
FEET
FIGURE
3.21B

that the area is the head both of a large block slide that moved during the Loma Prieta earthquake and of a large, pre-existing block slide. Earthquake-induced displacements across individual cracks and scarps in this area were 10 inches or less.

The zone of cracks and scarps next downslope crosses Old San Jose Road approximately 1,800 to 2,000 feet north, 1,100 feet north, and 300 feet north of its intersection with Redwood Lodge Road (fig. 3.21). This zone forms an arcuate pattern, concave downslope in plan view. The southern part of this zone is at the base of an older bedrock scarp, and the slope between this zone and the creek channel to the west has a benched topographic profile. Both the older scarp and the benched profile are additional indicators of previous landslide movement. Direct evidence of previous landslide movement at this locality was also documented by SCC road-repair records that describe repeated landslide damage to Redwood Lodge Road (table 2.2 and fig. 2.7). Earthquake-related displacements of 1 to 12 inches measured across individual cracks in this zone were not consistent in direction.

The zone of cracks and scarps farthest downslope trends west-northwest along and downslope from Redwood Lodge Road, between Old San Jose Road and Long Branch Gulch (fig. 3.21). This zone, which is 1,900 feet long, is the most continuous of the three main zones of cracks and scarps in the landslide complex.

The location of the northeastern boundary of the landslide complex is poorly determined, but it is inferred to be at least as far northeast as the northeastern limits of the three prominent zones of cracks and scarps (fig. 3.21); the landslide complex is thus at least 2,100 feet wide. The southwestern (downslope) boundary is likewise not marked by any surface features, but the position and pattern of the westernmost cracks and scarps suggest that the landslide complex extends to the creek at the base of the slope (fig. 3.21). The landslide complex is thus on the order 2,700 feet long and has an area of at least 92 acres. The average slope through the landslide complex is on the order of 15 to 20°.

Two wells within the boundaries of the landslide complex were reported to have been damaged by the earthquake--well #159, at a depth of 90 feet and well #38, at an unknown depth--while four wells (#35, 36, 37, and 40 in fig. 3.21), with depths between 150 and 370 feet, were reported to have been undamaged (Brumbaugh, 1990). The two damaged wells are both near the margins of the

landslide complex. The four reportedly undamaged wells are farther from these landslide margins but within the landslide complex; the lack of reported disturbance to these wells could indicate either a basal shear surface locally deeper than the wells or local displacements too small to cause damage.

On the map of Cooper-Clark and Associates (1975), nearly all of the Upper Redwood Lodge Road landslide complex was shown as being underlain by a pre-existing complex of three landslide deposits; two of these were designated as "definite" and one was not labeled as to whether definite, probable, or questionable (figs. 2.8 and 3.7). Approximately the southern half of the area of the earthquake-induced landslide complex downslope from Redwood Lodge Road was also portrayed on the USGS geologic quadrangle map as being underlain by a landslide deposit (fig. 2.4). Other evidence of previous landslide activity in this area has been described above.

Bedrock underlying the Upper Redwood Lodge landslide complex belongs to the Rices Mudstone Member of the San Lorenzo Formation (mudstones and sandstones), under the northeastern part, and to the Vaqueros Sandstone, under the southwestern part (fig. 2.4). These rocks lie between the axis of the Laurel Anticline and the axis of the Glenwood Syncline and may locally dip to the southwest, stand vertical, or be overturned to the northeast (fig. 2.4).

11. Long Branch Landslide

The Long Branch landslide is immediately west of Long Branch Gulch and the Upper Redwood Lodge Road landslide complex (plate 3.3 and fig. 3.21). Ground cracks within the Long Branch landslide consist of three, approximately concentric sets of scarps and cracks that are concave downslope in plan view (plate 3.3 and fig. 3.21). The main scarp is the longest and farthest upslope of these sets; it extends 600 feet across the steep bank of the creek and downslope to within 50 feet of the stream channel. The landslide is therefore inferred to extend the additional distance downslope to the channel itself. The landslide thus delineated is approximately 400 feet long and 600 feet wide and encompasses an area of 5 acres. Measurements across cracks indicated at least 18 inches of downslope displacement. No landslide deposits were shown within the area of this landslide on either the map of Cooper-Clark and Associates (1975; see fig. 3.7) or the USGS geologic quadrangle map

(fig. 2.4). Bedrock underlying the landslide is mapped as Vaqueros Sandstone, which may incline toward the southwest, stand vertical, or be overturned to the northeast, according to nearby dips (fig. 2.4).

12. Stetson Road Landslide

The Stetson Road landslide, which crosses Stetson Road 0.4 miles east-northeast of its intersection with Old San Jose Road, is on the southwest-facing flank of Skyland Ridge, upslope from Hester Creek (plate 3.4 and fig. 3.22). The average slope here is on the order of 20°. The landslide was delineated by an arcuate, concave-downslope zone of scarps and cracks that are partly en echelon. This zone defines the head and at least the upper parts of both flanks of the landslide. The landslide interpreted as being partly bounded by this zone is at least 650 feet long, 1,500 feet wide, and 11 acres in area. The downslope extent of the landslide is undetermined, but it may extend downslope to Hester Creek; if so it is significantly larger than 11 acres. A small zone of cracks near the creek (plate 3.4 and fig. 3.22) could be part of this landslide but more probably marks a smaller, unrelated feature. Displacements measured across the arcuate, landslide-related zone of ground cracks indicated downslope movement was between 12 and 24 inches. The two cracks striking approximately N55°W that intersect the right flank of the landslide (plate 3.4 and fig. 3.22) were probably structurally controlled.

The map of Cooper-Clark and Associates (1975) did not show an older landslide deposit in the area of ground cracks, but, if the landslide extends downslope to the creek, it may involve material from a "probable" landslide deposit (figs. 2.8 and 3.7). The head of the Stetson Road landslide is underlain by the Rices Mudstone Member of the San Lorenzo Formation (mudstones and sandstones), and the rest of the landslide is underlain by Vaqueros sandstones (fig. 2.4). Rocks of both formations here dip toward or are overturned toward the northeast (fig. 2.4).

13. Amaya Ridge Landslide

The Amaya Ridge landslide is on the southwestern flank of Amaya Ridge, 0.7 miles east of Old San Jose Road and 0.5 miles north of the confluence of Hester Creek and Caldwell Gulch (plate 3.4 and

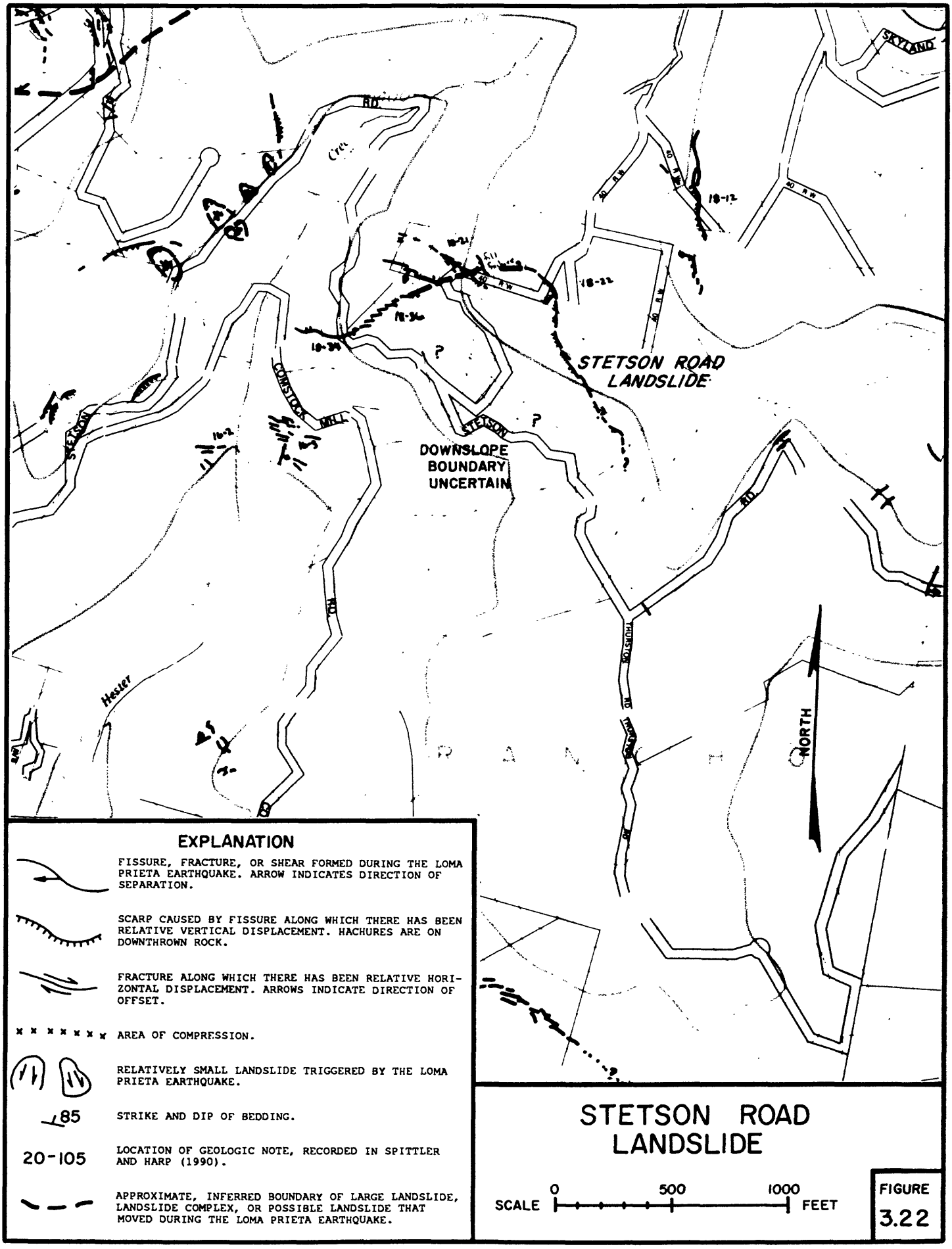
STETSON ROAD LANDSLIDE
DOWNSLOPE BOUNDARY UNCERTAIN
COMSTOCK MILL
STETSON
SKYLAND
NORTH
EXPLANATION
FISSURE, FRACTURE, OR SHEAR FORMED DURING THE LOMA PRIETA EARTHQUAKE. ARROW INDICATES DIRECTION OF SEPARATION.
SCARP CAUSED BY FISSURE ALONG WHICH THERE HAS BEEN RELATIVE VERTICAL DISPLACEMENT. HACHURES ARE ON DOWNTHROWN ROCK.
FRACTURE ALONG WHICH THERE HAS BEEN RELATIVE HORIZONTAL DISPLACEMENT. ARROWS INDICATE DIRECTION OF OFFSET.
AREA OF COMPRESSION.
RELATIVELY SMALL LANDSLIDE TRIGGERED BY THE LOMA PRIETA EARTHQUAKE.
85
STRIKE AND DIP OF BEDDING.
20-105
LOCATION OF GEOLOGIC NOTE, RECORDED IN SPITTLER AND HARP (1990).
APPROXIMATE, INFERRED BOUNDARY OF LARGE LANDSLIDE, LANDSLIDE COMPLEX, OR POSSIBLE LANDSLIDE THAT MOVED DURING THE LOMA PRIETA EARTHQUAKE.
STETSON ROAD LANDSLIDE
SCALE 0 500 1000 FEET
FIGURE 3.22

fig. 3.23). This area contains two sets of ground cracks and associated features. The northwestern set consists of a relatively continuous, arcuate zone of cracks that are concave downslope in plan view, and a nearly straight compression feature farther downslope, to the southwest. These features are interpreted to be, respectively, the main scarp and toe of a landslide approximately 400 feet long, 800 feet wide, and 4 acres in area. Measurements across the main scarp indicated local downslope displacements of 3 to 40 inches or more.

To the southeast is a zone of cracks and scarps that is linear to slightly arcuate, parallel to the western crack set, and en echelon to it (fig. 3.23). The latter set of cracks and scarps is approximately 1,000 feet long and is not associated with any mapped compression feature. The relation of these cracks and scarps to the landslide to the northwest has not been clearly determined; the southeastern set of cracks and scarps may be the main scarp of a separate landslide, an easterly and upslope extension of the other landslide, or structurally controlled ground cracks produced by some other process. One displacement measurement across a crack in this set (at locality 4-112 in plate 3.4 and figure 3.23) indicated movement of 6 to 8 inches downslope, to the southwest. The area between this set of cracks and the base of the slope encompasses 11 acres; this area is portrayed as a "possible landslide" on plate 3.4 and fig. 3.23.

Both the southeastern and the northwestern sets of scarps and cracks are near breaks in slope; the slopes above them are relatively steep and the slopes below them are comprised of a broad, gently sloping bench, 300 feet wide and several hundred feet long. A topographic profile surveyed down the slope through the northwestern set of cracks shows that the average slope inclination is 22° and that the inclination of the steep segment above the break in slope is 24°. Marshy areas just below the base of the steep stretch of slope indicate a local ground-water level near the surface. Such topographic and ground-water characteristics are typical of landslide deposits. The northwestern landslide is within an area that was designated as a "questionable" landslide deposit on the map of Cooper-Clark and Associates (1975; fig. 3.7), and the southeastern set of cracks and scarps closely follows the trace of a larger, older landslide scarp shown on that map (fig. 2.8). Bedrock underlying these areas belongs to the Purisima Formation (sandstones and siltstones), and mapping in the vicinity indicates that these rocks dip to the southwest (fig. 2.4).

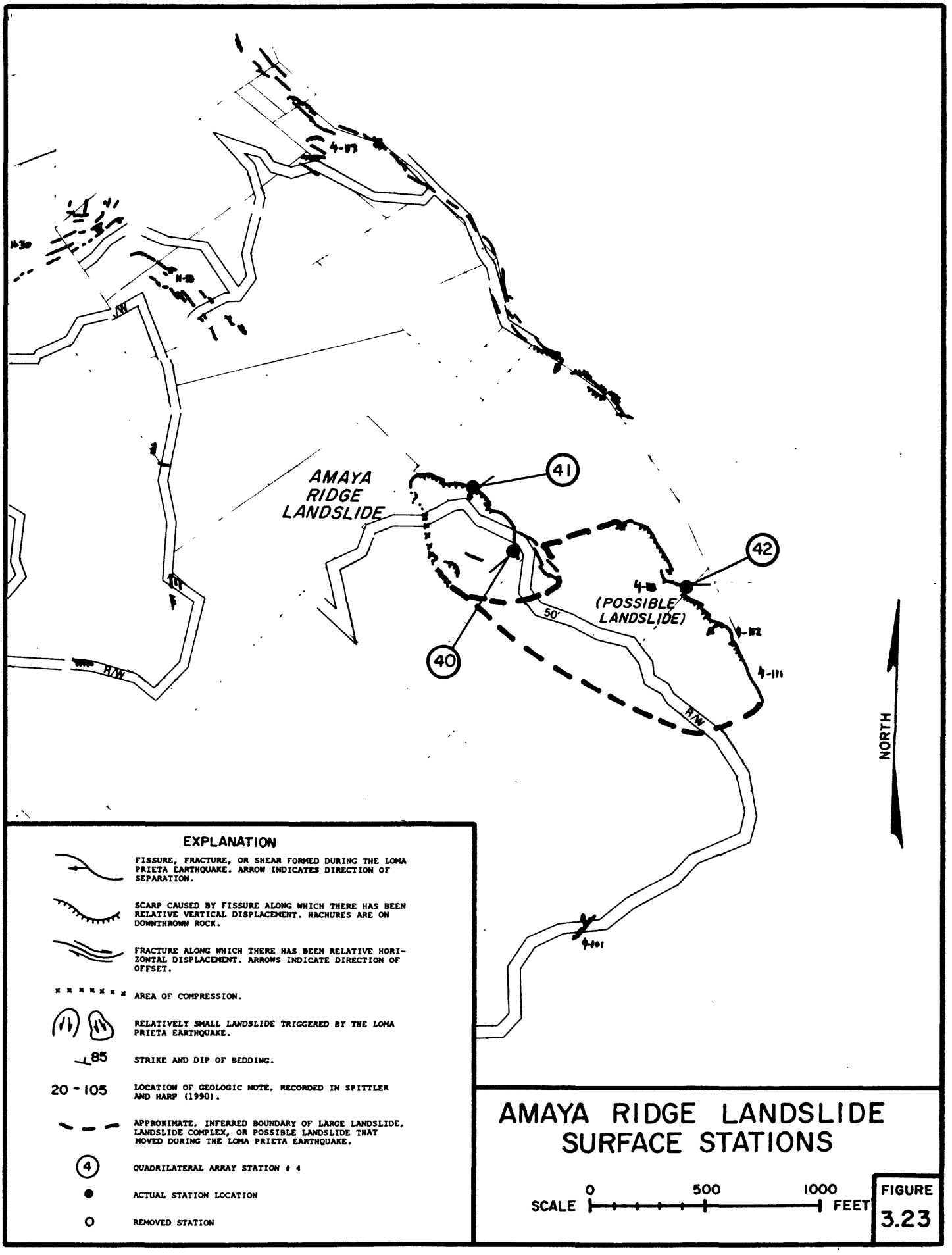

AMAYA RIDGE LANDSLIDE SURFACE STATIONS

SCALE 0 500 1000 FEET

FIGURE 3.23

14. Hester Creek North Landslide

The Hester Creek North landslide is on the eastern bank of Hester Creek, 0.8 miles northwest of the confluence of Hester Creek and Caldwell Gulch and 700 feet east of Old San Jose Road (plate 3.3 and fig. 3.24). The feature interpreted as the main scarp is an almost continuous scarp that is arcuate and concave-downslope and bounds an area approximately 200 feet long and 300 feet wide that covers 1 acre (plate 3.3 and fig. 3.24). The location of the landslide toe is uncertain; the landslide may extend as far downslope as Hester Creek, encompassing an additional 2 acres. Measurements across the main scarp suggested that 12 to 31 inches of downslope displacement had taken place.

The average slope in the area of the landslide is 25°. The slope on which this landslide occurred has produced many previous landslides during periods of winter rainfall (Griggs and others, 1990) and is underlain by material that is part of a "questionable" landslide deposit, according to the map of Cooper-Clark and Associates (1975; see fig. 3.8). Bedrock underlying the landslide consists of Purisima Formation sandstones and siltstones (fig. 2.4). This area is on the southwest limb of the Glenwood Syncline, where the regional dip is to the northeast, but the nearest dip information, judged questionable by Clark and others (1989), suggests dip locally may be toward the southwest (fig. 2.4).

15. Hester Creek South Landslide

The Hester Creek South landslide is on the eastern bank of Hester Creek, 600 feet south of the Hester Creek North landslide. This southern landslide is larger and has a more complex set of cracks and scarps defining its crown, head, and upper flanks (plate 3.3 and fig. 3.24). Included within the landslide area are a nearly continuous main scarp, crown cracks upslope from the main scarp, and at least two internal scarps; these features together with the channel of Hester Creek, which is inferred to be the downslope limit of the landslide, enclose an area, approximately 600 feet long and 600 feet wide, that covers approximately 7 acres. The average slope in the area of this landslide is on the order of 25° to 30°. One measurement at a point on the southern part of the main scarp

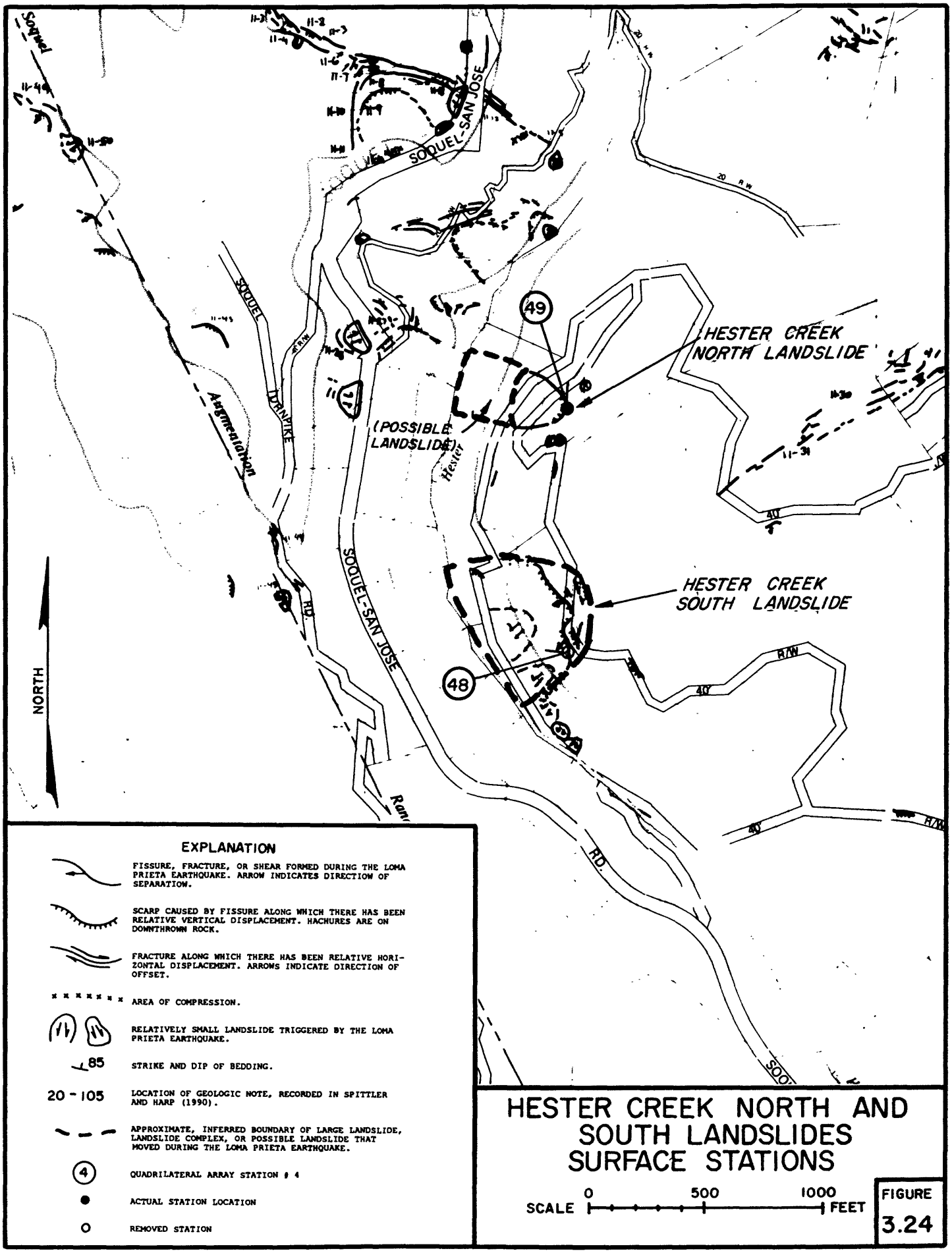

HESTER CREEK NORTH AND SOUTH LANDSLIDES SURFACE STATIONS

SCALE 0 500 1000 FEET

FIGURE 3.24

(quadrilateral array #48 on fig. 3.24) indicated downslope displacement in the range between 4 and 10 inches. Three smaller landslides adjoin the southern flank of the Hester Creek South landslide (plate 3.3 and fig. 3.24). As with the Hester Creek North landslide, the slope on which the Hester Creek South landslide occurred has produced many previous landslides during periods of winter rainfall (Griggs and others, 1990) and is included in an area underlain by part of a "questionable" landslide deposit, according to the map of Cooper-Clark and Associates (1975; see fig. 3.7).

Bedrock underlying the Hester Creek South landslide consists of Purisima Formation sandstones and siltstones on the southwest limb of the Glenwood Syncline (fig. 2.4). The regional dip in this area is also to the northeast, but the nearest dip information, judged questionable by Clark and others (1989), suggests dips locally may be toward the southwest. The Zayante fault passes 500 feet southwest of the landslide (fig. 2.4).

16. Lower Redwood Lodge Road Landslide

The Lower Redwood Lodge Road landslide is along the West Branch of Soquel Creek, just south of the confluence of Burns and Laurel creeks and 1,600 feet east of the junction of Laurel, Schultheis, and Redwood Lodge roads (plate 3.1 and fig. 3.25). The head and flanks are defined by an arcuate scarp and the toe by a zone of disturbed ground low on the slope. The landslide is approximately 600 feet long, 900 feet wide, and 6 acres in area. This area has experienced landslide activity in recent years, and a pre-existing landslide scarp, more than 10 feet high, near the main scarp, shows that the earthquake-induced landslide reactivated an older landslide deposit. The average slope in this area is on the order of 20° to 25°. The area in and around the landslide was designated as a "questionable" landslide deposit on the map of Cooper-Clark and Associates (1975; see fig. 3.7). Bedrock belongs to Rices Mudstone Member of the San Lorenzo Formation, which is made up of mudstones and sandstones; the rocks locally either dip vertically or are overturned steeply to the northeast (fig. 2.4).

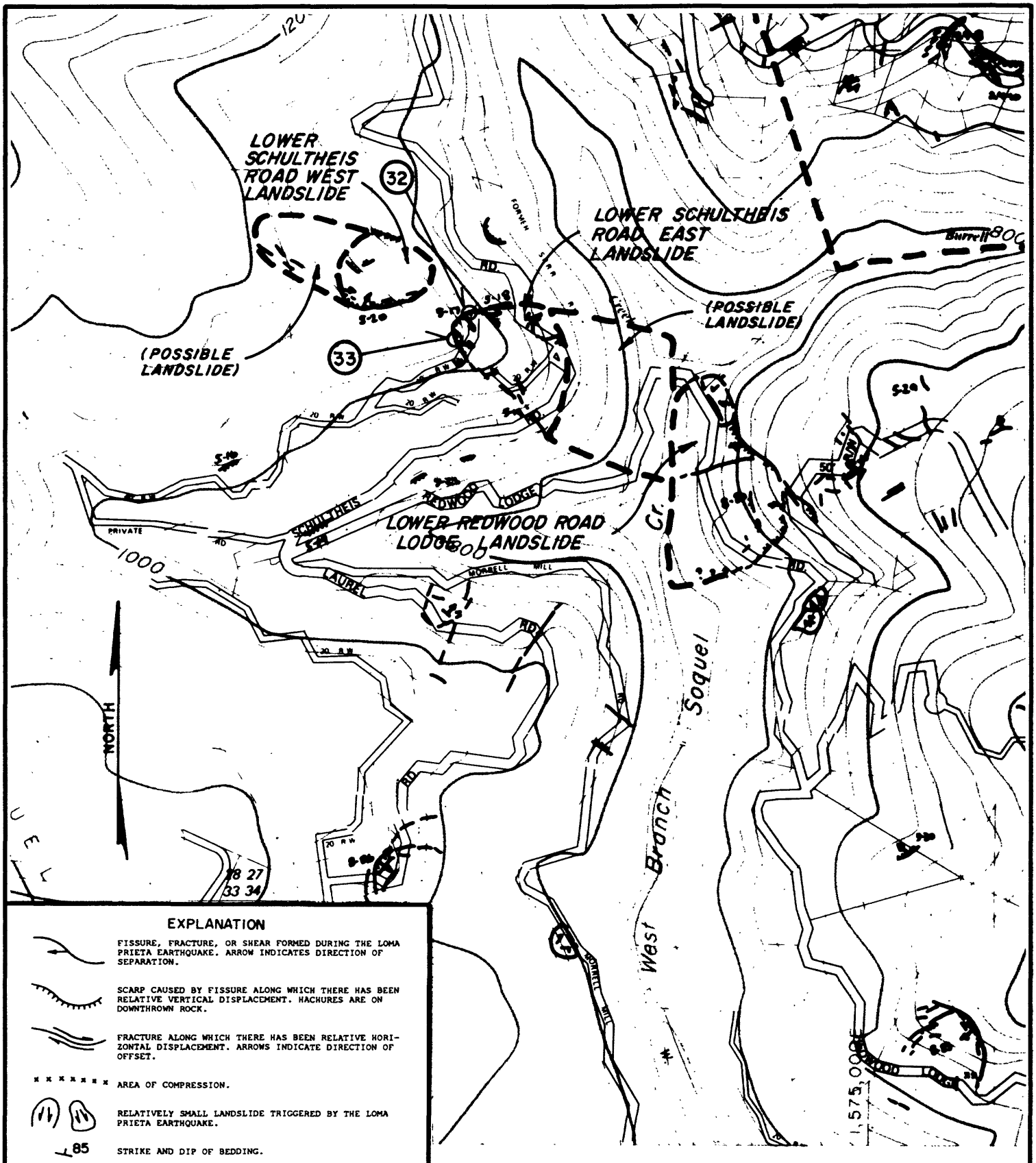

EXPLANATION

- FISSURE, FRACTURE, OR SHEAR FORMED DURING THE LOMA PRIETA EARTHQUAKE. ARROW INDICATES DIRECTION OF SEPARATION.
- SCARP CAUSED BY FISSURE ALONG WHICH THERE HAS BEEN RELATIVE VERTICAL DISPLACEMENT. HACHURES ARE ON DOWNTHROWN ROCK.
- FRACTURE ALONG WHICH THERE HAS BEEN RELATIVE HORIZONTAL DISPLACEMENT. ARROWS INDICATE DIRECTION OF OFFSET.
- AREA OF COMPRESSION.
- RELATIVELY SMALL LANDSLIDE TRIGGERED BY THE LOMA PRIETA EARTHQUAKE.
- 85 — STRIKE AND DIP OF BEDDING.
- 20 - 105 — LOCATION OF GEOLOGIC NOTE, RECORDED IN SPITTLER AND HARP (1990).
- APPROXIMATE, INFERRED BOUNDARY OF LARGE LANDSLIDE, LANDSLIDE COMPLEX, OR POSSIBLE LANDSLIDE THAT MOVED DURING THE LOMA PRIETA EARTHQUAKE.
- (4) — QUADRILATERAL ARRAY STATION # 4
- ● — ACTUAL STATION LOCATION
- ○ — REMOVED STATION

LOWER REDWOOD LODGE ROAD LANDSLIDE AND LOWER SCHULTHEIS ROAD EAST AND WEST LANDSLIDES SURFACE STATIONS

SCALE 0 500 1000 FEET

FIGURE 3.25

17. Lower Schultheis Road East Landslide

The Lower Schultheis Road East landslide is in Laurel township, on the east-facing nose of a ridge immediately northeast of the intersection of Schultheis, Redwood Lodge, and Laurel roads (plate 3.1 and fig. 3.25). A nearly continuous scarp, arcuate and concave-downslope, which extends approximately 250 feet across the slope, is taken as defining the crown, head, and upper flanks of the landslide. On both flanks, cracks extend 300 to 400 feet downslope from this scarp to Schultheis Road. The landslide thus defined is approximately 500 feet long and 400 feet wide and encompasses approximately 4 acres. No surface features marking the landslide toe were observed, and the landslide may extend an additional 500 feet downslope to the creek channel, encompassing an additional 7 acres. Measurements of downslope displacements at several points along the main scarp were in the range between 2 and 27 inches.

The average slope where this landslide occurred is 20°, and the slope has a benched topographic profile, suggesting previous landslide activity. According to SCC road-repair records (table 2.2 and fig. 2.7), landslide activity in this area in 1982 destroyed a stretch of the road and stranded some residents, who had to be evacuated. The roadway has continued to slide since 1983, and cumulative movement between 1983 and the 1989 earthquake was estimated to have been at least 2 feet (table 2.2). On the map of Cooper-Clark and Associates (1975), the area of the Lower Schultheis Road East landslide was designated as being underlain by a "questionable" landslide deposit (fig. 3.7). Bedrock in this area belongs to the Rices Mudstone Member of the San Lorenzo Formation, which is made up of mudstones and sandstones. Local bedrock dips are either vertical or overturned steeply to the northeast (fig. 2.4).

18. Lower Schultheis Road West Landslide

The Lower Schultheis Road West landslide is on the crest and north flank of the ridge in Laurel township that also contains the Lower Schultheis Road East landslide (plate 3.1 and fig. 3.25). The crown of the western landslide is 400 feet west of the crown of the eastern landslide.

The main scarp of the Lower Schultheis Road West landslide is a slightly arcuate crack-and-graben feature, approximately 300 feet

long (figs. 3.25 and 3.26). For part of its length this scarp is south of the ridge crest, and so part of the ridge crest is involved in the landslide and has been displaced to the north. Observations along the main scarp indicated that the landslide moved 12 to 18 inches. A set of discontinuous cracks west of this scarp suggests that the landslide may extend an additional 300 feet in that direction (plate 3.1 and fig. 3.25). These cracks are also subparallel to the strike of the bedrock in this area, suggesting that they and, by extension, the better-developed main scarp to the east, may also have been structurally controlled. A 100-foot-long, linear compression feature, approximately 350 feet down the northern flank of the ridge from the main scarp, is taken as marking part of the landslide toe (fig. 3.25). The landslide thus defined is at least 350 feet long, 350 feet wide, and 3 acres in area; if the landslide also encompasses the area of cracking to the north and extends as far downslope as the compression feature, its area may be as large as 5 acres. The average slope of the ridge flank is 15° to 20°.

Subsurface exploration, consisting of direct observations in two 30-inch-diameter boreholes, 12 and 37 feet downslope from the main scarp, revealed a basal shear surface at a depth of 15 feet. Material along this shear surface consisted of a layer of soft, slickensided clay, 1/2 to 2 inches thick. A second, deeper shear surface may also have been penetrated by the upslope borehole at a depth of 25 feet. This potential shear surface was marked by intensely fractured rock (William Cotton and Associates, Inc., 1990, unpublished data). A pre-existing shear surface, corresponding to the 1989 main scarp, was exposed and documented in a trenching investigation (Rogers E. Johnson and Associates, 1991, unpublished data).

The area within and adjacent to the Lower Schultheis Road West landslide exhibits several features almost certainly associated with shallow, pre-earthquake landslides, and the topography of the ridge and the meadow immediately to the north suggests that deep-seated landslide movements have also occurred here in the past. On the map of Cooper-Clark and Associates (1975), the area containing the Lower Schultheis Road West landslide was designated as being within a "questionable" landslide deposit (fig. 3.7). Bedrock consists of mudstones and sandstones of the Rices Mudstone Member of the San Lorenzo Formation and probably dips vertically (fig. 2.4).

FIGURE 3.26 – Part of ground–crack and graben feature that delineates the main scarp of the Lower Schultheis Road West landslide. Stretch of scarp in photograph shows approximately 12 to 18 inches of primarily extensional movement, with a smaller vertical (down to north) component. View is toward the east. Ridge crest at this locality is to the left (north) of the photograph and thus is involved in the landslide.

E. References Cited

Brumbaugh, R., 1990, Santa Cruz well history survey: Santa Cruz, Calif., Report to Santa Cruz County Planning Department.

Clark, J. C., Brabb, E. E., and McLaughlin, R. J., 1989, Geologic map and structure sections of the Laurel 7-1/2' quadrangle, Santa Clara and Santa Cruz counties, California: U.S. Geological Survey Open-File Map 89-676, scale 1:24,000.

Cooper-Clark and Associates, 1975, Preliminary map of landslide deposits in Santa Cruz County, California, *in* Seismic Safety Element: Santa Cruz County Planning Department, scale 1:62,500.

Griggs, G. B., Rosenbloom, N. A., and Marshall, J. S., 1990, Investigation and monitoring of ground cracking and landslides initiated by the October 17, 1989 Loma Prieta earthquake: Santa Cruz., Calif., Gary B. Griggs and Associates, Final Report to the U.S. Army Corps of Engineers.

Manson, M. W., Keefer, D. K., and McKittrick, M. A., compilers, 1991, Landslides and other geologic features in the Santa Cruz Mountains, California, resulting from the Loma Prieta earthquake of October 17, 1989: California Division of Mines and Geology, Preliminary Report 29 (in press).

McLaughlin, R. J., Clark, J. C., Brabb, E. E., and Helley, E. J., in press, Geologic map and structure sections of the Los Gatos 7 1/2' Quadrangle, Santa Clara County California: U.S. Geological Survey Open-File Map.

Spittler, T. E., and Harp, E. L., compilers, 1990, Preliminary map of landslide features and coseismic fissures in the Summit Road area of the Santa Cruz Mountains triggered by the Loma Prieta earthquake of October 17, 1989: U.S. Geological Survey Open-File Report 90-688, 53 p. + 3 maps, scale 1:4,800.

U.S. Geological Survey Staff, 1989, Preliminary map of fractures formed in the Summit Road-Skyland Ridge area during the Loma Prieta, California, earthquake of October 17, 1989: U.S. Geological Survey Open-File Report, 89-686, 1 sheet, scale 1:12,000.

Varnes, D. J., 1958, Landslide types and processes, *in* Eckel, E. B., ed., Landslides and engineering practice: National Academy of Sciences Highway Research Board Special Report 29, p. 20-47.

Varnes, D. J., 1978, Slope movement types and processes, *in* Schuster, R. L., and Krizek, R. J., eds., Landslides--Analysis and control: National Academy of Sciences Transportation Research Board Special Report 176, p. 11-33.

William Cotton and Associates, Inc., 1990, Schultheis Road and Villa Del Monte areas geotechnical exploration Santa Cruz County, California: Los Gatos, Calif., William Cotton and Associates, Report for U.S. Army Engineers, 2 vols.

Youd, T. L., and Hoose, S. N.., 1978, Historic ground failures in northern California triggered by earthquakes: U.S. Geological Survey Professional Paper 993, 177 p.

CHAPTER IV. ORIGIN OF STRUCTURALLY CONTROLLED FRACTURES TRIGGERED BY THE LOMA PRIETA EARTHQUAKE AND THEIR RELATION TO LANDSLIDES

A. Introduction

The initial efforts by geologists to locate surface fault-rupture from the Loma Prieta earthquake were frustrated largely due to the confusing pattern of landslide-related fractures and numerous other fractures that displayed features generally considered to be uncharacteristic of the San Andreas fault. Instead of predominantly left-stepping, right-lateral (relative displacement of material on the opposite side of the fracture to the right) fractures confined to the mapped trace of the San Andreas fault, fractures were distributed throughout a wide zone southwest of the fault, along the south side of Summit Ridge. This zone was approximately 1.5 miles wide, transverse to the ridge crest, and 5 miles long, parallel to the ridge, approximately between Hutchinson Road and Skyland Ridge (plates 3.1-3.4). Instead of the expected primarily right-lateral displacements, most fractures were primarily extensional, and components of left-lateral slip (relative displacement of material on the opposite side of the fracture to the left) were more common than right-lateral.

1. Lithology and Structure

The geologic and structural settings of the Summit Ridge area were described in Chapter II and shown in figure 2.4. The lithologic setting of Summit Ridge itself is dominated by three Tertiary-age formations: the Butano Sandstone, San Lorenzo Formation, and Vaqueros Sandstone. These units are predominantly weakly cemented sandstones, siltstones, mudstones, and shales. According to the most recent geologic mapping in this area (Clark and others, 1989, with landslide boundaries revised by McLaughlin and Clark, 1990, unpublished data; McLaughlin and others, in press), the overall trend of bedding and structure strikes northwest-southeast. The average strike of bedding throughout the area is between N30°W and N80°W. The rocks are intensely folded, as noted in Chapters II and III, and dips are typically steep. Locally the rocks dip to the

southeast, dip to the northeast, are vertical, or are overturned to the northeast (fig. 2.4).

Several major geologic structures pass through the area (fig. 2.4): The Laurel Anticline trends approximately N45°W through the south flank of Summit Ridge and is truncated by the Butano fault approximately 1.7 miles southeast of the California State Highway 17-Summit Road intersection. This fault, which splits off the San Andreas fault approximately 1,600 feet northwest of the Old San Jose Road-Summit Road intersection, traverses the Summit Ridge area northwest from there with local strikes between N60°W and N75°W.

From a point approximately 2,300 feet north of where the Laurel Anticline is truncated by the Butano fault, the axis of the Summit Syncline, trending N60°-65°W, extends southeastward to approximately 1,000 feet west of Morrell Road. There the synclinal axis is truncated by an unnamed fault, trending N45°W, which also offsets the Butano fault in a left lateral sense. In the Villa Del Monte and Morrell Road areas, several faults striking approximately N45°W extend across the Butano fault and the Summit Syncline. Most of these faults are less than 0.6 miles in mapped length and produce little or no offset of structures that they cross.

Several graben features are present near the crest of Summit Ridge. These grabens are subparallel to the ridge and have local relief of 5 to 20 feet across their scarps. Renewed displacement occurred on portions of the graben-bounding scarps during the Loma Prieta earthquake, evidenced by fractures with vertical displacements of several inches to as much as 1 foot. Three of the most obvious grabens are located near Summit Road (plate 4.1). The westernmost of these features is approximately 200 feet southeast of Old Summit Road and approximately 2,500 feet east of Highway 17. This graben is part of the extended "Tranbarger fracture" zone, in the Old Santa Cruz Highway area. There, earthquake-induced fractures formed on both margins of the graben near its northeastern limit, where it is approximately 50 feet wide. To the southwest, the graben width increases to approximately 300 feet within a horizontal distance of 600 feet. Measured vertical displacements produced during the earthquake varied from 1 to 6 inches. (Spittler and Harp, 1990).

Another visible linear depression along Summit Road is adjacent to and southwest of the 1,400-foot-long fracture that

extends southeast from the Melody Lane-Summit Road intersection, crossing Summit Road twice. The long fracture along the northeast margin of this depression is the only significant earthquake-induced fracture associated with it. Its maximum displacement is approximately 1 foot (Spittler and Harp, 1990). As discussed in section IVB3, no single origin is obvious for this graben-like feature.

Beginning at the Summit Road-Old Santa Cruz Highway intersection, a third, 100- to 150-foot-wide, graben extends approximately 800 feet to the southwest, along the southwest side of Summit Road. The trend of this graben is N45°W, diverging from the trend of Summit Road by about 5°. Both southwest- and northeast-facing scarps have formed there on fractures triggered by the earthquake, which had vertical displacements ranging from 2 to 14 inches (Spittler and Harp, 1990). Within this graben, earthquake-induced fractures were not wholly coincident with the graben margins but also formed southwest- and northeast-facing scarps within the graben itself.

2. Fracture Characteristics

There are three fundamental modes of crack development in brittle solids. These modes, which refer to the relative movement of the two sides of the crack with respect to the direction of fracture propagation, are illustrated in figure 4.1. Fractures that are predominantly extensional are represented by Mode I. Within landslides, such cracks are most commonly in head areas where extension is predominant and near toes where extension occurs because of convexities (bulging) or lateral movement of material. Mode II cracks are typical of strike-slip displacement. Within landslides, these cracks most commonly develop along the flanks. Mode III cracks are most commonly found in and around the heads of landslides where rotation or vertical shear is dominant over extension and propagates laterally. In tectonic settings, Mode III fractures are manifest as normal or reverse faults propagating laterally (Lawn and Wilshaw, 1975). Other characteristics of fractures, such as orientation, continuity, and relation to slope geomorphology, and implications regarding origins, are discussed in the following section.

Extension was the predominant mode of displacement across the structurally controlled fractures throughout the study area. Even

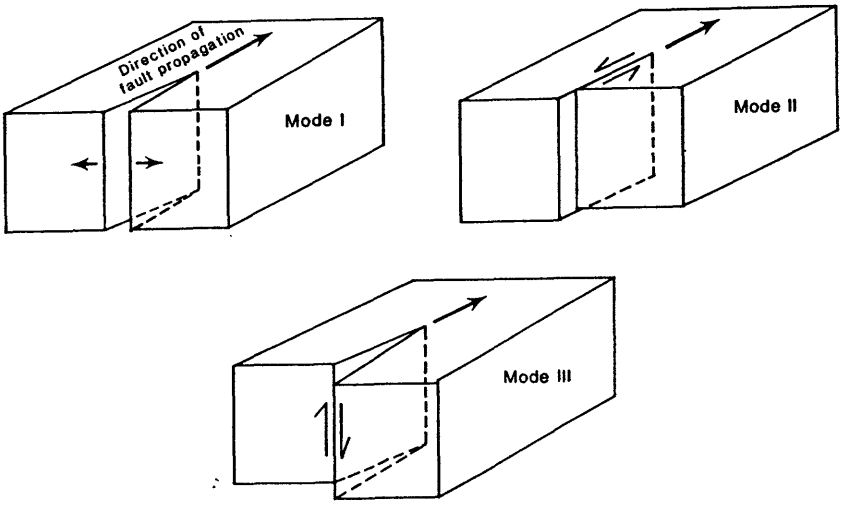

Figure 4.1. Mode I, II, and III fractures and relative movement causing deformation (after Lawn and Wilshaw, 1975). Mode I fractures separate in extension, perpendicular to direction of crack propagation. Displacement on Mode II fractures is perpendicular to fracture front (tip of crack). Fractures of this type can exhibit normal, reverse, or strike-slip displacements. Displacement on Mode III fractures is parallel to fracture front. This type of fracture is common to landslide main scarps that propagate laterally.

those fractures that displayed lateral and (or) vertical offsets generally lacked slickensides or surficial ridges of disturbed ground ("mole tracks") that are created by movement that is primarily shear. Although both left- and right-lateral displacements occurred, left-lateral displacements were more common. Furthermore, large displacements were uncharacteristic of structurally controlled fractures not also associated with landslides; displacements not associated with landslides were typically less than 20 inches. A few such fractures displayed displacements exceeding 3.5 feet, but most displacements exceeding 2 feet were on fractures associated with landslide movement. Cumulative displacements across fracture zones within landslides were as large as 8.1 feet.

B. Fracture Origins

The fractures or "ground cracks" that occurred in the Summit Ridge area as a result of the Loma Prieta earthquake were mapped by a multiagency team of geologists from federal, state, and county agencies, universities, and private consulting firms, as was discussed in Chapters I and III. This mapping was compiled by Spittler and Harp (1990) at a scale of 1:4,800. The method, accuracy, and limitations of this mapping were discussed in Chapter III. The maps in Spittler and Harp (1990) were used as the basis for plates 4.1-4.4 of this current report and as templates to produce other figures in this chapter. Criteria described in this section were used to discriminate between fractures primarily related to the movement of landslides and fractures primarily related to structural features such as bedding or faults. On plates 4.1-4.4 major fractures interpreted as being primarily related to landslides are differentiated from those judged to have been produced primarily by separation along other structural discontinuities; a few major fractures and fracture zones are designated as being related to both types of processes because it is evident that both landslide and regional structure contributed significantly to their formation. Relatively short ground cracks, whether within or outside landslide boundaries, were not individually categorized. Analyses of ground-crack patterns were carried out primarily on data from plates 1 and 2 of Spittler and Harp (1990).

1. Fractures Related To Landslide Movement

The typical association of fractures of different modes and orientations with the different parts of a landslide is well documented (Varnes, 1978) and forms a basis for relating fractures to landslides or other causes. The relation of fractures to slope morphology and to each other is also important in making such a determination. Large landslides in the Summit Ridge area and the fractures associated with them were described in Chapter III, which contains a discussion of general criteria for identifying such landslides; however, to facilitate the discussion of fracture origins, criteria used to differentiate landslide fractures from structurally controlled fractures produced by other processes are discussed in greater detail in the following sections.

a. Orientation: The orientation and shape of a fracture are of primary importance in evaluating origin. As shown in figures 3.1 and 3.2, if the main scarp and both flanks of a rotational slump or block slide are completely defined by fractures, those cracks will commonly describe a horseshoe-shaped arc opening to the downslope direction (although, as discussed in Chapter III, main scarps of block slides may be only gently curved or relatively straight--fig. 3.2). Therefore, in general, fractures related to these scarps may have a range in trends of as much as 180° on a single landslide. On the southwest flank of Summit Ridge, major fractures associated with landslides had trends that spanned the full possible range, even though the full range of possible trends was not observed on most individual landslides.

b. Trend Variability: Fractures associated with landslide main scarps are typically arcuate, or curved. If the main scarp or flanks are exceptionally long, however, these fractures may be relatively straight for much of their length. Most (but not all) fractures associated with landslides in the Summit Ridge area were in zones that remained straight for less than approximately 350 feet, and most exceptions to this limit were associated with the largest landslides.

c. Amounts of Displacement: Displacements measured across fractures within landslides in the Summit Ridge area were commonly larger than across fractures not associated with landslides. Fracture displacements outside of landslide boundaries were typically less than 20 inches, whereas displacements of more than 2 feet across individual cracks were not uncommon within landslides.

d. Directions of Displacement: Within a landslide mass that has a completely developed main scarp and flanks, vertical, right-lateral, and left-lateral senses of displacements may be more or less equally represented. In the Summit Ridge area, this was not true within all landslides, because cracks defining flanks of landslides were not equally developed. However, throughout the study area, displacements across fractures along landslide flanks were relatively consistent--right-lateral along the right flanks and left-lateral along the left flanks.

2. Fractures Controlled By Regional Structure

The origin or origins of fractures in the Summit Ridge area not associated with landslides has not been positively determined. However, most of these fractures are probably openings induced by earthquake shaking along bedding surfaces or along other structures with trends parallel to bedding. Most fractures in the Summit Ridge area outside the boundaries of well-defined landslides are parallel or nearly parallel to bedding, as depicted on the most recent 1:24,000-scale USGS geologic quadrangle maps of the Los Gatos and Laurel quadrangles (Clark and others, 1989, with landslide boundaries revised by McLaughlin and Clark, 1990, unpublished data; McLaughlin and others, in press); most of these fractures and most bedding planes have trends and strikes between N30°W and N80°W (compare fig. 2.4 and plates 4.1-4.4). To identify those fractures that were related primarily to regional structure and to differentiate them from those primarily related to landslides, the same categories of characteristics were used as discussed in the previous section for landslide-related cracks.

a. Orientation: Most fractures associated with regional geologic structure had trends between N30°W and N80°W. The trends of landslide-related fractures, as previously stated, had a much wider range of trends. Figures 4.2 and 4.3 are rose diagrams showing ranges of trends of fractures judged to be related primarily to regional structure for the areas covered in plates 1 and 2, respectively, of Spittler and Harp (1990). (Data are from Spittler and Harp, 1990, and Ponti and Wells, in press.) Figures 4.2 and 4.3 show that the greatest numbers of fractures in the area of plate 1 of Spittler and Harp (1990) trend approximately N35°W, whereas the trends of those fractures in the area of plate 2 of Spittler and Harp (1990) cluster around N45°W.

b. Displacement Trends and Directions of Displacement: Figures 4.4 and 4.5 are rose diagrams showing the azimuths of displacement vectors across fractures outside landslide boundaries in the areas covered by plates 1 and 2, respectively, of Spittler and Harp (1990). (Data are from Spittler and Harp, 1990, and Ponti and Wells, in press.) The displacements shown are totals of all displacements measured for each azimuth. The displacement azimuths in figure 4.4 show maxima that are slightly counterclockwise from being perpendicular to the fracture trend maxima in figure 4.2. Comparison of figures 4.2 and 4.4 shows that the displacements across the fractures are mostly extensional (normal to the fracture-trend maxima) with a small component of left-lateral displacement. Comparison of figures 4.3 and 4.5 shows that the fracture-trend maxima and the displacement-vector maxima are virtually perpendicular to each other, indicating that most displacements across fractures in the area of plate 2 of Spittler and Harp (1990) were extensional.

The sense of vertical displacement across fractures was not, in itself, a determining factor in establishing origin. Both landslides and other, structurally controlled, processes produced fractures with relative vertical displacements that were down on the downslope-side. In addition, a few fractures with the upslope side displaced relatively downward were found within landslide masses.

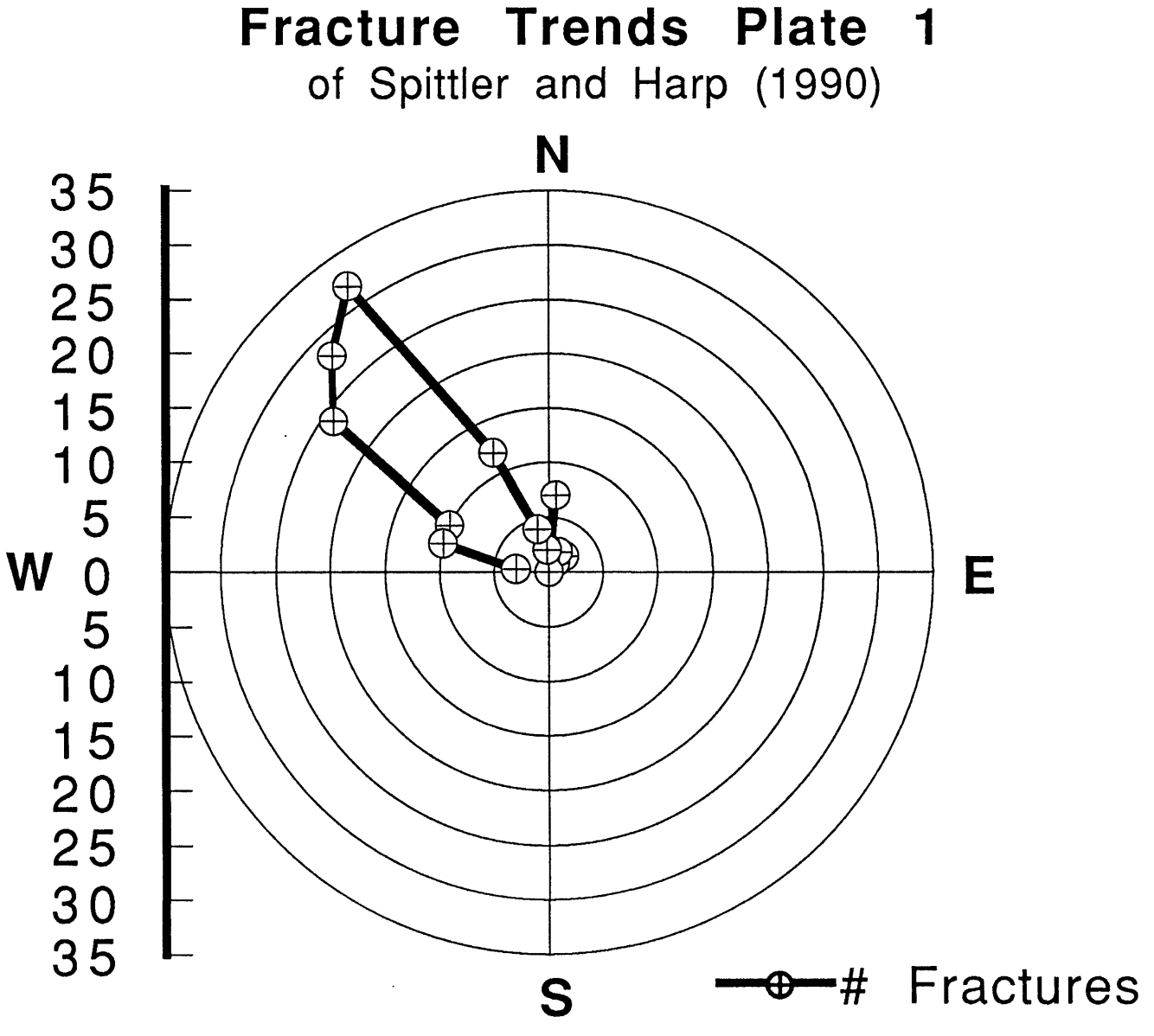

Figure 4.2. Rose diagram showing cumulative trends of fractures inferred to be related to regional structure within area covered by plate 1 of Spittler and Harp (1990).

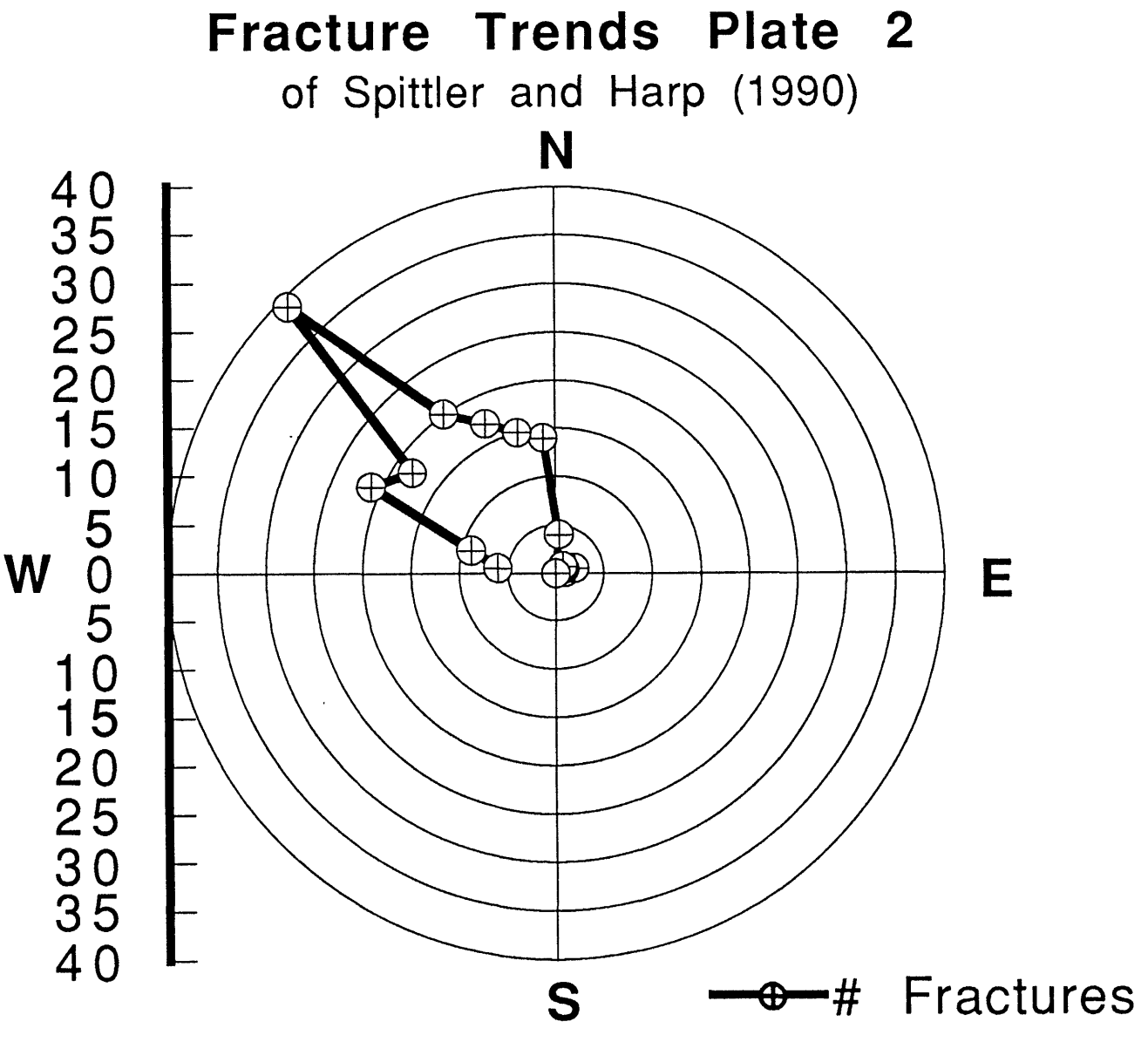

Figure 4.3. Rose diagram showing cumulative trends of fractures inferred to be related to regional structure within area covered by plate 2 of Spittler and Harp (1990).

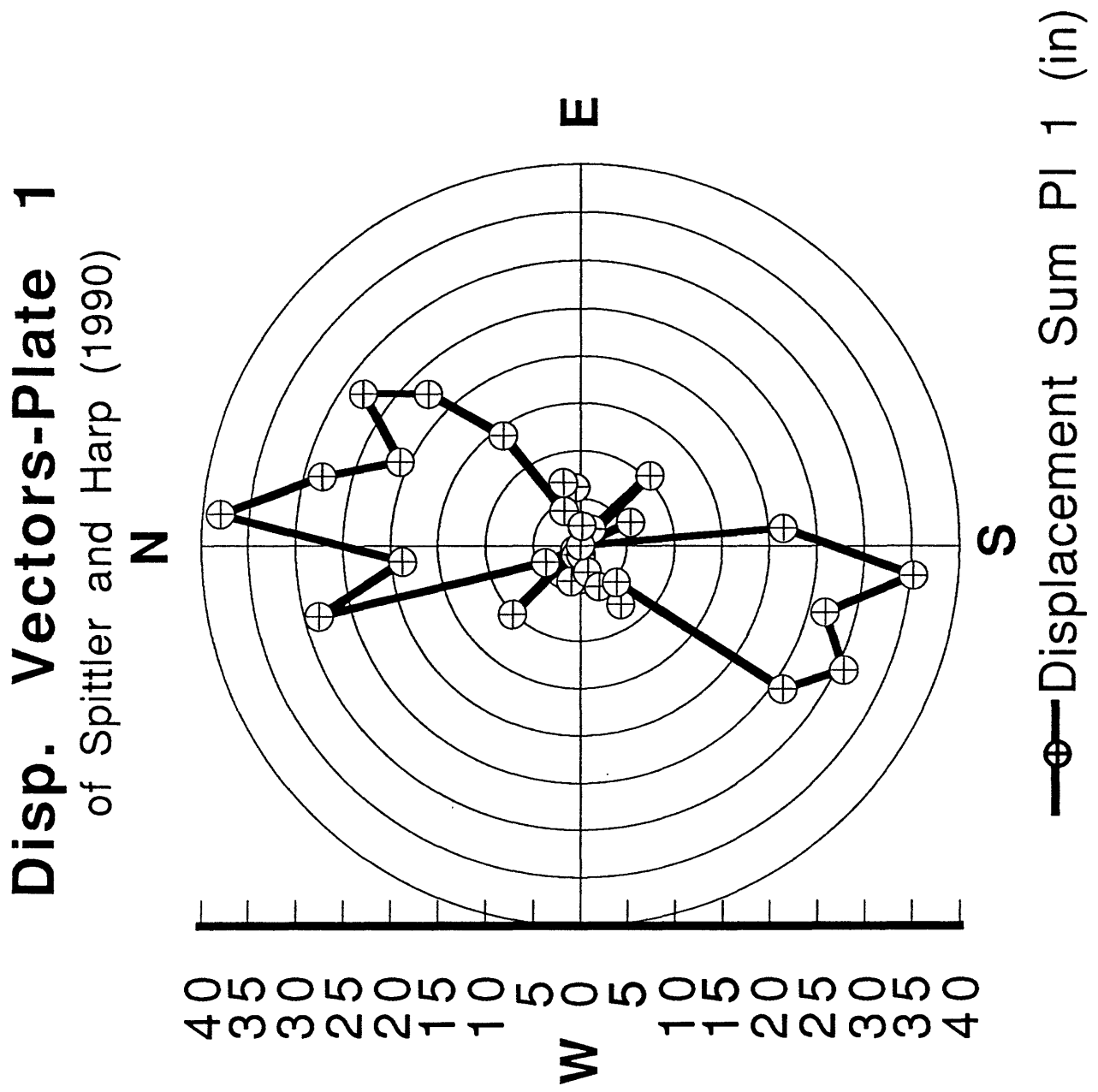

Figure 4.4. Rose diagram showing amounts of dispacement summed from all measurements with a given azimuth across all fractures inferred to be related to regional structure within the area covered by plate 1 of Spittler and Harp (1990).

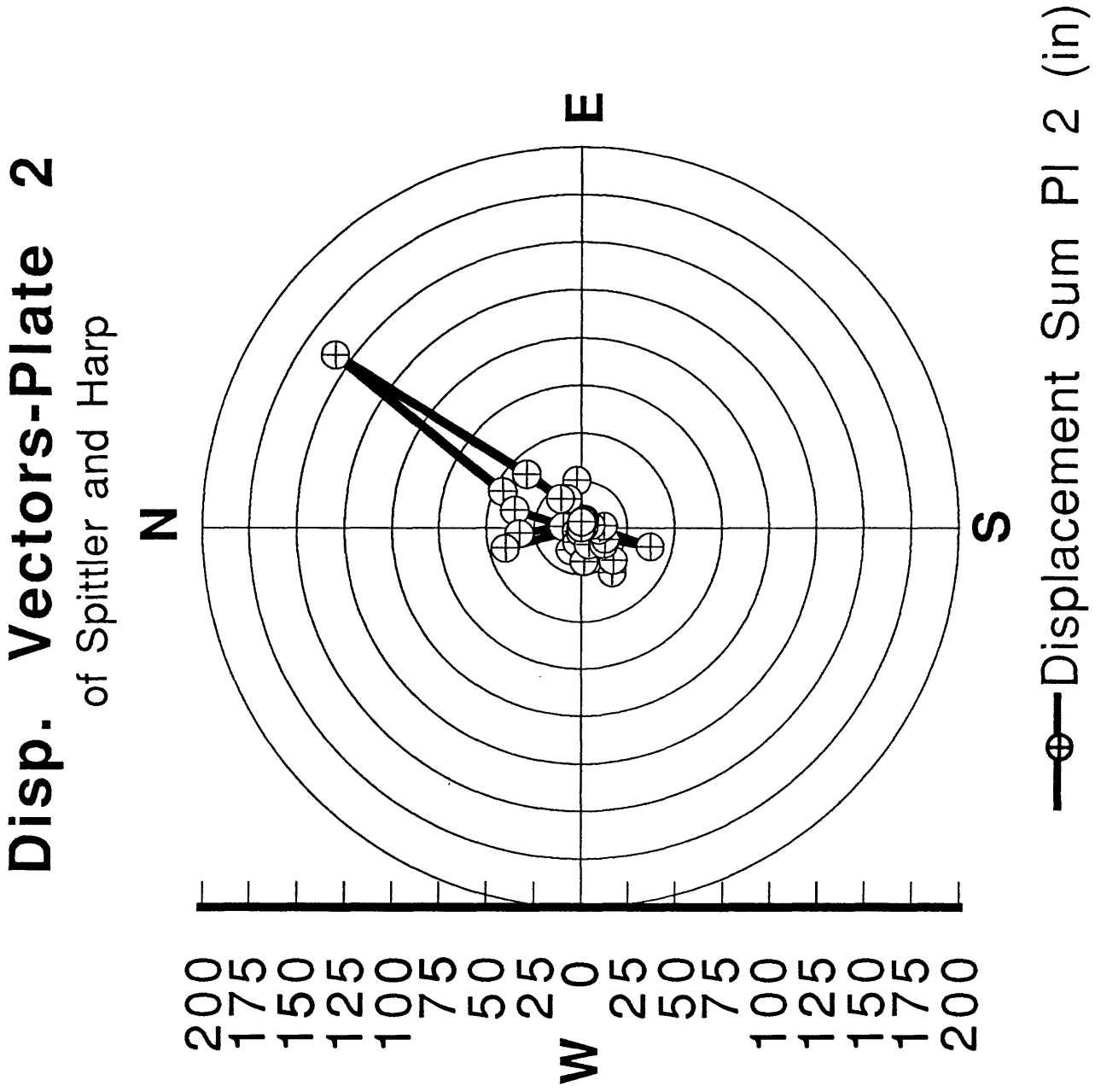

Figure 4.5. Rose diagram showing amounts of dispacement summed from all measurements with a given azimuth across all fractures inferred to be related to regional structure within the area covered by plate 2 of Spittler and Harp (1990).

c. Amounts of Displacement: The amounts of displacement across fractures outside landslide boundaries tended to be lower than displacements across fractures within landslides. As stated above, displacements across fractures related to regional structure were generally less than 20 inches, whereas displacements of more than 2 feet across individual cracks within landslide masses were not uncommon.

3. Fractures Of Undetermined Origin

The criteria described in the previous two sections allowed interpretation of the overall geometries of most major fracture zones in the Summit Ridge area and enabled discrimination between landslide and other, structurally controlled origins. However, several of the longest fracture zones within the area of the plate 1 of Spittler and Harp (1990) may be due to either, or both, causes. These fracture zones show characteristics typical both of fractures related to regional structure and of large landslide scarps.

a. "Tranbarger fracture" in the Old Santa Cruz Highway area: As noted in Chapter III, the "Tranbarger fracture," which received much attention in the first few days after the Loma Prieta earthquake, crossed Summit Road 2,100 feet east of Highway 17 (point A in Figure 4.6). From its northwestern end, it was mapped as extending approximately 2,200 feet to the southeast, with an average trend of N55°W that changed locally to slightly west of north where the fracture crossed Old Summit Road (U.S. Geological Survey Staff, 1989; Plafker and Galloway, 1989).

Figure 4.6, a portion of plate 4.1, shows this fracture and several other fractures, approximately parallel and to the southwest, which formed a zone approximately 600 feet wide along Summit Road. To the southeast, this zone was approximately 400 feet wide at Old Summit Road (B in fig. 4.6) and less than 100 feet wide at a point 650 feet farther southeast. Figure 4.6 shows this fracture zone continuing southeastward from this latter point to the southeast, expanding to a 400-foot-wide zone and ending near Old Santa Cruz Highway (C in fig. 4.6). The average trend of this somewhat discontinuous zone of fractures was N45°W. The zone extended for more than 4,000 feet and was thus the longest such zone in the

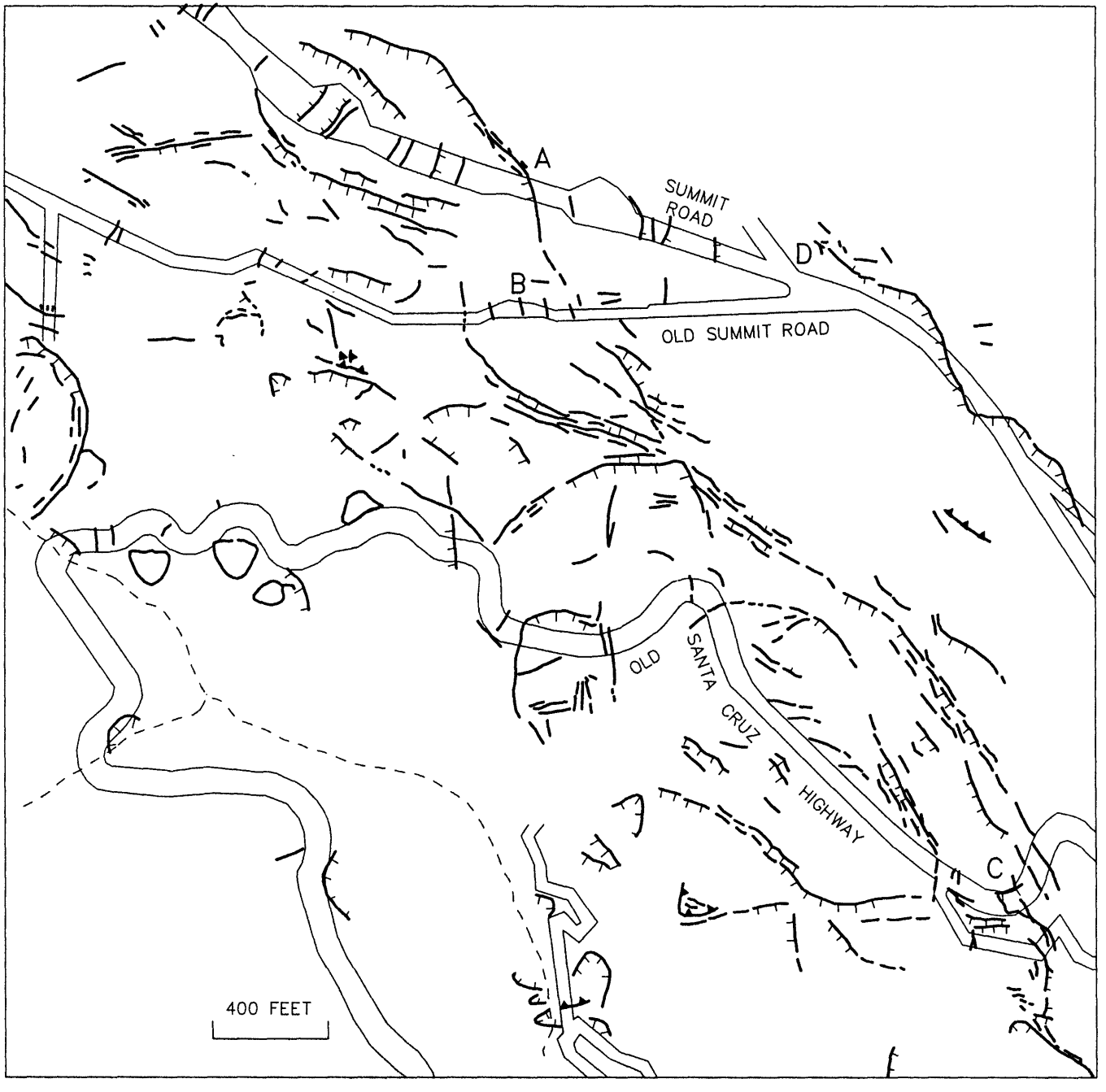

FIGURE 4.6 -- Ground cracks in part of plate 4.1 in Old Santa Cruz Highway area. Letters indicate specific localities discussed in text. Map symbols are the same as in plate 4.1.

Summit Ridge area. Trends of individual fractures in the zone were between N10°W and N65°W .

Near the northwestern limit of this zone, the vertical displacements across fractures were consistently downslope-side downward. Vertical displacements were generally less than 5 inches. Southeast of Old Summit Road, the zone was complex in terms of amounts and directions of displacements. There, several grabens formed. Farther southeast, upslope-facing and downslope-facing scarps faced away from each other, creating a horst (locally high block of ground). Still farther southeast, near the end of the zone, is another narrow graben. Vertical displacements in these areas were in the range between 2 inches and 2 feet, with an average vertical displacement of approximately 6 inches. Extension across fractures in this area was typically approximately 6 inches, and horizontal shear displacements were typically left-lateral and in the range between 1 inch and 2.5 feet.

The trend of this zone of fractures was parallel to the regional trend of bedding, and its extent, left-lateral shear component, and upslope-facing scarps are characteristics associated with structurally controlled fractures. However, the graben-forming scarps may also be part of a zone of fractures developing along the main scarp of a landslide; the left-lateral shear displacements were not large compared to the vertical displacements in most places, and the 4,000-foot-long fracture zone could well be the main scarp of a large landslide affecting much of the southwest slope of Summit Ridge. Because the fractures within this zone were developed along the regional trend, their origin is thus ambiguous. It cannot presently be determined with certainty whether the fractures in this zone merely developed along bedding planes due to seismic shaking, whether they indicate graben formation due to extension of the ridge crest in response to fault slip of combined right-lateral shear and high angle thrust, or whether they have developed in response to landslide movement along a large main scarp aligned parallel to regional structure.

b. 1,400-Foot-Long Fracture in the Old Santa Cruz Highway area: Another long fracture at least approximately parallel to the regional structural trend extends for approximately 1,400 feet southeast along Summit Road from near the Melody Lane-Summit Road intersection (D in fig. 4.6). The fracture intersects

Summit Road approximately 650 feet from its northwestern end; southeast of there, the fracture strikes parallel to the southwestern edge of Summit Road for approximately 200 feet and then recrosses Summit Road and continues parallel to the road for an additional 450 feet. The overall trend of this fracture is N40°W, and the trend varies locally from approximately N15°W to approximately N80°W. Throughout most of its length, this fracture is a single discontinuity with vertical displacements of as much as 1 foot, down to the southwest (downslope).

As with the "Tranbarger fracture" zone, this fracture has most of the characteristics of an opening along the regional structural trend. However, it also has characteristics of the main scarp of a large landslide. Unlike the "Tranbarger fracture" zone, the vertical displacement across this fracture was consistently downslope-side down, except for a few localities near the northwestern end where small (1 inch or less) vertical displacements occurred that were in the opposite sense (upslope-side down).

Ponti (1990, personal communication) has interpreted the displacement across this fracture as deformation along bedding on the northeast limb of the Summit Syncline, the axis of which trends N60°-65°W. He suggests that this fracture, as well as others in the vicinity, may reflect slippage along bedding surfaces as beds on both limbs of the syncline moved toward the center of the syncline. He further suggests that movement of beds toward the syncline center may be due to a slight opening of the syncline in response to NE-SW extension of the hanging wall (the block above the earthquake-generating fault rupture) resulting from the thrust component of the fault slip.

Whereas this postulated origin for the 1,400-foot-long fracture is consistent with vertical displacements along its length, this proposed explanation does not fit well with data from other fractures on the southwest limb of the syncline that have southwest-facing scarps, indicating movement of material in the opposite direction, away from the syncline center. In addition, the local topographic high is to the southwest of the center of the syncline. If movement on cracks in this area reflects gravitational movement toward the center of the syncline, then more northeast-facing fractures should have developed to the southwest of the topographic high, showing northeastward movement of beds on the southwest limb of the syncline.

A trench dug across the 1,400-foot-long fracture at a locality on the southwest side of Summit Road (Trench #1, described in Chapter V) showed that the fracture dips 45° to 63°SW. Data from the trench as well as surface data suggest that this feature could be the main scarp of a large, deep-seated landslide involving much of the southwest slope of Summit Ridge in this area. If both this fracture and those comprising the "Tranbarger fracture" zone are related to landslide movement, then the fracture along Summit Road would be a main scarp near the ridge top and the "Tranbarger fracture" zone would be a zone of internal scarps farther downslope and within a large landslide involving a major portion of the southwest flank of Summit Ridge between California Highway 17 and Old Santa Cruz Highway. An additional possibility is that this 1,400-foot-long fracture is related to a fault mapped at approximately the same location and with the same overall trend (McLaughlin and others, in press; see fig. 2.4). The fault, as mapped, extends beyond the present fracture, approximately 0.2 miles farther northwest and slightly more than 0.6 miles farther southeast. At present, the evidence is not conclusive as to the origin of this fracture, and any one, or possibly all, of these origins may be applicable.

C. Interpretation Of Structural and Landslide Fracture Patterns

Many fractures on Summit Ridge created by the Loma Prieta earthquake exhibited a complex interaction between landslide processes and processes responsible for the orientation and spacing of regional structures (such as bedding surfaces, joints, and faults). Of the two generic fracture groups, the landslide-related fractures evidently were superimposed on, and therefore postdate, the regional network of structural features.

1. Effect Of Regional Structure On Landslides

The spacing and orientation of regional structures within the area covered by plates 1 and 2 of Spittler and Harp (1990) evidently affected the shape and location of many of the margins of the larger landslides. Several examples of this are discussed below:

a. Upper Morrell Road landslide: This landslide, on the south flank of Summit Ridge, approximately 1,200 feet east of Taylor Gulch, shows a strong influence of regional structure on the location and shape of fractures forming its margins. Figure 4.7 shows that the zones of fractures forming the main scarp are aligned with fractures along the regional trend (N55°-60°W) for as much as 800 feet.

The fractures that formed the right flank of this landslide curved to the southwest from the main scarp area and trend approximately N20°E where they crossed Morrell Road. At that point, the fractures were predominantly right-lateral with approximately 2 feet of horizontal displacement and 6 to 10 inches of vertical displacement down to the southeast. Approximately 75 feet to the southwest along this fracture zone, its trend abruptly swung clockwise to N60°W (B in fig. 4.7), parallel to the regional structure. Immediately west of this trend change, the fracture became predominantly extensional and several upslope-facing scarp segments were present; maximum displacements on these were 2 inches. At this trend change, the fracture zone ceased to exhibit landslide characteristics and took on the attributes of fractures associated with regional structure.

b. Villa Del Monte area: Several zones in the Villa Del Monte area showed the interaction of the regional structure with the development of landslide fractures. Near the junction of Skyview Terrace and Bel Air Court, a fracture zone trending N50°W formed part of an internal landslide scarp (A in fig 4.8). This fracture zone was parallel to the trend of the regional structure. In a manner similar to the Upper Morrell Road landslide, the right flank of this fracture zone curved counterclockwise to the southwest to a trend of about N20°E.

Near the junction of Sunset Drive and Evergreen Lane, as well as immediately north of this intersection, are several fractures that are parallel to the regional structural trend but also display characteristics of fractures forming the main scarp of a large, deep-seated landslide. Most of this zone trends approximately N65°W, but the fracture near point B on figure 4.8 curves counterclockwise to a trend of N45°E as displacements change from being predominantly extensional to primarily right-lateral. The changes in trend and

FIGURE 4.7 -- Ground cracks in part of plate 4.2 in Morrell Road area. Letters indicate specific localities discussed in text. Map symbols are the same as in plate 4.2.

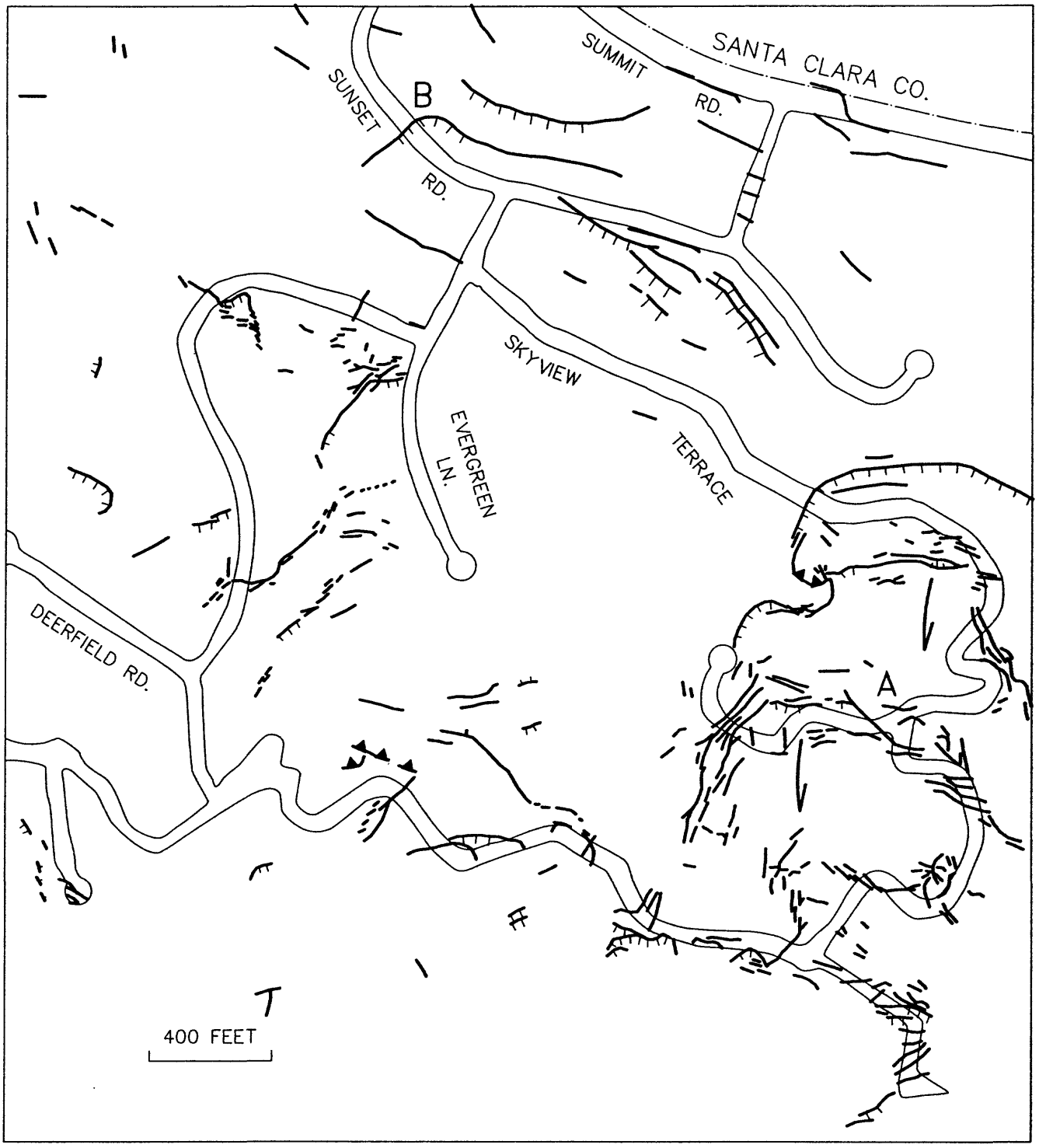

FIGURE 4.8 -- Ground cracks in part of plate 4.1 in Villa Del Monte area. Letters indicate specific localities discussed in text. Map symbols are the same as in Plates 4.1 and 4.2.

displacements along this fracture are common features of the transition from the main scarp to the right flank of a landslide.

One effect of the regional system of structural discontinuities on the shape of landslides along the south flank of Summit Ridge is to produce a consistent asymmetry in their horizontal dimensions. Generally, the right flanks are more completely developed than the left flanks, as, for example, in the Upper Morrell Road landslide (figs. 3.17 and 4.7) and in the Burrell landslide complex (fig. 3.10 and locality D in fig. 4.7). Another example of asymmetry, in the Villa Del Monte area (A in fig. 4.8), was described above.

c. Other Examples and Summary: Many other fractures approximately parallel to regional geologic structures extend across landslide boundaries or through landslides, evidently affecting the shapes of the landslides. The Burrell landslide complex (D in fig. 4.7) exhibits a N50°W-trending, structurally controlled fracture cutting through one of the main scarps in the landslide complex and continuing into the landslide. At point E in figure 4.7, a similar situation exists: A N50°W- to N67°W-trending fracture cuts across the Taylor Gulch landslide. Another example of structurally controlled fractures cutting across a landslide occurs on the Stetson Road landslide (fig. 3.22; plates 3.4 and 4.4), where fractures striking N60°W cut through the northwestern part of the main scarp and the right flank.

As these examples show, the pattern of fractures triggered by the Loma Prieta earthquake on the southwest slopes of Summit and Skyland ridges reveals an interaction between landslides triggered by the earthquake and a regional system of structural discontinuities, most likely bedding planes and faults that are subparallel to bedding. The interaction of the regional structure and landslides takes two forms. One form involves the influence that the spacing and orientation of the regional fractures have on the location and shape of fractures forming landslide boundaries, such as main scarps and flanks. This form also imparts an asymmetry to landslide shape in that fractures outlining left flanks of landslides are commonly poorly formed compared to fractures outlining right flanks. In several cases, the left flanks of landslides formed along fractures parallel to the regional network and were long and straight whereas fractures forming the right flanks were arcuate. The other

common form of interaction involves the cross-cutting of landslides by structurally controlled fractures.

D. Similarity Of Fractures in the Summit Ridge Area To Those Produced In Other Earthquakes

The pattern of cracks formed on the southwest slopes of Summit and Skyland ridges by the Loma Prieta earthquake exhibits some striking similarities to the fracture patterns produced in three other recent earthquakes--the 1986 Palm Springs, California; 1980 Irpinia, Italy; and 1980 El Asnam, Algeria, earthquakes all produced extensive zones of distributed fracturing and (or) reactivated landslides along and near the traces of the causative faults. These three earthquakes are discussed here to present additional context for evaluating the ground cracks and deformation patterns in the Summit Ridge area.

1. The Palm Springs, California, Earthquake

The July 8, 1986, Palm Springs earthquake (M_L 5.9) produced an extensive network of fractures in a diffuse zone along both sides of the Banning fault. This zone extended for 5.4 miles along the fault and was 300 to 1,000 feet wide on either side. Discontinuous fractures and landslides were most abundant and displacements were greatest where slopes were steepest within this zone, but gentle slopes and nearly level ground also were fractured. The fractures on nearly level ground were probably related to fault slip and not to slope movement. Intensely fractured ground along ridge crests was also a common feature within the fracture zone (Morton and others, 1989).

Much of the fracturing produced within the zone along the Banning fault was interpreted to have been caused by shallow gravitational slope movements (i.e., landslides) induced by the seismic shaking. However, because of the pattern of strong shaking and its distribution with respect to the fracture zone, strong shaking alone did not appear to explain the spatial frequency of fractures along the fault trace. Morton and others (1989) concluded that this

anomalous zone of ground fractures was a localized surficial response to static shear strain induced near the fault trace by rupture at depth. Their model, based on elastic dislocation theory, predicted that the surface fractures not caused by slope movements extended no deeper than 330 feet and that the fault rupture at depth extended only to within 2.4 miles of the surface and was not connected to the surface fractures.

The major difference between the fracture pattern created by the Palm Springs earthquake and that created by the Loma Prieta earthquake was the presence of fractures and slope failures on both sides of the Banning fault trace. By contrast, on Summit Ridge, most of the observed ground cracking was confined to the southwest side of the ridge or, at least, to the hanging wall of the San Andreas fault zone.

Similarities between the Palm Springs earthquake and the Loma Prieta earthquake are the respective source mechanisms, which were both right-lateral with a thrust component, and linear zones of discontinuous fractures away from the fault traces. In some respects, the Palm Springs earthquake is evidently a smaller analog of the Loma Prieta earthquake; both earthquakes induced many slope failures as well as fractures that were related, if not connected to, the subsurface fault ruptures. Indeed, the fractures created approximately parallel to regional trends of geologic structures by the Loma Prieta earthquake may have been generated as a response to strain caused by the fault dislocation at depth and not simply to shaking.

2. The Irpinia, Italy, Earthquake

The November 23, 1980, earthquake (M_S 6.9) that struck the Irpinian region of the Appenine Mountains in Italy produced landslides and ground fractures throughout a large area of the epicentral region (Cotecchia, 1982; Carrara and others, 1986). Many large, deep slump-and-earth-flow complexes were reactivated in Tertiary-aged flysch units; Pliocene-Quaternary clayey deposits; and fractured, marly and clayey limestones. Some of the landslides reactivated by this earthquake were reported to have exhibited continued slow movement for several months after the event.

Dramis and others (1982) described the effects of the earthquake within an area of 720 square miles, centered approximately 24 miles northwest of the epicenter, where more than 30 large landslides and approximately 100 large fractures were observed. In that area, the orientation of the fractures and the slopes on which the landslides were reactivated corresponded to directions parallel and perpendicular to the main northwest-trending Appenine structure.

The source mechanism for the Irpinian earthquake was that of a normal fault, typical of the extensional tectonics of the region (Cotecchia, 1982), which contrasts with the strike-slip and thrust mechanism of the Loma Prieta earthquake. No surface fault-rupture that could be established as being primary was found in the epicentral region.

In contrast to the relatively low ground-water levels in the Summit Ridge area at the time of the Loma Prieta earthquake, ground-water levels in the epicentral region of the Irpinian earthquake were high prior to and during the main shock, and many landslides reactivated by the earthquake continued to move for several months afterwards (Cotecchia and others, 1986). Additional landslides, as well as other coseismic fissures, were also widely scattered throughout a large area. Large landslides, with volumes of more than 40 million cubic yards, were reactivated as far as 48 miles from the epicenter.

3. The El Asnam, Algeria Earthquake

A recent earthquake showing perhaps even more similarities to the Loma Prieta earthquake in production of off-fault surface cracks, was the October 10, 1980, El Asnam earthquake in Algeria (M_S 7.3). That earthquake generated a 25-mile-long zone of primary surface rupture with local trends between N45°E and N80°E. The primary rupture was somewhat discontinuous over the 25 miles, but distances between individual fractures in the zone were generally less than 300 feet. The surface fault displacement was predominantly thrust with some left-lateral slip along the southern portion of the fault trace (fig. 4.9; Philip and Meghraoui, 1983; Sorriso-Valvo, 1986). The source mechanisms indicated a northward dip of approximately 50° (Ouyed and others, 1981). Few fractures developed south of the trace, on the footwall. However, along the

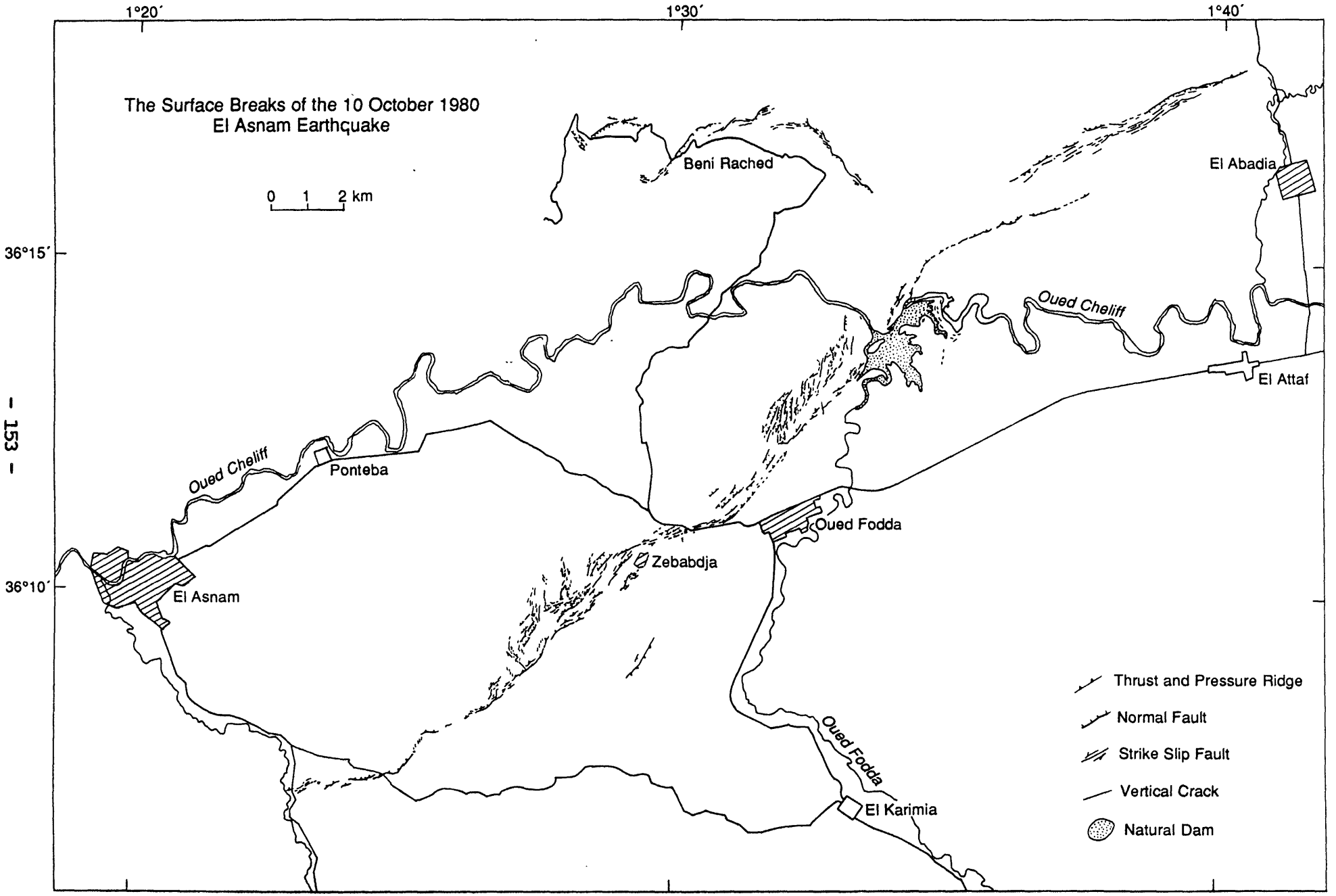

Figure 4.9. Map showing ground cracks from the October 10, 1980, El Asnam, Algeria, earthquake (after Philip and Meghraoui, 1983).

hanging wall near the main trace, were a variety of compressional and extensional fractures and landslides (rotational slumps) in a zone as wide as 0.6 miles.

Features that were compressional were evidently related to deformation at the leading edge of the thrust and the regional stress field associated with it. Pressure ridges south, or in front of, the thrust were observed in places where the thrust became imbricate and divided into multiple dislocations. Extension fractures, perpendicular to the fault trace and parallel to the inferred regional direction of maximum principal stress, were found primarily on the hanging wall side.

Several large rotational slumps were created where the surface of the hanging wall near the thrust fault was uplifted and folded. Landslide scarps were created immediately adjacent to the hanging-wall side of the fault and parallel to it, as the hanging wall was uplifted and brought into extension by folding in material near the ground surface (fig. 4.10).

Extension features parallel to the fault trace occurred both as simple extension cracks with little relative displacement and as large graben features (fig. 4.11). Other extensive grabens formed en echelon, with their long dimensions oriented at an angle of approximately 35° to the fault trace (Figs. 4.9 and 4.12). The en echelon pattern was right-stepping, consistent with extensional formation within a zone of left-lateral shear. Here, as in the case of the graben features previously discussed, vertical displacement occurred in response to extension being generated at the convex surface of arched or folded deposits in the hanging wall of the thrust (fig. 4.12).

Many large slumps and block slides were triggered as far as approximately 5 miles from the main fault trace. The most massive landslide occurred approximately 4.2 miles north of the main fault trace and involved an area of 5.8 square miles; this landslide was so large that it could as well be considered as being a gravity-slide tectonics feature (figs 4.9 and 4.13).

The similarities in the patterns of fractures and landslides produced by the El Asnam and Loma Prieta earthquakes are striking. Both earthquakes had source mechanisms made up of both thrust and strike-slip displacement components. Also, most of the off-fault fractures and landslides generated were confined to the hanging

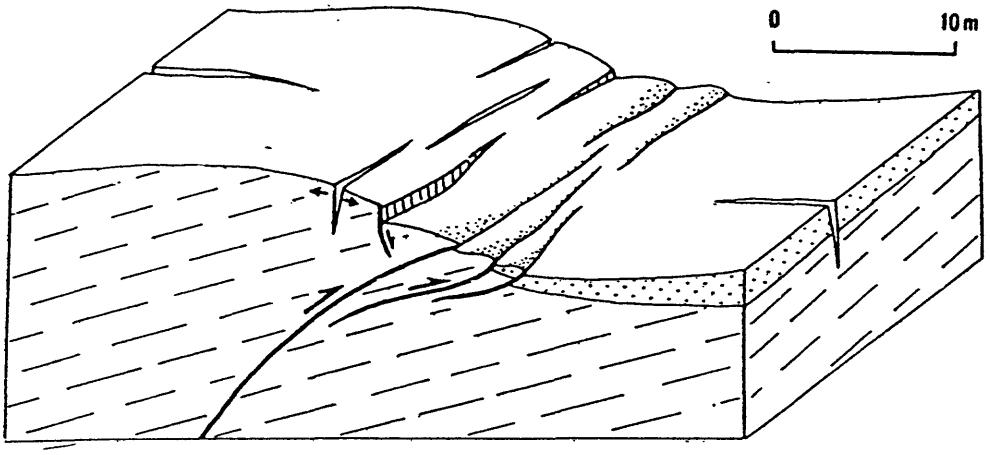

Figure 4.10. Conceptual block diagram showing relationships of pressure ridges, extension fractures, and slump scarps to main fault break in El Asnam earthquake (from Philip and Meghraoui, 1983).

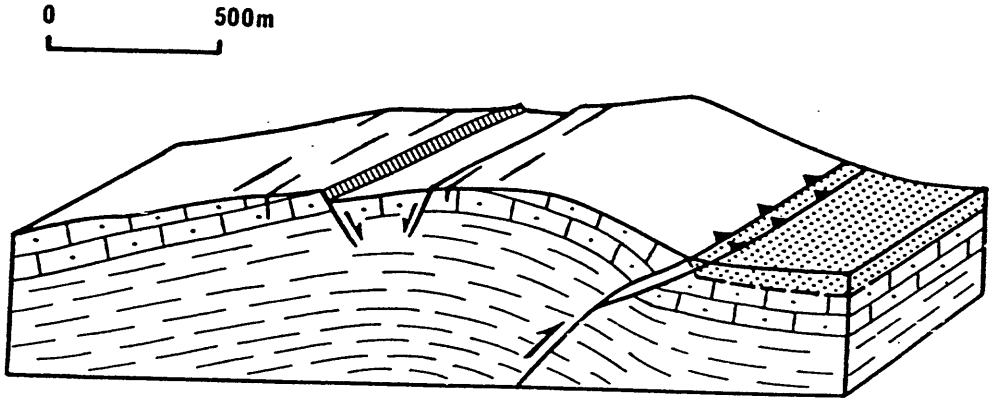

Figure 4.11. Conceptual block diagram showing relationships of graben features to main fault break in El Asnam earthquake (from Philip and Meghraoui, 1983).

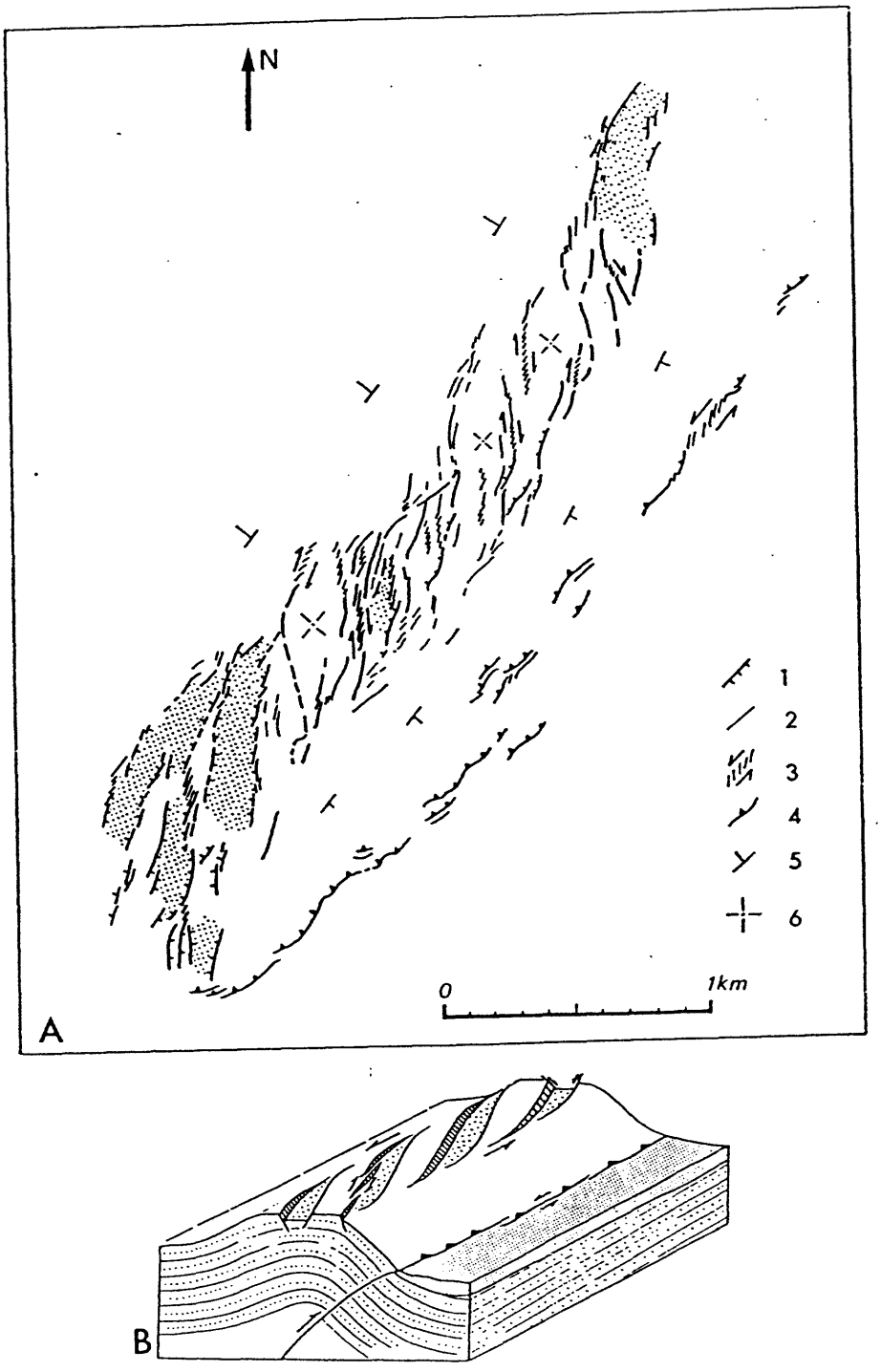

Figure 4.12. A. Map of a section of the main fault trace from the 1980 El Asnam earthquake showing en echelon graben features aligned at an angle approximately 35° to the fault trace. B. Conceptual block diagram showing relationship of en echelon graben features to the fault and to sense of horizontal shear present at this section of the fault break (from Philip and Meghraoui, 1983).

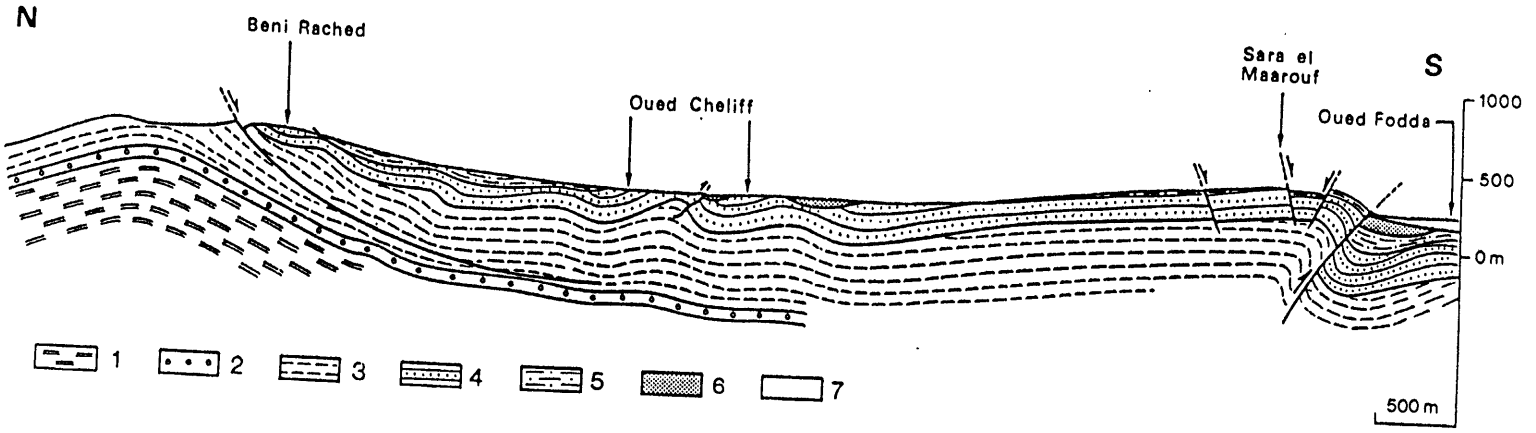

Figure 4.13. Cross section through large landslide to the north of the main fault break from the El Asnam earthquake. 1. Tortonian marls, 2. Tortonian sandstones, 3. Messinian marls, 4. Lower Pliocene sandstones and calcarenites, 5. Upper Pliocene conglomerates, 6. Old Quaternary conglomerates, 7. Recent Quaternary alluvium (from Philip and Meghraoui, 1983).

walls of the respective faults. In addition, both earthquakes produced hundreds of discontinuous extension fractures with little vertical or horizontal shear and with orientations subparallel to the main fracture zones.

The formation of graben features on the hanging walls of the thrust blocks in both earthquakes suggests that their formation also may be similar. The basic model of arching due to local uplift within the hanging wall causing extension and local normal fault-type displacement seems to be realistic and applicable in both cases although the magnitude of earthquake-induced displacement across graben margins was relatively small in the Loma Prieta earthquake.

Differences between the two earthquakes are also evident. The fault slip associated with the Loma Prieta earthquake was primarily strike-slip whereas that of the El Asnam earthquake was primarily thrust, and the sense of strike-slip motion on the two faults was opposite. Bedding in near-surface rocks in the El Asnam area is subparallel to the ground surface and directly reflects the deformation of this and similar past earthquakes, whereas bedding in the Summit Ridge area is more highly deformed. Lastly, the El Asnam earthquake produced prominent surface fault-rupture with surface offsets commonly more than 6.6 feet and maximum tectonic uplift of the ground surface of more than 20 feet, whereas the Loma Prieta earthquake produced little, if any, primary fault rupture at the ground surface and maximum regional uplift of only approximately 22 inches (Anderson, 1990; see fig. 2.6).

Despite the obvious differences between these two earthquakes, the patterns of surface fracturing and landslide generation were comparable in general if not in particular. The lack of vegetative cover and the greater fault displacements in Algeria permitted more complete observations of the relations between source mechanism and fracture patterns than was possible in the Santa Cruz Mountains. Although the orientations of lithologic units in the Summit Ridge area are not strictly coincident with surface morphology or geometry, the patterns of fracture and landslides produced by the Loma Prieta earthquake as well as the patterns of older landslide scarps and grabens appear to be consistent with mechanisms involving arching and extension within the hanging wall of a high-angle thrust and accompanying gravitational slope failure.

E. Summary

The systematic mapping of fractures triggered by the October 17, 1989, Loma Prieta earthquake revealed a complicated pattern that was inconsistent with the pattern previously expected from ground rupture in the San Andreas fault zone. The fractures were widely distributed on the southwest side of Summit Ridge, in a broad zone approximately 1.5 miles wide and 5 miles long, extending from near the California Highway 17-Summit Road intersection to Skyland Ridge.

The fracture patterns indicated that many landslides were triggered or reactivated by the earthquake and that most non-landslide fractures were aligned parallel to the regional trend of bedding or other structures. On the basis of the orientation, direction and amount of displacement, relation to adjacent landforms, and degree of curvature, most of the major fractures were separated into landslide-related or structure-related categories. Except for a short zone of fractures near the junction of Old San Jose and Summit Roads, none of the fractures were considered to be primary fault rupture.

The influence of the regional geologic structure was apparent in the trend and shape of many landslide margins. Main scarps of several large landslides developed along discontinuities that are part of the regional structure--probably mostly bedding surfaces. A distinct asymmetry was imparted to the shapes of many of the large landslides in that many right flanks were arcuate where they connected to their main scarps, whereas left flanks were typically straight, parallel to regional geologic structures, and not arcuate at points of intersection with main scarps. Some structurally-related fractures extended across landslide margins and through landslides with little deviation.

Two of the longest fracture zones--the "Tranbarger fracture" zone and another parallel to and east of it, along Summit Road--have many characteristics of landslide main scarps and may be associated with a landslide involving a large portion of the southwestern flank of Summit Ridge, yet these fracture zones also developed parallel to the regional structural trend and may have originated along bedding surfaces.

Finally, the Loma Prieta earthquake was similar to other recent earthquakes in production of off-fault fractures and landslides triggered near the faults. The 1986 Palm Springs, California; 1980

Irpinia, Italy; and 1980 El Asnam, Algeria, earthquakes produced extensive off-fault fractures and landslides. Extensional grabens and landslides developed as a result of the El Asnam earthquake, a thrust event with accompanying left-lateral shear displacement, and relations between thrusting, extensional arching, graben formation, fracture patterns, and landslide development in that earthquake appear to be analogous to relations between these phenomena in the Summit Ridge area, associated with the Loma Prieta earthquake (fig. 4.14).

F. References Cited

Carrara, A., Agnesi, V., Macaluso, T., Monteleone, S., and Pipitone, G., 1986, Slope movements induced by the Southern Italy earthquake of November 1980, Proceedings of the International Symposium on Engineering Geology Problems in Seismic Areas, v. 2, International Association of Engineering Geology, Bari, Italy, 1986, p. 237-250.

Clark, J.C., Brabb, E.E., and McLaughlin, R.J., 1989, Geologic map and structure sections of the Laurel 7.5 ' quadrangle, Santa Clara and Santa Cruz Counties, California: U.S. Geological Survey Open-File Map 89-676, scale 1:24,000.

Cotecchia, V., and Del Prete, M., 1986, Stability of Senerchia detrital plaque and Serra dell'Acquara mudslide, *in* Cotecchia, V., Luongo, G., Pagliarulo, R., Salvemini, A., Santagati, G., and Ventrella, A., eds., Proceedings of the International Symposium on Engineering Geology Problems in Seismic Areas-Post Symposium Technical Tour Excursion Guidebook, International Association of Engineering Geology, Bari, Italy, p. 30-33.

Cotecchia, V., 1982, Phenomena of ground instability produced by the earthquake of November 23, 1980, in southern Italy, Proceedings IV Congress International Association of Engineering Geology, India, v. VIII, p. 151-164.

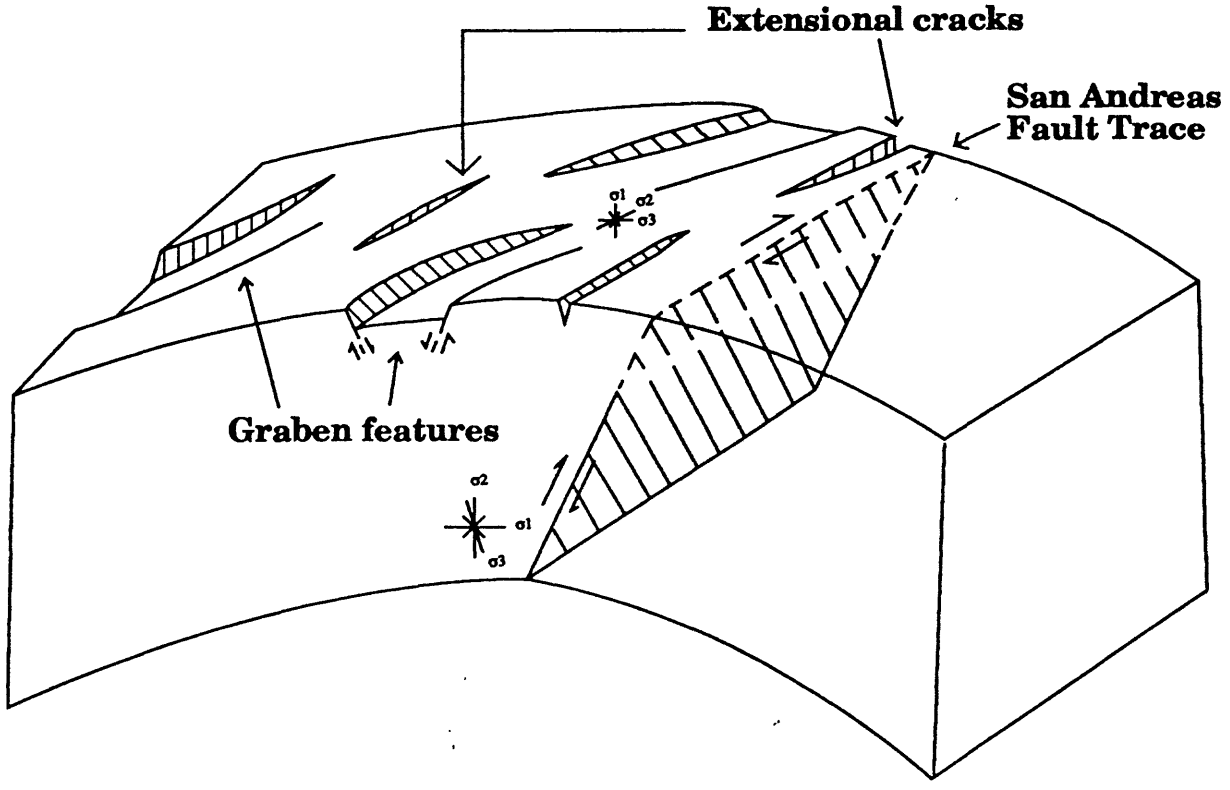

Figure 4.14. Conceptual block diagram showing relations between graben features and extension fractures in the Summit Ridge area and movement on the San Andreas fault zone as indicated by the source mechanism of the Loma Prieta earthquake.

Dramis, F., Prestininzi, A., Cognigni, L., Genevois, R., Lombardi, S., 1982, Surface fractures connected with the southern Italy earthquake (November 1980)-Distribution and geomorphological implications: Proceedings IV Congress International Association of Engineering Geology, India, v. VIII, p. 55-66.

Lawn, B.R., and Wilshaw, T.R., 1975, Fracture of brittle solids, Cambridge University Press, Cambridge, 204 p.

McLaughlin, R.J., and Clark, J.C., in preparation, Geologic map of the Los Gatos 7.5' quadrangle, Santa Clara County, California, U.S. Geological Survey Open-File Map.

Morton, D.M., Campbell, R.H., Jibson, R.W., Wesson, R.L., and Nicholson, C., 1989, Ground fractures and landslides produced by the North Palm Springs, California, earthquake of July 8, 1986, *in* Sadler, P.M., and Morton, D.M., eds., Landslides In A Semi-Arid Environment, v. 2, p. 183-196.

Ouyed, M., Meghraoui, M., Cisternas, A., Deschamps, A., Dorel, J., Frechet, J., Gaulon, R., Hatzfeld, D., and Philip, H., 1981, Seismotectonics of the El Asnam earthquake, Nature, v. 292, p. 26-31.

Philip, H., and Meghraoui, M., 1983, Structural analysis and interpretation of the surface deformations of the El Asnam earthquake of October 10, 1980, Tectonics, v. 2, p. 17-49.

Plafker, G., and Galloway, J. P., eds., 1989, Lessons learned from the Loma Prieta, California, earthquake of October 17, 1989: U.S. Geological Survey Circular 1045, 48 p.

Ponti, D.J., and Wells, R.E., 1990, Origin of surface ruptures that formed in the Santa Cruz Mountains, California during the Loma Prieta earthquake, Seismological Research Letters, Eastern Section of the Seismological Society of America, v. 61, p. 17.

Ponti, Daniel J., and Wells, Ray E., (in press), Off-fault ground ruptures in the Santa Cruz Mountains, California: Ridge-top spreading vs. tectonic extension during the 1989 Loma Prieta earthquake: Bulletin of the Seismological Society of America, 40 ms. p.

Sorriso-Valvo, M., 1986, Landslide activity in the area of the El-Asnam 1980 earthquake (Algeria): Engineering Geology Problems in Seismic Areas, International Association of Engineering Geology, Bari, Italy, v. XXI, p. 292-304.

Spittler, T.E., and Harp, E.L., 1990, Preliminary map of landslide features and coseismic fissures triggered by the Loma Prieta earthquake of October 17, 1989: U.S. Geological Survey Open-File Report, 90-688, 3 pls., 31p.

U.S. Geological Survey Staff, 1989, Preliminary map of fractures formed in the Summit Road-Skyland Ridge area during the Loma Prieta, California earthquake of October 17, 1989, U.S. Geological Survey Open-File Report 686, 1 sheet, scale 1:12,000.

CHAPTER V. TRENCHING INVESTIGATIONS

Trenching is an investigative technique that utilizes excavations to examine geologic structures. Trenching is often carried out to evaluate faults, since fault movement characteristically causes deformation of older deposits, or causes new deposits to form, all of which may be visible in the sidewall of an excavation. Information gained from examining the deposits exposed in the trench can be used to learn about the past behavior of the fault. Such knowledge then forms the basis for predictions of future behavior. Trenching is one means through which geologists can evaluate the hazards from geologic processes and potentially extend the historical record of ground displacements into prehistoric times.

The techniques used in trenching are not just applicable to faulting, but to any geologic process that affects sediment deposition, or alters the pattern of existing deposits. This chapter discusses the application of trenching to structures responsible for ground-cracking during the Loma Prieta earthquake. The chapter is divided into two sections: a report on a geologic trenching investigation that was conducted under the auspices of the TAG, and a review of previous trenching investigations contained in geologic reports on file with SCC. The purpose of the studies described in both these sections was the same: to examine sub-surface exposures in the study area for information that may be useful in evaluating geologic hazards.

In the most fundamental sense, the process consists of answering simple questions: can the various types of cracks observed during the earthquake be identified in the sub-surface? What do they look like? Can they be identified at depth? If so, how deep? How large are they? Have displacements occurred across them in the past? If so, how much and how often? Could their locations have been predicted in advance? Could the amount of movement that occurred on these cracks have been predicted? Answers to these questions allow one to make judgments about the hazards to existing or future development. More importantly, they may permit the risks from recognized hazards to be reduced or eliminated.

A. Trenching Investigation of Co-seismic Ground Cracking

1. Introduction

To help assess the hazard associated with co-seismic ground displacements (including landslides) in the study area, a trenching program was undertaken to document past behavior of the geologic structures associated with ground deformation during the Loma Prieta earthquake. Exploratory trenches were excavated at two sites selected by the TAG. Both sites were selected because they were associated with well-defined crack systems, their geologic settings suggested that they contained the youthful geologic deposits needed in the analysis, and access was provided by the land owners.

The goal of this trenching investigation was to determine, to the extent possible, the age, magnitude, and frequency of occurrence of past ground-cracking events. The first trench was excavated across a ground crack following the 1,400-foot-long scarp along Summit Road in the Old Santa Cruz Highway area. The trench was located adjacent to Summit Road, approximately 1 mile southeast of the intersection of that road and California Highway 17 (fig. 5.1). As discussed in Chapters III and IV, this ground-cracking feature has characteristics consistent with an origin as a landslide scarp, a structurally controlled ground crack, or both.

The second trench was excavated across a crack that follows the main scarp of a conspicuous, older landslide in the Burrell landslide complex, on the southwest side of Summit Road, approximately 2.5 miles southeast of the intersection of Summit Road and California Highway 17 (fig. 5.2). This older landslide was depicted as a "definite" landslide deposit on the map of Cooper-Clark and Associates (1975).

2. Methodology

This study concerns only the movement history of the geologic structures and associated ground cracks that were investigated. Although a landslide or other origin may be mentioned in the text, determining the specific driving mechanism or process was not the primary concern of the trenching investigations. What is important is

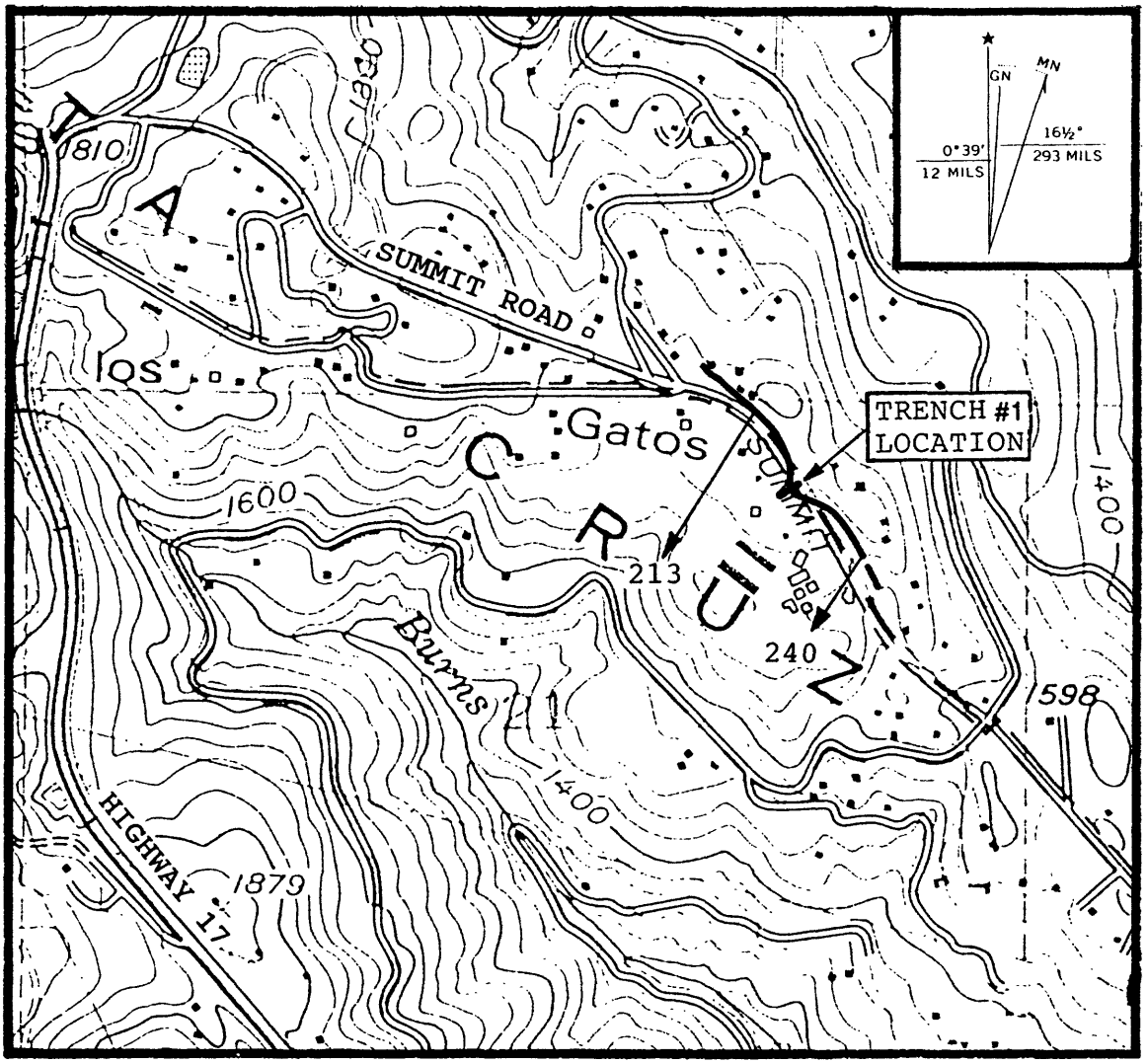

SCALE

1000 0 1000 2000 3000 FEET

213 ← mm OF TOTAL DISPLACEMENT

BASE MAP FROM U.S. GEOLOGICAL SURVEY LOS GATOS QUADRANGLE, 7.5- MINUTE SERIES. CRACKS FROM U.S.GEOLOGICAL SURVEY OPEN FILE REPORT 89-686.

MAP SHOWING LOCATION OF TAG TRENCH #1

FIGURE 5.1

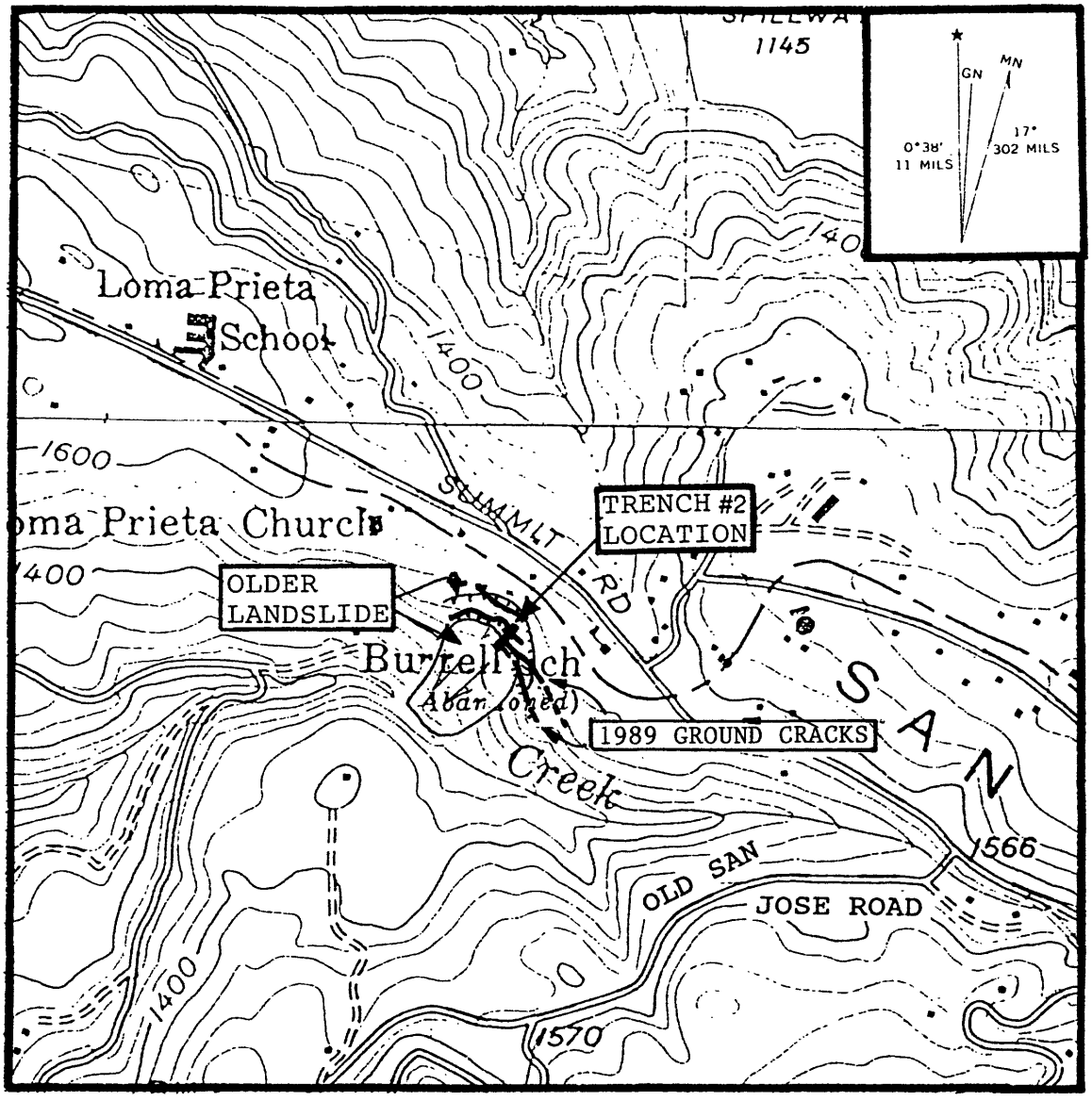

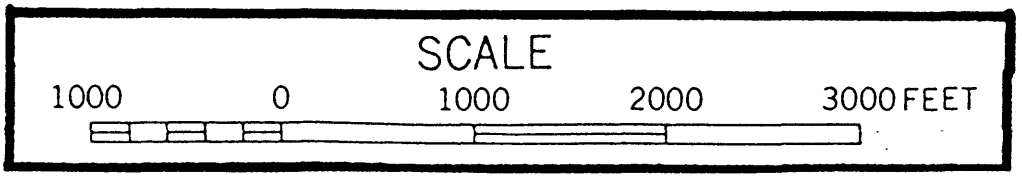

BASE MAP FROM U.S. GEOLOGICAL SURVEY LAUREL AND LOS GATOS QUARDANGLES, 7.5-MINUTE SERIES, LANDSLIDE FROM COOPER-CLARK AND ASSOCIATES, 1975. CRACKS FROM PRELIMINARY GROUND CRACK MAP, SANTA CRUZ COUNTY PLANNING DEPARTMENT.

MAP SHOWING LOCATION OF TAG TRENCH # 2

FIGURE 5.2

that during recent geologic history these structures have been subject to repeated small movements, in which each identifiable movement produced a steep scarp, or step, in the ground surface, often accompanied by an open crack or "fissure." Because of the steepness of these scarps, they are rapidly eroded and debris is deposited at the base of the scarp and (or) within the fissure.

In ideal cases, where individual movements have been sufficiently large and infrequent, a record of each movement may be preserved as an identifiable layer of debris overlying deposits from previous movements, and underlying deposits of subsequent movements. A trench excavated across such a structure may reveal those debris layers preserved in the sedimentary record. If the ages of individual layers can be determined, it is possible to discover approximately when each movement took place, and thus to determine how frequently such displacements have occurred. The stratigraphic record may also be analyzed to find and quantify the displacements associated with past movements.

The information produced from these studies is termed the movement history. Based on the movement history, it is possible in an ideal case to estimate, in a statistical fashion, the time and size of the next movement. Because the geologic record in the two trenches was less than ideal, the present study did not provide detailed movement histories on either of the structures examined. Nevertheless, the trenches did provide useful and important information for evaluating risk in the study area.

3. Analytical Dating Program

To provide age control on the stratigraphy and structural relationships observed in the trenches, nine samples were submitted for carbon-14 radiometric dating to the Center for Accelerator Mass Spectrometry, Lawrence Livermore National Laboratory, Livermore, California. Seven samples were obtained from trench #1, and two from trench #2. All dating was carried out under the supervision of Dr. John S. Vogel, a specialist in carbon-14 dating. Five of the dates were taken from charcoal or decaying plant matter and four were taken from bulk low-carbon soil. All samples were pre-treated to remove carbonates, root hairs, or other potential contaminants, and then were burned to produce CO_2 gas for dating. Only the light fraction (matter with specific gravity less than approximately 2.0)

from the soil samples was processed for dating. The results of the dating program are summarized in table 5.1.

B. Trench #1

As described in Section VA, trench #1 was excavated across a large scarp that trends along the crest of Summit Ridge, nearly parallel to Summit Road (fig. 5.1). The ground crack that parallels this scarp is arcuate in plan view, concave towards the southwest. The ground crack crosses Summit Road at two closely spaced locations near its mid-point, forming a local, southwest-facing salient. The trench location coincides with this salient and with a localized topographic depression formed on the down-dropped (southwest) side of the scarp. The axis of this depression is a former alignment of Summit Road. Therefore, the surface topography at this location had been previously altered by grading.

Displacement measurements taken at two locations along the ground crack yielded a consistent direction of S32°W for the slip vector, and a net slip of 0.7 to 0.8 feet. The scarp showed approximately 0.6 feet of vertical separation and 0.4 feet of horizontal separation where crossed by the trench alignment.

Bedrock in this vicinity was mapped by McLaughlin and others (in press) as Vaqueros Sandstone, a sequence of thick-bedded to massive, yellowish-gray, fine- to coarse-grained arkosic sandstone with a thick glauconitic sandstone bed in the lower part. This mapping indicates that the trench site lies on the southwest dipping limb of the Summit Syncline, adjacent to and slightly northeast of the synclinal axis (fig. 2.4). The orientation of bedrock in the trench was very weakly expressed. Dip, inferred from oriented mica flakes and an irregular lens of siltstone, was approximately 45°SW.

1. Trench Description

Approximately 100 linear feet of backhoe trench, 36 inches wide, were excavated. The trench varied in depth along its length from 11 to 18 feet and extended across the scarp and the adjacent topographic depression. The trench exposure, depicted on plate 5.1, revealed Vaqueros sandstones and shales offset in a normal sense by

TABLE 5.1: AGE DATING REPORT

CENTER FOR ACCELERATOR SPECTROMETRY

Lawrence Livermore National Lab

CAMS #	Indentification		delta 13_c	D 14_c	+	Age yrs B.P.	+
838	CC-1-11	charcoal	-25	-710.2	8.6	9950	240
839	CC-1-13	charcoal	-25	-712.2	3.9	10000	110
840	CC-1-1	leaf	-25	169.5	11.7	Modern	
841	CC-1-15	charcoal	-25	- 3.9	9.7	<130	
842	CC-1-17	charcoal	-25	-53.9	10.2	450	90
843	CC-1-19	low density soil fraction	-25	-160	18.2	1400	180
844	CC-1-16	low density soil fraction	-25	37.0	12.0	Modern	
845	CC-2-12	low density soil fraction	-25	-325.9	11.9	3170	150
n/a	CC-2-13	low density soil fraction	n/a	n/a	n/a	2000	140

Notes:

1) Delta 13_c values are the assumed values according to Stuiver and Polach (Radiocarbon, v. 19, p. 355, 1977) when given without the decimal places. Values measured for the material itself are given with a single decimal place.

2) The quoted age is in radiocarbon years using the Libby half life of 5568 years and following the conventions of Stuiver and Polach (ibid.).

3) Charcoal, leaf and twig samples were pretreated by the usual wash in 0.1N HCI to remove carbonates, 3-4 washes in 0.1N NaOH until the solution remained translucent (to remove humic acids), followed by a re-acidification in 0.1N HCI. CAMS 843-845 were measured on the soil fraction which was less than 2.0 mg/ml in density, primarily charcoal, separated from the bulk, dried soil using a solution of sodium polytungstate. The floated material was visually inspected for root hairs and was washed in 0.1N HCI. The samples were deemed too small for repeated hydroxide washes.

a southwest dipping shear surface. ("Normal" displacement denotes that the block of material above a shear surface moved down relative to the block below.) A sequence of colluvial deposits approximately 12 feet thick overlies the relatively down-dropped block. Figure 5.3 depicts a generalized geologic cross section through the trench.

The shear surface is a sharply defined parting surface lined with a 1/8-inch-thick layer of gray clay and a band of iron-oxide staining. The shear surface strikes N30°W to N35°W in the trench, with the dip increasing with depth from 45°SW to 63°SW. The upper part of the shear surface thus appeared to be approximately parallel to bedding as best as could be determined. Slickensides were observed on the shear surface raking 76 to 77° to the southeast, corresponding to a slip vector with a trend and plunge of S30°W, 60°SW. (The "rake" is the angle between strike--a horizontal line lying within the plane--and the line in question, measured in the plane.) Movement therefore appears to be dominantly normal, dip-slip, with a slight left-lateral (horizontal) component. Although movement appears to be occurring along bedding surfaces, the slip vector points directly downhill, rather than directly down dip. It has been suggested (Dan Ponti, U.S. Geological Survey, personal communication, 1990) that the left-lateral component of slip is a result of divergence between the downslope direction and dip direction. This explanation is consistent with observations, and it implies that the cracking was being driven by gravity (and therefore by landslide movement) and not by relief of tectonic forces on a deep-seated failure surface.

Normal displacement on the shear surface was evidently accompanied by headward rotation of the down-dropped block, forming a topographic basin at the site (fig. 5.3). No evidence for a matching boundary structure on the southwest side of the basin was observed in the field nor is one required to explain the geometry of existing deposits.

A family of arching, secondary fractures radiates away from the shear surface into the bedrock and the colluvial sediments on the down-thrown block, visible on plate 5.1 as a series of faint, curving lines between stations 10 and 40. Parts of these fractures were open at the time of the investigation and were clearly the result of small dislocations produced by the Loma Prieta earthquake. The relatively shallow inclination of the shear surface near the top of the trench,

FIGURE 5.3

TOPOGRAPHIC PROFILE AND GENERALIZED CROSS SECTION, TAG TRENCH #1

TOPOPGRAPHIC PROFILE DRAWN THROUGH TAG TRENCH #1

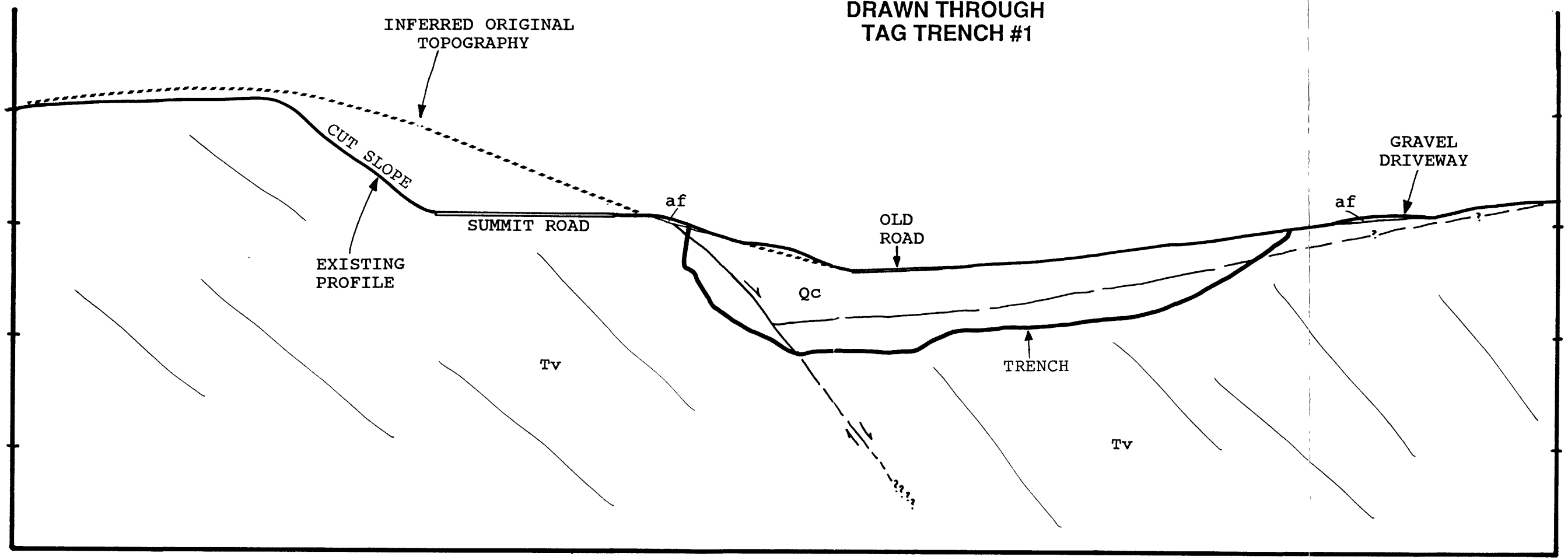

af ARTIFICIAL FILL

Qc COLLUVIUM

Tv VAQUEROS SANDSTONE

SCALE (FEET)

0 20 40

H = V

1/91

compared to its steeper dip at depth, evidently restrained downward movement of the surficial soils. These fractures, therefore, probably formed as a result of bridging of the near-surface soils over the zone of shear. Open voids were created along the arches defined by the fractures as the underlying sediments slipped without the same restraint.

Relative compression over the crests of the arches, or "bridges" formed by these secondary cracks resulted in a few apparent thrust-type displacements, one of which clearly offsets unit $1C_2$ in a reverse sense near station 20.5 (plate 5.1). Several of these fractures also offset the main shear surface slightly where they intersect. The larger of these secondary fractures are filled with a fine, powdery, horizontally laminated silt that infilled voids formed by earlier episodes of movement; this silt was probably transported and deposited by ground water.

A series of faint, poorly defined shear surfaces was observed parallel to the primary shear surface in bedrock within the down-dropped block (See note 15 on plate 5.1, near station 15). These shears are truncated at the bedrock/colluvium contact, indicating movement on these fractures occurred prior to the offset responsible for accumulation of the colluvial wedge.

2. Movement History

The long-term displacement history on the shear surface in this trench is demonstrated by analysis of the colluvial wedge overlying the relatively down-dropped block. A detailed description of the colluvium and associated soil horizons was made at station 39 in the trench. This description defined two buried soils, represented by B horizons corresponding to units $1D_2$ and $1D_3$, in addition to the modern soil horizon, units $1A_4$ and $1A_5$ (plate 5.1). All three soils were formed in a depositional basin on the down-dropped block. The two buried B soil horizons merge and appear to pinch out laterally toward the edges of the basin. All three soils show only weak development. Soil-horizon descriptors are shown on plate 5.1 at station 39; elsewhere in the trench logging, some of the individual soil horizons were grouped into composite units for simplicity.

The presence of the buried soil horizons is an indicator of depositional history, because the soils demonstrate changes in the

rate of sedimentation taking place on the block on the down-dropped side of the shear surface. Soil profiles require a relatively stable ground surface to form. Therefore, they indicate periods when the rate of sediment influx was low. Changes in the rate of sediment influx at this site may have been caused by either of two primary factors: changes in climate, principally in the amount of precipitation, and changes in local relief due to displacement on the shear surface that was noted in the trench. If the variations in sediment influx are related to displacement on the shear surface, then the soil horizons indicate significant, long term variations in displacement rate. Otherwise, they reflect climatic changes that may be of scientific interest, but tell little about the movement history of the structure. It was not possible to determine with certainty which of these two factors was primarily responsible for changes in the rate of deposition at the trench site. However, it is clear that deposition of the colluvium is ultimately being driven by offset on the shear surface, since colluviation is taking place into a basin created by displacement across this surface.

The following sections describe the early depositional history of the colluvial wedge, as suggested by the soil stratigraphy, and the recent movement history of the shear surface, as deduced from young colluvial deposits.

a. Depositional Episode, Event #1: Initial deposition of colluvium evidently began approximately 10,000 years ago, as indicated by dating of charcoal samples CC-1-11 and CC-1-13 (table 5.1 and plate 5.1) from the base of the colluvial wedge. Deposition occurred more rapidly than the rate of soil formation, and included deposition of 6 to 7 feet of colluvium. The lack of stratigraphy or additional soil horizons in these deposits suggests that the depositional process was relatively uniform colluviation.

b. Soil-Forming Episode, Event #2: Following this depositional episode was a hiatus in deposition, or at least a substantial decrease in sedimentation rates, during which time a soil profile developed on the section, consisting of A and E horizons (now included in unit $1D_2$), and a B horizon (unit $1D_3$). No quantitative assessment of the time required to form this soil was prepared. However, based on comparison with dated soil profiles elsewhere

and the carbon-14 dates obtained from the trench, a time scale of several hundred to, at most, a few thousand years is considered to be appropriate.

c. Depositional Episode, Event #3: The first period of relative quiescence was followed by a second period of deposition that included accumulation of an additional 2 feet of colluvium.

d. Soil Forming Episode, Event #4: A second soil profile, now buried, formed on the colluvium, partially overlapping the first soil. Unit $1C_2$ and $1D_2$ comprise the E and B horizons, respectively, of the newer soil, with the newer B apparently forming on the A and E horizons of the earlier soil. This soil signals a second period of relative stability of the surface, again on a time scale of several hundred to a few thousand years.

The two buried argillic soil horizons denoted by units $1D_2$ and $1D_3$ on plate 5.1 merge and then appear to die out as they approach the shear surface. The upper portion of unit $1D_1$ also has a weak argillic character and probably represents a continuation of $1D_2$ and $1D_3$ towards the shear surface; however, $1D_1$ lacks the distinctive characteristics used to map $1D_2$ and $1D_3$ to the southwest.

e. Depositional Episode, Event #5: Following formation of the second buried soil horizon, colluvial deposition resumed, but at rates slow enough to permit formation of the modern cumulic soil horizons. Total sediment accumulation during this episode amounted to approximately 4 feet of colluvium adjacent to the shear surface and 2 feet of colluvium in the center of the basin. This most recent depositional history is associated with a more detailed record of displacement on the shear surface, visible as a series of colluvial wedges and colluvium-filled older fissures adjacent to the shear surface.

Units $1A_2$ and $1A_3$ (plate 5.1) clearly show thickening of the colluvial sediments on the relatively down-dropped side of the shear surface in the trench, indicating progressive offset along the shear

surface through time. This thickened colluvial wedge is separated from the corresponding sediments on the relatively upthrown side of the shear surface by a seam of vertically oriented deposits that represent older crack-fill sediments ($1B_1$, $1B_2$, $1B_2'$, and $1B_3$, plate 5.1). The youngest crack fill, $1B_1$, dates from the 1989 earthquake. The other crack fill sediments are progressively older and less well defined and were not correlated with specific older events.

Units $1A_2$ and $1A_3$ were identified by subtle but distinct differences in fabric and structure and are separated by a distinct contact marked by an alignment of small sandstone pebbles and some localized laminae of fine, light-colored sand. In addition, several shears that penetrate unit $1A_3$ are truncated at the contact with $1A_2$. No internal structure that might suggest further subdivision of these units was observed. These two units are therefore interpreted to represent two movement episodes, separated by a longer time interval.

The base of unit $1A_3$ is displaced approximately 4 feet (measured vertically) from the base of unit $1A_1$, indicating that approximately that amount of movement has taken place on the crack system since the most recent episode of colluvial deposition began. The base of unit $1A_2$ is displaced somewhat less than 2 feet from the base of unit $1A_1$. Two carbon-14 dates were obtained from these deposits, one each from units $1A_2$ and $1A_3$. These dates were used to constrain the rate of displacement on the crack system. The following sections outline the movement history suggested by observations in the trench.

f. Movement 1: Renewed movement on the shear surface resulted in offset of the base of unit $1C_2$ and deposition of colluvium as a single layer, now represented roughly by all or portions of units $1A_1$, $1A_3$, and $1A_4$. Carbon from a soil sample obtained approximately 1 foot above the lower contact of unit $1A_3$ yielded a radiometric age of $1{,}400 \pm 180$ years before present (ybp) (See table 5.1). This date indicates that the event which led to resumption of relatively rapid colluvial deposition occurred somewhat prior to that time, probably on the order of a few hundred years (between 250 and 600 years prior, based on calculations of average sedimentation rates derived for the colluvial wedge).

g. **Movement 2:** A second movement or series of movements offset unit $1A_3$ from unit $1A_1$ and led to the deposition of unit $1A_2$. This episode of movement probably coincided with beginning of formation of the series of older crack-filling sequences visible on plate 5.1 as units $1B_2$ and 1B3. A carbon-14 date from a piece of charcoal located approximately 0.8 feet above the lower contact of unit $1A_2$ yielded a date of less than 130 ybp. Because of the limitations of carbon-14 dating in very recent materials, this date may be accepted as an indication that the material is young--approximately 300 years old or less--but should not be construed as a precise age. Using the range of sedimentation rates calculated for the trench, and an age range for the sample of 0 to 300 years, this date suggests that deposition of unit $1A_2$ began between approximately 200 and 800 years ago, with an older age considered more likely. This approximate age is compatible with the 1400 ybp age found by carbon-14 dating of a sample in the underlying deposit.

h. **Movement 3 (Recent Movement):** The most recent episode of movement displaced unit $1A_2$. An approximate vertical separation of 1.8 feet was measured assuming that unit $1A_2$ was originally continuous with unit $1A_1$. Evidence for two recent movements is discernable. The most recent is the offset of 0.6 feet caused by the Loma Prieta earthquake. An earlier displacement is suggested by the fill layer (Af_1) overlying the area on the downthrown side of the most recent ground cracking. This fill layer is not represented by a corresponding fill layer on the upthrown block. This indicates that the fill was placed against a pre-existing escarpment, either one left from a previous displacement on the shear surface, or one resulting from cultural disturbances (grading). It is possible that the fill was placed against a cut made during grading rather than against a pre-existing scarp. However, three observations argue against this interpretation. First, the edge of the fill wedge coincides precisely in location with previous ground cracking on both sides of the trench. Second, an oak tree, approximately 3 feet in diameter, is growing adjacent to the trench; the presence of this tree precludes any grading by heavy equipment at this location. Finally, the cumulative vertical separation measured on the lower contact of unit $1A_2$ is the same as the sum of the 1989 separation and the height of the scarp against which the fill was

placed. Therefore, it is believed that the older scarp represents displacement that occurred relatively recently, probably during the 1906 earthquake, since it is unlikely that the scarp would have been preserved for a much longer period of time.

3. Summary and Discussion

Deposition of colluvium on the down-dropped side of the shear surface in the trench commenced approximately 10,000 years before present. The colluvial wedge preserves evidence for three episodes of relatively rapid colluviation, separated by two periods of soil formation. The third episode of deposition, which continues at present, commenced between approximately 1650 and 2000 years before present, as estimated from carbon-14 dates combined with calculated sedimentation rates.

Three separate episodes of displacement were discerned in the colluvial section formed in response to the third major period of movement. The first is marked by offset of the youngest buried E horizon (unit $1C_2$) prior to approximately 2000 to 1650 ybp, followed by deposition of unit $1A_3$. The second is distinguished by offset of unit $1A_3$ by approximately 2 feet and deposition of unit $1A_2$ sometime after 1400 ybp, possibly between 200 and 800 ybp. The third definitive displacement episode offset unit $1A_2$ by slightly less than 2 feet. This displacement includes approximately 0.6 feet of vertical separation during the 1989 Loma Prieta earthquake, and an additional 1.2 feet of vertical separation prior to that. Circumstantial evidence points to the 1906 San Francisco earthquake as the most logical choice for that earlier event. Note that the number of movement episodes indicated by the stratigraphic record represents a minimum number of actual movement events. From this evidence, therefore, a minimum of four displacements in the last 2000 to 1650 years took place.

If the supposition concerning a 1906 event is correct, vertical separation on the ground surface at that time was approximately 1.2 ft, almost twice the displacement that occurred in 1989. This difference in displacement is consistent with the larger magnitude of the 1906 earthquake and with the reported differences between observed 1906 and 1989 displacements at other localities.

Cumulative displacement on the shear surface throughout the

Holocene cannot be precisely evaluated, because no single pre-Holocene datum occurs on both sides of the structure. However, total Holocene throw (vertical separation) on the shear surface can be approximated from the topographic profile through the trench if one assumes that: (1) erosion rates at the crest of the ridge are small and therefore the present ridge-crest elevation approximates the early Holocene surface, and (2) the bedrock surface on the downthrown block was originally continuous with that on the upthrown block. The separation measured in this manner is approximately 40 feet and is shown diagrammatically in figure 5.4. This throw translates to dip separation of approximately 60 feet and an average slip rate of approximately 6 feet per 1,000 years, or approximately eight Loma Prieta type events per 1,000 years.

The slip rate determined from offset data in the recent colluvial deposits shows a large range because of uncertainty about the time at which displacement of unit $1A_3$ began. Using a maximum age of 1400 ybp and a cumulative dip separation on the basal contact of unit $1A_3$ of 6 feet, a slip rate of 4.25 feet per thousand years is calculated. A minimum age for offset of unit $1A_3$ is less constrained. Using a best-estimate minimum age for beginning of deposition of unit $1A_2$ of 500 ybp, a slip rate of 12 feet per thousand years is determined. While not precise, these rates bracket the likely long-term rate.

Based on preceding observations, movement on the shear surface observed in the trench probably has been episodic, rather than uniform through time. If one presumes, for the sake of discussion, that movements on the shear surface were entirely co-seismic, a range of recurrence intervals can be calculated from different assumptions regarding single-event slip magnitudes. If the total dip slip of 0.8 feet that occurred in 1989 were the characteristic event for this structure and total dip slip in the last 10,000 years were approximately 60 feet, then the total slip implies approximately 75 events in the last 10,000 years, or a long-term average of one per 133 years. If it is assumed that the buried soils in the trench represent two periods of quiescence on the shear surface as long as few thousand years each, the actual frequency of events during periods of movement may have been as much as double the long-term average, or one event per 67 years.

In contrast, if one computes recurrence intervals for a characteristic event such as that suggested by the inferred offset in

FIGURE 5.4

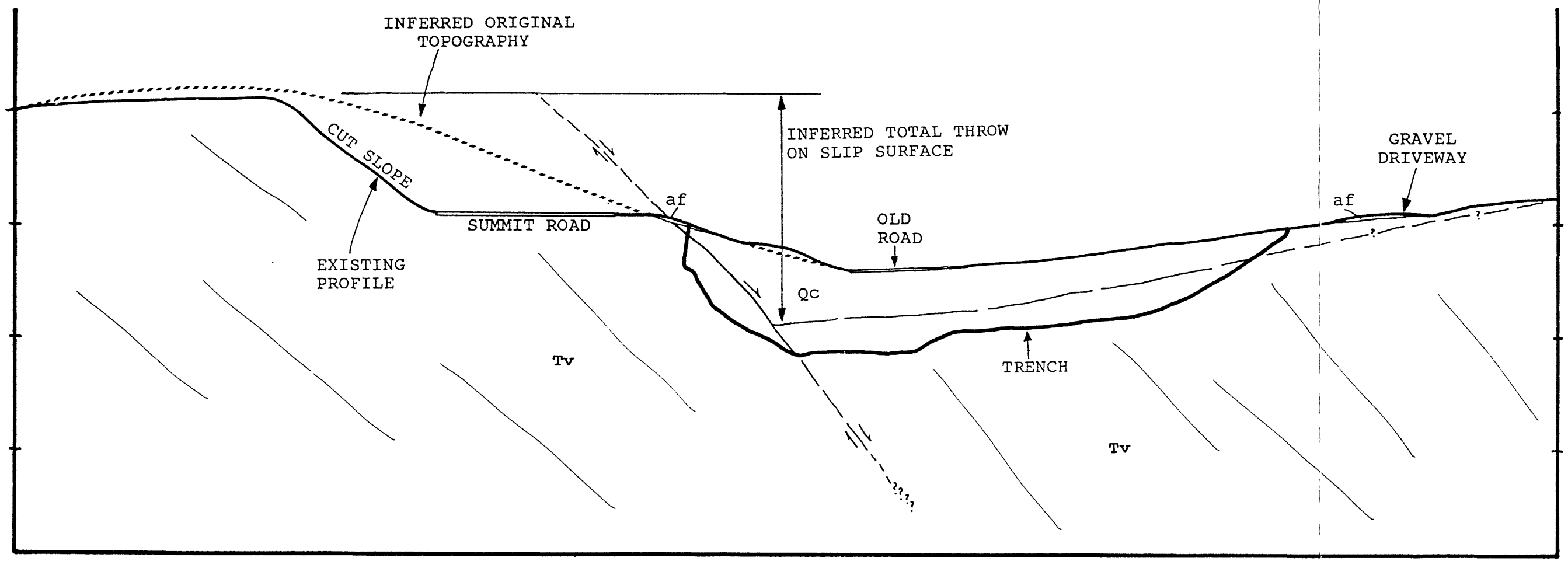

af ARTIFICIAL FILL

Qc COLLUVIUM

Tv **VAQUEROS SANDSTONE**

SCALE (FEET)

0 20 40

H = V

TOPOPGRAPHIC PROFILE DRAWN THROUGH TAG TRENCH #1

TOPOGRAPHIC PROFILE

TAG TRENCH #1

1/91

1906 (a dip separation of approximately 1.6 feet), one computes a long-term average of one event per 266 years; in this case, assuming the buried soils correlate with quiescent periods as long as a few thousand years each yields an average recurrence during active periods as short as one event per 133 years. None of the observations made in the trench demonstrated that movements on the shear surface were entirely co-seismic. However, this discussion of recurrence intervals has been included to point out the similarity between calculated earthquake recurrence intervals based on information gained in the trench and predicted recurrence intervals for earthquakes on relevant segments of the San Andreas fault from other sources, such as the Working Group on California Earthquake Probabilities (1988, 1990).

The information obtained from this trench, while not definitive, provides valuable insight into the movement history of the shear surface and associated scarp. Evidence for repeated past displacements on the shear surface identified in the trench is unequivocal, although the inferred times and amounts are imprecise. The range of displacements defined by the offset observed in 1989 and that postulated for 1906 is probably a realistic range for co-seismic offsets, since the 1906 event probably represents the upper limit of ground shaking intensity and duration in this locality.

There is no way to be certain that all displacements on the shear surface are associated with earthquakes. If the main shear surface in this trench is associated with a landslide, it is possible that movement can be triggered by causes other than earthquakes. Displacement could, for example, be triggered by climatic conditions such as intense or prolonged rainfall. In this case, one could not place upper limits on potential amounts of displacement, because landslides may move many tens of feet or more in a single episode of movement. Nevertheless, information from the trench suggests that movements in the last 2,000 years or so have been episodic and have involved limited, incremental displacements.

C. Trench #2

Trench #2 was excavated across ground cracks that follow the main scarp of a large, old landslide in the Burrell landslide complex, on the southwest flank of Summit Ridge (fig. 5.2). The ground cracks resulting from the Loma Prieta earthquake, which occurred at the

break in slope between the main scarp and the pre-existing landslide deposit, had been largely obliterated by grading before the beginning of field work, but observers who visited the site shortly after the earthquake reported large ground cracks, some with more than 1 foot of displacement. The primary ground crack around the head of the landslide mass was still visible where it crossed the trench alignment. It showed 3 to 4 inches of horizontal extension and a small amount of vertical separation. A second set of cracks within the main body of the landslide reportedly showed several inches of extension at a location south of the trench.

The trenching site is situated on bedrock mapped as the mudstone member of the Butano Sandstone (Clark and others, 1989), a sequence of dark gray, thin-bedded, nodular mudstones with interbedded arkosic sandstones. Bedding was not visible in the trench. The site is approximately 600 feet southwest of the main trace of the San Andreas fault.

1. Trench Description

A backhoe trench, 80 feet long and 36 inches wide, was excavated across the break in slope at the head of the pre-existing landslide deposit (plate 5.2). In contrast to trench #1, stratigraphic relationships exposed in the trench were relatively simple. The trench exposed a shear surface dipping 32°SW, with a strike of approximately N40°W. Bedrock below the shear surface is dark gray shale. Above the shear surface, bedrock is broken and disaggregated sandstone and shale, interpreted as landslide debris (See descriptions on plate 5.2). Overlying this rock debris is a wedge of colluvial materials, deposited at the base of the older scarp, and a layer of mixed colluvium and rock blanketing the gently sloping surface of the old landslide deposit (plate 5.2).

Cracks crossed the trench at stations 19 and 25. The fissure at station 19 was observed at the surface to have approximately 3 to 4 inches of horizontal extension. The fissure at station 25, which was not observed at the surface, showed a maximum extension of approximately 0.5 inches in the subsurface. The larger crack was associated with approximately 0.7 feet of dip separation and some headward rotation on a sandstone/shale contact in the landslide debris. Since this displacement is larger than that caused by the

Loma Prieta earthquake, one or more previous movements on this crack are indicated, either as a result of an earlier earthquake or the initial movement of the landslide. No convincing evidence for older soil-filled cracks was observed in this zone, so it is considered likely that most, if not all, of the prior movement on this crack occurred during a single episode.

The bedrock within the landslide mass is broken and disaggregated to the extent that the fractures cannot be traced downward in the section as discrete shears. Rather, they diffuse into distributed shears and minor rotations among the blocky landslide debris.

Within the colluvial wedge in the head of the landslide are several distinguishable units, appearing as alternating coarse and fine-grained layers on plate 5.2. These units are inferred to have been deposited by sheet wash and, probably, small debris falls or flows. To help provide a graphic image of the mapped units, all clasts larger than approximately 0.2 feet in diameter are shown on plate 5.2. The surficial sediments observed in the trench (unit 1) consist of fine-grained colluvial sediments with relatively high organic content. Underlying units, with the exception of unit 5, consist of poorly sorted or unsorted angular clasts, sand, and silt with relatively low organic content. This texture suggests rapid deposition and rapid burial.

Unit 5 is similar in appearance to unit 1 and is interpreted to be a result of a previous period of slow sedimentation. Unit 5 is clearly offset along a steeply dipping shear zone, although the shear zone itself is poorly expressed as distributed offset within coarse-grained sediments. The overlying unit 3 must also be offset, since the present inclination of this bed is too steep to have been a surface of deposition. Most or all of unit 2A was deposited subsequent to displacement of unit 3. A slight inflection at the base of unit 2A' and a thickening of unit 1 over this zone of displacement indicates that an additional period or periods of movement occurred. Cumulative dip separation on the more discretely displaced contacts at the base of the colluvial section is 1.5 to 1.7 feet. No evidence for displacement on this feature due to the Loma Prieta earthquake was observed.

A carbon-14 date on a soil sample collected approximately 0.2 to 0.3 feet above bedrock (at the unit 5/5A contact; see plate 5.2) yielded a date of 3,170 $\pm$ 150 ybp. This sample should approximate

the age of the original landslide movement fairly closely. This age is compatible with the state of preservation of the surficial landslide features.

A second soil sample from unit 2A yielded an age of 2000 ± 140 ybp. The base of unit 2A follows the offset geometry of unit 3, whereas the upper surface of the unit conforms to the geometry of overlying beds, and therefore post-dates the initial displacement of units 3, 4, and 5. It is not possible to tell whether unit 2A was deposited entirely after initial displacement of unit 3, or whether the lower portion of unit 2A was already in place at the time of the initial movement. Nevertheless, this date closely constrains the timing of the initial movement indicated by offset of units 3, 4, 5, and 5A.

2. Discussion

The first displacement on the landslide, inferred from these studies, occurred shortly before deposition of the first coarse-grained colluvial units on the landslide mass, approximately 3,150 ybp. This event was probably the initial landslide failure and may have involved movements of tens of feet. Following this first displacement, relatively slow deposition of a fine-grained colluvial unit (unit 5) and then rapid deposition of the coarse-grained layers of units 4 and 3 occurred. These depositional events were followed by reactivation of the landslide slightly before 2,000 ybp, with an estimated dip separation on the foregoing units of approximately 1 foot. This event was followed by rapid deposition of units 2A and 2A' and then relatively slow deposition of unit 1. Thickening of units 1 and 2 at the same place as the displacement of units 4 and 5 indicates a small additional offset of this zone of approximately 0.5 to 0.7 feet. The present ground surface shows no inflection at this point, and therefore this second movement is not due to the Loma Prieta earthquake.

Based on these observations, it is concluded that the landslide has moved at least three times following its initial failure, including movement in 1989. This number of movements is a minimum, because each episode of offset preserved in the stratigraphic record could have been produced by more than one movement on the shear surface, and because some displacement events may have left no record in the portion of the landslide examined in the trench.

Cumulative throw on shear surfaces in the trench in the last 3,000 years (following the initial landslide formation) appears to have been less than 3 feet.

D. Review of Previous Geologic Reports

All previous geologic reports from the Summit Ridge area filed with SCC before mid-November 1990 were examined for possible subsurface data on earthquake-induced ground cracks. The purpose of this review was to determine whether the ground cracks and other types of ground deformation associated with the earthquake could have been predicted in advance by appropriate geologic investigations. Reports examined included those completed before the earthquake as well as those completed afterwards.

Out of a total of 81 available reports, 24 were judged to include useful records of subsurface exposures and were thus selected for more detailed review. One additional geologic report, conducted for the Loma Prieta Elementary School, on the north side of Summit Road, in Santa Clara County, was also included in the review because its geologic setting is identical to adjacent portions of Santa Cruz County included within the study area. A list of the reports reviewed is shown in table 5.2. Locations of the parcels for which the reports were written are shown in figure 5.5.

Most of the reviewed reports contained either clear or probable evidence of ground cracking that pre-dated the Loma Prieta earthquake; of the 24 reports reviewed from SCC files, 14 contained clear evidence of previous ground cracking, five contained probable evidence for previous cracking, three were indeterminate, and two contained no evidence of previous ground cracks.

Of the two reports that contained no evidence for previous ground cracks, one did not include any trenches placed to intercept existing ground cracks or surface lineaments. The second report stated that no evidence of pre-existing ground cracks existed where the cracks caused by the Loma Prieta earthquake crossed the trench, although relations depicted in one of the trenches suggests that pre-existing cracks were present nearby. The "indeterminate" category was applied to sites where information on the trench log couldn't be interpreted or was judged to be incomplete. The "probable" category was used where information included on the trench logs or in the

TABLE 5.2: PREVIOUS GEOLOGIC REPORTS WITH SUBSURFACE DATA

Post Earthquake Reports

APN#	ADDRESS	FIRM	EVIDENCE OF PREVIOUS MOVEMENT
97-101-32	25295 Old San Jose Rd.	APPLIED SOIL MECHANICS	No evidence of previous movement.
96-271-09	24620 Miller Rd.	UPP GEOTECHNOLOGY	Evidence of previous movement.
96-291-07	23430 Sunset Dr.	J.W. LEONARD, C.E.	Indeterminate
96-131-36	23080 Summit Rd.	JO CROSBY and ASSOC.	Probable
96-151-13	23700 Morrell Cut Off	WM. COTTON and ASSOC.	Evidence for previous movement.
96-311-23	23484 Bel Aire Ct.	JO CROSBY and ASSOC.	Indeterminate
98-281-12	25200 Adams Rd.	MICHELUCCI and ASSOC.	Probable
98-151-04	15052 Stetson Rd.	GEOFORENSICS	Indeterminate
98-271-11	25734 Adams Rd.	ROBERTSON GEOTECHNICAL	Evidence for previous cracks.
97-161-03	25507 Old San Jose Rd.	FREEMAN-KERN ASSOC.	No ground cracks on site.
96-292-34	23048 Evergreen Ln.	UPP GEOTECHNOLOGY	Evidence for previous ground cracks.
97-071-20	16000 Redwood Lodge Rd.	HYDRO-GEO CONSULTANTS	Probable
96-283-06	18338 Las Cumbres	COTTON & ASSOC.	Evidence for previous ground cracks.
96-382-04	22494 Citation Dr.	GEOFORENSICS	Evidence for previous ground cracks.
96-131-22	23136 Summit Rd.	FOXX-NIELSEN and ASSOC.	Evidence for previous ground cracks.
96-111-01	23201 Old Santa Cruz Hwy.	PACIFIC GEOTECHNICAL	Evidence for previous ground cracks.
97-231-09	16010 Stetson Rd.	WEBER and ASSOC.	Evidence for older ground cracks.

TABLE 5.2 (continued)

APN#	ADDRESS	FIRM	EVIDENCE OF PREVIOUS MOVEMENT
97-231-10, 11	16020 Stetson Rd. 16060 Stetson Rd.	WEBER and ASSOC.	Evidence for older ground cracks.
97-231-12, 13	16026 Stetson Rd. 16044 Stetson Rd.	WEBER and ASSOC.	Evidence for older ground cracks.
96-061-11	17774 Old Summit Rd.	WEBER and ASSOC.	Evidence for older ground cracks.
		Pre-Earthquake Reports	
96-281-13	23426 Sunset (or Summit?) Rd.	K.W. PRICE (two reports)	Probable
96-121-21	Schultheis Rd.	WEBER and ASSOC.	Probable
95-021-21	Summit Rd.	JCP ENGINEERS	Evidence for older ground cracks.
SANTA CLARA COUNTY	23845 Summit Rd. (LOMA PRIETA SCHOOL)	JOHNSON & ASSOC.	Definite evidence for previous ground cracks.

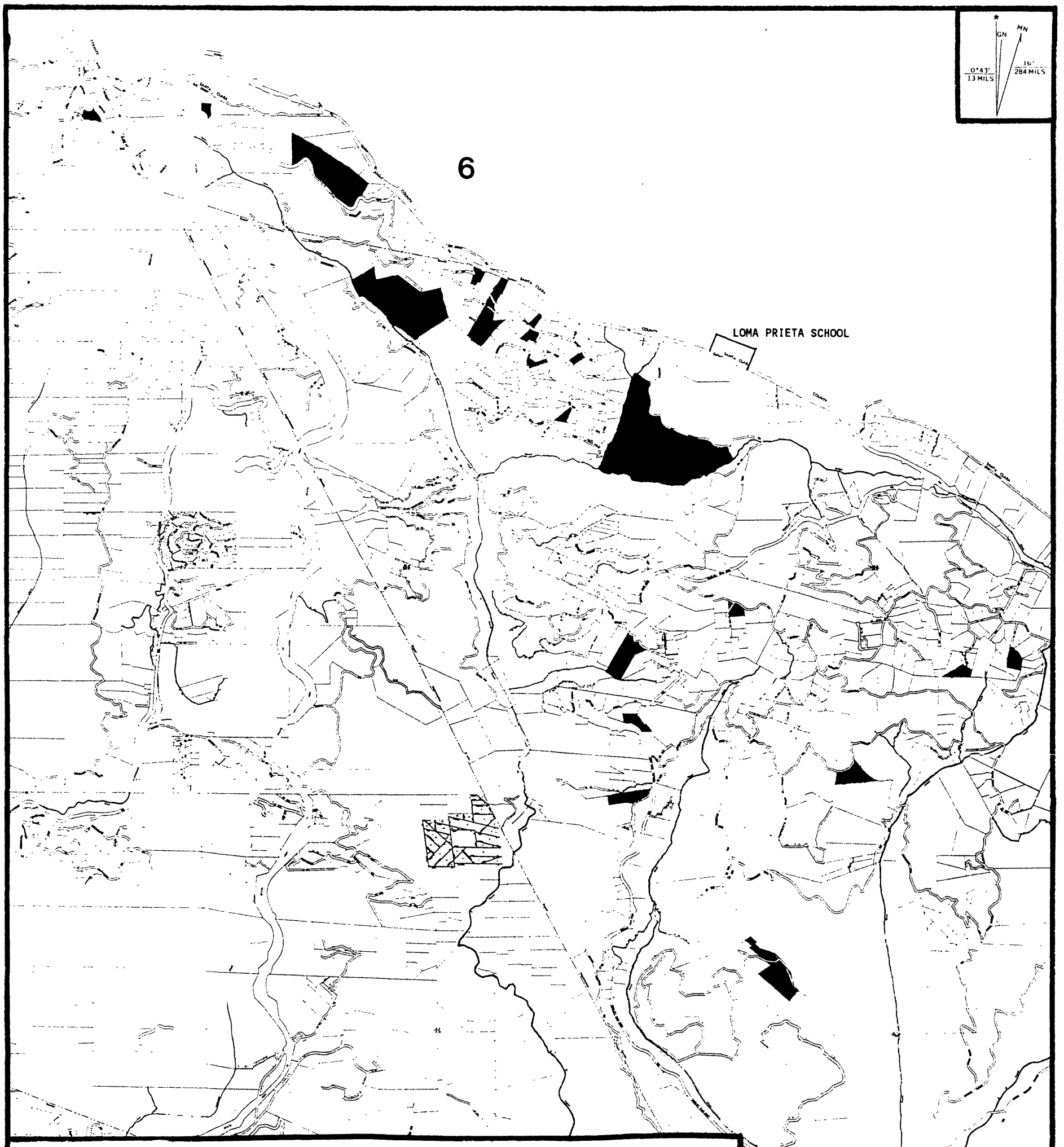

Base map from County of Santa Cruz parcel maps 6 and 11.

MAP SHOWING LOCATION OF PARCELS INCLUDED IN THE REVIEW OF GEOLOGIC REPORTS

FIGURE 5.5

report text was suggestive of previous ground-cracking episodes, but such information was not discussed by the report author(s). Those sites considered to have definite evidence for previous ground cracks are those where relations shown in the trench logs require previous movements or where the report author(s) specifically stated that previous movement was in evidence. However, the categorization of sites into definite, probable, or indeterminate categories represents the judgement of authors of this report and does not necessarily reflect the judgements of the authors of the original reports reviewed herein.

The following sections review three case histories to illustrate the type of subsurface relations observed in trenches and to describe associations between subsurface expressions and displacements during the Loma Prieta earthquake. The amount of information reviewed for this study was too great to be included here; the three case histories were selected to help illustrate the conclusions presented at the end of this section. It should be noted, however, that the conclusions are based on the entire data base, rather than only on the three cases presented here. These case histories include one pre-earthquake investigation for the Loma Prieta School and two post-earthquake studies.

1. Example 1: Case History of Pre-earthquake Investigation for Loma Prieta School

Geologic investigations for the Loma Prieta School were mandated by the Office of the California State Architect, as directed by the Alquist-Priolo Act, to evaluate the potential ground-rupture hazard due to faulting. The school is located on the northeast side of Summit Road, approximately 2.5 miles east of California Highway 17 (fig. 5.6). The investigation, conducted by Rogers E. Johnson and Associates, consisted of more than 1,200 linear feet of backhoe trench, excavated in two phases. The first phase comprised approximately 600 linear feet of trenching and covered the width of the school facilities. This first phase identified four potentially active fault strands, two of which demonstrably offset soil horizons. The second phase was intended to provide more precise control on the locations of these faults where they were projected under existing school facilities. The second phase of trenching identified additional faults, another two of which showed clear evidence for Holocene offsets.

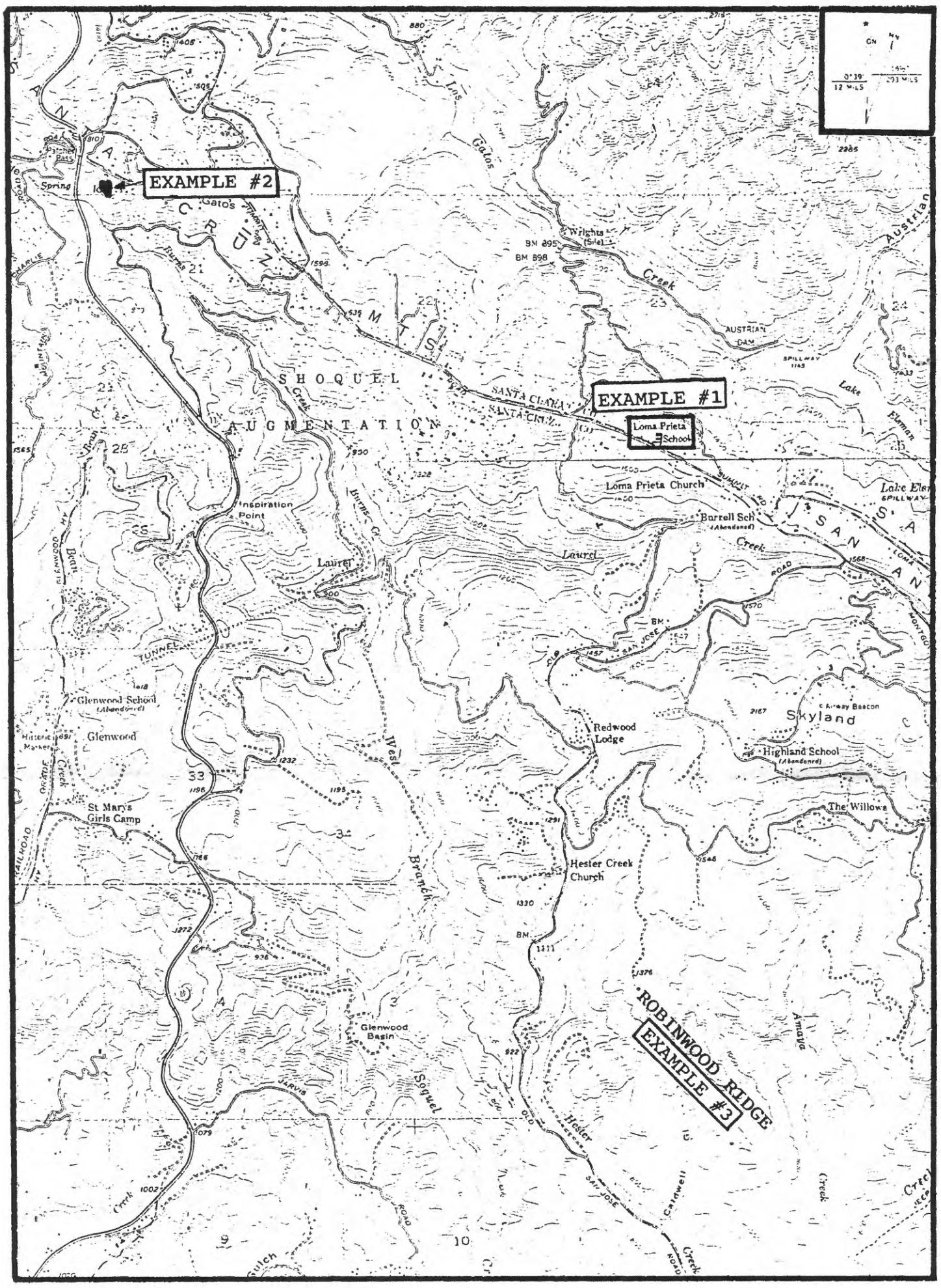

Base map from USGS Laurel and Los Gatos Quadrangles, 7.5 minute series.

	MAP SHOWING LOCATIONS OF CASE HISTORY EXAMPLES	FIGURE 5.6

The school site was extensively graded prior to construction. Therefore, all Quaternary deposits had been stripped from many of the areas trenched, leaving no datum with which to evaluate fault activity. A significant number of the faults identified in the trenches therefore could not be evaluated with regard to Holocene activity.

Prior to grading, the site was characterized by a set of alternating ridges and valleys, all with northwest trends, approximately parallel to the San Andreas fault. Figure 5.7 is a simplified site map showing the school buildings and trenches, and the locations of faults with demonstrable offset of Quaternary strata. The fault locations coincide with topographic breaks and appear to follow the margins or axes of troughs that existed prior to grading for the school.

Figure 5.8 and plate 5.3 are logs of trenches #10 and 13, respectively. Trench #13 (plate 5.3) shows a colluvium-filled basin, or half graben, formed by down-dropping and rotation of blocks along two well-defined slip surfaces at one edge. No slickensides were noted along the slip surfaces, but consistent normal separations on strata were observed. Both slip surfaces showed evidence for more than one episode of movement. Carbon-14 dates on bulk soil samples indicated that approximately 2.5 feet of normal separation has occurred on the easternmost slip surface in the last 2,000 to 4,700 years. A more detailed discussion of the faulting and the dating program was given by Johnson and Associates (1989).

The log of trench #10 (fig. 5.8) depicts a type of subsurface expression of faulting common in the Summit Ridge area. The zone of offset is not marked by any clearly recognizable shear surface. Rather, the zone of offset is recognized by a near-vertical, indistinct contact between weathered bedrock and colluvium. The lack of a well-defined slip surface is probably due to the extensional character of the displacements. In this case, the contrast between weathered bedrock and colluvium is not vivid, and the offset was not recognized during the initial trench # logging. This exposure highlights the caution that must be exercised when examining subsurface exposures in environments such as this.

Displacement of the ground surface during the Loma Prieta earthquake occurred along the trend of the slip surfaces recognized in trench #13. This deformation was not uniform along the projected surface fault trace, but was greatest in the vicinity of classroom building 2 and evidently decreased to the northwest and southeast.

FIGURE 5.7

SIMPLIFIED SITE PLAN

FOR LOMA PRIETA SCHOOL
EXAMPLE #1 LOCATION

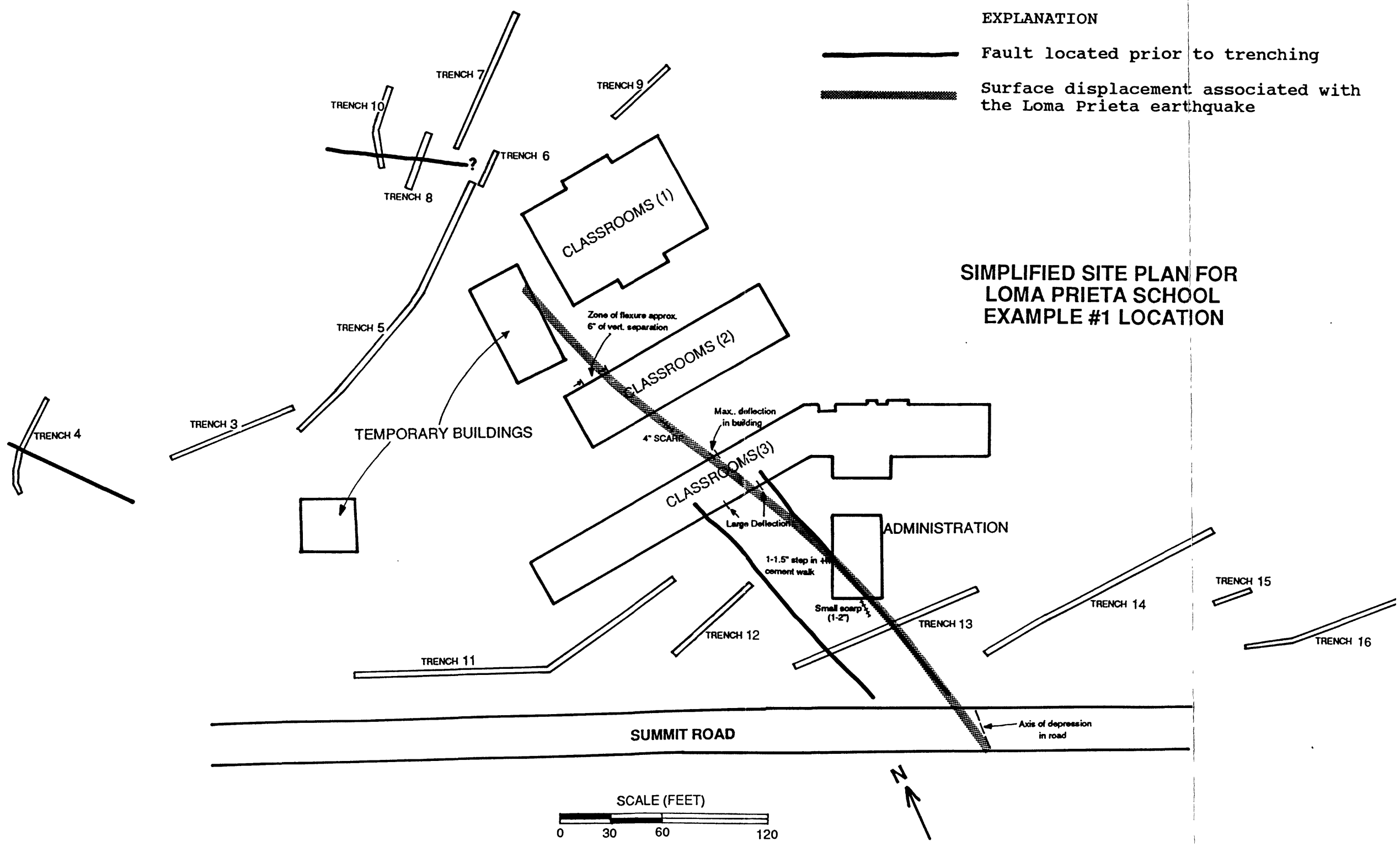

EXPLORATORY TRENCH 10

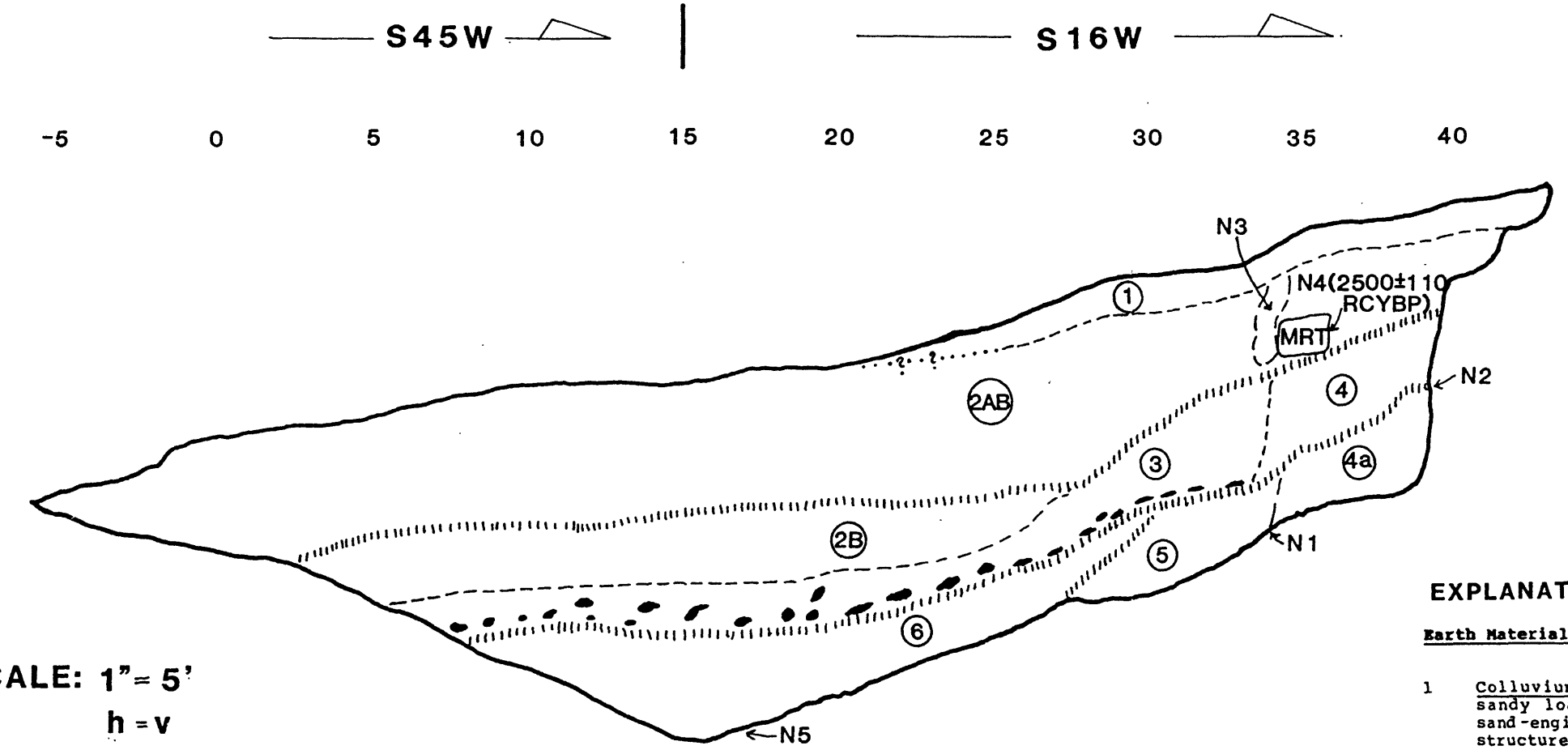

SCALE: 1"= 5'
h = v

Notes

N1 - Subvertical color contact oriented N57°W (cross trench strike).

N2 - Gradational contact over approximately 6 inches.

N3 - Zone of very loose material, abundant burrows, and deep root penetration.

N4 - Mean residence time sample: BETA-29852, 2500± 110 radiocarbon years before present.

N5 - Sharp subvertical contact on opposite trench wall. Not apparent on logged wall.

Symbols

— — — —	Contact, approximate
- - - - - - - -	Contact, very approximate
.....	Contact, gradational
.....	Contact, indistinct
▬ ▬ ▬ ▬	Clasts > 2 inches in diameter
MRT	Area sampled for mean residence time dating

EXPLORATORY TRENCH LOG #10 FOR LOMA PRIETA EXAMPLE #1 LOCATION

EXPLANATION

Earth Materials

1 Colluvium: 10YR 3/2; slightly sticky, slightly plastic; sandy loam (Soil Conservation Service nomenclature); silty sand-engineering texture; loose; weak, subangular blocky structure.

2AB Colluvium: 10YR 4/4 and 7.5-10YR 5/6; very mottled with organic staining; slightly sticky to sticky, slightly plastic to plastic; loam (Soil Conservation Service nomenclature), clayey sand-engineering texture; moderate, medium-coarse subangular blocky structure; few-common, moderately thick ped face clay films; highly bioturbated; moist; 5% gravel; lower contact gradational over about 4 to 6 inches (soil AB horizon).

2B Colluvium: Similar to unit 2AB except slight clay increase and mottling decreases in unit 2B (soil B horizon).

3 Colluvium: 10YR 5/4; sticky, plastic; sandy clay loam (Soil Conservation Service nomenclature), clayey sand-sandy clay-engineering texture; moderate, medium-strong, coarse subangular blocky structure; thick ped face and pore clay films; hard; dry; denser than unit 2AB. Prominent stone line at base of unit, lower contact gradational over about 1 foot.

4 Sandstone: 10YR 6/4 matrix; fractured, deeply weathered; fine-medium grained; matrix is slightly sticky, slightly plastic; sandy loam (Soil Conservation Service nomenclature), silty sand-engineering texture; weak, fine subangular blocky structure, common cobbles and gravels (15 to 20%), especially at contact with unit 2AB.

4a Sandstone: 10YR 6/5 matrix; fine grained sandstone, friable. Similar to unit 4 except unit 4a is less weathered.

5 Silty sandstone: 2.5Y to 10YR 7/6, fine-grained matrix, less weathered than unit 4a.

6 Same character as unit 4.

FIGURE 5.8

The deformation occurred as flexure of the ground surface, northeast-side down, probably as a result of normal slip at depth. Maximum vertical displacement was approximately 6 inches and occurred across a zone of flexure 10 to 15 feet wide. The examination of earthquake damage took place more than one year after the earthquake, so deformation could only be recorded where preserved by existing structures. Although the trend of the faulting in trenches 8 and 10 (fig. 5.7) is different from that in trench #13, the offset in trenches #8 and 10 lies directly on the projections both of the faults in trench #13 and of the ground-surface deformation resulting from the earthquake. These features are also aligned along the trough that predated the school. For these reasons, the fault orientations in trenches #8 and 10 are considered to be a result of a change in strike of the fault or faults mapped in trench #13. No ground deformation associated with the fault that offsets soil horizons in trench #4 was identified (fig. 5.7).

2. Example 2: Case History of Post-earthquake Investigation for a Single Family Residence (APN 96-061-11, Table 5.2)

A single family residence adjacent to Old Summit Road near the intersection of Summit Road and California Highway 17 (fig. 5.6), was severely damaged by strong seismic shaking and ground cracking. A plan map showing the pattern of ground cracking on the property is depicted on figure 5.9. Several ground cracks occurred in an arcuate zone; these displayed southwestward movement, with extensional displacements of 1 to 12 inches and vertical displacements of 0 to 10 inches. Trenches #17B and 18 (fig. 5.9 and plate 5.4) were excavated across this crack system. Trench #17B reveals a large, colluvium-filled graben formed by normal displacement on bounding slip surfaces. At least three episodes of displacement are required by stratigraphic relationships. However, a comparison between the displacement due to the Loma Prieta earthquake and the much larger cumulative displacement across the graben suggests numerous episodes of movement. In trench #18, stratigraphic displacements of bedrock, soil horizons, and older generations of infilled ground cracks also indicate several episodes of movement.

In trench #17B, a 6-inch-wide ground crack at the surface could not be traced into the subsurface. The crack may have been at least partially destroyed during excavation of the trench. However,

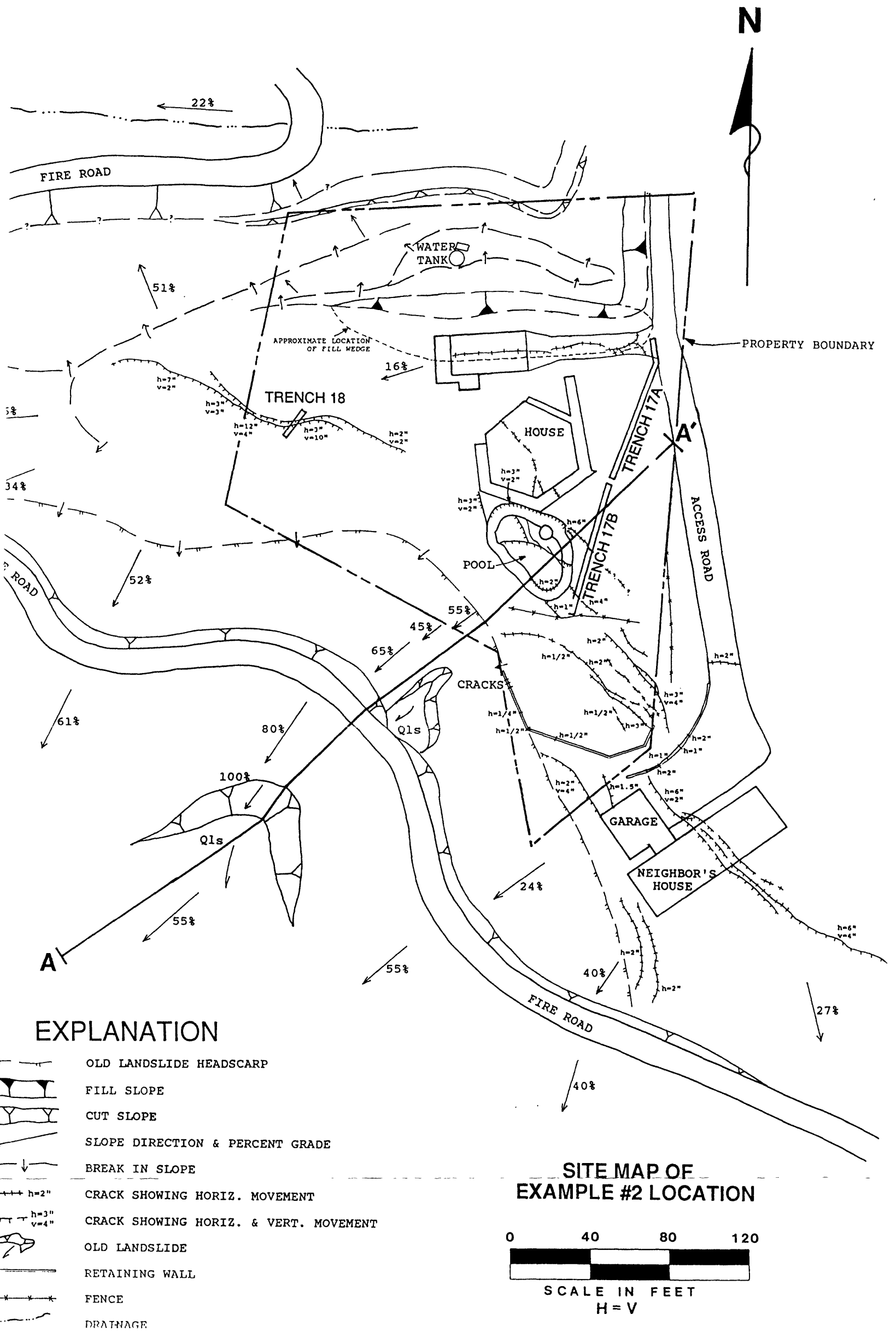

EXPLANATION

- OLD LANDSLIDE HEADSCARP
- FILL SLOPE
- CUT SLOPE
- SLOPE DIRECTION & PERCENT GRADE
- BREAK IN SLOPE
- h=2" — CRACK SHOWING HORIZ. MOVEMENT
- h=3" v=4" — CRACK SHOWING HORIZ. & VERT. MOVEMENT
- OLD LANDSLIDE
- RETAINING WALL
- FENCE
- DRAINAGE

SITE MAP OF EXAMPLE #2 LOCATION

0 40 80 120

SCALE IN FEET
H = V

	GEOLOGIC SITE MAP **EXAMPLE #2 LOCATION**	FIGURE 5.9

the subsurface material here (unit 2 in plate 5.4) is a very loose, featureless granular material, which accommodated extension as distributed shear throughout the unit, except at the surface. Identical behavior has been observed in loose, granular sediments at other locations. Therefore, the disappearance of ground cracks, even very large ones, at shallow depth cannot be taken as evidence that no deeper-seated failure has occurred. This point seems particularly important to note at sites where the potential for catastrophic slope failure is being evaluated. In more cohesive materials, such as those depicted in trench #18, surficial cracks persist into the subsurface (plate 5.4).

Trench #17A is a northward continuation of trench #17B (fig. 5.9 and plate 5.4). A second colluvium-filled basin was observed in this trench. Although no ground cracks were observed at the surface in this area (except for those due to fill failure under the driveway), careful inspection of slip surfaces exposed in the trench revealed 1/8 to 1/4 inches of extension across shear "g" (plate 5.4). A mean residence time carbon-14 date at the base of unit 2 of approximately 6,000 ybp provides an estimate of the duration of the processes responsible for forming and filling this basin. Like the Loma Prieta School site, this parcel was graded to form a level pad before development. Historical aerial photographs and old topographic maps, however, indicate a pre-existing ridge through the central portion of the site corresponding to the bedrock high located between the two grabens. The axes of the adjacent topographic troughs are coincident with basins identified in the trenches.

3. Example 3: Case history of Post-earthquake Investigation at Robinwood Ridge (APN 97-231-09, Table 5.2)

Robinwood Ridge is a long, narrow, northwest-trending ridge in the southeast part of the area covered by this report (fig. 5.6). Five contiguous parcels were investigated, covering a stretch of the ridge top approximately 0.33 miles long. The investigation included 12 trenches comprising approximately 500 linear feet of backhoe trench. The complete geologic maps and trench logs are too voluminous to reproduce here. However, two trench logs and a small portion of the mapped area are included for illustrative purposes, and observations made in all the trenches are summarized in this section.

In general, observed ground cracks were associated with evidence of previous movement in the subsurface, commonly expressed as zones of fine, parallel, discontinuous fractures or shears that form a "shear fabric" with a grain parallel to the recent ground cracks. The shear fabric is frequently accompanied by older, infilled ground cracks that appear as thick and continuous veins or discontinuous, thin stringers of darker fill material. There may be little or no observable displacement of stratigraphic markers where movement is primarily extensional, but large vertical separations occur elsewhere. The log of trench #19 (plate 5.5, shown in plan view on fig. 5.10) shows features associated with both types of movement. At the northeast margin of the trench, near station 4, is a zone characterized mainly by extensional displacement (the northeast-dipping surface showing normal separation of units 3B and 3C notwithstanding). The unit 1A boundary is not displaced across this zone but appears to be subsiding into a void created by extension. Several of the larger voids mapped in the section truncate downward against fractures parallel to the ground surface. These relations suggest formation of the voids by translation of near-surface materials parallel to the ground surface. Infilled older fissures show that several episodes of movement have occurred. In contrast to this type of deformation, a large, discrete, vertical displacement of the B soil horizon is observed at station 8.

Some ground cracks crossed by trenches were not observed in the subsurface, nor was visible evidence of earlier episodes of ground cracking found at these localities. Such areas were associated only with smaller cracks having less than 1 to 2 inches of total displacement in relatively loose, granular materials. By contrast, in some other localities where clear evidence for large, older ground cracks existed, no ground cracking occurred during the Loma Prieta earthquake.

Exploratory trench #20 (plate 5.5) portrays an observation unique among the results of the review of post-earthquake trenching investigations: in contrast to trench #19 and other trenches included in the review, the crack observed in trench #20 exhibits a large displacement at the surface resulting from the Loma Prieta earthquake, yet it is regarded as highly unlikely that any evidence for prior movement would have been observed had trenching been conducted prior to the earthquake. The slight shear fabric depicted on the trench log (plate 5.5) is weakly expressed and could have formed in the recent event. This is the only example of a large-

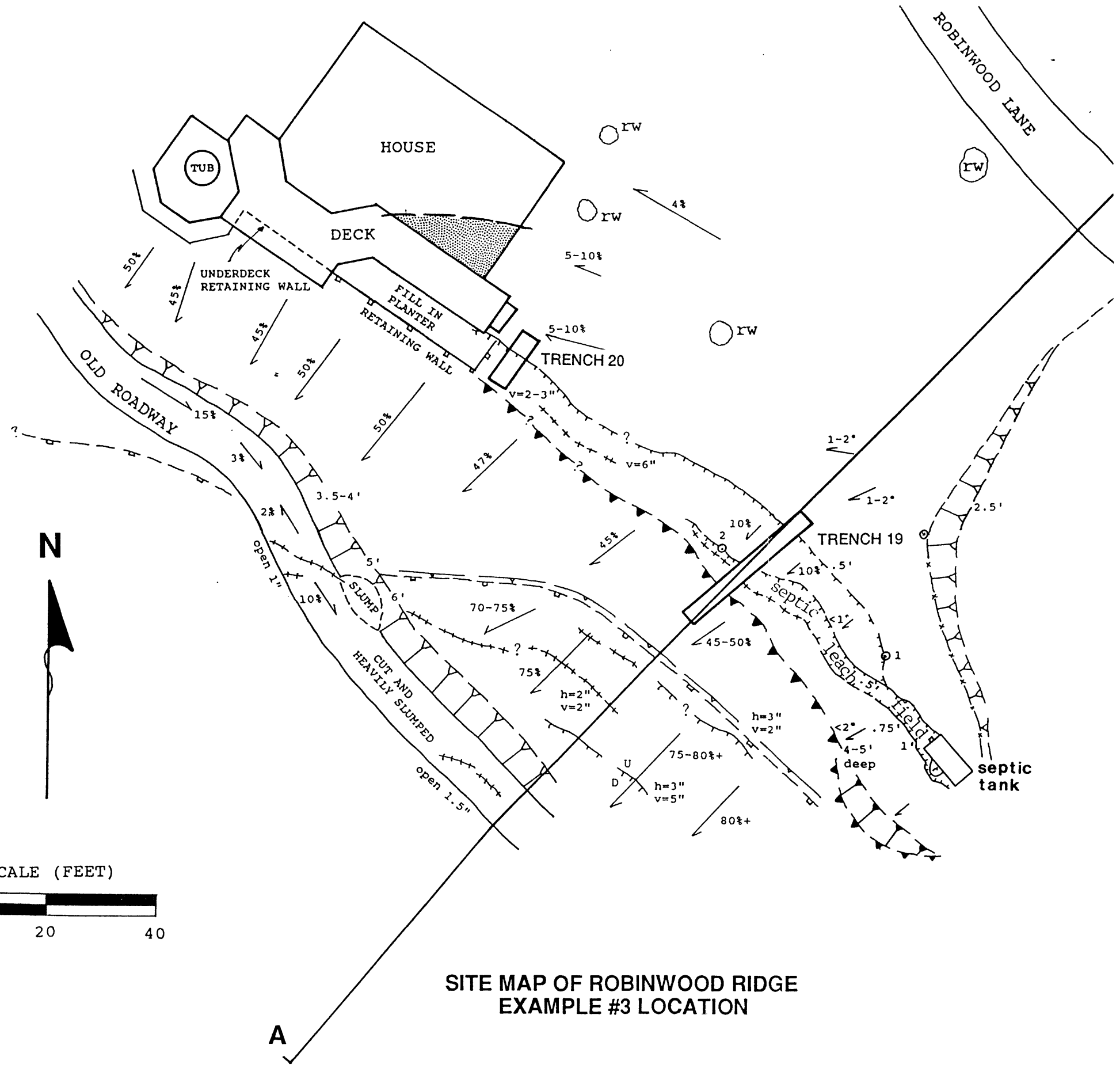

EXPLANATION

- SCARP horiz. & vert. offset
- .5 HEIGHT OF SCARP
- CRACK horiz. offset only
- FILL SLOPE
- CUT SLOPE
- BREAK IN SLOPE
- FENCE
- INFERRED OLDER LANDSLIDE HEADSCARP
- ⊙ FENCE POST WITH TAPE
- ○~ REDWOOD TREES

⊙1. Vertical offset is 0, horizontal offset, or crack width, is 3".

⊙2. The scarp dies into a crack or 2 parallel cracks. Too much cover.

SITE MAP OF ROBINWOOD RIDGE
EXAMPLE #3 LOCATION

FIGURE 5.10

GEOLOGIC SITE MAP

ROBINWOOD RIDGE
EXAMPLE #3 LOCATION

displacement crack (with 3 to 12 inches of extension) that did not exhibit clear evidence in the subsurface of previous movement.

4. Discussion

The preceding examples were selected to provide a brief overview of the types of subsurface expression associated with ground cracks caused by the Loma Prieta earthquake, and to describe evidence for the following conclusions, which have necessarily been generalized from a volume of observations too large to be presented in their entirety. Based on this review, the following three conclusions are drawn:

1. Almost without exception, ground cracks exhibiting large displacement resulting from the Loma Prieta earthquake (more than 1 to 2 inches of extension, and (or) more than 1/2 to 1 inch of vertical displacement) showed clear evidence of prior movement in the subsurface; ground cracks exhibiting smaller earthquake-related displacements were commonly, but not ubiquitously, associated with clear subsurface evidence of prior movement. Therefore, using appropriate investigative techniques, it appears possible to predict the probable locations of most relatively large ground cracks relatively accurately.

2. Not all ground cracks with prior displacements observed in the subsurface were reactivated by the earthquake. Therefore, the ground cracking pattern resulting from the Loma Prieta earthquake cannot, by itself, be used to evaluate the potential for future displacement.

3. Areas of repeated large-scale ground displacements, even those not reactivated during the Loma Prieta earthquake, are commonly, if not ubiquitously, associated with visible topographic expressions.

E. References Cited

Clark, J.C., Brabb, E.E., and Mclaughlin, R.J., 1989, Geologic map and structure sections of the Laurel 7.5' Quadrangle, Santa Clara and Santa Cruz Counties, California: U.S. Geological Survey Open-File Map 89-676, scale 1:24,000.

Cooper-Clark and Associates, 1975 Preliminary map of landslide deposits in Santa Cruz County, California: *in* Seismic Safety Element: Santa Cruz County Planning Department, scale 1:62,500.

Rogers E. Johnson and Associates, 1989; Fault investigation report, Loma Prieta Elementary School, Santa Clara County, California, (Phases 1 and 2): Santa Cruz, California, Rogers E. Johnson and Associates.

U.S. Geological Survey Staff, 1989, Preliminary map of fractures formed in the Summit Road-Skyland Ridge area during the Loma Prieta, California, earthquake of October 17, 1989: U. S. Geological Survey Open-File Report, 89-686, 1 sheet, scale 1:12,000.

Working Group on California Earthquake Probabilities, 1988, Probabilities of large earthquakes occurring in California on the San Andreas fault: U.S. Geological Survey Open File Report 88-398.

Working Group on California Earthquake Probabilities, 1990, Probabilities of Large Earthquakes in the San Francisco Bay Region, California: U.S. Geological Survey Circular 1053, 51 p.

CHAPTER VI. SURFACE MONITORING

Cracks associated with the heads and flanks of 12 selected landslides and landslide complexes were monitored for 18 months after the Loma Prieta earthquake to measure any post-earthquake movement. Use of two types of instrumentation--stake arrays and strain gages--allowed both periodic measurements at many localities and more detailed and continuous measurements at a few selected points.

The persistence of below-average rainfall conditions in the Santa Cruz Mountains during the initial post-earthquake ground-crack monitoring period (December 1989-June 1990) prevented adequate evaluation of slope stability under conditions of high rainfall or elevated ground-water levels. The monitoring program was therefore reinitiated in December 1990 and continued through July 1991 to again attempt to document any renewed movement across the ground cracks and to provide a potential warning system during the second winter/spring rainy season following the Loma Prieta earthquake. Data on this ground-surface monitoring program are taken from Griggs and others (1990) and Griggs and Marshall (1991).

A. Instrumentation and Methods

1. Quadrilateral Stake Arrays

The first instrumentation system consisted of 51 quadrilateral-shaped arrays of four stakes each (fig. 6.1) placed across cracks and scarps along the heads and flanks of large landslides. Locations of these arrays are shown on figures 3.8, 3.9, 3.11, 3.13, 3.17, 3.21, 3.23, 3.24, and 3.25. The general method of using quadrilateral stake arrays to monitor landslide movement is described by Baum and others (1988). In many localities on large landslides in the Summit Ridge area, zones of cracks as much as 160 feet wide were present, and this condition involved judgement, as well as some subjectivity, in selecting positions for stakes. At most localities, the largest (i.e., widest, deepest and (or) longest) crack was selected, although that crack was not necessarily the most headward or outermost. At other

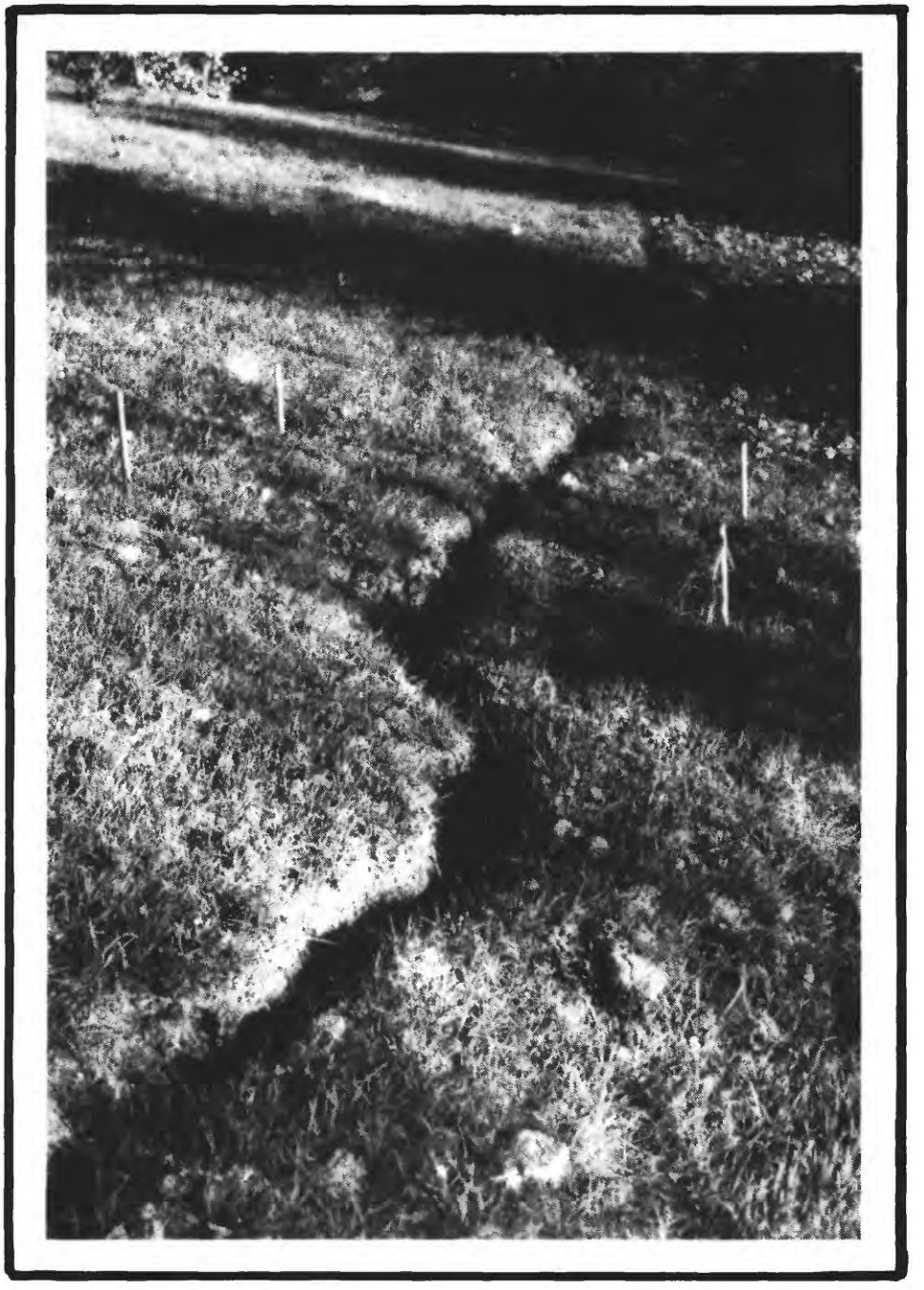

FIGURE 6.1 –Photograph of typical quadrilateral stake array (from Griggs and others, 1990).

localities, the most headward or outermost crack was selected even though it was neither very wide nor deep. At still other localities, stake arrays spanned several cracks. As a result, the arrays monitored a wide variety of scarp or crack features.

Stakes in the arrays were 30-inch-long sections of 0.75-inch-diameter steel pipe, and each array consisted of four stakes driven approximately 24 inches into the ground (fig. 6.1). The stakes were arranged with two on each side of the crack and were lettered clockwise "A" through "D" with "A" and "B" on the upslope side. Stakes were set at least 20 inches away from crack edges, and, depending on crack size and geometry, distances between stakes were typically in the range between 3 and 10 feet. Where arrays spanned several cracks, distances between stakes were as much as 23 feet, but such placement was avoided wherever possible to minimize measurement error.

A metric fiberglass tape was used to measure distances between stakes. Arrays were consistently measured beginning at stake "A" and proceeding through each of the six possible legs within each quadrilateral (four sides and two diagonals). Distances recorded were rounded to the nearest centimeter (0.4 inches). Repeated measurements of two control arrays placed in level, uncracked ground showed measurement accuracy to be 1 centimeter (0.4 inches). Arrays were measured every 15 to 20 days and after significant rainfall.

A field survey at the time the second winter of monitoring was initiated in December 1990 indicated that of the 51 original quadrilateral arrays, 13 were either damaged, removed, or abandoned. During the second monitoring phase, most of the remaining 38 arrays were checked at least once a month, and sometimes as often as once a week during the period of heavy rainfall in March 1991. Two new quadrilateral arrays were installed during the March storms at sites of renewed cracking.

2. Strain Gages

The second ground-crack monitoring system consisted of four pairs of potentiometer-based strain gages linked to continuously recording data loggers. These systems were positioned across selected scarps considered especially sensitive to movement (and where instrument security could be maintained) in the Upper

Schultheis, Villa Del Monte, and Morrell Road areas; locations of the strain gages are shown in figs. 3.11, 3.13, and 3.17. Use of data loggers allowed continuous monitoring of movement.

Each strain gage consisted of a nylon line stretched across the scarp between two wooden stakes (fig. 6.2). One end of the line was fixed to the top of the downhill stake with a nail; the other end was wound around a pulley on the uphill stake and attached to a counterweight, which maintained tautness in the line. Any displacement across the scarp turned the pulley, and this revolution was sensed electronically by a rotary potentiometer that formed the axis of the pulley. The data logger, programmed to record every 30 minutes, transformed the signal into a linear distance (with resolution of 0.5 millimeters, or 0.02 inches). In addition, to compensate for possible effects related to temperature change, the data logger recorded air temperatures inside the data-logger enclosure every half hour.

All four strain-gage systems operating during the first monitoring phase were removed from the field at the end of June 1990. At the beginning of the second phase of monitoring in mid-December 1990, three of the systems--Morrell, Schultheis, and Sunset in Villa del Monte--were overhauled in preparation for reinstallation at their original locations. Throughout the first study phase, monitoring at the Schultheis and Morrell strain-gage installations was repeatedly interrupted by animal traffic. To prevent this type of disturbance during the second study phase, fences were placed around these two instruments. The Deerfield strain-gage site was abandoned to increase the efficiency of the monitoring program and concentrate on the three locations considered most likely to show renewed landslide movement.

B. Results of Monitoring Program

1. First Monitoring Period: December 1989-June 1990

During the initial 7-month monitoring period from December 1989 through June 1990, no significant cross-crack displacements were recorded at any of the quadrilateral or strain-gage sites. During this monitoring period, however, rainfall was exceptionally low; total rainfall in the Summit Ridge area during the 1989-1990

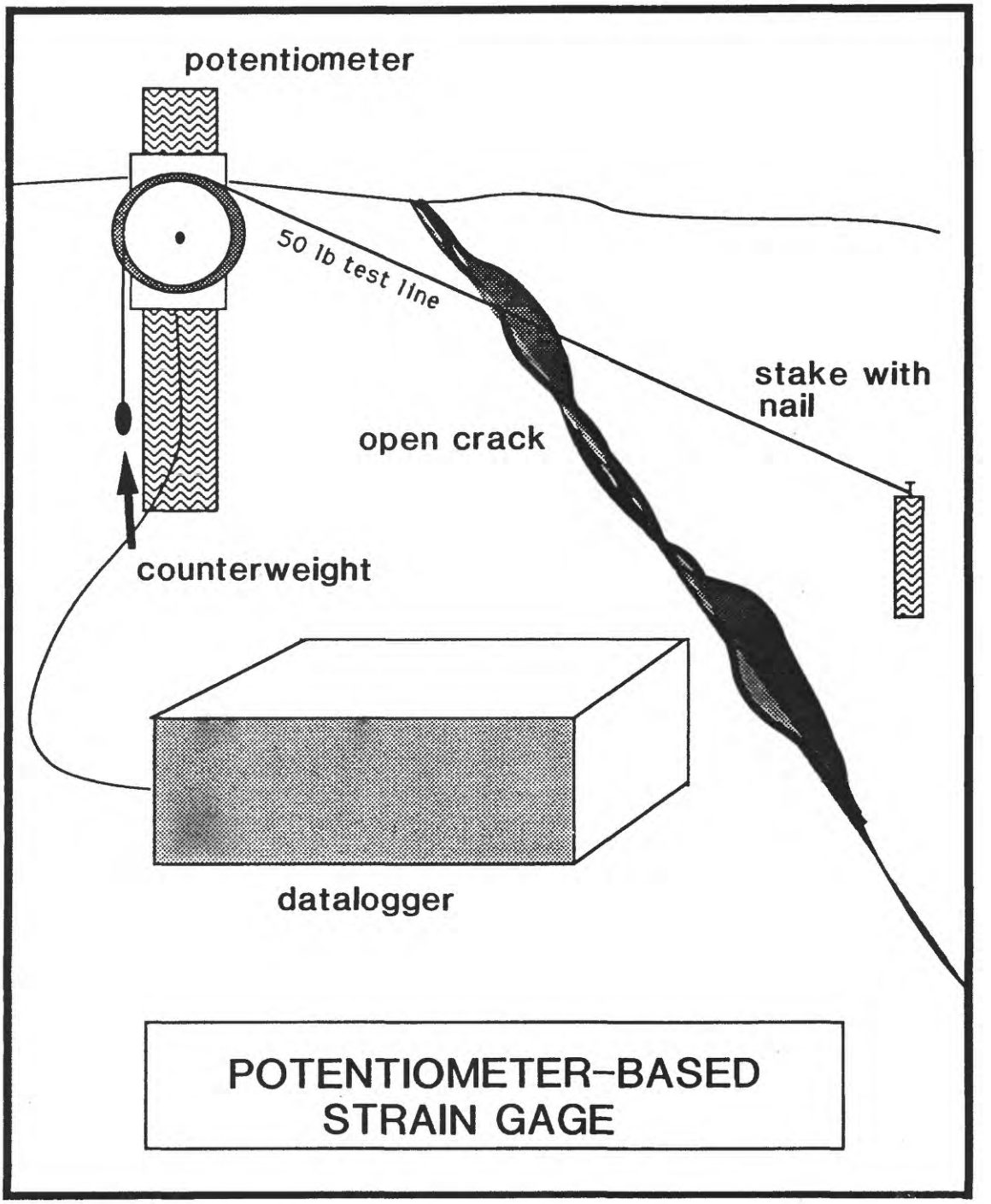

FIGURE 6.2 –Conceptual sketch of strain-gage system (from Griggs and others, 1990).

winter was only approximately 30 inches, or 67 percent of normal, and this winter followed three other exceptionally dry winters (See Section IIB and fig. 2.3). The lack of recorded displacements thus gave no indication about potential for renewed landslide movement during wetter periods.

Only approximately 4 inches of rain fell during the first 50 days of monitoring, from December 1, 1989, through January 19, 1990. The subsurface soil and bedrock exposed in cracks were visibly dry during this period. During this time interval, many ground cracks were covered or filled by property owners or by the San Jose Conservation Corps. An additional 2 to 4 inches of rain fell in the Summit Area between mid-January and mid-February, 1990, yet measurements in mid-February again showed no significant movement across any of the cracks.

Another more intense storm in mid-February 1990, however, produced 3 to 4 inches of rain in 3 days, and measurements at 18 of the 51 quadrilateral stations following this event showed contractions of 0.8 to 1.6 inches on at least one leg of the quadrilateral. Strain-gage data from the Villa Del Monte landslide complex indicated that the onset of the contraction correlated with the onset of rainfall, with virtually no time lag (fig. 6.3). The direct correlation between rainfall and reduction in cross-crack distance at the quadrilateral sites indicated that the soils at these sites were expanding as they took up water. This pattern was consistently documented at a number of widely-spaced sites during a number of subsequent precipitation events.

An additional 1 to 2 inches of rain fell in the first 3 days of March, 1990, and this rainfall produced additional contraction across monitored cracks at six of the quadrilateral stations. Strain-gage data again showed a close correlation between onset of precipitation and onset of contraction, and a comparison of the strain-gage data from the Upper Morrell Road and Upper Schultheis Road landslides, which are 1.7 miles apart, showed a nearly identical contraction response to this March rainfall event (fig 6.4). These strain-gage data also showed cycles of expansion and contraction, with amplitudes in the range between 0.08 and 0.20 inches, that evidently correlate with daily temperature fluctuations.

April 1990 was relatively dry, but May was a relatively wet month for that time of year (the third wettest May in 112 years of record in the city of Santa Cruz), and 5 to 10 inches of rain fell in the

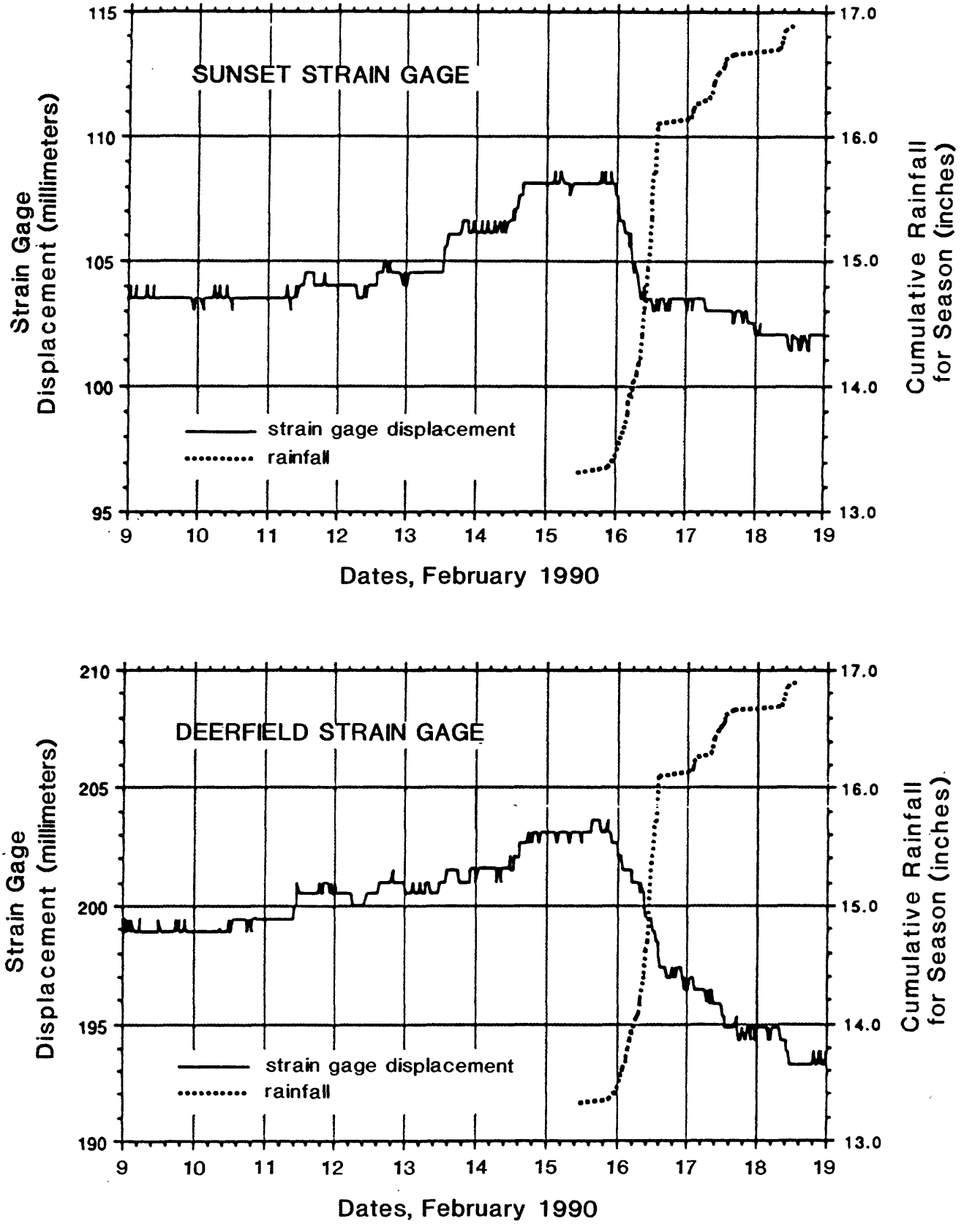

FIGURE 6.3 –Rainfall and displacements recorded by two strain gages on Villa Del Monte landslide complex. February 9 through February 18, 1990 (Modified from Griggs and others, 1990).

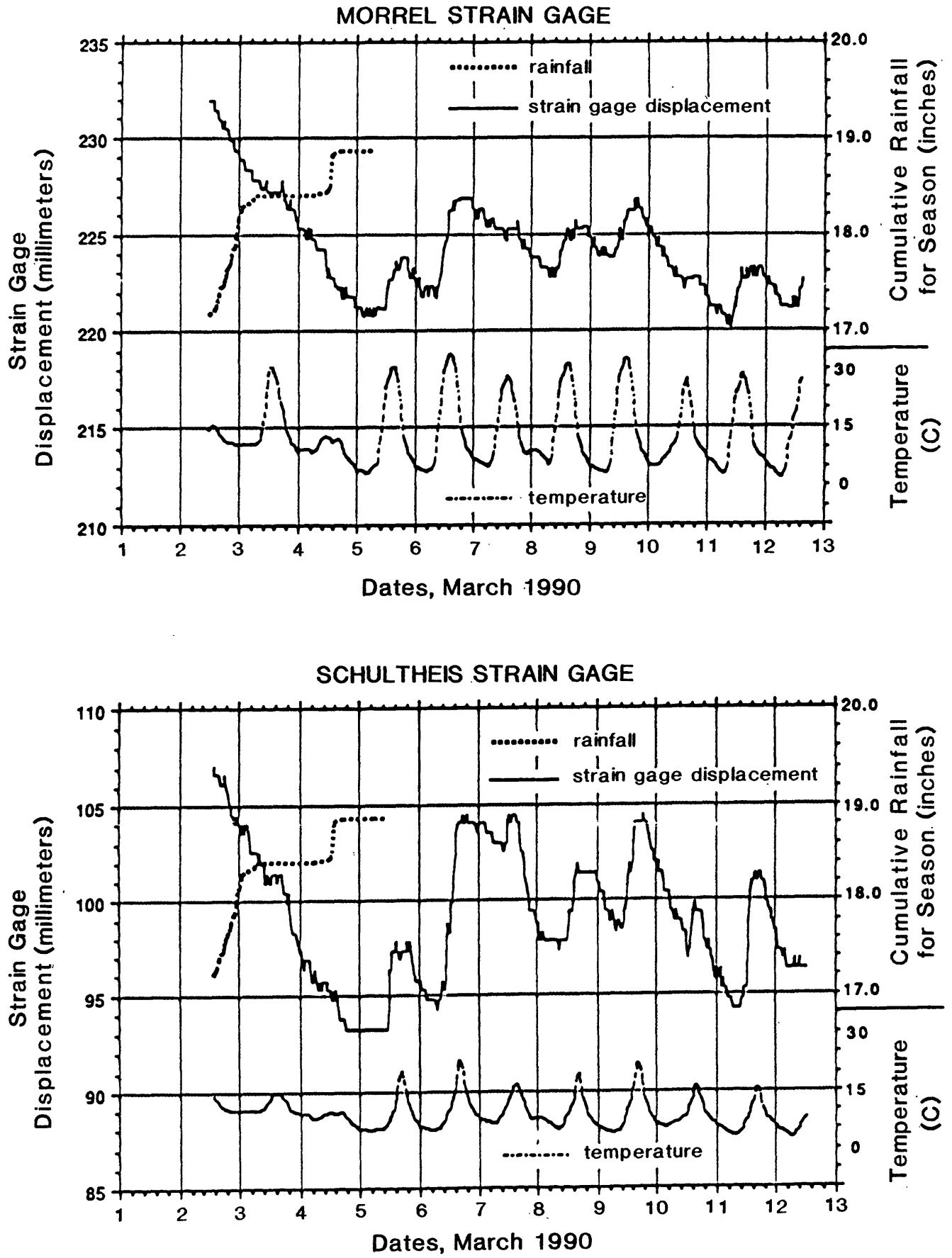

FIGURE 6.4 –Rainfall, temperature, and displacements recorded by two strain gages on Upper Schultheis Road and Upper Morrell Road landslides, March 1 through March 12, 1990 (Modified from Griggs and others, 1990).

Summit Ridge area. Soils were dry prior to this, however, and this rain did not cause any measurable displacements at the 51 quadrilateral sites.

Complete records of the quadrilateral-array measurements and selected plots of the strain-gage data for the initial 7-month monitoring period were presented by Griggs and others (1990).

2. Second Monitoring Period: December 1990-July 1991

The rainfall in the Summit Ridge area during most of the period between the earthquake and the end of the 1991 summer was substantially below normal. Total rainfall during the 1989-1990 winter was 30 inches, 67 percent of average (See Section IIB) and total rainfall from July 1, 1990, through February 25, 1991, was only 6.72 inches (table 6.1). However, an exception to the pattern of dry conditions occurred from February 26 through March 26, 1991, when approximately 26 inches of rain fell during a 29-day period (table 6.1). During and after this period of high rainfall, new or reactivated surface cracking was observed in parts of the Upper Schultheis Road, Upper Morrell Road, and Hester Creek North landslides, and the Villa Del Monte landslide complex ; movements were recorded by quadrilateral arrays, strain gages and inclinometers; and ground-water levels rose within slopes monitored with piezometers. The remainder of this section summarizes the surface observations and measurements and discusses their implications for slope behavior. Subsurface inclinometer and piezometer measurements are discussed in Chapter VII.

Overall dry conditions characterized the Santa Cruz Mountains during the 5 months between the end of the first monitoring phase in June 1990 and the beginning the second monitoring phase in December 1990. The second winter season following the Loma Prieta earthquake began with a series of small storms that generated 2.2 inches of rain in the study area from December 10 through 19, 1990, and an additional 0.6 inches of rain in the first week of January 1991. As documented during the previous winter of monitoring, quadrilaterals and strain gages typically indicated 0.4 to 0.8 inches of cross-crack contraction during these wet periods, as the soils expanded with intake of moisture, followed by a similar amount of extension during the post-storm desiccation period.

TABLE 6.1: BURRELL RAINFALL, JULY 1, 1990-JUNE 30, 1991

Date (1990-1991)	Daily Rainfall (Inches)	Cumulative Rainfall (Inches)
1-Jul--18-Nov		0.93
19-Nov	0.01	0.94
20-Nov	0.02	0.96
25-Nov	0.40	1.36
10-Dec	0.57	1.93
14-Dec	0.55	2.48
15-Dec	0.38	2.86
18-Dec	0.19	3.05
19-Dec	0.15	3.20
6-Jan	0.21	3.41
7-Jan	0.09	3.50
8-Jan	0.32	3.82
9-Jan	0.01	3.83
1-Feb	0.99	4.82
2-Feb	1.02	5.84
4-Feb	0.88	6.72
26-Feb	0.05	6.77
27-Feb	2.15	8.92
28-Feb	1.68	10.60
1-Mar	0.66	11.26
2-Mar	2.17	13.43
3-Mar	5.30	18.73
4-Mar	1.13	19.86
10-Mar	0.90	20.76
12-Mar	1.08	21.84
13-Mar	0.06	21.90
14-Mar	0.11	22.01
16-Mar	1.00	23.01
17-Mar	1.82	24.83
19-Mar	1.00	25.83
20-Mar	0.41	26.24
21-Mar	0.15	26.39
23-Mar	1.07	27.46
24-Mar	3.80	31.26
25-Mar	1.35	32.61
26-Mar	0.39	33.00
1-Apr	0.17	33.17
19-Apr	0.45	33.62
20-Apr	0.10	33.72
24-Apr	0.02	33.74
30-Apr	0.03	33.77

13-May	0.05	33.82
26-Jun	0.01	33.83
27-Jun	0.20	34.03
28-Jun	0.64	34.70

These relatively dry conditions in the Santa Cruz Mountains changed beginning in late February 1991. A series of storms, which lasted through most of March 1991, produced approximately 26 inches of rain in the Summit Ridge area, in contrast to the 2.8 inches of rain that had fallen during the preceding 3 months (table 6.1). These storms generated more than 13 inches of rain from February 26 through March 4, 1991; 2.15 inches of rain from March 10 through 14; and an additional 2.82 inches of rain on March 16 and 17. Continued sporadic storm activity from March 19 through 21 produced 1.66 inches of rain in the area, and a powerful storm, which lasted from the night of March 23 through the morning of March 25, produced approximately 5 more inches of rain (table 6.1 and fig. 6.5). An additional 1.74 inches of rain fell in the Summit Ridge area on March 25 and 26 during the final rainfall event of the March 1991 storm period (table 6.1 and fig. 6.5). Among other effects, this series of storms triggered several small- to moderate-sized landslides in the Summit Ridge area (K. M. Schmidt, D. K. Keefer, and E. L., Harp, 1990, unpublished data).

Ground-crack monitoring was intensified during this storm series, with measurements and field observations made at monitored sites on March 5, 15, 19, 25, and 27, following each individual storm event. The quadrilateral-array data indicated that significant net changes in cross-crack distance (more than 1 centimeter, or 0.4 inches) occurred at 16 of the 38 monitored sites during the March storm period. Measurements made at 14 of these sites showed net contraction, while the changes recorded at two sites showed net extension.

A comparison of rainfall data with both quadrilateral-array and strain-gage records indicated that the observed displacements occurred concurrently with the three most intense rainfall events of the March storm period, which occurred March 2-4, 16-17, and 23-25 (fig. 6.5) The strain-gage record is essentially a mirror image of the piezometric record of ground-water levels shown in figure 6.5, indicating synchronous responses to the March 1991 rainfall. Field observations suggested that the recorded displacements reflected three different general types of movement at the array sites: (1) local expansion or creep of soils induced by increased soil moisture, (2) local sloughing of crack margins, and (3) renewed cracking along scarps related to local readjustment or to headward extension of the monitored landslide masses.

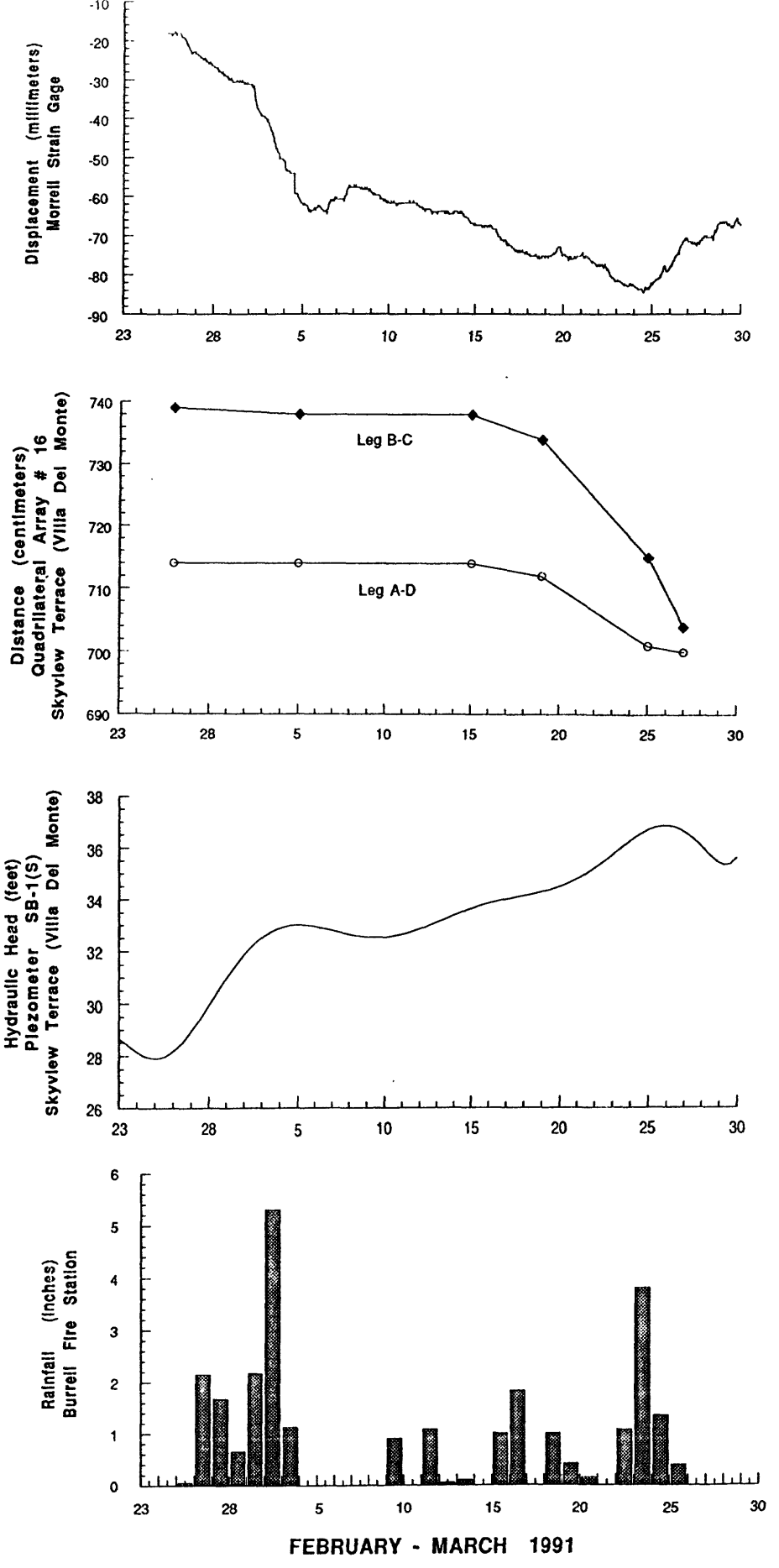

FIGURE 6.5--Comparison of rainfall with example records from strain gage, quadrilateral array, and piezometer; late February-March, 1991, Summit Ridge area.

3. Renewed Cracking Along Landslide Scarps in March 1991

During the March 1991 storm period, renewed cracking and local displacement occurred along scarps associated with four of the monitored landslide masses in the study area: Upper Schultheis Road, Villa Del Monte, Upper Morrell Road, and Hester Creek North. This was the first landslide-related extensional movement recorded at any of the ground-surface monitoring sites since the monitoring program began in December 1989, 2 months after the Loma Prieta earthquake. Cracks on the Upper Morrell Road landslide were probably related to movement of relatively small, shallow blocks of ground and will not be discussed further. Cracking on the other three landslides and landslide complexes is described in more detail in the following sections.

a. Upper Schultheis Road landslide: The first evidence of renewed cracking along any of the landslide scarps in the Summit Ridge area was discovered on March 5, 1991, immediately following the first storm of the March rainy period. A set of newly formed en echelon cracks was observed through a repaired section of Schultheis Road, where the road crosses the main scarp of the Upper Schultheis Road landslide. The 0.4- to 0.8-inch-wide cracks had lengths of between 5 and 10 feet, and showed as much as 0.8 inches of downslope vertical displacement. Observations made on March 15 and 19, following additional rain, revealed increases of 0.4 to 0.8 inches in crack widths and vertical displacements and increases in crack lengths of 1.6 to 3.3 feet.

Field observations made on March 25, following additional heavy rains, revealed significant renewed cracking upslope from the main scarp formed during the Loma Prieta earthquake (fig. 6.6). Because these fresh cracks did not occur along the traces of the pre-existing, earthquake-induced cracks, renewed displacement was not detected at nearby quadrilateral arrays #51 or #52 or by the adjacent Schultheis strain gage.

Extending eastward from the main scarp produced by the Loma Prieta earthquake, the fresh crack formed a broad, 100-foot-long arc, concave-downslope, that crossed a dirt access road and entered a small gully. From there, the new crack was traced approximately 50

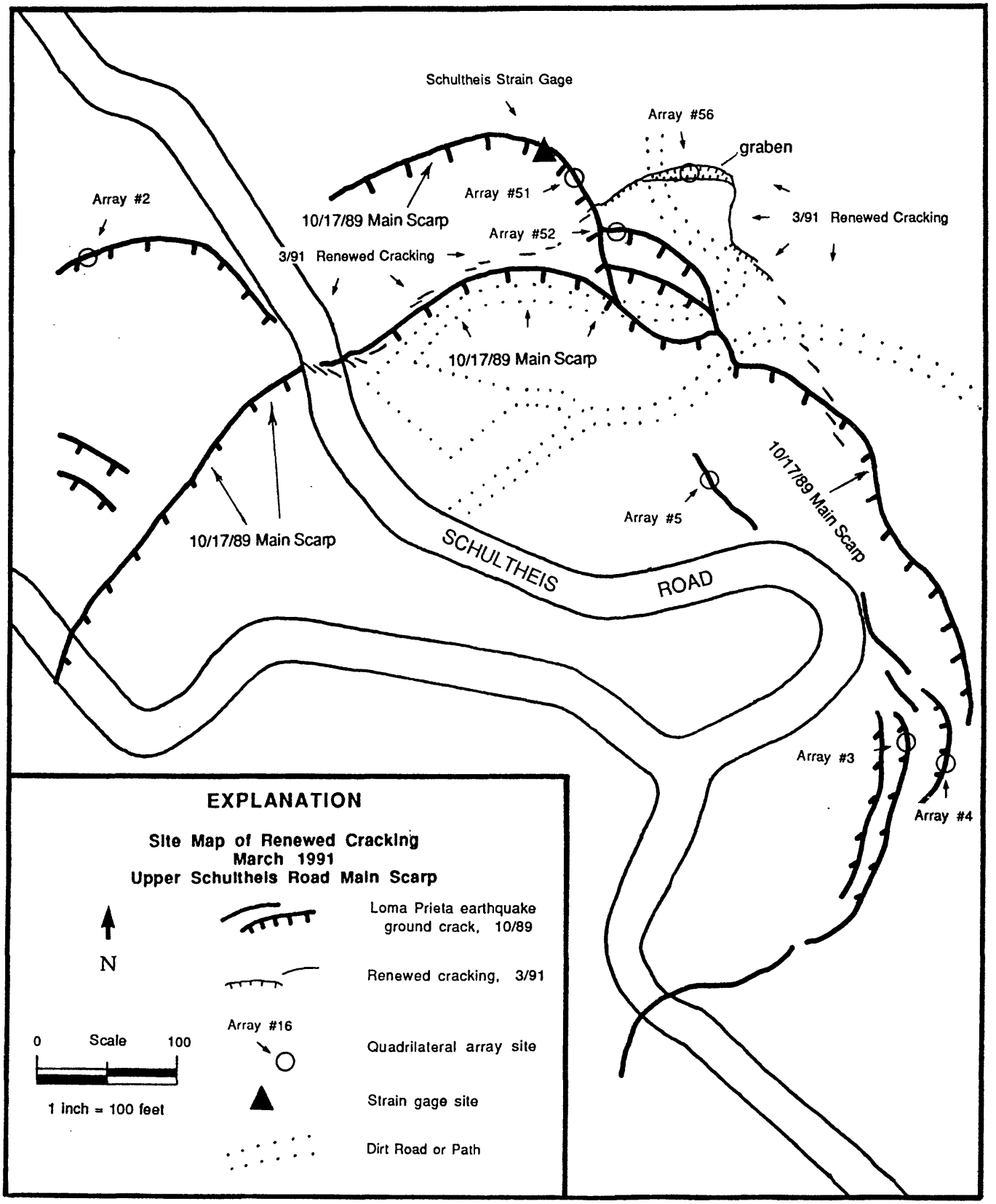

FIGURE 6.6--Area around main scarp of Upper Schultheis Road landslide showing mapped ground cracks and scarps resulting from the Loma Prieta earthquake; ground cracks, scarps and graben formed during period of heavy rainfall in March, 1991; and locations of quadrilateral arrays and strain gage.

feet downslope, along the gully, to a point where its trend became more easterly; from there, the fresh crack continued eastward, across the slope, for an additional 30 to 50 feet, to a point where it was lost beneath the redwood duff. Between the earthquake-induced main scarp and the access road, the fresh crack feature consisted of a single crack, approximately 50 feet long and 2 to 4 inches wide, showing 2 to 4 inches of vertical displacement. Between the access road and the gully, the cracking consisted of a 50-foot-long, 6- to 10-foot-wide graben, which reached a depth of approximately 20 inches at its center and showed net vertical displacements of 8 to 12 inches between its upslope and downslope margins. The continuation of the cracking from the end of the graben down the axis of the gully was barely discernible; however, the eastward extension of cracking from the gully consisted of several, 4- to 8-inch-wide, en echelon cracks showing as much as 4 inches of vertical displacement.

At several locations upslope from the main scarp of the Upper Schultheis Road landslide, a significant quantity of storm runoff was observed flowing into the newly formed cracks. A new quadrilateral array (#56) was installed on March 27, 1991, across the newly formed graben. Remeasurement of this array 2 weeks later, on April 11, indicated 1.2 inches of downslope extension. Subsequent measurements at this site on April 18, 23, and 30 and May 8 indicated no additional changes in cross-crack distances. However, field observations made during those visits revealed evidence of minor, partly en echelon, cracking in several locations along the main scarp between the western limit of this renewed cracking and the locality with renewed cracking on Schultheis Road. Similar, partly en echelon cracks were also observed trending downslope from the eastward margin of this renewed cracking, along the eastern portion of the main scarp formed during the Loma Prieta earthquake (fig. 6.6). A final measurement on July 6, 1991, indicated no additional changes at array #56. The other arrays nearby (arrays #3, 4, 51 and 52 in fig. 6.6) also showed no significant changes between May 8 and July 7, 1991.

The zone of cracking induced by the March 1991 rainfall thus extends in a discontinuous, partly en echelon, arcuate and concave-downslope pattern for more than 500 feet across the slope. The crack pattern indicates headward migration and local reactivation of cracking along the earthquake-induced main scarp of the Upper Schultheis Road landslide.

b. Villa Del Monte landslide complex (Upper Skyview Terrace area): The first evidence of renewed cracking and displacement along the major scarp near Upper Skyview Terrace (fig. 6.7) was detected on March 19, 1991. Measurements made at quadrilateral array #16, positioned across this prominent scarp, indicated 0.4 to 0.8 inches of contraction on all four cross-crack quadrilateral legs. An inspection of the area around array #16 revealed that the observed contraction was the result of extension across a newly formed crack, less than 3 feet upslope from the array site and oriented subparallel to the pre-existing scarp (fig. 6.7) This 0.8- to 2.0-inch-wide crack, which formed sometime between March 15 and 19, showed no vertical displacement. The crack was traceable at least 30 feet eastward from the array site, until lost beneath the thick brush upslope from the scarp. Minor (less than 0.4 inches wide) en echelon cracking was also observed in the pavement of upper Skyview Terrace, where that road crossed the scarp near array site #16.

Measurements made at array #16 on March 25, following additional heavy rain, revealed additional cross-crack contractions of 4.3 to 7.5 inches. The new crack noted on March 19 appeared unchanged; however, a significantly larger crack, approximately 3 feet farther upslope, had formed between March 19 and 25. This new crack, 2 to 6 inches wide and showing 2 to 6 inches of downslope vertical displacement, was oriented subparallel to the pre-existing scarp and could be traced continuously approximately 130 feet eastward through thick brush to a dirt access trail. From that point, the crack was traceable for another 250 feet eastward, but showed only discontinuous expression as a 2- to 6-inch-wide crack with vertical displacements of as much as 6 inches. Although this crack was not traceable very far west of array #16, the previously minor cracking in the road had increased noticeably.

On March 27, additional renewed cracking was observed above the scarp, and another, discontinuous crack had developed downslope from the new cracks. This newest crack, which was an average of 2 inches wide and showed as much as 2 inches of vertical displacement, was traceable for 13 feet, trending obliquely uphill from the edge of the original scarp and passing between stakes A and B of quadrilateral array #16 (inset in fig. 6.7). Quadrilateral measurements revealed 4.3 inches of contraction on the two cross-

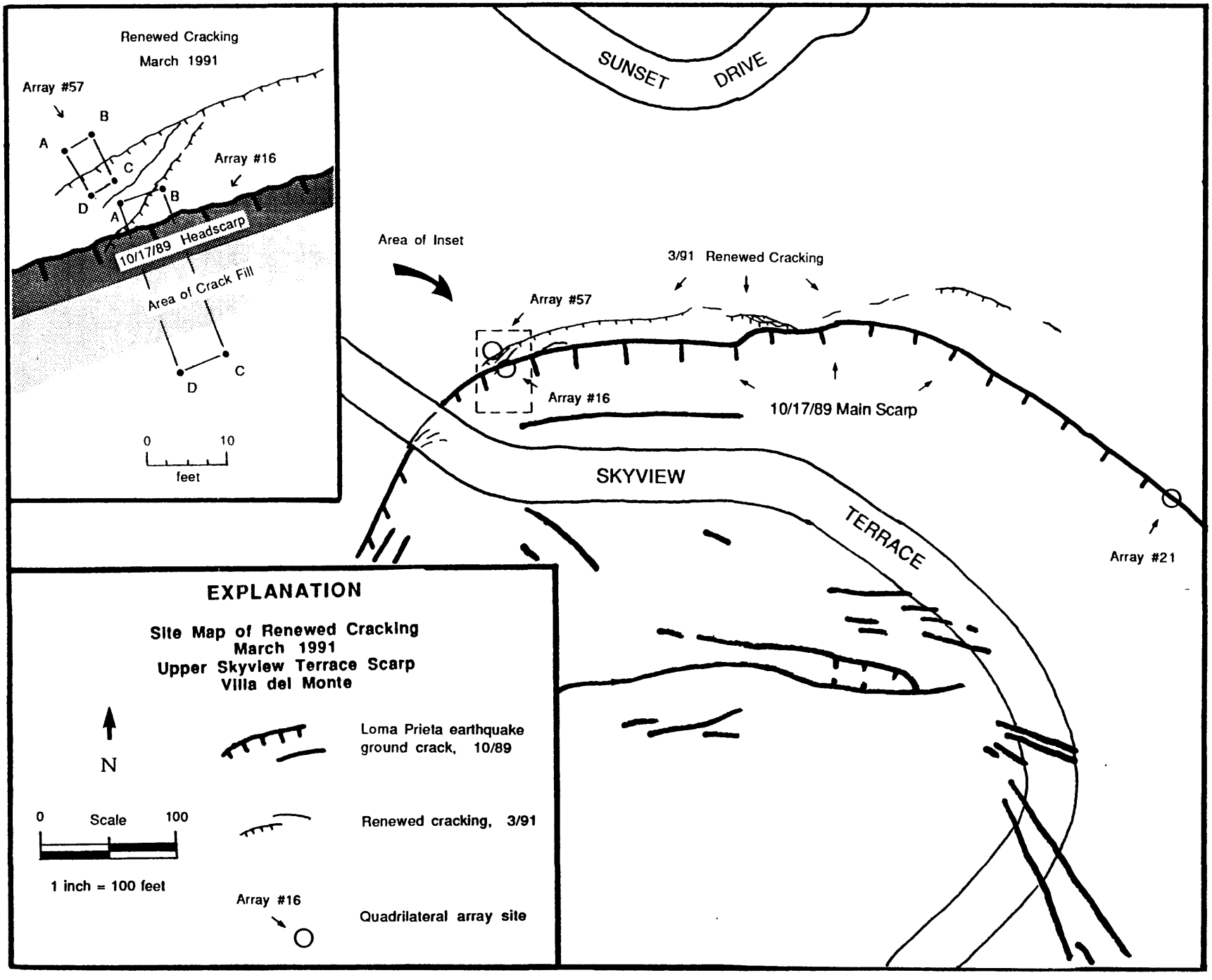

FIGURE 6.7--Upper Skyview Terrace area of Villa Del Monte, showing mapped ground cracks and scarps resulting from the Loma Prieta earthquake; ground cracks and scarps formed during period of heavy rainfall in March, 1991; and locations of quadrilateral arrays.

crack legs involving stake B (i.e., legs BC and BD) and no significant change on the two legs involving stake A (i.e., legs AC and AD). During the March 27 visit to this site, a new quadrilateral array (#57) was installed across the extensive new crack first observed on March 25 (inset in fig. 6.7). Subsequent measurements made at both arrays #16 and #57 on April 11, 18, and 23 and May 8 indicated no additional movement at this locality. A final visit on July 6 revealed that stake D had been removed from array #16, but measurements from the remaining stakes indicated no change from the May 8 readings. All but one of the measurements at the new array, #57, on July 6, were within 0.8 inches of the May 8 readings.

The zone of renewed cracking in the upper Skyview Terrace area extends discontinuously for about 500 feet across the slope, eastward from Skyview Terrace. The cracking appears to represent approximately 25 to 50 feet of upslope migration of the major scarp that formed in this area during the Loma Prieta earthquake.

c. Hester Creek North landslide: Renewed displacement was first detected along the main scarp of the Hester Creek North landslide (fig. 3.24) on March 19, 1991. Quadrilateral measurements at array #49 indicated 0.8 inches of extension between March 15 and 19. On March 25, measurements at this site revealed an additional 0.8 inches of extension. During the March 25 visit to this site, renewed minor cracking was observed across the dirt access road, located downslope from array #49, at both localities where the road crosses the main scarp. These continuous cracks averaged 0.4 to 0.8 inches in width and showed slight vertical displacements.

C. Discussion

While the series of heavy storms that struck the Santa Cruz Mountains during March 1991 triggered several small- to moderate-sized slope failures throughout the Summit Ridge area, no large, catastrophic failures were reported. However, renewed cracking and displacement were detected for the first time since the Loma Prieta earthquake along or near the main scarps of four monitored landslides and landslide complexes: Upper Schultheis Road, Villa Del Monte, and Hester Creek North, and Upper Morrell Road. This renewed cracking probably was caused by local readjustment and

local headward extension of the landslide masses associated with elevated ground-water levels, which were in turn a result of the heavy rainfall in March 1991.

It is important to note that while the March 1991 storms generated approximately 26 inches of rainfall in the Summit Ridge area, total annual rainfall was still significantly below average, as it had been for the preceding 4 years. Thus, the renewed cracking, inferred to have been associated with local readjustment and local upslope extension of the landslide masses, occurred within the larger context of a fifth year of drought in the Summit Ridge area, which has a historically demonstrated potential for significantly higher rainfall (See Section IIB and fig. 2.3). Therefore, while the ground-surface monitoring program provided information on the response of these slopes to a short period of high precipitation, the long term stability of these slopes under conditions of average or above-average annual rainfall still remains untested.

D. References Cited

Baum, R. L., Johnson, A. M., and Fleming, R. W., 1988, Measurement of slope deformation using quadrilaterals: U.S. Geological Survey Bulletin 1842-B, 23 p.

Griggs, G. B., Rosenbloom, N. A., and Marshall, J. S., 1990, Investigation and monitoring of ground cracking and landslides initiated by the October 17, 1989 Loma Prieta earthquake: Santa Cruz., Calif., Gary B. Griggs and Associates, Final Report to the U.S. Army Corps of Engineers.

Griggs, G.B. and Marshall, J.S., 1991, Ground Crack Monitoring Program- December 1990-July 1991. Report to the Army Corps of Engineers.

CHAPTER VII. SUBSURFACE EXPLORATION AND MONITORING--UPPER SCHULTHEIS ROAD LANDSLIDE AND VILLA DEL MONTE LANDSLIDE COMPLEX

A. Subsurface Exploration

The Upper Schultheis Road landslide and Villa Del Monte landslide complex were selected for detailed study of subsurface conditions, monitoring, laboratory testing of materials, and quantitative stability analyses. The Upper Schultheis Road landslide was selected because of the infrastructure present and because landslide features were particularly well expressed there; the Villa Del Monte landslide complex was selected because of the infrastructure and relatively dense development and population.

Subsurface exploration within these two landslide areas included the drilling of 18 small-diameter boreholes, which were visually logged, sampled, and instrumented. The information developed by the drilling program was used, together with other surface and subsurface data, to construct three geologic cross sections and three geotechnical cross sections through these landslide areas.

In addition, a seismic reflection and refraction geophysical survey was carried out on the Upper Schultheis Road landslide on an experimental basis. Results of this survey were not fully interpreted in time for inclusion in this report; preliminary results were discussed by Williams and King (1990).

Inclinometers, for measuring subsurface movement, and piezometers, for measuring ground-water levels and pore-water pressures, were installed in the boreholes. Data from the piezometers were used together with data from water wells to analyze ground-water conditions.

One additional instrument for monitoring movement--a borehole tiltmeter--was installed on an experimental basis in the Upper Schultheis Road landslide. The tiltmeter showed negligible movements during the period the instrument was monitored, which lasted from March 28 through August 7, 1990; details concerning tiltmeter installation, monitoring, and results were discussed by Horath (1990).

Representative samples from the two landslide areas were tested in the laboratory, and results of laboratory tests (see Appendix A) were combined with other types of data to perform quantitative slope-stability analyses (see Chapter VIII) to help evaluate the likely future stability or instability of these areas.

The program of drilling, sampling, logging, and placement of piezometers and inclinometers was carried out by William Cotton and Associates, Inc., of Los Gatos, Calif. under contract to the COE and was described in detail in their report (William Cotton and Associates, Inc., 1990). The interpretation of findings by William Cotton and Associates, Inc. was reviewed and in some cases modified during this study.

1. Location and Purpose of Boreholes

Locations for boreholes in the Upper Schultheis Road and Villa Del Monte areas shown in figures 7.1 and 7.2 were selected by William Cotton and Associates, Inc., in consultation with the TAG. Locations were determined to some extent by the locations of previously surveyed transect lines. The purpose of the drilling program was threefold: (1) to allow the installation of downhole instrumentation (inclinometers and piezometers) to monitor potential future movements and ground-water conditions, (2) to acquire soil and rock samples for laboratory testing, and (3) to characterize the subsurface geologic conditions in the study areas. Complete logs of the boreholes, drilled between December 18, 1989 and March 9, 1990, were presented in the report by William Cotton and Associates, Inc. (1990, v. 2, Appendix F), and data regarding drilling dates, total depths, and the types of drill rigs used are included in table 7.1.

Geotechnical cross sections developed during the present study from the drilling combined with other data are shown in figures 7.3, 7.4, and 7.5. Data on intervals sampled and sample recovery are summarized in figure 7.6. Geologic cross sections along the same lines as the geotechnical cross sections are shown in figures 7.7, 7.8, and 7.9.

In the Upper Schultheis Road area, five boreholes were drilled to depths of 82.5 to 250 feet beneath the ground surface in the locations shown in figure 7.1. Two boreholes (SR-1 and SR-1A) were drilled near the crown of the landslide, one (SR-2) near water well

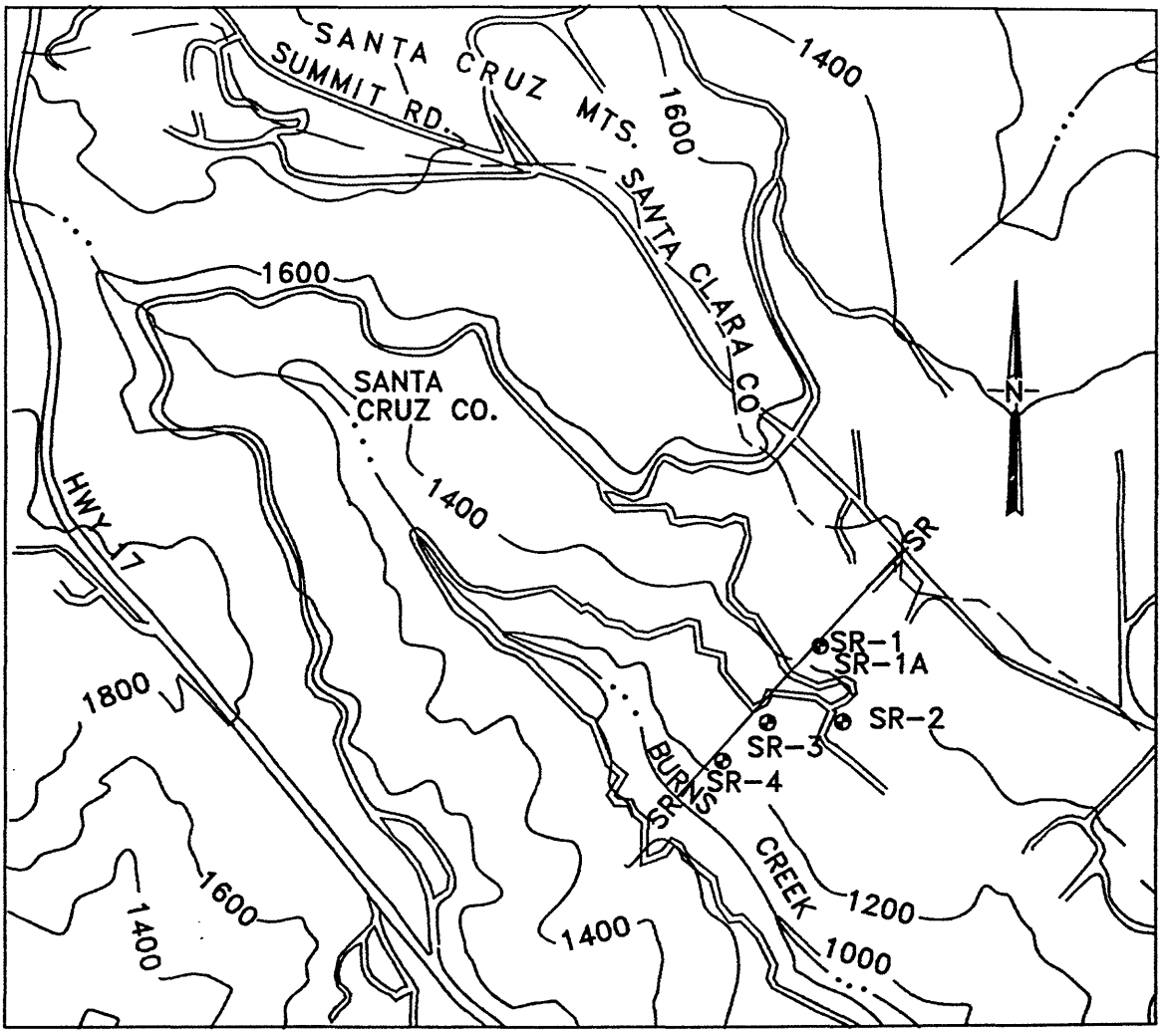

Figure 7.1 Locations of borings in the Schultheis Road area

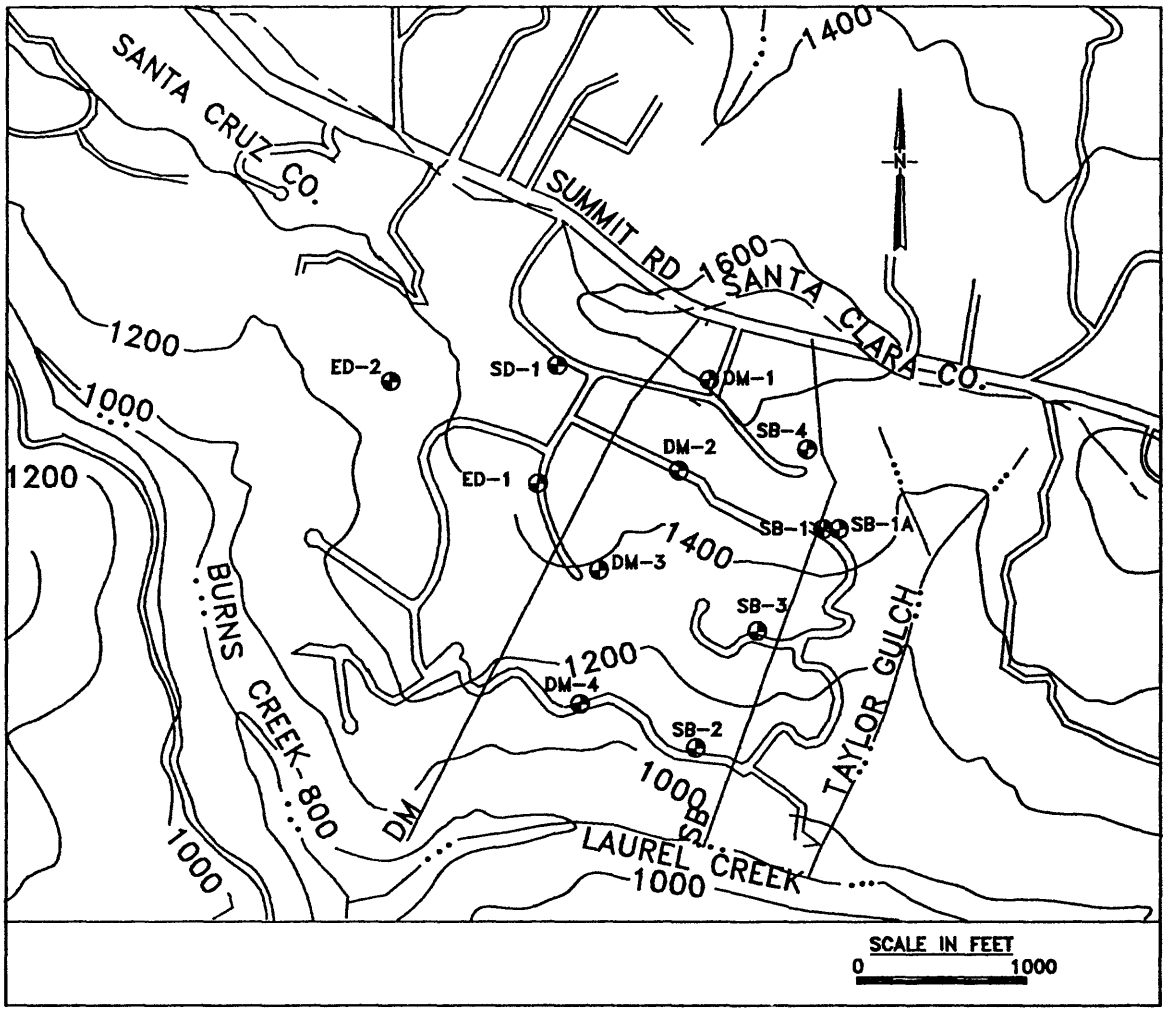

LEGEND

⊕ BORING
SD-1

NOTE: MAP BASED ON USGS LOGS GATOS AND LAUREL QUADRANGLE MAPS DATED 1953, PHOTOREVISED 1980.

BORING LOCATIONS TAKEN FROM WILLIAM COTON AND ASSOCIATES, INC.(1990)

Figure 7.2 Locations of borings in the Villa Del Monte area

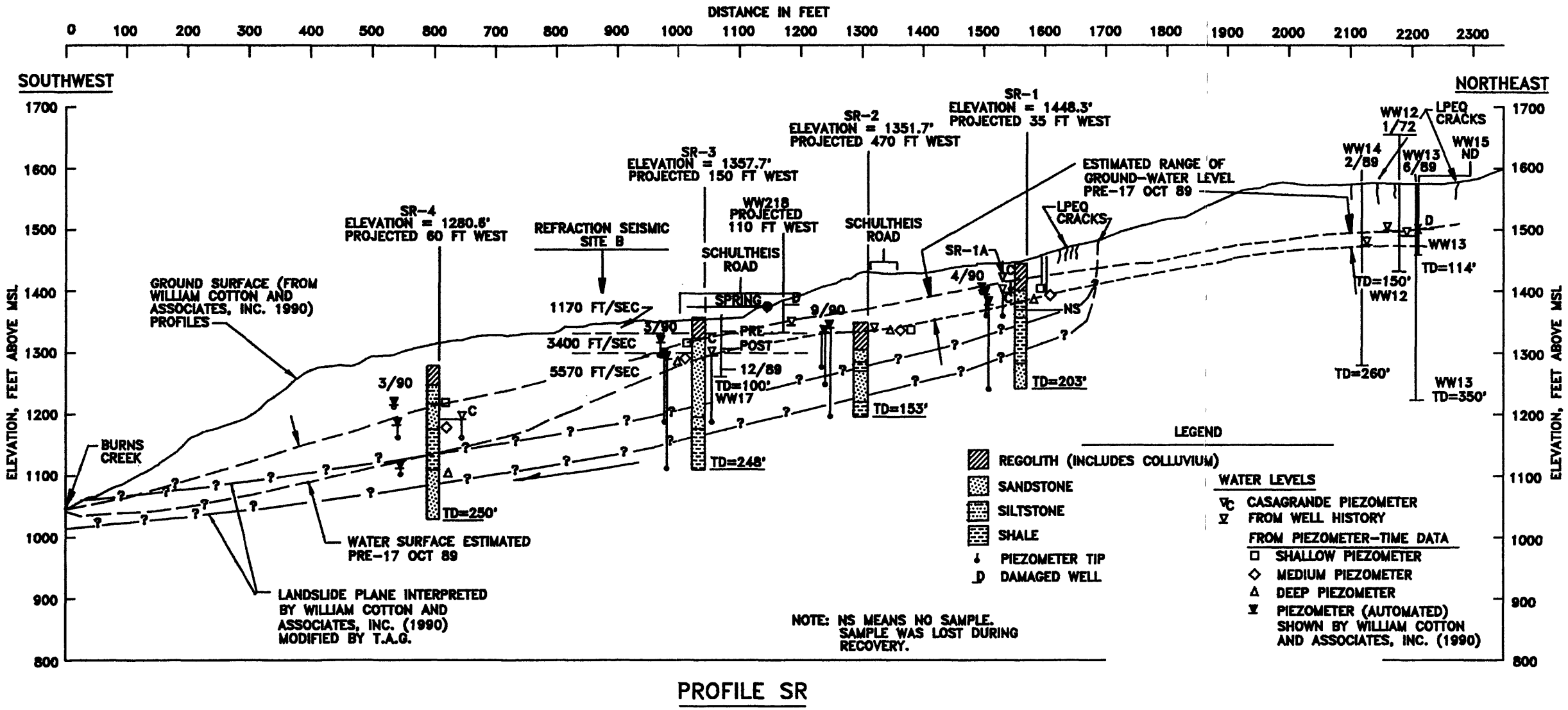

PROFILE SR

Figure 7.3 Geotechnical Profile SR for the Schultheis Road area

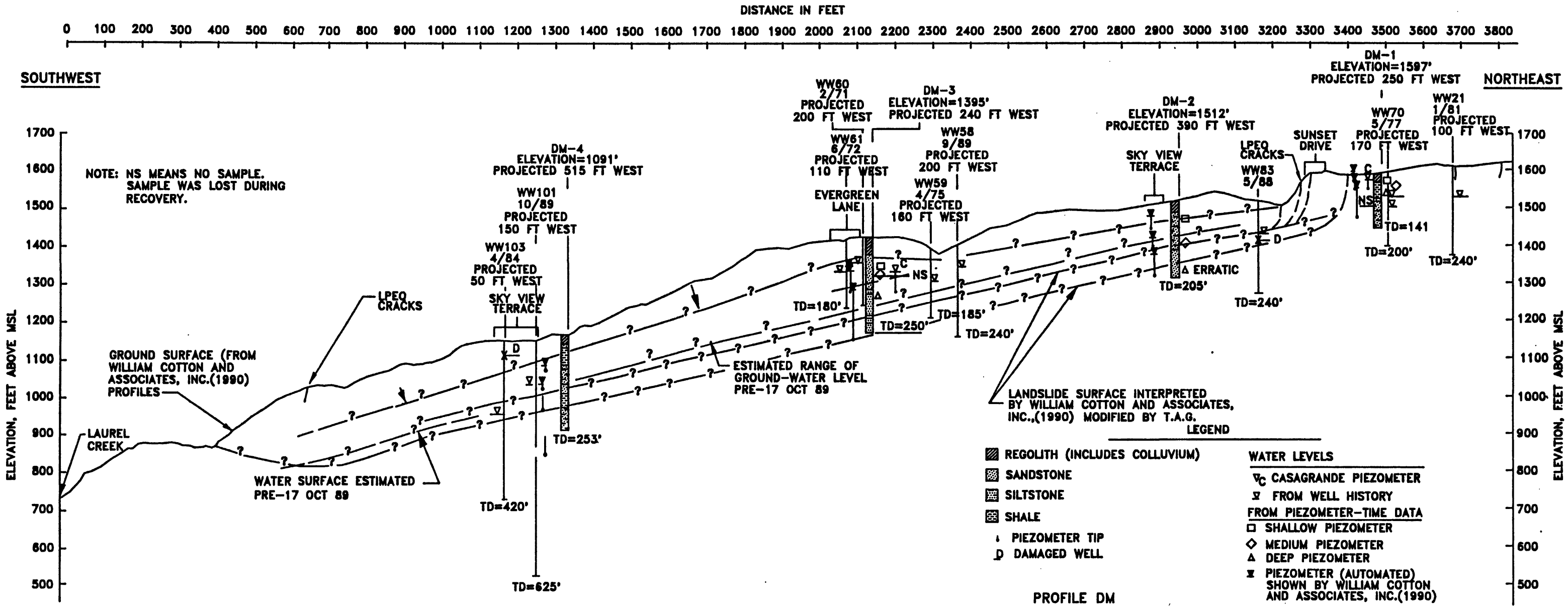

Figure 7.4 Geotechnical profile DM, Villa Del Monte area

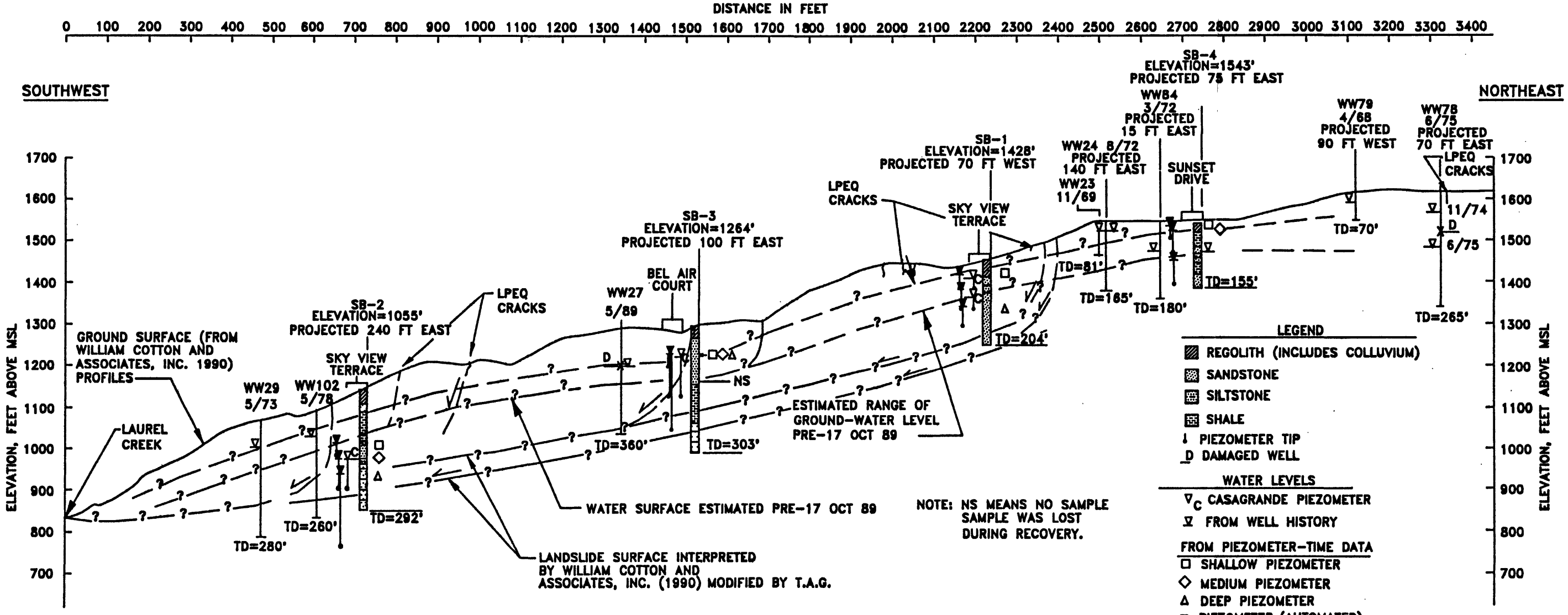

Figure 7.5 Geotechnical profile SB, Villa Del Monte area

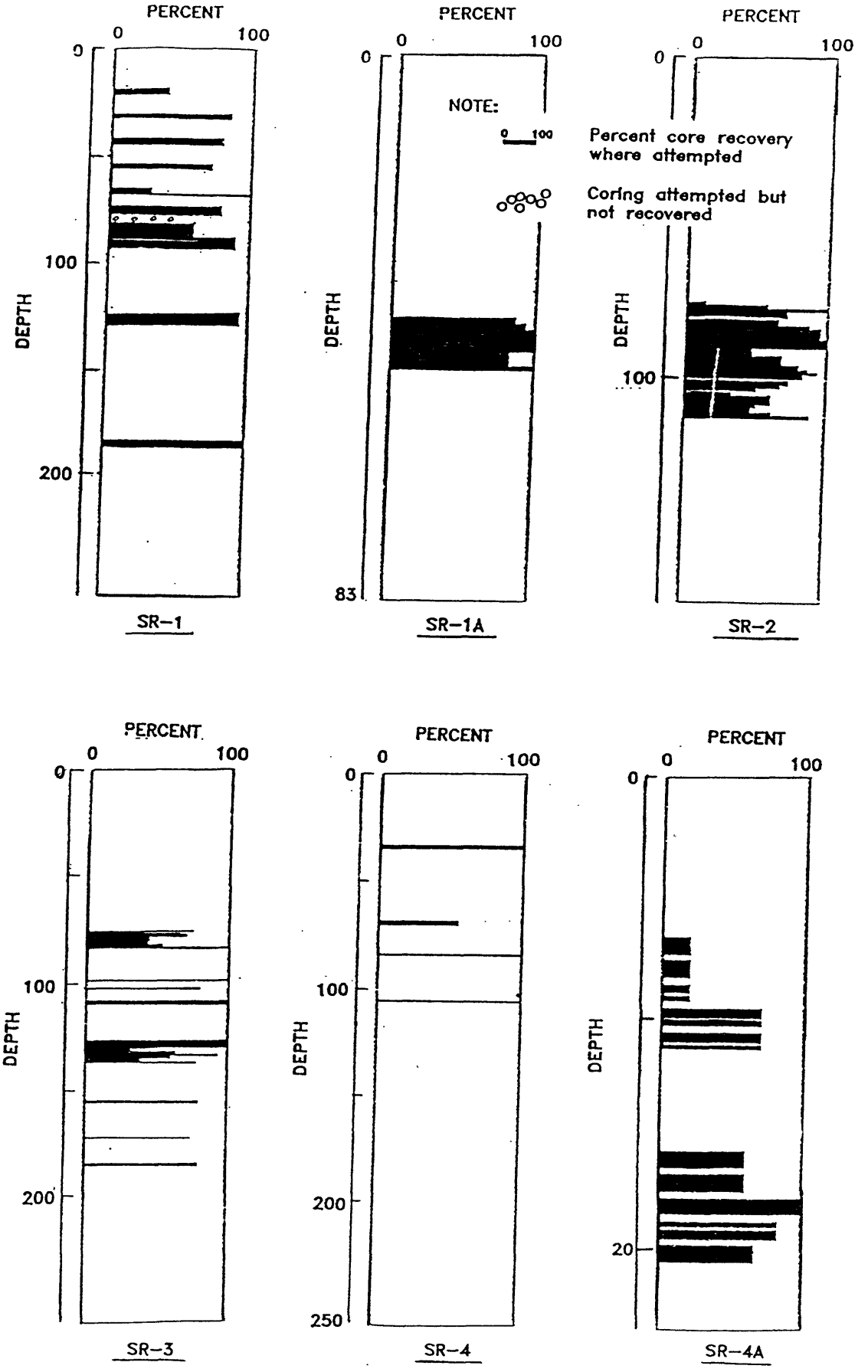

Figure 7.6(a). Percent core recovery versus depth, borings SR-1, SR-1A, SR-2, SR-3, SR-4, SR-4A.

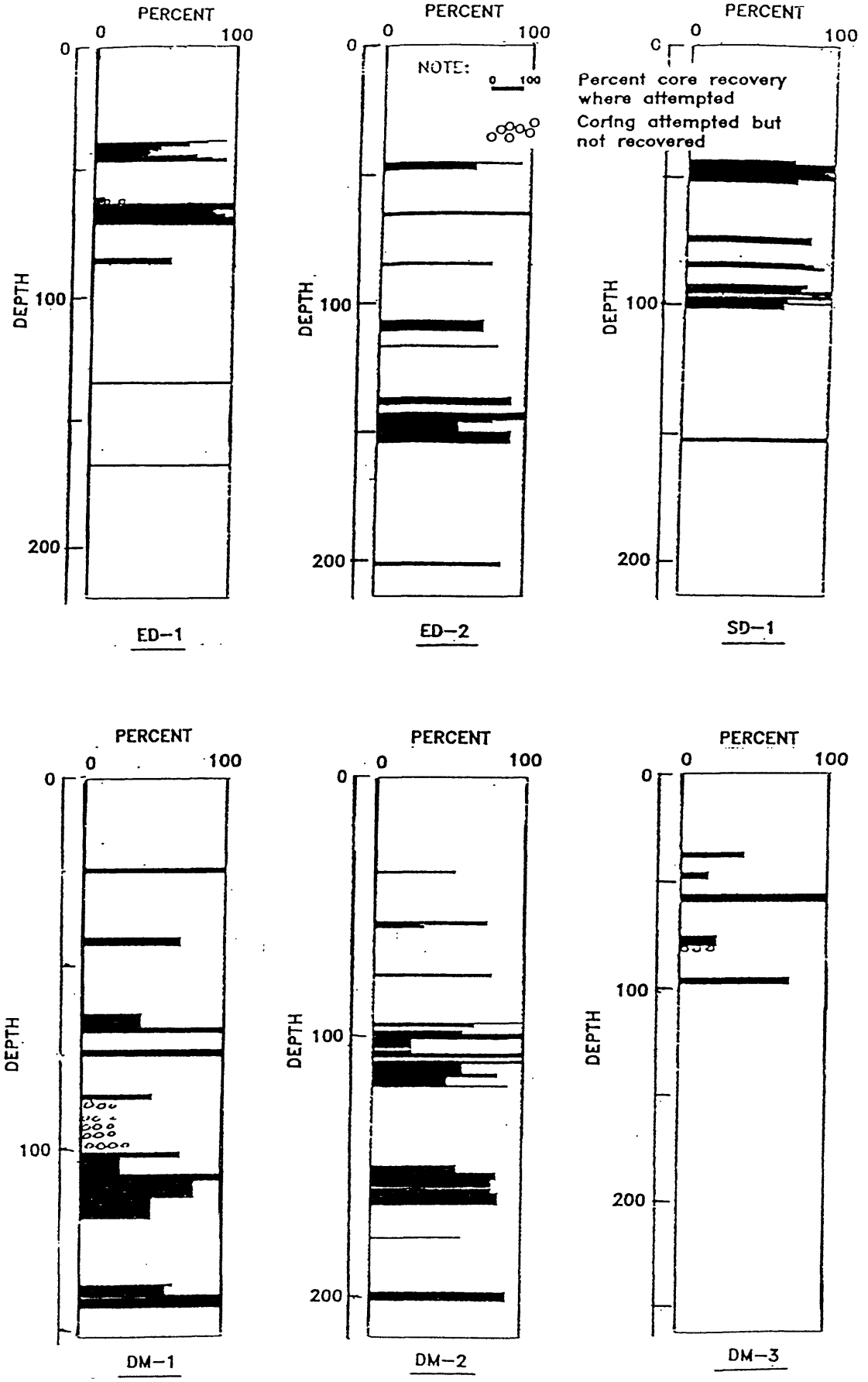

Figure 7.6 (b). Percent core recovery versus depth, borings ED-1, ED-2, SD-1, DM-1, DM-2, DM-3.

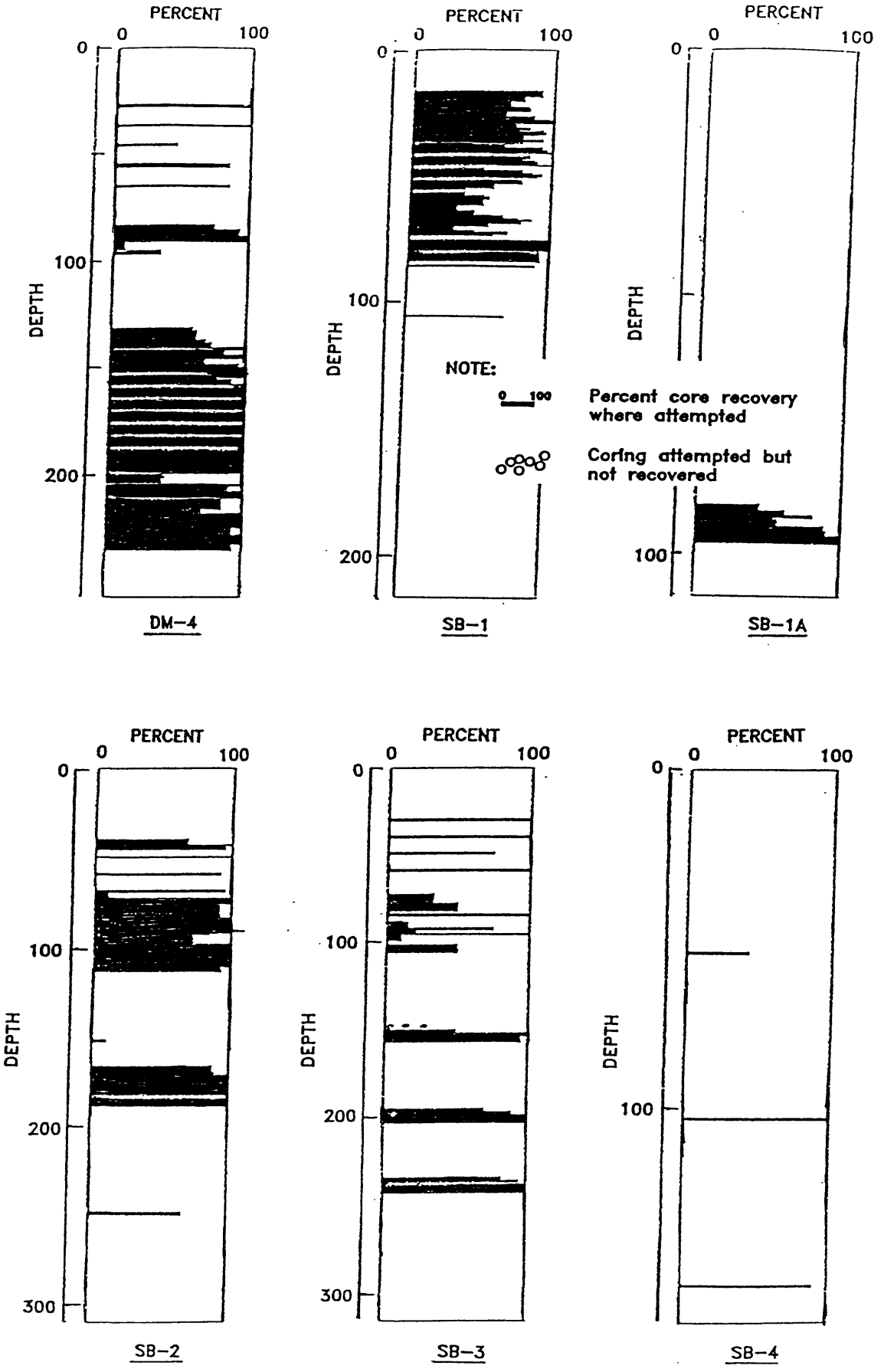

Figure 7.6(c). Percent core recovery versus depth, borings DM-4, SB-1, SB-1A, SB-2, SB-3, SB-4.

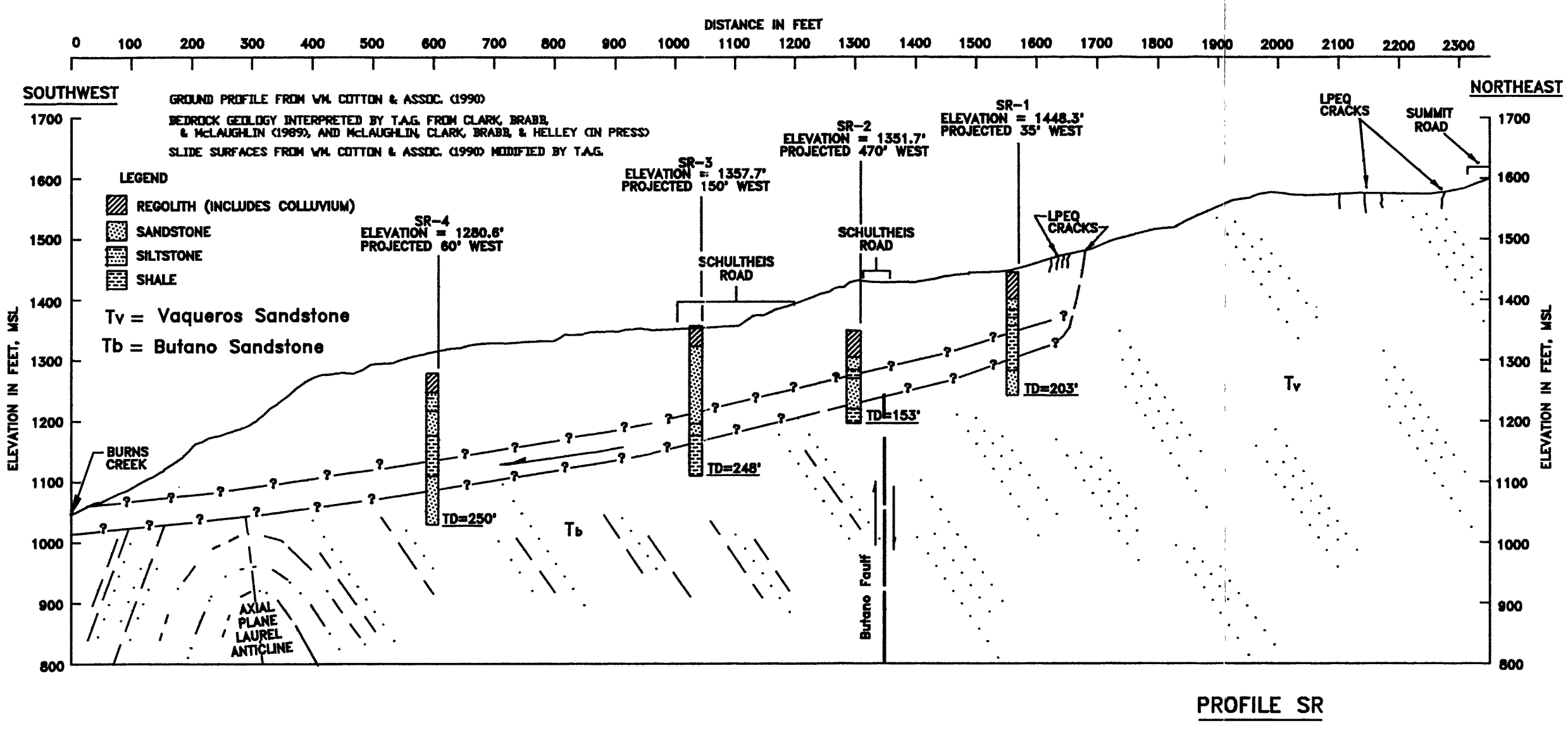

PROFILE SR

Figure 7.7 Geologic cross section along SR profile

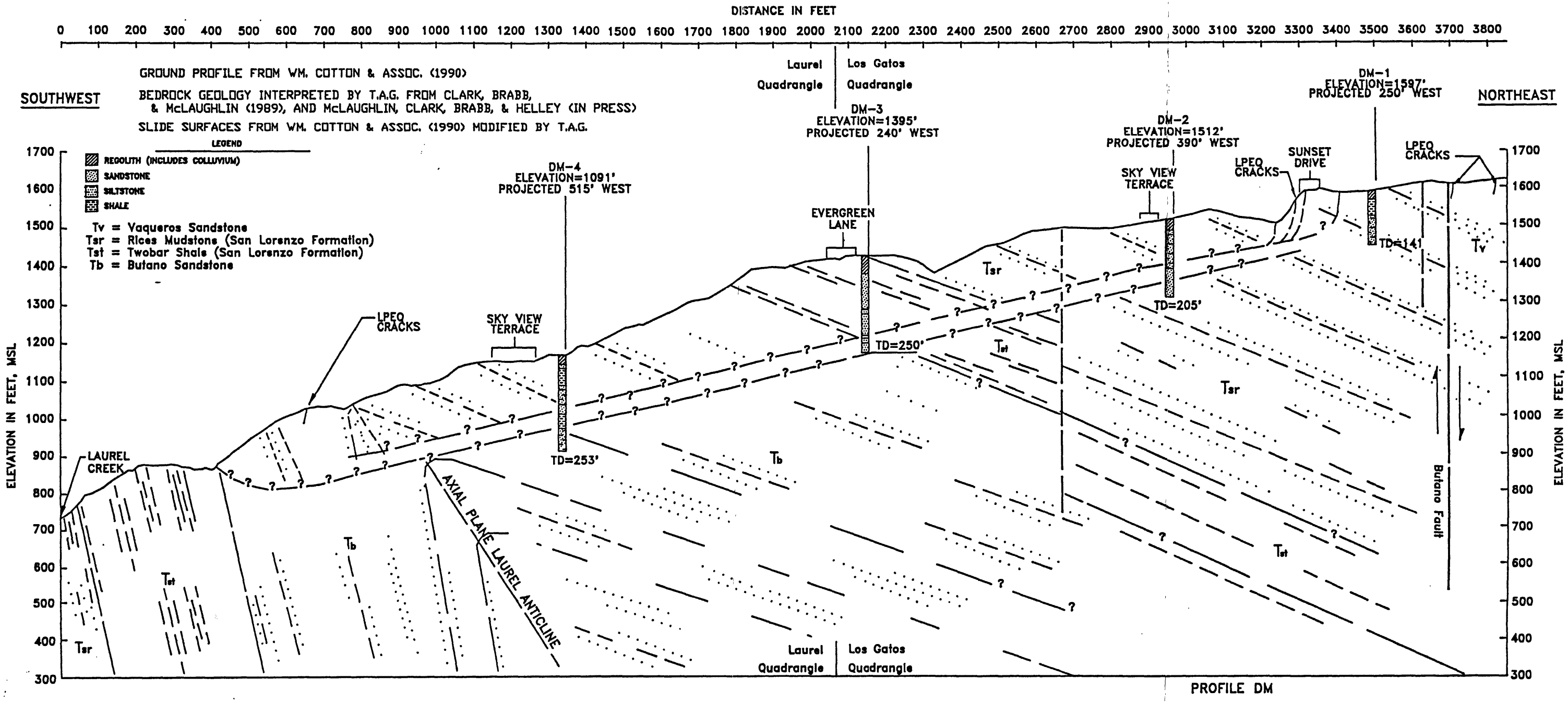

Figure 7.8 Geologic cross section along DM profile

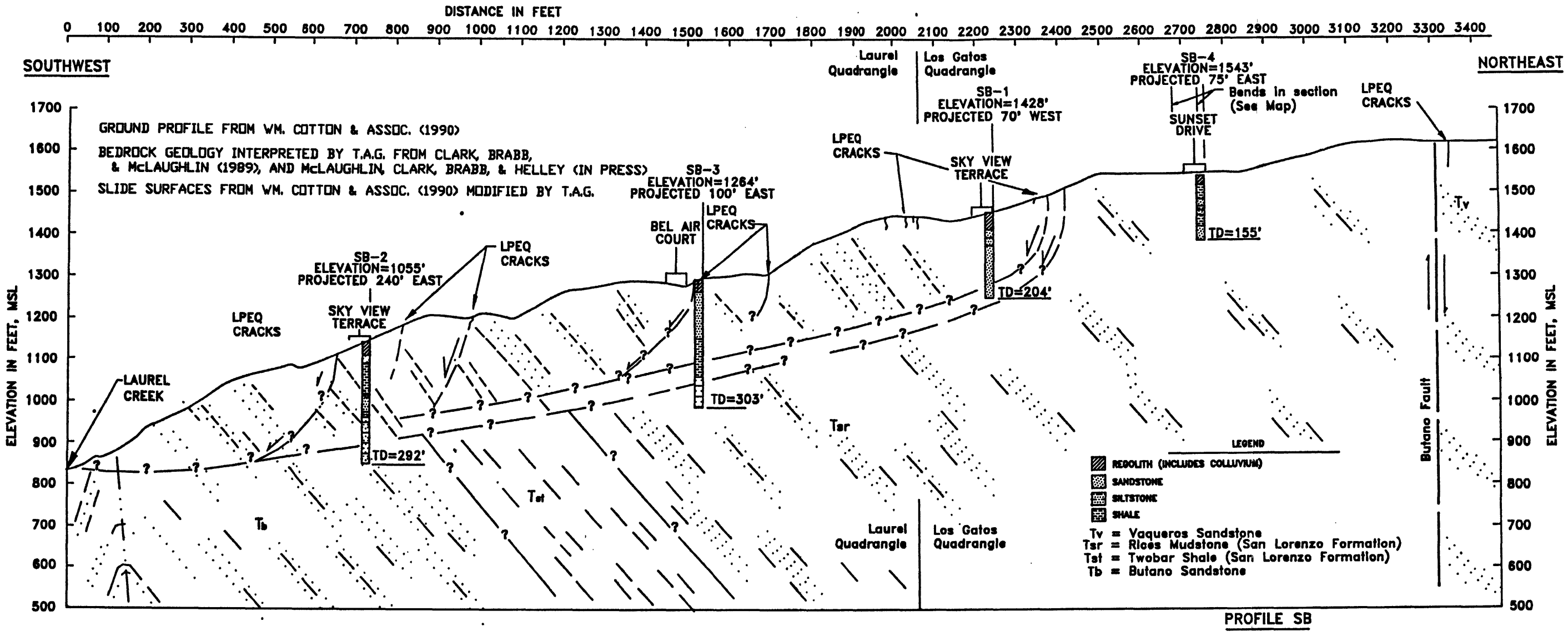

Figure 7.9 Geologic cross section along SB profile

TABLE 7.1: GENERAL INFORMATION ON BORINGS, UPPER SCHULTHEIS AND VILLA DEL MONTE AREAS
(Depths in Feet, dates 1989/1990)

Boring Number	Total Depth	Dates Start	Dates Finish	Drilled by	Bottom of Inclinometer Casing	Initial Inclinometer Reading	Piezometer Depths Shallow	Piezometer Depths Medium	Piezometer Depths Deep	Casagrande Piezometer Depths
SR-1	203	12/18	12/22	Pitcher	200	1/8/90	39.5	79.5	198	
SR-1A	82.5	12/29	01/02	Pitcher	--	--	--	--	--	38 and 77.2
SR-2	153.5	01/03	01/05	Pitcher	150	1/9/90	69.5	99.5	149.5	--
SR-3	248	01/08	01/02	Pitcher	250	3/19/90	59.5	169.5	240	175
SR-4	250	01/29	03/13	Pitcher	244	3/19/90	66	116	176	116
ED-1	208	01/17	01/23	Pitcher	200	2/1/90	49.5	94.5	199	--
ED-2	202	01/23	01/30	Pitcher	200	3/8/90	55	109.5	199.5	--
SD-1	203	01/40	01/10	Pitcher	200	1/12/90	38.8	95	188.8	--
DM-1	141	01/29	01/31	AllTerrain	140	3/14/90	39.5	61	139.5	61
DM-2	205	01/15	01/23	Pitcher	200	2/27/90	69.5	119.5	199.5	--
DM-3	250	01/30	03/09	Pitcher	250	3/14/90	60	120	250	120
DM-4	253	01/18	01/25	AllTerrain	250	2/14/90	70	130	250	--
SB-1	204	12/21	12/30	Pitcher	200	1/9/90	38	90	130	--
SB-1A	100	01/02	01/03	Pitcher	--	--	--	--	--	37 and 89.7
SB-2	292	01/02	01/10	AllTerrain	290	3/13/90	69.5	149.5	289	150
SB-3	303	01/10	01/18	AllTerrain	300	3/13/90	69.5	139.5	219.5	138
SB-4	155	01/11	01/12	Pitcher	150	3/1/90	35	69.5	149.5	--
SB-4A	20	01/15	01/15	Pitcher	--	--	--	--	--	--

#141, which had been reported damaged at a depth of 97 feet (Brumbaugh, 1990), one (SR-3) near the center of the landslide, and one (SR-4) relatively low on the slope. Data from these boreholes were used to construct cross sections depicting subsurface geotechnical and geologic conditions. The location of the cross-section line is shown in figure 7.1, and the geotechnical and geologic cross sections themselves are shown, respectively, in figures 7.3 and 7.7.

In the Villa Del Monte landslide complex, 13 boreholes were drilled to depths of 20 to 303 feet beneath the ground surface in the locations shown in figure 7.2 Six boreholes were drilled in the Upper Skyview Terrace-Bel Air Court area: two boreholes (SB-4 and SB-4A) upslope from the zone of concentrated ground-cracking, two boreholes (SB-1 and SB-1A) immediately downslope from the upper margin of this zone, one borehole (SB-3) near the center of the zone, and one borehole (SB-2) near the downslope margin. Likewise, three boreholes were drilled in the Sunset Drive area (SD-1, DM-1, and DM-2), one borehole (DM-4) was drilled in the Lower Skyview Terrace area, one borehole (ED-1) was drilled in the Deerfield Road area, one borehole (ED-2) was drilled to the west of this area, and one borehole (DM-3) was drilled in the relatively uncracked area in the interior of the Villa Del Monte landslide complex (fig. 7.2). Data from these boreholes were used to construct two geotechnical cross sections and two geologic cross sections depicting subsurface conditions. Locations of the cross-sections lines are shown in figure 7.2, and the cross-sections themselves are shown in figures 7.4 , 7.5, 7.8 and 7.9.

2. Drilling and Sampling Methods

All boreholes were drilled with rotary-wash drill rigs by Pitcher Drilling Company of Palo Alto and All Terrain Drilling of Roseville. The rotary-wash setup consists of a drill bit attached to a series of hollow drill rods. Fluid is pumped through the drill rods to the drill bit where it enters the borehole. The fluid picks up the soil and rock pieces (cuttings) loosened by the bit and travels up the borehole to the surface, where it is collected in a large tub. A series of baffles in the tub allows the cuttings to settle out of the fluid. Samples of these cuttings are also captured in a screen, visually classified, and logged by an engineering geologist. The fluid is then recirculated. Where the soil or rock contains open fractures, drilling fluid can enter the fractures and be lost. This results in the fluid not

returning to the surface. This phenomenon is termed "losing circulation" and is noted on the borehole logs (William Cotton and Associates, Inc., 1990, v. 2, Appendix F) as indicative of highly fractured rock.

The drilling rate is determined by monitoring and timing the advance of the drill bit into the ground. The drilling rate can be influenced by many factors, including the type and condition of the drill bit, the pressure exerted on the drill rod, and the speed with which the bit is rotated. However, the drilling rate is also indicative of the relative physical condition of the subsurface materials and consequently provides an additional source of subsurface data. In general, when the drilling rate becomes faster, the material being drilled is softer and (or) more fractured than the overlying material.

Decisions concerning which materials to sample were based on several factors. To examine the lithology and physical condition of all types of rock and soil encountered during subsurface exploration, samples generally were taken when changes in cuttings or drilling rates indicated changes in material or physical condition. Because landslide basal rupture surfaces are typically associated with fractured or soft material, sampling was also attempted when circulation was lost or when drilling rates became particularly high. In addition, sampling intervals were targeted at potential rupture surfaces identified on preliminary cross sections developed by William Cotton and Associates, Inc., prior to drilling.

Two types of samplers, Pitcher Barrel and rock core, were available on the drill rigs provided by Pitcher Drilling Company. The Pitcher Barrel sampler can retrieve relatively undisturbed Shelby tube samples of soil or soft rock approximately 30 inches long. The Shelby tube, which is 3 feet long, has an outside diameter (OD) of 3 inches, and an inside diameter (ID) of 2-7/8 inches, is slowly pushed into the earth while a core barrel rotates around it, relieving the friction along the outside of the liner. Where the rock was too hard to use Shelby tubes, rock core barrels were used. Rock core samplers were NX (2-1/8 inches ID) and HW (Christiansen Diamond Products NQ version, 2-2/5 inches ID), tip-and side-circulating barrels with diamond or carbide bits. The rock core barrels are attached to the drill rod and advanced by pushing on the drill rod while the entire barrel rotates and cuts around the sample. When the barrel is lifted out of the hole, a core-catching device secures the disturbed sample inside the barrel.

The sampling methods available on the All Terrain drill rigs were the Pitcher Barrel sampler and a 94-mm-wireline punch, drill, and core system. The wireline system employed a core barrel (3.71 inches OD and 2.56 inches ID) lowered by wires, through the hollow drill stem, to the bottom of the hole. The coring process is similar to that previously described, except that when the sampling is completed, the barrel (with disturbed samples inside) can be disengaged and retrieved using the cables, eliminating the need to pull all of the drill rod out of the hole after each core interval.

Samples obtained by rock core barrels were logged and classified in detail in the field and stored in core boxes. Representative Pitcher Barrel samples were also extruded in the field and logged in detail to characterize the physical condition of the material during drilling. These disturbed samples, if still relatively intact, were then trimmed and returned to the tubes. Both the extruded and unextruded Pitcher Barrel samples were sealed at both ends with wax, capped and taped, and transported to the laboratory facility for safekeeping. Extruded samples not replaced into the Shelby tubes were stored in core boxes. Unextruded tube samples were X-rayed to obtain information regarding lithologic contacts or shear surfaces.

In the 18 boreholes, total drilling was approximately 3,500 linear feet. Sampling was attempted in approximately 20 percent of this total. The intervals sampled and the recovery rate in each interval are shown in figure 7.6, and a summary of drilling results is given in table 7.2. The sample recovery techniques permitted detailed descriptions of the rock and soil conditions when sample recovery was good. However, the weakest zones encountered in these areas, which were those most likely to contain landslide shear surfaces, were also the zones where material was most likely to be lost owing to grinding and washing during drilling.

3. Subsurface Materials and Interpretation of Landslide Depths

Examination of samples and cuttings showed that five different earth materials, derived from the geologic formations in the Upper Schultheis Road and Villa Del Monte areas, can be identified, as follows:

TABLE 7.2: SOIL AND ROCK RECOVERY DATA FROM BORINGS, UPPER SCHULTHEIS AND VILLA DEL MONTE AREAS
(Depths in Feet)

Boring	Total Depth	Depth of Regolith	Feet Cored	Feet Not Cored	Percent Cored	Overall Recovery in Cored Interval(s), %	Dominant Rock Types*	Remarks
SR-1	203	43	42	161	21	70	Sandstone, Shale	
SR-1A	82.5	82.5	9	74	11	94	Sandstone, Shale	
SR-2	153.5	36.5	36	118	23	71	Sandstone, Shale	Sheared mixtures of rock and clay (in recovered core), may represent failure zones: 89.0-89.75, 95.0-96.6, 97.5-99.25. A damaged water well is nearby.
SR-3	248	32	28	220	11	73	Sandstone, Shale	
SR-4	250	26.5	6	244	2	85	Sandstone, Siltstone, Silty Shale	
ED-1	208	31.5	27	181	13	72	Sandstone, Silty Shale	
ED-2	202	11	35	167	17	74	Sandstone, Siltstone	
SD-1	203	16	28	175	14	89	Siltstone	
DM-1	141	19	59	82	42	51	Siltstone, Shale	
DM-2	205	2	53	152	26	72	Siltstone; Sandstone	

TABLE 7.2 (continued)

DM-3	250	0.5	24	226	10	50	Sandstone; Siltstone	
DM-4	253	3	136	117	54	87	Shale, Sandstone; Siltstone	
SB-1	204	43	70	134	34	77	Sandstone, Siltstone	
SB-1A	100	43	8	92	8	77	Siltstone, Shale, Sandstone	
SB-2	292	31	87	205	30	88	Shale; Siltstone, Sandstone	Two major zones of good core recovery document extensive crushed material moderate to steep dips, sheared zones, rapidly varying rock types
SB-3	303	30	76	227	25	62	Sandstone; Shale; Siltstone	
SB-4	155	18	3	152	2	77	Shale, Sandstone	
SB-4A	20	18	10	10	50	57	(Dominantly Regolith)	

*Commas = roughly equal occurrences. 1 semicolon = major type followed by minor. 2 semicolons = dominant rock in respective sections of boring.

* Colluvium: surficial soils that have evolved as a result of weathering, downslope creep, and other slope-movement processes.

* Regolith: highly weathered and fractured bedrock materials that have been subjected to cyclic changes in ground-water levels and slope-movement processes. This material contains angular, weathered, gravel-to-boulder sized rock fragments with varying amounts of soil matrix.

* Sandstone: predominantly medium gray to dark gray and composed of very-fine-grained to medium-grained quartz sand with varying amounts of cement. Bedding is generally massive and typically cannot be determined by examination of samples. Overall, the most competent material encountered during subsurface exploration. Typically hard with low intergranular porosity and permeability.

* Shale: predominantly dark-yellow-brown shale composed of clay- and silt-sized particles. Commonly fissile (i.e., easily splits into very thin slabs or sheets generally parallel to bedding). In general, the most highly fractured material encountered during the drilling operations. Samples often contained a high percentage of clay matrix.

* Siltstone: varies in color from gray to dark-yellow-brown and is composed mainly of silt-sized particles. Bedding is also typically fissile. This unit was intermediate between sandstone and shale in degree of fracturing.

Figures 7.3, 7.4, and 7.5 show geotechnical information, which was developed during the subsurface investigation, as discussed below. Figures 7.7, 7.8 and 7.9 are companion cross sections to figures 7.3, 7.4 and 7.5, respectively, and show geologic information, which was developed as part of this study from recent published and unpublished geologic quadrangle maps of the USGS (Clark, Brabb, and McLaughlin, 1989, with landslide boundaries revised by McLaughlin and Clark, 1990, unpublished data; McLaughlin and Clark, in press). The principal difference between the geologic cross sections presented herein and those in William Cotton and Associates, Inc.,

(1990) is the inclusion of information from the recent USGS maps; these maps present interpretations of the regional geology that differ significantly from the earlier interpretations that were generally available at the time when the cross sections of William Cotton and Associates, Inc., (1990) were developed.

It is important to note that despite the presence of recently prepared regional geologic maps, the work performed by William Cotton and Associates, Inc., and the work performed in the present in their study, the detailed geologic structure of Summit Ridge and adjacent areas is not well understood. Deep soils and regolith, dense vegetation, and landslide deposits obscure the underlying bedrock. Consequently, the distribution of rock units and the geologic structure can only be approximated, and the distribution and structure of the bedrock shown on cross sections must be regarded as interpretive.

To determine the likely depths of landslides in the Villa Del Monte and Upper Schultheis Road areas, data from exploratory drilling logs, drilling rates, geologic maps, maps of ground cracks and other surface features, and water-well damage reports were initially analyzed by William Cotton and Associates, Inc. (1990) and reviewed and locally modified during this study.

To prepare the cross sections showing basal rupture surfaces, data from boreholes and water wells were projected in plan view along lines perpendicular to the sections. Tops of boreholes were plotted in the vertical plane at the surveyed elevations. Boreholes were projected into cross sections from as far away as 670 feet, but data from boreholes projected more than approximately 100 feet were judged by William Cotton and Associates, Inc., (1990, v. 1, p. E4) to be less representative of conditions along the cross sections than data from closer boreholes. Water-well data were also projected onto the cross sections, but neither the locations nor the elevations of individual water wells were established as accurately or as precisely as the boreholes. The mapped location of each water well is estimated to be within approximately 100 feet of its actual location, and the cross sections only portray water wells that are located less than approximately 200 feet from the section. For interpretive purposes, the tops of the projected water wells were plotted at the ground surface on the cross sections.

Limitations in the data, including the wide spacing and small diameter of the boreholes, lack of continuous sampling, and absence

of supporting exploration techniques, such as downhole geophysical logging, precluded a more precise or definite characterization of the basal portions of the landslides. In addition, the degree of development of specific shear surfaces within the basal zones shown is not well determined. However, the probable basal rupture zones shown on the cross sections (figs. 7.3, 7.4, 7.5, 7.7, 7.8, 7.9) were established from several types of data that are generally consistent, and these zones were determined warrant the additional testing and analyses discussed in Chapters VIII and Appendix A. In addition to these relatively deep, basal shear zones shown in the cross sections, note that shallower zones of soft, crushed, sheared, or highly fractured rock, rock containing clay seams, and zones of lost circulation were encountered in the boreholes, and thus additional, shallower and (or) more localized shear surfaces or zones may also be present.

B. Monitoring for Post-earthquake Movement Using Inclinometers

Inclinometers were installed to detect and monitor possible post-earthquake slope movements and to better define, if possible, the depths of landslide basal rupture surfaces. These instruments were placed in 15 boreholes in the Upper Schultheis Road and Villa Del Monte areas. Boreholes in which inclinometer casing was installed are listed in table 7.1 and located in figures 7.1 and 7.2. The instruments and their installation are discussed in detail by William Cotton and Associates, Inc., (1990, v. 1, p. 23-25). The type of inclinometer casing selected for installation was a SINCO™ 2.75-inch OD CPI quadri-grooved ABS casing with self-aligned O-ring sealed couplings. The probe used to monitor verticality deflections in the casings was a SINCO™ Digitilt Sensor with a sensitivity of one part in 10,000. This sensor is a waterproof, biaxial, digital inclinometer probe with a 24-inch wheel spacing. The sensor was connected to an ISIS™ conditioner and automatic data collector managed by a Packard Bell™ laptop computer.

The inclinometer casings are manufactured in 10-foot-long sections and contain four interior grooves opposed at 90°. The casing sections were connected with couplings (such that the grooves were aligned) and lowered to the bottom of the borehole, with one groove oriented downslope. This direction is defined as the "A+" direction, and the azimuth located at 90° to A+ is defined as the "B+" direction.

The annulus between the casing and the borehole was then grouted with Portland cement mix containing 5 percent bentonite.

The inclinometer is monitored by lowering the probe to the bottom of the casing (fig. 7.10). The wheels of the probe are opposed at 180°, and fit into the grooves in the casing oriented upslope and downslope. The probe measures the angle that the casing deviates from vertical in the A+ direction. The probe is then raised 2 feet (the length of the probe), and the process is repeated until the probe reaches the top of the casing. Following this, the probe is rotated 180° and lowered to the bottom of the casing once again, and readings are taken in the A- direction. The probe is then rotated 90° and again 180°, and readings are taken in the B+ and B- directions. The resulting data file contains four readings (two in each plane) for every 2 feet of depth. The first set of data taken for a particular inclinometer is termed the "initial" or "base" reading. Subsequent readings are acquired at time intervals judged sufficient to characterize any potential landslide movement.

After the data acquisition is complete, a computer software program averages the difference between the A+ and A- readings, and the B+ and B- readings. The program then subtracts the initial reading set from a subsequent set (chosen by the user) to produce a graph which shows the horizontal deflection since the initial reading as a function of depth. Measurements from the 15 installed inclinometer casings, showing cumulative deflections between the initial readings, and readings in May 1990, November 1990, and March 1991, respectively, are plotted in figures 7.11(a)-(o). Dates of initial readings are given in table 7.1.

Overall, the movements recorded by the inclinometers did not indicate renewed or ongoing displacements with depth. The only displacement that exceeded instrument system error of 0.25 inches of deflection per 100 vertical feet did so by the very small amounts of approximately 0.5 to 0.75 inches at depths of 50 and 100 feet, respectively, in boring DM4 (fig. 7.11d). This could indicate either small post-earthquake movement of the landslide mass or more localized movement toward the steep creek bank, near to and downslope from the instrument. The latter interpretation is supported by the lack of identifiable landslide movement in the other inclinometers. Further, the small deflections occurred in both the positive and negative directions. The small movements and variable directions suggest that settlement of the grout around the

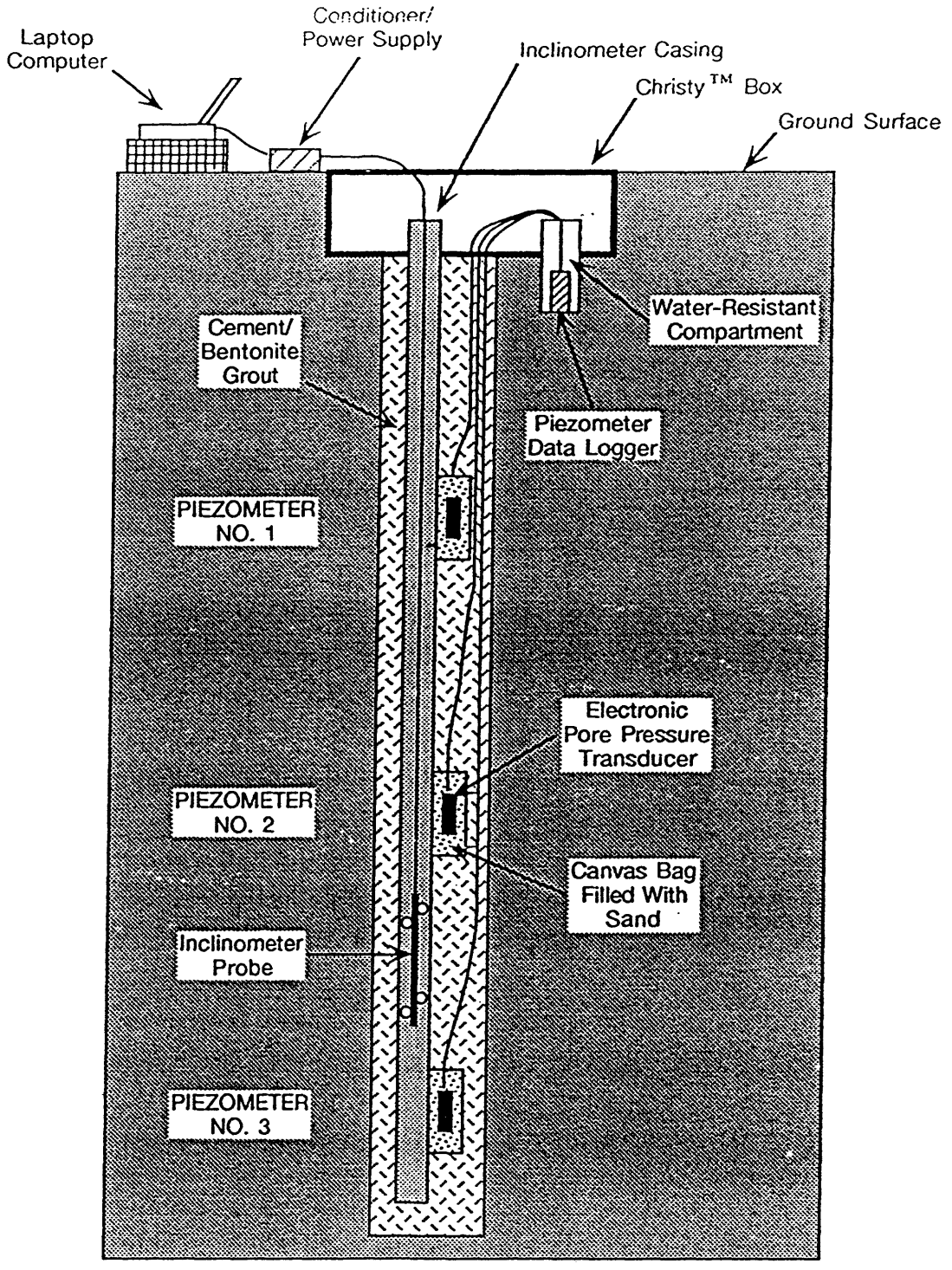

Figure 7.10 Schematic diagram of borehole instrumentation, Schultheis Road and Villa Del Monte Areas (from William Cotton and Associates, 1990).

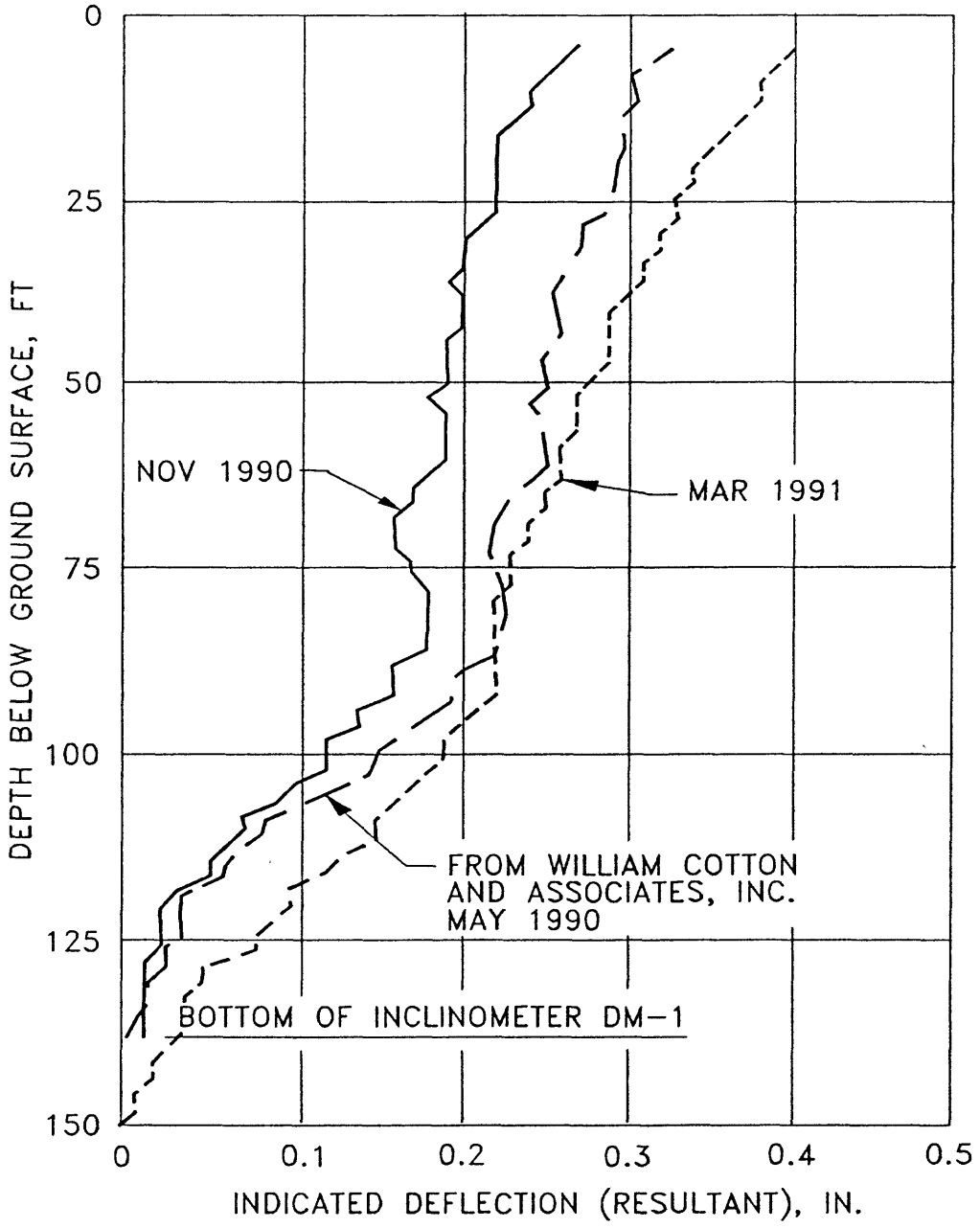

Figure 7.11(a). Inclinometer data for DM-1 (May and November 1990 and March 1991).

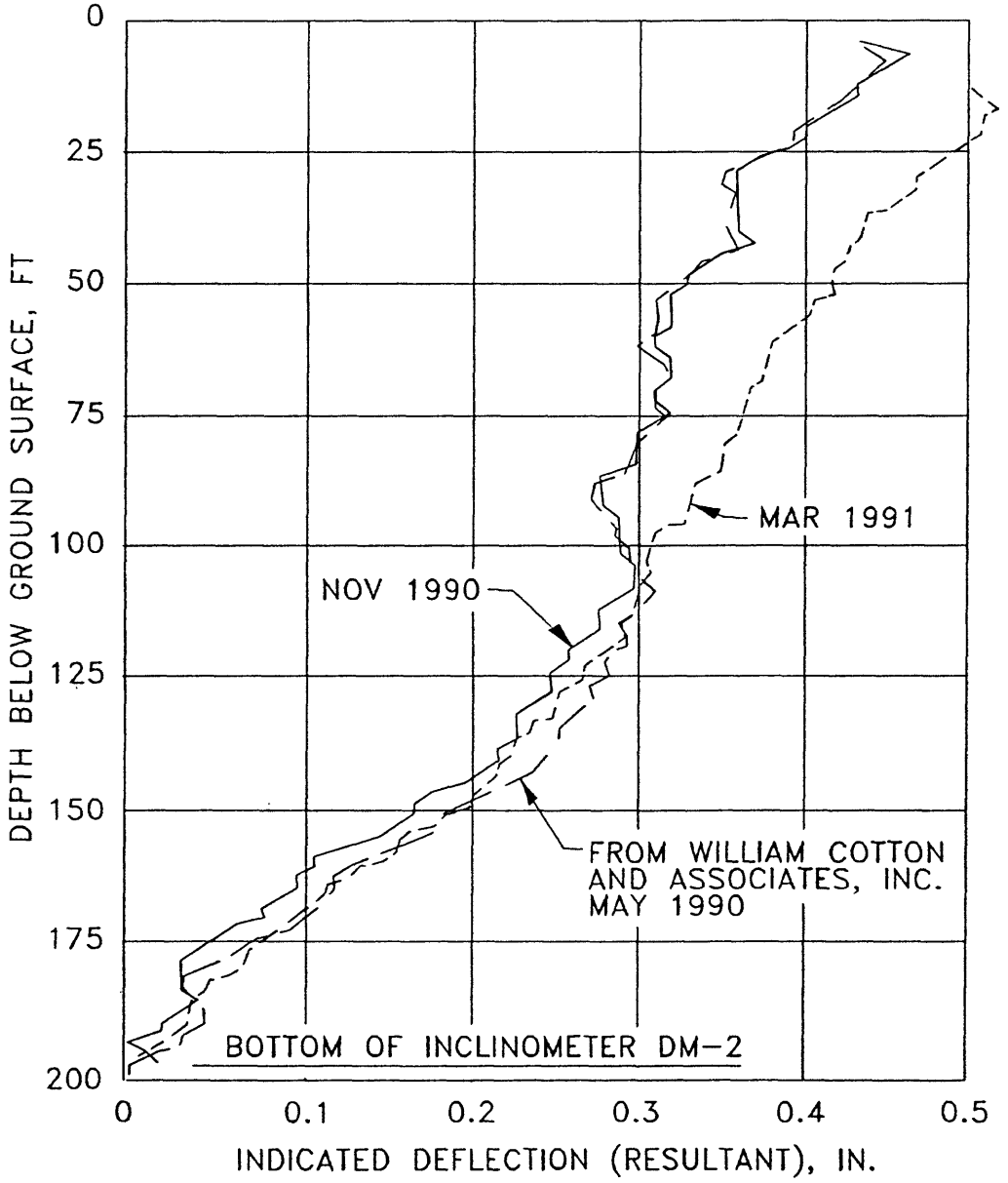

Figure 7.11(b). Inclinometer data for DM-2 (May and November 1990 and March 1991).

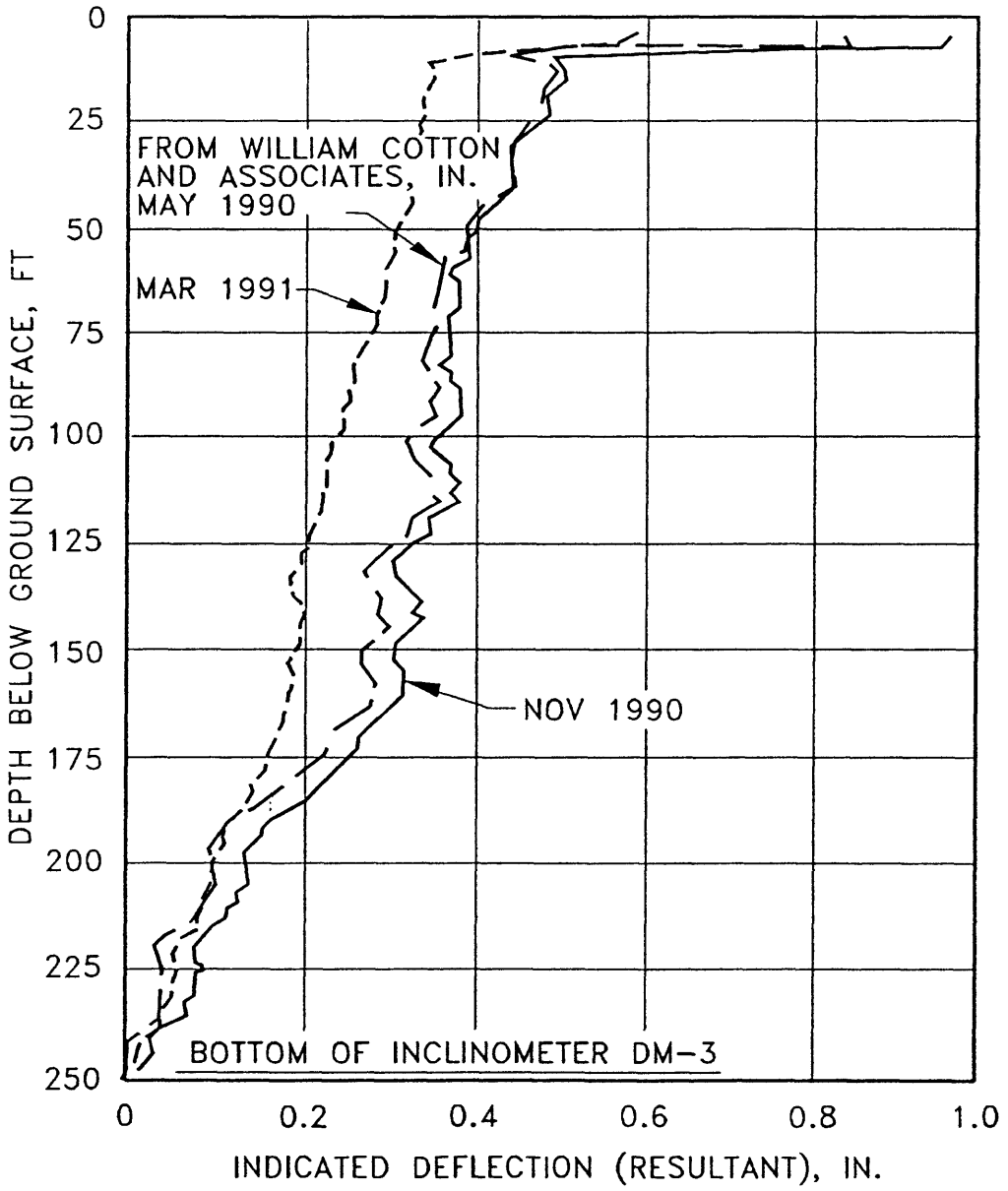

Figure 7.11(c). Inclinometer data for DM-3 (May and November 1990 and March 1991).

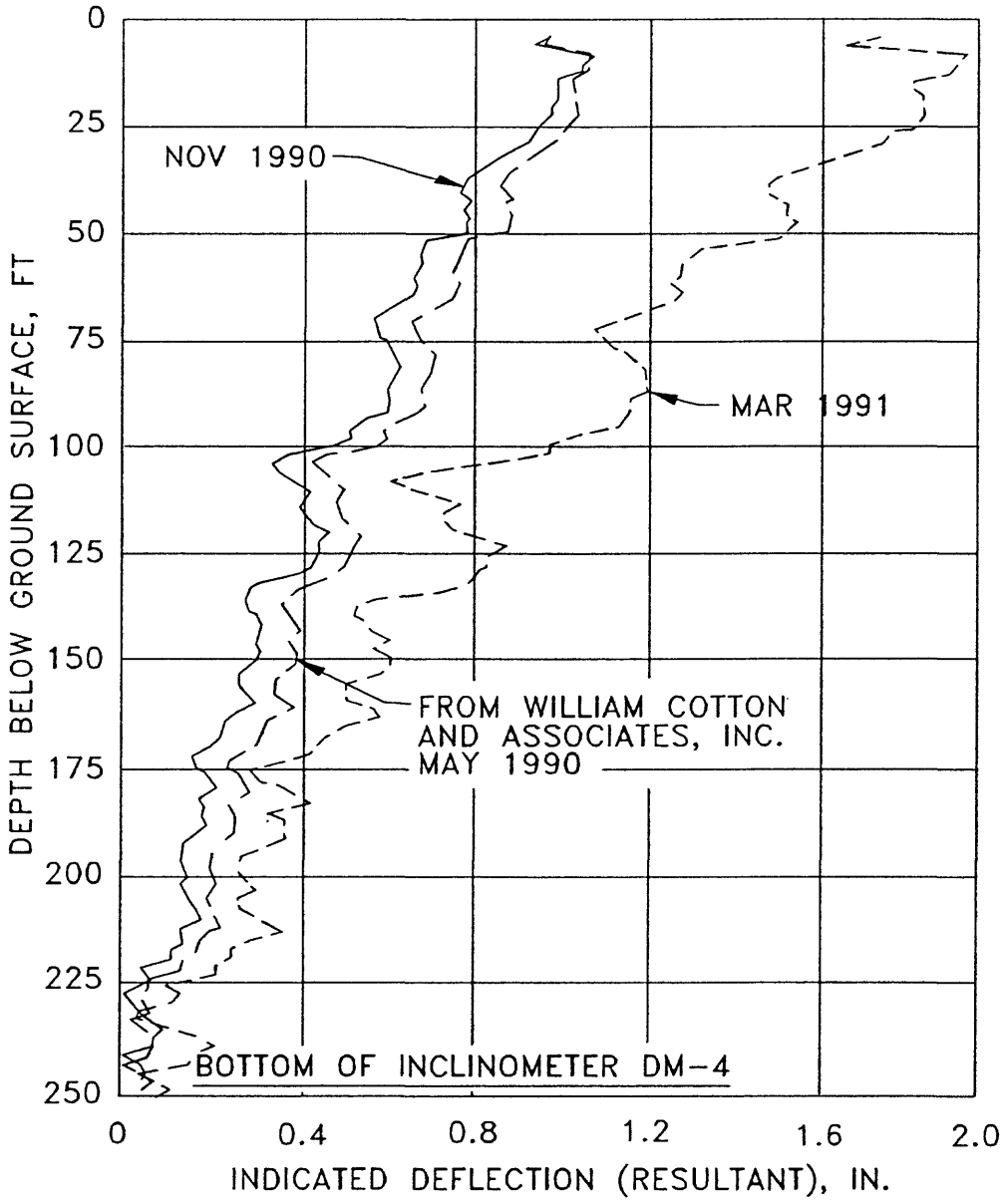

Figure 7.11(d). Inclinometer data for DM-4 (May and November 1990 and March 1991).

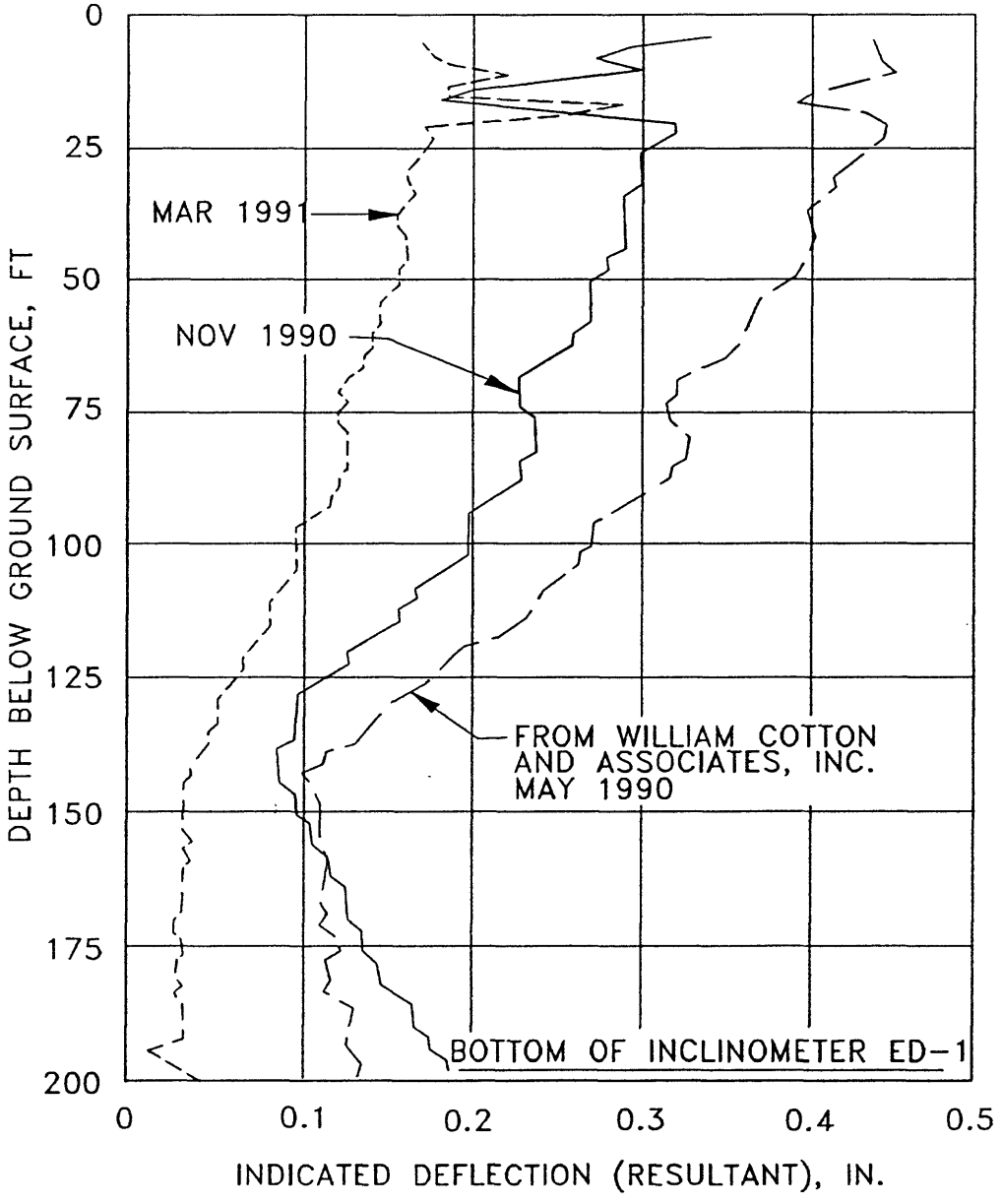

Figure 7.11(e). Inclinometer data for ED-1 (May and November 1990 and March 1991).

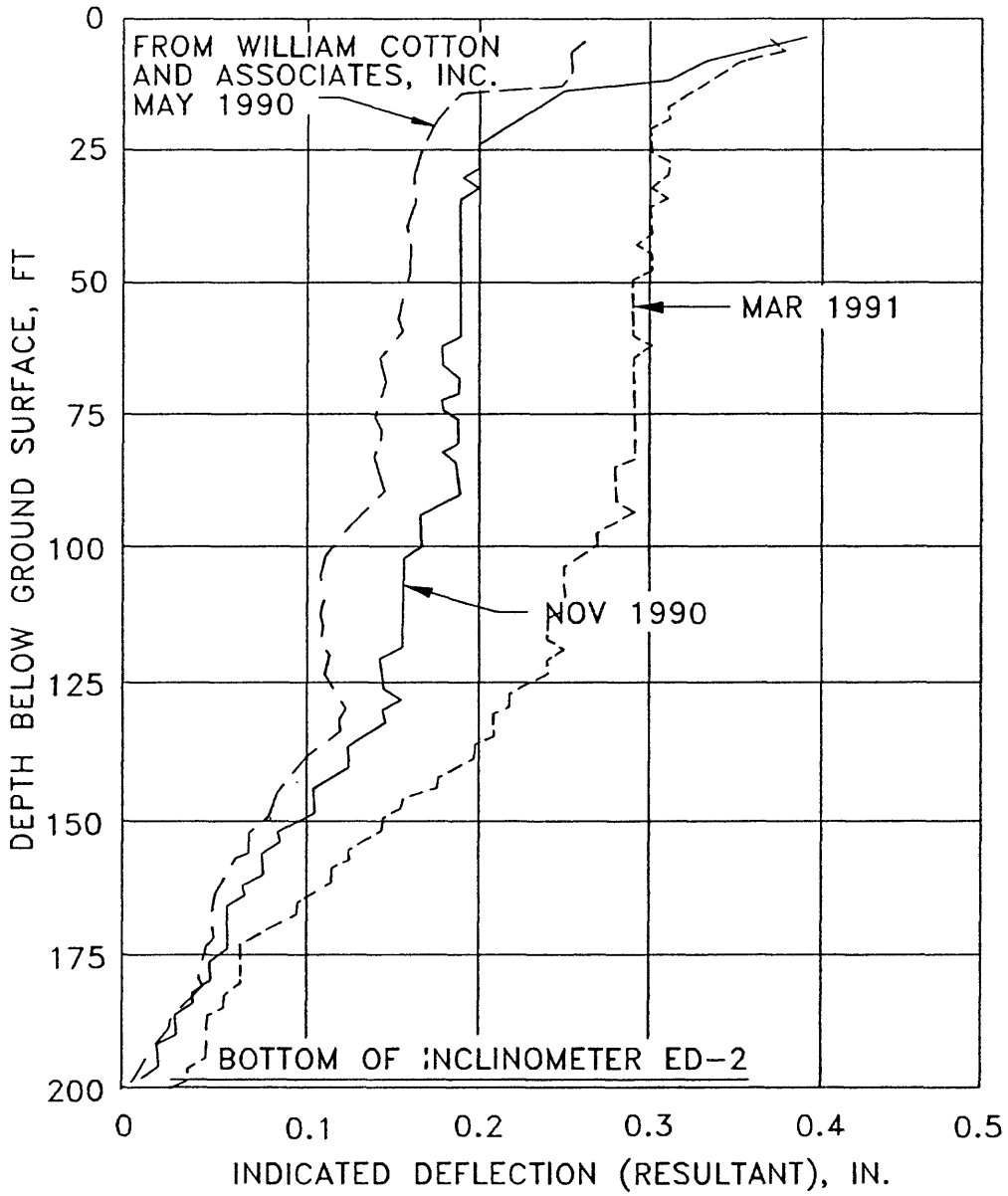

Figure 7.11(f). Inclinometer data for ED-2 (May and November 1990 and March 1991).

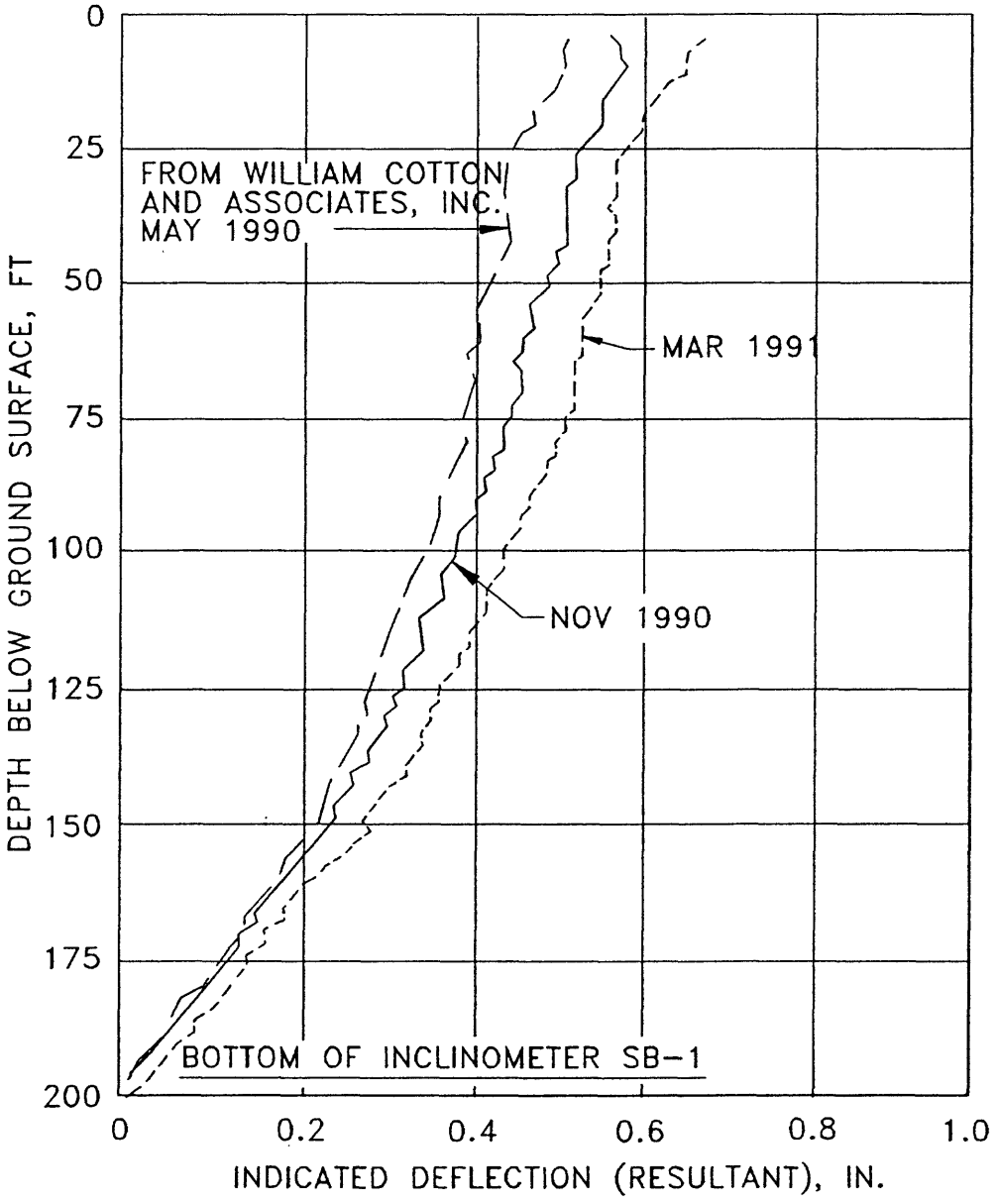

Figure 7.11(g). Inclinometer data for SB-1 (May and November 1990 and March 1991).

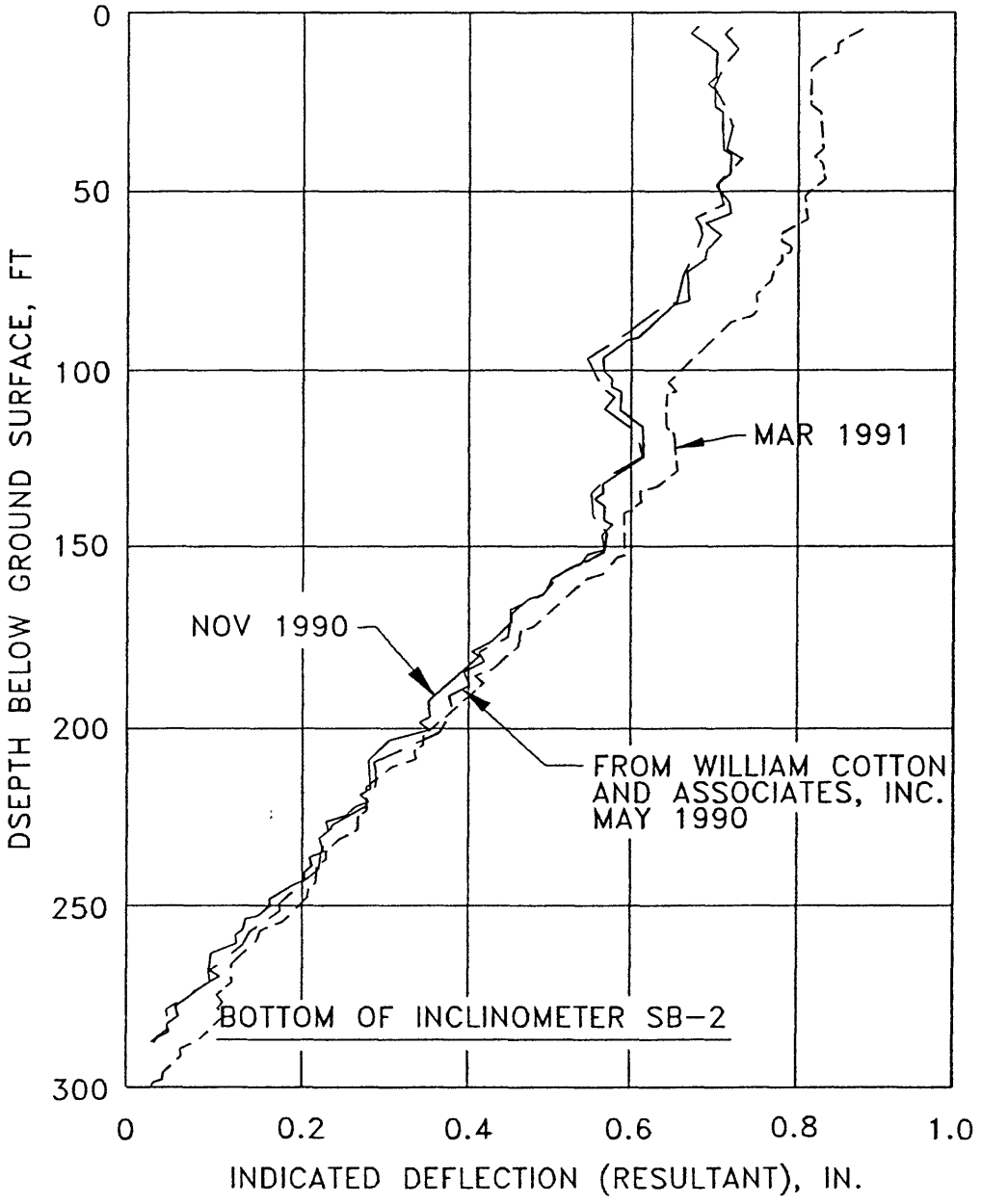

Figure 7.11(h). Inclinometer data for SB-2 (May and November 1990 and March 1991).

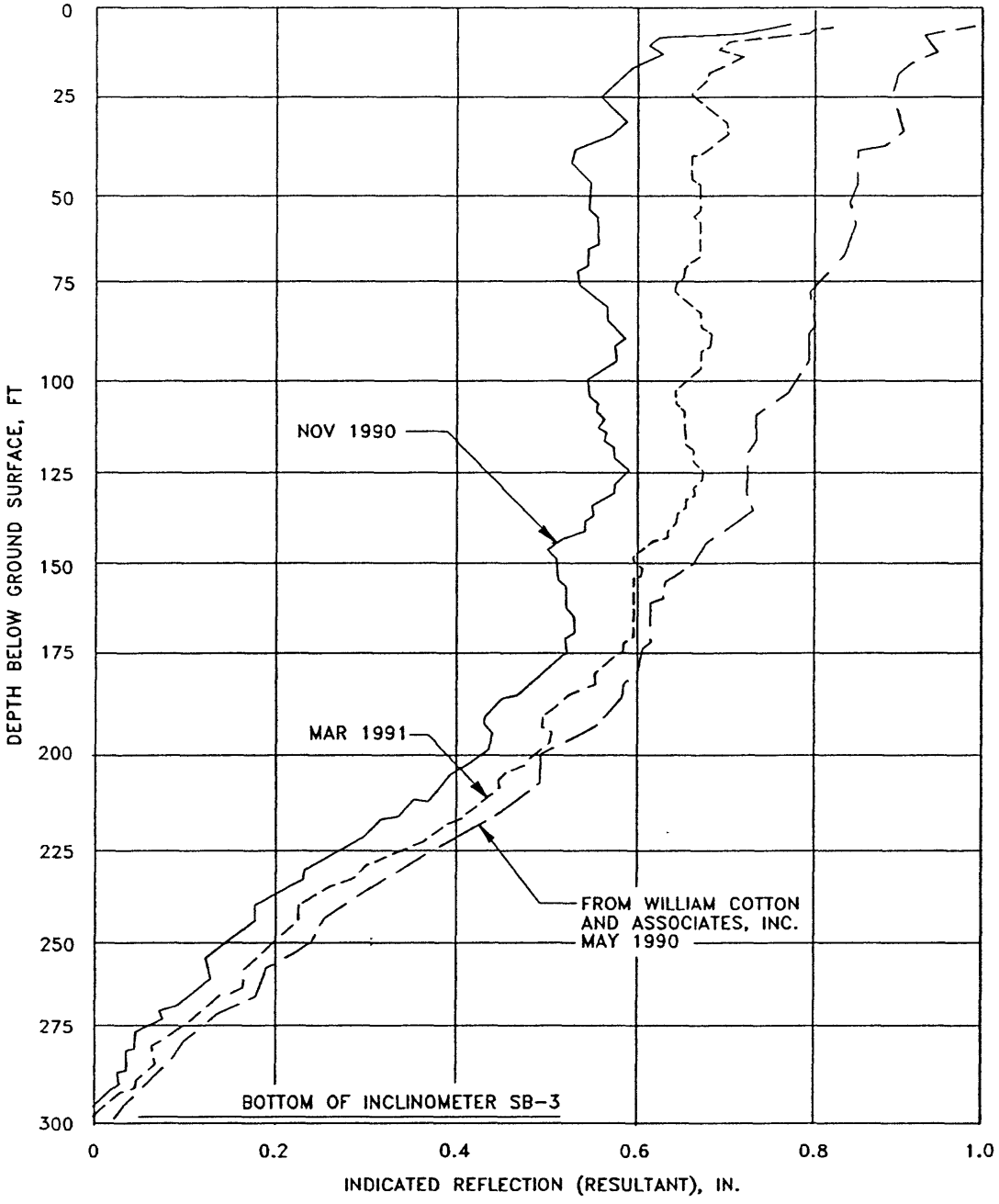

Figure 7.11(i). Inclinometer data for SB-3 (May and November 1990 and March 1991).

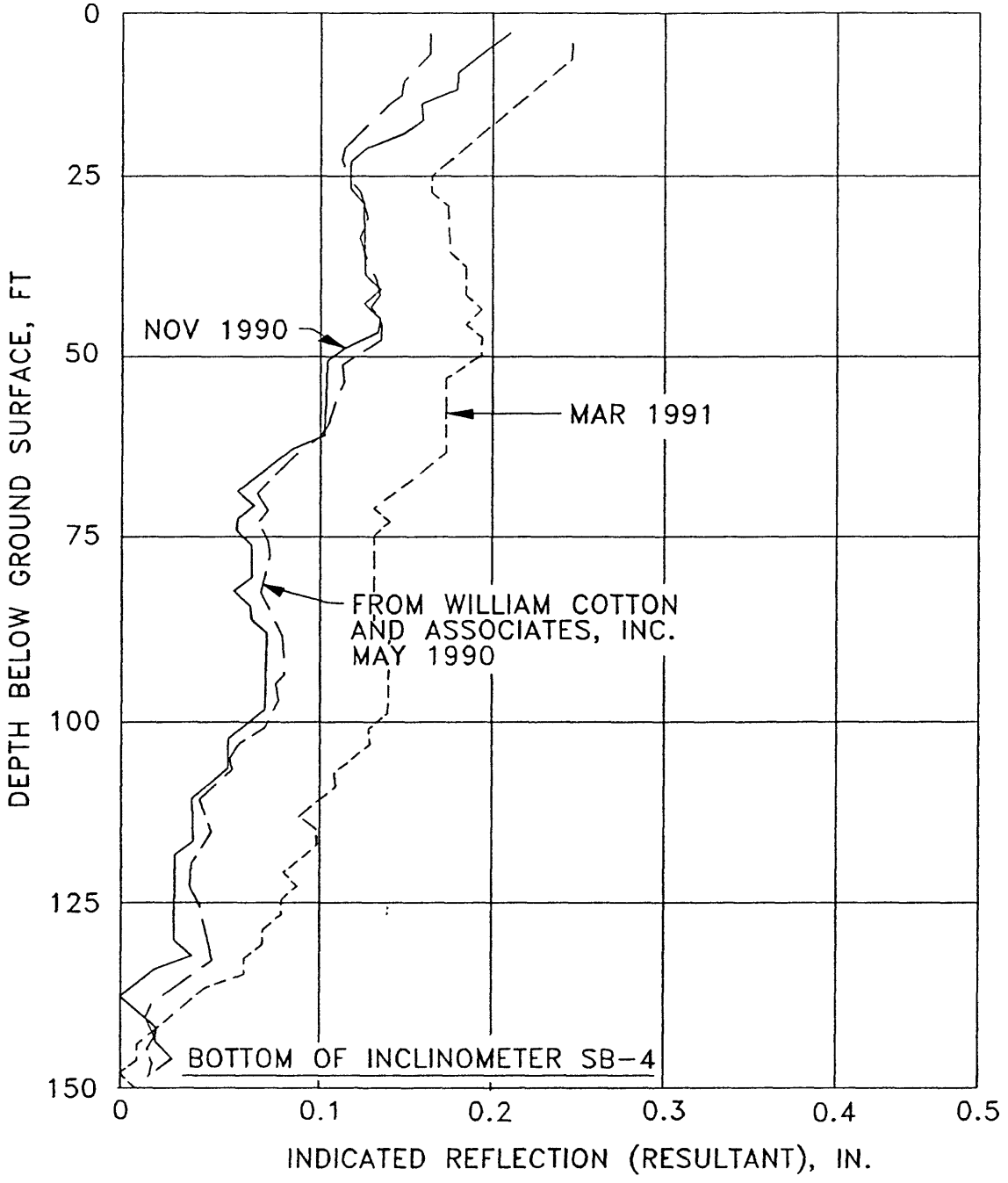

Figure 7.11(j). Inclinometer data for SB-4 (May and November 1990 and March 1991).

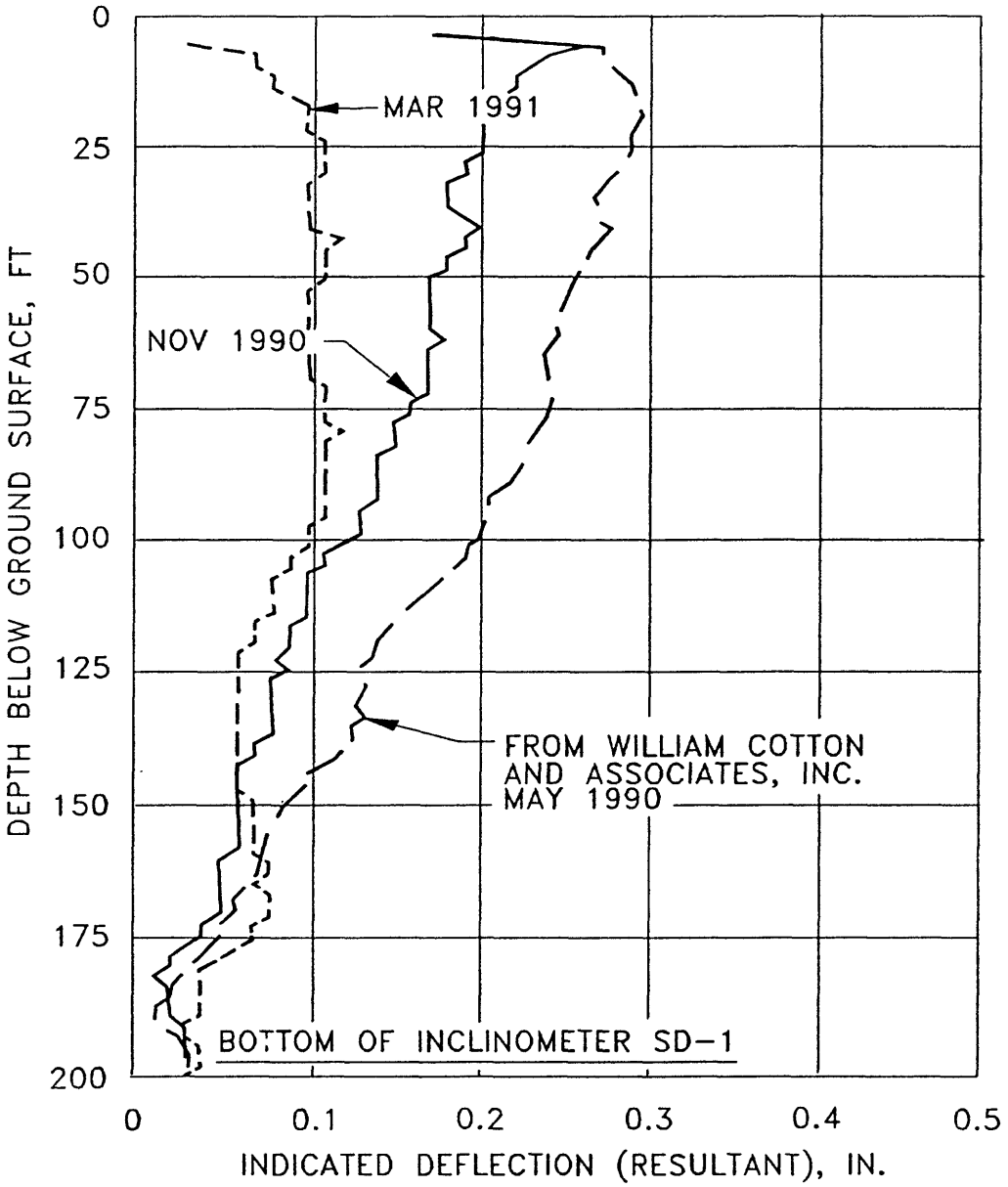

Figure 7.11(k). Inclinometer data for SD-1 (May and November 1990 and March 1991).

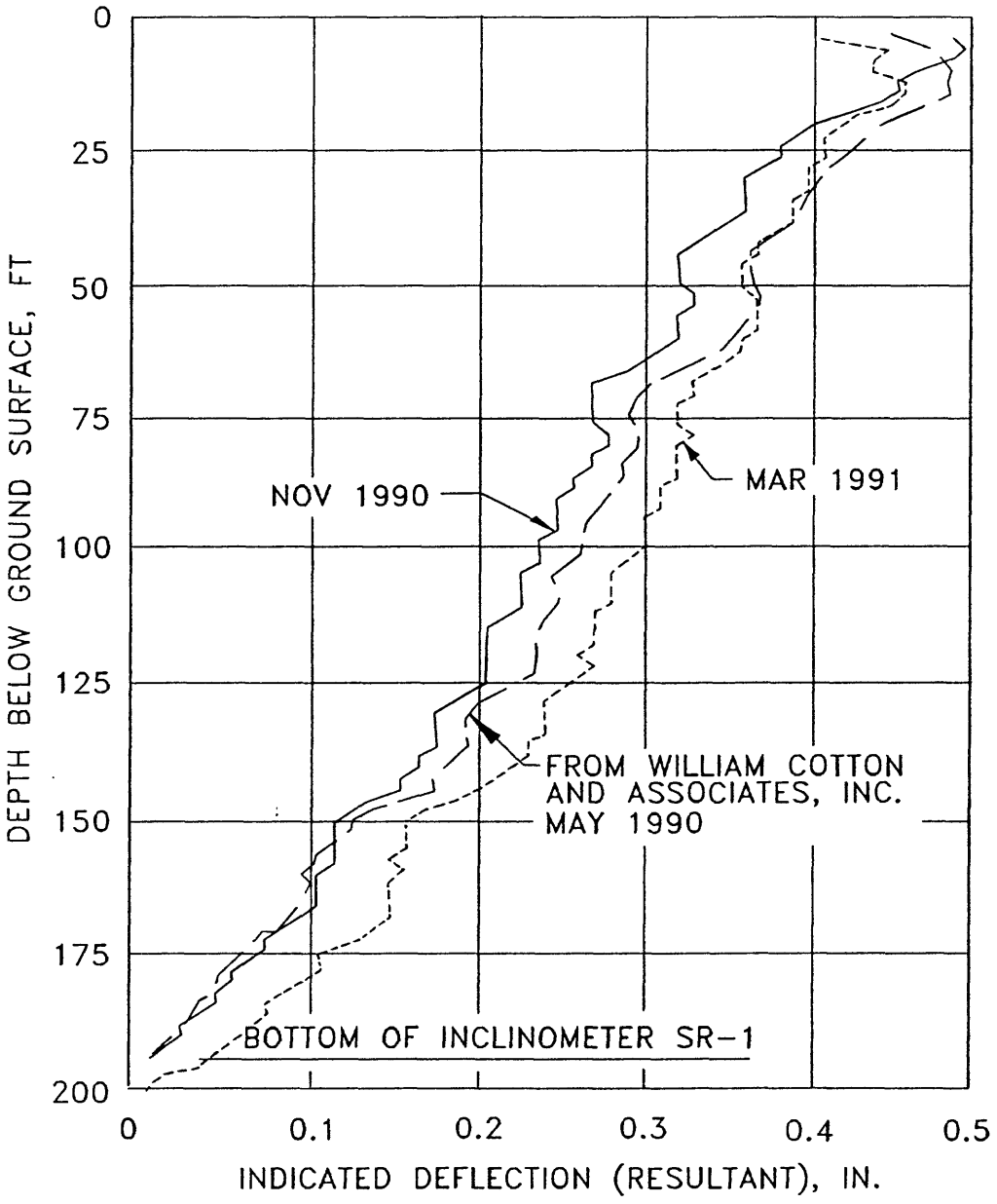

Figure 7.11(1). Inclinometer data for SR-1 (May and November 1990 and March 1991).

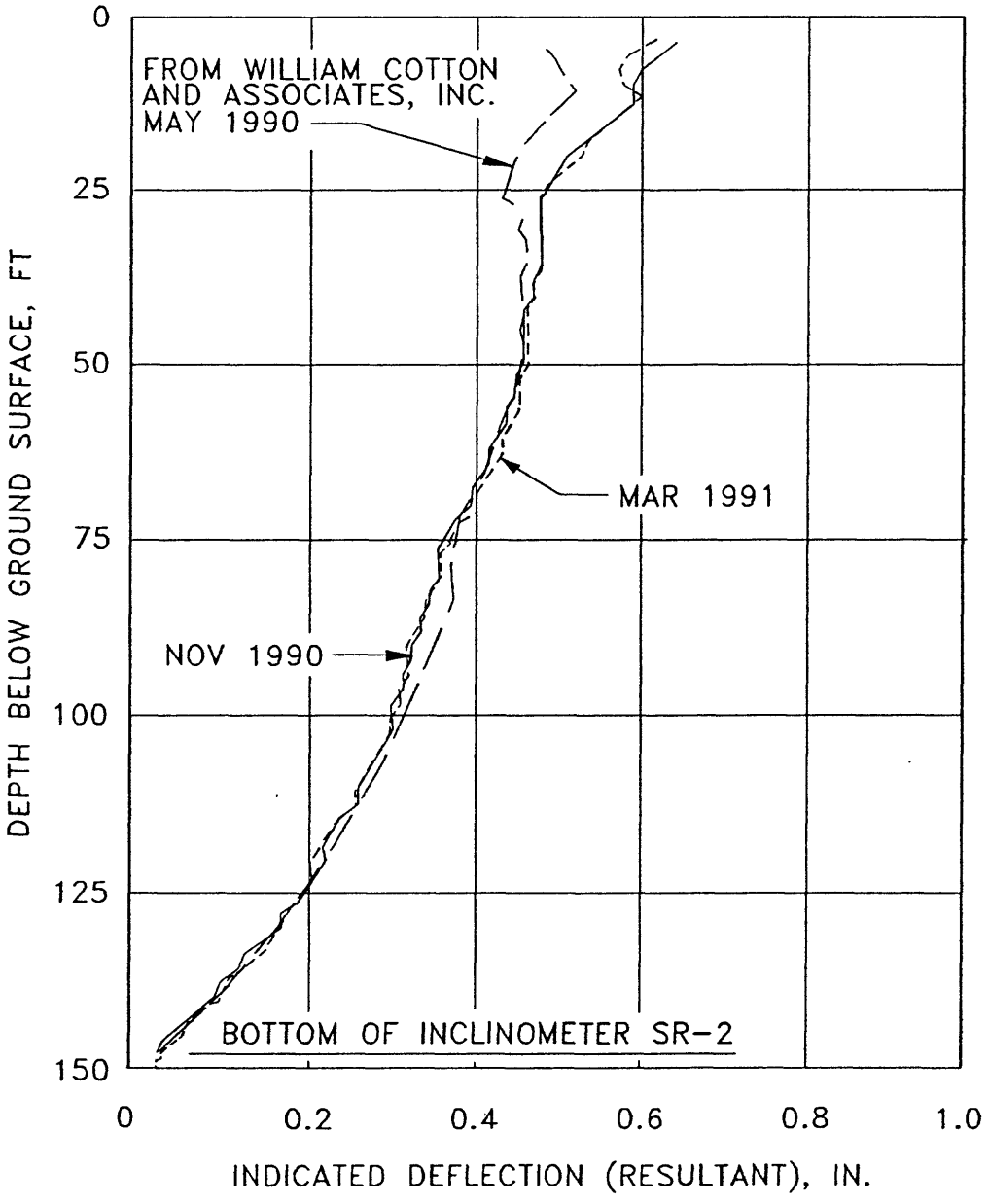

Figure 7.11(m). Inclinometer data for SR-2 (May and November 1990 and March 1991).

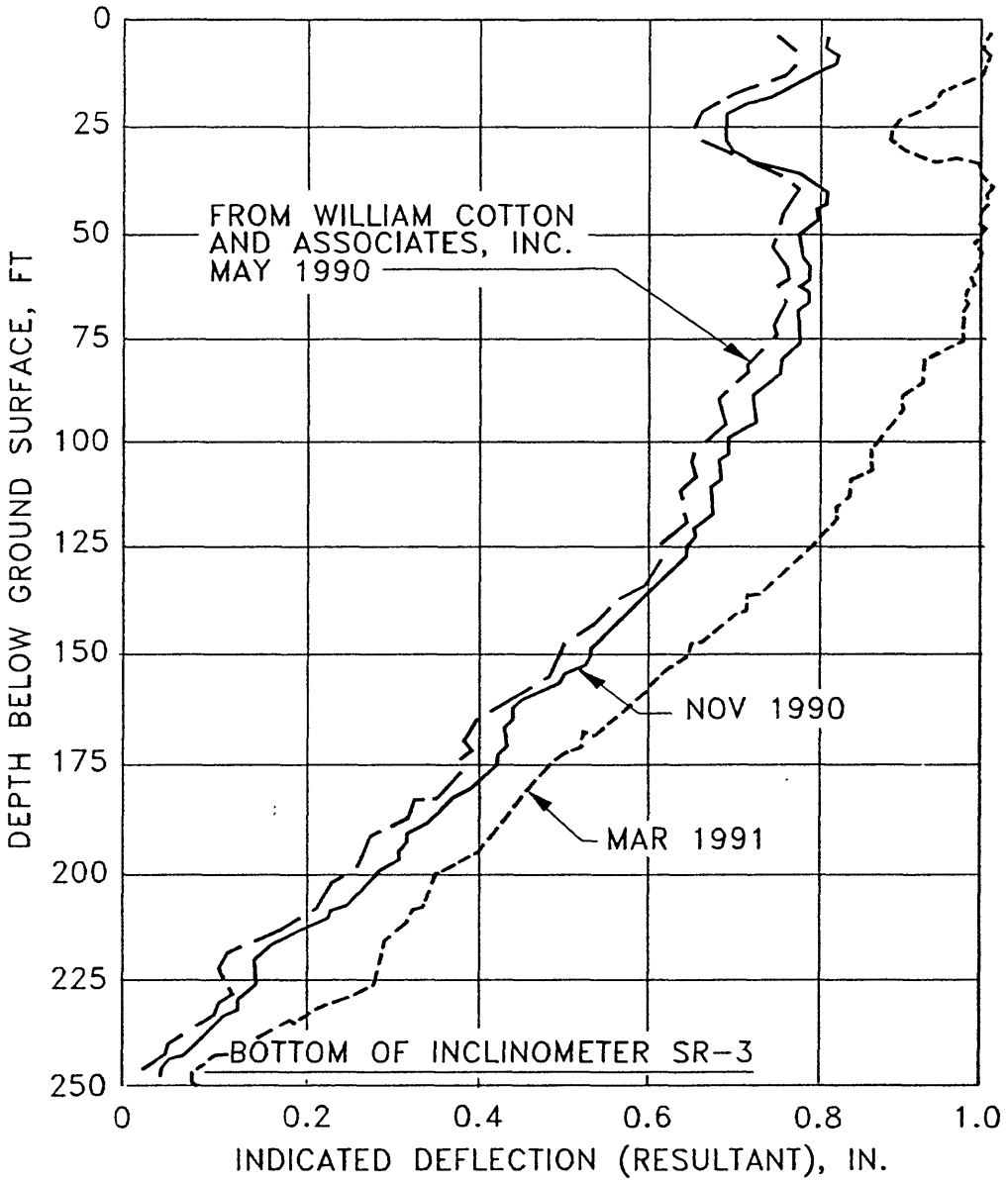

Figure 7.11(n). Inclinometer data for PSR-3 (May and November 1990 and March 1991).

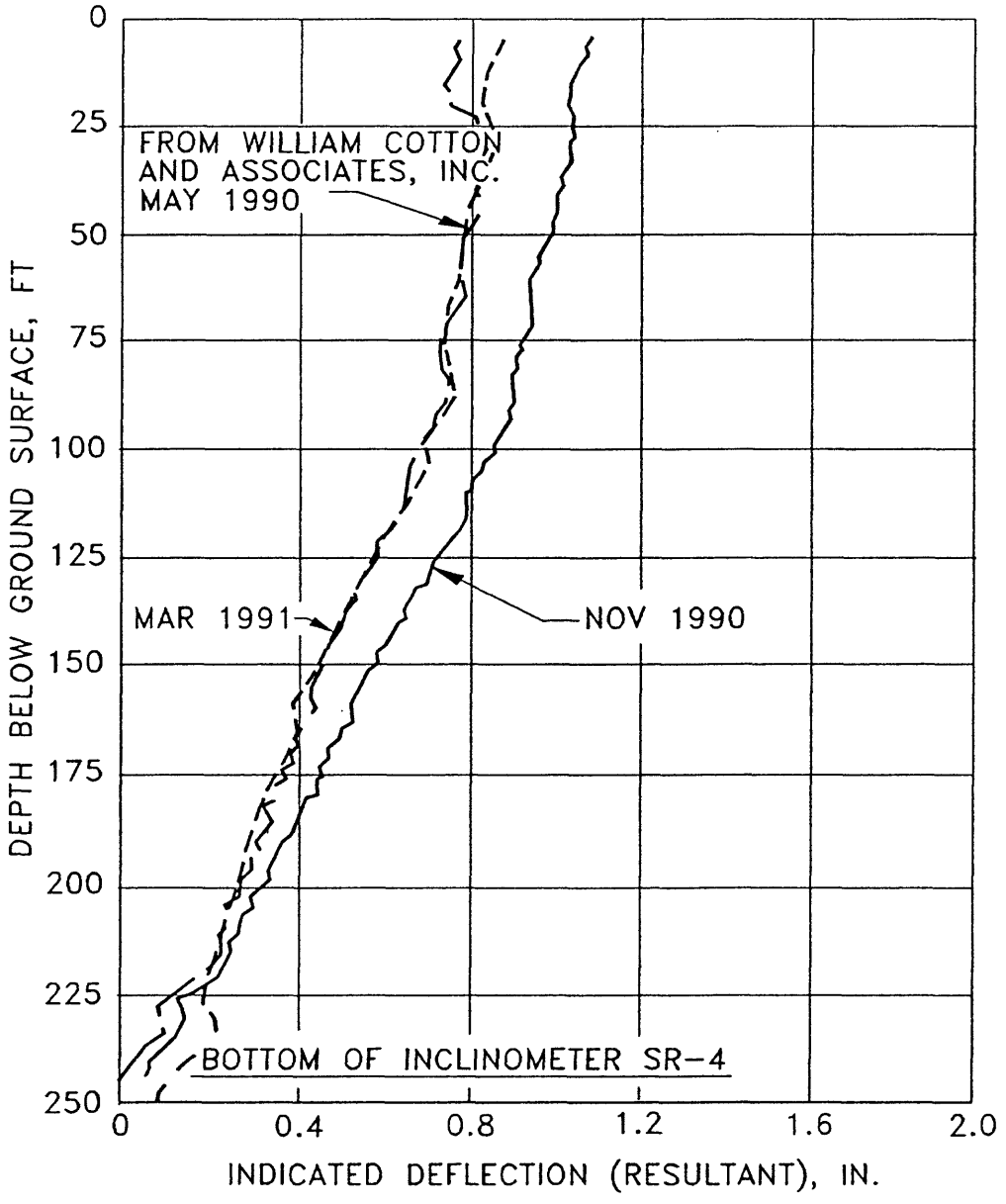

Figure 7.11(o). Inclinometer data for PSR-4 (May and November 1990 and March 1991).

inclinometer casings, squeezing of the soft materials around the casings, and (or) fluctuations in ground-water levels were the probable cause(s) of the small deflections.

C. Ground-Water Levels

Piezometers were installed in the boreholes in the Upper Schultheis Road and Villa Del Monte areas to monitor ground-water levels within the slopes. Data from these instruments were supplemented by a survey of water levels in wells to determine likely pre-earthquake ground-water levels for use in slope-stability analyses.

Piezometers installed in most boreholes were of the electronic strain-gage type, which can provide automatic, continuous recording of data. The piezometers were Thor™ Model DPXE instruments with a pressure range of 100 pounds per square inch and an overrange capacity of 1.5 times. The piezometers were installed in canvas socks, which were filled with sand and secured onto the outside of the inclinometer casings (fig. 7.10). The piezometers were sealed by the impermeable grout used to emplace the inclinometer casings. Three such piezometers were installed in all boreholes except SR-1A, SB-1A, and SB-4A (table 7.1). Depths of the piezometer tips were selected to characterize the expected range of ground-water conditions and to provide data on pore-water pressures at the projected depths of the landslide basal shear surfaces. The piezometers were connected to Thor™ Model SDEE-03A, 3-channel dataloggers. These data loggers were programmed and data were recorded using a Packard Bell™ laptop computer. Records from the strain-gage type piezometers are shown in figures 7.12(a-o).

To monitor the performance of the strain-gage piezometers, Casagrande-type, open-standpipe piezometers (fig. 7.13) were installed at two depths each in boreholes SR-1A and SB-1A and at depths near the intermediate strain-gage piezometer tips in boreholes DM-1, DM-3, SB-2, SB-3, SR-3, and SR-4 (table 7.3). Data from the Casagrande piezometers generally agree well with the data from the adjacent strain-gage piezometers (Compare tables 7.3, table 7.4, and fig. 7.12).

Ground-water levels in the Upper Schultheis and Villa Del Monte areas rose in response to the period of heavy rainfall in the

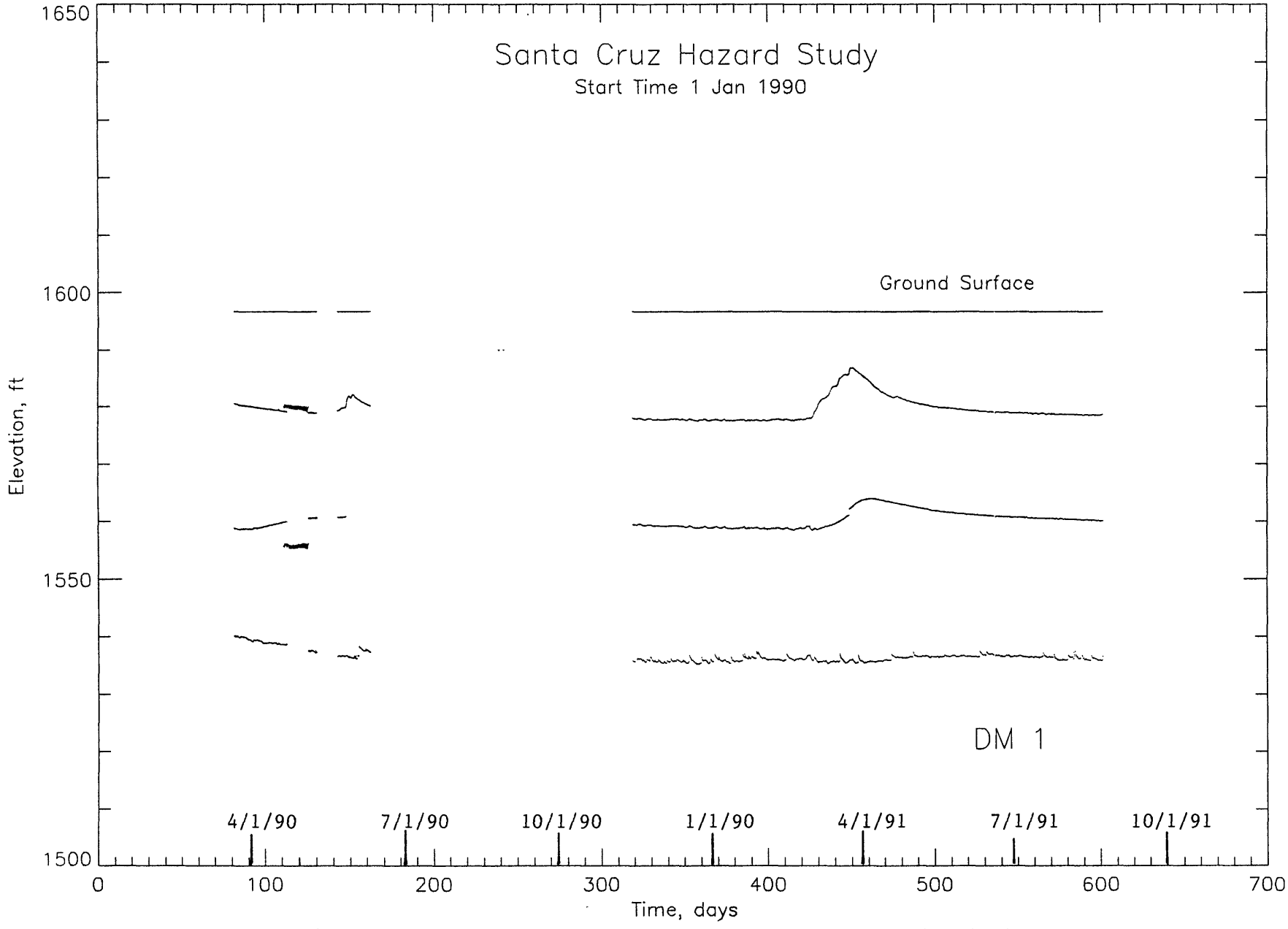

Figure 7.12(a) DM-1 piezometric-surface elevations vs. time, 1990-1991; shallow, medium, and deep piezometers

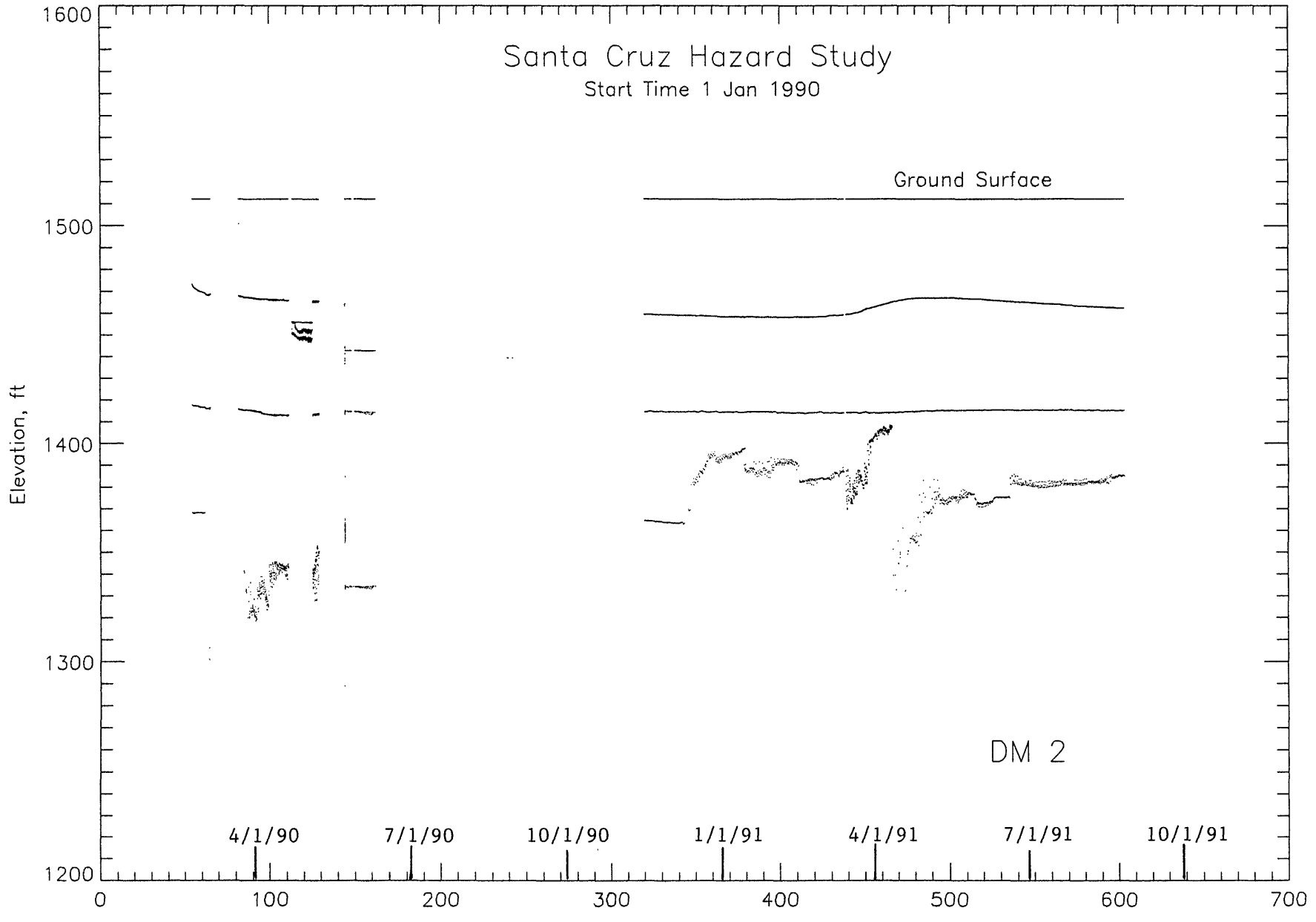

Figure 7.12(b) DM-2 piezometric-surface elevations vs. time, 1990-1991; shallow, medium, and deep piezometers

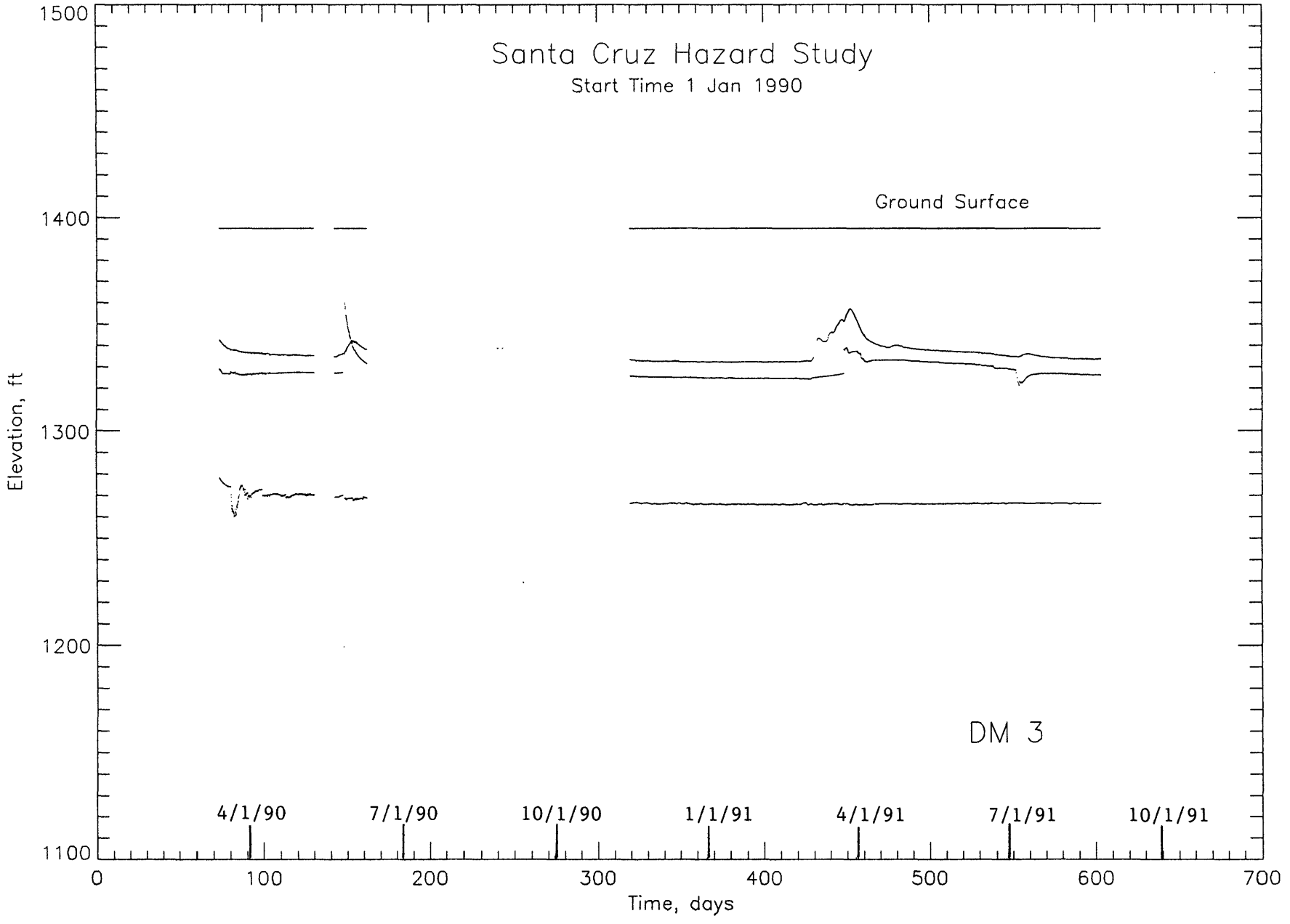

Figure 7.12(c) DM-3 piezometric-surface elevations vs. time, 1990-1991; shallow, medium, and deep piezometers

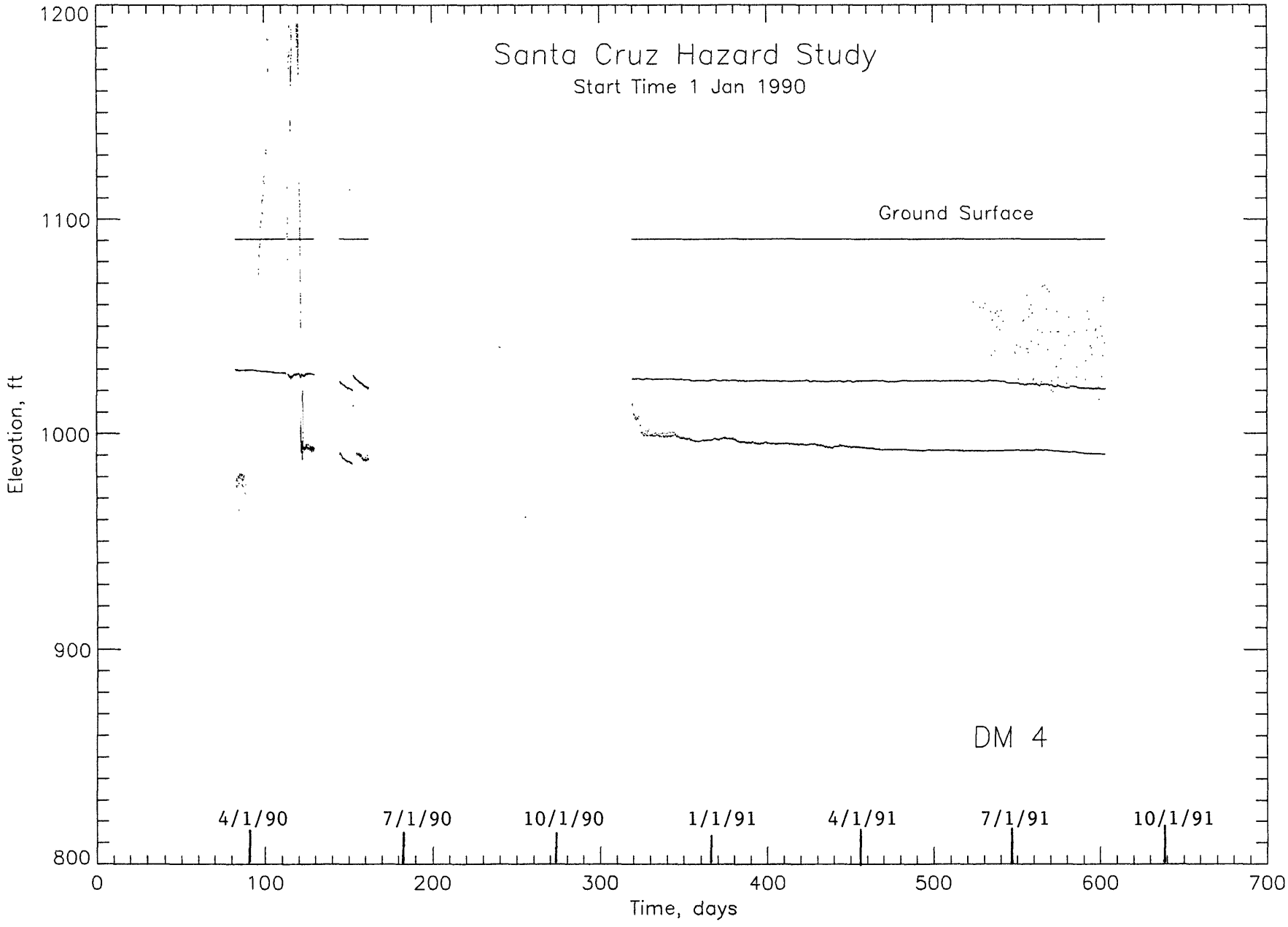

Figure 7.12(d) DM-4 piezometric-surface elevations vs. time, 1990-1991; shallow and medium piezometers. Deep piezometer malfunctioned at all times.

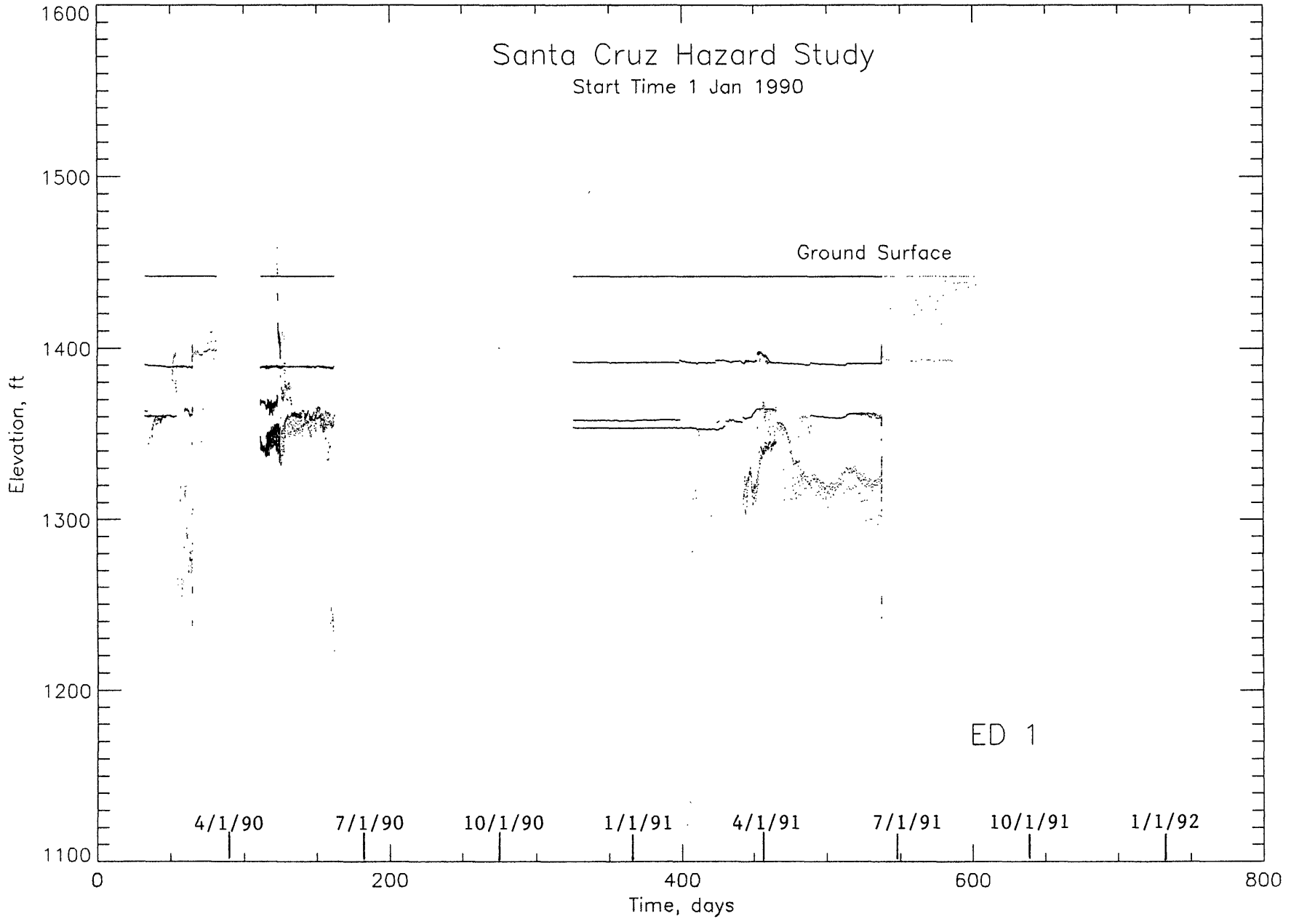

Figure 7.12(e) ED-1 piezometric-surface elevations vs. time, 1990-1991; shallow, medium, and deep piezometers

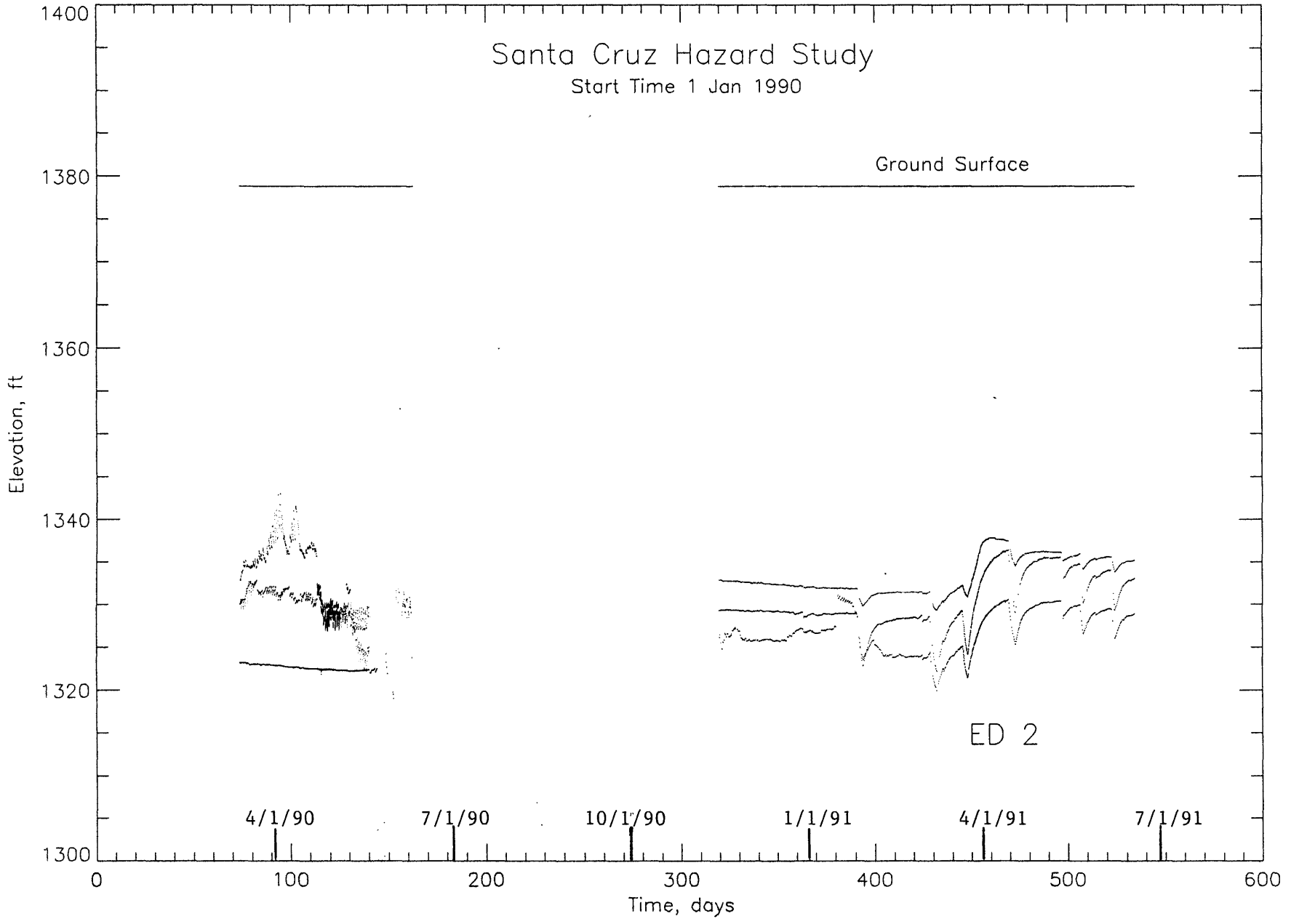

Figure 7.12(f) ED-2 piezometric-surface elevations vs. time, 1990-1991; shallow, medium, and deep piezometers

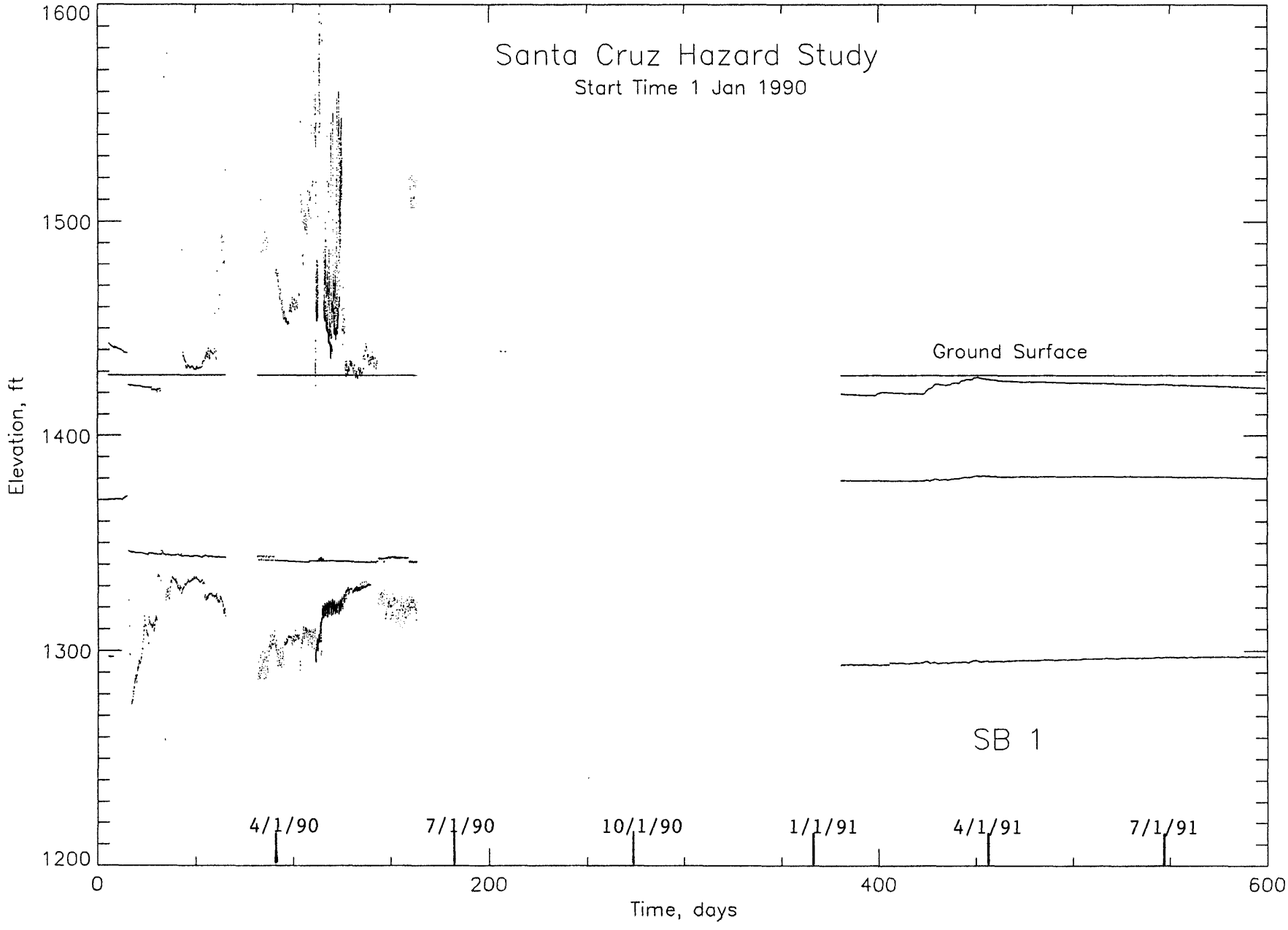

Figure 7.12(g) SB-1 piezometric-surface elevations vs. time, 1990-1991; shallow, medium, and deep piezometers

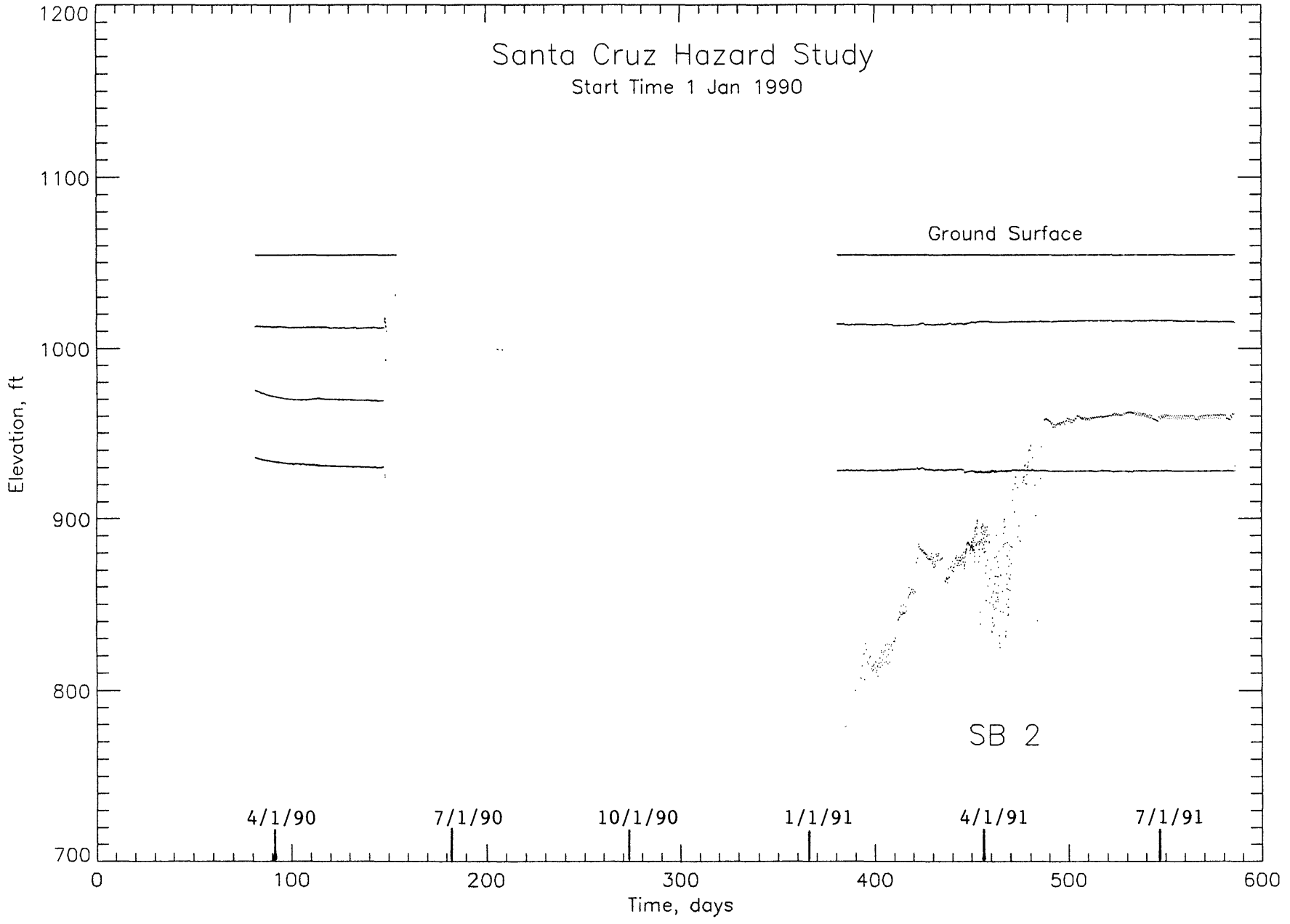

Figure 7.12(h) SB-2 piezometric-surface elevations vs. time, 1990-1991; shallow, medium, and deep piezometers

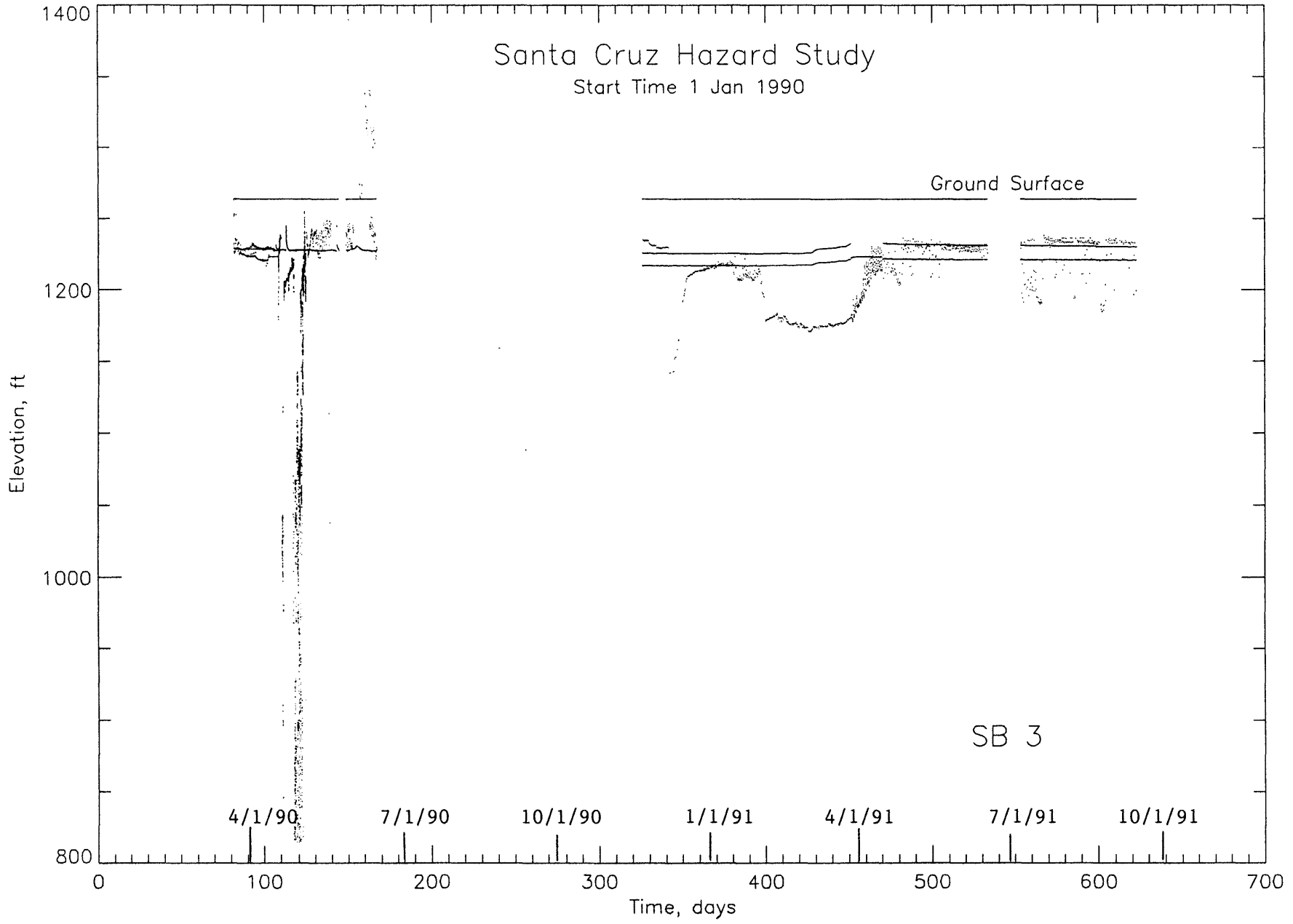

Figure 7.12(i) SB-3 piezometric-surface elevations vs. time, 1990-1991; shallow, medium, and deep piezometers

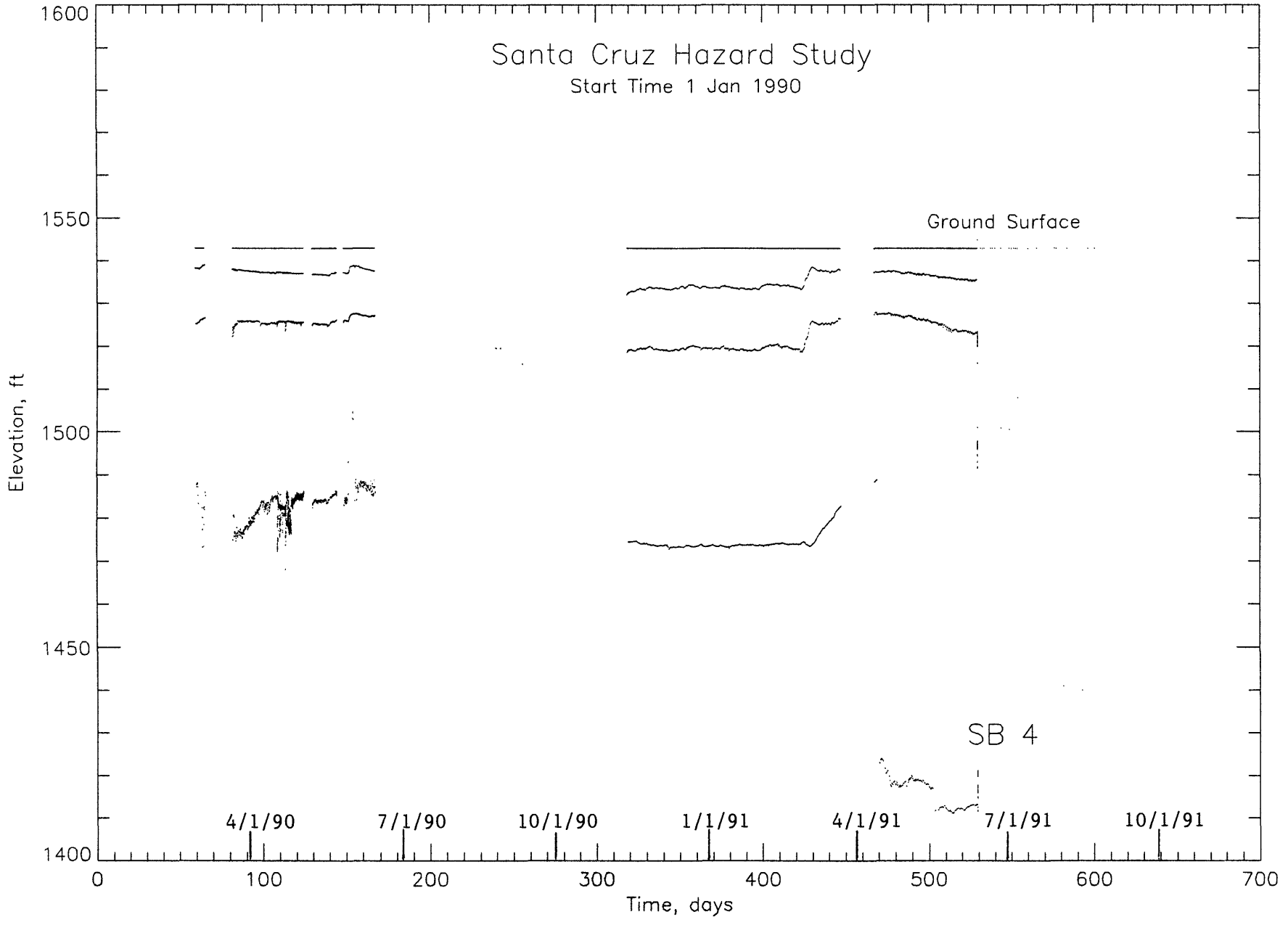

Figure 7.12(j) SB-4 piezometric-surface elevations vs. time, 1990-1991; shallow, medium, and deep piezometers

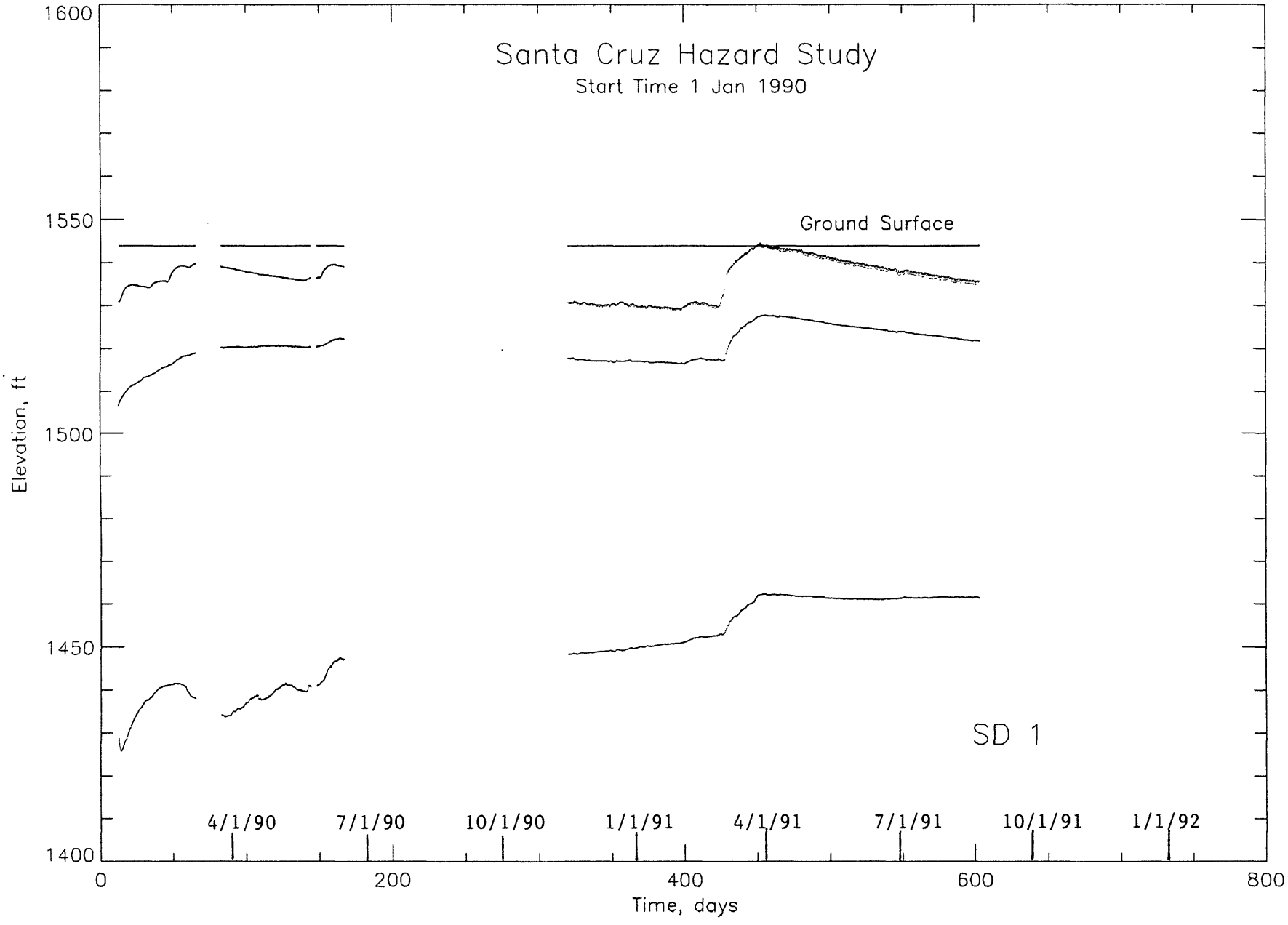

Figure 7.12(k) SD-1 piezometric-surface elevations vs. time, 1990-1991; shallow, medium, and deep piezometers

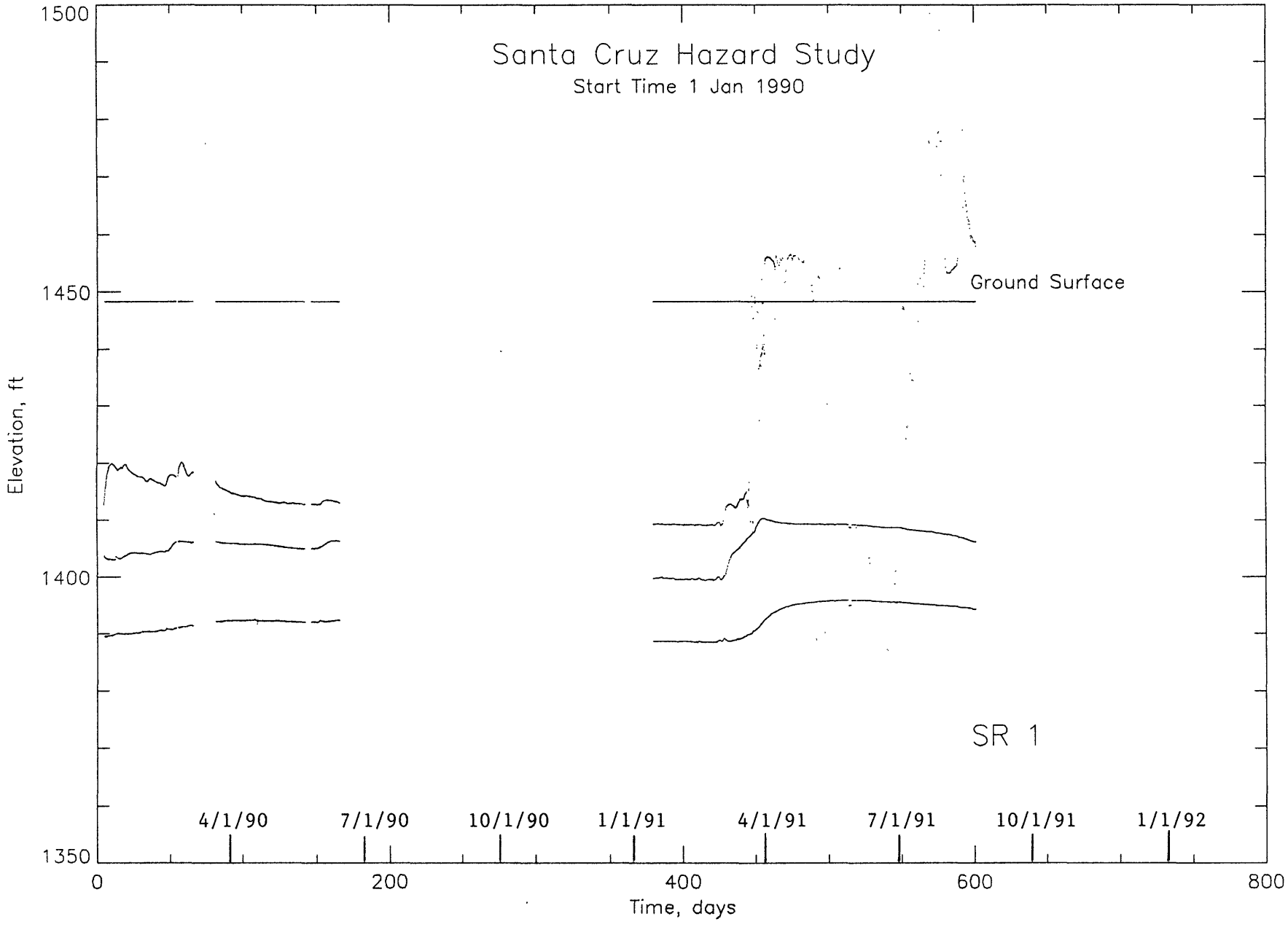

Figure 7.12(1) SR-1 piezometric-surface elevations vs. time, 1990-1991; shallow, medium, and deep piezometers

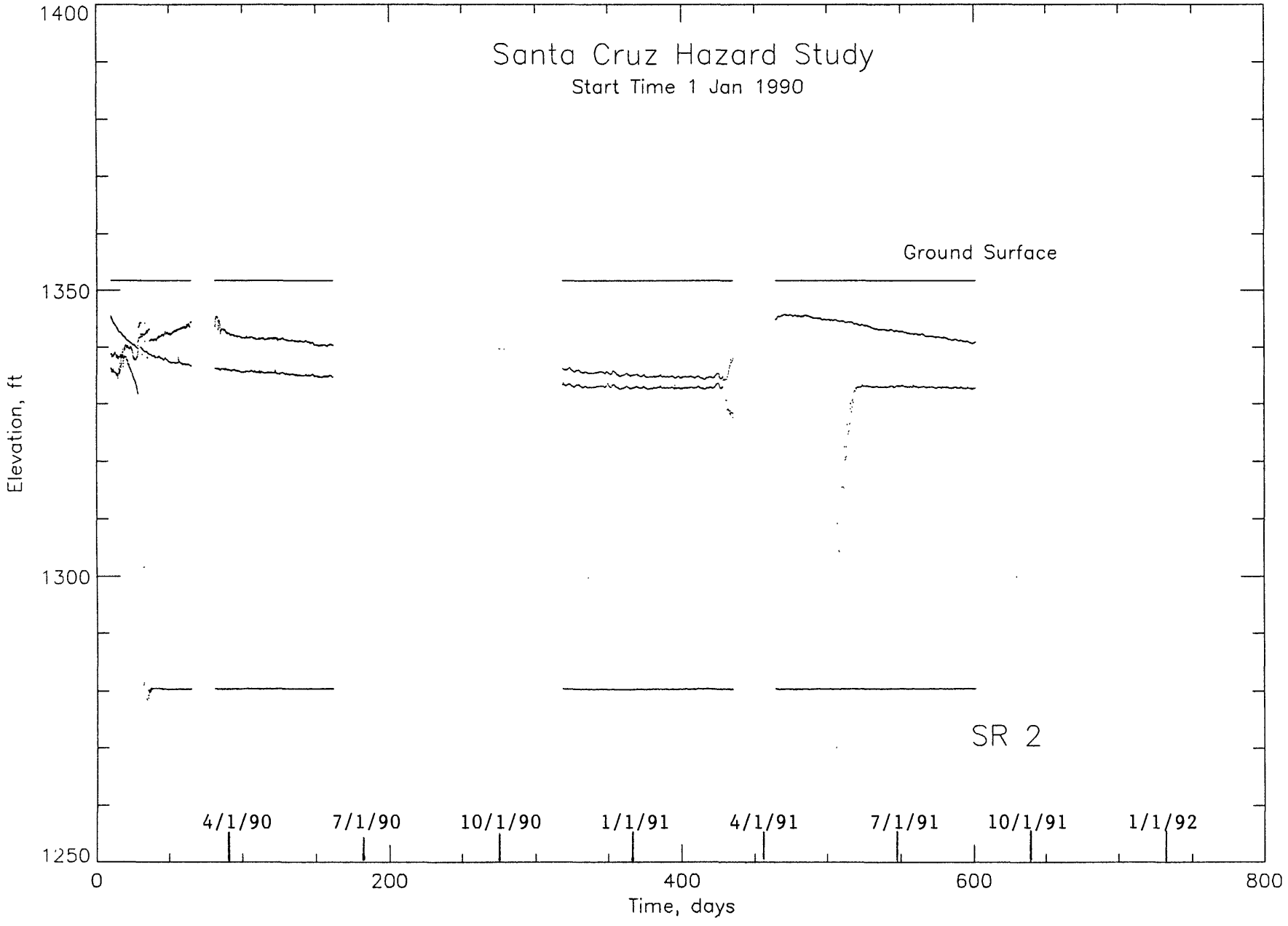

Figure 7.1(m) SR-2 piezometric-surface elevations vs. time, 1990-1991; shallow, medium, and deep piezometers. The lowest, flat trace is from the shallow piezometer and represents instrument malfunction.

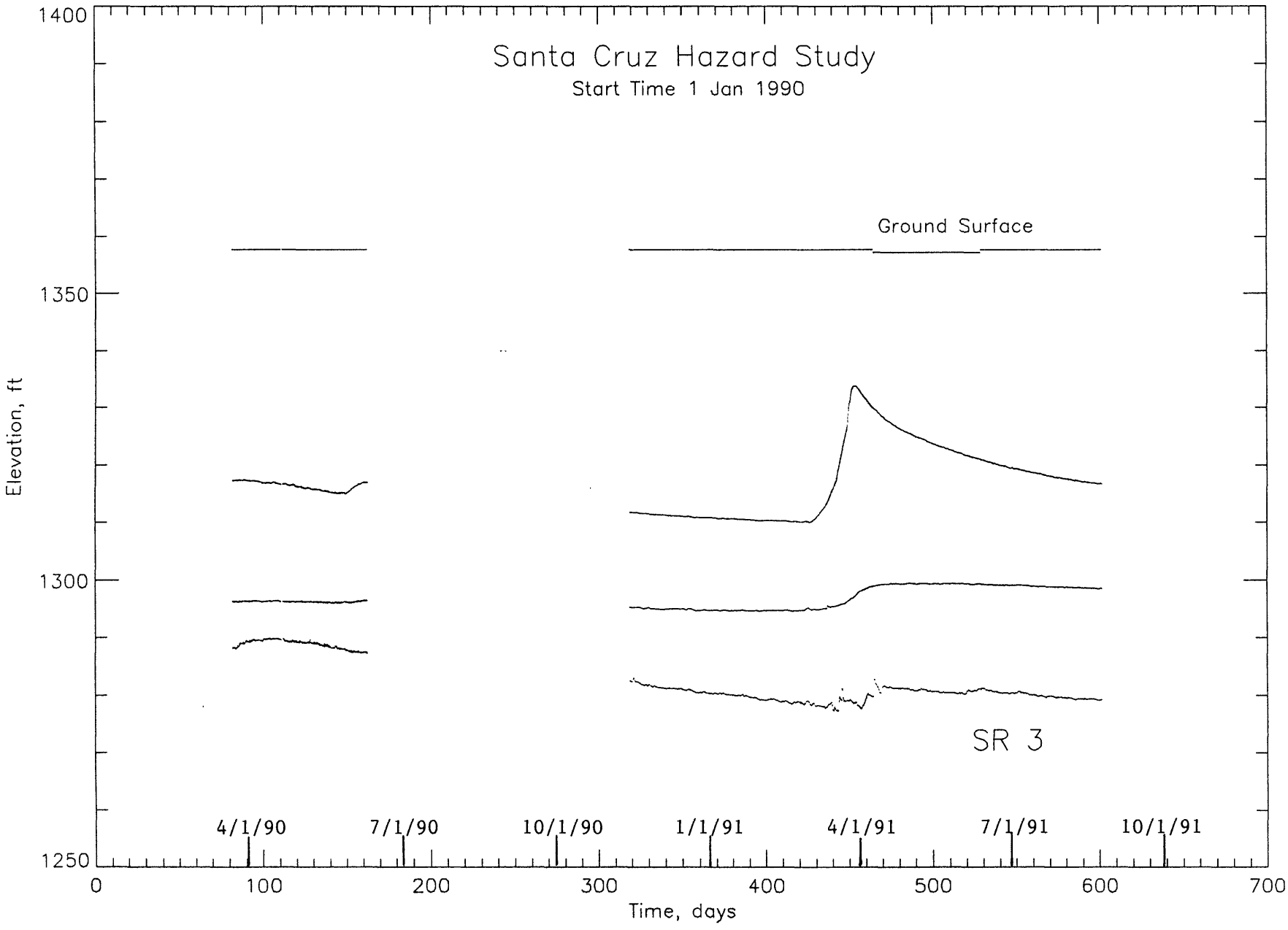

Figure 7.12(n) SR-3 piezometric-surface elevations vs. time, 1990-1991; shallow, medium, and deep piezometers

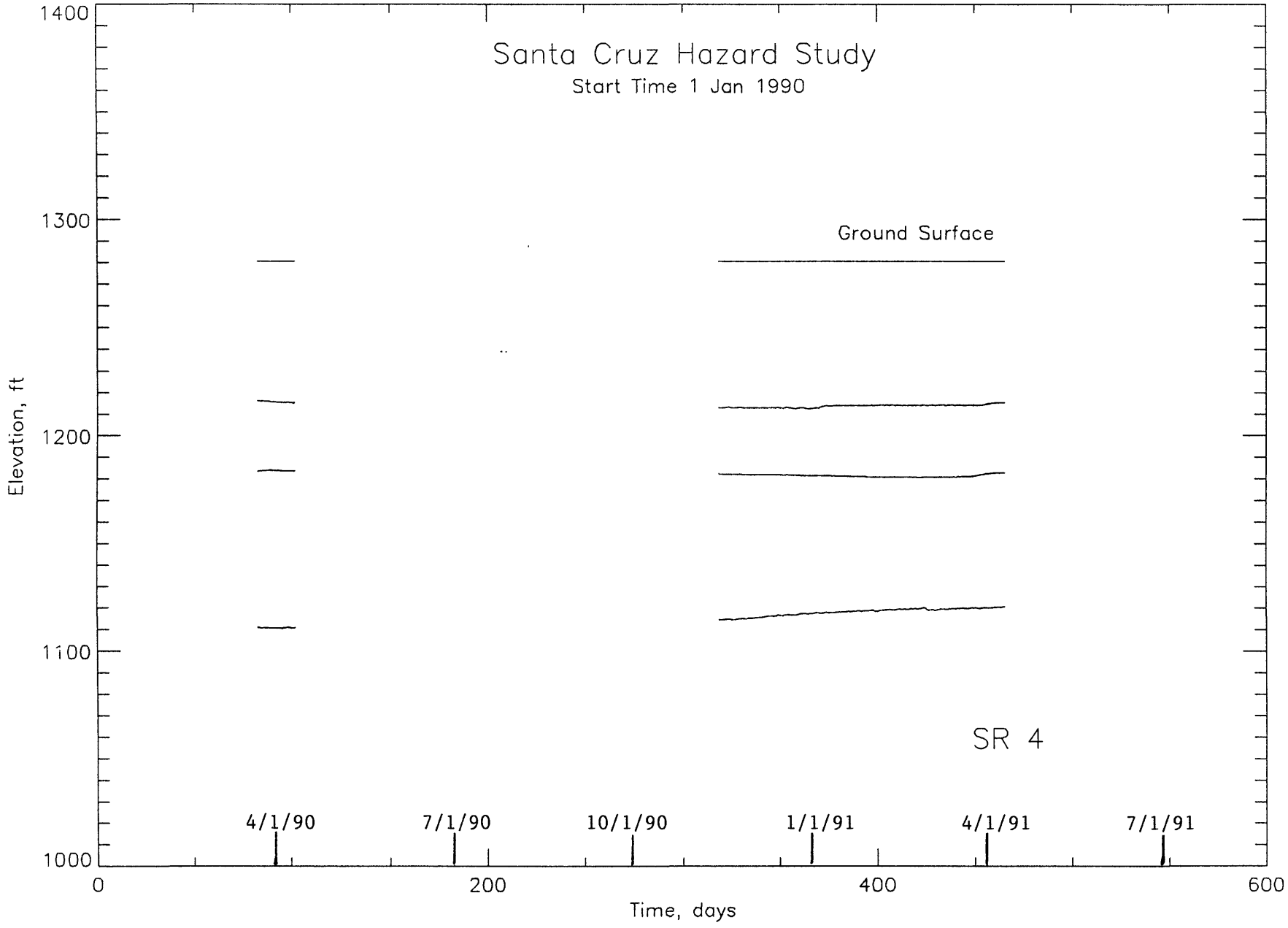

Figure 7.12(o) SR-4 piezometric-surface elevations vs. time, 1990-1991; shallow, medium, and deep piezometers

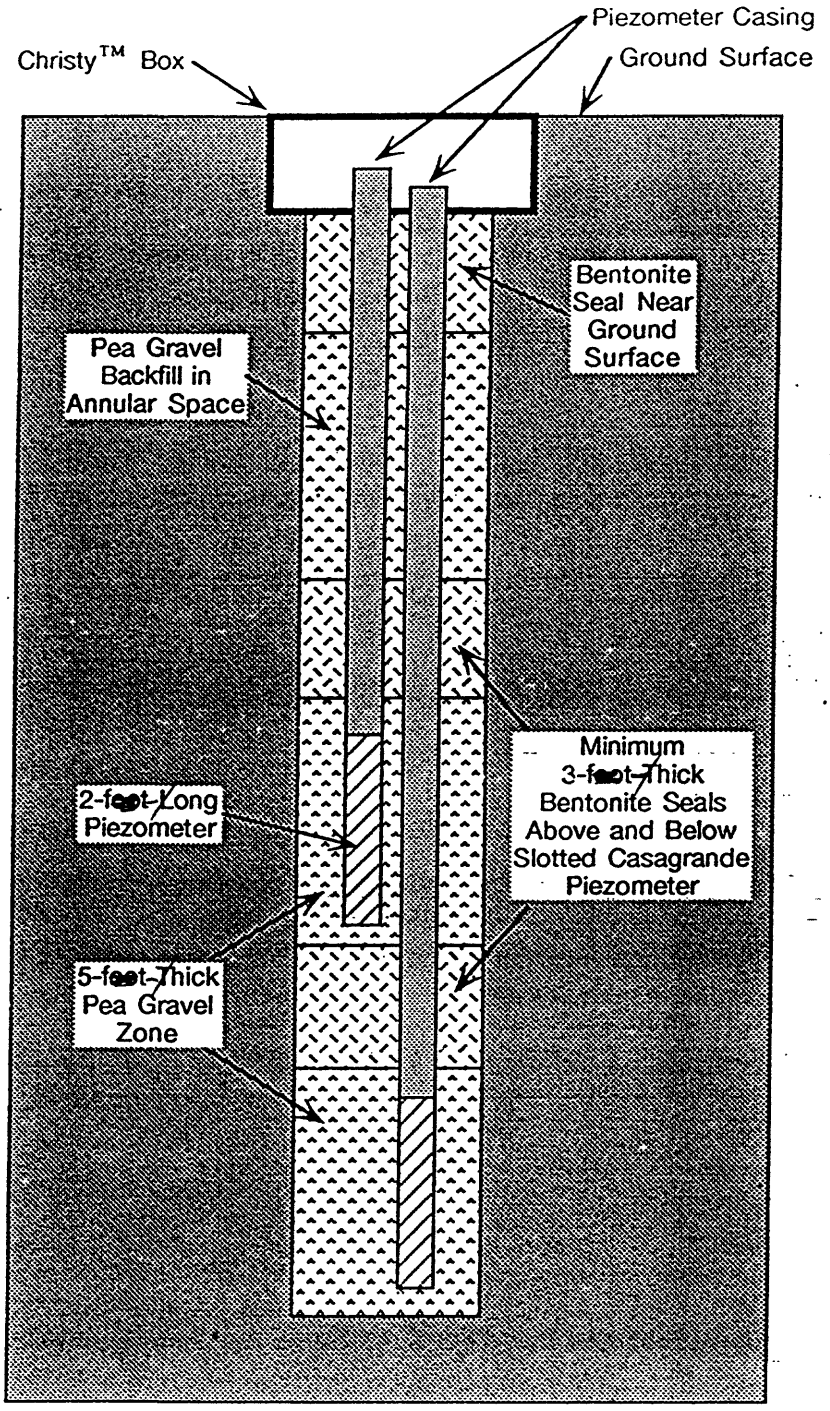

Figure 7.13 Schematic diagram of Casagrande piezometer, Schultheis Road and Villa Del Monte Areas (from William Cotton and Associates, 1990).

TABLE 7.3: CASAGRANDE PIEZOMETER DATA
(Depths in feet; measurements by R. Brumbaugh)

Borehole No.	DM-1	DM-3	SB-2	SB-3	SR-1A	SR-1A	SR-3	SR-4	SB-1A	SB-1A
Tip Depth	61	120	150	138	18.0	77.2	175	116	37.0	89.7
11/13/90	--	--	--	--	26.9	43.4	--	--	--	--
11/14/90	36.2	--	--	--	--	--	61.8	85.5	--	--
11/15/90	--	68.7	80.0	--	--	--	--	--	--	--
11/16/90	38.0	--	--	--	--	--	--	--	--	--
11/20/90	--	--	--	38.0	--	--	--	--	6.9	57.9
01/04/91	--	--	--	--	25.1	45.2	--	--	5.0	39.8
03/14/91	38.0	--	--	--	21.9	74.1	--	--	--	--
03/18/91	--	69.2	--	--	--	--	--	--	--	--
03/19/91	--	--	--	--	--	--	62.1	99.6	--	--
03/22/91	--	--	80.5	--	--	--	--	--	37	89.7
03/27/91	--	--	--	32.2	--	--	--	--	--	--
06/17/91	--	--	82.7	33.0	--	--	--	--	--	--
06/19/91	--	59.0	--	--	--	--	--	--	--	--
06/20/91	36.8	--	--	--	--	--	--	--	--	--
06/21/91	--	--	--	--	23.8	40.0	58.7	99.5	--	--

Table 7.4
Groundwater Fluctuation, 1991

Piezometer	Fluctuation for Shallow Piezometer Tip (maximum groundwater elevation), ft	Fluctuation for Medium Piezometer Tip (maximum groundwater elevation), ft	Fluctuation for Deep Piezometer Tip (maximum groundwater elevation), ft	Comments
PDM 1	+5.5 (1583)	+5.2 (1564)	+1.0 (1537)	Casagrande data missed peak but otherwise agrees well
PDM 2	+8.8 (1467)	+1 (1415)	-10 (1375	
PDM 3	+14 (1346)	+9 (1333)	N/C (1265)	Casagrande data caught initial rise; didn't agree with 6/91 (+5 ft)
PDM 4	N/C (1025)	-4 (996.5)	N/C (1400)	
PED 1	N/C (1391)	+8 (1362)	Bad (1360)	
PED 2	(+5) (1335)	N/C (1335)	(+7) (1330)	
PSB 1	+7 (1427)	+2 (1381)	+3 (1297)	
PSB 2	+3 (1016)	+2 (962)	+1 (930)	Casagrande data indicated +5 to +8 ft over PSB 2
PSB 3	Bad - N/C (-)	+7 (1233)	+5 (1222)	Casagrande data caught peak (6 ft increase)
PSB 4	+5 (1539)	+8 (1528)	+9 (1483)	
PSD 1	+13 (1543)	+11.5 (1527.5)	+12 (1462)	

Table 7.4 (continued)

Piezometer	Fluctuation for Shallow Piezometer Tip (maximum groundwater elevation), ft	Fluctuation for Medium Piezometer Tip (maximum groundwater elevation), ft	Fluctuation for Deep Piezometer Tip (maximum groundwater elevation), ft	Comments
PSR 1	+3 (1413)	+10 (1410)	+8 (1396)	Casagrande data indicated +13.5 over PSR 1 (shallow) Casagrande confirmed rise to 10 ft PSR 1 (medium)
PSR 2	N/C (1281)	+6 (1341)	+2 (1335)	
PSR 3	+20 (1330)	+5 (1300)	+2 (1282)	Casagrande data confirmed rise to 1300
PSR 4	N/C (1215)	N/C (1182)	+2 (1120)	

N/C = No Change

spring of 1991 (table 6.1). The range of dates of initial groundwater rise due to the spring 1991 rains for the shallow, medium, and deep strain-gage piezometers were:

Piezometer Depth	Time Range of Initial Rise	Average Time of Initial Rise
Shallow	Feb. 24 to Mar. 4, 1991	Mar. 1, 1991
Medium	Feb. 26 to Apr. 10, 1991	Mar. 7/8, 1991
Deep	Feb. 4 to Apr. 20, 1991	Mar. 6, 1991

These times reflect a relatively rapid ground-water response to the rainfall, particularly to that in February and early March.

The ground-water fluctuations shown in table 7.4 were derived from figure 7.12 and from table 7.3. The groundwater elevations from the strain-gage piezometers increased the following amounts during March through June 1991:

Piezometer Depth	Range of Rise in Ground-Water Level	Average Rise in Ground-Water Level
Shallow	0 to 20 feet	5.6 feet
Medium	0 to 11.5 feet	4.4 feet
Deep	0 to 12 feet	3.0 feet

While the piezometer records are somewhat erratic and discontinuous, there is generally good agreement in data obtained by the two types of piezometers (tables 7.3 and 7.4), which increases the confidence in drawing conclusions.

The geotechnical cross sections, figures 7.3-7.5, show two water levels from individual piezometers--one from the period around March 1990, taken from the report of William Cotton and Associates, Inc., (1990), and one derived from those plots in figure 7.12 that were judged to indicate the predominant water level for an interval of good-quality data within the monitoring period. Each borehole had three electronic piezometers installed, with tips at different

depths. In most boreholes, the three piezometer tips sensed different water levels, as is typical in areas of such complex geologic conditions.

Standing water levels in wells are listed in table 7.5; these data indicate the water levels at the times the wells were developed, as long ago as 1966. These standing water levels are influenced by the well-drilling technique as well as the hydrologic properties of the surrounding geologic material. In the Summit Ridge area, well drillers typically use air for drilling and well development, and typically the final stage in development is surging. Well development with air can draw the water level in the well down many feet whereas surging allows the well to recover, so that the water level in the well is more indicative of that in the geologic material. Wells drilled near each other in different years (42 and 42A; 50 and 50A; 78 and 78A; and 104 and 104A in table 7.5) show differences of as much as 85 feet in standing water levels. Whereas these data may reflect topographic differences to some degree, they also suggest that substantial variations in ground-water levels over time are likely possible in the Summit Ridge area.

The immediate pre-earthquake ground-water levels, estimated from both piezometers and wells, are shown in figures 7.3-7.5 In general, data from the piezometers were given more weight in these determinations than data from the water wells because all of the piezometers were emplaced under controlled conditions, had precise horizontal and vertical control on their locations, and were sealed so as to sense the water level only within a specific unit, and because many of the water-well data are from many years before the earthquake. Nevertheless, the agreement between the piezometer and water-well data was relatively good. Along cross-sections SR and DM (figs. 7.3 and 7.4) and along part of cross-section SB (fig. 7.5) a range of estimated ground-water levels, rather than a single level, is shown to account for the range in piezometric readings and well data. Not enough data are available to analyze the effects of the current 5-year-long drought on water levels.

TABLE 7.5 STANDING WATER LEVELS RECORDED IN WELL SURVEY
(Data from Brumbaugh, 1990; locations of some wells shown in figures 3.6, 3.8, 3.10, and 3.18)

Well Number	Standing-water levels (feet below ground surface)	Well Number	Standing-water levels (feet below ground surface)
1		46	100
2	200	47	90
3		48	80
4		49	30
5		50	120
6	45	50A	60
7	90	51	200
8	140	52	70
9		53	70
10	160	54	
11	280	55	
12	78	56	70
13	90	57	495
14	100	58	60
15		59	90
16		60	65
17	25	61	90
18	25	62	
19		63	
20	120	64	
21	60	65	50
22	75	66	85
23	23	67	
24	30	68	
25		69	70
26	140	70	92
27	90	71	59.5
28		72	42
29	65	73	
30	70	74	
31	150	75	52
32	15	76	65
33		77	25
34	180	78	135
35	70	78A	50
36		79	25
37	120	80	80
38	13	81	
39	60	82	90
40	120	83	90
41	240	84	20
42	100	85	33
42A	120	86	
43	52	87	70
44		88	
45	190	89	

D. References Cited

Brumbaugh, R., 1990, Santa Cruz well history survey: Santa Cruz, Calif., Report to Santa Cruz County Planning Department.

Clark, J. C., Brabb, E. E., and McLaughlin, R. J., 1989, Geologic map and structure sections of the Laurel 7-1/2' quadrangle, Santa Clara and Santa Cruz counties, California: U.S. Geological Survey Open-File Map 89-676, scale 1:24,000.

Horath, F., 1990, Summary of tiltmeter data, slope movement investigation, Schultheiss Road landslide: Santa Cruz, Calif., Applied Geomechanics, Inc., Report for U.S. Army Corps of Engineers, 14 p.

Geologic map and structure sections of the Los Gatos 7 1/2' Quadrangle, Santa Clara County California: U.S. Geological Survey Open-File Map.

William Cotton and Associates, Inc., 1990, Schultheis Road and Villa Del Monte areas geotechnical exploration Santa Cruz County, California: Los Gatos, Calif., William Cotton and Associates, Inc., Report for U.S. Army Engineers, 2 vols.

Williams, R. A., and King, K. W., 1990, Summary of seismic-reflection/refraction investigations on Schultheis Road landslide, Santa Cruz County: Golden, Colo., U. S. Geological Survey, Technical letter dated August 17, 1990, 5 p.

CHAPTER VIII. SLOPE STABILITY AND DEFORMATION ANALYSES--UPPER SCHULTHEIS ROAD LANDSLIDE AND VILLA DEL MONTE LANDSLIDE COMPLEX

A. Introduction and Scope

The Upper Schultheis Road landslide and Villa Del Monte landslide complex were modeled in slope stability and deformation analyses first to back-calculate static (no earthquake) and dynamic (earthquake) strengths of the slope materials. These back-calculated strengths were then used in the slope stability and deformation analyses to estimate the stability of the slopes under higher ground-water conditions and the displacements that could occur in future earthquakes.

Back-calculated strengths are preferred to laboratory test results in this case because they represent the strength of in situ materials averaged over the entire sliding surface at full-scale stress conditions. Laboratory tests were performed on selected samples as described in Appendix A. These laboratory results represent point estimates of strength for samples that are likely to be stronger than those actually found along a potential shear surface. This happens because high quality, undisturbed specimens of extremely weak, fractured materials are difficult to obtain in the field and test in the laboratory. Consequently, the specimens that were suitable for laboratory testing in this investigation were typically of the stronger materials and were not representative of the average strength along a potential shear surface.

The slope stability and deformation analyses were calibrated using observed past performance of the slopes. The past performance of the slopes against which the models were calibrated are:

Condition (a): The slopes are generally stable under deep ground-water conditions and static loading as observed during periods of drought and low rainfall before and after the 1989 Loma Prieta earthquake.

Condition (b): Deep basal sliding surfaces of large areal extent are stable to marginally stable under elevated ground-water conditions and static loading, since areally extensive sliding of this type has not been observed during past periods of high rainfall.

Condition (c): Shallow sliding surfaces of limited areal extent are marginally stable to unstable under elevated ground-water conditions and static loading, as observed from localized slope movements experienced in the slopes during past periods of high rainfall.

Condition (d): The severe earthquake ground shaking caused by the 1989 Loma Prieta earthquake triggered instability of deep basal sliding surfaces of large areal extent and resulted in downslope displacements as large as approximately 8 feet. This occurred during a period of drought when the ground-water levels were relatively deep.

The models were developed to reflect condition (a) above, and then slope stability for conditions (b) and (c) were computed. The computed safety factors against sliding were consistent with the observed past performance of the slopes for conditions (b) and (c) above. Thus, it was concluded that the models provided reasonable estimates of averaged static strengths of the slope materials.

The slope stability and deformation models were then adjusted to represent the dynamic loading case in condition (d) above. The computed dynamic strengths from this case were compared to the estimated static strengths, and it was found that the dynamic strengths reflected typical levels of strength degradation associated with dynamic loading and displacements on the order of several feet (Idriss, 1985; Seed, 1987). Thus it appears that the analytical models provided realistic estimates of both static and dynamic strengths of the slope materials.

The laboratory-measured strengths on the weakest samples that were tested were assumed to represent high ground-water, large displacement conditions. These minimum laboratory strengths were slightly greater than the back-calculated static strengths, as expected, since typically only the higher strength materials can successfully be sampled and tested with the techniques used in this investigation.

The back-calculated static and dynamic strengths were then used to develop charts and procedures from which slope displacements caused by future earthquakes and ground-water conditions could be estimated. For example, the analyses indicated that had the ground-water levels been significantly higher when the 1989 Loma Prieta earthquake occurred, then the maximum displacements could have been three times as large or more; i.e., on the order of at least 25 feet rather than 8 feet.

This chapter describes the slope stability and displacement models that were developed, and presents the resulting charts and procedures for use in analysis of slope stability for a range of earthquake and ground-water conditions.

B. Stability and Deformation Approach

In the Newmark sliding-block deformation analyses adopted for this study, the part of a slope displaced by earthquake shaking was idealized as a rigid block sliding on an inclined plane, as originally proposed by Newmark (1965). Since 1965, a number of researchers (Goodman and Seed, 1966; Ambraseys and Sarma, 1967; Sarma, 1975; Franklin and Chang, 1977; Hynes, 1979; Makdisi and Seed, 1979; Sarma, 1979; Wilson and Keefer, 1983; Hynes and Franklin, 1984; Idriss, 1985; Wilson and Keefer, 1985) have developed Newmark's conceptual model into a widely used, practical procedure for estimating permanent, earthquake-induced deformation of slopes.

A conventional, limit-equilibrium slope-stability analysis with slight modifications was used to determine the shearing resistance along a failure surface. Because the base motions may be amplified upon being propagated upward through a slope, consideration of the dynamic (earthquake) response of the slope was incorporated to account for amplified accelerations in the slope. The shearing resistance determined in the limit-equilibrium slope-stability analysis was then used to determine the relative displacement that will accumulate along a slide surface for a representative group of earthquake ground-motion histories. Each of these steps is described in greater detail below.

C. Limit-Equilibrium Slope-Stability Analyses

1. Method Used

In the limit-equilibrium slope stability analysis that is used, the sliding mass is idealized as a rigid block with earthquake and gravitational body forces tending to push the block downslope, and shear forces developed from the frictional strength of the earth materials along the sliding surface, tending to hold the block in place. By solving for equilibrium of the block, it is possible to determine the limiting values of forces required to prevent movement of the block. Although actual earthquake body forces change with time during a seismic event, in a limit equilibrium analysis they are idealized as a constant horizontal acceleration, termed a pseudo-static horizontal acceleration, k_h, expressed as a fraction of gravity, and applied at the center of gravity of the sliding mass. The value of k_h that causes the factor of safety against sliding of the slope to equal unity is termed the yield acceleration, k_y. A parametric study was performed to determine values of k_y and static ($k_h = 0$) safety factors against sliding for a range of frictional shear strength values and ground-water conditions. A two-dimensional, force-equilibrium method using Lowe and Karafiath's side force assumption was used for the slope-stability calculations (Lowe and Karafiath, 1960). The programs used were UTEXAS2 (Edris and Wright, 1987) and UTEXAS3 (Wright, 1990). A unit weight of 134.5 pounds per cubic foot was used as an average estimate for all materials in the slopes, based on laboratory test results presented in Appendix A.

2. Geometry of Failure Masses

An analysis of the field evidence used to estimate the geometry of the failure masses and locations of the shear surfaces was described in earlier chapters of this report. Several sliding surface locations were assumed in the slope stability analyses ranging from deep surfaces (greater than approximately 100 feet) to fairly shallow surfaces (approximately 50 feet or less). This range provided (1) insight about the controlling mechanism of failure acting in the slope during sliding caused by the Loma Prieta 1989 earthquake, (2) an indication of the sensitivity of the results to possible slip surface

locations, and (3) information about potential slope stability during future rainfall and earthquake events.

A single cross section, denoted SR, was selected through the Upper Schultheis Road landslide area, as shown in figures 7.1 (plan) and 7.3 (section). Two cross sections, denoted DM and SB, were chosen through the Villa del Monte landslide complex, as shown in figures 7.2 (plan) and 7.4-7.5 (sections). At the time the slope stability computations were performed, the deep-seated basal shear surfaces estimated by William Cotton and Associates, Inc. (1990) were the best estimates of sliding mass geometry and were used in the analyses. These estimated surface locations are shown in figures 8.1-8.3 for sections SR, DM, and SB, respectively; they differ slightly from the surfaces shown in figures 7.3-7.5, but the results of the slope stability analyses are relatively insensitive to these minor differences. The additional assumed shear surfaces are shown in figures 8.4-8.6 for sections SR, DM, and SB, respectively.

3. Ground-water Levels

A range of water-level conditions was assumed in the analyses to simulate the range from the 1989-1990 drought conditions to high ground-water levels, such as may be caused by intense or long-duration rainfall. Monitoring of ground-water levels was discussed in greater detail in Chapter VII. A key step in the stability analyses was to estimate the pore-water pressures that existed in the slope just prior to the earthquake; it is estimated that the piezometric levels measured during the spring of 1990 were indicative of those that existed just prior to the earthquake. Since no significant rainfall occurred in the area for several months prior to the earthquake, and the winter and spring months of 1990 had a similar rainfall environment, it is estimated that transient effects related to the earthquake had passed and the ground-water regime had again reached a steady-state condition similar to that before the earthquake. Estimated ground-water levels along the three analyzed sections are shown in figures 7.3-7.5. Due to the complex stratigraphy, it was expected that the in situ pore-pressure fields are also complex. However, for the purposes of analysis, hydrostatic pore-water pressure fields were used as an approximation of the in situ conditions.

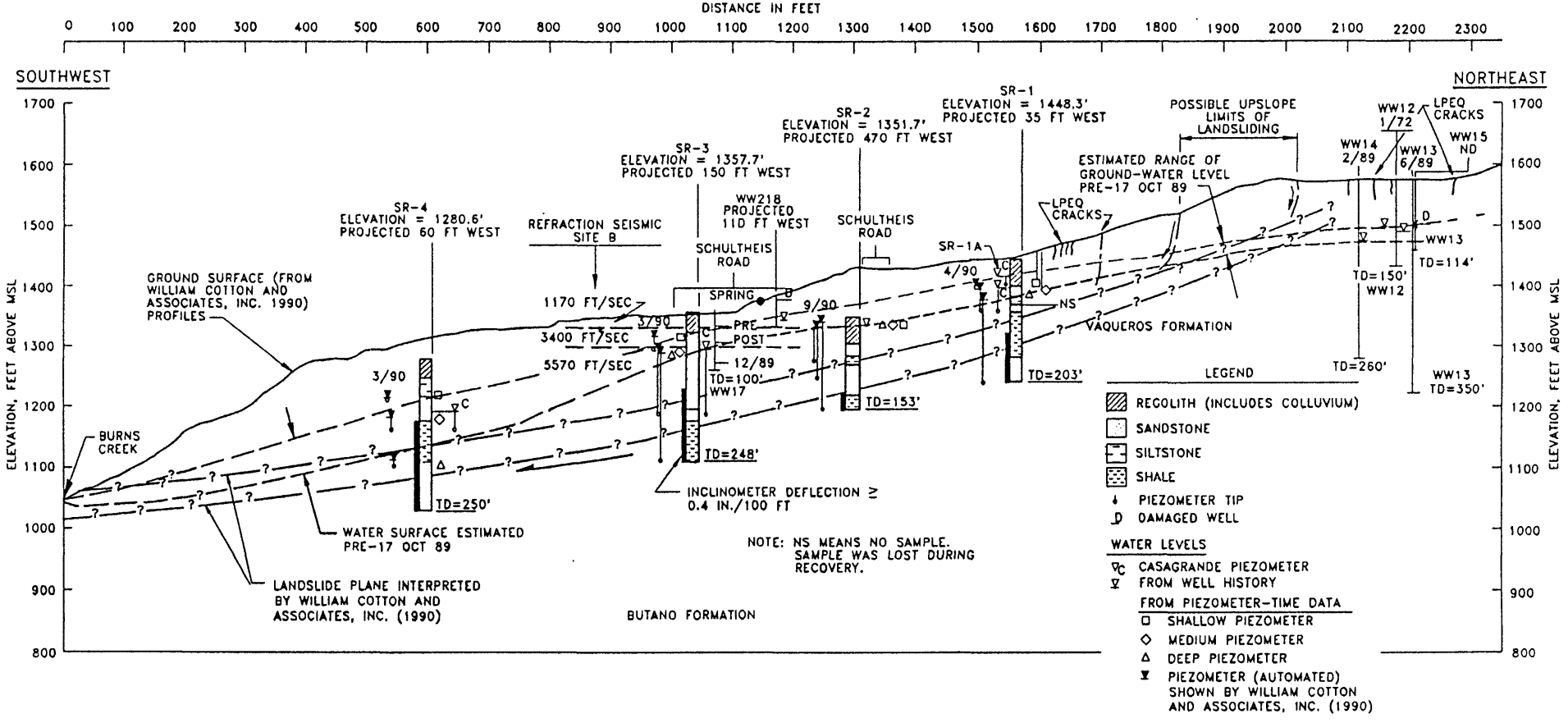

FIGURE 8.1 - Estimated Upper and Lower Locations of Basal Shear Surfaces for Section SR, Upper Schultheis Road Landslide, from William Cotton and Associates, Inc. (1990)

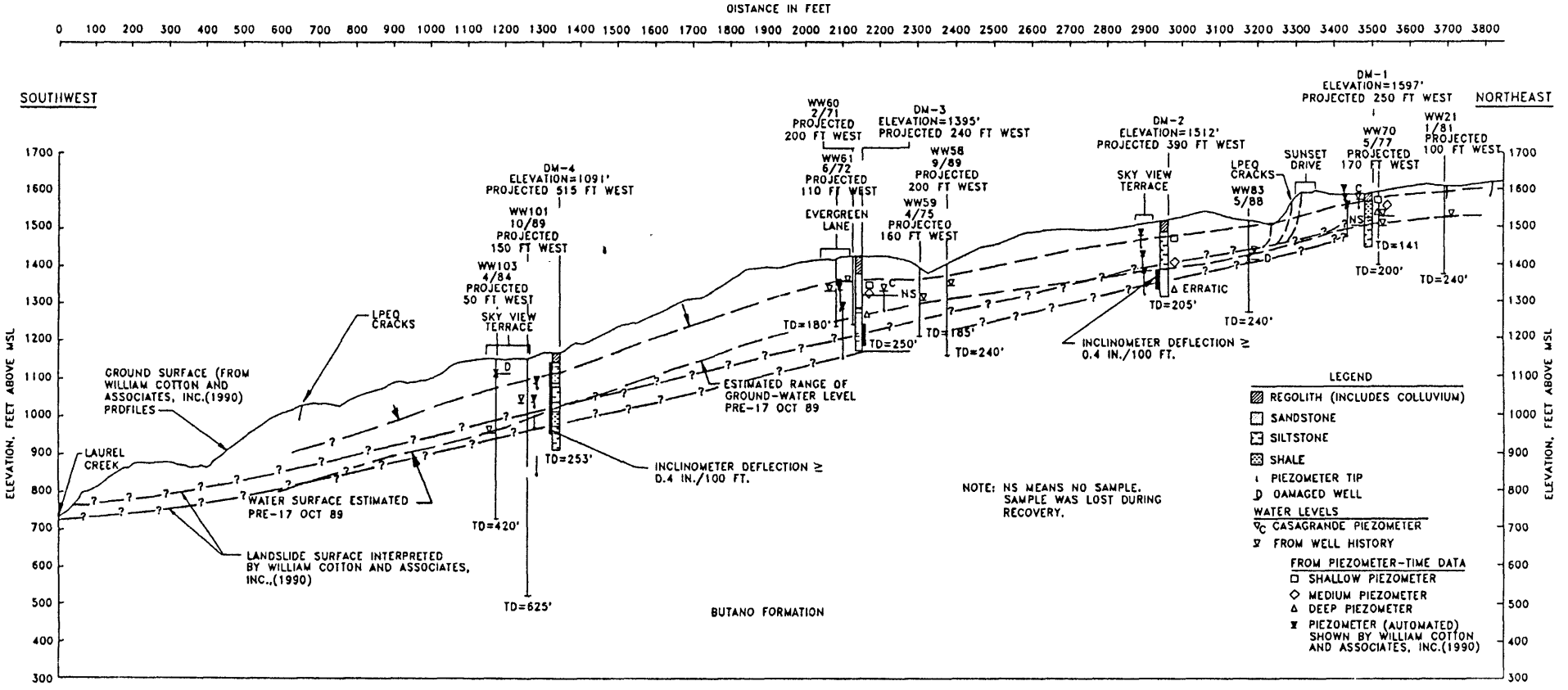

FIGURE 8.2 - Estimated Upper and Lower Locations of Basal Shear Surfaces for Section DM, Villa Del Monte Landslide Complex, from William Cotton and Associates, Inc. (1990)

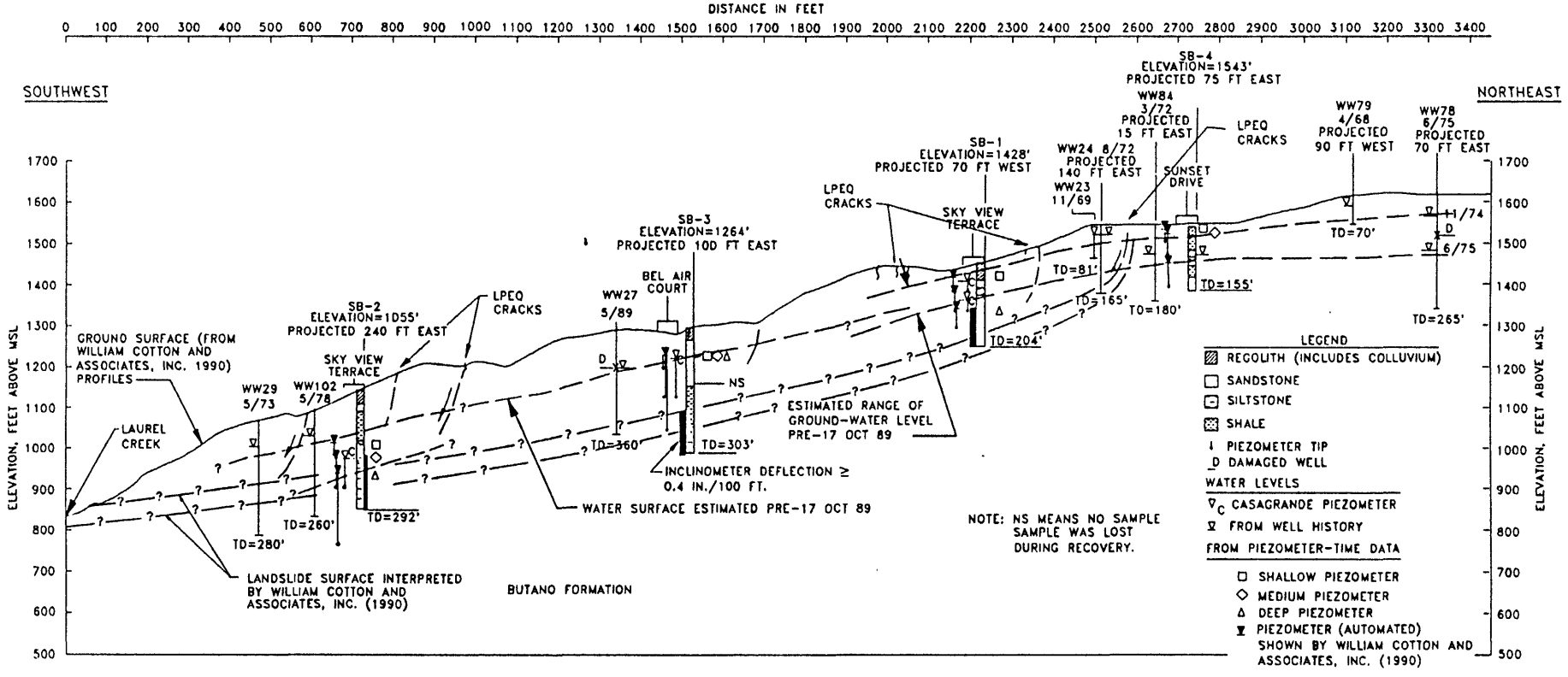

FIGURE 8.3 - Estimated Upper and Lower Locations of Basal Shear Surfaces for Section SB, Villa Del Monte Landslide Complex, from William Cotton and Associates, Inc. (1990)

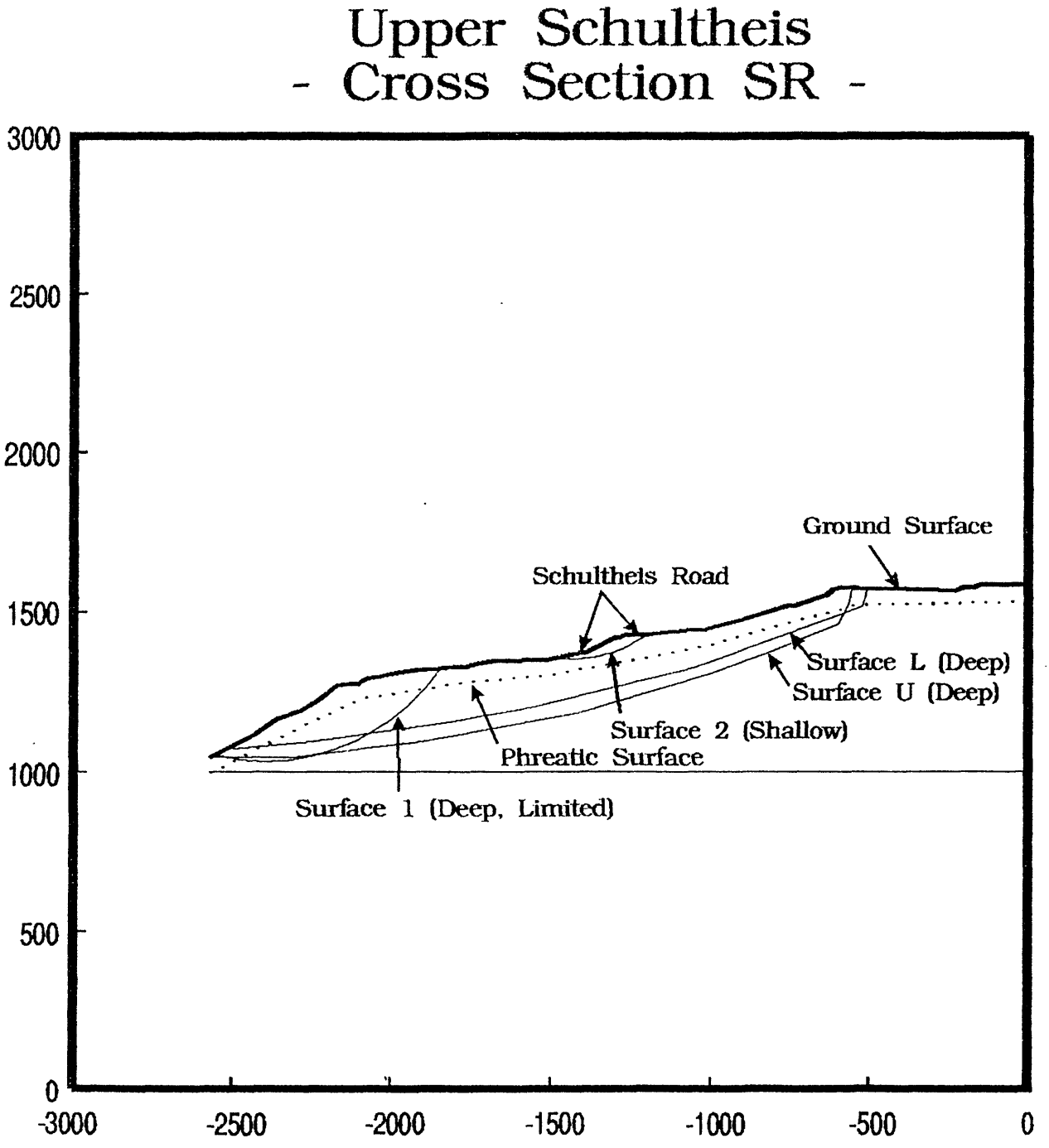

FIGURE 8.4 - Assumed Locations of Shallow and Deep Sliding Surfaces for Section SR, Upper Schultheis Road Landslide

Villa Del Monte
- Cross Section DM -

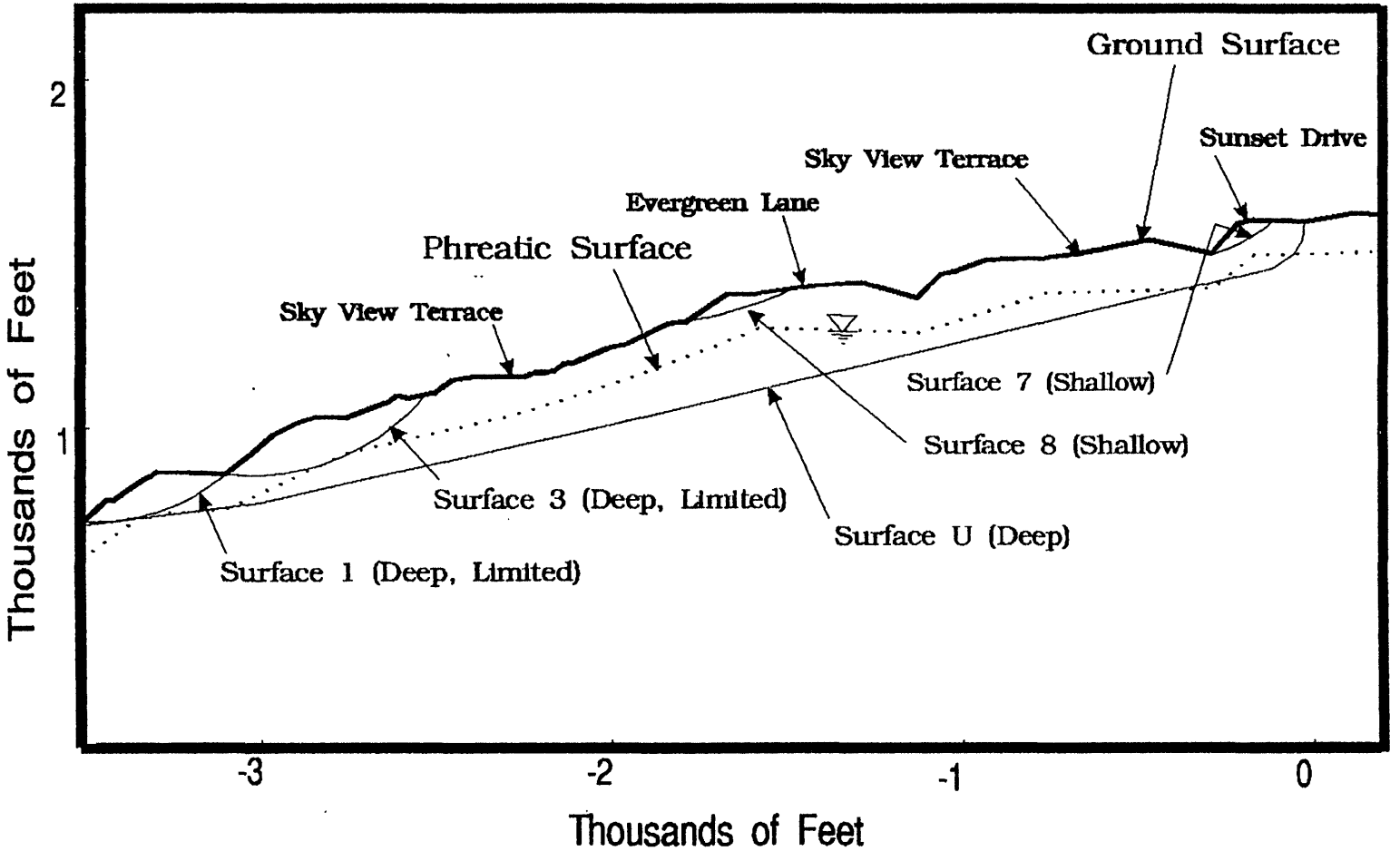

FIGURE 8.5 - Assumed Locations of Shallow and Deep Sliding Surfaces for Section DM, Villa Del Monte Landslide Complex

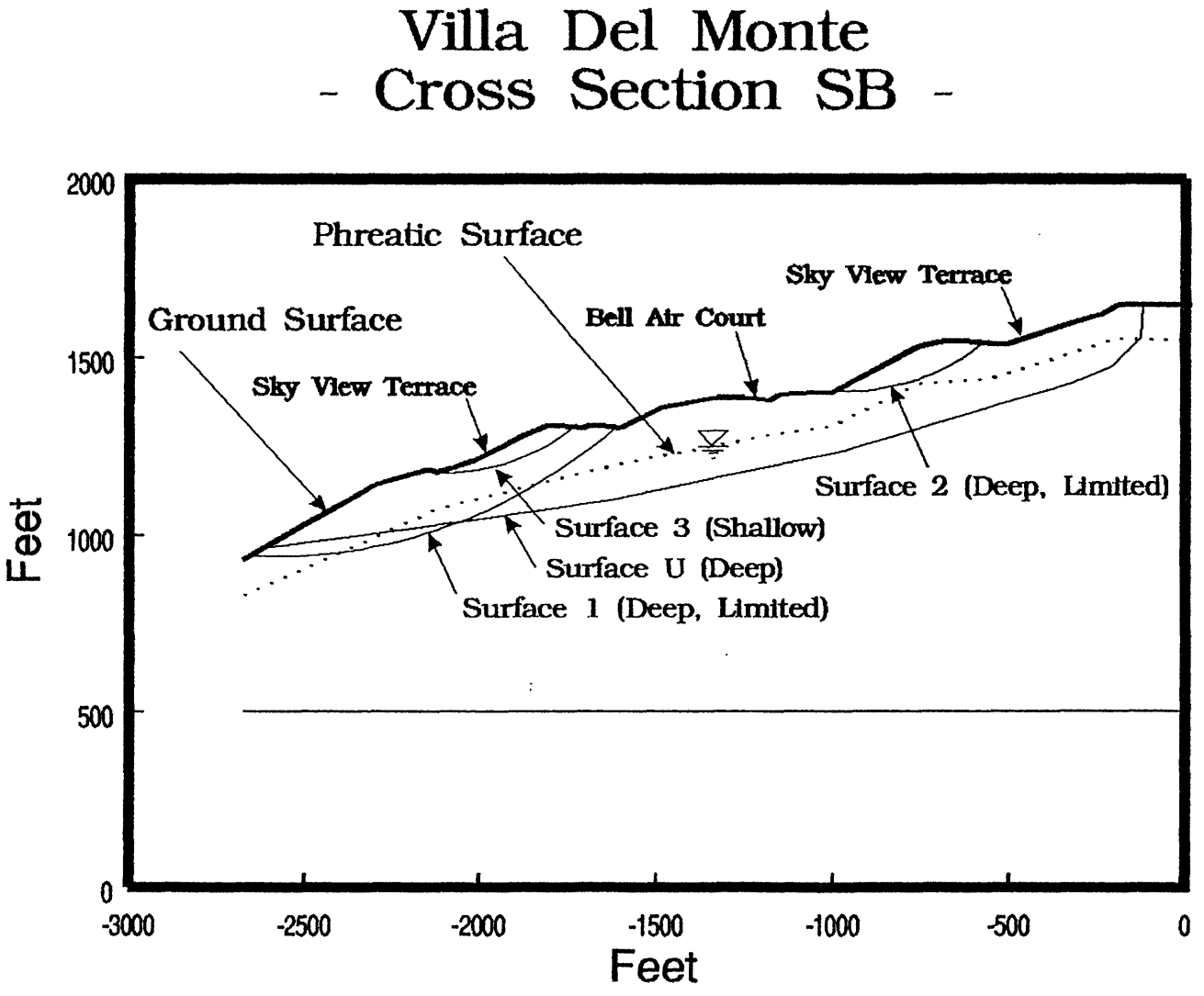

FIGURE 8.6 - Assumed Locations of Shallow and Deep Sliding Surfaces for Section SB, Villa Del Monte Landslide Complex

In the Upper Schultheis Road landslide (fig. 7.3), a hydrostatic ground-water level at a depth of 50 feet was used to represent pre-earthquake pore-water pressure conditions. Analyses were conducted for hydrostatic ground-water levels ranging from 0 to 50 feet below the ground surface to represent the effects of low to high rainfall.

In the Villa del Monte area (figs. 7.4 through 7.5), the pre-earthquake ground-water level was assumed to be at a depth of 100 feet, and analyses were conducted for hydrostatic ground-water levels ranging from 200 to 0 feet below the ground surface for sensitivity analyses and to represent ground-water conditions for low to high rainfall.

4. Shear Strength

Friction angles represented the shear strength in the stability computations. Friction angles ranging from 10° to 40° were used in the parametric studies.

5. Parametric Results from Slope Stability Calculations

The sliding masses bounded by deep-seated basal shear surfaces shown in figures 8.1-8.3 were analyzed in a detailed parametric study for a wide range of shear strength values and ground-water levels. The resulting relations determined between k_y (the value of horizontal acceleration which results in a factor of safety against sliding equal to one), mobilized friction angle, and ground-water level are shown in figures 8.7-8.12. Minimum values of friction angle required for static stability for the range of ground-water levels correspond to $k_y = 0$ in these plots and range from 11° to 24°. These figures were used to estimate the in situ strength mobilized during earthquake-induced sliding and critical levels of ground-water increase, as described below, in this chapter. Slope stability results for the additional assumed shallow and deep shear surfaces are presented later in this chapter.

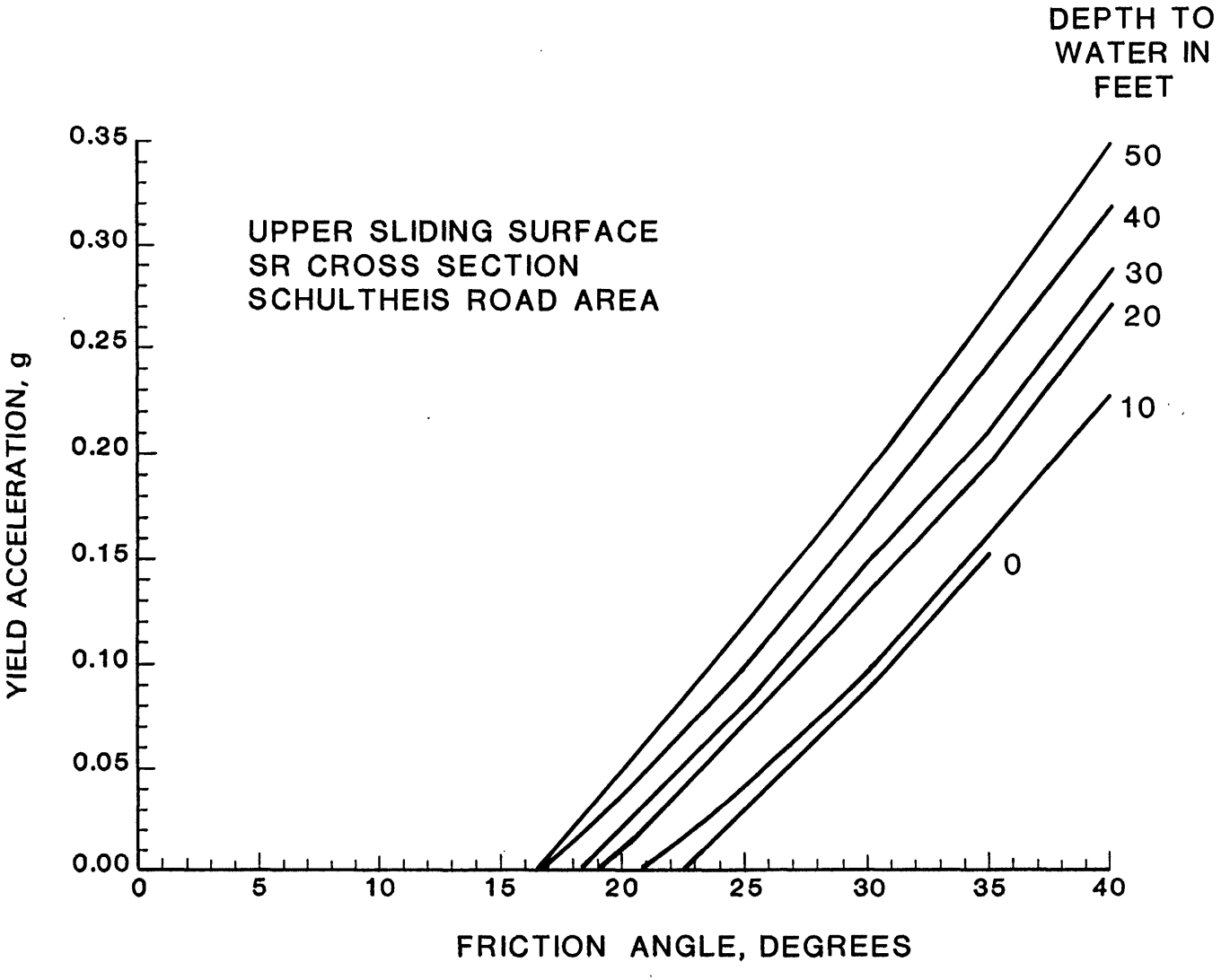

FIGURE 8.7 - Relation Between Mobilized Friction Angle, Depth to Water Table, and Yield Value of Horizontal Acceleration for Upper Basal Shear Surface, Section SR, Upper Schultheis Road Landslide

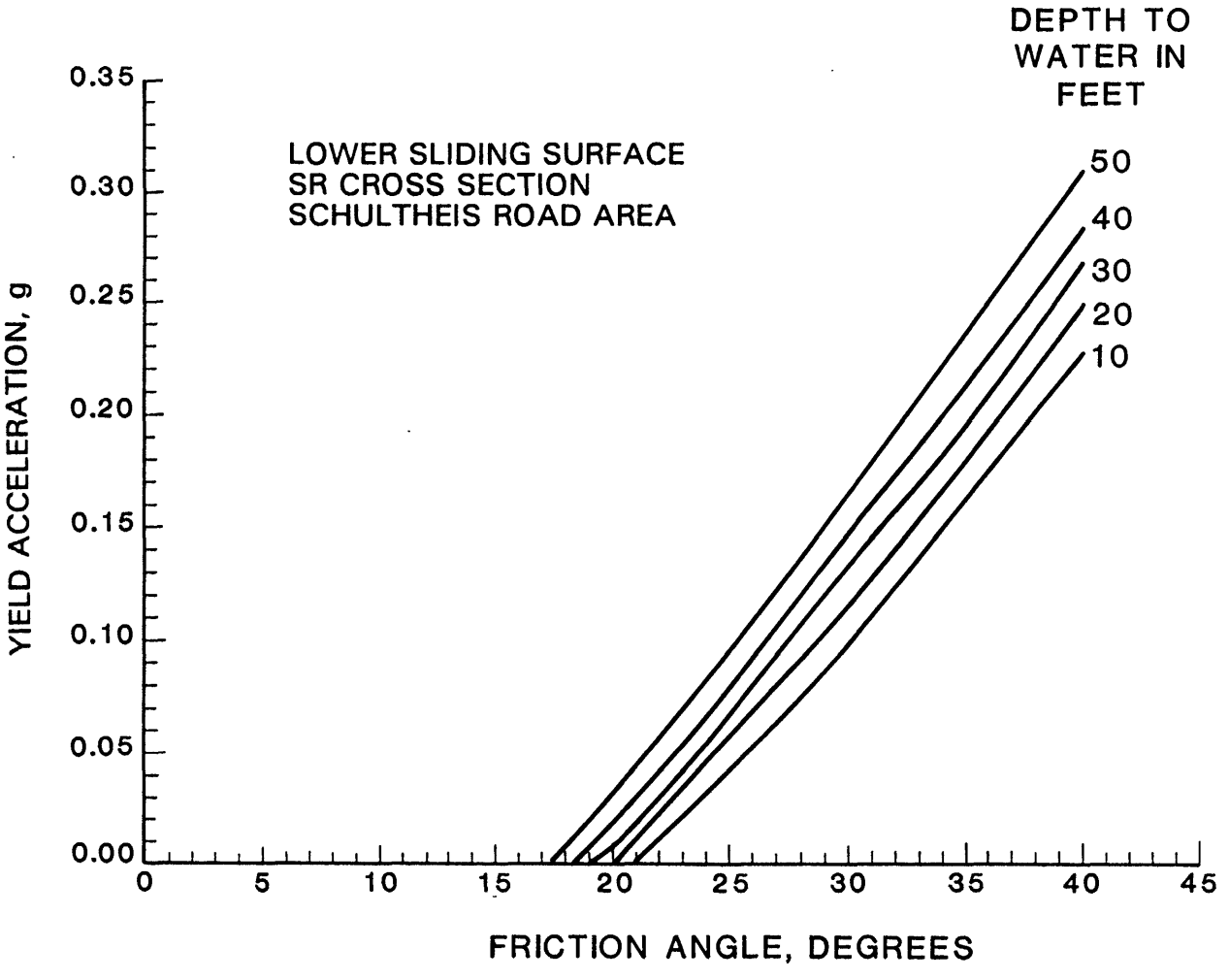

FIGURE 8.8 - Relation Between Mobilized Friction Angle, Depth to Water Table, and Yield Value of Horizontal Acceleration for Lower Basal Shear Surface, Section SR, Upper Schultheis Road Landslide

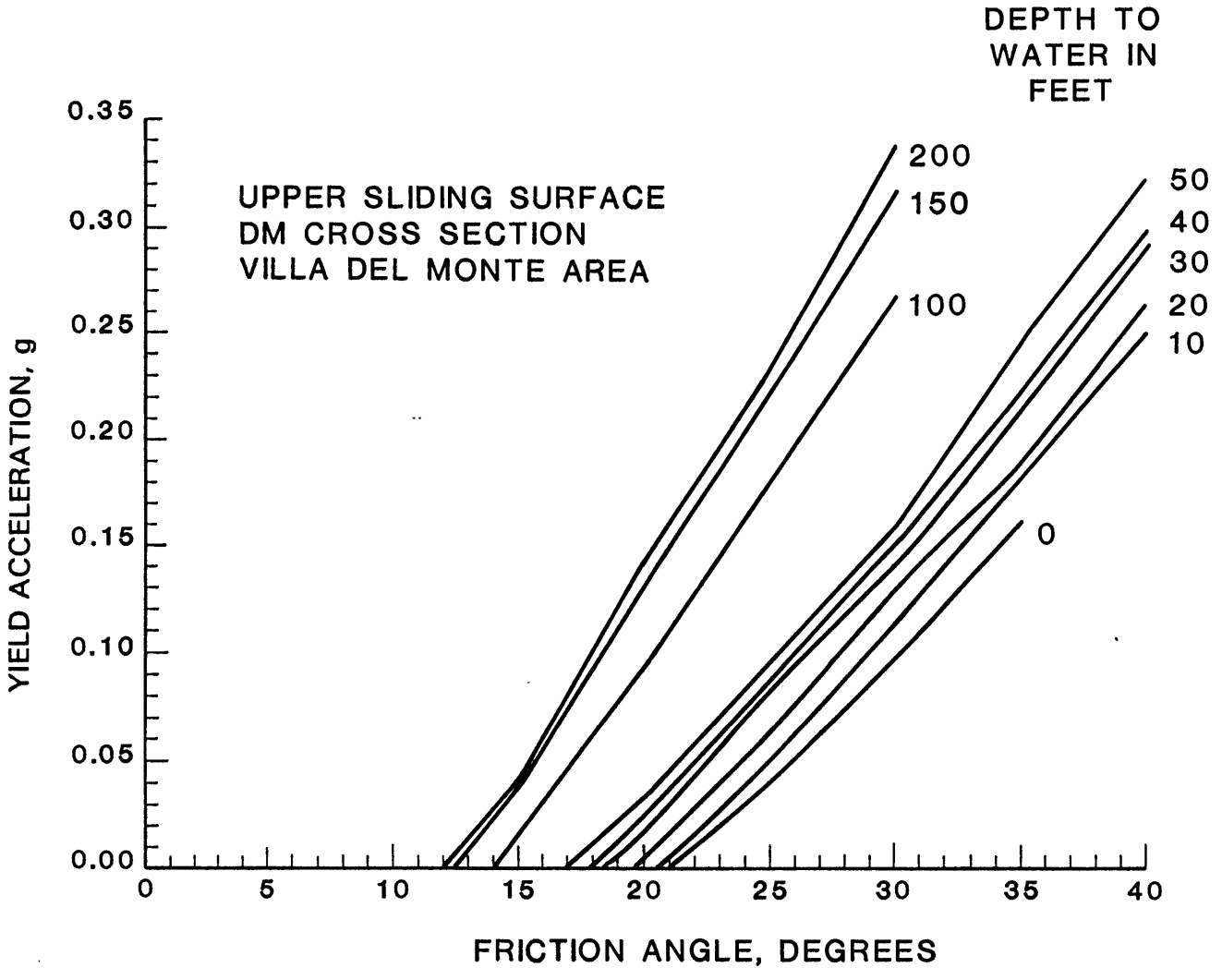

FIGURE 8.9 - Relation Between Mobilized Friction Angle, Depth to Water Table, and Yield Value of Horizontal Acceleration for Upper Basal Shear Surface, Section DM, Villa Del Monte Landslide Complex

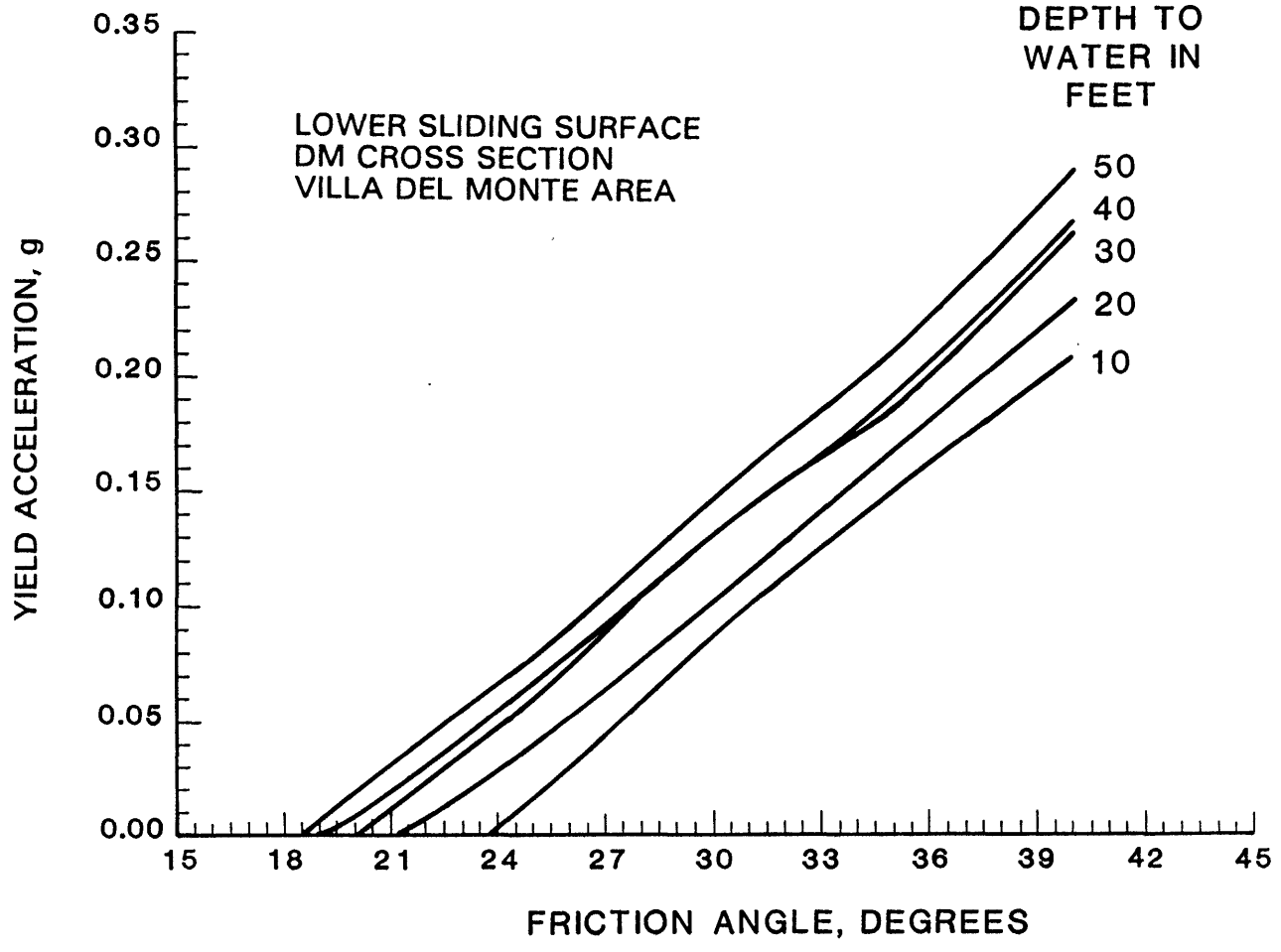

FIGURE 8.10 - Relation Between Mobilized Friction Angle, Depth to Water Table, and Yield Value of Horizontal Acceleration for Lower Basal Shear Surface, Section DM, Villa Del Monte Landslide Complex

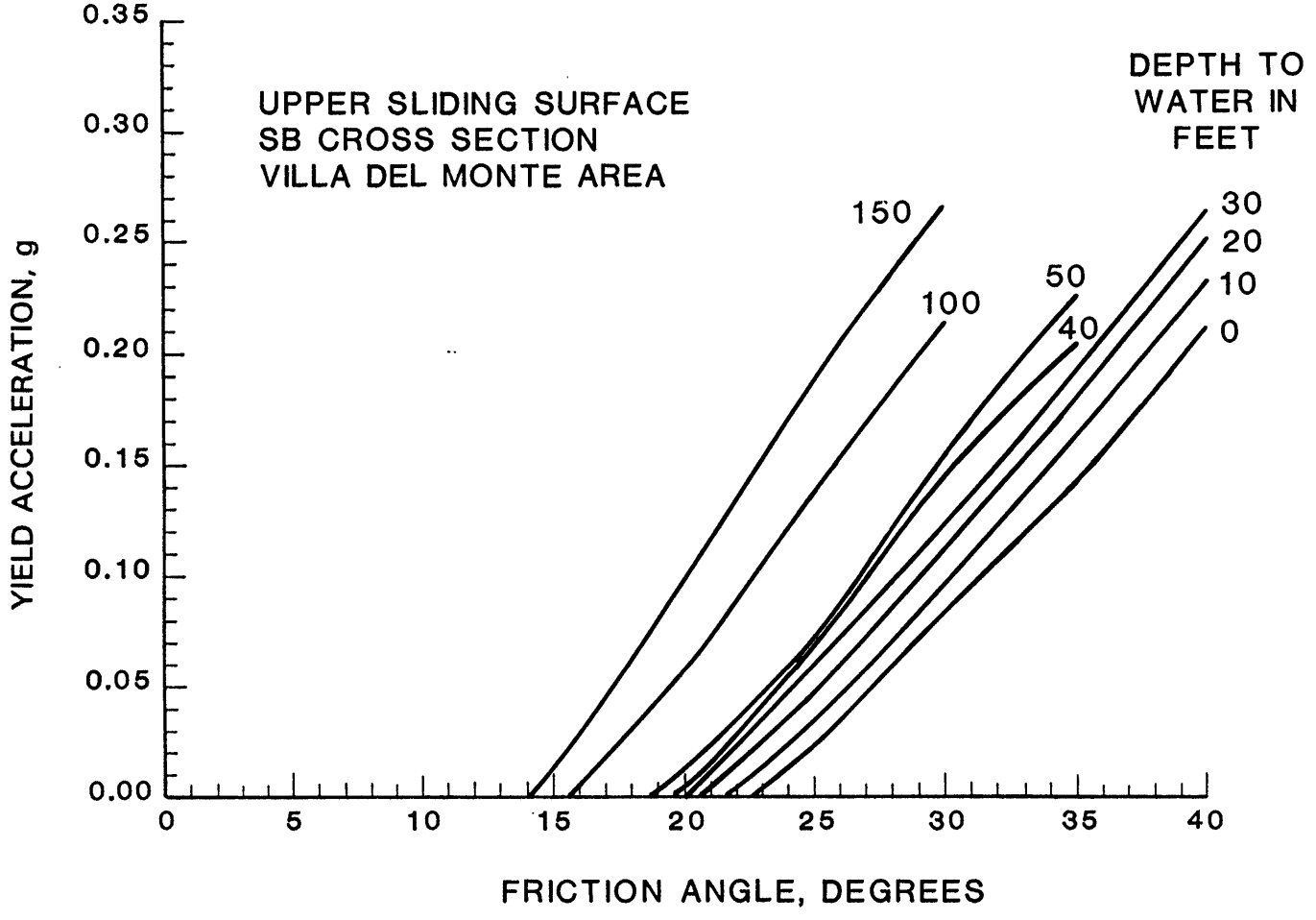

FIGURE 8.11 - Relation Between Mobilized Friction Angle, Depth to Water Table, and Yield Value of Horizontal Acceleration for Upper Basal Shear Surface, Section SB, Villa Del Monte Landslide Complex

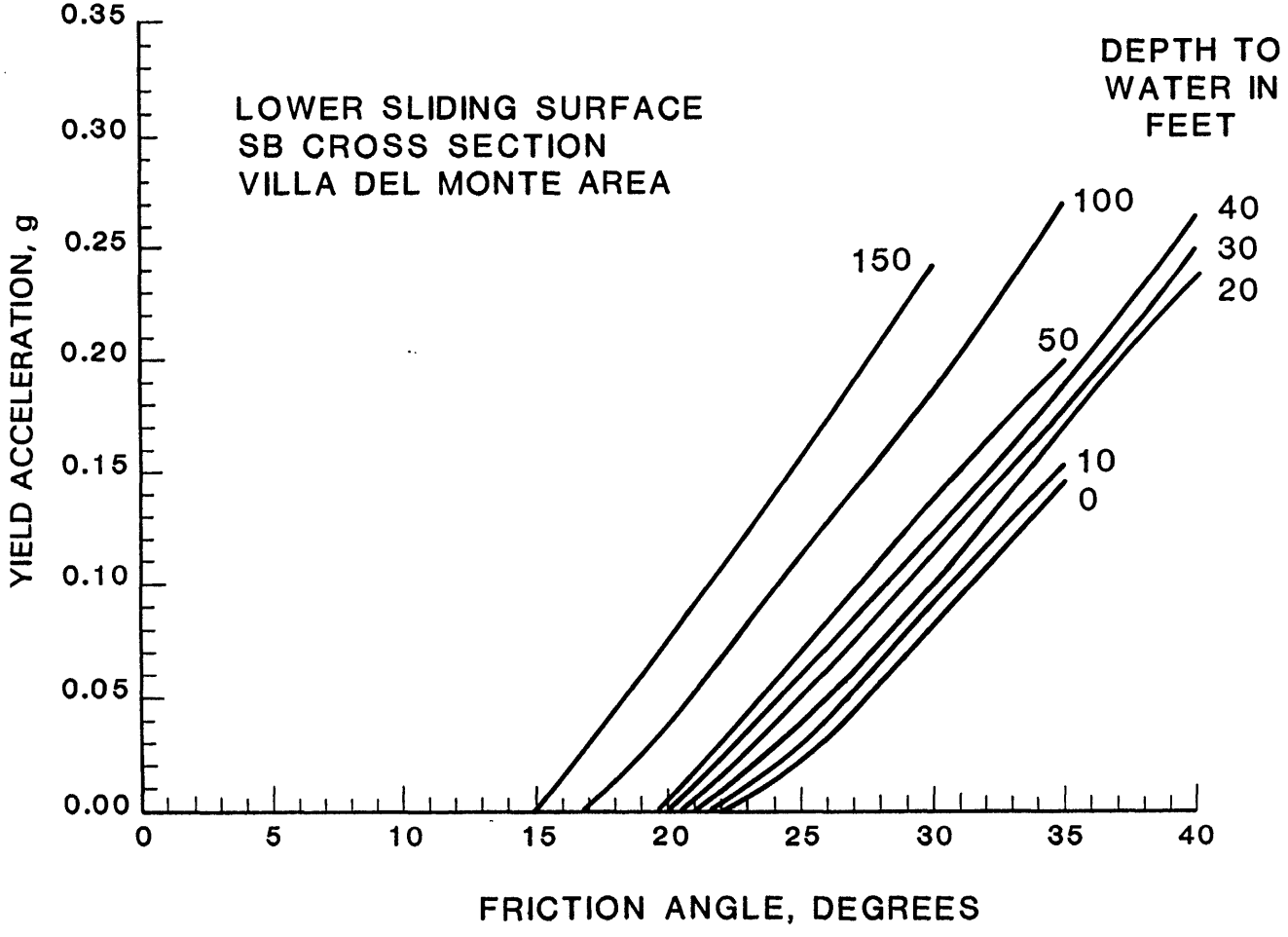

FIGURE 8.12 - Relation Between Mobilized Friction Angle, Depth to Water Table, and Yield Value of Horizontal Acceleration for Lower Basal Shear Surface, Section SB, Villa Del Monte Landslide Complex

D. Estimated Ground Motion and Slope Amplification

The next step in the Newmark analysis was to estimate the ground motions (accelerations) that were generated at the base and crest of the mountain by the Loma Prieta event, particularly the peak horizontal ground accelerations. No strong-motion instruments were located in the immediate area. Two California strong-motion instrument stations were close to the epicenter of the earthquake--Corralitos, to the south, at an epicentral distance of approximately 10 kilometers, and Lexington Dam, to the north, at an epicentral distance of approximately 18 kilometers (Shakal and others, 1989). The records from these stations were provided by the TAG. The peak horizontal ground accelerations at Corralitos for the 1989 Loma Prieta event were 0.48 and 0.63 g. At Lexington Dam (left abutment), the peak horizontal ground accelerations were 0.41 and 0.44 g.

The Upper Schultheis Road landslide and Villa del Monte landslide complex are located approximately 10 kilometers north of the earthquake epicenter. Numerous attenuation charts have been developed from California earthquake data to relate peak ground motions to epicentral distance. The Krinitzsky, Chang, and Nuttli (1988) acceleration attenuation chart shown in figure 8.13 was used for this study. It is based on a large body of California data, and indicates that a peak horizontal ground acceleration of about 0.63 g would be estimated for a magnitude 7 earthquake occurring at a distance of10 kilometers; about 0.40 g would be estimated at a distance of 18 kilometers. Since the recorded peak acceleration (maximum of two horizontal records) at Corralitos located at the same distance as the slide areas and the predicted value from a large body of California data both result in a peak acceleration of 0.63 g, it was concluded that the observed values at Corralitos of 0.48 and 0.63 g were realistic estimates of the peak motions at a rock outcrop in the study area.

The possible amplification of these motions as they propagated upward through the slope to the ridge crest was estimated from consideration of typical values from analytical studies and field observations of natural slopes and embankments, and from a simplified shear-beam numerical model described by Makdisi and Seed (1979). Typically, analytical studies and field observations have indicated that natural slopes and embankments amplify peak base (toe-of-slope) accelerations, a, by factors ranging from

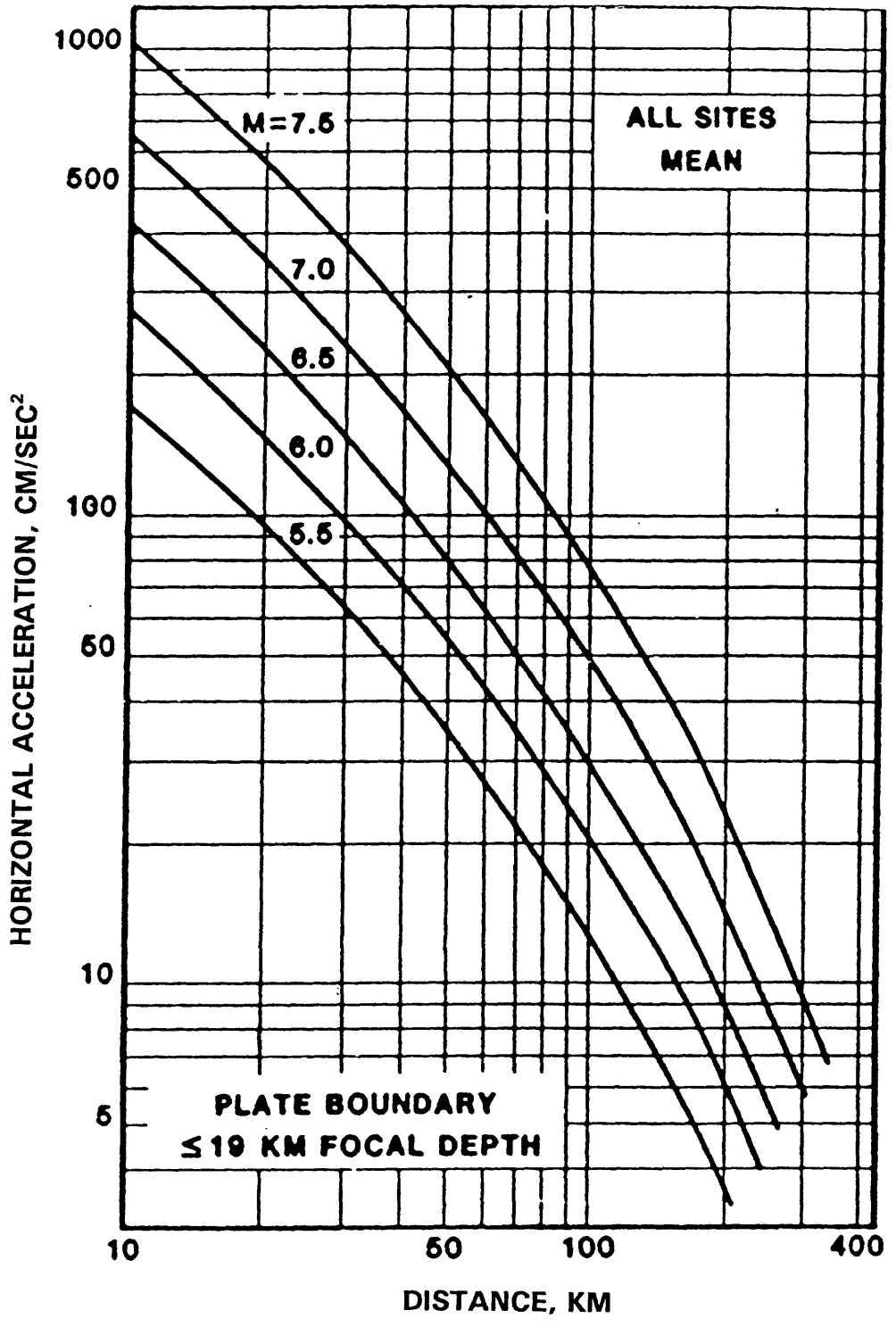

FIGURE 8.13 - Attenuation of Peak Ground Acceleration with Distance. Average Curves for All Site Types for Plate Boundary Seismic Events with Focal Depths Less than 19 km, from Krinitzsky, Chang, and Nuttli (1988)

approximately 1 to 4 to obtain peak crest accelerations, ü. In special cases, amplification factors greater than 4 have been observed in the field (based on data from Hynes and Franklin, 1984; and the Corps of Engineers Strong-Motion network). At high levels of acceleration, embankment amplification factors tend to approach unity, as shown in figure 8.14 (from Harder, 1991). Simplified shear-beam models tend to yield fairly high amplification factors; values of 4 to 5 were computed in this case. A range of amplification values was used in the sensitivity analysis shown in table 8.1 to estimate the pseudo-static dynamic acceleration, k_{max}, most appropriate to represent the earthquake motions in the deformation calculations.

The yield acceleration, k_y, from the slope-stability analyses is compared to the mass-averaged acceleration, k_{max}, induced by the earthquake in the sliding mass. The acceleration k_{max} can be thought of as the equivalent pseudo-static acceleration applied by the earthquake, and k_y represents the resistance to sliding from the strength of the slope materials. Values of k_{max} vary in a manner similar to peak accelerations in a mountain. Generally, peak accelerations will increase from the toe to the crest of the mountain and will decrease with depth from the ground surface into the mountain. Thus, for sliding masses that span nearly the full height of a mountain, computation of k_{max} involves averaging peak accelerations along the slope surface from the toe to the crest of the mountain, and k_{max} will generally decrease as the sliding surface of interest passes through deeper materials in the mountain. For short, shallow sliding masses near the crest of the slope, k_{max} will have a value very similar to the peak crest acceleration. Both shear-beam and finite-element numerical analyses have been used in earlier studies (Sarma, 1979; Makdisi and Seed 1979) to develop generalized charts to compute representative values of k_{max} for a range of sliding mass shapes, slope stiffnesses, and geometries (which affect amplification), and incoming earthquake ground motions.

The value of k_{max} should range from about 0.75 to 1.5 times the base motion on the basis of numerous dynamic finite element analyses of slopes (Idriss, 1968; Idriss, 1991). The chart for estimating k_{max} from embankment and slope crest peak accelerations (ü) developed by Seed and Makdisi (1979) is shown in figure 8.15. This chart indicates that deep-seated slides typically have ratios of k_{max} to crest acceleration of about 0.20 to 0.45, depending on the amount of amplification of the accelerations in the mountain. Based on the sensitivity analysis shown in table 8.1,

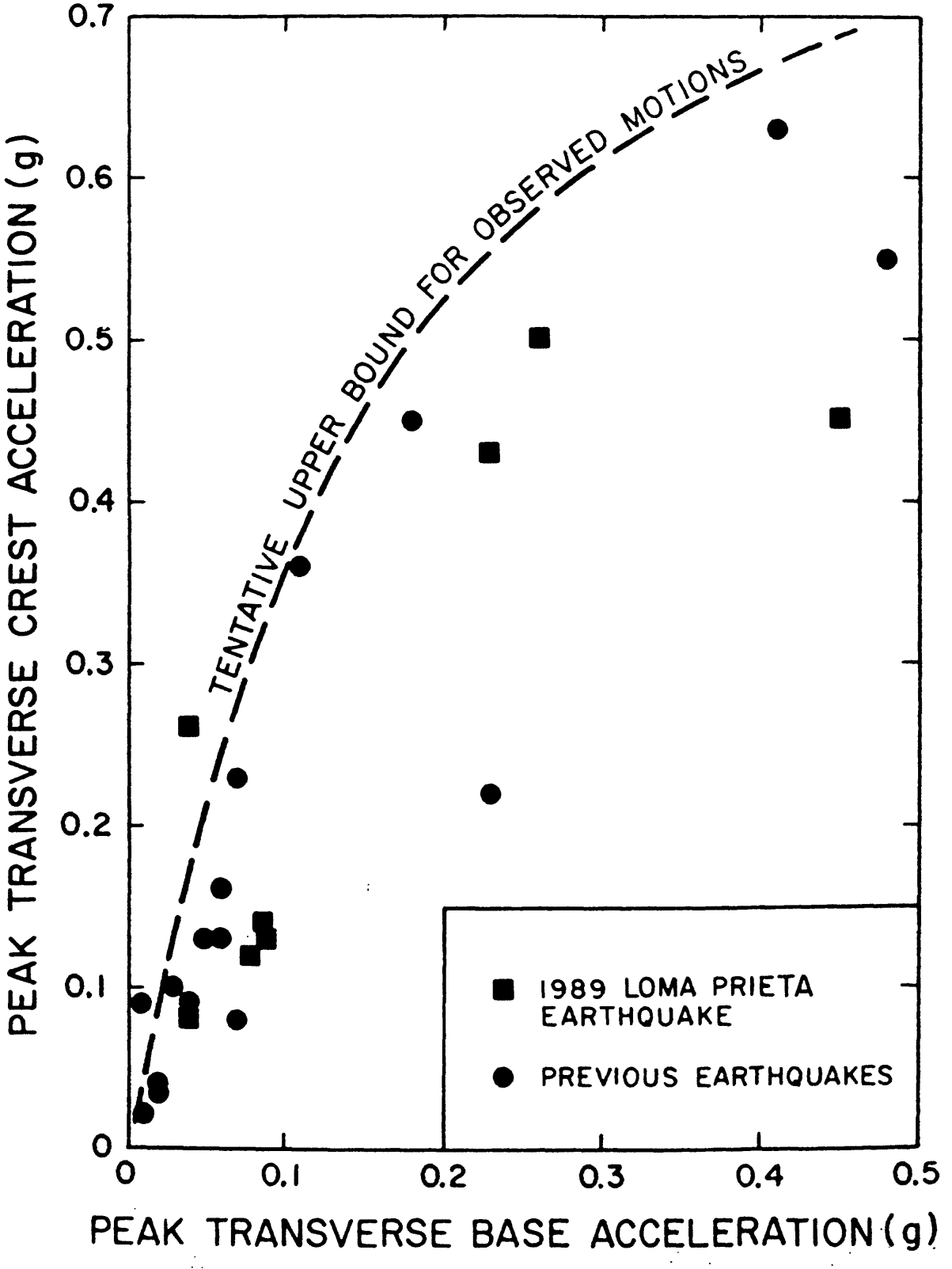

FIGURE 8.14 - Comparison of Peak Base and Crest Transverse Accelerations Measured at Earth Dams (from Harder 1991)

Table 8.1

Sensitivity Analysis of Dynamic Load, K_{max}

Acceleration, g				
Base a	Crest ü	Ratio ü/a	Dynamic Load Ratio K_{max} / ü	Dynamic Load K_{max}, g
0.4	2.4	6	0.20	0.48
0.4	2.0	5	0.25	0.50
0.4	1.6	4	0.30	0.48
0.4	1.2	3	0.35	0.442
0.4	0.8	2	0.40	0.32
0.48	1.44	3	0.35	0.50
0.5	2.5	5	0.25	0.63
0.5	2.0	4	0.30	0.60
0.5	1.5	3	0.35	0.53
0.5	1.0	2	0.40	0.40
0.6	2.4	4	0.30	0.72
0.6	1.8	3	0.35	0.63
0.6	1.2	2	0.40	0.48
0.63	1.26	2	0.40	0.50
0.7	2.1	3	0.35	0.74
0.7	1.4	2	0.40	0.56

Based on sensitivity analysis above,
K_{max} = 0.5 to 0.6 g selected for displacement computations

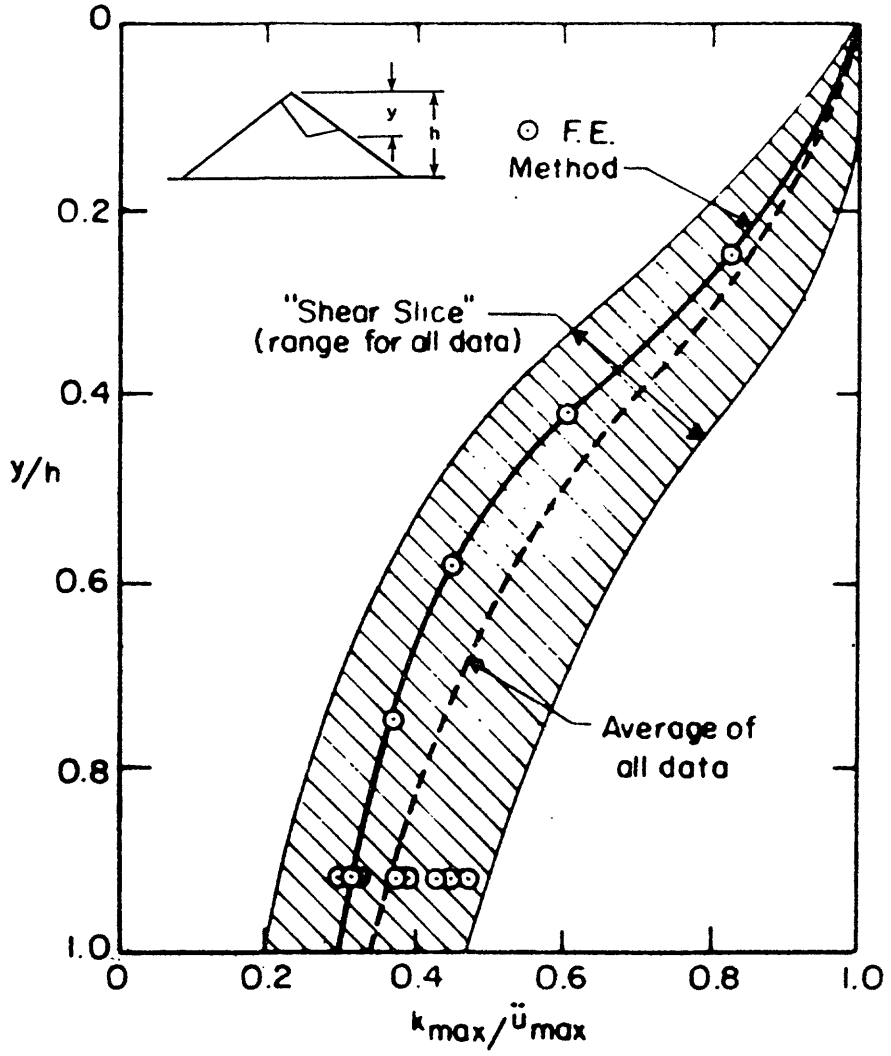

FIGURE 8.15 - Relation between Acceleration Ratio k_{max} / u_{max} (averaged dynamic load to peak crest acceleration) and Relative Height of Sliding Surface (y/h)

values of k_{max} of 0.5 to 0.6 seem to best represent the dynamic load for the 1989 Loma Prieta event. These values were used in the deformation calculations described next.

E. Deformation Calculations, Estimated Field Strengths, and Calculation of Static (Non-Earthquake) Stability

Charts of the relative displacement, u, that can accumulate between a sliding block and an inclined plane for a range of ratios of k_y/k_{max} have been developed by Franklin and Chang (1977), Seed and Makdisi (1979), and Hynes and Franklin (1984), based on many earthquake accelerograms. The Seed and Makdisi (1979) curves were selected for this study. Generalized displacement curves from Seed and Makdisi (1979) for earthquake magnitudes of 6.5 and 7.5 are shown in figure 8.16. An average curve for magnitude 7 earthquakes was estimated from these curves and used to back-calculate mobilized strength. This estimated curve and upper and lower bounds are shown in figure 8.17.

The deformations observed in the field were analyzed to estimate the displacement of the center of gravity (CG) of the sliding masses for the various failure surfaces. The TAG recommended using both upper-bound and average displacements, based on a sum of observed displacements along each cross section analyzed. The displacements used are listed in table 8.2; these displacements were compiled from data in Spittler and Harp (1990); William Cotton and Associates, Inc. (1990); and David K. Keefer and Randall W. Jibson (unpublished data). The total displacement is approximately the cumulative value of downslope displacements observed along the ground surface along and near the limits of a section. Because the sliding mass is compressed during movement, the TAG estimated that the CG displacement might best be associated with about half of the total displacement. Thus, half of the total displacement was defined as the average displacement and represented the best estimate for back-calculation of strength.

The estimated CG displacements were analyzed with the sliding-block model to determine the mobilized shear strength in the field and to estimate the ground-water rise that would lead to static slope instability. The computations are shown in tables 8.3 and 8.4 for upper and lower deep-seated basal shear surfaces (three upper sliding surfaces and two lower sliding surfaces) identified in figures

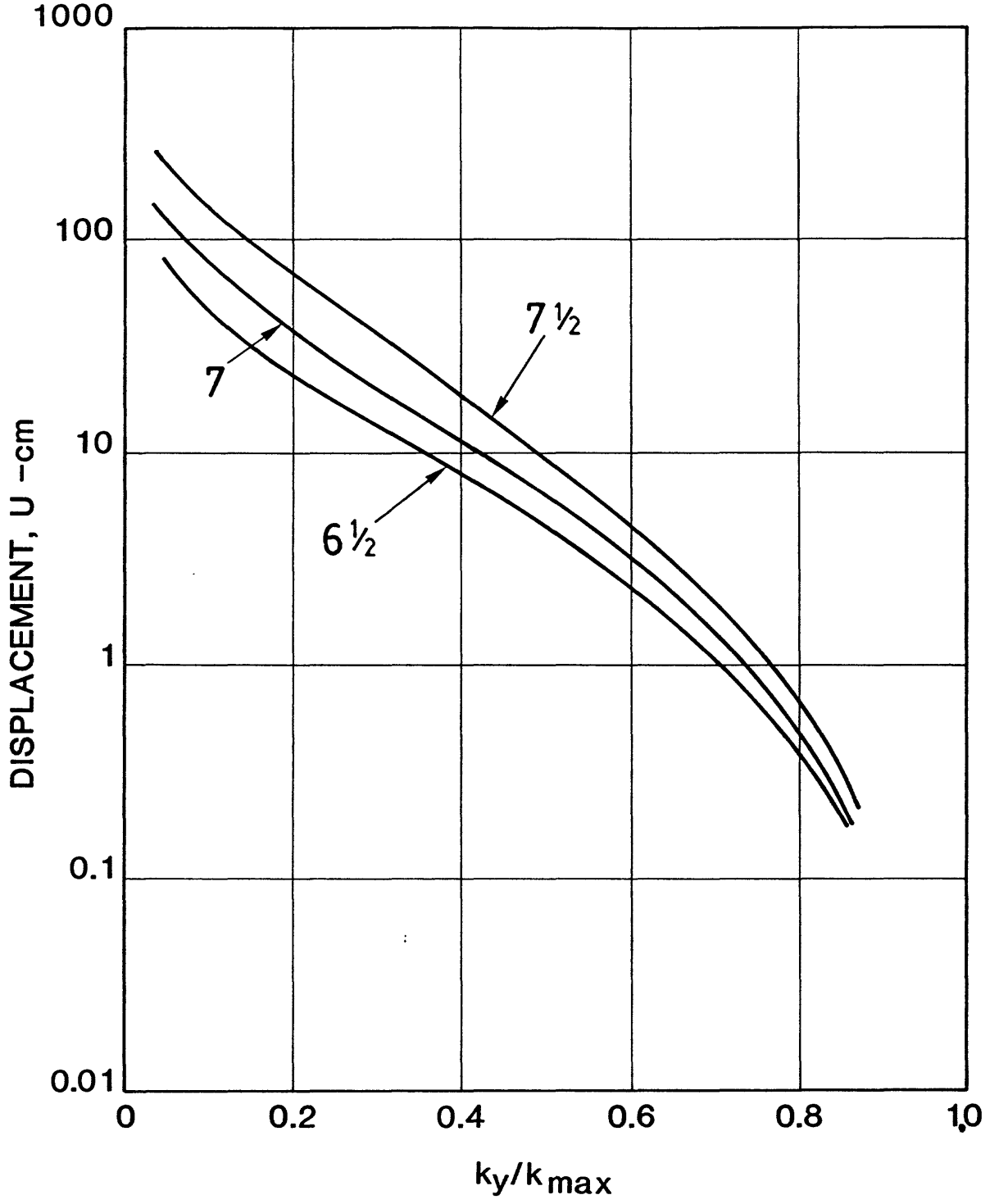

FIGURE 8.16 - Relation Between Accumulated Newmark-Sliding-Block Displacement, U, and Acceleration Ratio, k_y/k_{max}, for Magnitude 6.5, 7 (Interpolated), and 7.5 Earthquakes after Makdisi and Seed (1979)

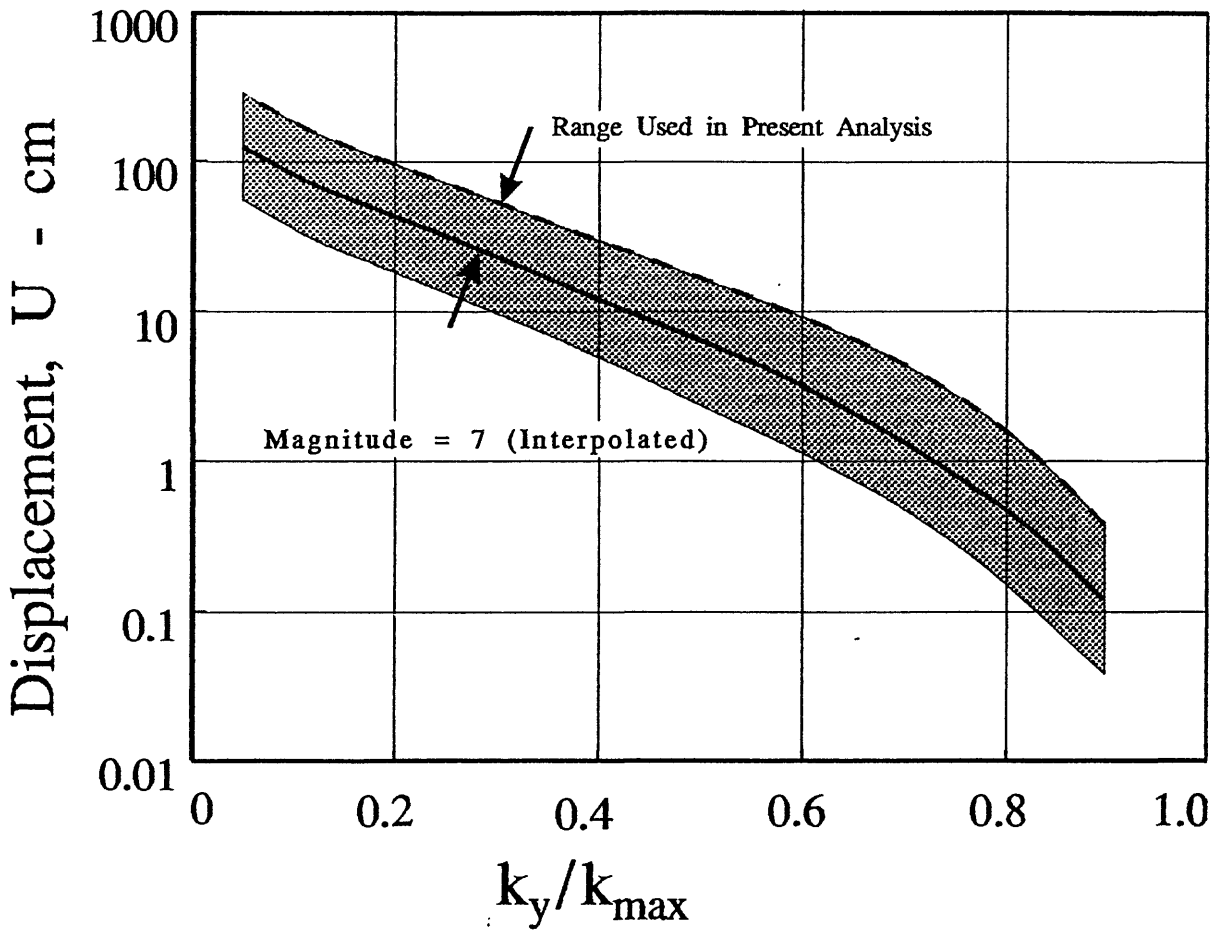

FIGURE 8.17 - Average and Range for Relation Between Accumulated Newmark-Sliding-Block Displacement, U, and Acceleration Ratio, k_y/k_{max}, for Interpolated Magnitude 7 Earthquakes after Makdisi and Seed (1979)

Table 8.2

Summary of Slope Displacements
Provided by the T.A.G.

Section	Displacement			
	Total		Average	
	in.	cm	in.	cm
Villa del Monte				
DM	28	72	14	36
SB	44	111	22	36
Schultheis Road				
SR	96	244	48	122

Table 8.3

Displacement Computations for Villa del Monte Landslide Complex and Upper Schultheis Road Landslide

Section (U-upper, L-lower surfaces)*	Dynamic Load K_{max} g	Total Displacement u in.	cm	Ratio K_y / K_{max}	Yield Acceleration K_y g	Mobilized Friction ϕ'_{mob} degrees	Average Displacement u in.	cm	Ratio K_y / K_{max}	Yield Acceleration K_y g	Mobilized Friction ϕ'_{mob} degrees
Villa del Monte											
DM-U	0.5	28	72	0.11	0.055	17.6	14	36	0.21	0.105	20.7
DM-U	0.6	28	72	0.11	0.066	18.3	14	36	0.21	0.126	22
SB-U	0.5	44	111	0.06	0.03	17.8	22	55.5	0.15	0.075	21
SB-U	0.6	44	111	0.06	0.036	18.3	22	55.5	0.15	0.09	22
SB-L	0.5	44	111	0.06	0.03	19.3	22	55.5	0.15	0.075	22.5
SB-L	0.6	44	111	0.06	0.036	19.8	22	55.5	0.15	0.09	23.5
Schultheis Road											
SR-U	0.5	96	244	0.03	0.015	17.6	48	122	0.05	0.025	18.3
SR-U	0.6	96	244	0.03	0.015	17.8	48	122	0.05	0.03	18.6
SR-L	0.5	96	244	0.03	0.015	18.6	48	122	0.05	0.025	19.4
SR-L	0.6	96	244	0.03	0.018	18.9	48	122	0.05	0.03	19.8

* Surfaces identified in Figures 8.1 - 8.3

Table 8.4

Summary of Mobilized Dynamic Friction, Static Stability, and Critical Ground-Water Depths

Pre-Quake Ground-Water Conditions

Section*	Estimated Ground-Water Depth at Time of Quake, ft	Dynamic Load K_{max}, g	Displacement u, in.	Displacement u, cm	Mobilized Friction ϕ'_{mob}, degree	Friction Required for Static Stability $\phi'_{req.}$, degrees	Factor of Safety Against Sliding** FS_s	Ground-Water Depth That Would Trigger Static Instability**, ft	Critical Change in Ground-Water Depth**, ft
DM-U	100	0.5	28	72	17.6	14	1.27	45	55
DM-U	100	0.6	28	72	18.3	14	1.33	30	70
DM-U	100	0.5	14	36	20.7	14	1.52	10	90
DM-U	100	0.6	14	36	22	14	1.62	>0	>100
SB-U	100	0.5	44	111	17.8	15.5	1.15	70	30
SB-U	100	0.6	44	111	18.3	15.5	1.19	60	40
SB-U	100	0.5	22	55.5	21	15.5	1.38	15	85
SB-U	100	0.6	22	55.5	22	15.5	1.46	5	95
SB-L	100	0.5	44	111	19.3	16.9	1.15	55	45
SB-L	100	0.6	44	111	19.8	16.9	1.19	45	55
SB-L	100	0.5	22	55.5	22.5	16.9	1.36	>0	>100
SB-L	100	0.6	22	55.5	23.5	16.9	1.43	>0	>100

(Continued)

Table 8.4

Summary of Mobilized Dynamic Friction, Static Stability, and Critical Ground-Water Depths

Section*	Pre-Quake Ground-Water Conditions: Estimated Ground-Water Depth at Time of Quake, ft	Dynamic Load K_{max}, g	Displacement u, in.	Displacement u, cm	Mobilized Friction ϕ'_{mob}, degree	Friction Required for Static Stability $\phi'_{req.}$, degrees	Factor of Safety Against Sliding** FS_s	Ground-Water Depth That Would Trigger Static Instability**, ft	Critical Change in Ground-Water Depth**, ft
SR-U	50	0.5	96	244	17.6	16.5	1.07	35	15
SR-U	50	0.6	96	244	17.8	16.5	1.08	35	15
SR-U	50	0.5	48	122	18.3	16.5	1.12	30	20
SR-U	50	0.6	48	122	18.6	16.5	1.14	30	20
SR-L	50	0.5	96	244	18.6	17.2	1.09	35	15
SR-L	50	0.6	96	244	18.9	17.2	1.11	30	20
SR-L	50	0.5	48	122	19.4	17.2	1.14	25	25
SR-L	50	0.6	48	122	19.8	17.2	1.16	20	30

* Surfaces identified in Figures 8.1 - 8.3

** Based on dynamic strengths

8.1-8.3. Back-calculated dynamic friction angles for the additional assumed surfaces shown in figures 8.4-8.6 are listed in tables 8.5 and 8.6.

The computed mobilized friction angles for deep basal sliding surfaces ranged from approximately 16° to 19° for the Upper Schultheis Road landslide and from about 18° to 23° for the Villa del Monte landslide complex. These back-calculated strengths are from dynamic loading conditions and are typically lower than the strength actually available for static loading conditions. The calculations shown in the last three columns of table 8.4 were performed to obtain conservative estimates of the stability of the slopes and critical rises in ground-water levels for triggering slope instability under static conditions. These conservative results indicated that a ground-water rise of 15 to 30 feet, from a depth of 50 feet to 20 to 35 feet below the ground surface in the Upper Schultheis Road landslide, would result in renewed landslide movement without earthquake shaking. At Villa del Monte, the range of computed critical ground-water levels was broader; the results suggested that some analyzed sliding masses would become statically unstable with a ground-water level increase of as little as 30 feet, while others would remain stable with rises of more than 100 feet (which would require artesian conditions.) Computed static factors of safety using dynamic strengths, with estimated pre-earthquake ground-water levels, were in the range of 1.07 to 1.16 for the Upper Schultheis Road landslide and 1.15 to 1.62 for the Villa del Monte landslide complex. These results are summarized in table 8.4. These safety factors for the low 1989-1990 ground-water levels are all quite low, but greater than unity, even when the low dynamic strengths are used in the computations.

The strengths and static stability conditions discussed above are back-calculated from a dynamic loading event. Usually, there is some degradation of strength caused by dynamic loading of geologic materials, especially if they are below the water table. To estimate the amount of strength degradation, the additional assumed sliding masses shown in figures 8.4-8.6 were analyzed. The surfaces were chosen based upon critical locations of slope geometry and roadway locations. Two cases were analyzed to determine (1) the friction angle that would have been mobilized during the 1989 Loma Prieta event, and (2) the friction angle required to have a static factor of safety against sliding of unity if the water table is near the surface of the slope, at a depth of approximately 10 feet. These results are

Table 8.5

Calculated Friction Angles for Shallow Failure Surfaces Shown in Figures 8.4 - 8.6

Failure Surface Designation	Friction Angle Back-Calculated From Loma Prieta Earthquake (degrees)	Friction Angle Required for Static F.S = 1 With Water Table Near Surface (degrees)
SR-2	19	33
DM-7	33	>40
DM-8	20	22
SB-3	22	26

Table 8.6

Calculated Friction Angles for Deep Failure Surfaces Shown in Figures 8.4 - 8.6

Failure Surface Designation	Friction Angle Back-Calculated From Loma Prieta Earthquake (degrees)	Friction Angle Required for Static F.S. = 1 With Water Table Near Surface (degrees)
SR-1	25	32
SR-U	18	22
SR-L	16	22
DM-1	20	29
DM-3	21	27
DM-U	20	23
SB-1	22	29
SB-2	19	22
SB-U	18	22

listed in table 8.5 for shallow (approximately 50 feet or less) surfaces and table 8.6 (approximately 100 feet or more) surfaces.

Localized movements have been observed in these slopes after periods of heavy rains. The strengths of the materials in the slope were probably at least as high as the values calculated for static conditions with the water table near the surface and the factor of safety against sliding equal to one. If this were not the case, large failures would have been expected to be seen as the water table rose at times in the past. Instead, localized slope movements have been observed during wet weather, indicating a factor of safety near one. The strength values in tables 8.5 and 8.6 indicate that the friction angles for the static high-water-table case are larger than those necessary to produce the observed displacements during the 1989 Loma Prieta earthquake. Therefore, in order to satisfy both conditions, the strength of the slope materials must have degraded due to the shaking of the earthquake.

Degradation of strength is most likely to occur in saturated conditions. The materials along shallow surfaces were not saturated at the time of the earthquake. All of the deep failure surfaces had some of their lengths at or below the water table. Therefore, it is most likely that materials along deep surfaces experienced strength degradation. It was therefore concluded that deep-seated sliding surfaces were more likely to have been responsible for the landslide activity in the Upper Schultheis Road and Villa del Monte areas, with a reduction in strength occurring in the materials along the deep surfaces due to earthquake shaking.

Another approach was used to estimate the strength of the materials in the slope under static loading conditions. It is known that the slopes were stable before the 1989 Loma Prieta earthquake, with the ground-water table at a depth of about 50 feet in the Upper Schultheis Road area and about 100 feet in the Villa del Monte area. A factor of safety against sliding of 1.5 was used as a reasonable estimate for the static factor of safety of the slopes for these ground-water conditions. A series of slope stability calculations was performed using these additional slip surfaces to determine the strengths required to have a static factor of safety against sliding of 1.5. These strengths were then used to compute the static factor of safety against sliding with the water table near the surface. The results of these calculations are shown in table 8.7. As can be seen from this table, the friction angles thus generated seem reasonable in

Table 8.7

Estimated Static Friction Angles for
Deep Surfaces Shown in Figures 8.4 - 8.6

Failure surface designation	Friction angle required for static F.S. = 1.5 with a deep water table (degrees)	Factor of safety water table at ground Surface
SR-1	35	1.09
SR-U	26	1.18
SR-L	24	1.10
DM-1	24	0.81
DM-3	26	0.94
DM-U	23	1.01
SB-1	28	0.98
SB-2	25	1.16
SB-U	23	1.03

that they provide a low factor of safety against sliding after the water table has risen significantly. This correlates well with the observations of localized movements during periods of high water table.

In summary, the strengths back-calculated from the Loma Prieta event probably underestimate the available strength of the materials in the slope for the static case of a rise in ground-water levels because of strength degradation of saturated materials due to dynamic loading. The static strengths are likely to be greater than the back-calculated dynamic values and approximately equal to or less than the static values listed in tables 8.5-8.7. Also, if ground-water levels rise, slope movements may involve both shallow and deep surfaces.

F. Sliding During Future Earthquakes with Higher Ground-Water Levels

The Newmark sliding-block calculation procedure demonstrated in table 8.3 can be used in conjunction with the yield accelerations in figures 8.7 through 8.12 to estimate the potential for further deep-seated sliding-block displacement in future earthquakes with higher ground-water levels. For example, displacement computations that simulate occurrence of a Loma Prieta-type event with higher ground-water levels indicate that displacements on a deep-seated shear surface along cross section SB, in the Villa del Monte landslide complex, might have been two to three times greater than they actually were if the ground-water level had been at a depth of 50 feet rather than 100 feet during the earthquake. This is determined by observing in the last column in table 8.3 that the average mobilized friction angle for the slip surface denoted SB-U was approximately 21°. One then enters figure 8.4 at a friction angle of approximately 21° to find the value of k_y corresponding to a water-table depth of 50 feet, by intersecting this contour. The corresponding value of k_y is approximately 0.03. Then, one can compute the ratio k_y/k_{max} using a value of k_{max} equal to 0.5 for a nearby magnitude 7 event. The resulting ratio is 0.03/0.5 = 0.06. One then enters the displacement chart in figure 8.16 at a ratio value of 0.06. For a magnitude 7 event, this yields a displacement value of about 43 inches (110 centimeters). This displacement value is twice as large as the estimated average observed value of 22

inches (55 centimeters) during the Loma Prieta event when the water table was at a depth of approximately 100 feet.

If an earthquake occurs when water tables are higher in the slopes, more materials will be saturated and likely to suffer some degradation of strength due to earthquake shaking; consequently, for these conditions, slope instability may not be limited to areally extensive, deep-seated basal shear surfaces, but may also include shallower surfaces and deep surfaces with more limited lateral extents.

To investigate this possibility further, the slip surfaces shown in figures 8.3-8.6 were analyzed to determine k_y for three water-table depths: (1) the water-table depth at the time of the Loma Prieta event (50 feet for Upper Schultheis Road and 100 feet for Villa del Monte), (2) a 50-percent rise in water table (25 feet for Upper Schultheis Road and 50 feet for Villa del Monte), and (3) a water table at a depth of 10 feet for both slide areas. In these calculations, the undegraded strengths shown in table 8.7 were used. The values of k_y were then used to compute displacements for a Loma Prieta type event. The resulting values are listed in table 8.8. In this case, the lower bound of the displacement chart shown in figure 8.17 was used to reflect the shorter-than-average duration of this event. These calculated displacements are for conditions similar to those during the Loma Prieta earthquake, but do not consider any strength degradation. Comparing these displacements with the reported field displacements shows that these calculations underestimate the observed displacements. The calculated total displacements are on the average about 16 inches(40 centimeters) when in fact the slopes moved a total of about 30 to 100 inches (72 to 244 centimeters) or about 50 inches (125 centimeters). Thus, without accounting for strength degradation, the evaluation method used in this case underestimates displacements by about a factor of 3. This factor is applied for estimating displacements during future earthquakes, again to account for possible degradation of the saturated slope materials due to earthquake loading.

Displacements were calculated for certain postulated scenarios. For these cases, the upper range indicated in figure 8.17 was used for estimating displacement as a function of k_y/k_{max}. These analyses were conducted for three water-table depths as follows: (1) water tables at depths of 100 feet in the Villa del Monte area (cross sections DM and SB) and 50 feet in the Upper Schultheis Road area

Table 8.8

Computed Slope Displacements with No Strength Degradation

(Surfaces Identified in Figures 8.4 - 8.6)

Failure Surface Designation	Yield Acceleration Based on Friction Angles Listed in Table 8.7	K_{max} (g's)	K_y/K_{max}	Calculated Displacement in.	cm
SR-1	0.150	0.5	0.300	24	9
		0.6	0.250	32	13
SR-U	0.100	0.5	0.201	44	17
		0.6	0.167	51	20
SR-L	0.100	0.5	0.199	44	17
		0.6	0.166	51	20
DM-1	0.136	0.5	0.272	38	11
		0.6	0.227	38	15
DM-3	0.147	0.5	0.294	24	9
		0.6	0.245	32	13
DM-U	0.104	0.5	0.209	44	17
		0.6	0.174	51	20
SB-1	0.145	0.5	0.290	24	9
		0.6	0.242	32	13
SB-2	0.138	0.5	0.276	28	11
		0.6	0.230	25	10
SB-U	0.108	0.5	0.217	38	15
		0.6	0.181	48	19

(cross section SR), which were approximately the depths to water at the time of the Loma Prieta earthquake; (2) water tables at depths of 50 feet in the Villa del Monte area and 25 feet in the Upper Schultheis Road area; and (3) water tables at a depth of 10 feet, to represent a major rise in the water table due to wet conditions. The calculated displacements were multiplied by a factor of 3, as discussed above, to obtain the estimated displacements, which are presented in table 8.9.

The displacements in scenario 3, indicated to be at least 28 feet, had very small ratios of k_y/k_{max}, and hence fell into an area of figure 8.17 beyond the limits of the curves presented. Therefore, those displacements can only be assumed to be at least that of the smallest ratio of k_y/k_{max} represented. The displacements from these three scenarios represent long-duration magnitude 7 events with k_{max} of 0.5 to 0.6.

The occurrence of an earthquake when the water table is near the surface in the slopes could result in large displacements if the epicenter is close to the landslide areas. The meaning of "close" varies with the magnitude of the earthquake and the depth to the water table at the time of the event. For the relatively deep water tables that existed during the Loma Prieta event, a magnitude 7 epicenter would need to be at least as close as approximately 10 miles (16 kilometers) to cause calculated slide displacement on Villa del Monte slopes of more than a foot; for the Upper Schultheis Road area, the magnitude 7 epicenter could be as far away as about 25 miles (40 kilometers) and still cause this magnitude of displacement. It should be noted that the southern end of the Hayward-Calaveras fault is approximately 25 miles away from the Summit Ridge study area.

G. Summary and Conclusions

Slope-stability and deformation analyses of the Upper Schultheis Road landslide and Villa del Monte landslide complex were performed to back-calculate the strengths mobilized in the slopes during the 1989 Loma Prieta earthquake, and to use this and other field performance information to assess the potential for future movement caused by earthquakes, rainfall, or a combination of the two. Both shallow and deep block sliding were analyzed using a limit-equilibrium pseudo-static slope stability procedure (Lowe and

Table 8.9

Estimated Displacements for Postulated Scenarios
(Surfaces Identified in Figures 8.4 - 8.6

Failure Surface Designation	Scenario 1: Water at 100 ft in.	cm	Water at 50 ft in.	cm	Scenario 2: Water at 50 ft in	cm	Water at 25 ft in.	cm	Scenario 3: Water at 10 ft in.	cm
SR-1			76	194			65	165	230	585
SR-L			120	306			215	545	312	792
SR-U			120	306			194	494	250	635
DM-1	80	204			165	419			>340	>863
DM-3	76	194			144	365			>340	>863
DM-U	109	278			241	612			>340	>863
SB-1	76	194			165	419			>340	>863
SB-2	80	204			157	398			>340	>863
SB-U	109	278			215	545			>340	>863

Karafiath 1960) and a Newmark sliding-block deformation analysis (Newmark 1965). These analyses indicated the following:

a) It is likely that the saturated slope materials suffered some degradation of shear strength due to earthquake shaking. Strengths back-calculated from observations of the Loma Prieta earthquake can be used to assess future earthquake stability, but are likely to underestimate the available strength for static loading conditions.

b) The analyses confirm that deep-seated basal shear surfaces were the likely controlling failure mechanism for these landslide areas in the Loma Prieta event, since these deeper materials were saturated and subject to earthquake-induced strength degradation. It is unlikely that the controlling slope failure mechanism for these landslide areas in the Loma Prieta event was shallow slip surface movement (shallower than about 50 feet), since these materials were well above the water table and would not be likely to have suffered earthquake-induced strength degradation.

c) If there is a significant rise in ground-water levels, slope failure mechanisms may include shallower and deeper slip surfaces of limited areal extent. Large slope failures have not been observed in this area during past heavy rainfall events, but rather have involved small movements on sliding masses of limited extent. This past field performance of the slopes and the analyses indicate that the factor of safety against sliding for such surfaces is close to one when the water table is near the ground surface (within about 10 feet).

d) If there is a significant rise in ground-water levels and another earthquake shakes the slopes, the slope failure mechanisms may include deep basal shear surfaces of large areal extent as well as shallow and deep surfaces of limited areal extent. This is because the shallower slope materials would then be saturated and subject to earthquake-induced strength degradation.

e) If the Loma Prieta event had occurred when the water table was higher, maximum slope displacements might have been on the order of 25 feet rather than 8 feet. This level of displacement was indicated for deep basal shear surfaces as well as the shallow

and deep surfaces of limited extent for a nearby magnitude 7 earthquake event.

Consequently, the analyses indicated that deep-seated basal-shear slide masses could become marginally stable when the ground water rises to within about 20 feet of the ground surface at the Upper Schultheis Road landslide area and to within about 30 feet of the ground surface at the Villa del Monte landslide complex. If the ground-water rises to within about 10 feet of the ground surface, the slopes could become marginally stable against deep-seated, large-scale, basal shear sliding; the computed factors of safety against sliding for this case ranged from about 1 to 1.2. The analyses also indicated that shallow and deep surfaces of more limited areal extent may possibly become unstable to marginally stable if the ground water rises to within 10 feet of the ground surface; the computed safety factors in this case ranged from about 0.8 to 1.1. However, if an earthquake occurs nearby when the water table is high, there may be extensive damage.

H. References Cited

Ambraseys, N. N., and Sarma, S. K., 1967, The response of earth dams to strong earthquakes: Geotechnique, v. 17, No. 2., pp 181-213.

Edris, E. V., and Wright, S. G. 1987, User's guide: UTEXAS2 slope stability package, v. 1: Instruction Report GL-87-1, U. S. Army Engineer Waterways Experiment Station, Vicksburg, Miss.

Franklin, A. G., and Chang, F. K., 1977, Earthquake resistance of earth and rockfill dams; permanent displacements of earth embankments by Newmark sliding block analysis: Miscellaneous Paper S-71-17, Report 5, U. S. Army Engineer Waterways Experiment Station, Vicksburg, Miss.

Goodman, R. E., and Seed, H. B., 1966, Earthquake-induced displacements in sand embankments: Journal of the Soil Mechanics and Foundations Division, American Society of Civil Engineers, v. 92, no. SM2, p 125-146.

Harder, L.F. Jr., 1991, Performance of earth dams during the Loma Prieta earthquake: Proceedings of the Second International Conference on Recent Advances in Geotechnical Earthquake Engineering and Soil Dynamics, Shamsher Prakash, ed., March 11-15, 1991, St. Louis, Missouri, p. 1613-1629.

Hynes, M. E., 1979, Dynamic analysis of earth embankments for the Richard B. Russell Dam and Lake Project: Final Report Prepared for U. S. Army Engineer District, Savannah, Georgia.

Hynes, M. E., and Franklin, A. G., 1984, Rationalizing the seismic coefficient method: Miscellaneous Paper GL-84-13, U. S. Army Engineer Waterways Experiment Station, Vicksburg, Miss.

Idriss, I. M., 1968, Finite element analysis for the seismic response of earth banks: Journal of the Soil Mechanics and Foundations Division, American Society of Civil Engineers, New York, NY, no. 3, p. 617-636.

Idriss, I. M., 1985, Evaluating seismic risk in engineering practice: Proceedings of the Eleventh International Conference on Soil Mechanics and Foundation Engineering, San Francisco, CA, August 12-16, 1985, v. 1, p. 255-320.

Idriss, I. M., 1990, Review comments in letter dated 10 July 1991, to Dr. M.E. Hynes, USAE Waterways Experiment Station, Vicksburg, Miss.

Krinitzsky, E. L., Chang, F. K., and Nuttli, O. W. 1988, Magnitude-related earthquake ground motions: Bulletin of the Association of Engineering Geologists, v. 25, no. 4, p. 399-423.

Lowe, J., III, and Karafiath, L., 1960, Stability of earth dams upon drawdown: Proceedings, First Panamerican Conference on Soil Mechanics and Foundation Engineering, Mexico City, v. 2, p. 537-552.

Makdisi, F. I., and Seed, H. B., 1979, Simplified procedure for estimating dam and embankment earthquake-induced deformations: Journal of the Geotechnical Engineering Division, American Society of Civil Engineers, v. 104, no. GT7, p. 849-867.

Newmark, N. M., 1965, Effects of earthquakes on dams and embankments: Geotechnique, v. 15, no. 2, p. 139-160.

Sarma, S. K., 1975, Seismic stability of earth dams and embankments: Geotechnique, v. 25, no. 4, p. 743-761.

Sarma, S. K., 1979, Response and stability of earth dams during strong earthquakes: Miscellaneous Paper GL-79-13, U.S. Army Engineer Waterways Experiment Station, Vicksburg, Miss.

Seed, H.B., 1987, Design problems in soil liquefaction: Journal of Geotechnical Engineering, American Society of Civil Engineers, New York, NY, no. 8, pp. 824-845.

Shakal, A., Huang, M., Reichle, M., Ventura, C., Cao, T., Sherburne, R., Savage, M., Darragh, R., and Peterson, C., 1989, CSMIP strong-motion records from the Santa Cruz Mountains (Loma Prieta), California earthquake of 17 October 1989: California Division of Mines and Geology, California Strong Motion Instrumentation Program, Report OSMS 89-06, 195 p.

Spittler, T. E., and Harp, E. L., compilers, 1990, Preliminary map of landslide features and coseismic fissures in the Summit Road area of the Santa Cruz Mountains triggered by the Loma Prieta earthquake of October 17, 1989: U. S. Geological Survey Open-File Report 90-688, 53 p. + 3 maps, scale 1:4,800.

William Cotton and Associates, Inc., 1990, Schultheis Road and Villa Del Monte areas geotechnical exploration Santa Cruz County, California: Los Gatos, Calif., William Cotton and Associates, Inc., Report for U.S. Army Engineers, 2 vols.

Wilson, R. C., and Keefer, D. K. 1983, Dynamic analysis of a slope failure from the 6 August 1979 Coyote Lake, California, Earthquake: Bulletin of the Seismological Society of America, v. 73, no. 3, p. 863-877.

Wilson, R. C., and Keefer, D. K. 1985, Predicting areal limits of earthquake-induced Landsliding, in Ziony, J. I., ed., Earthquake Hazards in the Los Angeles region--an earth-science perspective: U.S. Geological Survey Professional Paper 1360, p. 317-494.

Wright, S. G. 1990, UTEXAS32 (UNIVERSITY OF TEXAS ANALYSIS OF SLOPES -- VERSION 3): a computer program for slope stability calculations: Geotechnical Engineering Software GS90-1, Geotechnical Engineering Center, The University of Texas at Austin.

CHAPTER IX. GEOLOGIC HAZARDS EVALUATION

A. Introduction

This analysis uses information from the geologic studies and slope-stability modeling discussed in previous chapters to evaluate the potential for the occurrence of hazardous geologic conditions in the study area at some time in the future. The evaluation considers both the potential consequence of a particular geologic event and the likelihood or probability that such an event will occur. This hazard evaluation is concerned with the present study area, a time period of 50 to 100 years (the typical design life of a structure), and the processes of (1) landsliding, whether under seismic or nonseismic conditions, and (2) other, earthquake-induced ground cracking.

The primary goals of this geologic hazard evaluation are:

1. To evaluate the potential for future ground displacements,

2. To define the regions where future displacements will most likely occur,

3. To define the conditions under which future ground displacements are most likely to occur, and

4. To define the relative hazards to life and (or) property from potential future ground displacements.

The hazard evaluation is based on observable, documented conditions, including historic events, current conditions, and the geologic record, combined with predictive slope-stability analyses. In all stages of the evaluation, multiple lines of evidence were used to analyze data and to draw conclusions. The evaluation is based on information synthesized from (1) surface mapping of ground cracks and other surface features resulting from the Loma Prieta earthquake, (2) geomorphologic analysis, (3) geologic mapping, (4) surface and subsurface monitoring of individual landslides and

landslide complexes, (5) exploratory trenching of ground-crack features, (6) drilling of small-diameter borings, (7) evaluation of water-well data, (8) material testing, and (9) slope-stability modeling. This use of a variety of data sources ensured that neither the analysis nor the conclusions were based on only one type of evidence.

Limitations of this hazard evaluation are:

*It applies only to the landslides and ground cracks that have been identified and described in this report or in the referenced literature.

*It is not site-specific. Unless otherwise stated, this evaluation of geologic hazards should not be construed to apply to any particular structure or locality, and this hazard evaluation cannot and should not substitute for site-specific geologic and geotechnical investigations.

*Not all potential geologic hazards have been evaluated to the same degree, and not all landslides, landslide complexes, or areas of other ground cracking been subjected to the same level of investigation.

B. Factors Controlling Ground Displacement

1. Seismic Shaking

The severity and duration of seismic shaking exert significant control on ground movement and deformation during earthquakes. The seismic shaking in a given area, in turn, is a function of such parameters as the earthquake magnitude, distance of the area from the fault rupture, earthquake mechanism, depth to the hypocenter, and site-specific ground conditions. Within the study area, future large earthquakes on either the San Francisco Peninsula segment or the Southern Santa Cruz Mountains segment of the San Andreas fault will almost certainly cause high levels of seismic shaking.

a. San Francisco Peninsula segment of San Andreas fault: For the time period in question (50-100 years) the potential is high that a large earthquake will occur on the San Francisco Peninsula segment of the San Andreas fault. The Working Group on California Earthquake Probabilities (1990) estimates that there is a 23 percent probability for a magnitude 7 earthquake to occur on this segment of the San Andreas fault within the next 30 years. Because the southeastern end of this segment lies within approximately 2 miles of the study area, severe seismic shaking related to a large earthquake along this segment of the fault can reasonably be expected within the time period covered by this hazard evaluation.

b. Southern Santa Cruz Mountains segment of San Andreas fault: Because this segment produced the Loma Prieta earthquake, most of the stress accumulated along this segment during this century is believed to have been released. Therefore, it is less likely that a large earthquake will occur along this segment during the next 30 years. The Working Group on California Earthquake Probabilities (1990) estimated that the probability of a magnitude 7 earthquake on this segment in the next 30 years is less than 1 percent. Although the Working Group on California Earthquake Probabilities (1990) did not calculate an earthquake probability for a period of 50-100 years, they calculated the recurrence interval for earthquakes on this fault segment to be between 84 $\pm$ 24 years and 100 $\pm$ 24 years. Therefore, it is highly probable that another earthquake similar to the Loma Prieta earthquake will occur along the Southern Santa Cruz Mountains segment of the San Andreas fault within the next 100 years.

c. Other faults: In addition to earthquakes along the San Andreas fault, large earthquakes along other faults, including the Zayante, Butano, Sargent-Berrocal, San Gregorio, and Hayward faults, could subject the study area to moderate to high levels of seismic shaking. The probability that an earthquake within the next 100 years on one of these faults will cause shaking in the study area comparable to that during the Loma Prieta event is relatively low, but not zero.

2. Ground Water

Ground-water conditions generally also exert significant control on the stability of slopes, both during seismic shaking and under nonseismic conditions. Within the study area, ground-water conditions have been measured and analyzed, but the available information is not sufficient to quantify relations between amount, intensity, and (or) duration of rainfall and consequent rises in ground-water levels within slopes. Such relations are difficult to determine because (1) the subsurface hydrology is complex and variable throughout the study area, (2) the hydrology may have been locally altered by the earthquake in unknown ways, and (3) total annual rainfall for the past five years (three years pre-earthquake and two years post-earthquake) has been significantly below average.

Owing to the below-average rainfall, direct measurement of slope response under conditions of above-average precipitation has been impossible. Consequently, it is not known how high or how fast ground-water levels can rise within the study area under conditions of above-average annual rainfall. Therefore, it has not been possible to calculate probabilities of encountering particular ground-water levels either within individual landslides or within the study area in general. However, direct piezometric measurements during the spring of 1991 did show that ground-water levels within monitored parts of the study area rose rapidly in response to a relatively short period of heavy rainfall. In addition, the historical record in the Santa Cruz Mountains suggests that ground-water levels can rise substantially and rapidly in response to prolonged and (or) intense rainfall.

C. Historical Perspective

The geologic history of the slopes in the study area provides an indication of the expected performance of the slopes under similar conditions in the future. Data from geomorphic studies, exploratory trenching of ground cracks and landslides, historical reports, and the observed performance of slopes under a variety of conditions also provide information for the interpretation of future slope-stability and ground-cracking potential. As indicated by these studies,

repeated movement has occurred on large landslides and other ground-crack features in the study area. In addition, movement has often occurred repeatedly along the same crack features. In most cases, these repeated movements cannot be unequivocally associated with either past earthquake events or high ground-water levels, and so they may have been triggered by either or both.

Of primary concern for the hazard evaluation are conditions that can trigger renewed movement of landslides and ground cracking: elevated ground-water levels and seismic shaking. The estimated performance of the slopes in the study area, based on the historical and geologic records, is described below, first for static (nonseismic) conditions and second for the condition of severe seismic shaking.

1. Static Conditions

a. Low ground-water levels: The historical record indicates that the hazard of slope failure or ground cracking in the study area, either within or outside of existing landslides, is low when ground-water levels are low and there is no seismic shaking.

b. High ground-water levels: Early in the last decade, particularly in 1981-82, 1982-83, and 1985-86, annual precipitation was substantially above average in the study area, yet extensive slope damage, associated with movement of the large landslide masses, was not reported. Landslides in the study area that were reported during those periods were apparently small compared to the largest of the landslides triggered by the Loma Prieta earthquake. These smaller landslides, however, did cause localized damage in some cases.

The geomorphology of the area, the movement history revealed by the exploratory trenching studies, and the slope-stability analyses all agree with the observation that deep-seated movement of areally extensive landslides did not occurred during those high-rainfall years. This, in turn, suggests a low probability for the occurrence of landslides as large as the largest Loma Prieta-triggered landslides

under static conditions, even with elevated ground-water levels. However, evaluation of the geomorphology also indicates that some slow, intermittent movements of large landslides within the study area have occurred in the geologic past. These geomorphic observations additionally suggest that if movement of large landslides within the study area were to occur during periods of high ground-water levels and static conditions, the movements would probably generally be slow. However, it is beyond the present state of the art of landslide analysis to predict accurately the velocity of a landslide or the extent of break-up of the moving material, and it is thus impossible to guarantee that catastrophic failure will not occur under static conditions.

The historical record indicates that shallow, surficial slope failures (including debris flows and localized slumps) often occur in the Santa Cruz Mountains as a result of high ground-water levels under static conditions. The ground cracking and probable loosening of surface materials that took place during the Loma Prieta earthquake may have locally elevated the potential for rainfall-induced debris flows or shallow slumps. However, the overall effect of the Loma Prieta earthquake on the potential for shallow slumps and debris flows in the study area is probably minor. Although the geologic hazards from these types of landslides are not included in the present evaluation, such hazardous conditions can be readily identified and evaluated in smaller-scale, site-specific studies.

Ground cracks not associated with landslides may also pose a geologic hazard, since they may reopen or display renewed movement. The potential for such reopening or renewed movement is greatest during severe seismic shaking, and relatively low during static conditions, even with high ground-water levels. It is possible that some of these ground cracks may eventually cause additional landsliding in the study area, but it is not possible to determine the probability of such an event.

2. Seismic Conditions

The Loma Prieta earthquake provided an historical example of the amount of slope failure and associated damage that can occur in the study area during a large, nearby earthquake that occurs when ground-water levels are relatively low. Similar slope failure and associated damage and deformation are likely to occur during future

earthquakes of similar size on either the San Francisco Peninsula segment or Southern Santa Cruz Mountains segment of the San Andreas fault or, possibly, on other nearby faults, that occur when ground-water levels are low.

Information available about the performance of slopes in the study area during the larger 1906 earthquake is less complete and precise. Available reports indicate that the earthquake followed a period of high rainfall and that the earthquake triggered abundant landslides throughout the Santa Cruz Mountains. Within the study area, these reports indicate that many landslides occurred, including some that were relatively large.

D. Probability of Future Ground Displacement

Ground cracks and landslides in the study area caused by the Loma Prieta earthquake were widespread and resulted in substantial damage to buildings. No deaths in the study area were attributable to either ground displacements or earthquake effects, but numerous injuries did occur. A principal goal of this study is to determine the likelihood that future ground displacements could pose a threat to life and property. Two major factors that determine the level of hazard are:

* (1) The inherent potential for an individual site to experience ground displacement. This is based on the intrinsic, or site-specific, properties of the site itself, including characteristics of the geology, topography, vegetation, and hydrology.

* (2) The frequency of occurrence of those conditions, such as seismic shaking or rises in ground-water levels, that act upon the site and could trigger ground failure. These are the extrinsic properties.

1. Intrinsic Properties

Exploratory trenching investigations performed as part of this study and other trenching studies in the Santa Cruz Mountains

indicate that displacements have repeatedly occurred along the same fracture or crack systems. In addition, most of the large earthquake-induced landslides and landslide complexes in the study area involved material from previously-identified, pre-existing landslide deposits. These observations indicate that future ground displacements will probably occur to a large degree along features that experienced displacement in the past. Based on the present study, the relative likelihood that sites in the study area with certain properties will experience future ground displacements is ranked as follows (from highest potential to lowest):

a. Areas upon existing surface fractures or fissures shown on the "Preliminary Map of Landslide Features and Coseismic Fissures in the Summit Road Area of the Santa Cruz Mountains Triggered by the Loma Prieta Earthquake of October 17, 1989" (Spittler and Harp, 1991);

b. Areas upon fractures identifiable in subsurface trench studies, which show a history of former ground cracking but which were not reactivated during the Loma Prieta earthquake;

c. Areas along the trend of or immediately upslope from mapped fissures;

d. Other areas within the identified landslide masses shown on plates 3.1-3.4 of this report;

e. Areas beyond the landslides triggered by the Loma Prieta earthquake that were mapped as definite, probable, or questionable landslide deposits on the "Preliminary Map of Landslide Deposits in Santa Cruz County, California," (Cooper-Clark and Associates, 1975);

f. Other parts of the study area not included in a-e above.

The location of earthquake-induced landslides and ground cracks and the displacements associated with them were consequences both of the local severity of seismic shaking and of the local site conditions. A future large earthquake, which produced a different local pattern of shaking in the study area, would probably

also produce a pattern of landslides and ground cracks that also differed in detail from that produced in 1989. However, such an earthquake would probably produce displacements across many of the same fractures that underwent displacement in the Loma Prieta earthquake as well as many others. Because not every ground crack will break during every earthquake, it is not possible to develop a precise map of the study area that would show areas where displacements would or would not occur. Site-specific, subsurface studies, however, can show whether a site has experienced past ground displacements and is therefore more likely to experience ground displacements in future earthquakes than sites that have not failed in the past.

2. Extrinsic Properties

The potential for ground displacements is based on both the physical conditions of a site (intrinsic properties) and extrinsic factors such as rainfall and seismic shaking that have the potential to trigger future ground movement. Specific parameters important in determining whether a slope will fail are pore-water pressures and the severity of seismic shaking.

Pore-water pressures within the slopes in the study area are determined by several mechanisms relating to ground-water recharge and discharge; of these the most important general determinant of variations in pore-water pressure with time is precipitation. The Loma Prieta earthquake occurred during an extended drought when the cumulative rainfall was significantly less than normal. Under normal rainfall conditions, ground-water levels (and, thus, pore-water pressures) will be higher than those in October 1989, when the earthquake occurred. Neither rainfall amounts nor patterns can be precisely predicted; neither can absolute relations between rainfall and ground-water levels be quantified. However, observed positive correlations between rainfall amounts and raised ground-water levels, particularly as measured during the spring of 1991, indicate that pore-water pressures and ground-water levels would almost certainly be substantially higher in the study area following prolonged wet periods, such as occurred in the winters of 1981-82, 1982-83, and 1985-86.

The severity of seismic shaking that a site experiences during an earthquake is correlated with the earthquake magnitude, the

hypocentral depth, the distance of the site from the hypocenter, the earthquake mechanism, and the site geology. The Loma Prieta earthquake demonstrated the effects of an 11-mile-deep, M_S 7.1, oblique-slip earthquake, with an epicentral location 4.1 miles southeast of the study area, that occurred during a prolonged drought. Future earthquakes would produce different patterns of ground cracking and landslides, not only due to variations in seismic shaking, but also due to variations in ground-water levels and other site-specific conditions.

Earthquakes both smaller and larger than the Loma Prieta event could also cause landslides and ground cracks in the study area. Larger, more distant earthquakes producing stronger and longer-duration shaking, for example, could trigger landslide movement and in the study area. Similarly, near-field (very close and (or) shallow) earthquakes smaller than the Loma Prieta earthquake could also trigger landslides, particularly when ground-water levels are high.

3. Hazards to Life and Property

The principal hazard to both life and property from ground displacements in the study area would probably be the failure (collapse, fire, etc.) of residential structures. Evaluation of historic ground displacements and the modeling of probable future movements indicate the following relative levels of potential hazards under nonseismic and seismic conditions within the study area:

a. High ground-water levels without seismic shaking: The hazard to life and property from large, deep-seated landslides triggered solely by high ground-water (without seismic shaking) is relatively low, but not zero. The potential for catastrophic failure from such landslides is also low. The level of hazard varies throughout the study area. Shallow, fast-moving debris flows and relatively small slumps and other types of landslides may occur under these conditions, causing a localized hazard, but evaluation of that hazard is beyond the scope of the present study.

b. Seismically-triggered failures: The hazard to life and property for seismically-triggered ground displacements on large, deep landslides, as investigated in this study, is related to both ground-water levels and the severity of shaking.

Seismic shaking and ground-water levels similar to those during the Loma Prieta earthquake: If similar seismic shaking occurs during a time when ground-water levels in slopes are similarly low, a similar level of hazard will exist: a relatively low probability for loss of life, and a high to very high probability of severe property damage. The potential for catastrophic slope failure is low, but not zero.

Seismic shaking similar to the Loma Prieta earthquake and high ground-water levels: If seismic shaking similar to that generated by the Loma Prieta earthquake were to occur when ground-water levels were relatively high, the potential for ground displacements and landslide movement is greater, and therefore the hazard to life and property would both be increased, probably significantly, over that of the Loma Prieta earthquake.

Seismic shaking greater than the Loma Prieta earthquake: If a great earthquake (M_S 8.0 or larger) were to occur on the San Andreas fault in the Santa Cruz Mountains, the hazard to both life and property would be significantly greater than that during the Loma Prieta earthquake, regardless of the ground-water conditions. If such an earthquake occurred during very high ground-water conditions, the hazards to life and property would be greatly increased, and the results could be catastrophic.

Seismic shaking less severe than in the Loma Prieta earthquake: If earthquake shaking in the study area were weaker than in 1989, either because a future earthquake is smaller or farther away, there may still be a significant

hazard to property, and probably a low hazard for loss of life. The specific level of hazard would depend to a large degree on the magnitude of the event and its distance from the study area. However, shaking intensities significantly lower than those generated by the Loma Prieta earthquake that occur when ground-water levels are low probably pose a relatively low level of hazard from ground displacements.

Synopsis of estimated hazards during future seismic shaking: The following matrix summarizes the estimated hazard of future ground displacements, including landslide movement, relative to their occurrence in the Loma Prieta earthquake, as a function of severity of seismic shaking and ground-water levels:

		SEVERITY OF SHAKING	
		Similar to Loma Prieta earthquake	**Greater than Loma Prieta earthquake**
GROUND-WATER LEVELS	**Low (as during Loma Prieta earthquake)**	APPROXIMATELY SAME HAZARD	HIGHER HAZARD
	Higher than during Loma Prieta earthquake	HIGHER HAZARD	MUCH HIGHER HAZARD

E. Summary

In summary, the highest potential for property damage, injury, and death from ground cracking and large, deep-seated landslides would occur during severe seismic shaking, particularly if ground-water levels were significantly higher than during the Loma Prieta earthquake. A great earthquake combined with high ground-water levels could result in widespread landsliding, with potentially

catastrophic consequences. However, based on the historical and geologic record, we believe that the potential for this is relatively low during the time period under consideration.

Under nonseismic conditions, the potential for renewed movement of large, deep-seated landslides is evidently low, based on the historical record, even during periods of high ground-water levels. Consequently, the greatest potential for damage, injury, and death is associated with the occurrence of large earthquakes, which are intermittent, episodic events that are essentially unpredictable as to the future dates of occurrence.

F. References Cited

Cooper-Clark and Associates, 1975, Preliminary map of landslide deposits in Santa Cruz County, California, *in* Seismic Safety Element: Santa Cruz County Planning Department, scale 1:62,500.

Spittler, T. E., and Harp, E. L., compilers, 1990, Preliminary map of landslide features and coseismic fissures in the Summit Road area of the Santa Cruz Mountains triggered by the Loma Prieta earthquake of October 17, 1989: U.S. Geological Survey Open-File Report 90-688, 53 p. + 3 maps, scale 1:4,800.

Working Group on California Earthquake Probabilities, 1990, Probabilities of large earthquakes in the San Francisco Bay region, California: U.S. Geological Survey Circular 1053, 51 p.

CHAPTER X. CONCLUSIONS

The October 17, 1989, Loma Prieta earthquake (magnitude 7.1) was the largest seismic event in the San Francisco Bay-Monterey Bay region since 1906. The 1989 earthquake produced abundant ground failures throughout an area of approximately 5,400 square miles. Observations from many earthquakes throughout the world have revealed that most earthquakes as large as the Loma Prieta event are accompanied by significant ground failure, including landsliding. Within the Summit Ridge area, near the ruptured segment of the San Andreas fault, the earthquake generated severe shaking, a number of large landslides, and abundant ground cracks associated with the landslides, with the regional geologic structure, or both.

In the study area, the earthquake caused movement of at least 18 large landslides and landslide complexes, with surface areas of more than 1 acre each, as well as numerous smaller landslides. The largest landslide complex mapped had a surface area of approximately 210 acres. The largest landslides were along the south flank of Summit Ridge and in the Redwood Lodge area. The large landslides were recognized and differentiated from other areas of ground cracks based on the overall patterns of the cracking and other surface features, as described in Chapter III (Section IIIB).

Many of the ground cracks in the Summit Ridge area produced by the Loma Prieta earthquake were related to the regional geologic structure. Some of these cracks were also associated with the landslides, but many were not. The structurally controlled ground cracks were recognized and differentiated from non-structurally controlled landslide cracks primarily on the basis of:

* *Linearity:* Structurally produced cracks were typically linear over greater distances than were non-structurally controlled landslide cracks;

* *Orientation:* Most cracks of structural origin had trends between N30W and N80W, approximately parallel to the recognized structural trends in the underlying rocks. Landslide cracks exhibited a wider range of trends;

**Amounts of displacement:* Displacements across most structurally produced cracks (that were not also associated with a landslide) were less than 20 inches, whereas displacements across landslide cracks could be either less than or greater than 20 inches;

**Orientations of displacement:* Displacements across structurally produced cracks were typically extensional, whereas displacements associated with landslides were extensional across main scarps, but primarily left- or right-lateral along left and right flanks, respectively.

In some parts of the Summit Ridge area, cracks of structural origin were intermixed with landslide cracks, and, in other areas, landslide boundaries and internal scarps and cracks formed along structurally produced cracks that presumably originated earlier in the shaking. These relations account in part for the irregular shapes of some of the large landslides.

The large earthquake-induced landslides in the study area had downslope displacements ranging from somewhat more than 1 foot to 8.1 feet. The landslides had features, including generally discontinuous boundary cracks and poorly formed toes, that are consistent with such displacements that are relatively small compared to the great lengths of the landslides.

Calculated tectonic uplift of the ground surface accompanying the Loma Prieta earthquake in the study area was on the order of 6 to 22 inches. Along the south flank of Summit Ridge, where most of the largest landslides occurred, differential tectonic uplift was on the order of only a few inches, with the base of the ridge probably being uplifted 4 to 8 inches more than the crest. Displacements of most landslides substantially exceeded the local uplift, and, in the case of Summit Ridge, the tilt of the ground surface imparted by uplift was in the direction opposite to the landslide displacements. Similarly, in other parts of the Summit Ridge study area, the measured displacements of landslides were too large and (or) were in the wrong directions to be attributable to the calculated tectonic uplift. Thus, tectonic uplift cannot account for the observed landslide displacements.

Because the specific patterns of ground cracking and ground failure from an earthquake depend on the specific characteristics of the earthquake as well as on site-specific geologic and ground-water conditions at the time of the event, it is not presently possible from the available information for us to develop a precise map that would differentiate between safe/stable and unsafe/unstable areas in the Summit Ridge area. However, based on the available data and analyses, general areas of potential hazard have been ranked as follows, from most hazardous to least hazardous:

a. Areas upon existing surface fractures or fissures shown on the Preliminary Map of Landslide Features and Coseismic Fissures (Spittler and Harp, 1991);

b. Areas upon fractures identifiable in subsurface trench studies, which show a history of former ground cracking but which were not reactivated during the Loma Prieta earthquake;

c. Areas along the trend of or immediately upslope from mapped fissures;

d. Other areas within the identified landslide masses;

e. Areas beyond the landslides triggered by the Loma Prieta earthquake that were mapped as definite, probable, or questionable landslide deposits on the "Preliminary Map of Landslide Deposits in Santa Cruz County, California," prepared in 1975;

f. Other parts of the Summit Ridge area not included in a-e above.

Primary regional factors leading to hillside instability in the Summit Ridge area include weak, locally fractured, and locally deeply weathered earth materials, moderate to locally steep slopes, locally thick mantles of residual and colluvial soils, variable (but generally shallow) ground-water conditions, erosional undercutting by adjacent creeks, periods of intense and (or) long-duration rainfall, and repeated seismic shaking.

Large portions of the Summit Ridge area have been recognized as having been affected by large landslides since the area was first systematically mapped. More recent geologic mapping has confirmed the existence of these pre-earthquake landslide masses. In addition, as noted in Chapter II (Section IIG), virtually all of the geologic consultants who had worked in the Summit Ridge area prior to the earthquake recognized the landslide origin of the irregular benched topography. These consultants concluded that these were "old" or "ancient" landslides, which probably formed during prior large historic or prehistoric earthquakes, or perhaps during a wetter climatic period than at present. Approximately half of the consultants stated that the potential for reactivation of these large landslide masses was low to moderate, and approximately half of the consultants judged that the masses could be remobilized by strong seismic shaking.

At least 16 of the 18 large, recognized landslides and landslide complexes in the study area that moved during the Loma Prieta earthquake were partly or completely within features identified as definite, probable, or questionable landslide deposits on the "Preliminary Map of Landslide Deposits in Santa Cruz County, California" prepared in 1975. In addition, at least 13 of the 20 large, pre-existing landslide deposits identified on the 1975 map in the area were partially reactivated during the Loma Prieta earthquake. Thus, the 1975 landslide map was a relatively good indicator of the general locations of large earthquake-induced landslides, although the specific boundaries of the individual landslides differed.

Landslides have previously been documented in the Santa Cruz Mountains in association with past large earthquakes, particularly the great 1906 San Francisco earthquake, which had a magnitude of 8.3. Reports documenting the effects of that earthquake suggest that landsliding and ground cracking in and around the Summit Ridge area (as well as throughout the rest of the Santa Cruz Mountains) were more widespread and severe in 1906 than in 1989. This finding is consistent with the wetter conditions preceding the 1906 earthquake, the larger earthquake magnitude, and the more severe shaking associated with that event.

In addition to the landslides that took place during the 1906 earthquake, many additional landslides occurred in the Santa Cruz Mountains during heavy rainfall later in 1906 and in 1907. More detailed observations in another part of the region affected by the

1906 earthquake (Marin County) suggest that water entering earthquake-generated cracks caused significant numbers of landslides during this time period, as described in Chapter II (Section IIG).

Numerous landslides have also been triggered without seismic shaking throughout the Santa Cruz Mountains, including the study area, during other periods of heavy rainfall, such as occurred in January 1982 and February 1986. Reviews of historical reports, scientific literature, and road-repair records, suggest that landslides in the Summit Ridge area that are associated with rainfall (but not with seismic shaking) are generally smaller and, presumably, shallower than the largest of the landslides and landslide complexes that moved during the Loma Prieta earthquake. These rainfall-induced landslides, however, have included several fluid, fast-moving debris flows that can be particularly hazardous locally because of their high velocity and relatively long distance of transport. The earthquake-induced ground cracking that occurred in 1989 may have locally increased the debris-flow hazard.

Landslide movements occurred in the Summit Ridge area during the 1989 Loma Prieta earthquake despite drought conditions, which caused exceptionally low ground-water levels within the slopes. Annual rainfall in the area during the three winters preceding the earthquake was respectively, 71 percent, 56 percent, and 64 percent of the long-term average of 45 inches. Drought conditions also persisted for the 2 years after the earthquake, when annual rainfall was 67 percent and 78 percent of normal, respectively. Post-earthquake drought conditions have precluded direct observation of the behavior of the slopes affected by the 1989 landslides under conditions of above-average annual rainfall.

In contrast to these drought conditions, historical rain-gage records from the area show that maximum annual rainfall can be as much as 87 inches, almost double the average and triple the amount received in the year preceding the earthquake. The dry ground conditions preceding and during the 1989 earthquake limited the extent and severity of landsliding. A similar earthquake occurring during wetter conditions, when ground-water levels in slopes were higher, would almost certainly produce more extensive and severe landslide activity.

While the probability of another magnitude 7 earthquake on the southern Santa Cruz Mountains segment of the San Andreas fault

within the next 30 years is judged to be low (less than 1 percent), the probability of a magnitude 7 earthquake on the adjacent San Francisco Peninsula fault segment is judged to be relatively high (23 percent in the next 30 years), and the southern end of this segment is located just north of California Highway 17, approximately 2 miles from the Summit Ridge area.

A magnitude 7 earthquake on this segment of the fault would almost certainly produce landslide effects similar to those produced by the Loma Prieta earthquake if it occurred when ground-water levels beneath slopes were at similar levels. A larger earthquake or another magnitude 7 event occurring in wetter conditions would probably produce more severe and damaging landslide effects. Other faults in and near the study area that could produce earthquakes as large as the Loma Prieta event include the Zayante fault and the Sargent-Berrocal fault zone.

A review of both pre- and post-earthquake geologic reports that involved trenching in the Summit Ridge area showed that most or all earthquake-induced ground cracks with large displacements (more than 1 to 2 inches of extension and (or) 1/2 to 1 inch of vertical displacement) exhibited clear evidence of prior subsurface movement. However, this review also showed that not all cracks with prior displacement were offset during the Loma Prieta earthquake. Thus, the pattern of ground cracks resulting from the earthquake cannot be used by itself to determine where all displacements might take place during future earthquakes. During such a future event, displacements or ground fractures could occur in additional zones that produced no cracks in 1989. Trenching of two ground-crack features as part of the present investigation revealed a history of repeated movements during the recent geologic past.

A drilling program, consisting of 18 boreholes, was carried out in the Upper Schultheis Road and Villa Del Monte areas to characterize subsurface geologic conditions, obtain samples for testing, and install downhole instruments (inclinometers and piezometers). The drilling program revealed that subsurface conditions were complex; several different types of geologic materials and numerous zones of broken, fractured, and (or) sheared rock are present. Interpretive cross sections have been prepared, which are consistent with information from the drilling program as well as from surficial geomorphology and ground-crack patterns. These cross sections show that relatively deep basal shear surfaces

likely are present under these landslide features. However, because of the complexity of the subsurface conditions and the limitations in available exploration methods, significant uncertainly still exists concerning the specific nature and locations of basal shear surfaces. Therefore, the slope-stability modeling that was undertaken considered a wide variety of potential landslide geometries and shear surfaces, including both shallow and deep-seated examples.

A program of surface monitoring of ground cracks associated with 12 large landslides and landslide complexes was initiated in December 1989 and continued through July 1991 to detect and document any additional, post-earthquake displacements. The program utilized a combination of 51 quadrilateral arrays and eight strain gages placed across main scarps and landslide flanks. No significant extensional movements across any of the cracks was detected during the relatively dry 14-month period ending in January 1991. However, a sequence of storms in February and March of 1991 dropped approximately 26 inches of rain on the Summit Ridge area within a 29-day period. During this time, localized surface cracking occurred on parts of the Upper Schultheis Road, Upper Morrell Road, and Hester Creek North landslides, and the Upper Skyview Terrace-Bel Air Court area of the Villa Del Monte landslide complex. Maximum movement recorded across surface cracks and (or) surface monitoring arrays was 5 to 8 inches. The longest surface crack, which opened near the main earthquake-induced scarp in the Upper Skyview Terrace-Bel Air Court area of Villa Del Monte, was approximately 600 feet long. This and the other observed cracks were judged to have resulted from local readjustments of portions of the landslide masses due to the prolonged rainfall, primarily through the process of upslope scarp migration. Such local readjustments will likely continue during future winters that have precipitation at least approaching average.

The period of high rainfall and observed landslide cracking in the spring of 1991 coincided with a period of rising ground-water levels, as monitored by piezometers in the Upper Schultheis Road and Villa Del Monte areas. Ground-water levels measured by individual piezometers during this period rose as much as 20 feet; average rise in ground-water level was 5.6 feet as measured in shallow piezometers, 4.4 feet as measured in medium-depth piezometers, and 3.0 feet as measured in deep piezometers. These rises in ground-water level were associated with both a month-long period of very high rainfall and with below-average annual rainfall

during a 5-year drought. While these data indicate that significant changes in ground-water levels are possible within these slopes, extrapolation to other short- or long-term rainfall cycles requires additional data and analysis.

Results of an inclinometer survey carried out in April 1991 support the finding that the observed 1991 cracking and associated movement were of a localized rather than throughgoing nature. Of the 15 inclinometers in the Upper Schultheis Road and Villa del Monte areas, the four that showed deflections greater than system error showed very small deflections of variable direction. These deflections can be accounted for by settlement of the casings and densification effects due to ground-water fluctuations.

Slope-stability analyses carried out for the Upper Schultheis Road landslide and the Villa Del Monte landslide complex calculated static (non-seismic) strengths of the slope materials for the low ground-water levels that exist in the slopes during extended periods of low rainfall. The back-calculated static strengths are consistent with the observed good performance (i.e., no movement) of the slopes under low-ground-water/low-rainfall conditions; the back-calculated strengths are also consistent with typical static strength of similar materials known from engineering experience in the Santa Cruz Mountains.

The slope-stability analyses additionally indicate that some degradation of the strength of the slope materials likely occurred due to the seismic shaking. Because such strength degradation is usually more severe for materials below the water table, the analysis thus also suggests that the modeled landslide features moved on relatively deep-seated shear surfaces during the Loma Prieta earthquake.

Under non-seismic conditions when ground-water levels are near the ground surface, slope-stability analyses and historical observations of the slopes in the Upper Schultheis Road and Villa Del Monte areas indicate that the slopes are marginally stable for deep-seated shear surfaces of large areal extent (as defined in Chapter VIII) and marginally stable to unstable for shallow and deep-seated shear surfaces of limited areal extent. Consequently, the analyses indicate that large landslide displacements (perhaps tens of feet) are likely to occur if strong seismic shaking occurs in these areas when ground-water levels are near the ground surface. The precise magnitudes of the displacements will, of course, depend on several

factors including the severity of shaking and ground-water conditions at the time.

APPENDIX A. LABORATORY TESTING PROGRAM-- GEOLOGIC MATERIALS OF THE UPPER SCHULTHEIS ROAD LANDSLIDE AND VILLA DEL MONTE LANDSLIDE COMPLEX

A. Purpose and Scope

This chapter presents the results of laboratory tests performed by the COE South Pacific Division Laboratory (SPDL) on samples of geologic materials obtained from the Upper Schultheis Road and Villa Del Monte landslide areas. These samples were obtained by William Cotton and Associates, Inc. (1990) as described above, in Chapter VII. The laboratory testing program was planned by the COE Waterways Experiment Station (WES).

The testing program had four major purposes: (1) to observe the diversity of material types and ranges of material properties encountered in the subsurface, (2) to estimate a representative unit weight for use in slope-stability analyses, (3) to provide point strength estimates of the materials in the slope for comparison with mobilized strengths back-calculated in the slope-stability analyses, and (4) to indicate stress-strain behavior of the materials at the depths of the estimated basal shear surfaces to provide a context for estimating long-term behavior. Such objectives can only be achieved in full if the samples recovered from the subsurface investigation represent the spectrum of conditions in the subsurface. As discussed above in Chapter VII, the boring logs indicated that core was recovered from only a part of each boring, either because the field investigators elected not to sample certain intervals, or because core recovery in an interval was poor. Samples for testing were selected by SPDL and WES with these objectives and limitations in mind.

Selected samples were subjected to classification and index tests including grain-size analyses (mechanical and hydrometer), Atterberg liquid and plastic limits, specific gravity of solids, natural water content, and moist and dry unit weights. A few triaxial and direct-shear strength tests were performed to obtain estimates of point strength and stress-strain behavior. Boring logs and laboratory examinations showed that the sampled slopes were composed of colluvium, regolith, siltstone, sandstone, and shale. These materials included intact rock; highly fractured, sheared and brecciated rock; highly weathered, soil-like materials; and colluvium. This chapter

describes the handling and inspection of these samples, testing procedures, and results.

B. Sample Handling and Inspection and Test Procedures

Samples obtained from the field investigation consisted of unextruded tube samples, cores extruded and deposited in corrugated plastic boxes, and extruded material in resealable plastic bags, also deposited in the boxes. The samples were shipped to SPDL and stored. The unextruded cores were stored in a humidity-and-temperature-controlled environment, but the cores in the boxes were not. The period between extraction from the field and initial testing in the laboratory was approximately 7 months.

Extruded core and bag samples were visually inspected by TAG members and personnel from COE District, San Francisco, COE Division, San Francisco, and WES. Eighty-eight unextruded tube samples were x-rayed to examine their contents. Front and side (90° offset) views were taken of each tube. Two sets of x-rays were made--one set was deposited with William Cotton and Associates, Inc. and the other, reproduced from this set, with SPDL. These visual and x-ray inspections provided qualitative information about the diversity and condition of the materials extracted from the slopes. SPDL also provided 47 color photographs of the open boxes of extruded core samples.

A preliminary copy of the field investigation report by William Cotton and Associates, Inc., dated June 1990, contained a suggested schedule of testing. As part of this list, six triaxial and 11 direct-shear tests on specific samples were proposed. This list and the visual and x-ray inspections helped WES and SPDL make final selections of samples for the strength-testing program. Samples that appeared to have been sheared and that could have been from landslide basal rupture surfaces were selected.

All tests were performed using procedures described in U.S. Army Corps of Engineers Manual EM-1110-2-1906 (1970); these procedures are generally similar to those defined by the American Society for Testing and Materials (ASTM). Classification tests included grain-size (mechanical and hydrometer) analyses and Atterberg liquid and plastic limit determinations. Index tests

included specific gravity, water content, and unit-weight determinations.

C. Soil Classification Tests

1. Grain size

Plates 1 through 7 show the results of 14 mechanical grain-size analyses performed on weathered, soil-like samples from depths of 15 to 140 feet. Additional testing notes are shown on plates 8 and 9. The results of the two hydrometer tests, which measured the clay-size fraction of samples, are plotted in plate 10.

2. Atterberg liquid and plastic limits

Atterberg liquid- and plastic-limit tests are performed to distinguish between cohesive and cohesionless soils. The selection of samples for these tests was difficult, because many samples contained material transitional (in terms of weathering) between soil and rock. Consequently, prior to testing, some samples required grinding as described in EM-1110-2-1906 (1970, p. III-5). Liquid and plastic limits were determined for a total of 38 samples. The results are listed in plates 1-7 and summarized in the plasticity chart in figure 1, used to classify the fine-grained soils. Thirty-five of the fine-grained samples were classified as lean clay (CL) according to the Unified Soils Classification System (USCS). Two samples were classified as silty clay-clayey silt (CL-ML), and one was classified as highly plastic clay (CH).

The grain-size and Atterberg-limit data were used to classify the soil samples as sandy clay, silty sand, silty clay, or clayey sand. Rock types were classified by visual inspection. Visual logs are presented in plates 11-26.

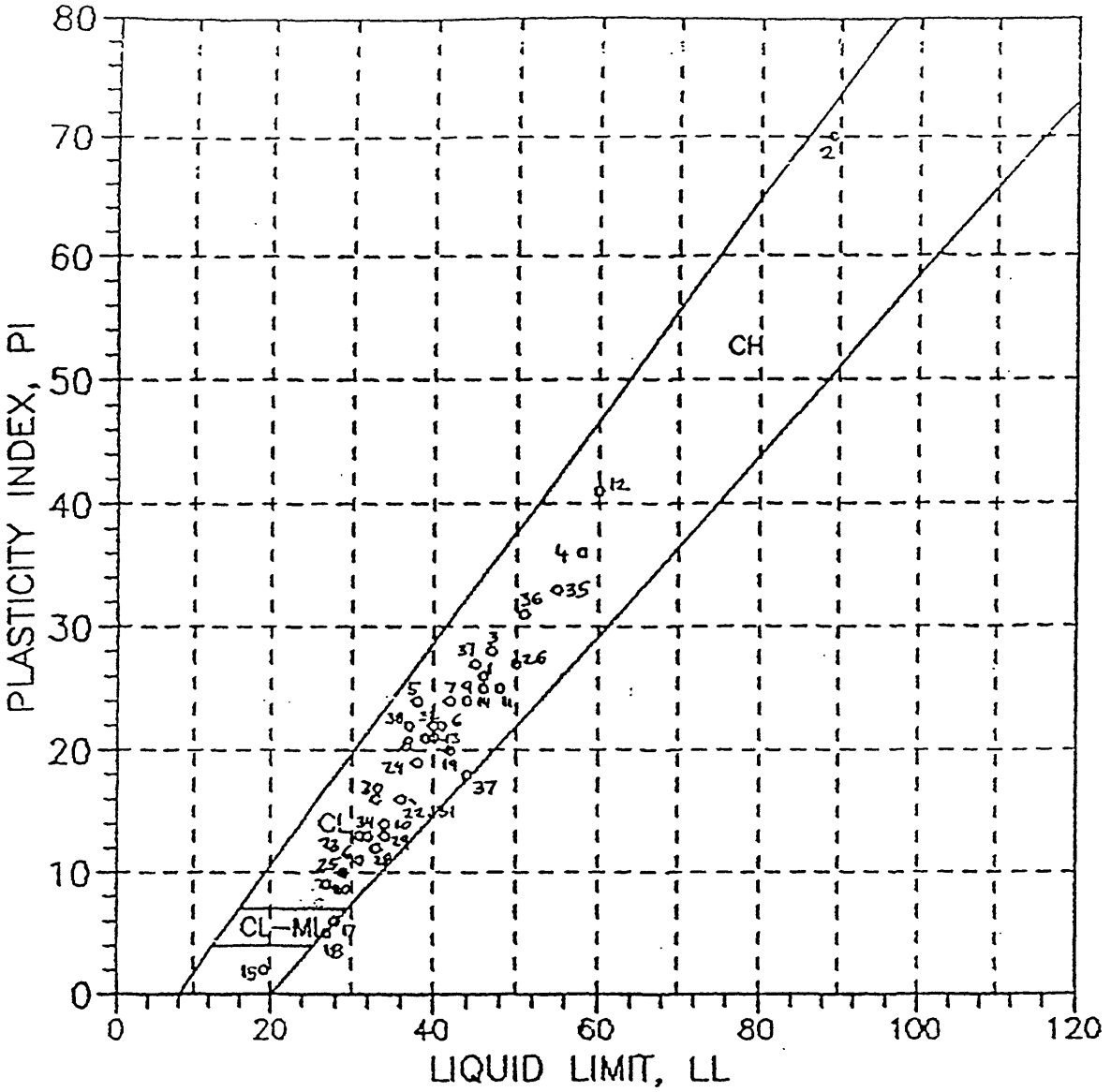

LEGEND

1- DM-1	20.3 FT	13 ED-2	145.0 FT	27 SB-4	150.5 FT
2 DM-1	70.7 FT	14 ED-2	196.4 FT	28 SD-1	45.9 FT
3 DM-1	100.0 FT	15 ED-2	197.3 FT	29 SD-1	49.0 FT
4 DM-4	20.25 FT	16 SB-1	15.0 FT	30 SD-1	73.8 FT
5 DM-4	30.5 FT	17 SB-1	15.7 FT	31 SD-1	81.6 FT
6 DM-4	40.0 FT	18 SB-1	23.5 FT	32 SD-1	98.2 FT
7 DM-4	50.35 FT	19 SB-1	56.3 FT	33 SR-1	59.7 FT
8 DM-4	60.0 FT	20 SB-1	68.5 FT	34 SR-1	65.5 FT
9 DM-4	195.0 FT	21 SB-1A	91.96 FT	35 SR-1	104.0 FT
10 ED-1	38.5 FT	22 SB-2	41.45 FT	36 SR-1	151.2 FT
11 ED-1	58.75 FT	23 SB-2	66.90 FT	37 ED-1	61.0 FT
12 ED-2	139.0 FT	24 SB-2	167.2 FT	38 SR-2	89.5 FT
		25 SB-3	80.00 FT		
		26 SB-4	50.0 FT		

Figure 1. Results of Atterberg Limit Tests Plotted on Plasticity Chart for Classification of Soil Type

D. Index tests

1. Specific gravity

Specific-gravity tests were conducted to determine void ratios from water-content and density test results (presented below), to analyze the hydrometer data, and as an indicator of component minerals of the soil or rock. Forty-two specific-gravity tests were performed. The results for the Upper Schultheis area are plotted in figure 2 and for the Villa Del Monte area in figure 3. The values of specific gravity that were measured varied little with depth, and were typically between 2.63 to 2.78. Table 1 lists the measured specific-gravity values along with water-content and density data.

2. Water content

The water content is an indicator of material density and, for cohesive soils, of strength characteristics. For example, water contents for rocks are usually much smaller than those for soils. Water contents were determined in conjunction with moist and dry unit weights and specific gravity for selected extruded cores and bag samples. Water contents and dry unit weights for extruded cores are shown in figures 7.9 through 7.19, which also show geological information and drilling rates from boring logs. Water content values between 0.3 and 30 percent were measured. These water contents probably underestimated the actual conditions in situ due to the 7-month interval between sampling and testing and the manner in which the samples were stored. However, representative values of in situ water content and moist unit weight, determined from samples extruded from tubes in the laboratory for strength tests (tables 2 and 3), were only slightly higher than and compare well with the data shown in table 1.

3. Unit weights

Three typical samples of siltstone, sandstone, and shale were selected and tested by SPDL in August 1990 for preliminary estimation of the moist and dry unit weights of the slope materials. The results are listed in table 7.2. Moist and dry unit weights were

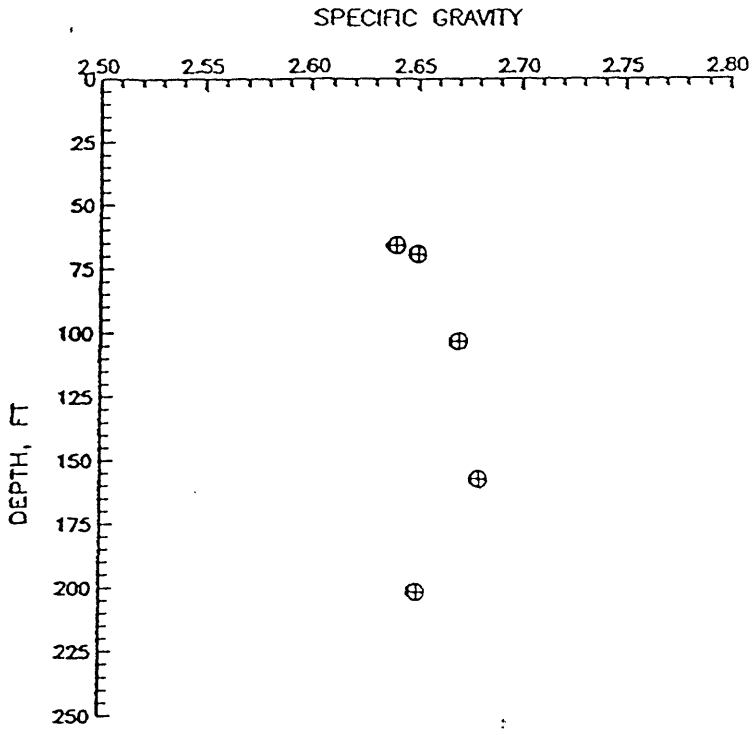

Figure 2. Specific Gravity Values for Samples from Upper Schultheis Area Plotted Versus Depth

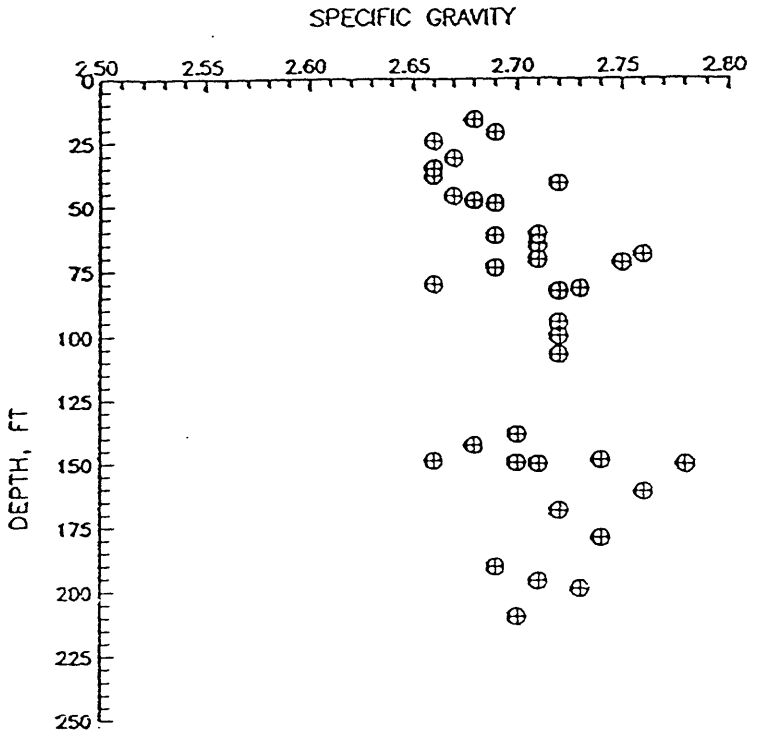

Figure 3. Specific Gravity Values for Samples from Villa Del Monte Area Plotted Versus Depth

Table 1

Density and Water Content Index Test Results for
Extruded Samples From Upper Schultheis and Villa Del Monte Areas

Boring	Depth Interval, ft	Material Description	Specific Gravity	Dry Unit Weight, pcf	Water Content, percent	Moist Unit Weight, pcf
ED-1	31.5-32.9	Sand	2.67		9.9	
ED-1	34.5-34.9	Sandy Silt	2.66	124.7	11.5	139.04
ED-1	38.4-38.6	Lean Clay	2.66	113.01	7.8	121.82
ED-1	65.0-65.3	Soft Sandstone	2.71	117.8	14.8	135.23
ED-1	80.0-81.4	Sand		118.8	13.1	134.36
ED-2	61.2-61.5	Shale	2.69	118.6	14.7	136.03
ED-2	80.3-80.6	Sandstone		124.6	9.7	136.68
ED-2	139.0-139.4	Clay	2.7	130.5	6.5	138.98
ED-2	145.5-145.9	Sandstone		138.2	5.5	145.80
ED-2	148.7-149.1	Fractured Shale	2.74			
ED-2	196.4-196.8	Fractured Shale	2.71	125.8	6.9	134.48
ED-2	197.3-197.7	Fractured Shale		124.4	12.1	139.45
SB-1	15.0-15.3	Clayey Sand		119.0	12.3	133.64
SB-1	15.7-16.2	Clayey, Silty Sand		118.3	14.0	134.86
SB-1	17.0-17.6	Silty Sand		116.2	15.9	134.67
SB-1	17.6-18.2	Silty Sand		128.4	9.4	140.46
SB-1	23.5-24.0	Clayey, Silty Sand		126.6	1.9	129.00
SB-1	24.1-24.7	Silty Sand		114.8	15.8	132.94
SB-1	47.8-48.1	Silty Sand	2.68	125.2	11.6	139.72
SB-1A	91.9-92.2	Fractured Shale		127.0	9.4	138.93
SB-2	41.5-41.9	Fractured Shale		133.2	8.7	144.78
SB-2	66.6-67.4	Fractured Shale		124.3	7.8	133.99
SB-2	81.0-85.0	Fractured Shale	2.72	120.4	10.0	132.44
SB-2	100.5-100.7	Fractured Shale		124.4	7.4	133.60
SB-2	167.2-167.7	Fractured Shale		127.2	7.9	137.25
SB-2	242.7-243.0	Siltstone		159.9	1.7	162.62
SB-3	41.0-41.5	Silt		104.8	21.8	127.64
SB-3	80.0-80.2	Clay	2.66	124.8	11.8	139.53
SB-3	190.7-191.1	Shale	2.69	148.2	4.0	154.12

Table 1
(Continued)

Boring	Depth Interval, ft	Material Description	Specific Gravity	Dry Unit Weight, pcf	Water Content, percent	Moist Unit Weight, pcf
SB-4	50.0-50.5	Fractured Shale		143.3	6.3	152.33
DM-1	20.2-20.5	Fractured Shale	2.69	116.2	16.2	135.02
DM-1	61.2-61.4	Fractured Shale	2.71	132.0	6.5	140.58
DM-1	70.8-71.1	Fractured Shale	2.71	120.7	11.0	133.98
DM-1	100.2-100.5	Fractured Shale	2.72	126.9	8.4	137.55
DM-2	71.5-72.2	Shale	2.72	120.6	14.6	138.21
DN-2	94.6-94.9	Shale	2.72	126.9	7.4	136.29
DM-2	107.4-107.7	Siltstone	2.72	136.0	6.4	144.70
DM-2	149.2-149.5	Sandstone	2.66	135.2	6.8	144.39
DM-3	30.8-31.1	Sandstone	2.67	125.2	6.0	132.71
DM-3	40.5-40.8	Fractured Shale		105.5	15.4	121.74
DM-3	90.4-90.8	Fractured Shale		124.9	13.4	141.63
DM-4	20.0-20.3	Fractured Shale		111.3	18.5	131.89
DM-4	30.5-30.8	Fractured Shale		114.0	17.7	134.17
DM-4	40.0-40.3	Fractured Shale	2.72	122.7	13.9	139.76
DM-4	50-0-50.3	Fractured Shale		127.6	11.3	142.02
DM-4	60.0-60.3	Fractured Shale		132.5	10.2	146.01
DM-4	81.0-81.5	Sandstone		165.1	1.0	166.75
DM-4	148.7-149.0	Fractured Shale		135.6	7.7	146.04
DM-4	150.4-150.7	Shale with Sandstone	2.78	126.8	10.0	139.48
DM-4	161.6-162.0	Shale	2.76	127.4	7.7	137.46
DM-4	168.7-169.0	Shale	2.72	150.0	4.7	157.05
DM-4	182.2-182.5	Shale		125.4	12.8	141.45
DM-4	191.0-191.3	Soft Shale		130.5	8.7	141.85
DM-4	195.0-195.25	Fractured Shale		119.0	12.3	133.63
DM-4	200.0-200.2	Shale		124.3	9.9	136.60
DM-4	208.3-208.6	Siltstone		155.9	1.4	158.08
DM-4	210.2-120.5	Siltstone	2.71	150.0	3.1	154.65
DM-4	217.4-217.7	Shale		149.9	4.3	156.34

Table 1
(Concluded)

Boring	Depth Interval, ft	Material Description	Specific Gravity	Dry Unit Weight, pcf	Water Content, percent	Moist Unit Weight, pcf
DM-4	228.2-228.8	Shale		151.4	4.3	157.91
DM-4	230.7-231.0	Soft Shale		130.5	8.9	142.11
SB-4	150.5-150.9	Fractured Shale	2.71	129.5	8.9	141.03
SD-1	45.9-46.4	Fractured Sandstone and Shale	2.67	126.9	10.9	140.73
SD-1	49.0-49.8	Fractured Sandstone and Shale	2.69	122.2	11.9	136.74
SD-1	81.6-82.2	Fractured Shale	2.73	119.1	14.3	136.13
SD-1	98.2-98.85	Fractured Shale		118.5	14.7	135.91
SR-1	59.7-60.5	Sand		113.5	16.2	131.88
SR-1	65.5-65.8	Shale	2.64	121.7	10.9	134.72
SR-1	69.0-71.0	Sand and Shale	2.65			
SR-1	104.0-105.2	Shale		115.3	13.9	131.33
SR-1	151.2-152.0	Shale	2.68	123.8	12.4	139.15
SR-1	202.0-202.3	Fractured Sandstone	2.65	146.0	0.3	146.43
SR-3	76.3-76.6	Soft Sandstone		131.1	9.8	143.95
SR-3	103.8-104.0	Sandstone	2.67	124.3	7.6	133.74
SR-3	105.0-105.3	Sandstone		158.2	0.8	159.46

Table 2
Density and Water Content Measurements for
Undisturbed Samples Used in Triaxial Tests

Boring	Depth Interval ft	Material Description	Water Content, percent	Dry Unit Weight, pcf	Moist Unit Weight, pcf
SB-1	10.0-12.3	Sandstone	15.5	115.5	133.4
ED-1	61.0-62.3	Fractured Shale	21.0	104.3	126.2
SR-2	78.5-79.5	Sand	15.3	116.5	134.3
SB-1A	88.5-89.7	Siltstone and Shale Breccia	11.5	124.6	138.9
SR-3	180.0-181.2	Fractured Shale	16.3	109.0	126.8
SB-1A	90.0-90.7	Fractured Siltstone	11.2	122.5	136.2
ED-1	31.5-32.9	Sandstone	18.1	112.3	132.6
DM-2	91.0-91.4	Soft Siltstone	8.7	131.2	142.6

Table 3

Density and Water Content Test Results
from Preliminary Tests

Boring	Depth Interval, ft	Visual Classification		Dry Unit Weight, pcf	Water Content, percent	Moist Unit Weight, pcf
		Field	Laboratory			
SB-2	34.0-34.5	Sandstone	Siltstone	152.7	3.7	158
SB-1	26.3-26.9	Sandstone	Shale	115.2	15.5	133
DM-2	71.5-72.5	Siltstone	Dense Sand	117.8	15.9	136

eventually determined for a large number of samples representing a broader spectrum of materials present in the slope. Values of dry unit weight ranged from 110 to 167 pounds per cubic foot. Table 4 shows the manner in which these values were averaged to compute a representative value for the slope materials. Based on examination of all the unit weight information, a moist-unit-weight value of 134.5 pounds per cubic foot was selected for the stability analyses described in Chapter VIII.

E. Shear Strength Tests

The highly fractured, variably weathered, interbedded, and sheared sandstone, siltstone, and shale in the slope were very difficult to sample in the field; thus, obtaining high-quality undisturbed samples for meaningful laboratory strength testing was also difficult. Even samples in good condition were difficult to extrude, trim, and set up for laboratory strength testing without additional disturbance. Since the landslides themselves provided a full-scale field test of the shear strength of the basal shear surface materials in the slope, only a few laboratory strength tests were performed to provide point values for comparison with the back-calculated field strengths, obtained from the stability analyses. Samples of intact--unfractured, unsheared, and unweathered--rock were not tested because their strength almost certainly does not control stability of the slopes. The laboratory strength tests also provided an indication of the stress-strain behavior of the slope materials. Two types of tests were performed, direct-shear and triaxial tests. The measured effective friction angles and cohesion values (c) from these tests are listed in table 5.

1. Triaxial tests

These tests measure strength parameters, while simulating in situ stress and drainage conditions. In situ stress conditions for high ground-water levels were simulated in the laboratory tests to approximate conditions after intense rainfall. Two types of saturated, consolidated, undrained tests with pore-pressure measurements were performed. In one type of test, two samples were anisotropically consolidated to estimated overburden pressures corresponding to high ground-water levels and failed in compression

Table 4
Weighting Factors Used to Estimate
Representative Average Moist Unit Weight
of Landslide Materials

Boring	Weighting Factor, Percent	Moist Unit Weight, ft	
		Typical Value	Average
SB-2	49	133	
	51	136	134
DM-1	88	134	
	12	158	136
DM-4	95	134	
	5	158	135
ED-1	4	158	
	96	130	132
SR-4	3	158	
	33	120	
	64	130	127

Table 5
Shear-Strength Parameters from Laboratory Tests
on Undisturbed Samples of Slope Materials

Boring	Depth Interval, ft	Material Description	Type of Strength Test*	Effective-Stress Strength Parameters: Friction Angle, degrees	Effective-Stress Strength Parameters: Cohesion, psf
ED-1	58.5-59.0	Lean Clay	DSR	28	-
SR-2	89.5-90.5	Lean Clay	DSR	29	-
SB-1	10.0-12.3	Sandy Clay	CADLE	44	-
SR-2	78.5-79.5	Sand	CAULE	40	-
SR-2	99.5-100.4	Shale	DSR	9	2000
SR-3	180.0-181.2	Fractured Shale	CIUAC	25	440
ED-1	59.5-61.0	Fractured Shale	DSR	23	1200
ED-1	61.0-62.3	Fractured Shale	CIUAC	21	2100
SB-2	51.0-53.3	Siltstone and Shale	DSR	18 3	-
SB-1A	88.5-89.5	Siltstone and Shale Breccia	CAULE	47	-
SB-1A	90.0-90.7	Fractured Siltstone	CADLE	51	-
DM-2	91.0-91.4	Soft Siltstone	DS	45	-
ED-1	31.5-32.9	Sandstone	DS	45	-
ED-2	41.7-43.0	Sandstone	DS	-	7000*

*Legend:

DS = Direct shear (consolidated, drained, no reversal).
DSR = Direct shear (consolidated, drained, with reversal).
CIUAC = Triaxial shear, isotropic consolidation, undrained, compression loading.
CADLE = Triaxial shear, anisotropic consolidation, drained, compression unloading.
CAULE = Triaxial shear, anisotropic consolidation, undrained, compression unloading.

**Measured shear strength at a normal stress of 3000 psf.

unloading with no drainage of the sample allowed. This test represents a situation of unloading in which lateral confinement is reduced. In the other type of test, two samples were isotropically consolidated to estimated overburden pressures corresponding to high ground-water levels and failed in axial compression with no drainage allowed. This test represents a situation in which an additional load is imposed on the material. Tests of a third type were performed on two sand samples. In these tests, the samples were saturated and anisotropically consolidated, and then slowly sheared under compression unloading with full drainage.

The results from all three types of triaxial tests are shown in plates 27-40, figures 4-9 and table 5. The two undrained compression-loading tests were performed on fractured shale, one sample (fig. 4) from Upper Schultheis Road (US) Section SR (180-foot depth) and the other (fig. 5) from Villa Del Monte (VDM) Section ED (61-foot depth, refer to Chapter VII for cross sections). In both tests, the samples developed positive excess pore-water pressures upon shear, even though they were consolidated to confining stresses well below their pre-sampling in situ stress. The measured effective stress strength parameters ranged from 21° and c=1 ton per square foot to 25° and 0.2 tons per square foot. The two tests on fractured siltstone were anisotropically consolidated and sheared in compression-unloading; one was drained (fig. 6) and the other was undrained (fig. 8). Both samples were from VDM Section SB from a depth of about 90 feet. Both samples resulted in about the same effective stress strength parameters of 50° and c=0. The undrained test showed that the fractured siltstone developed negative excess pore-water pressures upon shear. The remaining two tests were on samples of sand (from US Section SR, depth 70 ft, fig. 8) and sandy clay (VDM Section SB, depth 10 feet, fig. 9). The sand developed some negative excess pore-water pressures and the resulting effective friction angle was 40° (c=0). The sandy clay was consolidated to a confining stress much higher than the pre-sampling in situ stresses and sheared under drained-unloading conditions. This sample exhibited a high effective friction angle of 44° (c=0). The effective stress paths (as defined by Lambe and Whitman, 1969) shown in figures 4-9 indicate that, after some initial excess pore-water pressure development, all the materials tested tended to dilate.

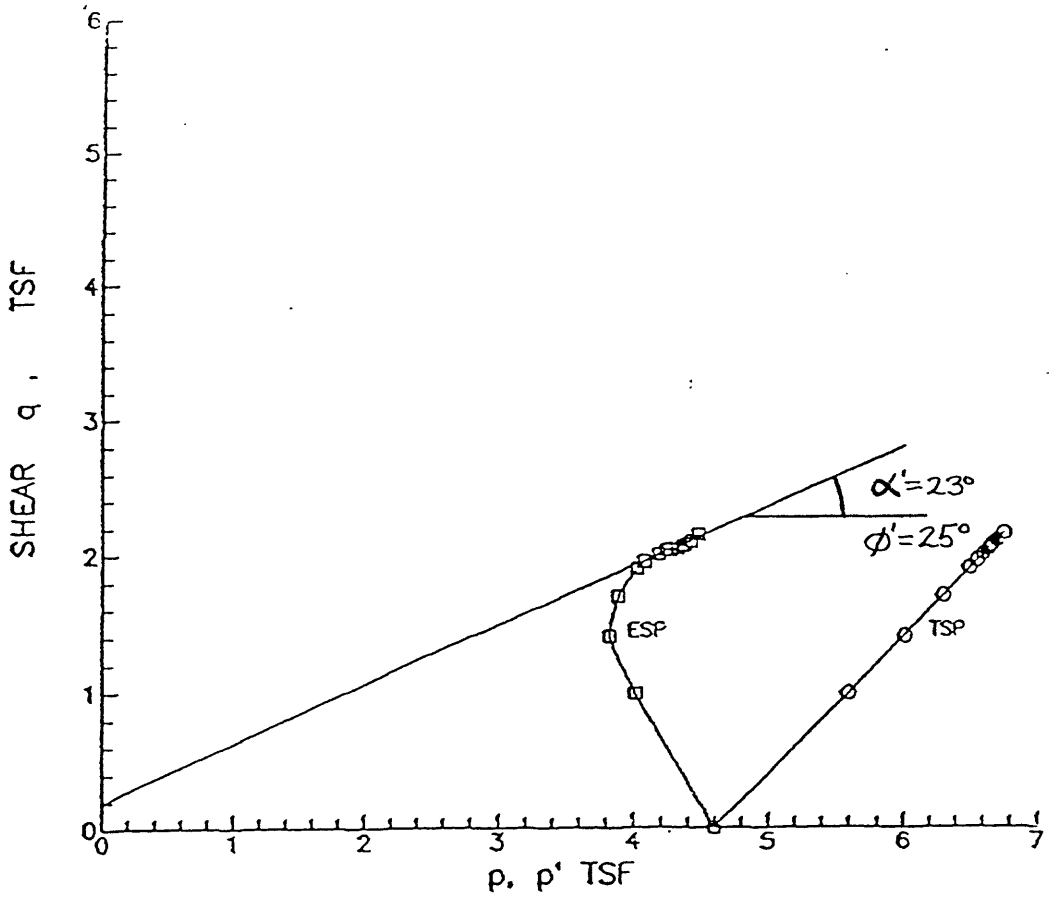

Figure 4. Total (TSP) and Effective (ESP) Stress Paths for Isotropically-Consolidated, Undrained, Compression-Loading Triaxial Shear Test on Sample of Grey Fractured Shale from Boring SR-3, Depth Interval 180-181.2 ft.

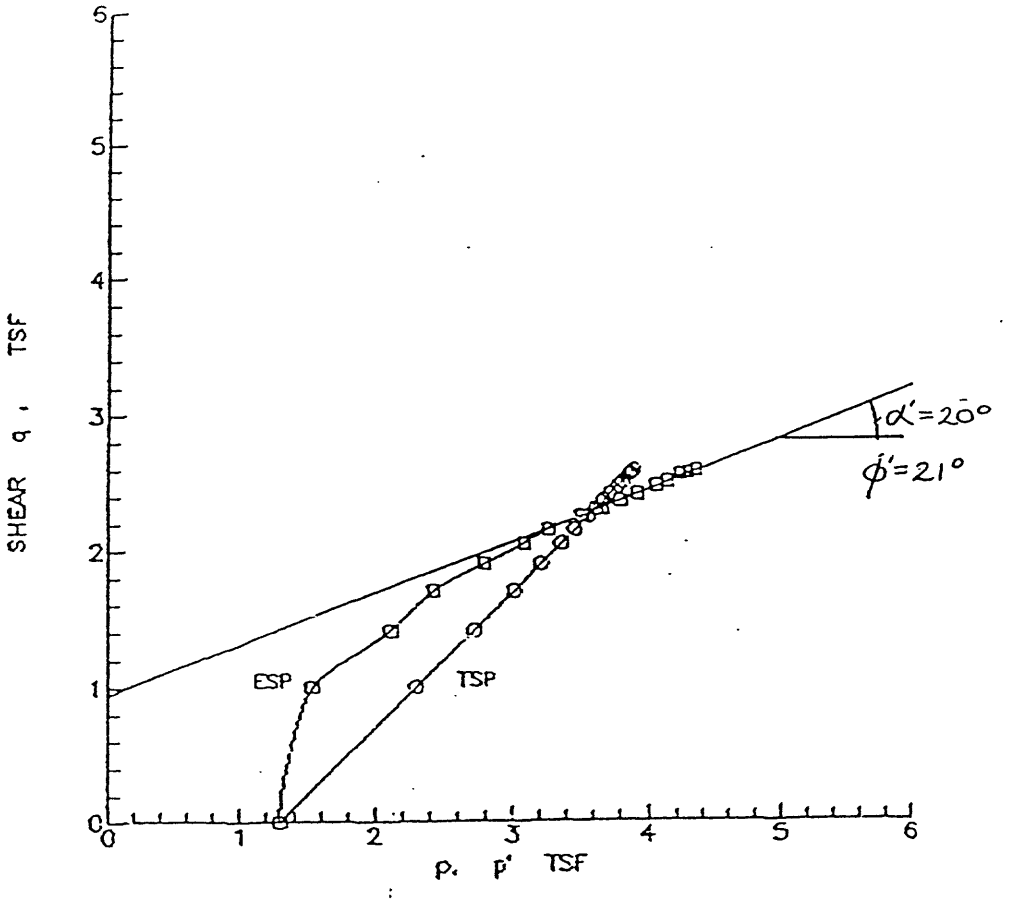

Figure 5. Total (TSP) and Effective (ESP) Stress Paths for Isotropically-Consolidated, Undrained, Compression-Loading Triaxial Shear Test on Sample of Brown Fractured Shale from Boring ED-1, Depth Interval 61.0-62.3 ft.

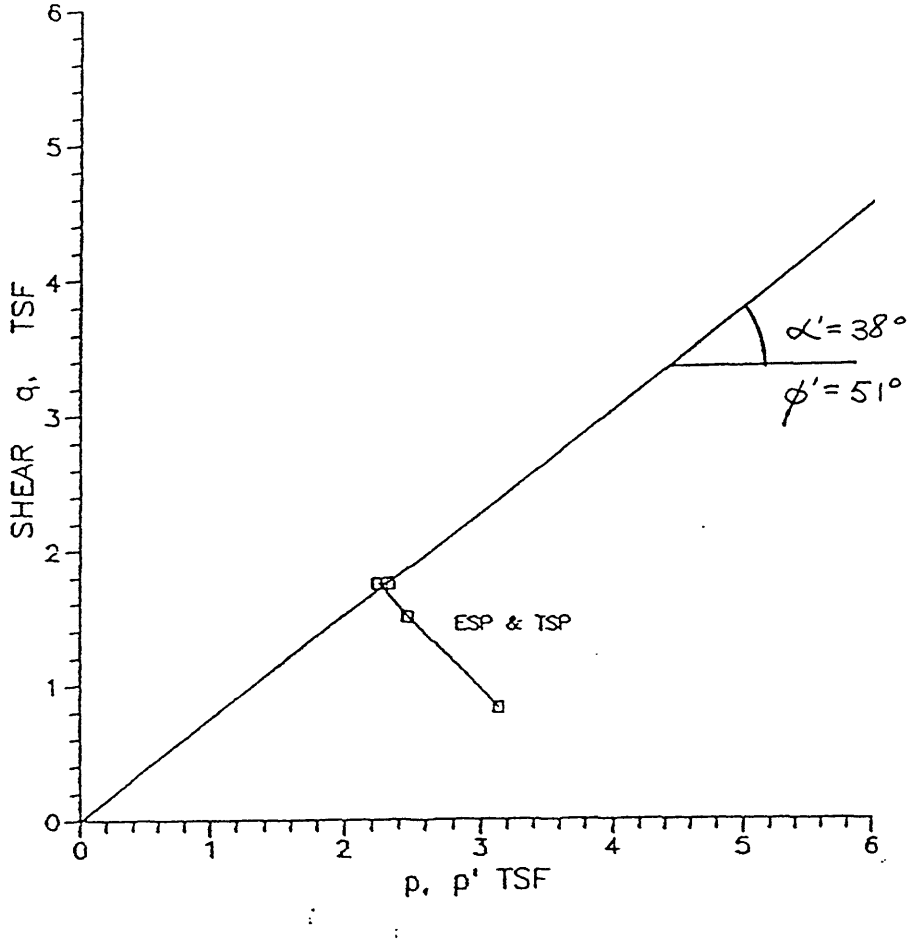

Figure 6. Total (TSP) and Effective (ESP) Stress Paths for Anisotropically-Consolidated, Drained, Compression-Unloading Triaxial Shear Test on Sample of Fractured Siltstone from Boring SB-1A, Depth Interval 90.0-90.7 ft.

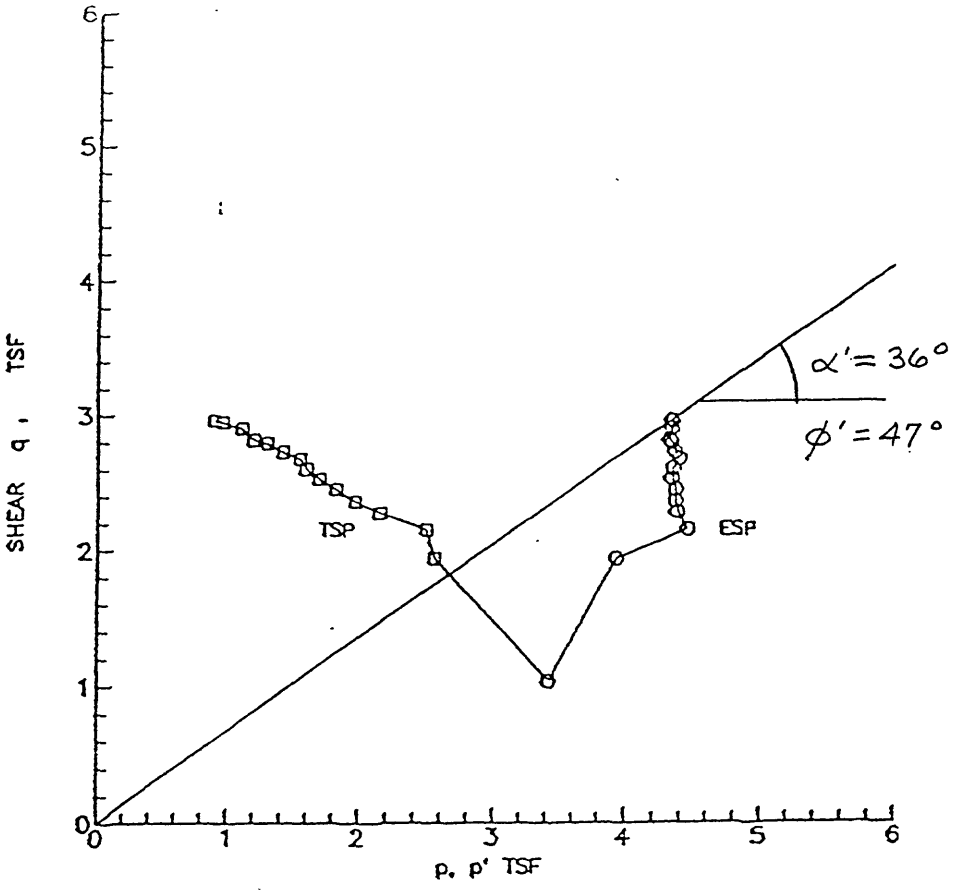

Figure 7. Total (TSP) and Effective (ESP) Stress Paths for Anisotropically-Consolidated, Undrained, Compression-Unloading Triaxial Shear Test on Sample of Siltstone and Shale Breccia from Boring SB-1A, Depth Interval 88.5-89.7 ft.

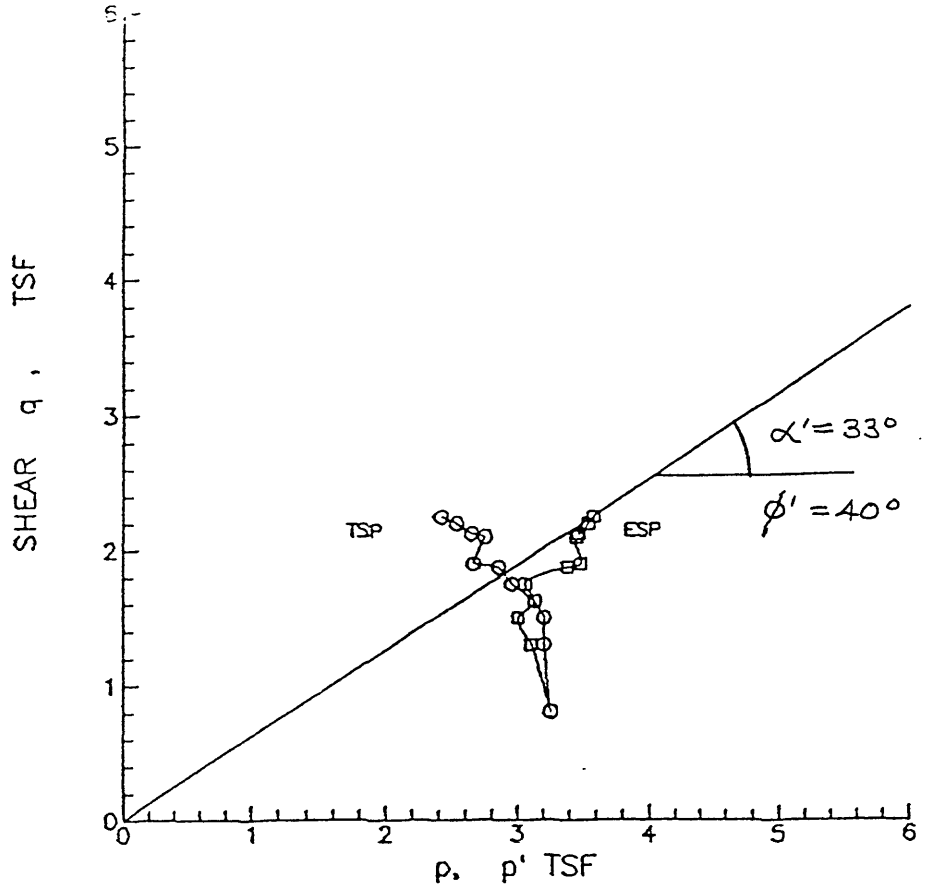

Figure 8. Total (TSP) and Effective (ESP) Stress Paths for Anisotropically-Consolidated, Undrained, Compression-Unloading Triaxial Shear Test on Sample of Sand from Boring SR-2, Depth Interval 78.5-79.5 ft.

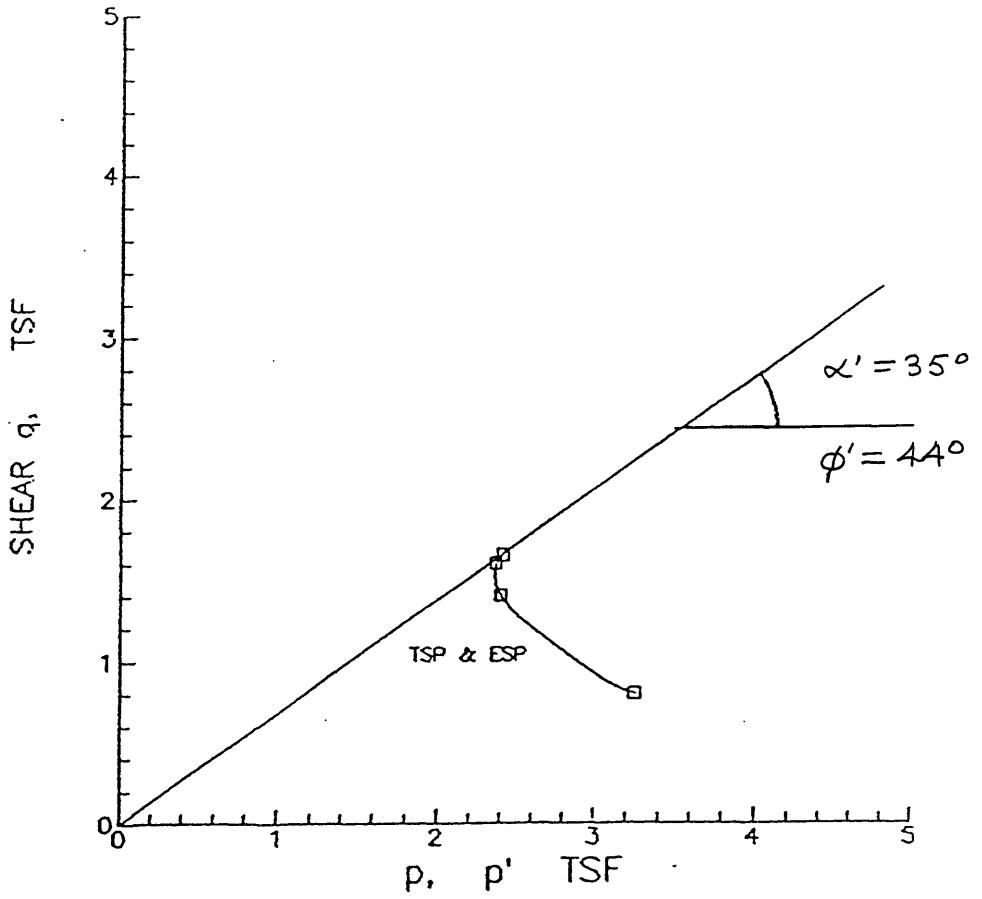

Figure 9. Total (TSP) and Effective (ESP) Stress Paths for Anisotropically-Consolidated, Drained, Compression-Unloading Triaxial Shear Test on Sample of Sandy Clay from Boring SB-1, Depth Interval 10.0-12.3 ft.

2. Direct-shear tests

These tests measured drained and large-displacement, shear-strength characteristics of samples. These tests are less expensive to perform than triaxial tests, but have several disadvantages. One of the major disadvantages is that the failure-plane location is forced by the testing equipment; this was a particular problem for the materials transitional between dense sand and soft sandstone. Failure planes were precut in samples of stiff clays, but usually could not be precut on sandy materials. In some tests, the direction of shear was reversed to measure large-strain, residual strength. Results from these tests complemented the triaxial testing. Normal stresses for tests ranged from 1 to 7 tons per square foot. Results are shown in plates 41-48 and in table 5. These data generally indicate a small reduction in strength with increased strain, except for one particularly weak sample of siltstone and shale from VDM Section SB (depth 51 feet).

F. Material Properties

The boring logs identified four basic groups of materials: regolith near the surface (locally includes colluvium), and sandstone, siltstone, and shale at greater depths. This section summarizes the classification, index, and strength properties measured in the laboratory for these four material groups.

The regolith, representing the immediate subsurface layer, includes a great variety of materials. These are silty clay; sand; sandy, clayey silt; and shale breccia. The transition between materials listed above is commonly indistinct, and the spatial variability of the materials is great.

Relatively intact siltstone had high strength parameters and a high density. The measured specific gravity of such siltstone was 2.78 which is within the range of typical values--2.17 to 2.83-- listed by Bowles (1988). Moist unit weights of the siltstone samples were between 131 and 158 pounds per cubic foot. In situ water contents were less than 9 percent. Fractured and soft (weathered) siltstone, present at a depth of about 100 feet in several boreholes, had effective friction angles that exceeded 40°.

Sandstone was found at several depths in both landslide areas investigated. The measured moist unit weights ranged from 131 to 167 pounds per cubic foot. This range compares with typical values for sandstone of 140 to 150 pounds per cubic foot (Bowles, 1988). Typical measured water contents were 15 to 18 percent, higher than expected for dense, intact material. The measured strength properties of sandstone are listed in table 5. The effective friction angle for this material was about 45 degrees.

Shale was the most common material in the samples. Shale was found in various samples in a solid, undamaged state, a fractured state, and as fragments mixed with sand and clay. Fractured shale samples had water contents of from 16 to 21 percent, as shown in table 2. The measured dry unit weights ranged from 126 to 146 pounds per cubic foot, which compare well with typical values of 100 to 140 pounds per cubic foot (Bowles, 1988). Effective friction angles typically exceeded 20° with corresponding cohesion exceeding 400 pounds per square foot. The direct-shear tests with reversal indicated some strength reduction with large strain, and one particularly weak sample was tested.

Sand samples had water contents typical for dense sand. Measured moist unit weights typically exceeded 130 pounds per cubic foot, a relatively high value. It is likely that the tested sand was a soft, weathered sandstone. The effective friction angle measured in one test was 40°, a value that compares well with typical values of 43 to 50° for dense sand listed by Bowles (1988).

Lean clay had a dry unit weight of 113 pounds per cubic foot and a water content of 8 percent, as tested on extruded samples. The corresponding saturated unit weight was 123 pounds per cubic foot. The low value of the measured water content was likely due to a loss of moisture from the bag sample and therefore probably did not represent water content in situ. The effective friction angle for the one sandy clay triaxial specimen was 44°, and for large strain conditions, the direct shear test strength was about 28° (c=0 for both triaxial and direct-shear test results). Typical values of effective friction angle for lean clay range from 20 to 42° (Bowles, 1988).

G. Summary

Laboratory tests on samples from the Upper Schultheis Road and Villa Del Monte areas were performed by SPDL. The tests included:

* Visual inspection of extruded samples
* X-ray inspection of unextruded tubes
* Mechanical grain-size analysis
* Hydrometer analysis
* Atterberg liquid and plastic limits
* Direct shear tests (with and without reversal)
* Saturated, consolidated triaxial tests (isotropic and anisotropic, loading and unloading, drained and undrained)

The classification tests showed that a wide variety of materials are present within the four material groups identified in the boring logs. The surface, regolith layer consisted of mixtures of silt, sand, clay, and shale breccia. The siltstone, sandstone, and shale rock materials ranged from weathered, soil-like materials to fractured and sheared materials, to intact rock. The many unit weight, water content, and specific-gravity tests performed resulted in a representative moist unit weight estimate of 134.5 pounds per cubic foot for both landslide areas. This value was used in slope-stability analyses, as discussed in Chapter VIII. The direct-shear strength tests indicated some reduction in strength to residual conditions should be expected if these materials undergo large strains. The effective stress paths from the triaxial tests indicated that the slope materials dilated at the stress levels tested.

H. References Cited

Bowles, J. E., 1986, Engineering properties of soils and their measurements, 3rd edition: New York, McGraw-Hill Book Company.

Lambe, T.W., and Whitman, R.V., 1969, Soil mechanics: New York, John Wiley and Sons, 553 p.

United States Army Corps of Engineers, 1970, Laboratory soils testing, engineering manual, EM 1110-2-1906, Department of the Army, Office of the Chief of Engineers.

William Cotton and Associates, Inc., 1990, Schultheis Road and Villa Del Monte areas geotechnical exploration Santa Cruz County, California: Los Gatos, Calif., William Cotton and Associates, Inc., Report for U.S. Army Engineers, 2 vols.

INDEX OF TESTING - PLATES 1 THROUGH 47 *

I. Soil Test Result Summary (Descriptions, Sieve Analyses, Atterberg Limits, Specific Gravities, Unit Weights, Water Contents).

Plate	*Borings*
1	*DM-1 through DM-2*
2	*DM-3 through DM-4*
3	*DM-4 through ED-1*
4	*ED-1 through SB-1*
5	*SB-1 through SB-3*
6	*SB-3 through SD-1*
7	*SR-1 through SR-3*
8	*Notes*
9	*Notes*

II. Gradation Curves (Hydrometers)

Plate	*Borings*
10	*ED-1 and SB-3*

III. Sample Log (Visual Observations)

Plate	*Borings*
11	*DM-1, Box 1*
12	*Box 2*
13	*DM-4, Box 1*
14	*Box 1*
15	*Box 9*
16	*ED-2, Box 2*
17	*Box 3*
18	*Box 3*

---

* From U. S. Army Engineer South Pacific Division Laboratory, March 1991. "Report of Soil Tests, Santa Cruz Landslide Study, Santa Cruz County, CA."

Plate	Borings (Continued from previous page)
39	SA-1A, S-3
40	Same as above

VI. Direct Shear

Plate	Borings
41	ED-1, Box-2
42	ED-1, Bag 5
43	SR-2, S-8
44	SR-2, S-12
45	SB-2, S-3

VII. Direct Shear (Repetitive)

Plate	Borings
46	ED-1, S-1
47	ED-2, S-1
48	DM-2

U.S. ARMY CORPS OF ENGINEERS, SOUTH PACIFIC DIVISION LABORATORY, SAUSALITO, CALIFORNIA

SOIL TEST RESULT SUMMARY

PROJECT: Santa Cruz - Loma Prieta DATE: January 1991

Division Number	Hole Number	Field Sample No.	Depth or Elevation From	To	Laboratory Description or Classification	GRAVEL PERCENT FINER 3/4	3/8	SAND #4	#8	#16	#30	#50	#100	FINE #200	Liquid Limit	Plasticity Index	GS -4	Dry Unit Weight (pcf)	Water Content %
112776	DM-1	BOX 1	20.0 20.2	20.6 20.5	Fractured Shale										46	25	2.69	116.2	16.2
112776	DM-1	BOX 1	39.0	39.5														152.0	3.1
112776	DM-1	BOX 1	61.2	61.4													2.71	132.0	6.5
112776	DM-1	BOX 1	64.9	65.2														125.1	10.6
112776	DM-1	BOX 1	70.7 70.8	71.2 71.1	Fractured Shale										89	70	2.71	120.7	11.0
112777	DM-1	BOX 2	82.2	82.5														165.2	2.2
112777	DM-1	BOX 2	99.2	99.4														130.9	4.6
112777	DM-1	BOX 2	100.0 100.2	100.4 100.5	Fractured Shale										47	28	2.72	126.9	8.4
112778	DM-1	BOX 3	132.0	132.3														126.6	5.9
112778	DM-1	BOX 3	133.5	133.7														131.3	8.6
112778	DM-1	BOX 3	138.7	139.0														135.9	4.9
112286	DM-2	BOX 1	71.5	72.2													2.75	120.6	14.6
112287	DM-2	BOX 2	94.6	94.9													2.72	126.9	7.4
112288	DM-2	BOX 3	107.4	107.7													2.72	136.0	6.4
112289	DM-2	BOX 4	149.2	149.5													2.66	135.2	6.8

SPD FORM 66A

PLATE 1

U.S. ARMY CORPS OF ENGINEERS, SOUTH PACIFIC DIVISION LABORATORY, SAUSALITO, CALIFORNIA

SOIL TEST RESULT SUMMARY

PROJECT: Santa Cruz - Loma Prieta

DATE: January 1991

Division Number	Hole Number	Field Sample No.	Depth or Elevation From	Depth or Elevation To	Laboratory Description or Classification	GRAVEL PERCENT FINER 3/4	3/8	SAND PERCENT FINER #4	#8	#16	#30	#50	#100	FINE #200	Liquid Limit	Plasticity Index	GS -4	Dry Unit Weight (pcf)	Water Content %
112291	DM-3	BOX 1	30.8	31.1				100	98	94	91	88	70	45			2.67	125.2	6.0
112291	DM-3	BOX 1	40.5	40.8														105.5	15.4
112292	DM-3	BOX 2	90.4	90.8														124.9	13.4
112293	DM-4	BOX 1	20.0 20.0	20.5 20.3	Fractured Shale										58	36		111.3	18.5
112293	DM-4	BOX 1	30.5 30.5	31.2 30.8											38	24		114.0	17.7
112293	DM-4	BOX 1	40.0 40.0	40.7 40.3	Fractured Shale										40	21	2.72	122.7	13.9
112293	DM-4	BOX 1	50.0 50.0	50.7 50.3	Fractured Shale										42	24		127.6	11.3
112293	DM-4	BOX 1	60.0 60.0	60.7 60.3	Fractured Shale										39	21		132.5	10.2
112294	DM-4	BOX 2	81.0	81.5														165.1	1.0
112296	DM-4	BOX 4	148.7	149.0													2.79	135.6	7.7
112297	DM-4	BOX 5	150.4	150.7													2.78	126.8	10.0
112298	DM-4	BOX 6	161.6	162.0													* 2.76	127.4	7.9
112298	DM-4	BOX 6	168.7	169.0													2.72	150.0	4.7
112779	DM-4	BOX 8	182.2	182.5														125.4	12.8
112779	DM-4	BOX 8	189.7	190.0														131.1	4.3

SPD FORM 66A

PLATE 2

U.S. ARMY CORPS OF ENGINEERS, SOUTH PACIFIC DIVISION LABORATORY, SAUSALITO, CALIFORNIA

SOIL TEST RESULT SUMMARY

PROJECT: Santa Cruz - Loma Prieta DATE: January 1991

Division Number	Hole Number	Field Sample No.	Depth or Elevation From	Depth or Elevation To	Laboratory Description or Classification	GRAVEL PERCENT FINER 3/4	3/8	SAND PERCENT FINER #4	#8	#16	#30	#50	#100	FINE #200	Liquid Limit	Plasticity Index	GS -4	Dry Unit Weight (pcf)	Water Content %
112780	DM-4	BOX 9	191.0	191.3														130.5	8.7
112780	DM-4	BOX 9	195.0 195.0	195.5 195.25	Fractured Shale										44	24		119.0	12.3
112780	DM-4	BOX 9	199.4	199.6													2.73	127.6	8.6
112299	DM-4	BOX 10	200.0	200.2														124.3	9.9
112299	DM-4	BOX 10	208.3	208.6														155.9	1.4
112300	DM-4	BOX 11	210.2	210.5													2.71	150.0	3.1
112300	DM-4	BOX 11	217.4	217.7														149.9	4.3
112301	DM-4	BOX 12	228.2	228.8														151.4	4.3
112781	DM-4	BOX 13	230.7	231.0														130.5	8.9
112302	ED-1	S-1	31.5	32.9				100	99	98	97	95	86	59			2.67		9.9
112307	ED-1	BOX 1	34.7 34.5	34.9 34.7	Sandy Silt (ML)							100	96	65			2.66	124.7	11.5
112307	ED-1	BOX 1	38.4	38.6	Lean Clay with Sand (CL)							100	97	82	34	14	2.66	113.01	7.8
112308	ED-1	BOX 2	58.5 59.5	59.0 61.0											48 60	25 33			
112309	ED-1	BOX 3	65.0	65.3													2.71	117.8	14.8
112309	ED-1	BOX 3	80.0 80.1	81.4 80.4												NP		118.8	13.1

SPD FORM 66A

PLATE 3

U.S. ARMY CORPS OF ENGINEERS, SOUTH PACIFIC DIVISION LABORATORY, SAUSALITO, CALIFORNIA

SOIL TEST RESULT SUMMARY

PROJECT: Santa Cruz - Loma Prieta DATE: January 1991

Division Number	Hole Number	Field Sample No.	Depth or Elevation From	Depth or Elevation To	Laboratory Description or Classification	GRAVEL PERCENT FINER 3/4	3/8	SAND #4	#8	#16	#30	#50	#100	FINE #200	Liquid Limit	Plasticity Index	GS -4	Dry Unit Weight (pcf)	Water Content %
112303	ED-1	S-2	75.3	75.7														133.8	3.2
112304	ED-1	S-3	61.0	62.3											44	18			
112311	ED-2	BOX 1	61.2	61.5													2.69	118.6	14.7
112312	ED-2	BOX 1	80.3	80.6														124.6	9.7
112312	ED-2	BOX 2	139.0 139.1	139.4 139.4	Sandy Fat Clay (CH)				100	99	99	98	92	60	60	41	* 2.70	130.5	6.5
112312	ED-2	BOX 2	145.5 145.3	145.9 145.7											40	21		138.2	5.5
112313	ED-2	BOX 3	148.7	149.1	Fractured Shale												2.74		
112313	ED-2	BOX 3	196.4	196.8	Fractured Shale										46	26	2.71	125.8	6.9
112313	ED-2	BOX 3	197.3	197.7	Fractured Shale										19	2		124.4	12.1
112782	SB-1	ST-3	15.0	15.3	Clayey Sand (SC)				100	99	99	95	69	41	31	11		119.0	12.3
112782	SB-1	ST-3	15.7 15.6	16.4 16.2	Silty Clayey Sand (SC-SM)			100	99	98	96	92	66	38	28	6	2.68	118.3	14.0
112783	SB-1	ST-4	17.0 17.0	17.6 17.3	Silty Sand (SM)			100	99	98	97	93	69	41		NP		116.2	15.9
112783	SB-1	ST-4	17.6 17.7	18.2 18.0	Silty Sand (SM)				100	99	98	93	61	33		NP		128.4	9.4
112784	SB-1	ST-8	23.5 23.7	24.3 24.0	Silty Clayey Sand (SC-SM)				100	99	97	85	47	25	27	5		126.6	1.9
112784	SB-1	ST-8	24.1 24.1	24.7 24.4	Silty Sand (SM)					100	99	93	70	42		NP	2.66	114.8	15.8

SPD FORM 66A

PLATE 4

U.S. ARMY CORPS OF ENGINEERS, SOUTH PACIFIC DIVISION LABORATORY, SAUSALITO, CALIFORNIA

SOIL TEST RESULT SUMMARY

PROJECT: Santa Cruz - Loma Prieta DATE: January 1991

Division Number	Hole Number	Field Sample No.	Depth or Elevation From	Depth or Elevation To	Laboratory Description or Classification	GRAVEL PERCENT FINER 3/4	GRAVEL PERCENT FINER 3/8	SAND PERCENT FINER #4	SAND PERCENT FINER #8	SAND PERCENT FINER #16	SAND PERCENT FINER #30	SAND PERCENT FINER #50	SAND PERCENT FINER #100	FINE #200	Liquid Limit	Plasticity Index	GS -4	Dry Unit Weight (pcf)	Water Content %
112789	SB-1	ST-23	47.8 47.8	48.0 48.1	Silty Sand (SM)				100	98	95	83	51	27		NP	2.68	125.2	11.6
112793	SB-1	ST-29	56.0	56.3														120.6	13.8
112793	SB-1	ST-29	56.3 56.35	56.8 56.8											42	20		128.7	8.5
112794	SB-1	S-38	68.5	69.1											27	9	2.76	NOTE 1	
112798	SB-1A	B-6	91.95 91.9	92.35 92.2	Fractured Shale Fractured Shale										47	28		127.0	9.4
112265	SB-2	ST-2	41.5	41.9	Fractured Shale										36	16		133.2	8.7
112267	SB-2	BOX 1	34.5	35.3														NOTE 1	
112268	SB-2	BOX 2	66.9 66.6	67.4 66.7	Fractured Shale										31	13		124.3	7.8
112269	SB-2	BOX 3	81.0	85.0													2.72	120.4	10.0
112271	SB-2	BOX 5	100.5	100.7	Fractured Shale													124.4	7.4
112272	SB-2	BOX 6	167.2 167.4	167.4 167.7	Fractured Shale Fractured Shale										38	19		127.2	7.9
112274	SB-2	BOX 8	242.7	243.0														159.9	1.7
112275	SB-3	BOX 1	20.6	21.9														107.7	19.3
112275	SB-3	BOX 1	41.0	41.5	Sandy Silt (ML)					100	99	98	89	66		NP		104.8	21.8
112276	SB-3	BOX 2	80.0	80.2	Sandy Lean Clay (CL)			100	97	93	91	89	81	58	29	10	2.66	124.8	11.1

SPD FORM 66A

PLATE 5

U.S. ARMY CORPS OF ENGINEERS, SOUTH PACIFIC DIVISION LABORATORY, SAUSALITO, CALIFORNIA

SOIL TEST RESULT SUMMARY

PROJECT: Santa Cruz - Loma Prieta

DATE: January 1991

Division Number	Hole Number	Field Sample No.	Depth or Elevation From	Depth or Elevation To	Laboratory Description or Classification	GRAVEL PERCENT FINER 3/4	3/8	SAND #4	#8	#16	#30	#50	#100	FINE #200	Liquid Limit	Plasticity Index	GS -4	Dry Unit Weight (pcf)	Water Content %
112277	SB-3	BOX 3	91.7	92.0														142.1	3.5
112278	SB-3	BOX 4	143.2	143.5														140.8	3.4
112278	SB-3	BOX 4	150.0	150.3													2.70	126.5	10.9
112279	SB-3	BOX 5	190.7	191.1													2.69	148.2	4.0
112279	SB-3	BOX 5	194.6	194.8														119.5	12.0
112280	SB-3	BOX 6	230.2	230.5														122.2	9.2
112280	SB-3	BOX 6	236.6	236.9														125.1	8.0
112281	SB-4	BOX 1	50.0	50.5	Fractured Shale										50	27		143.3	6.3
			50.0	50.2															
112281	SB-4	BOX 1	150.5	150.9	Fractured Shale										45	27	2.71	129.5	8.9
			150.6	150.8															
112317	SD-1	BOX 1	45.9	46.4	Fractured Sand-										33	12	2.67	126.9	10.9
			46.0	46.4	stone & Shale														
112317	SD-1	BOX 1	49.0	49.8	Fractured Sand-										34	13	2.69	122.2	11.9
			49.1	49.6	stone & Shale														
112317	SD-1	BOX 1	73.8	74.1											33	16	2.69	124.6	11.1
			73.6	73.8															
112318	SD-1	BOX 2	81.6	82.2	Fractured Shale										36	16	2.73	119.1	14.3
			81.8	82.0															
112319	SD-1	BOX 3	98.2	98.85	Fractured Shale										40	22		118.5	14.7
			98.5	98.7															
112319	SD-1	BOX 3	179.4	179.7													2.74	130.0	9.9

SPD FORM 66A

PLATE 6

U.S. ARMY CORPS OF ENGINEERS, SOUTH PACIFIC DIVISION LABORATORY, SAUSALITO, CALIFORNIA

SOIL TEST RESULT SUMMARY

PROJECT: Santa Cruz - Loma Prieta DATE: January 1991

Division Number	Hole Number	Field Sample No.	Depth or Elevation From	To	Laboratory Description or Classification	GRAVEL PERCENT FINER 3/4	3/8	SAND PERCENT FINER #4	#8	#16	#30	#50	#100	FINE #200	Liquid Limit	Plasticity Index	GS -4	Dry Unit Weight (pcf)	Water Content %
112804	SR-1	BOX 1	59.7	60.5											41	22		113.5	16.2
112804	SR-1	BOX 1	65.5	65.8											32	13	2.64	121.7	10.9
112805	SR-1	BOX 2	69.0	71.0											Visualed med. plastic		2.65	NOTE 1	
112806	SR-1	BOX 3	104.0 104.8	106.0 105.2											55	33		115.3	13.9
112807	SR-1	BOX 4	151.2 151.4	152.0 151.8											51	31	2.68	123.8	12.4
112808	SR-1	BOX 5	202.0	202.3													2.65	146.0	0.3
112221	SR-2	S-4	79.3	79.5				100	99	97	95	83	55	33		NP	2.65		
112225	SR-2	S-8	89.5 89.5	90.0 90.5		100	98	96	92	87	82	75	65	54	37	22	2.64		
112229	SR-2	S-12	100												39	22			
112246	SR-3	BOX 1	76.3	76.6														131.1	9.8
112247	SR-3	BOX 2	103.8	104.0													2.67	124.3	7.6
112247	SR-3	BOX 3	105.0	105.3														158.2	0.8

* Depth not certain

SPD FORM 66A

PLATE 7

U.S. ARMY CORPS OF ENGINEERS, SOUTH PACIFIC DIVISION LABORATORY, SUASALITO, CALIFORNIA

SOIL TEST RESULT SUMMARY

PROJECT: Santa Cruz - Loma Prieta DATE: January 1991

NOTES

1) The following samples were totally fragmented. No dry unit weight was possible.

112794	SB-1	S-38	68.5-69.1	
112267	SB-2	Box 1	34.5-35.3	
112805	SR-1	Box 2	69.0-71.0	(This sample was not large enough for the Atterberg tests. A visual of medium-plastic was made).

2) The following unit weights were done on hard rock:

112776	DM-1	Box 1	39.0-39.5	112274	SB-2	Box 8	242.0-243.0
112777	DM-1	Box 2	82.2-82.5	112279	SB-3	Box 5	190.7-191.1
112294	DM-4	Box 2	81.0-81.5	112808	SR-1	Box 5	202.0-202.3
112299	DM-4	Box 10	208.3-208.6	112247	SR-3	Box 2	105.0-105.3
112277	SB-2	Box 3	91.7-92.0				

3) The following Atterberg liquid and plastic limits were done on soft shale. They were generally prepared following the procedures outlined in EM 1110-2-1906 (Laboratory Soils Testing) dated 30 November 1970 with Change 2 dated 20 August 1986, Appendix III-25, Paragraph (1).

112776	DM-1	Box 1	(20.0-20.6), (70.7-71.2), (80.0-80.2)	112272	SB-2	Box 6	167.2-167.4
112777	DM-1	Box 2	100.0-100.4	112281	SB-4	Box 1	150.5-150.9
112293	DM-4	Box 1	(40.0-40.7), (50.0-50.7), (60.0-60.7)	112804	SR-1	Box 1	59.7-60.5
112780	DM-4	Box 9	195.0-195.5	112806	SR-1	Box 3	104.0-106.0
112312	ED-2	Box 2	(139.0-139.4), (145.5-145.9)	112807	SR-1	Box 4	151.2-152.0
112313	ED-2	Box 3	197.3-197.7				
112793	SB-1	ST-29	56.3-56.8				
112794	SB-1	S-38	68.5-69.1				
112798	SB-1A	Box 6	91.95-92.35				

SPD FORM 66A (MODIFIED)

PLATE 8

U.S. ARMY CORPS OF ENGINEERS, SOUTH PACIFIC DIVISION LABORATORY, SUASALITO, CALIFORNIA

SOIL TEST RESULT SUMMARY

PROJECT: Santa Cruz - Loma Prieta DATE: January 1991

NOTES (continued)

4) The following Atterberg liquid and plastic limits were done on shale. These samples were not blenderized due to the hardness of the material.

112794	SB-1	S-38	68.5-69.1
112265	SB-2	ST-2	41.5-41.9
112268	SB-2	Box 2	66.9-67.4
112317	SD-1	Box 1	(45.9-46.4), (49.1-49.8), (73.8-74.1)
112318	SD-1	Box 2	81.6-82.2
112804	SR-1	Box 1	65.5-65.8

SPD FORM 66A (MODIFIED)

PLATE 9

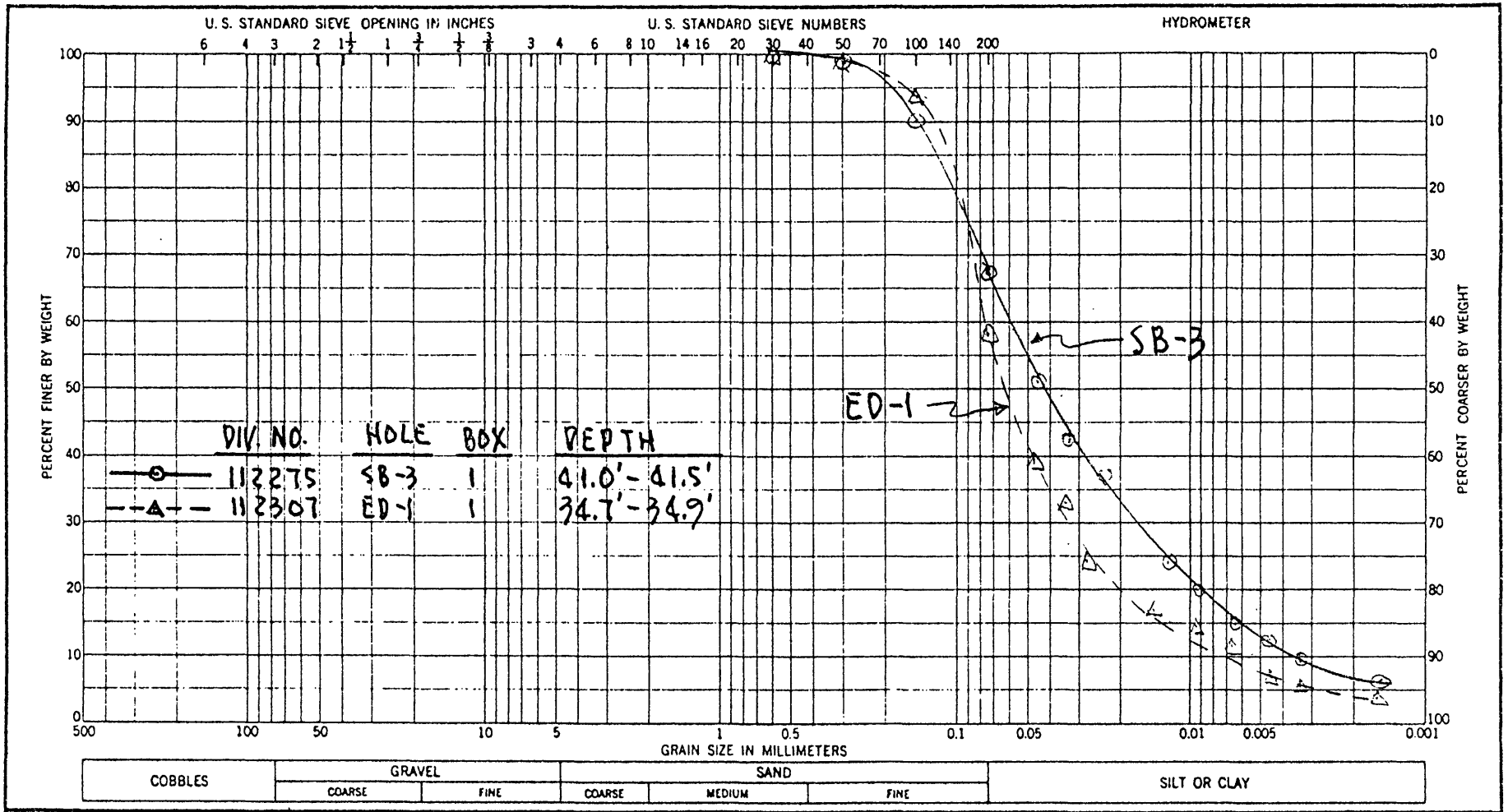

Sample No.	Elev or Depth	Classification	Nat w %	LL	PL	PI
112275	41.0'-41.5'	SANDY SILT (ML)				NP
112307	34.7'-34.9'					

GRADATION CURVES

Project SANTA CRUZ

Area

Boring No. ED-1 & SB-3

Date JAN 1991

ENG FORM 1 MAY 63 2087

PLATE 10

SAMPLE LOG

DISTRICT: PROJECT: Santa Cruz - Loma Prieta HOLE NO.: DM-1

REMARKS: SHEET 1 of 16

Division Number	Field Sample No.	Depth (Ft.)	Type & Condition of Sample, Remarks	Symbol	Classification of Soil
		20.0			
			Chunk density taken.		
112776	Box 1		Dark gray, wet, highly-fractured shale.		
			Dark gray, soft to hard, moist, highly-fractured shale.		
		21.0			
		22.0			
		70.0			
			Grayish-brown, soft to hard, damp, fractured shale.		
		71.0			

FORM 11

PLATE 11

SAMPLE LOG

DISTRICT: PROJECT: Santa Cruz - Loma Prieta HOLE NO.: DM-1

REMARKS: SHEET 2 of 16

Division Number	Field Sample No.	Depth (Ft.)	Type & Condition of Sample, Remarks	Symbol	Classification of Soil
		72.0			
		100.0			
112777	Box 2		Dark gray, soft to hard, damp, fractured shale.		

FORM 11

PLATE 12

SAMPLE LOG

DISTRICT: PROJECT: Santa Cruz - Loma Prieta HOLE NO.: DM-4

REMARKS: SHEET 3 of 16

Division Number	Field Sample No.	Depth (Ft.)	Type & Condition of Sample, Remarks	Symbol	Classification of Soil
		20.0			
112293	Box 1		Chunk density taken. Grayish-brown, soft to hard, wet, fractured shale.		
			Same but moist.		
		21.0			
		22.0			
		40.0			
			Chunk density taken 40.0-40.3 Dark gray, soft to hard, wet, fractured shale. Some slick surfaces.		
		41.0			

FORM 11

PLATE 13

SAMPLE LOG

DISTRICT: PROJECT: Santa Cruz - Loma Prieta HOLE NO.: DM-4

REMARKS: SHEET 4 of 16

Division Number	Field Sample No.	Depth (Ft.)	Type & Condition of Sample, Remarks	Symbol	Classification of Soil
		50.0			
112293 (cont'd)			Chunk density taken 50.0-50.4 Dark gray, soft to hard, wet, fractured shale. Some slick surfaces.		
		51.0			
		60.0			
			Dark gray, soft to hard, wet, fractured shale.		
		61.0			

FORM 11

PLATE 14

SAMPLE LOG

DISTRICT: | PROJECT: Santa Cruz - Loma Prieta | HOLE NO.: DM-4

REMARKS: | SHEET 5 of 16

Division Number	Field Sample No.	Depth (Ft.)	Type & Condition of Sample, Remarks	Symbol	Classification of Soil
		195.0			
112780	Box 9		Dark gray, soft to hard, moist, folded and fractured shale. Some with slick surfaces.		
		196.0			

FORM 11

PLATE 15

SAMPLE LOG

DISTRICT: PROJECT: Santa Cruz - Loma Prieta HOLE NO.: ED-2

REMARKS: SHEET 6 of 16

Division Number	Field Sample No.	Depth (Ft.)	Type & Condition of Sample, Remarks	Symbol	Classification of Soil
		139.0			
112312	Box 2		Sandstone		
			Mottled pale gray and dark gray, damp,		
	Box 2	140.0	folded and fractured shale and sandstone.		
		147.0			

FORM 11

PLATE 16

SAMPLE LOG

DISTRICT: PROJECT: Santa Cruz - Loma Prieta HOLE NO.: ED-2

REMARKS: SHEET 7 of 16

Division Number	Field Sample No.	Depth (Ft.)	Type & Condition of Sample, Remarks	Symbol	Classification of Soil
		147.0			
112313	Box 3				
			Dark olive-brown, soft to hard, fractured shale. Some with slick surfaces.		
		148.0			
			Chunk density 148.7-149.1		
		149.0			
		196.0			
			Dark olive-brown, highly-fractured shale.		
		197.0			

FORM 11

PLATE 17

SAMPLE LOG

DISTRICT: PROJECT: Santa Cruz - Loma Prieta HOLE NO.: ED-2

REMARKS: SHEET 8 of 16

Division Number	Field Sample No.	Depth (Ft.)	Type & Condition of Sample, Remarks	Symbol	Classification of Soil
		197.0			
112313			Depth continued from previous sheet.		
		198.0			

FORM 11

PLATE 18

SAMPLE LOG

DISTRICT: PROJECT: Santa Cruz - Loma Prieta HOLE NO.: SB-1A

REMARKS: SHEET 9 of 16

Division Number	Field Sample No.	Depth (Ft.)	Type & Condition of Sample, Remarks	Symbol	Classification of Soil
		91.0			
112798	Box 6	92.0	Gray, soft to hard, damp, highly-fractured shale.		

FORM 11

PLATE 19

SAMPLE LOG

DISTRICT: PROJECT: Santa Cruz - Loma Prieta HOLE NO.: SB-2

REMARKS: SHEET 10 of 16

Division Number	Field Sample No.	Depth (Ft.)	Type & Condition of Sample, Remarks	Symbol	Classification of Soil
		41.0			
112265	ST-2		Dark olive-brown, highly fractured, hard to soft shale, some with slick surfaces.		
			Chunk density 41.5-42.3.		
		42.0			
			Bottom of tube mangled and disturbed.		
		66.0			
		67.0			
112268	Box 2		Dark olive-brown, highly-fractured, soft to hard shale.		
		68.0			

FORM 11

PLATE 20

SAMPLE LOG

DISTRICT: PROJECT: Santa Cruz - Loma Prieta HOLE NO.: SB-2

REMARKS: SHEET 11 of 16

Division Number	Field Sample No.	Depth (Ft.)	Type & Condition of Sample, Remarks	Symbol	Classification of Soil
		99.0			
112171	Box 5				
			Gray, damp, soft to hard, highly fractured shale.		
		100.0			
		101.0			

FORM 11

PLATE 21

SAMPLE LOG

DISTRICT: PROJECT: Santa Cruz - Loma Prieta HOLE NO.: SB-2

REMARKS: SHEET 12 of 16

Division Number	Field Sample No.	Depth (Ft.)	Type & Condition of Sample, Remarks	Symbol	Classification of Soil
		166.0			
112272	Box 6		Dark olive-brown, soft to hard, highly-fractured shale.		
		167.0			
		168.0			

FORM 11

PLATE 22

SAMPLE LOG

DISTRICT: PROJECT: Santa Cruz - Loma Prieta HOLE NO.: SB-4A & SB-4

REMARKS: SHEET 13 of 16

Division Number	Field Sample No.	Depth (Ft.)	Type & Condition of Sample, Remarks	Symbol	Classification of Soil
		6.0			
112281	SB-4A				
	Box 1				
			Gray, damp, soft to hard, highly-fractured shale. (This depth was marked on the baggie not on the work order).		
		7.0			
		50.0			
	SB-4		Gray, soft to hard, moist, highly fractured shale.		
	B-4				
		51.0			

FORM 11

PLATE 23

SAMPLE LOG

DISTRICT: PROJECT: Santa Cruz - Loma Prieta HOLE NO.: SB-4A & SB-4

REMARKS: SHEET 14 of 16

Division Number	Field Sample No.	Depth (Ft.)	Type & Condition of Sample, Remarks	Symbol	Classification of Soil
		150.0			
112281 (cont'd)	SB-4 B-1	151.0	Gray, moist, soft to hard, highly-fractured shale.		
		152.0			

FORM 11

PLATE 24

SAMPLE LOG

DISTRICT: PROJECT: Santa Cruz - Loma Prieta HOLE NO.: SD-1

REMARKS: SHEET 15 of 16

Division Number	Field Sample No.	Depth (Ft.)	Type & Condition of Sample, Remarks	Symbol	Classification of Soil
		45.0			
112317	Box 1				
			Yellowish-brown, moist, soft to hard, fractured sandstone and shale.		
		46.0			
		49.0			
	Box 1		Yellowish-brown, moist, soft to hard, fractured sandstone and shale.		
		50.0			

FORM 11

PLATE 25

SAMPLE LOG

DISTRICT: PROJECT: Santa Cruz - Loma Prieta HOLE NO.: SD-1

REMARKS: SHEET 16 of 16

Division Number	Field Sample No.	Depth (Ft.)	Type & Condition of Sample, Remarks	Symbol	Classification of Soil
		81.0			
112318	Box 2				
			Brown, wet, soft to hard, fractured shale.		
		82.0			
		83.0			
		98.0			
112319	Box 3		Brown, damp. soft to hard, fractured shale.		
		99.0			

FORM 11

PLATE 26

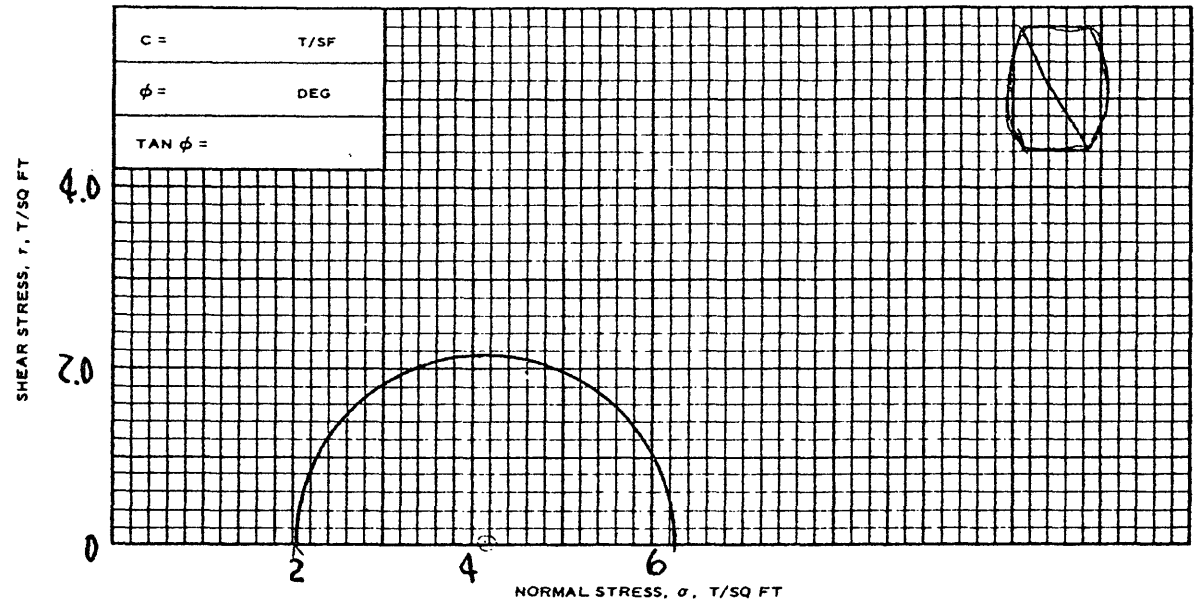

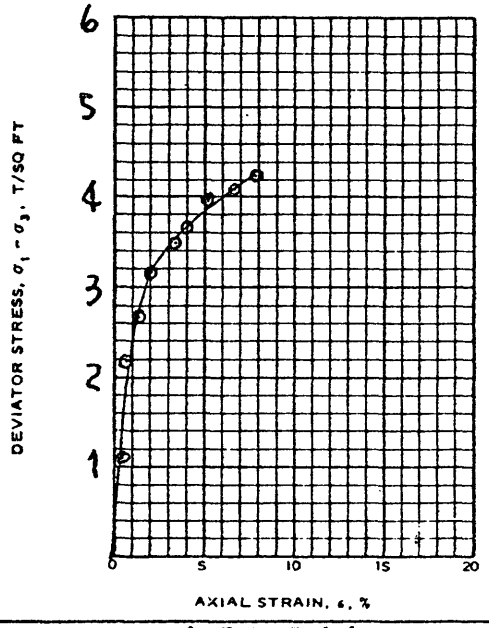

SPECIMEN NO.			112304			
INITIAL	WATER CONTENT, %	w_o	20.5			
	DRY DENSITY LB/ CU FT	γ_{d_o}	106.1			
	SATURATION, %	S_o	96.0			
	VOID RATIO	e_o	0.5700			
BEFORE SHEAR	WATER CONTENT, %	w_c	20.6			
	DRY DENSITY LB/CU FT	γ_{d_c}	107.4			
	SATURATION, %	S_c	100			
	VOID RATIO	e_c	0.5514			
	FINAL BACK PRESSURE, T/SQ FT	u_o	3.96			
MINOR PRINCIPAL STRESS, T/SQ FT		σ_3	2.04			
MAXIMUM DEVIATOR STRESS, T/SQ FT	$(\sigma_1 - \sigma_3)_{MAX}$		4.28			
TIME TO $(\sigma_1 - \sigma_3)_{MAX}$, MIN		t_f	360			
ULTIMATE DEVIATOR STRESS, T/SQ FT	$(\sigma_1 - \sigma_3)_{ULT}$		-			
INITIAL DIAMETER, IN.		D_o	2.88			
INITIAL HEIGHT, IN.		H_o	6.25			

CONTROLLED- STRESS TEST

DESCRIPTION OF SPECIMENS FRACTURED BROWN SHALE

LL	PL	PI	G_s
44	26	18	2.67

TYPE OF SPECIMEN UD

TYPE OF TEST Ā

REMARKS:

PROJECT SANTA CRUZ LANDSLIDE STUDY S-3

BORING NO. ED-1 SAMPLE NO.

DEPTH/ELEV 61.0' - 62.3'

LABORATORY SPDL DATE FEB 1971

TRIAXIAL COMPRESSION TEST REPORT

ENG FORM NO. 2089 REV JUNE 1970 PREVIOUS EDITION IS OBSOLETE

PLATE 27

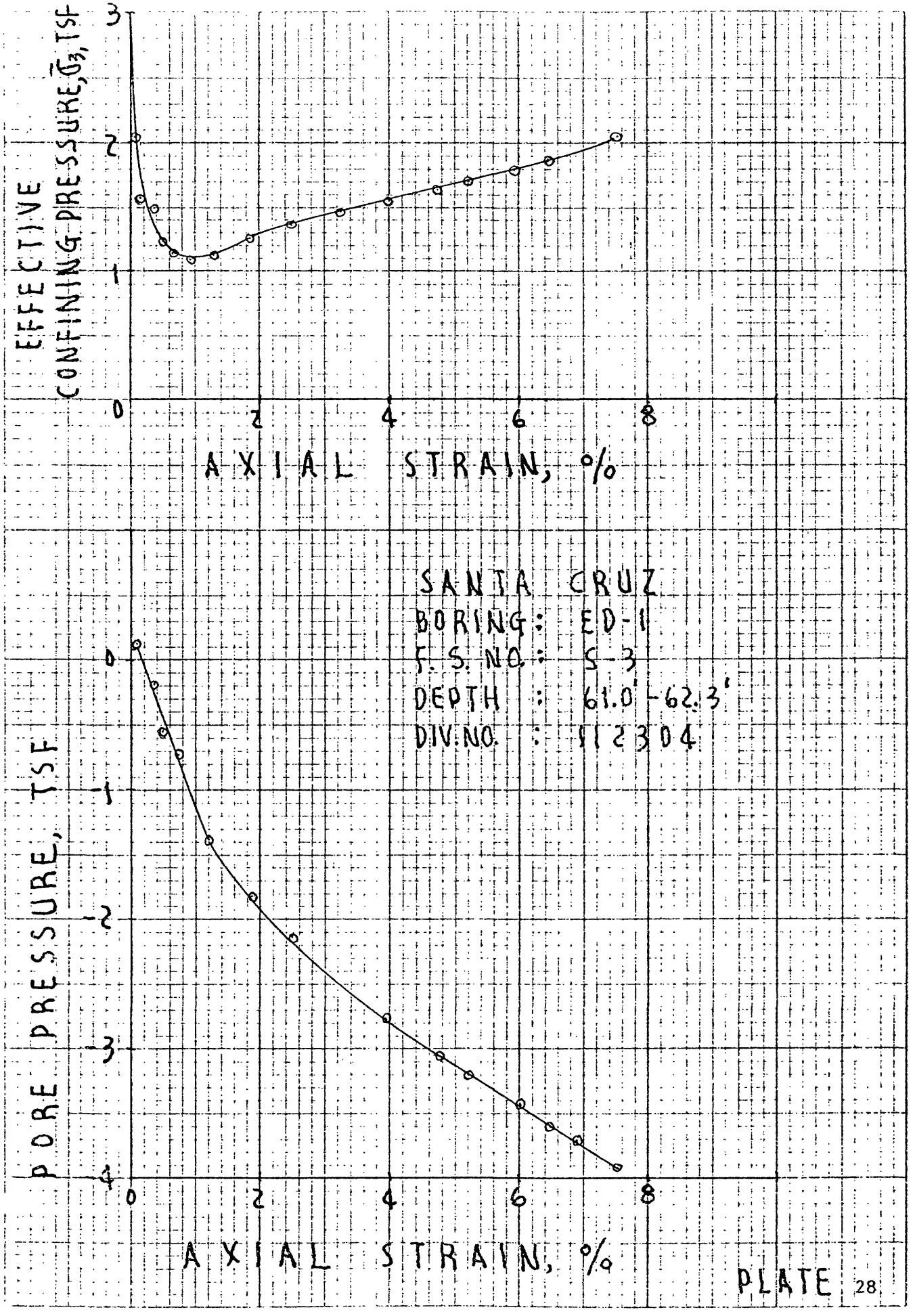
EFFECTIVE CONFINING PRESSURE, $\bar{\sigma}_3$, TSF
3
2
1
0
2
4
6
8
AXIAL STRAIN, %
SANTA CRUZ
BORING: ED-1
F.S. NO.: S-3
DEPTH : 61.0'-62.3'
DIV.NO. : 112304
PORE PRESSURE, TSF
0
-1
-2
-3
-4
0
2
4
6
8
AXIAL STRAIN, %

PLATE 28

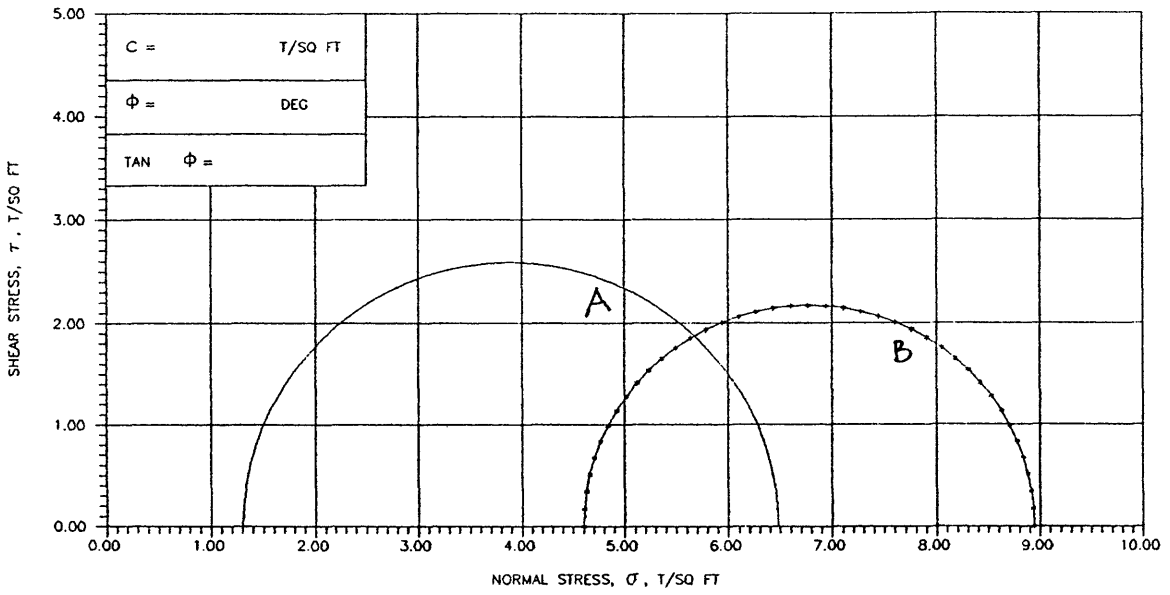

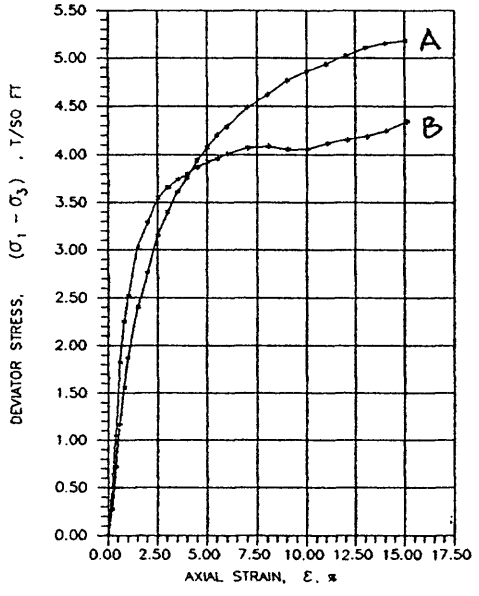

SPECIMEN NO.			A	B		
INITIAL	WATER CONTENT, %	w_o	21.0	14.3		
	DRY DENSITY LB/CU FT	γ_{d_o}	104.3	109.0		
	SATURATION, %	S_o	92	81		
	VOID RATIO	e_o	.615	.546		
BEFORE SHEAR	WATER CONTENT, %	w_c	21.4	15.5		
	DRY DENSITY LB/CU FT	γ_{d_c}	104.2	118.8		
	SATURATION, %	S_c	100	100		
	VOID RATIO	e_c	.583	.418		
	FINAL BACK PRESSURE, T/SQ FT	u_o	4.3	5.7		
MINOR PRINCIPAL STRESS, T/SQ FT		σ_3	1.3	4.6		
MAXIMUM DEVIATOR STRESS, T/SQ FT	$(\sigma_1 - \sigma_3)_{MAX}$		5.18	4.34		
TIME TO $(\sigma_1 - \sigma_3)_{MAX}$, MIN		t_f	420	416		
ULTIMATE DEVIATOR STRESS, T/SQ FT	$(\sigma_1 - \sigma_3)_{ULT}$		—	—		
INITIAL DIAMETER, IN.		D_o	2.84	2.80		
INITIAL HEIGHT, IN.		H_o	6.33	6.14		

CONTROLLED STRAIN TEST

DESCRIPTION OF SPECIMEN A, Fractured Shale, brown. B, Fractured Shale gray.

(A) 44 | PL 26 | PI 18 | G_S

TYPE OF SPECIMEN Undisturbed | TYPE OF TEST R

REMARKS

PROJECT Santa Cruz Landslide Study

	Boring No.	F.S. No.	Depth
A	ED-1	S-3	61'-62.3'
B	SR-3	S-13	180'-181.2'

BORING NO. | SAMPLE NO.

LABORATORY SPD | DATE Aug 90

TRIAXIAL COMPRESSION TEST REPORT

ENG FORM NO. 2089
REV. JUNE 1970

PLATE 29

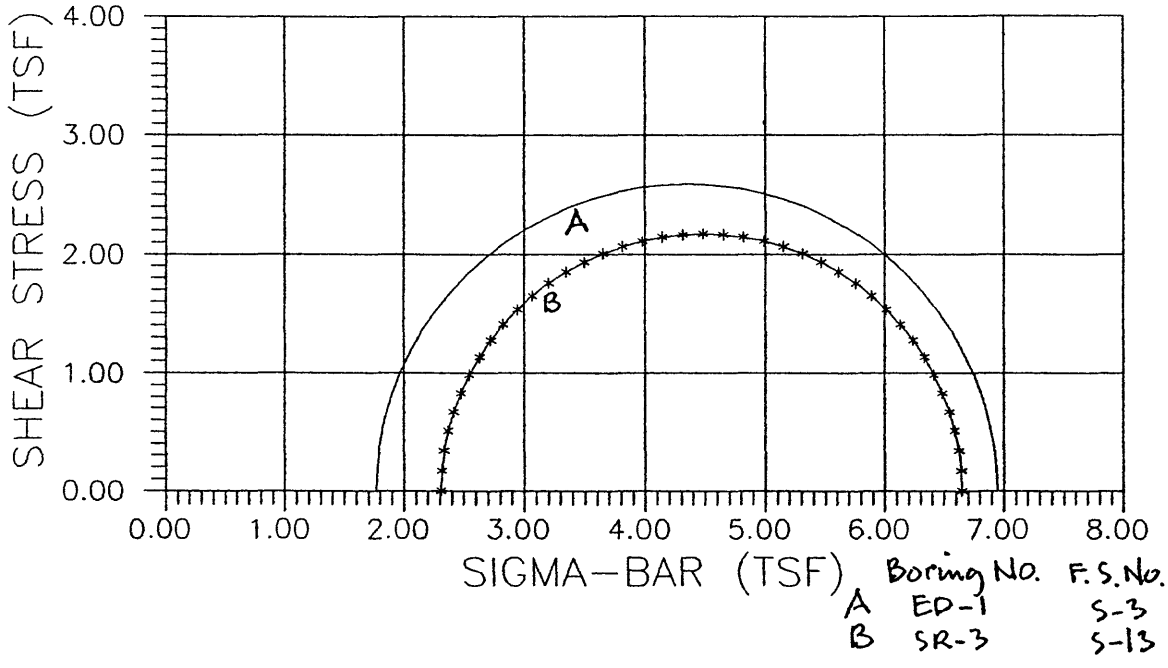

	Boring No.	F.S.No.	Depth
A	ED-1	S-3	61'-62.3'
B	SR-3	S-13	180'-181.2'

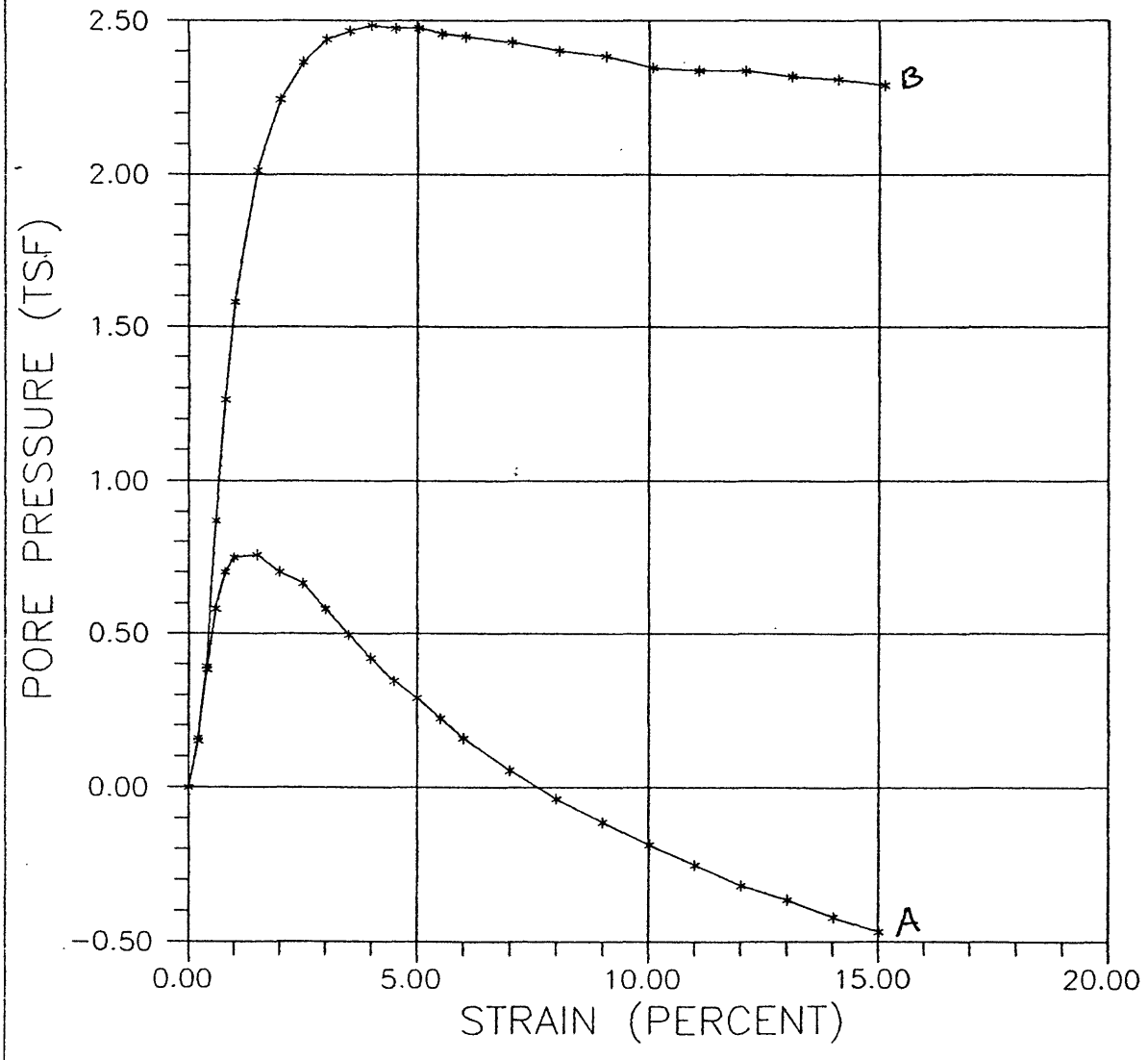

PLATE 30

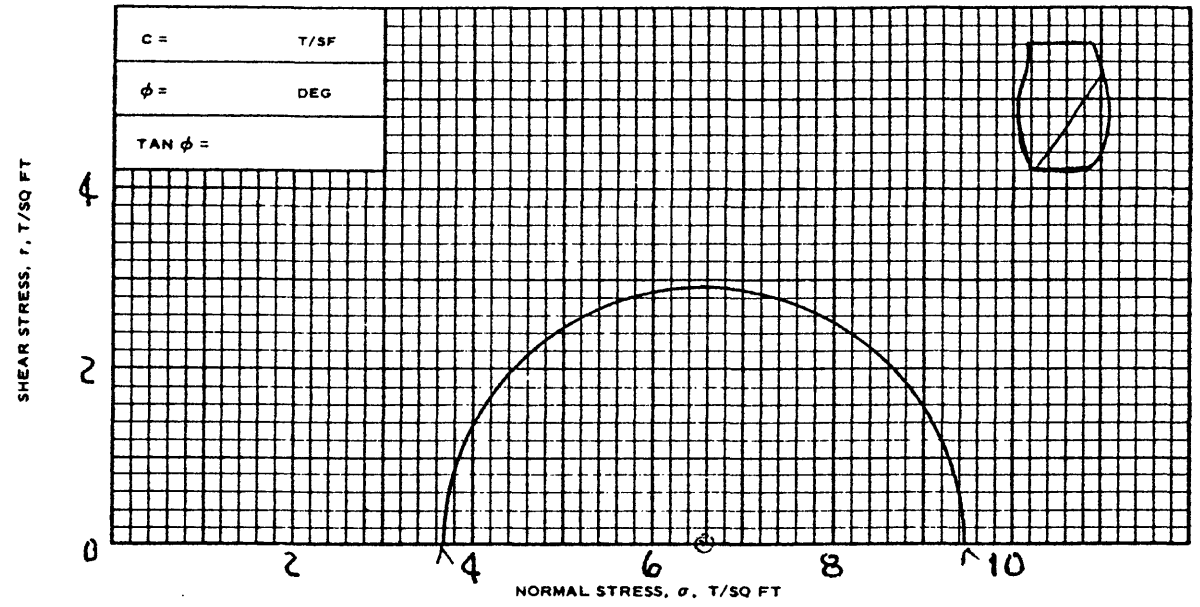

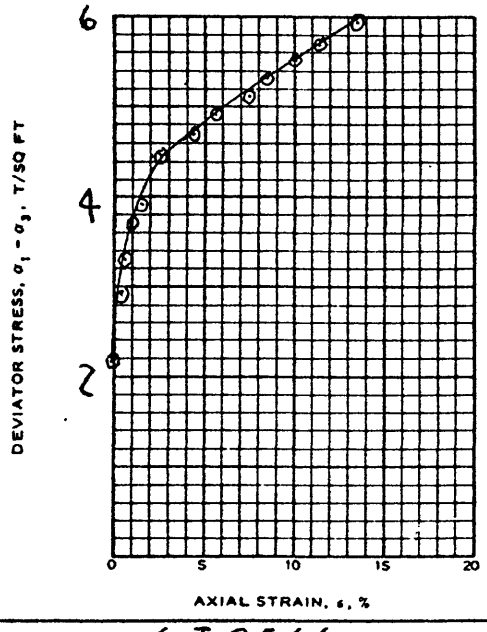

SPECIMEN NO. 112262						
INITIAL	WATER CONTENT, %	w_o	11.2			
	DRY DENSITY LB/ CU FT	γ_{d_o}	124.6			
	SATURATION, %	S_o	91			
	VOID RATIO	e_o	0.3266			
BEFORE SHEAR	WATER CONTENT, %	w_c	11.5			
	DRY DENSITY LB/CU FT	γ_{d_c}	126.8			
	SATURATION, %	S_c	100			
	VOID RATIO	e_c	0.3044			
	FINAL BACK PRESSURE, T/SQ FT	u_o	5.76			
MINOR PRINCIPAL STRESS, T/SQ FT		σ_3	2.35			
MAXIMUM DEVIATOR STRESS, T/SQ FT	$(\sigma_1 - \sigma_3)_{MAX}$		5.91			
TIME TO $(\sigma_1 - \sigma_3)_{MAX}$, MIN		t_f	1925			
ULTIMATE DEVIATOR STRESS, T/SQ FT	$(\sigma_1 - \sigma_3)_{ULT}$		-			
INITIAL DIAMETER, IN.		D_o	2.83			
INITIAL HEIGHT, IN.		H_o	6.12			

CONTROLLED- STRESS TEST

DESCRIPTION OF SPECIMENS SILTSTONE & SHALE REGOLITH

LL	PL	PI	G_s
36	20	16	2.65

TYPE OF SPECIMEN UD

TYPE OF TEST $\bar{R}$

REMARKS:

PROJECT SANTA CRUZ

BORING NO. SB-1A SAMPLE NO. S-2

DEPTH/ELEV 88.5' - 89.7'

LABORATORY SPDL DATE NOV. 1990

TRIAXIAL COMPRESSION TEST REPORT

ENG FORM NO. 2089
REV JUNE 1970 PREVIOUS EDITION IS OBSOLETE

PLATE 31

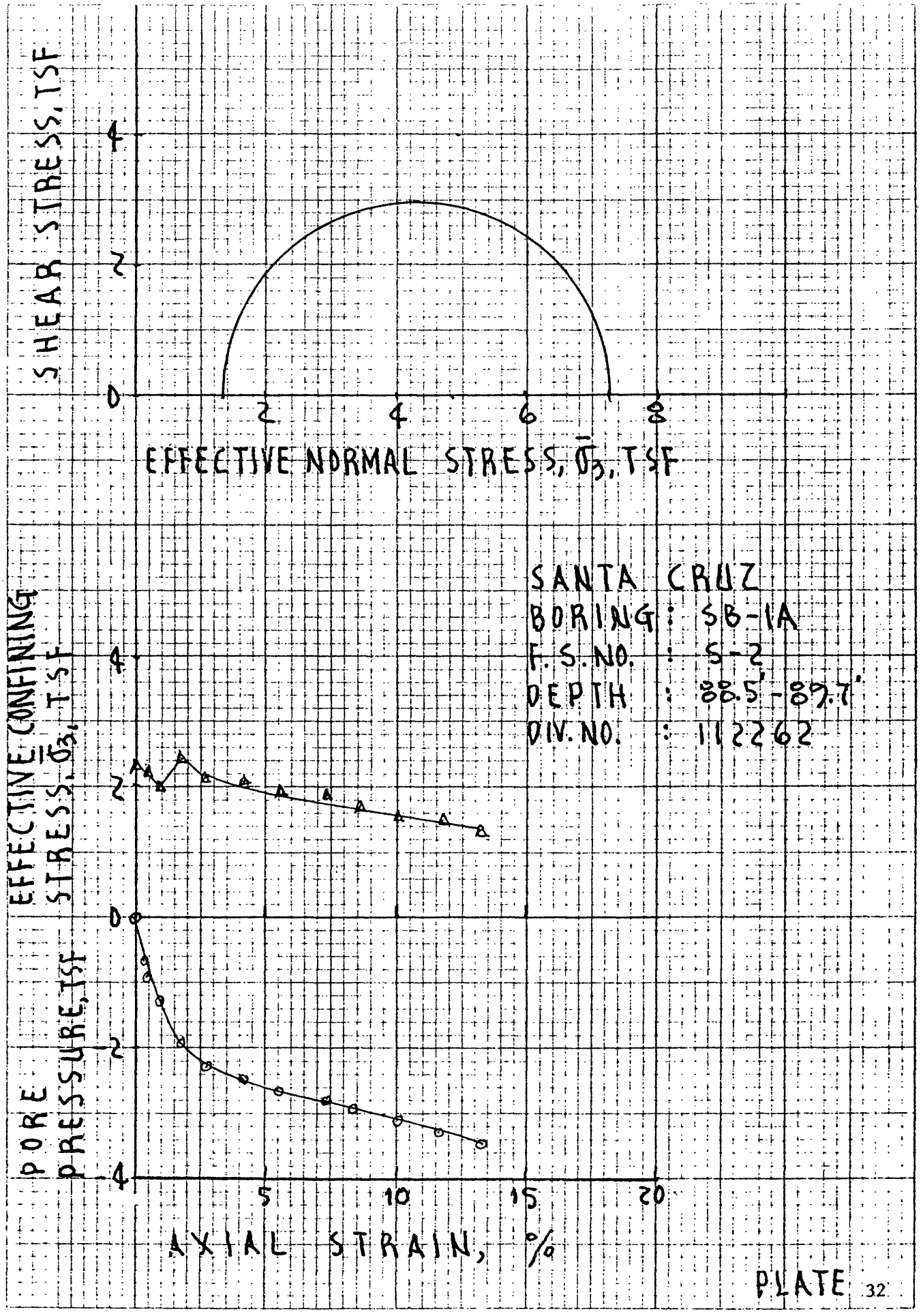
SHEAR STRESS, TSF
4
2
0
2
4
6
8
EFFECTIVE NORMAL STRESS, $\bar{\sigma}_3$, TSF
SANTA CRUZ
BORING: SB-1A
F.S.NO. : S-2
DEPTH : 80.5-80.7'
DIV.NO. : 112262
EFFECTIVE CONFINING PRESSURE, STRESS, $\bar{\sigma}_3$, TSF
PORE
4
2
0
2
4
5
10
15
20
AXIAL STRAIN, %

PLATE 32

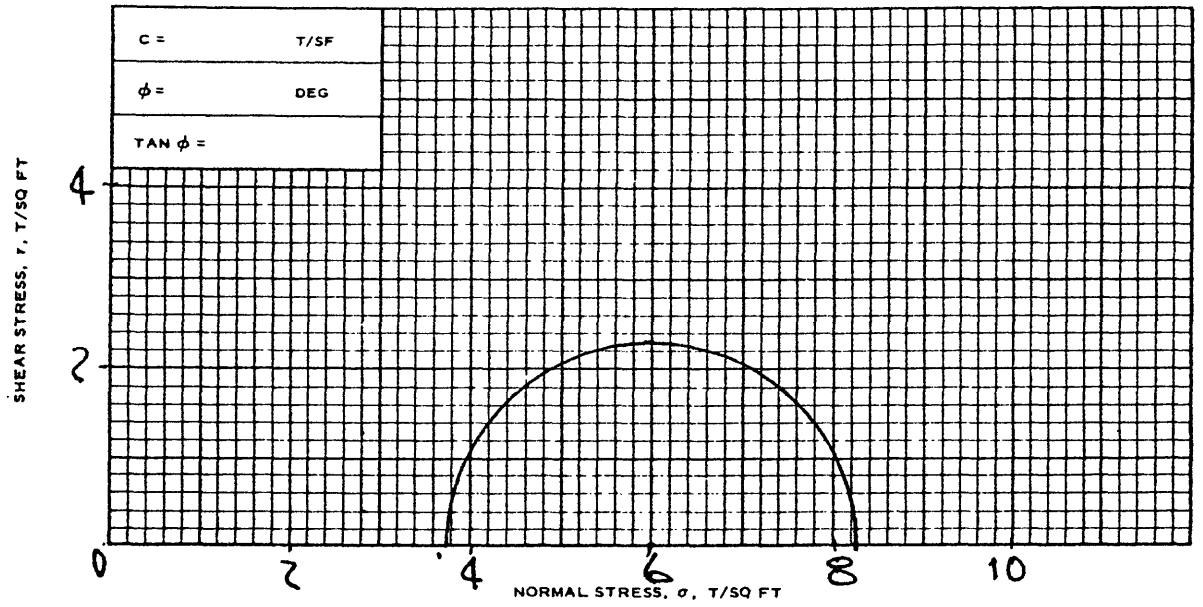

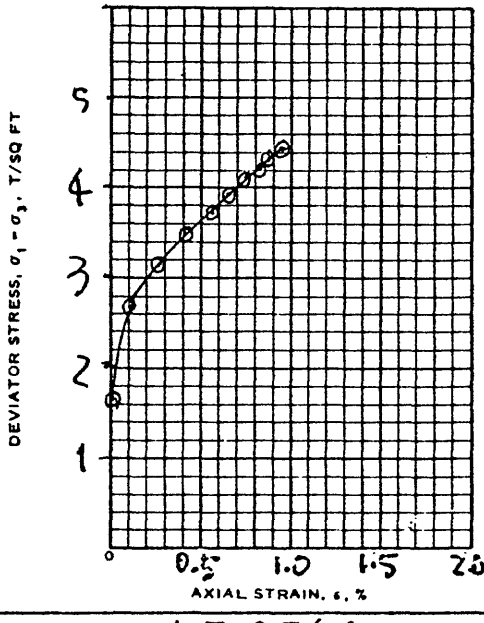

SPECIMEN NO.			112221			
INITIAL	WATER CONTENT, %	w_o	15.3			
	DRY DENSITY LB/ CU FT	γ_{d_o}	116.5			
	SATURATION, %	S_o	97			
	VOID RATIO	e_o	0.419			
BEFORE SHEAR	WATER CONTENT, %	w_c	15.4			
	DRY DENSITY LB/CU FT	γ_{d_c}	117.0			
	SATURATION, %	S_c	97			
	VOID RATIO	e_c	0.413			
	FINAL BACK PRESSURE, T/SQ FT	u_o	3.60			
MINOR PRINCIPAL STRESS, T/SQ FT		σ_3	3.74			
MAXIMUM DEVIATOR STRESS, T/SQ FT		$(\sigma_1 - \sigma_3)_{MAX}$	4.53			
TIME TO $(\sigma_1 - \sigma_3)_{MAX}$, MIN		t_f	330			
ULTIMATE DEVIATOR STRESS, T/SQ FT		$(\sigma_1 - \sigma_3)_{ULT}$	–			
INITIAL DIAMETER, IN.		D_o	2.81			
INITIAL HEIGHT, IN.		H_o	5.97			

CONTROLLED- STRESS TEST

DESCRIPTION OF SPECIMENS SAND

LL	PL	PI N.P.	G_s 2.65

TYPE OF SPECIMEN U D TYPE OF TEST R

REMARKS:

PROJECT SANTA CRUZ

BORING NO. SR-2 SAMPLE NO. S-4

DEPTH/ELEV 78.5' - 79.0'

LABORATORY SPD DATE NOV 1990

TRIAXIAL COMPRESSION TEST REPORT

ENG FORM NO. 2089 REV JUNE 1970 PREVIOUS EDITION IS OBSOLETE

PLATE 33

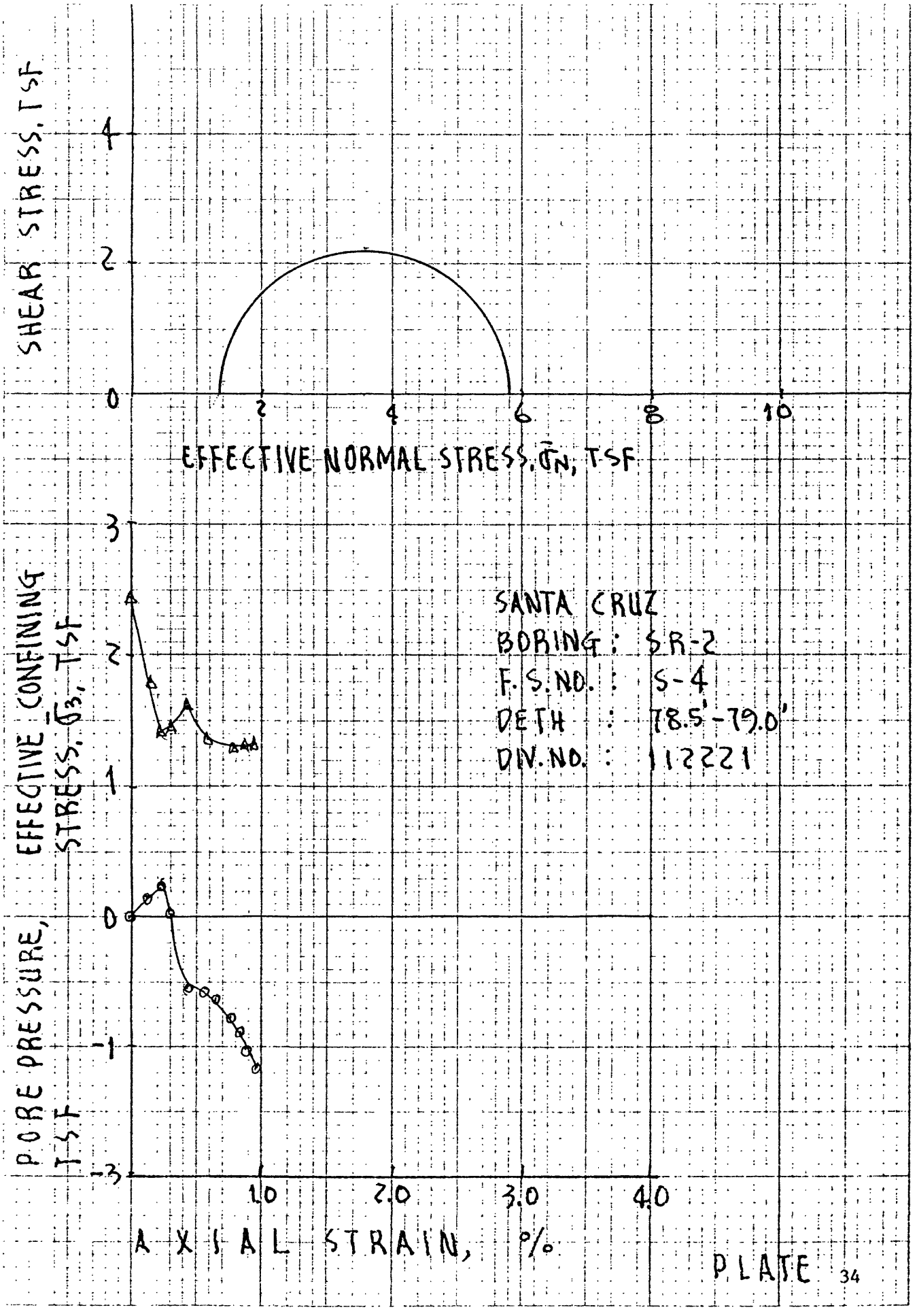
SHEAR STRESS, TSF
4
2
0
2
4
6
8
10
EFFECTIVE NORMAL STRESS, $\bar{\sigma}_N$, TSF
3
2
1
0
-1
-3
EFFECTIVE CONFINING STRESS, $\bar{\sigma}_3$, TSF
PORE PRESSURE, TSF
SANTA CRUZ
BORING : SR-2
F.S.NO. : S-4
DEPTH : 78.5'-79.0'
DIV.NO. : 112221
1.0
2.0
3.0
4.0
AXIAL STRAIN, %

PLATE 34

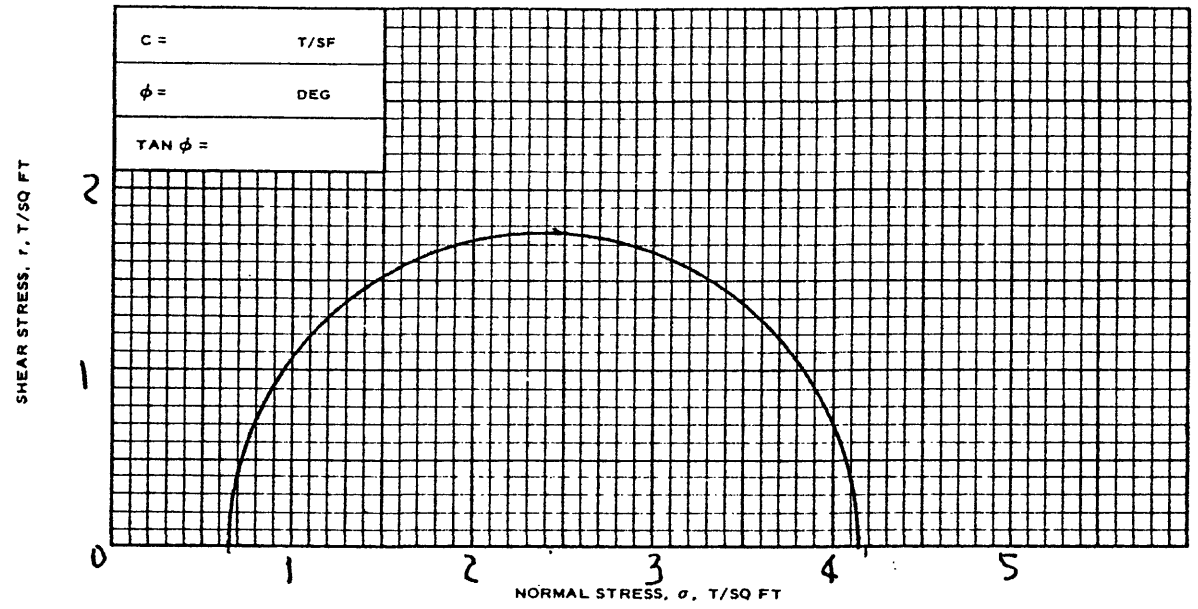

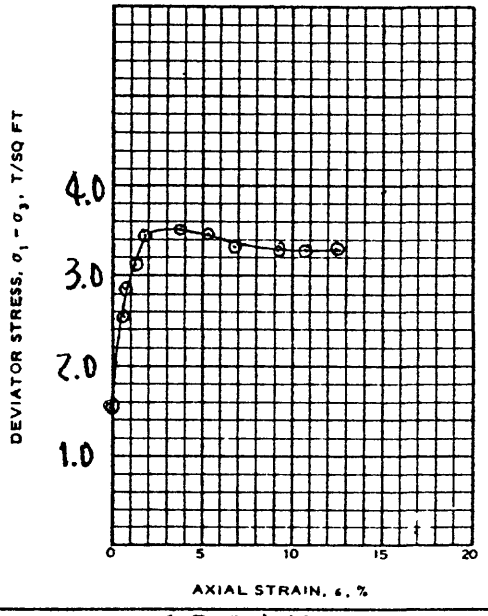

SPECIMEN NO.	112263					
INITIAL	WATER CONTENT, %	w_o	11.2			
	DRY DENSITY LB/ CU FT	γ_{d_o}	122.5			
	SATURATION, %	S_o	76			
	VOID RATIO	e_o	0.406			
BEFORE SHEAR	WATER CONTENT, %	w_c	13.9			
	DRY DENSITY LB/CU FT	γ_{d_c}	124.5			
	SATURATION, %	S_c	100			
	VOID RATIO	e_c	0.383			
	FINAL BACK PRESSURE, T/SQ FT	u_o	6.48			
MINOR PRINCIPAL STRESS, T/SQ FT		σ_3	0.65			
MAXIMUM DEVIATOR STRESS, T/SQ FT	$(\sigma_1 - \sigma_3)_{MAX}$		3.52			
TIME TO $(\sigma_1 - \sigma_3)_{MAX}$, MIN		t_f	220			
ULTIMATE DEVIATOR STRESS, T/SQ FT	$(\sigma_1 - \sigma_3)_{ULT}$		—			
INITIAL DIAMETER, IN.		D_o	6.08			
INITIAL HEIGHT, IN.		H_o	2.81			

CONTROLLED- STRAIN TEST

DESCRIPTION OF SPECIMENS FRACTURED SILTSTONE.

LL	PL	PI	G=2.76(EST)	TYPE OF SPECIMEN UD	TYPE OF TEST S

REMARKS:

σ_c = 33 psi
ANISOTROPICALLY
CONSOLIDATED TO
K_c = 55/33 = 1.67

PROJECT SANTA CRUZ

BORING NO. SB-1A SAMPLE NO. S-3

DEPTH/ELEV 90.0' - 90.7'

LABORATORY SPDL DATE DEC 1990

TRIAXIAL COMPRESSION TEST REPORT

ENG FORM NO. 2089 REV JUNE 1970 PREVIOUS EDITION IS OBSOLETE

PLATE 35

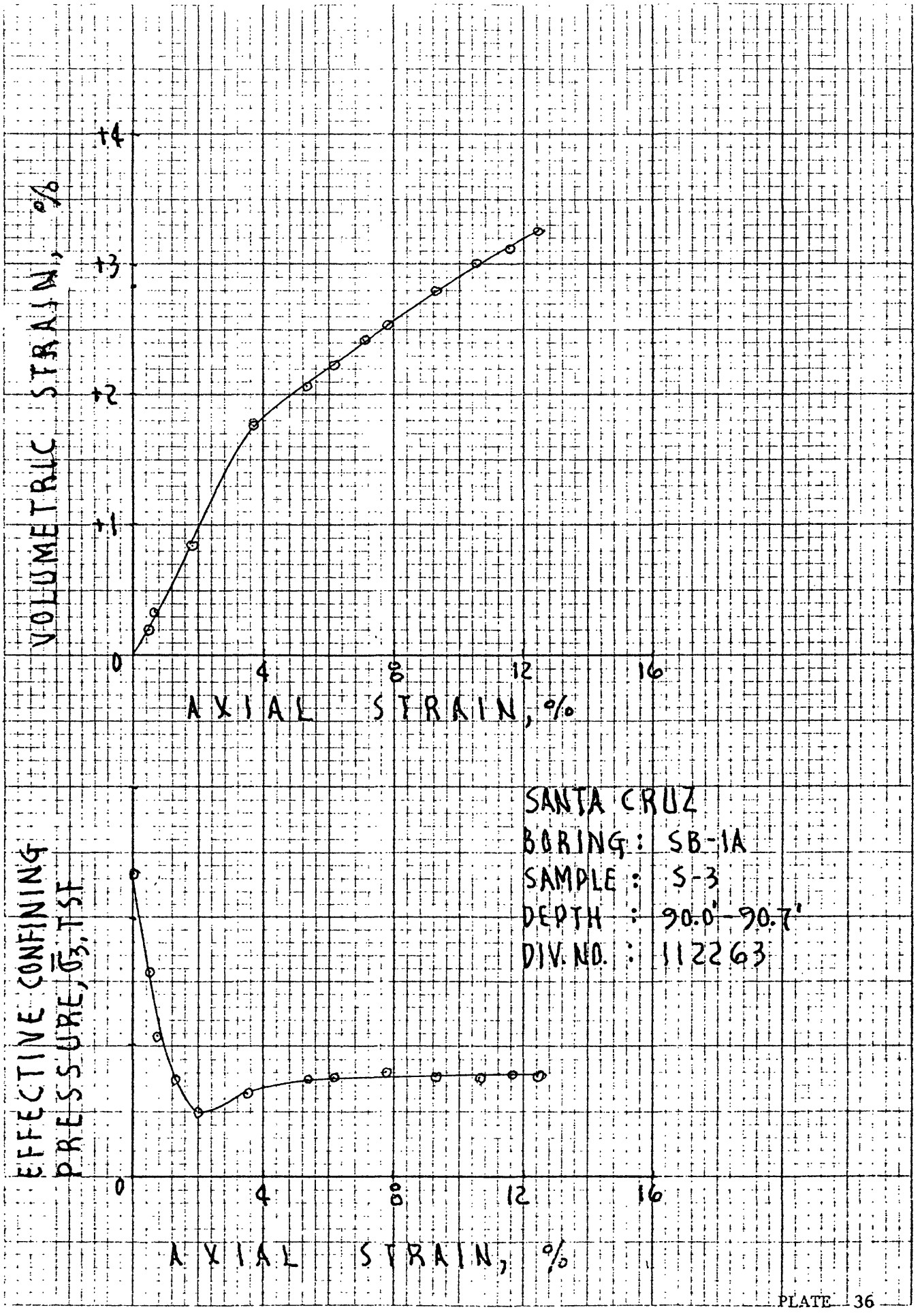
VOLUMETRIC STRAIN, %
+4
+3
+2
+1
0
4
8
12
16
AXIAL STRAIN, %
EFFECTIVE CONFINING PRESSURE, $\bar{\sigma}_3$, TSF
0
4
8
12
16
AXIAL STRAIN, %
SANTA CRUZ
BORING: SB-1A
SAMPLE: S-3
DEPTH: 90.0'-90.7'
DIV. NO.: 112263

PLATE 36

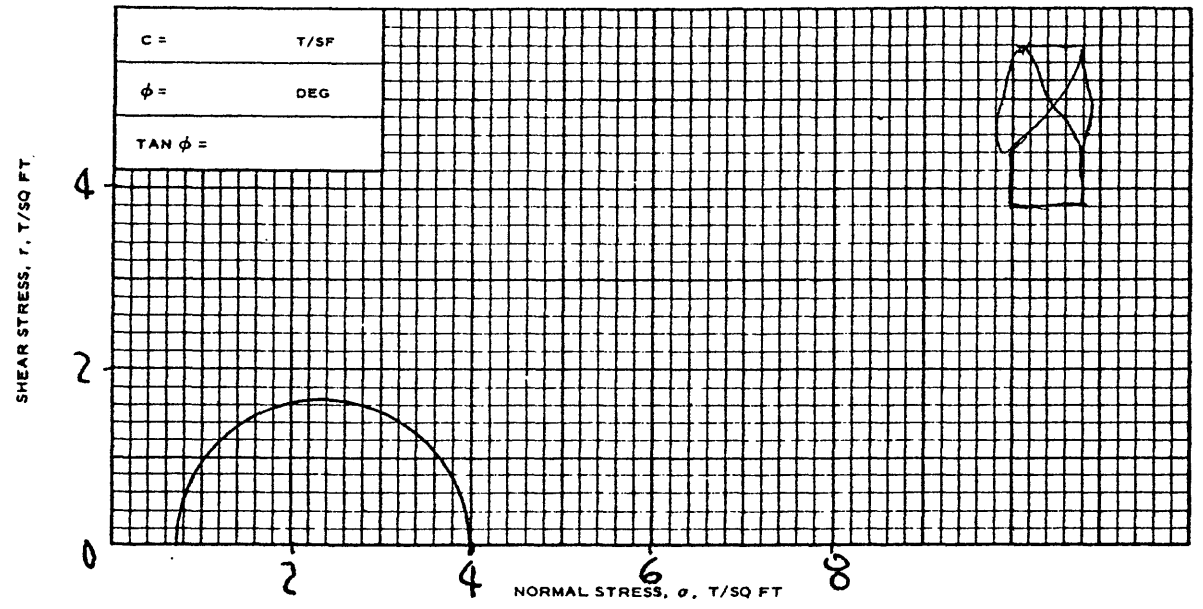

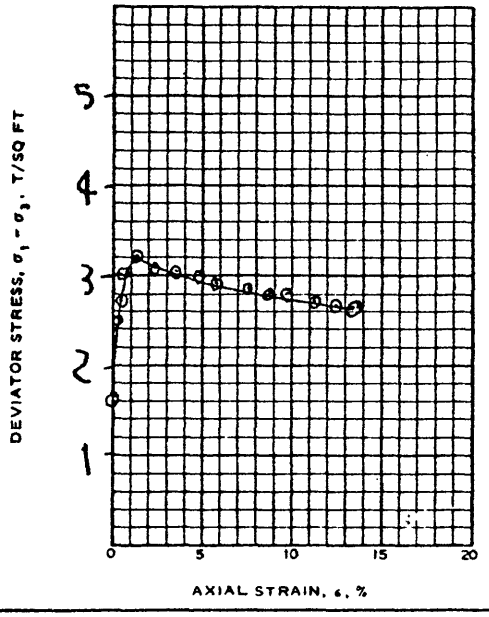

SPECIMEN NO.			112248			
INITIAL	WATER CONTENT, %	w_o	15.5			
	DRY DENSITY LB/ CU FT	γ_{d_o}	115.5			
	SATURATION, %	S_o	95			
	VOID RATIO	e_o	0.4315			
BEFORE SHEAR	WATER CONTENT, %	w_c	15.2			
	DRY DENSITY LB./CU FT	γ_{d_c}	117.2			
	SATURATION, %	S_c	100			
	VOID RATIO	e_c	0.4025			
	FINAL BACK PRESSURE, T/SQ FT	u_o	5.04			
MINOR PRINCIPAL STRESS, T/SQ FT		σ_3	0.72			
MAXIMUM DEVIATOR STRESS, T/SQ FT	$(\sigma_1 - \sigma_3)_{MAX}$		3.29			
TIME TO $(\sigma_1 - \sigma_3)_{MAX}$, MIN		t_f	1585			
ULTIMATE DEVIATOR STRESS, T/SQ FT	$(\sigma_1 - \sigma_3)_{ULT}$					
INITIAL DIAMETER, IN.		D_o	2.87			
INITIAL HEIGHT, IN.		H_o	6.14			

CONTROLLED- STRESS TEST

DESCRIPTION OF SPECIMENS

LL	PL	PI	G_s 2.65(EST.)	TYPE OF SPECIMEN UD	TYPE OF TEST S

REMARKS:

PROJECT SANTA CRUZ

BORING NO. SB-1 SAMPLE NO. ST-1

DEPTH/ELEV 10.0' - 12.3'

LABORATORY SPD DATE DEC 1990

TRIAXIAL COMPRESSION TEST REPORT

ENG FORM NO. 2089
REV JUNE 1970 PREVIOUS EDITION IS OBSOLETE

PLATE 37

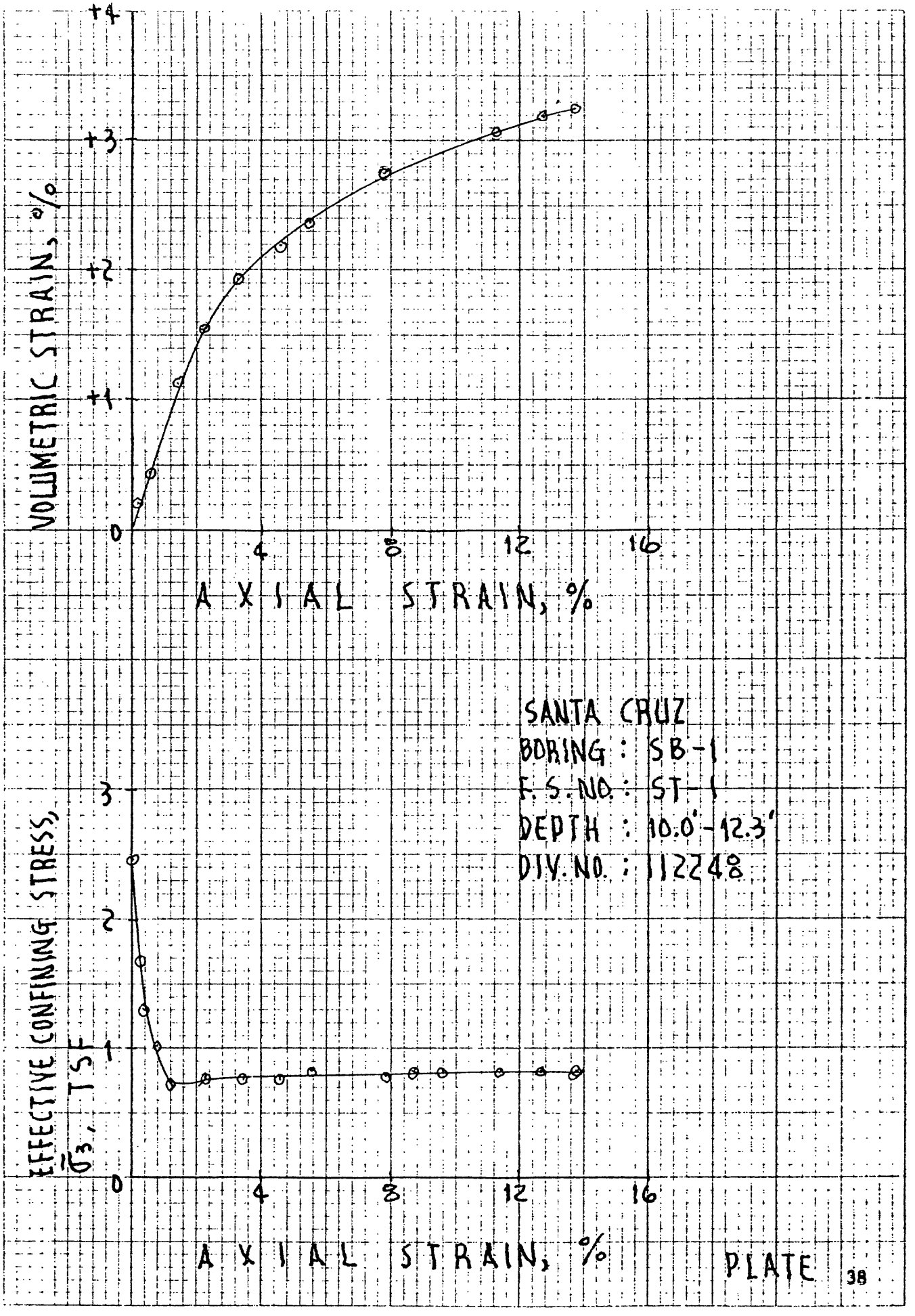
+4
+3
+2
+1
0
VOLUMETRIC STRAIN, %
4
8
12
16
AXIAL STRAIN, %
SANTA CRUZ
BORING : SB-1
F.S.NO. : ST-1
DEPTH : 10.0'-12.3'
DIV.NO. : 11224
3
2
1
0
EFFECTIVE CONFINING STRESS, $\bar{\sigma}_3$, TSF
4
8
12
16
AXIAL STRAIN, %

PLATE 38

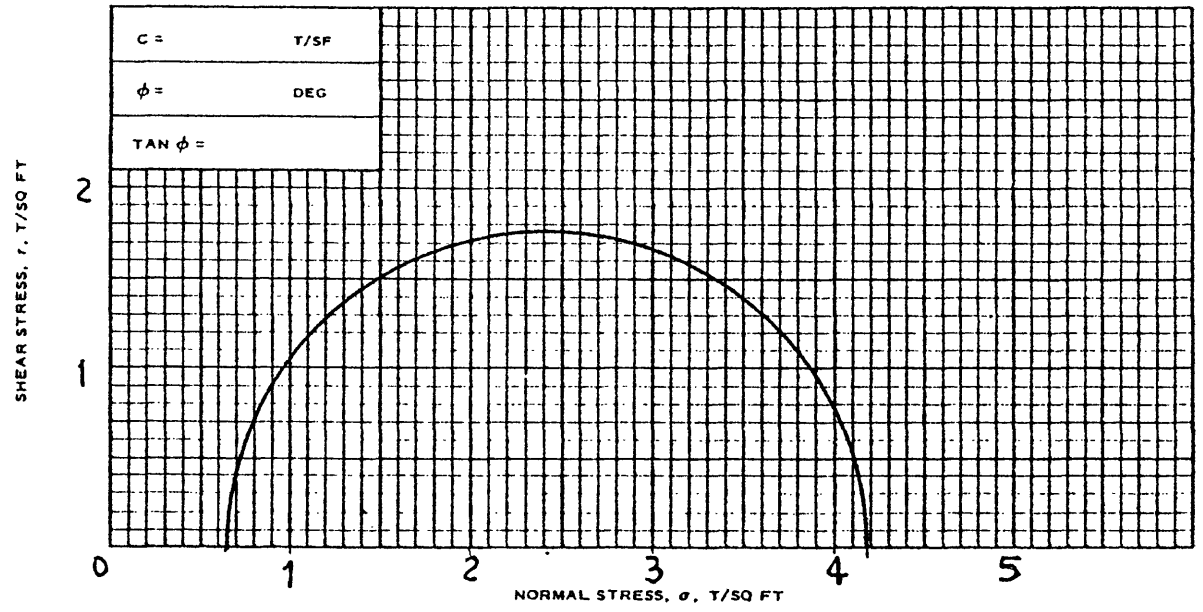

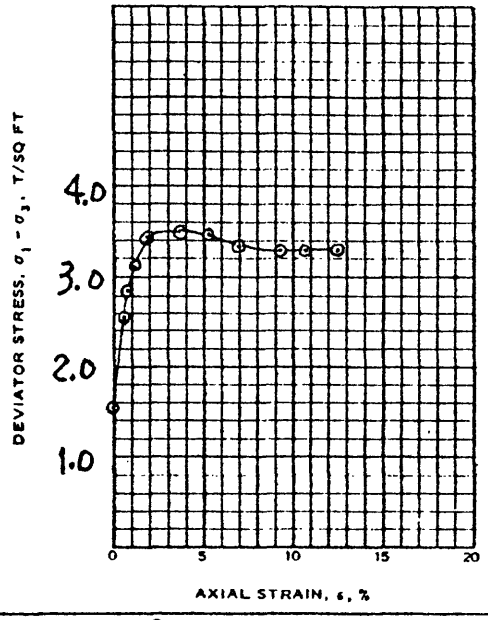

SPECIMEN NO. 112263						
INITIAL	WATER CONTENT, %	w_o	11.2			
	DRY DENSITY LB/ CU FT	γ_{d_o}	122.5			
	SATURATION, %	S_o	76			
	VOID RATIO	e_o	.406			
BEFORE SHEAR	WATER CONTENT, %	w_c	13.9			
	DRY DENSITY LB./CU FT	γ_{d_c}	124.5			
	SATURATION, %	S_c	100			
	VOID RATIO	e_c	.383			
	FINAL BACK PRESSURE, T/SQ FT	u_o	6.48			
MINOR PRINCIPAL STRESS, T/SQ FT		σ_3	0.65			
MAXIMUM DEVIATOR STRESS, T/SQ FT	$(\sigma_1 - \sigma_3)_{MAX}$		3.52			
TIME TO $(\sigma_1 - \sigma_3)_{MAX}$, MIN		t_f	220			
ULTIMATE DEVIATOR STRESS, T/SQ FT	$(\sigma_1 - \sigma_3)_{ULT}$		—			
INITIAL DIAMETER, IN.		D_o	6.08			
INITIAL HEIGHT, IN.		H_o	2.81			

CONTROLLED- STRAIN TEST

DESCRIPTION OF SPECIMENS FRACTURED SILTSTONE

LL	PL	PI	G_s 2.76 (EST.)	TYPE OF SPECIMEN UNDISTURBED	TYPE OF TEST "S"

REMARKS:

σ_c = 33 psi

ANISOTROPIC CONSOLIDATION TO 55/33 = 1.67

PROJECT SANTA CRUZ

BORING NO. SA-1A SAMPLE NO. S-3

DEPTH/ELEV 90' - 90.7'

LABORATORY SPD DATE DEC 1990

TRIAXIAL COMPRESSION TEST REPORT

ENG FORM NO. 2089 REV JUNE 1970 PREVIOUS EDITION IS OBSOLETE

PLATE 39

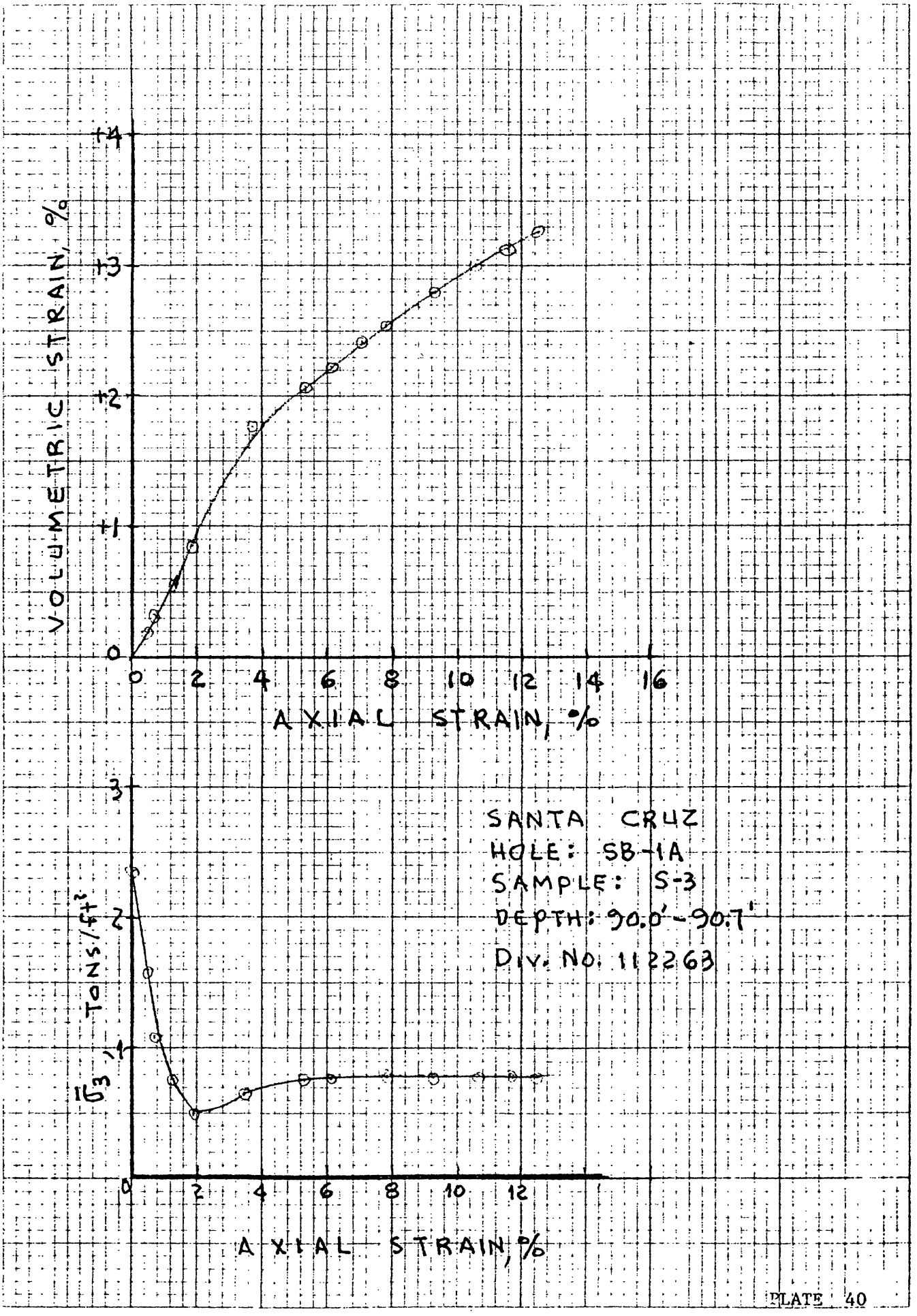
VOLUMETRIC STRAIN, %
+4
+3
+2
+1
0
0
2
4
6
8
10
12
14
16
AXIAL STRAIN, %
SANTA CRUZ
HOLE: SB-1A
SAMPLE: S-3
DEPTH: 90.0'-90.7'
DIV. NO. 112263
$\bar{\sigma}_3$, TONS/FT²
3
2
1
0
2
4
6
8
10
12
AXIAL STRAIN, %

PLATE 40

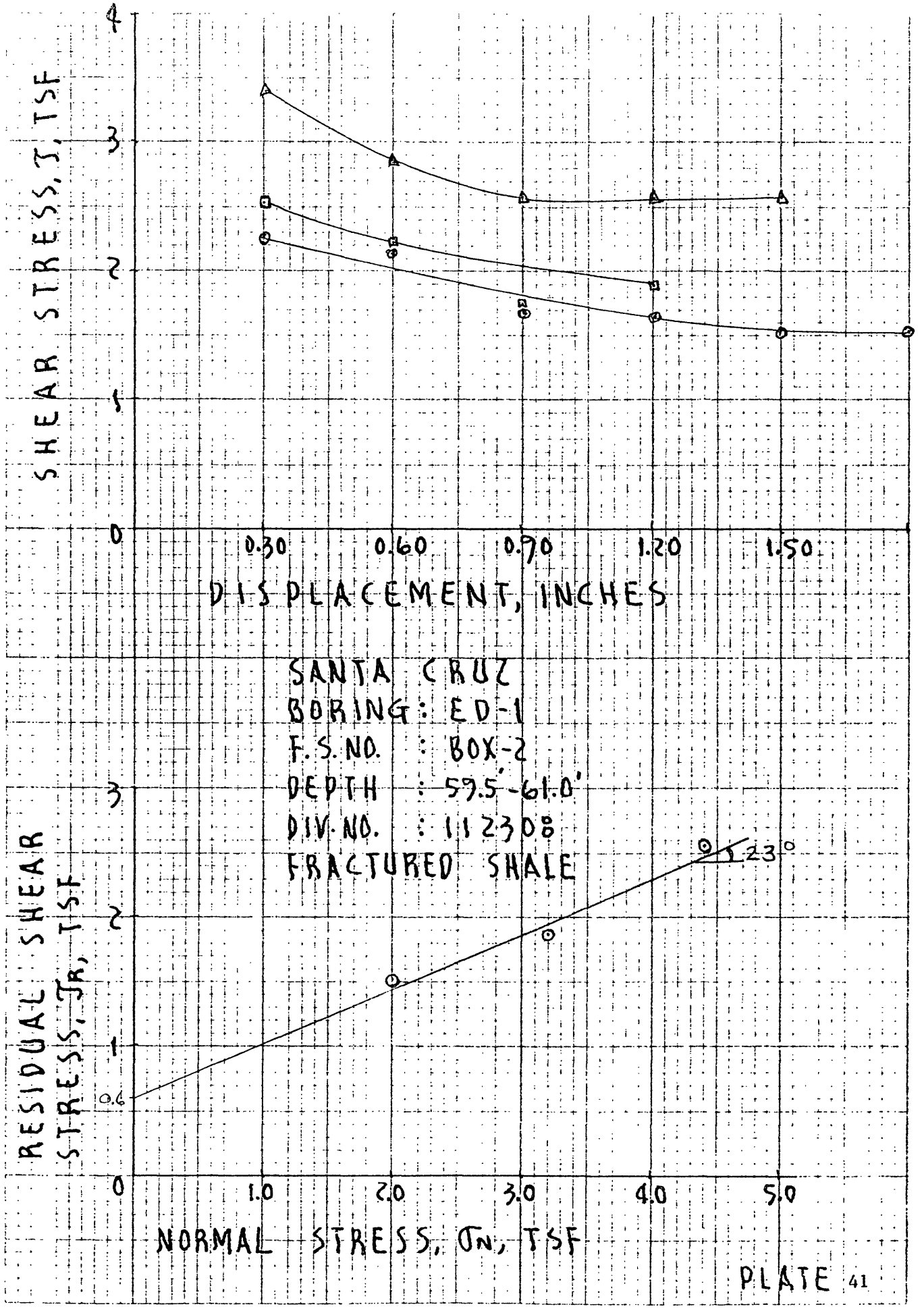
SHEAR STRESS, τ, TSF
4
3
2
1
0
0.30
0.60
0.90
1.20
1.50
DISPLACEMENT, INCHES
SANTA CRUZ
BORING: ED-1
F.S.NO. : BOX-2
DEPTH : 59.5'-61.0'
DIV.NO. : 11230
FRACTURED SHALE
RESIDUAL SHEAR STRESS, τR, TSF
3
2
1
0.6
0
23°
1.0
2.0
3.0
4.0
5.0
NORMAL STRESS, σN, TSF

PLATE 41

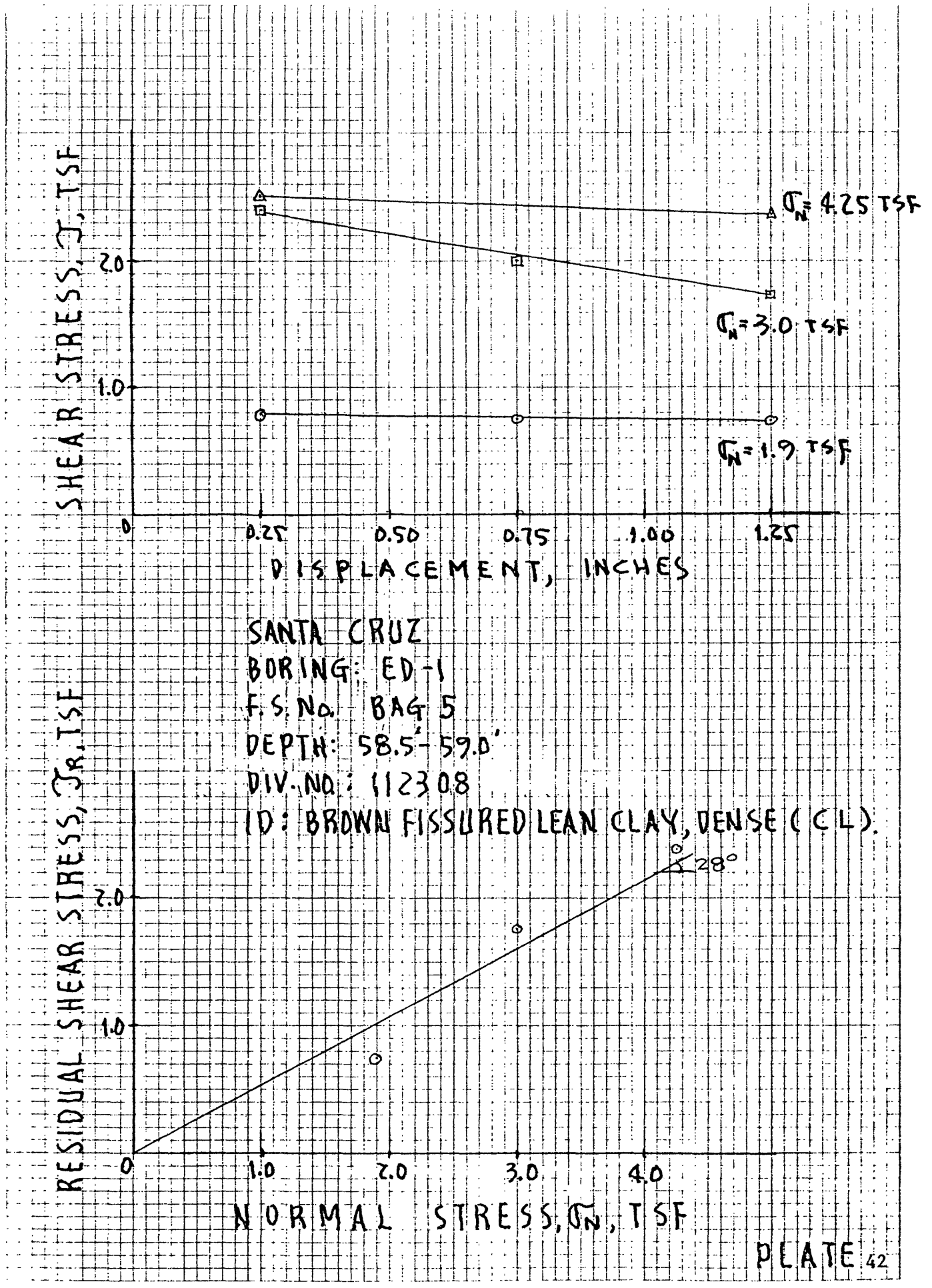
SHEAR STRESS, τ, TSF
2.0
1.0
0
0.25
0.50
0.75
1.00
1.25
DISPLACEMENT, INCHES
σN = 4.25 TSF
σN = 3.0 TSF
σN = 1.9 TSF
SANTA CRUZ
BORING: ED-1
F.S. No. BAG 5
DEPTH: 58.5'-59.0'
DIV. NO.: 112308
ID: BROWN FISSURED LEAN CLAY, DENSE (CL).
RESIDUAL SHEAR STRESS, τR, TSF
28°
2.0
1.0
0
1.0
2.0
3.0
4.0
NORMAL STRESS, σN, TSF

PLATE 42

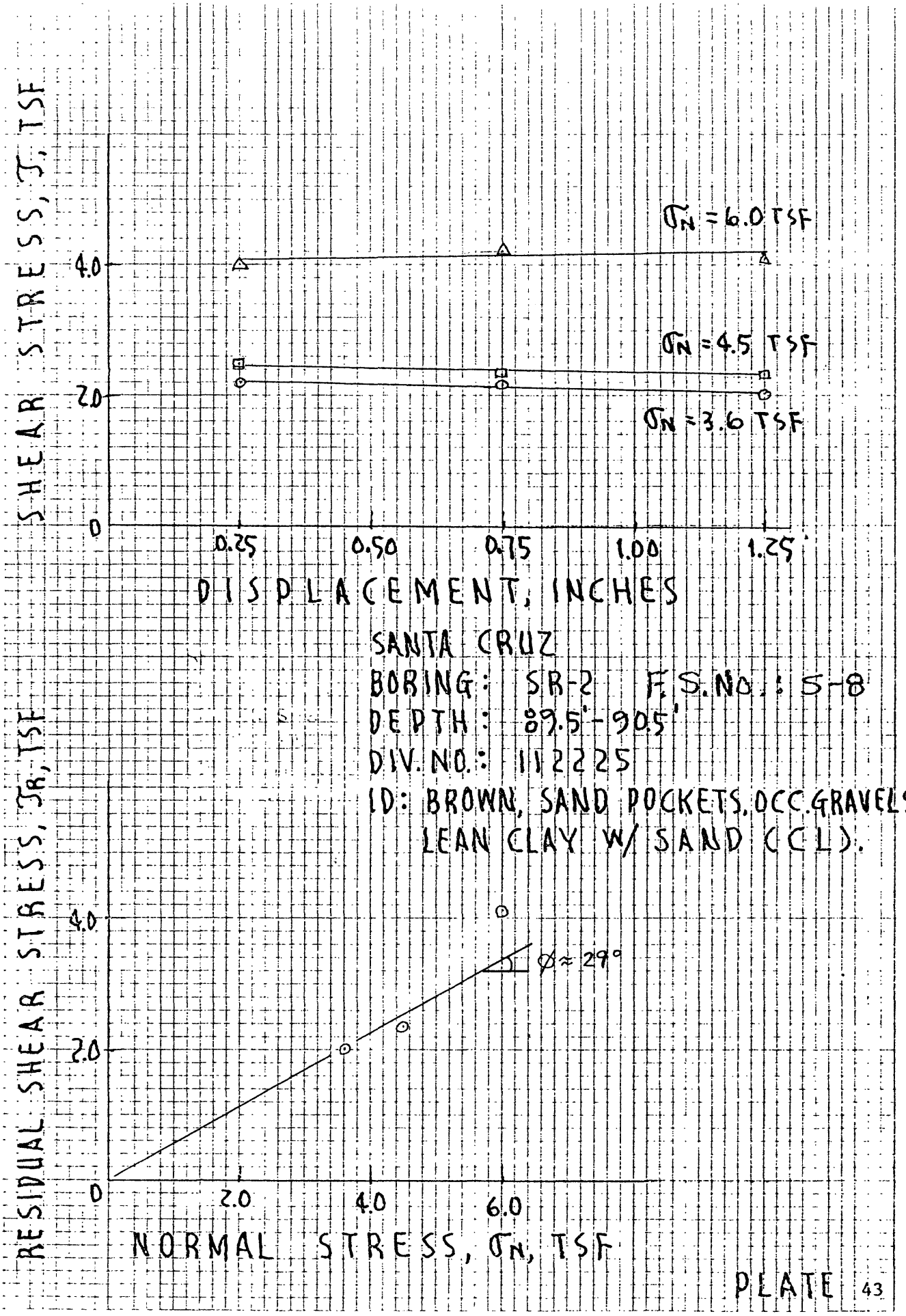
SHEAR STRESS, S, TSF
4.0
2.0
0
σ_N = 6.0 TSF
σ_N = 4.5 TSF
σ_N = 3.6 TSF
0.25
0.50
0.75
1.00
1.25
DISPLACEMENT, INCHES
SANTA CRUZ
BORING: SR-2 F.S.NO.: 5-8
DEPTH: 97.5'-90.5'
DIV.NO.: 112225
ID: BROWN, SAND POCKETS, OCC. GRAVELS, LEAN CLAY W/ SAND (CL).
RESIDUAL SHEAR STRESS, S_R, TSF
4.0
2.0
0
$\phi \approx 29°$
2.0
4.0
6.0
NORMAL STRESS, σ_N, TSF

PLATE 43

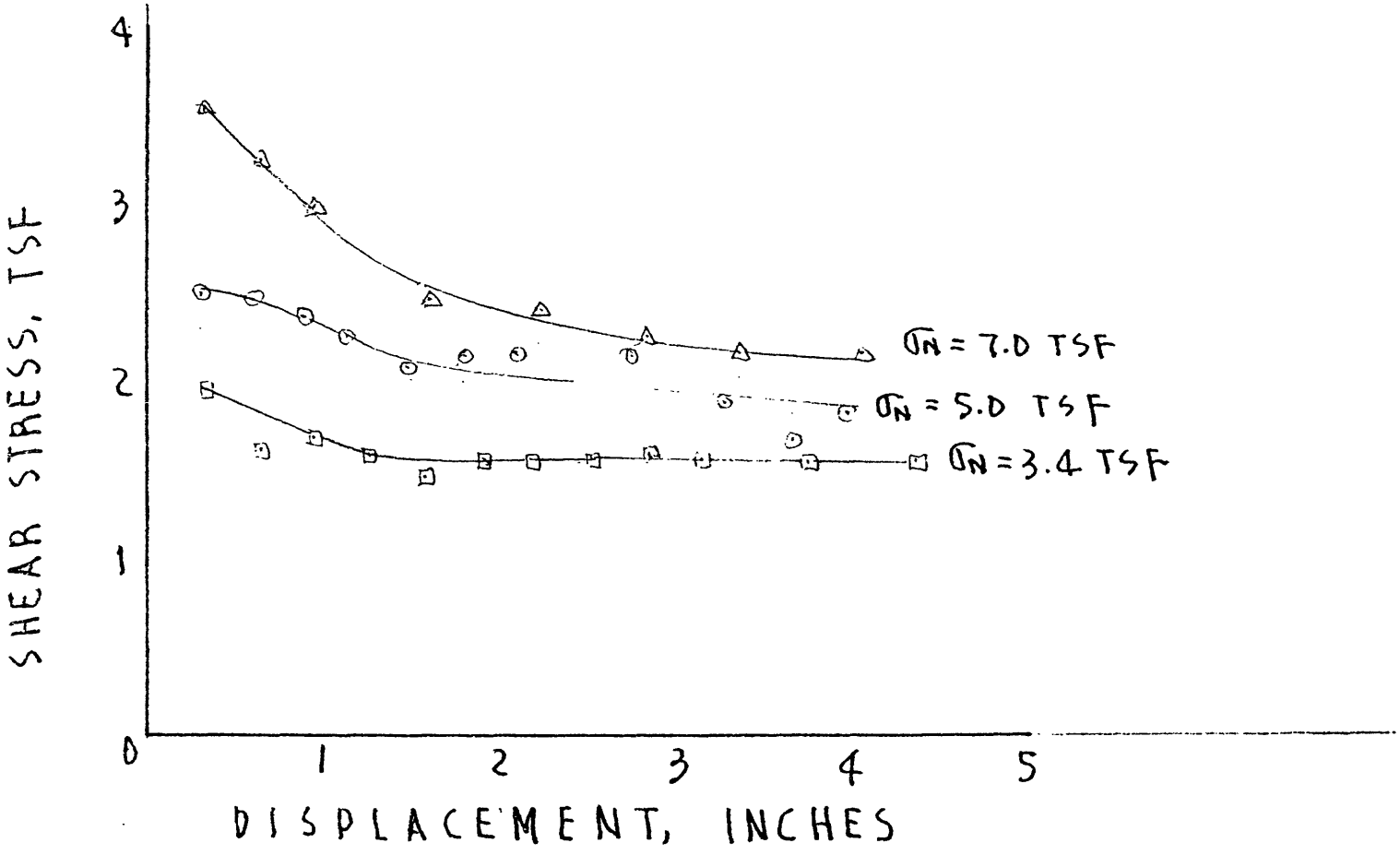

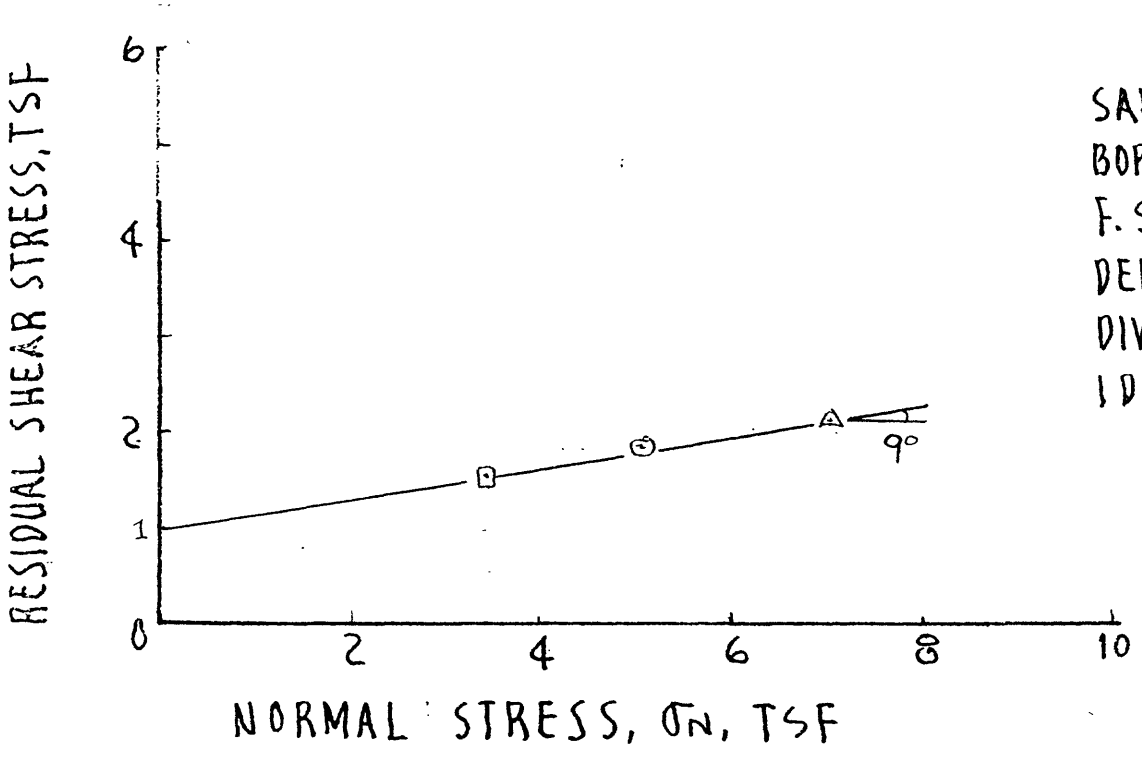

SANTA CRUZ
BORING: SR-2
F.S.NO.: S-12
DEPTH : 99.5'-100.4'
DIV.NO.: 112229
ID : SHALE

PLATE 44

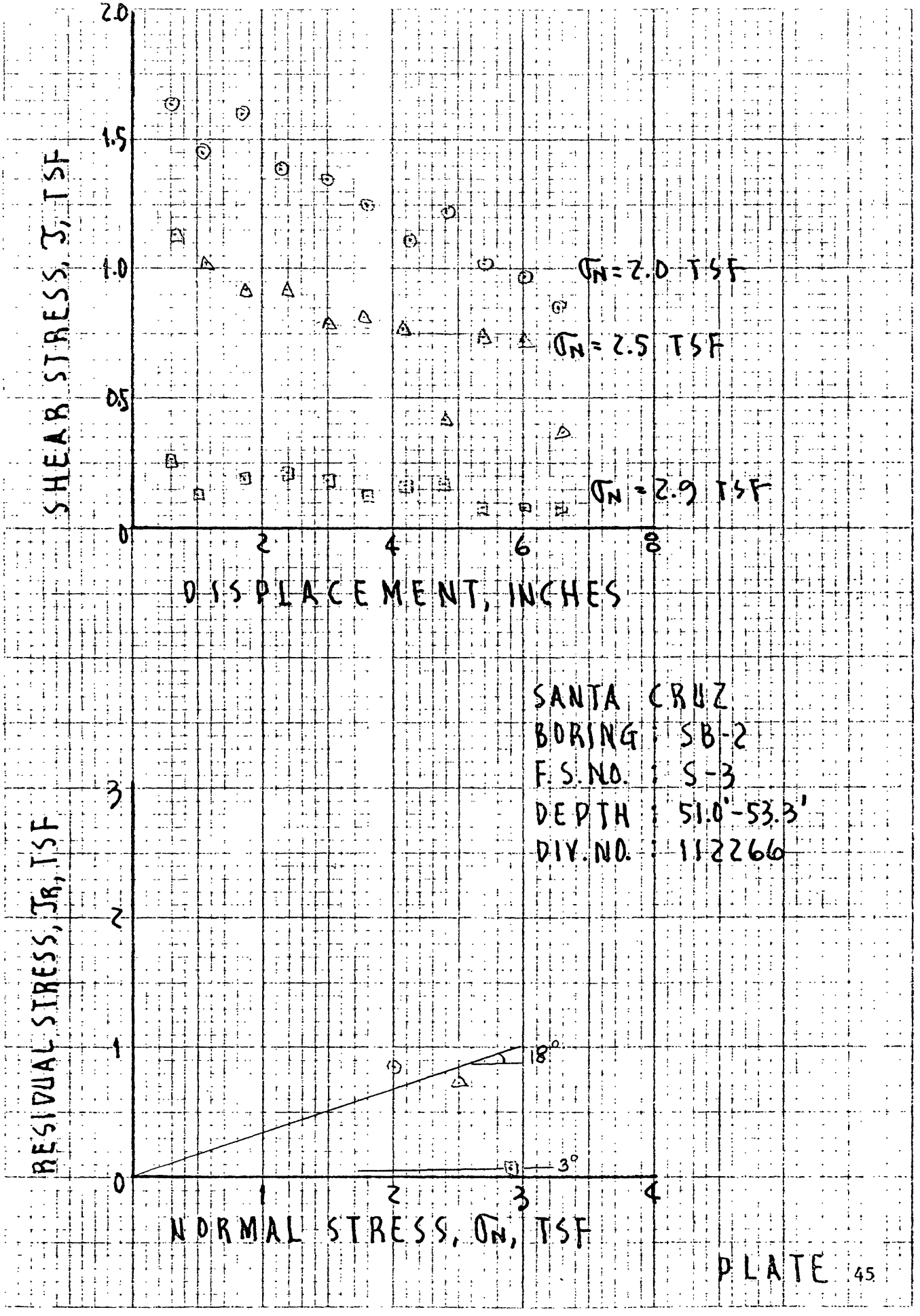
SHEAR STRESS, S, TSF
2.0
1.5
1.0
0.5
0
σ_N = 2.0 TSF
σ_N = 2.5 TSF
σ_N = 2.9 TSF
2
4
6
8
DISPLACEMENT, INCHES
SANTA CRUZ
BORING : SB-2
F.S.NO. : S-3
DEPTH : 51.0'-53.3'
DIV.NO. : 112266
RESIDUAL STRESS, S_R, TSF
3
2
1
0
18°
3°
1
2
3
4
NORMAL STRESS, σ_N, TSF

PLATE 45

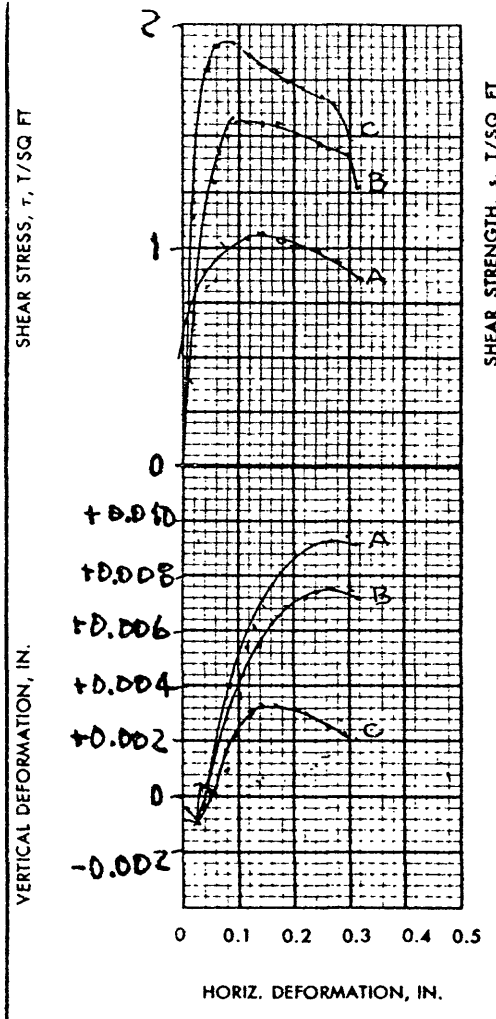

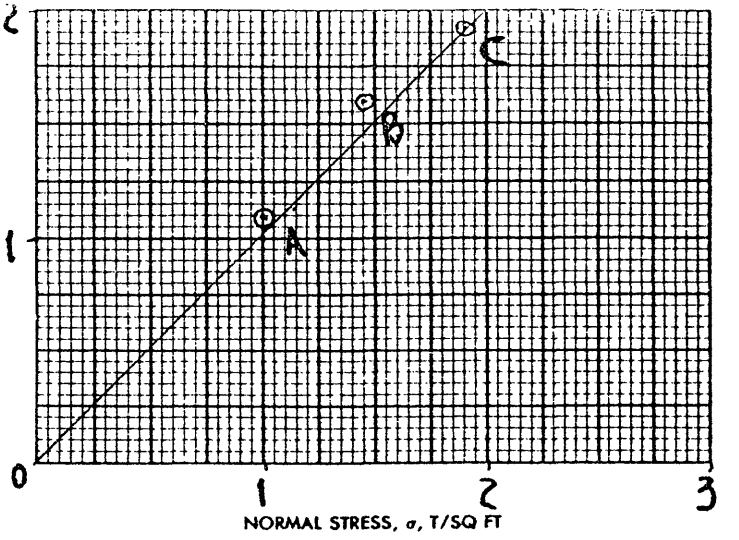

SHEAR STRENGTH PARAMETERS

$\phi' =$ 45°

TAN $\phi' =$ _____

$c' =$ 0 T/SQ FT

☐ CONTROLLED STRESS

☒ CONTROLLED STRAIN

TEST NO. 112302			A	B	C	
INITIAL	WATER CONTENT	w_o	18.1 %	13.0 %	13.5 %	%
	VOID RATIO	e_o	0.4830	0.5363	0.5410	
	SATURATION	S_o	100 %	64.7 %	66.6 %	%
	DRY DENSITY, LB/CU FT	γ_d	112.3	108.4	108.1	
VOID RATIO AFTER CONSOLIDATION		e_c	0.4299	0.5008	0.4946	
TIME FOR 50 PERCENT CONSOLIDATION, MIN		t_{50}	0.1	0.1	0.1	
FINAL	WATER CONTENT	w_f	16.9 %	19.5 %	18.7 %	%
	VOID RATIO	e_f	0.4502	0.5206	0.4992	
	SATURATION	S_f	100 %	100 %	100 %	%
NORMAL STRESS, T/SQ FT		σ	1.00	1.45	1.90	
MAXIMUM SHEAR STRESS, T/SQ FT		τ_{max}	1.09	1.59	1.92	
ACTUAL TIME TO FAILURE, MIN		t_f	240	180	180	
RATE OF STRAIN, IN./MIN			0.00053	0.00051	0.00047	
ULTIMATE SHEAR STRESS, T/SQ FT		τ_{ult}				

TYPE OF SPECIMEN UNDISTURED — 2.50 ~~IN. SQUARE~~ DIA. — 0.50 IN. THICK

CLASSIFICATION

LL	PL	PI		G. 2.67

REMARKS

PROJECT SANTA CRUZ

AREA

BORING NO. ED-1 SAMPLE NO. S-1

DEPTH EL 31.5-32.9' DATE 4 DEC 90

DIRECT SHEAR TEST REPORT PLATE 46

ENG FORM 2092 1 JUN 65 (EM 1110-2-1906) PREVIOUS EDITIONS ARE OBSOLETE (TRANSLUCENT) GPO : 1966 OP—214-943 PLATE IX-3

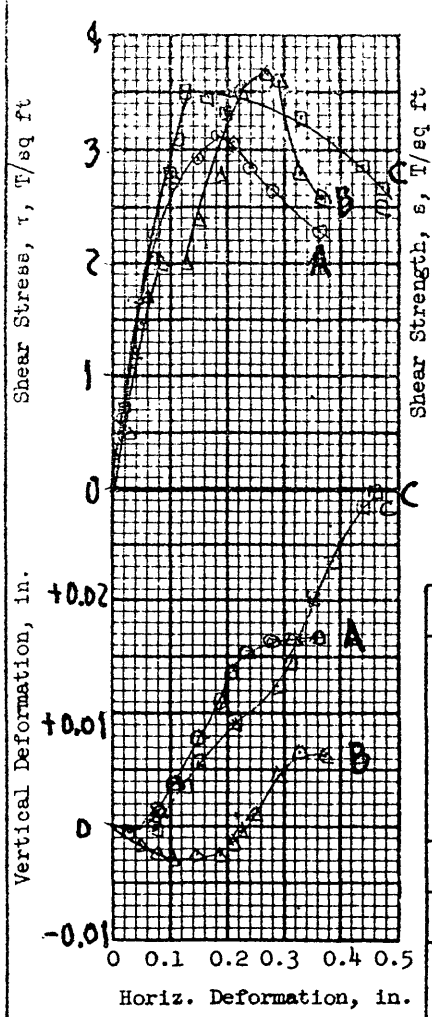

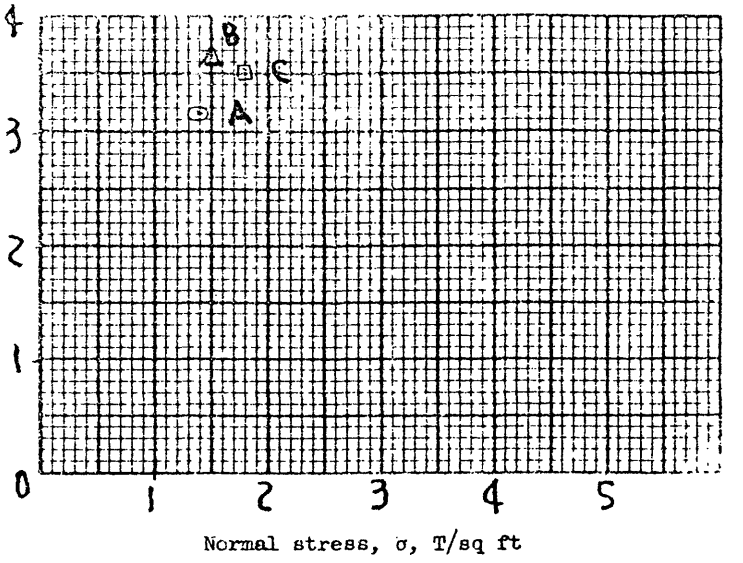

Test No. 112310			A	B	C	
Initial	Water content	w_o	6.3 %	19.6 %	13.0 %	%
	Void ratio	e_o	0.4894	0.5175	0.4847	
	Saturation	S_o	34.5 %	100 %	71.9 %	%
	Dry density, lb/cu ft	γ_d	112.3	110.2	112.6	
Void ratio after consolidation		e_c	0.4510	0.4717	0.4128	
Time for 50 percent consolidation, min		t_{50}	0.1	0.15	0.1	
Final	Water content	w_f	18.7 %	18.3 %	18.9 %	%
	Void ratio	e_f	0.5013	0.4905	0.5052	
	Saturation	S_f	100 %	100 %	100 %	%
Normal stress, T/sq ft		σ	1.40	1.50	1.80	
Maximum shear stress, T/sq ft		τ_{max}	3.17	3.69	3.53	
Actual time to failure, min		t_f	450	520	300	
Rate of strain, in./min			0.0004	0.005	0.004	
Ultimate shear stress, T/sq ft		τ_{ult}	–	–	–	

Shear Strength Parameters

ϕ' = _____ °

tan ϕ' = _____

c' = 3.5 T/sq ft

☐ Controlled stress

☒ Controlled strain

Type of specimen UNDISTURBED | 2.87 in. ~~square~~ DIAMETER | 0.50 in. thick

Classification

LL | PL | PI | | G_s 2.68

Remarks

Project SANTA CRUZ LANDSLIDE

Area

Boring No. ED-2 | Sample No. S-1

Depth El 41.7' - 43' | Date 05 DEC 1990

DIRECT SHEAR TEST REPORT PLATE 47

ENG FORM 2092 1 JUN 65 PREVIOUS EDITIONS ARE OBSOLETE D41491 PLATE IX-3

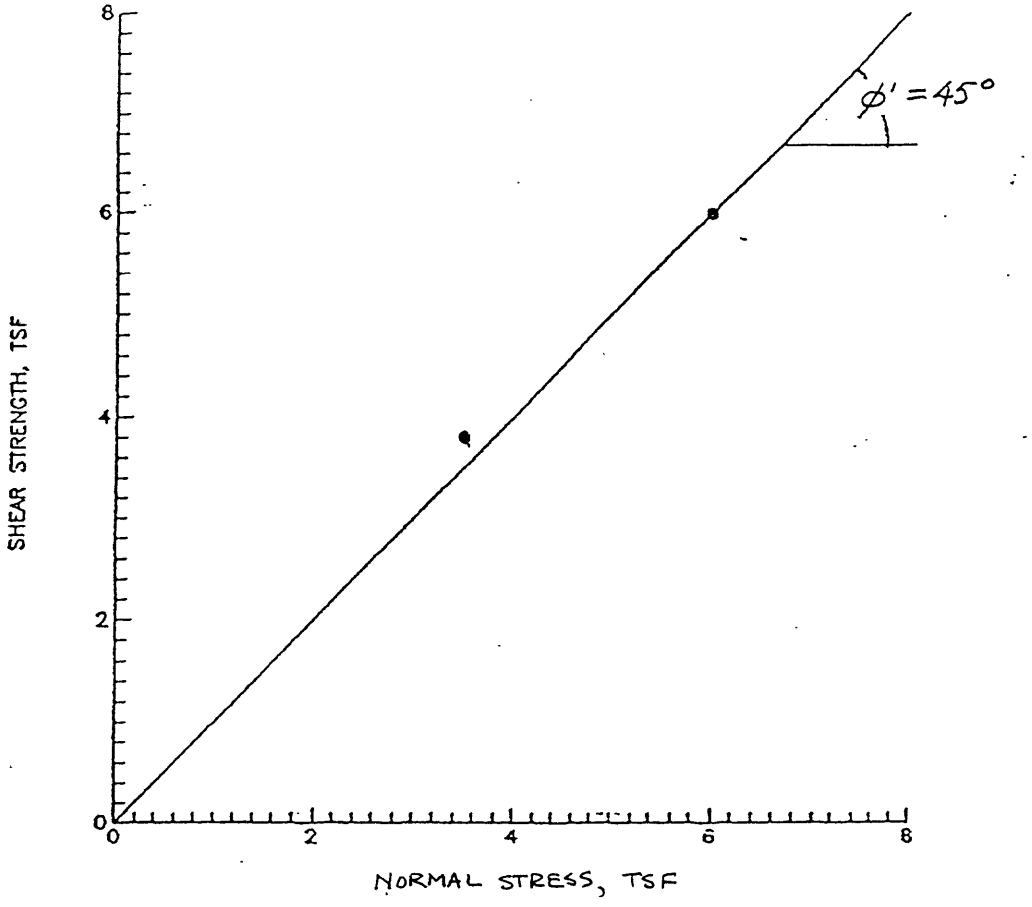

Results of Direct Shear Test on Undisturbed Specimen of Soft Siltstone from Boring DM-2, Depth Interval 91.0-91.4 ft

Plate 48